

# UNCLASSIFIED

AD NUMBER
ADB006505
NEW LIMITATION CHANGE
TO Approved for public release, distribution unlimited
FROM Distribution authorized to U.S. Gov't. agencies only; Test and evaluation; Jan 1975. Other requests shall be referred to the Commander, Frankford Aersenal, Attn: SARFA-MDS-D, Philadelphia, PA, 19137.
AUTHORITY
DA ltr, 17 Aug 1976.

THIS PAGE IS UNCLASSIFIED

AD

FA-TT-75005

ON THE ACCURACY OF FLECHETTES BY DYNAMIC  
WIND TUNNEL TESTS, BY THEORY AND  
ANALYSIS, AND BY ACTUAL FIRINGS

January 1975

Distribution limited to U.S. Government agencies  
only - Test and Evaluation - January 1975. Other  
requests for this document must be referred to  
Commander, Frankford Arsenal, ATTN: SARFA-MDS-D,  
Philadelphia, PA 19137.

DDC  
RECEIVED  
SEP 17 1975  
E



Munitions Development & Engineering Directorate

U.S. ARMY ARMAMENT COMMAND  
FRANKFORD ARSENAL  
PHILADELPHIA, PENNSYLVANIA 19137

## DISPOSITION INSTRUCTIONS

Destroy this report when it is no longer needed. Do not return it to the originator.

The findings in this report are not to be construed as an official Department of the Army position unless so designated by other authorized documents.

UNCLASSIFIED

SECURITY CLASSIFICATION OF THIS PAGE (When Data Entered)

REPORT DOCUMENTATION PAGE		READ INSTRUCTIONS BEFORE COMPLETING FORM
1. REPORT NUMBER FA-TT-75005	2. GOVT ACCESSION NO.	3. RECIPIENT'S CATALOG NUMBER
4. TITLE (and Subtitle) ON THE ACCURACY OF FLECHETTES BY DYNAMIC WIND TUNNEL TESTS, BY THEORY AND ANALYSIS, AND BY ACTUAL FIRINGS		5. TYPE OF REPORT & PERIOD COVERED Technical Engineering Report
7. AUTHOR(s) J.D. Nicolaides L.E. Lijewski (University of C.W. Ingram M.J. Garsik Notre Dame)		6. PERFORMING ORG. REPORT NUMBER
9. PERFORMING ORGANIZATION NAME AND ADDRESS Frankford Arsenal Attn: SARFA-MDS-D Philadelphia, PA 19137		8. CONTRACT OR GRANT NUMBER(s) DAAA25-71-C0447, Mod.P00002
11. CONTROLLING OFFICE NAME AND ADDRESS ARMCOM		10. PROGRAM ELEMENT, PROJECT, TASK AREA & WORK UNIT NUMBERS AMCMS: 662603.11.H7800 DA: 1W662603AH78
14. MONITORING AGENCY NAME & ADDRESS (if different from Controlling Office)		12. REPORT DATE January 1975
		13. NUMBER OF PAGES 358
		15. SECURITY CLASS. (of this report) UNCLASSIFIED
		16a. DECLASSIFICATION/DOWNGRADING SCHEDULE N/A
16. DISTRIBUTION STATEMENT (of this Report) Distribution limited to U.S. Government agencies only - Test and Evaluation January 1975. Other requests for this document must be referred to the Commander, Frankford Arsenal, Attn: SARFA-MDS-D, Philadelphia, PA 19137.		
17. DISTRIBUTION STATEMENT (of the abstract entered in Block 20, if different from Report)		
18. SUPPLEMENTARY NOTES Coordinator - Walter J. Schupp, SARFA-MDS-D.		
19. KEY WORDS (Continue on reverse side if necessary and identify by block number) Flechette Flash x-ray Dispersion Transitional ballistics Trajectory Supersonic wind tunnel Jump angle Flechette dispersion theory		
20. ABSTRACT (Continue on reverse side if necessary and identify by block number) The accuracy and dispersion of flechettes are investigated 1) by an exploratory firing program, 2) by a supersonic dynamic testing wind tunnel program, 3) by development of a theory for jump and dispersion for computer computation and analysis and 4) by precision range firings at Frankford Arsenal. The exploratory firing program reveals the importance of fin and body damage, the blast region, and sabotaging. The dynamic wind tunnel program		

DD FORM 1 JAN 73 1473

EDITION OF 1 NOV 65 IS OBSOLETE

UNCLASSIFIED

SECURITY CLASSIFICATION OF THIS PAGE (When Data Entered)



UNCLASSIFIED

SECURITY CLASSIFICATION OF THIS PAGE (When Data Entered)

20. ABSTRACT (Cont'd)

yields the static and dynamic aeroballistic stability coefficients on various flechette designs. The theory and analysis program has presented the effects of the initial launching conditions, the various stability coefficients and asymmetries and has provided accuracy criteria. Lastly, the flechette firing range program provided a correlation between theory and experiment which clearly suggests that high accuracy and low dispersion in flechettes is possible when optimum aerodynamic design is coupled with good saboting and minimization of blast.

UNCLASSIFIED

SECURITY CLASSIFICATION OF THIS PAGE (When Data Entered)

## TABLE OF CONTENTS

	page
INTRODUCTION . . . . .	2
DISCUSSION . . . . .	4
SUMMARY . . . . .	10
APPENDIX A	
Exploratory Flechette Firing Program	11
APPENDIX B	
Dynamic Supersonic Wind Tunnel Tests of Four-Flechette Configurations	17
APPENDIX C	
Dispersion Theory of High Fineness Ratio, Cruciform Fin Bodies	111
APPENDIX D	
Frankford Arsenal Experimental Ballistics Firing Program of Flechettes	339

## INTRODUCTION

The backbone of ballistics has been the spin stabilized projectile. Virtually, all ordnance from small arms to artillery has almost exclusively utilized the spin stabilized projectile over the last century. Its predecessor was the cannonball and spherical shot. Just as the elongated spin stabilized projectile yielded a marked improvement over the less efficient cannonball, so also fin stabilized ammunition offers great aeroballistic improvements over the spin stabilized projectile. It has only been in recent years that the fin stabilized projectile has come under serious consideration. Some success was achieved by the Germans during World War II with Naval projectile artillery. During the Korean War fin stabilized anti-tank ammunition was introduced which improved the effectiveness of the shape change because of its low spin. In recent years the accuracy of fin stabilized projectiles has improved due to the application of the Tricyclic Theory, the use of dynamic supersonic wind tunnel tests, and improved launching techniques. Because of their small size and the desire for very inexpensive manufacture, the flechette has not received the careful attention that it requires to achieve high accuracy. It is essential that manufacturing techniques, saboting techniques, launching techniques, blast suppression techniques, optimized aeroballistic design procedures, dynamic wind tunnel tests, accuracy theory studies, computer analysis, and precision firings all be undertaken and optimized to achieve good flechette accuracy and low dispersion.

The purpose of this study is to explore flechette design and performance with a view towards achieving high accuracy and low dispersion. Specifically, exploratory firing programs were carried out by Frankford Arsenal, by the Ballistics Laboratories and by the University of Notre Dame. The results of the Notre Dame Flechette Firing Program are summarized in Appendix A.

A dynamic wind tunnel testing program was also carried out by the university on various flechette designs so as to determine the essential static and dynamic aeroballistic stability coefficients. The results of this dynamic wind tunnel program are summarized in Appendix B.

Of particular importance is the development of a computer theory for flechette flight performance, accuracy and dispersion. This theory together with an extensive computer analysis is given in Appendix C. Finally, flechette firings were carried out in the precision range at Frankford Arsenal and a correlation of theory and experiment is also provided in Appendix C. along with a physical evaluation of dispersion.

Based on the theory, sabot design and launcher changes were made in order to reduce the values of those parameters which affect dispersion. A second series of firings were conducted and the analysis of the results is provided in Appendix D.

## DISCUSSION

### Exploratory Flechette Firing Program

The exploratory flechette firing program both at Frankford Arsenal and at the university have provided an opportunity to measure flechette spin, to measure flechette accuracy and dispersion, to identify fin damage and body damage due to stripper, to provide an approximate measure of dynamic stability at long range, to provide a first hand appreciation of the strong blast region and to concentrate on sabot design, separation, and transition all as affecting flechette flight performance and accuracy.

In addition a transition ballistic range was set up and optimized at Frankford Arsenal to obtain initial condition data using flash x-ray photography. A complete description of the set-up is provided in Appendix C.

BRL conducted free flight tests in their transonic Spark Range to obtain aerodynamic data on the various flechettes under consideration. These data were used in the preliminary development of the dispersion theory and are compared with the wind tunnel results in Appendix B.

## Dynamic Supersonic Wind Tunnel Tests of Four Flechette Configurations

In order to obtain both static and dynamic wind tunnel data on flechette configurations, special tests were carried out at the University of Notre Dame which utilizes its unique vertical down flow supersonic wind tunnel and utilizes its one-degree-of-freedom pitching dynamic support instrumentation. Four flechette configurations were constructed and tested. The data from these dynamic tests was measured on a photo-comparator and reduced and fitted by using the Wobble program. The Notre Dame data on  $CM_{\alpha}$  and  $CM_q + CM_{\dot{\alpha}}$  is in good agreement with the data obtained by the Ballistic Research Laboratory at small angles of attack and small mach numbers. At the larger angles of attack, the Notre Dame data is as much as four times larger as the BRL data in damping and as much as two times larger than the  $CM_{\alpha}$  data. Thus, the nonlinearities which have been uncovered in the dynamic wind tunnel tests are of considerable importance in evaluating flechette flight performance and in evaluating flechette accuracy and dispersion. No wind tunnel data was obtained on the important Magnus moment. This omission is considered extremely serious and it is recommended that future studies be carried out in

this area. It is also recommended that the aerodynamic characteristics of the different flechette designs be evaluated with a view towards improvement in performance and accuracy.

Preliminary tests were carried out in obtaining the rolling motion of flechettes at the various angles of attack and in obtaining three-degrees-of-freedom wind tunnel tests where models were able to freely pitch, yaw, and roll. The exploratory rolling tests were carried out in the supersonic wind tunnel at Picatinny Arsenal. Good success was obtained on the basic configuration at small angles of attack. At the large angles of attack the sting support mechanism bent and thus had to be redesigned. These rolling tests have demonstrated that it will be quite possible to obtain excellent free rolling motion performance of flechettes at small and large angles of attack using instrumentation at Picatinny Arsenal.

Three-degree-of-freedom dynamic wind tunnel tests were explored in a preliminary way in the Notre Dame vertical down supersonic wind tunnel. In these tests the model was able to freely pitch and yaw and the afterbody with fins was able to roll freely. The forebody however did not roll. The tests were of marginal success but suggested that complete success could be achieved with more effort. It is specifically suggested that the new 3-D testing procedures originally explored at Notre Dame be continued in the Picatinny Arsenal and/or the BRL wind tunnels.

It should be emphasized that the nonlinear aeroballistic dynamic stability coefficients obtained in the Notre Dame program represent a major finding which was extensively utilized in the performance analysis and accuracy computations. It is considered essential that all future flechette designs undergo complete dynamic wind tunnel testing and range firings in order to permit accurate computations of the true dynamic flight performance, accuracy and dispersion of flechettes.

#### Dispersion Theory of High Fineness Ratio, Cruciform Fin Bodies

A complete jump and dispersion theory is set forth for the free flight performance of flechettes. The six-degree-of-freedom equations of motion are coded for various computer computations which indicated that the flechette accuracy theory accurately predicts the jump and dispersion of flechettes.

In order to determine realistic values for the initial conditions of flight and for the actual dispersion of flechettes, test firings are carried out in order to obtain special experimental data. The raw experimental data is fitted by the least squares method and thereby placed into the form of initial flight conditions. These initial conditions are then applied to the theory. Six-degree-of-freedom numerical computations are used to evaluate the dispersion of eight test rounds. The good agreement between the theory and test firing results indicate that the methods of data analysis and the flechette accuracy theory together provide a precise means of predicting the dispersion of flechettes.



The analysis of the firing data indicates that the large initial conditions of flechette flight result from a strong impulse imparted to the flechette in the muzzle blast regime. It is found that if the transverse impulse imparted to the flechette is equal to an opposite angular impulse then the dispersion will be zero. Since these two impulses rarely balance and always exist, flechette dispersion is generally large. However, by controlling sabot design and muzzle blast, the transverse and angular momentums can be reduced and partially balanced thereby yielding excellent accuracy and low dispersion.

Of particular importance is the invalidation of the classical maximum yaw theory long used in exterior ballistics.

More specifically the complete jump and dispersion theory for flechettes has been reduced to three governing equations which represent flechettes having high, low and very low roll rates. These three theories were found to be accurate by evaluation against six-degree-of-freedom, numerical computations of the equations of motion. It was found therefore that they accurately predict the jump and dispersion of flechettes.

The computer program undertaken to evaluate the flechette accuracy theory includes 201 special case runs carried out in four parts. The first part validates the theory with respect to the aerodynamic restoring and damping moments. The effect of these moments on dispersion was found to depend on the initial conditions.

The second part validated the theory with respect to the aerodynamic Magnus force and moment. The effects on dispersion were found to be

very small and of no consequence unless the total dispersion of a particular round was of the same order of magnitude as a Magnus effect.

The third part validated the theory with respect to aerodynamic asymmetries (mass asymmetry, inertia asymmetry, etc.) and roll rate. All three theories were found to be validated in this phase and found to be quite accurate. Aerodynamic asymmetries causing a trim of  $1^{\circ}$  have little effect on the dispersion of fast rolling flechettes. Slower rolling flechettes were found to have in general increasingly large dispersion values as the roll rate decreased. It can be concluded that for flights which are prone to aerodynamic asymmetry and fin damage, a high roll rate is essential to low dispersion and increased accuracy.

The fourth part validates the theory with respect to gravity. The theory indicates a lateral contribution to dispersion from gravity in addition to the vertical contribution. However, for the flechette this lateral contribution was found to be minimum.

In general, the agreement between the flechette accuracy theory and the computer computations were excellent and account for the effect of the initial launching conditions as well as the static and dynamic stability coefficients and asymmetries. Further, simple equations are given in order to achieve the desired accuracy and optimization.

## SUMMARY

By an exploratory firing program, by a supersonic dynamic wind tunnel testing program, by the development of an accuracy theory for jump and dispersion, by computer computations and analysis, and by precision range firings at Frankford Arsenal, flechette accuracy and dispersion is explained, evaluated and improved.

The firing program revealed the importance of fin and body damage, the blast region and sabotaging. The dynamic wind tunnel program yielded values for the important static and dynamic stability coefficients. The flechette accuracy theory was confirmed by numerical integration of the 6-D equations on the high speed computer where the effects of initial conditions, stability coefficients and asymmetries was revealed and evaluated. Finally, by a flechette firing program in the new Frankford Arsenal Ballistics Range, excellent correlation between theory and experiment for flechette accuracy was obtained.

## APPENDIX A

### EXPLORATORY FLECHETTE FIRING PROGRAM

Two flechette firing programs were carried out at the University of Notre Dame. The first program was carried out in the Army Firing Range located under the football stands in the Rockne Stadium. In these first firing tests the actual flechette and its sabot were fired at full hypersonic velocity using a mann barrel with sabot stripper. The firings were carried out with the assistance of technical personnel from Frankford Arsenal and under the direct supervision of Army ROTC personnel stationed on the campus and responsible for the Firing Range. These firings revealed two very important discoveries. By firing through light drawing paper yaw cards and by examining the impression left by the passage of the flechette, it was possible to obtain a positive confirmation that the fins were being seriously damaged and/or bent by the stripper. This finding was transmitted to the cognizant Frankford Arsenal personnel where suitable corrective changes were initiated and finalized thereby eliminating the problem of fin damage.

The second major finding of the first flechette firing program, insofar as university investigators were concerned, was the recognition of the tremendously intensive and long muzzle blast regime. While a standard 22 projectile is fired in the range with little noise and little blast, the flechette system of basically the same weight but fired at large velocity yields a

tremendous concussion and a tongue of fire, blast and flame stretching some 3-4 feet. The importance of the recognition of the strong blast region lies in its effect in disturbing the flechette at launch and thereby contributing to inaccuracy.

The first firing program therefore revealed fin damage due to sabot strippers and a large blast region which contributed to jump and inaccuracy.

The second flechette firing program carried out at the university utilized an air gun in simple subsonic launchings. The range setup is shown in Figure 1. The purpose of this special firing setup was to explore various saboting techniques. In this program sabots of both pusher design and puller designs were investigated. Also body inset sabot designs were studied, see Figure 2. Representative target data is illustrated in Figure 3 where effects of sabot designs are clearly evident. Various flechette and sabot designs are shown in Figures 4 and 5.

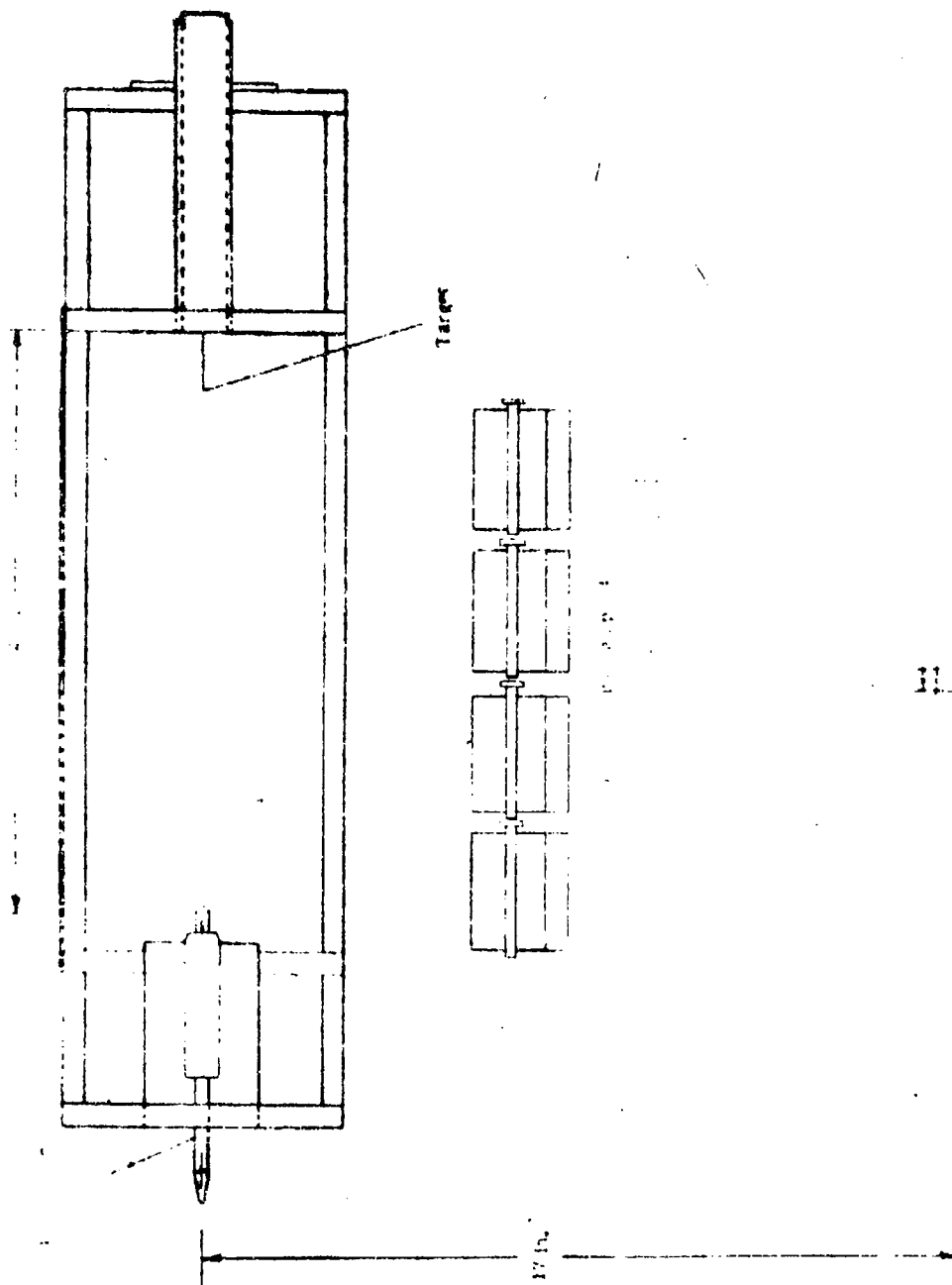


Figure 1. Subsonic Firing Range

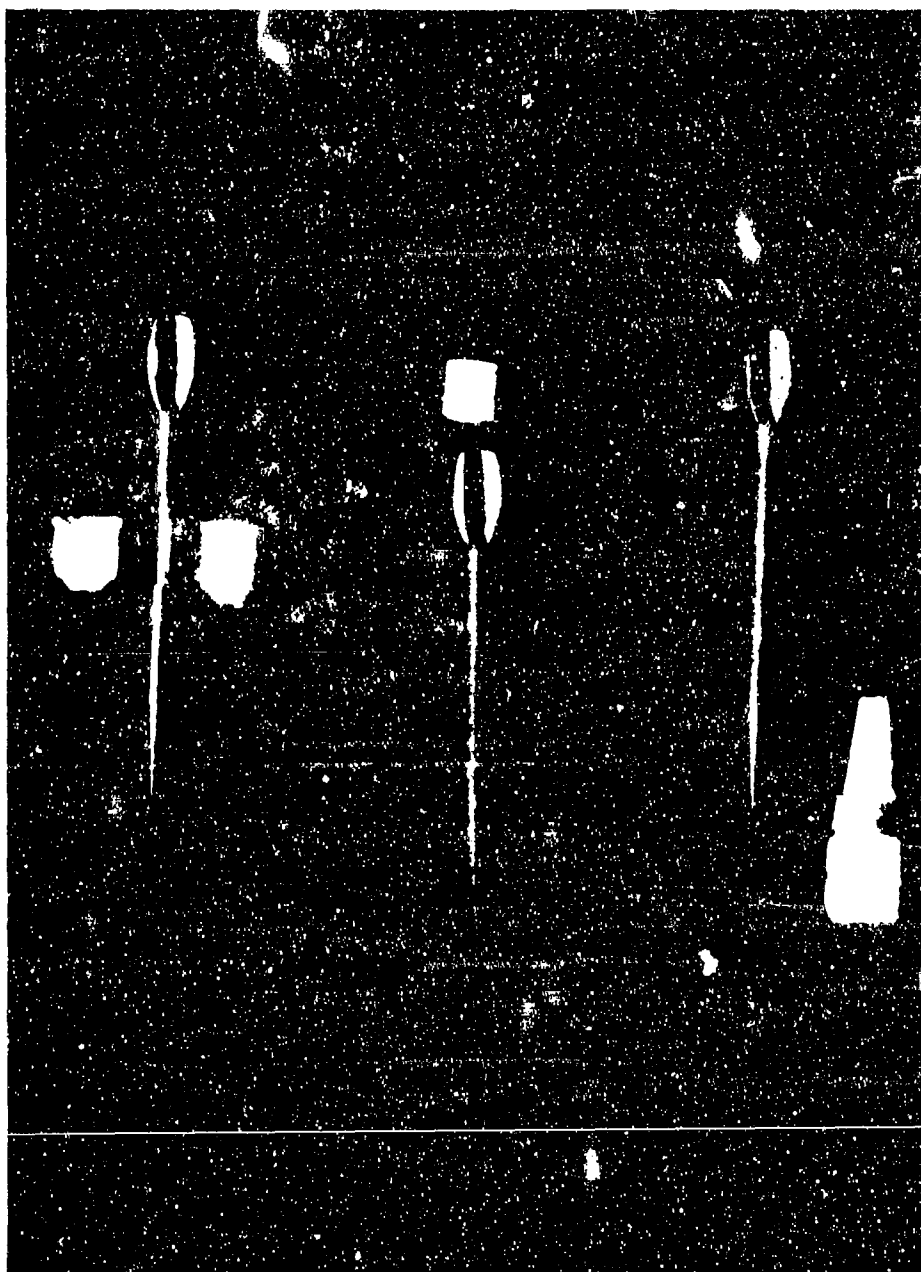


Figure 2. Flechette Sabot Designs

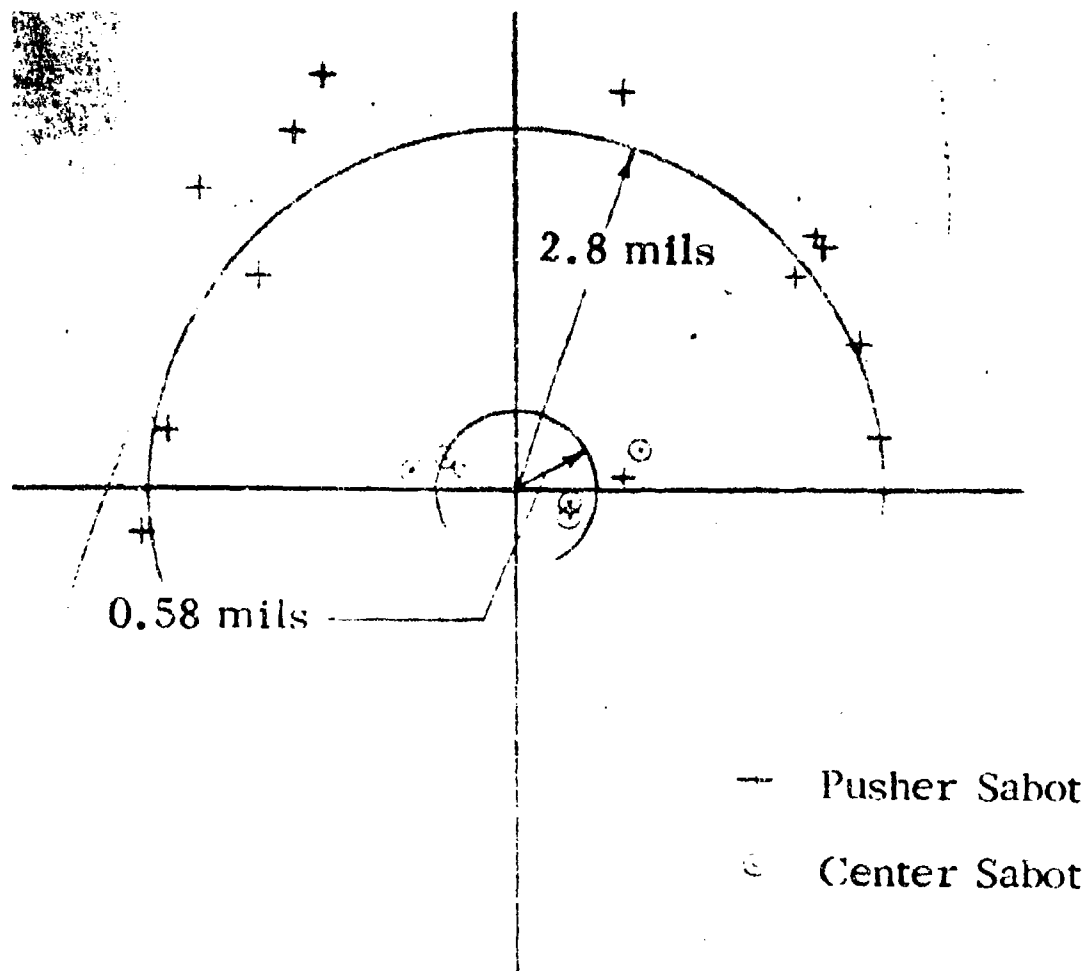
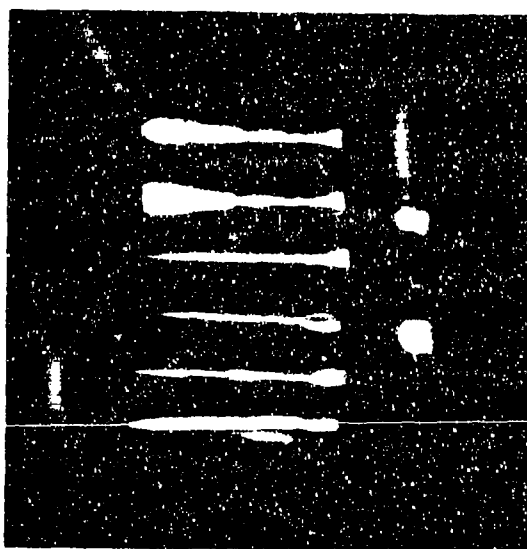


Figure 3. Comparison of Pusher and Center Sabot Results Flechette Testing





Figure 4. Producibility Sabot - R & D Flechette



5. Various Puller and Pusher Sabots and Flechette Configurations

## APPENDIX B

### DYNAMIC SUPERSONIC WIND TUNNEL TESTS OF FOUR-FLECHETTE CONFIGURATIONS

#### DYNAMIC SUPERSONIC WIND TUNNEL TESTING\*

#### ABSTRACT

The linear values of the static pitching moment stability coefficient,  $C_{M_\alpha}$ , and the damping moment stability coefficient,  $C_{M_q} + C_{M_{\dot{\alpha}}}$ , are determined versus angle of attack for four flechette designs. The program is carried out in a vertical supersonic wind tunnel using a one-degree-of-freedom dynamic testing technique. This method allows the model to go through free one-degree-of-freedom angular oscillations. Stability parameters are extracted from a film record of this motion and the stability coefficients are computed using the WOBBLE computer program. Good repeatability of the results is shown for low angle of attack.

---

\*Prepared by Michael Garsik.

# TABLE OF CONTENTS

	Page
TABLE OF CONTENTS . . . . .	18
LIST OF FIGURES . . . . .	20
LIST OF SYMBOLS . . . . .	23
INTRODUCTION . . . . .	25
AEROBALLISTIC THEORY . . . . .	29
Axis Systems . . . . .	29
Linear Theory . . . . .	29
Computation of Aerodynamic Stability Parameters . . . . .	37
Computation of Linear Stability Coefficients . . . .	37
EXPERIMENTAL TECHNIQUE . . . . .	39
One-Degree-of-Freedom Wind Tunnel Test Procedure . . . . .	39
One-Degree-of-Freedom Data Reduction Procedure . . . . .	53
Tunnel Velocity Measuring Technique . . . . .	53
ONE DEGREE-OF-FREEDOM TEST RESULTS . . . . .	59
One-Degree-of-Freedom Data Reduction . . . . .	59
One-Degree-of-Freedom Stability Coefficients . .	59
CONCLUSION . . . . .	94
APPENDIX A . . . . .	95

TABLE OF CONTENTS (concluded)

	Page
APPENDIX R . . . . .	96
APPENDIX C . . . . .	98

# LIST OF FIGURES

Number	Title	Page
1	Space Fixed Axis System . . . . .	30
2	Aeroballistic Axis System . . . . .	31
3	Static and Dynamic Fluid Forces . . . . .	33
4	Single-Degree-of-Freedom Motion . . . . .	38
5	Schematic of Ground Point . . . . .	40
6	Schematic of Olin . . . . .	41
7	Schematic of Swaged Point . . . . .	42
8	Schematic of Tracer . . . . .	43
9	Supersonic Wind Tunnel . . . . .	44
10	Flechette Mounted in Supersonic Wind Tunnel . . . . .	45
11	Exterior Support System . . . . .	46
12	Exterior Support System (Exploded View) . .	47
13	Retaining Mechanism . . . . .	51
14	Camera Set-Up . . . . .	52
15	Optical Comparator . . . . .	54
16	Reduction Coordinates . . . . .	55
17	Velocity Measurement Set-Up . . . . .	56
18	Representative Plot P.E. vs Time . . . . .	61
19	$\lambda_1$ vs Time (Ground Point) . . . . .	62
20	$\omega_1$ vs Time (Ground Point) . . . . .	63
21	$K_1$ vs Time (Ground Point) . . . . .	64

# LIST OF FIGURES (continued)

Number	Title	Page
22	$K_T$ vs Time (Ground Point) . . . . .	65
23	$\lambda_1$ vs Time (Olin) . . . . .	66
24	$\omega_1$ vs Time (Olin) . . . . .	67
25	$K_1$ vs Time (Olin) . . . . .	68
26	$K_T$ vs Time (Olin) . . . . .	69
27	$\lambda_1$ vs Time (Swaged Point) . . . . .	70
28	$\omega_1$ vs Time (Swaged Point) . . . . .	71
29	$K_1$ vs Time (Swaged Point) . . . . .	72
30	$K_T$ vs Time (Swaged Point) . . . . .	73
31	$\lambda_1$ vs Time (Tracer) . . . . .	74
32	$\omega_1$ vs Time (Tracer) . . . . .	75
33	$K_1$ vs Time (Tracer) . . . . .	76
34	$K_T$ vs Time (Tracer) . . . . .	77
35	$C_{M_\alpha}$ vs $\alpha$ (Ground Point) . . . . .	78
36	$(C_{M_q} + C_{M_\alpha})$ vs $\alpha$ (Ground Point) . . . . .	79
37	$C_{M_\alpha}$ vs $\alpha$ (Olin) . . . . .	80
38	$(C_{M_q} + C_{M_\alpha})$ vs $\alpha$ (Olin) . . . . .	81
39	$C_{M_\alpha}$ vs $\alpha$ (Swaged Point) . . . . .	82
40	$(C_{M_q} + C_{M_\alpha})$ vs $\alpha$ (Swaged Point) . . . . .	83
41	$C_{M_\alpha}$ vs $\alpha$ (Tracer) . . . . .	84
42	$(C_{M_q} + C_{M_\alpha})$ vs $\alpha$ (Tracer) . . . . .	85

# LIST OF FIGURES (continued)

Number	Title	Page
43	$C_{M_\alpha}$ vs Mach Number (Ground Point) . . . .	86
44	$(C_{M_q} + C_{M_{\dot{\alpha}}})$ vs Mach Number (Ground Point) . . . . .	87
45	$C_{M_\alpha}$ vs Mach Number (Olin) . . . . .	88
46	$(C_{M_q} + C_{M_{\dot{\alpha}}})$ vs Mach Number (Olin) . . . .	89
47	$C_{M_\alpha}$ vs Mach Number (Swaged Point) . . . .	90
48	$(C_{M_q} + C_{M_{\dot{\alpha}}})$ vs Mach Number (Swaged Point) . . . . .	91
49	$C_{M_\alpha}$ vs Mach Number (Tracer) . . . . .	92
50	$(C_{M_q} + C_{M_{\dot{\alpha}}})$ vs Mach Number (Tracer) . .	93

# LIST OF SYMBOLS

$a$  Local speed of sound (feet/second)

$a_T$  Total speed of sound (feet/second)

$C_{M_\alpha}$  Static pitching moment stability coefficient ( $\text{rad}^{-1}$ )

$$C_{M_\alpha} = \frac{M_{\dot{\alpha}} \alpha}{\alpha Q S d}$$

$C_{M_q}$  Damping moment stability coefficient ( $\text{rad}^{-1}$ )

$$C_{M_q} = \frac{M_q q}{Q S d \frac{qd}{2V}}$$

$C_{M_{\dot{\alpha}}}$  Damping moment stability coefficient due to aerodynamic lag ( $\text{rad}^{-1}$ )

$$C_{M_{\dot{\alpha}}} = \frac{M_{\dot{\alpha}} \dot{\alpha}}{Q S d \frac{\dot{\alpha} d}{2V}}$$

$C_{M_{\delta_\epsilon}}$  Aerodynamic asymmetry moment stability coefficient ( $\text{rad}^{-1}$ )

$$C_{M_{\delta_\epsilon}} = \frac{M_{\delta_\epsilon} \delta_\epsilon}{\delta_\epsilon Q S d}$$

$d$  Reference length, missile diameter (ft.)

$I = I_y = I_z$  Pitching moment of inertia (slugs/feet<sup>2</sup>)

$K_{1,2}$  Amplitude of nutation and precession arms (rad)

$K_3$  Trim mode (rad)

$L, M, N$  Moments about X, Y, Z aeroballistic axes (ft-lb)

$M_\alpha$  Pitching moment derivatives (ft-lbs/rad)

$M_{\dot{\alpha}}$  Damping moment derivative due to aerodynamic lag (ft-lbs sec/rad)



# LIST OF SYMBOLS (continued)

$M_q$	Damping moment derivative (ft-lbs sec/rad <sup>2</sup> )
$M_{\delta_\epsilon}$	Asymmetry moment derivative (ft-lbs/rad)
$p, q, r$	Angular rates about aeroballistic axes (rad/sec)
$Q$	Dynamic pressure $Q = \frac{1}{2} \rho U^2$ (lb/ft <sup>2</sup> )
$R$	Gas constant
$S$	Reference area, $S = \frac{\pi d^2}{4}$ (ft <sup>2</sup> )
$t$	Time (sec)
$T_t$	Total temperature °R
$U$	Total velocity (ft/sec)
$X, Y, Z$	Aeroballistic axes
$x, y, z$	Space-fixed axes
$\alpha$	Angle of attack (rad)
$\beta$	Angle of sideslip (rad)
$\theta, \psi, \phi$	Euler angles (rad or deg)
$\rho$	Air density (slugs/ft <sup>3</sup> )
$\lambda_{1,2}$	Damping rate (rad/sec)
$\omega_{1,2}$	Nutation and precession frequency (rad/sec)
$\gamma$	Ratio of specific heats, $\frac{c_p}{c_v}$
$\delta$	Phase angle (rad)

## INTRODUCTION

With the advent of more advanced analysis techniques<sup>1</sup> today's aerodynamicist has the power to achieve a better understanding of the free flight performance of a flight vehicle. Data such as angular motion, jump angle and dispersion can now be extracted from free flight data and studied<sup>2</sup> so that previously undetected instabilities and design failures can be corrected. Obviously from this there arises a clear need for development of free flight simulations.<sup>3,4</sup> The random method used in trying to solve the problems of stability and flight performance would prove dangerous and costly if full scale flight tests were conducted. It would be much cheaper and safer to experiment with new designs on models of the actual configuration. This presents the problems of simulating free flight motions so that data can be extracted and the new designs evaluated just as if the test were conducted on a full scale model in free flight.

Ballistic range firings was one of the initial attempts at a flight simulation technique. It involved taking photographs at various stations along a firing range of a model that had been launched from a gun. Because of the limitations on the types of motion that could be observed, the lack of control of initial conditions, and other limiting factors, it soon became apparent that a more sophisticated method of simulation was necessary. Attention was turned to the wind tunnel.

Attempts to study the angular motions of flight vehicles in the wind

tunnel began by mechanically reproducing them. This technique ran into several problems, in particular separating the driving mechanism response from the aerodynamic response and the fact that the technique is limited in that a mechanical response, rather than a free one, to the flow field is used. In recent years the most successful wind tunnel simulation technique, dynamic wind tunnel testing, has been developed.

Actually there are several types of dynamic wind tunnel testing. The free flight angular oscillation method exhibits complete six-degree-of-freedom motion and needs no external support system, however certain limitations to this technique do exist. The duration of the simulation is restrictive hence length of the "flight" is very short. Also, a lack of control of initial conditions prohibits the study of particular flight modes. Another method, that of constrained angular oscillations, eliminates these disadvantages at the expense of introducing new ones. The most predominate disadvantage is the interference effects of the support system on the response of the model to the flow field. This assumes that the problem of building an adequate support system can be solved. It is important to have control over the initial conditions and the length of the simulation run in order to simulate the free flight angular motions in the wind tunnel. Of course, the choice of which method to use depends on the careful consideration of the problem at hand and the experimental limitations which could be allowed and not interfere with the test being carried out.

With regard to the constrained angular oscillation technique and its use in the supersonic wind tunnel, several methods have been

developed. The gas bearing system is one that is ideally suited to the study of low fineness ratio, non-finned bodies such as projectiles. It does not lend itself to the study of high fineness ratio finned bodies quite as well. One of the drawbacks of this technique is the high cost of construction and maintenance of the system. The jewel bearing support system has been utilized in supersonic wind tunnel testing to observe the rolling motion of various models of flight vehicles. Such a system has been successfully employed in determining the roll damping moment and induced roll moment stability coefficients for different flight configurations.

This investigation is intended to determine the linear pitching moment and damping moment stability coefficients of four flechette configurations in a supersonic regime. The study was conducted under a contract awarded to the Department of Aerospace and Mechanical Engineering at the University of Notre Dame by Frankford Arsenal, Philadelphia, Pa. The contract deals with a study of the jump angle and dispersion of the flechette configurations. An underlying intent will be to document the constrained angular oscillation technique used in the supersonic wind tunnel tests.

In order to study the performance of the flechette configurations and to be able to predict their flight path, a basic understanding of the stability of the rounds must be obtained. Adequate stability prediction requires that techniques of flight simulation be used which will produce continuous results for supersonic conditions.

The actual steps taken in developing such a program of dynamic wind tunnel tests were: 1) adapting the one-degree-of-freedom free oscillation technique to the supersonic wind tunnel; 2) recording the one degree of freedom angular oscillations of the models in the supersonic wind tunnel by high speed photography techniques; 3) reducing the motion of the models to numerical values of angle of attack; 4) fitting the Aeroballistic Theory to the angular data obtained to determine the stability parameters  $K_{N,P}$ ,  $\lambda_{N,P}$ ,  $\omega_{N,P}$ ; <sup>5,6</sup> 5) computing the aerodynamic stability coefficients from Linear Theory using the stability parameters, model parameters, wind tunnel Mach number and density; 6) analyzing the interference of the support system by checking the repeatability of results.

To accomplish the goals set down a unique method of supporting the pure pitch flechette models are utilized.<sup>7</sup> It involved suspending the model in the test section of the University of Notre Dame's vertical supersonic wind tunnel and allowing it to go through free one-degree-of-freedom oscillations. The low friction in the system allowed continuous motions to be obtained and recorded and the stability coefficients to be extracted from the angular data.

## AEROBALLISTIC THEORY

### Axis Systems

Two basic axis systems are used. The space fixed axis system (Figure 1) is the system in which the data is recorded. The aeroballistic axis system (Figure 2) is the system in which the equations of motion are expressed. By choosing the x-axis of the space fixed system to coincide with the velocity vector the data is made directly compatible to the equations of motion. From Figures 1 and 2 it is seen that  $\theta = \alpha$  and  $q = \dot{\theta}$ . Care must be taken in extending this comparison beyond this point.

The linear theory for a missile constrained at its center of gravity for one-degree-of-freedom pure pitching is as follows.

### Linear Theory

In the development of the Linear Theory several assumptions are made:

1. Aerodynamic coefficients are constant
2. Velocity and density are constant
3. All angular motions except roll are small enough that the small angle approximations may be used:

$$\sin x = \tan x = x$$

$$\cos x = 1$$

4. The missile has mirror symmetry and trigonal or greater rotational symmetry.

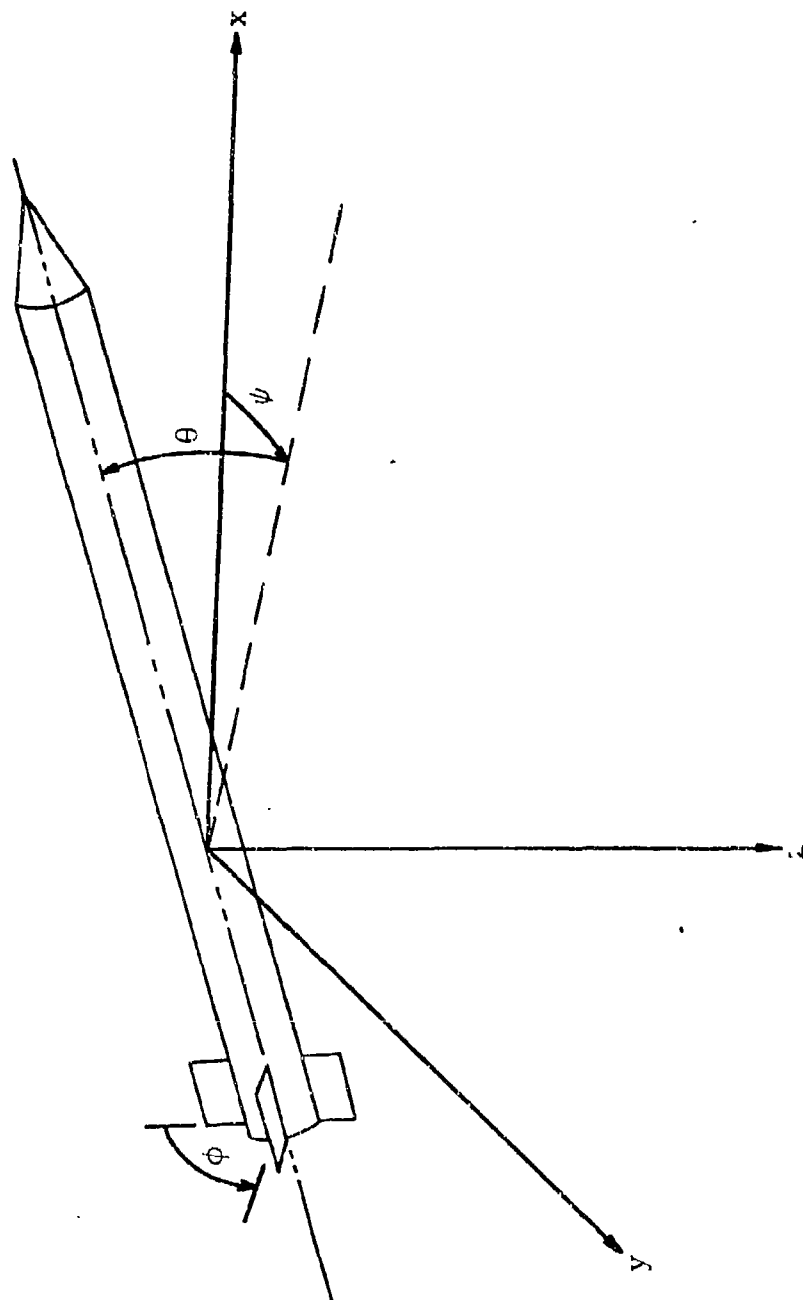


Figure 1. Space Fixed Axis System

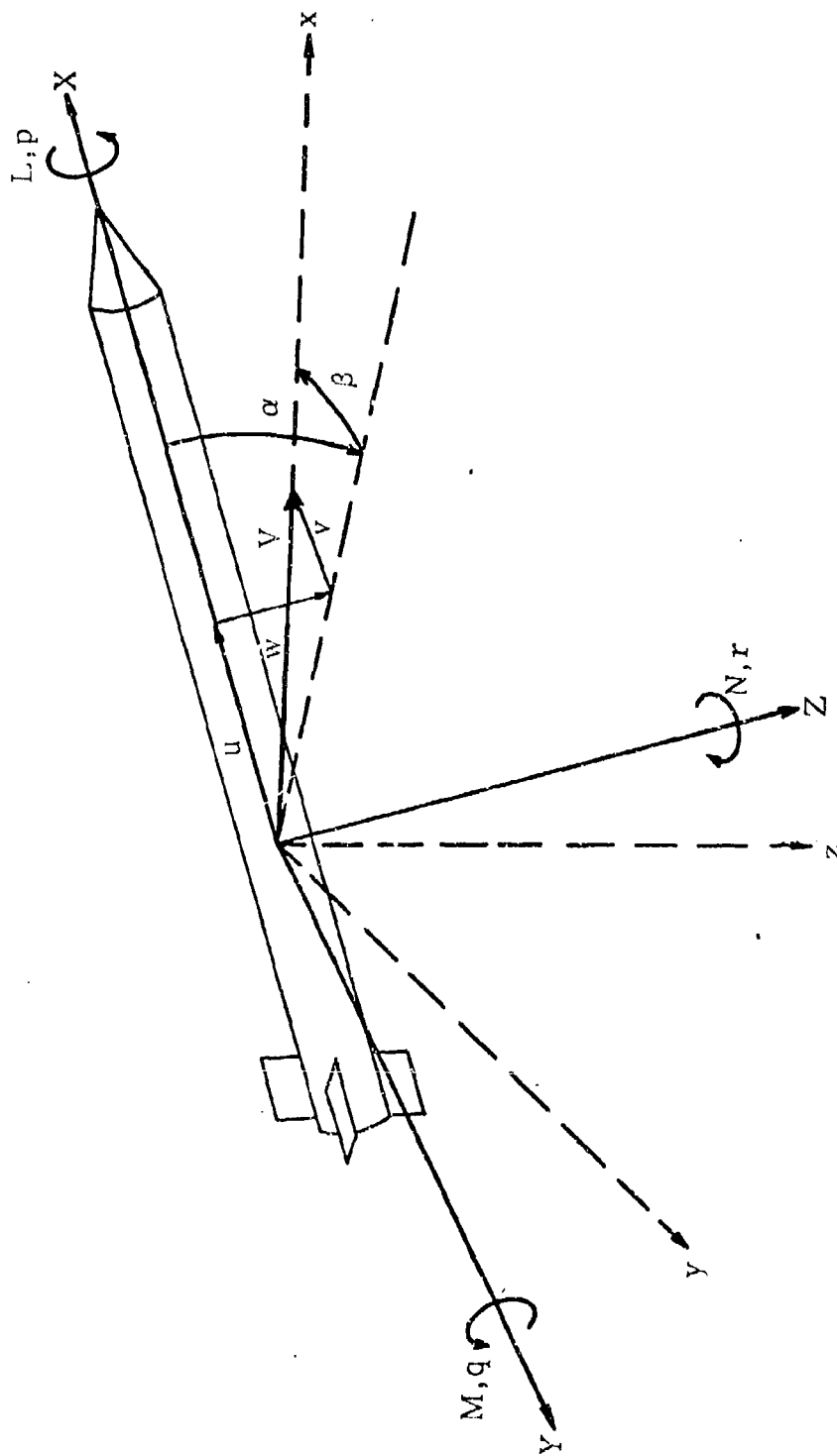


Figure 2. Aeroballistic Axis System



The fundamental differential equation of motion for the rotational motion is

$$M = I \ddot{\theta} \quad (1)$$

The sum of the acting aerodynamic moments, shown in Figure 3, which are assumed to vary linearly with angle of attack is

$$M = M_{\alpha} \alpha + M_q \dot{\alpha} + M_{\dot{\alpha}} \ddot{\alpha} + M_{\delta_{\epsilon}} \delta_{\epsilon} \quad (2)$$

where

$$\begin{aligned} M_{\alpha} &= C_{M_{\alpha}} \frac{1}{2} \rho U^2 S d \\ M_q &= C_{M_q} \left[ \frac{d}{2u} \right] \frac{1}{2} \rho U^2 S d \\ M_{\dot{\alpha}} &= C_{M_{\dot{\alpha}}} \left[ \frac{d}{2u} \right] \frac{1}{2} \rho U^2 S d \\ M_{\delta_{\epsilon}} &= C_{M_{\delta_{\epsilon}}} \frac{1}{2} \rho U^2 S d \end{aligned} \quad (3)$$

Because of the selection of the particular axis systems and their orientation, Equation 1 can be rewritten as

$$M = I \ddot{\alpha} \quad (4)$$

Equation 2 can be rewritten as

$$M = M_{\alpha} \alpha + M_q \dot{\alpha} + M_{\dot{\alpha}} \ddot{\alpha} + M_{\delta_{\epsilon}} \delta_{\epsilon} \quad (5)$$

Combining Equations 4 and 5 and rearranging

$$\ddot{\alpha} - \left[ \frac{M_q + M_{\dot{\alpha}} \ddot{\alpha}}{I} \right] \dot{\alpha} - \left[ \frac{M_{\alpha}}{I} \right] \alpha = M_{\delta_{\epsilon}} \delta_{\epsilon} \quad (6)$$

and



$$\alpha + N_1 \dot{\alpha} + N_2 \alpha = N_3 \quad (7)$$

where

$$\begin{aligned} N_1 &= - \left[ \frac{M_q + M_{\dot{\alpha}}}{I} \right] \\ N_2 &= - \left[ \frac{M_{\alpha}}{I} \right] \\ N_3 &= \left[ \frac{M_{\delta} \delta_{\epsilon}}{I} \right] \end{aligned} \quad (8)$$

Solving for the homogeneous solution to Equation 7 assume a solution of the form

$$\alpha = K e^{\phi t} \quad (9)$$

Differentiation of this yields

$$\dot{\alpha} = \phi K e^{\phi t} \quad \ddot{\alpha} = \phi^2 K e^{\phi t} \quad (10)$$

Substitute Equation 9 and 10 into the homogeneous form of Equation 7

$$\phi^2 K e^{\phi t} + N_1 \phi e^{\phi t} + N_2 e^{\phi t} = 0$$

$$\phi^2 + N_1 \phi + N_2 = 0$$

which has a solution of the form

$$\phi_{1,2} = - \frac{N_1}{2} \pm \frac{1}{2} \sqrt{N_1^2 - 4N_2} \quad (11)$$

For missiles in air the assumption that the products of stability derivatives are negligible when compared to themselves (i.e.  $N_1^2 \ll 4N_2$ )

can be made. This is generally a good assumption and will be made here. Hence Equation 11 can be written

$$\begin{aligned}\phi_{1,2} &= -\frac{N_1}{2} \pm i\sqrt{N_2} \\ &= \lambda_{1,2} + i\omega_{1,2}\end{aligned}\tag{12}$$

The homogeneous solution has the form

$$\alpha = K_1 e^{(\lambda_1 + i\omega_1)t} + K_2 e^{(\lambda_2 - i\omega_2)t}\tag{13}$$

where

$$\lambda_1 = \lambda_2 = \left[ \frac{d}{2u} \right] - \frac{1}{2} \rho U^2 S d \frac{C_{M_q} + C_{M_{\dot{\alpha}}}}{2I}\tag{14}$$

$$\omega_1 = \left[ \frac{C_{M_{\alpha}} \frac{1}{2} \rho U^2 S d}{I} \right]^{1/2}\tag{15}$$

$$\omega_2 = \left[ \frac{C_{M_{\alpha}} \frac{1}{2} \rho U^2 S d}{I} \right]^{1/2}\tag{16}$$

and

$$C_{M_{\alpha}} \approx -\frac{2 I \omega^2}{\rho U^2 S d}\tag{17}$$

$$(C_{M_q} + C_{M_{\dot{\alpha}}}) \approx \frac{8 I \lambda}{\rho U S d}\tag{18}$$

Solving for the particular part of the solution of Equation 7 consider the steady state case of no pitching, Equation 7 would be

$$N_2 \alpha = N_3$$

$$\alpha = \frac{N_3}{N_2} = - \frac{M_{\delta} \delta_{\epsilon}}{M_{\alpha}} = K_3 \quad (19)$$

This is the particular part of the solution of Equation 7. The complete solution is

$$\alpha = K_1 e^{(\lambda_1 + i\omega_1)t} + K_2 e^{(\lambda_2 + i\omega_2)t} + K_3 \quad (20)$$

where  $K_1$  and  $K_2$  are found from initial conditions and are

$$K_{1,2} = \frac{\dot{\alpha}_0 - \phi_{2,1} \alpha_0}{\phi_{1,2} - \phi_{2,1}} + \frac{\phi_{2,1} K_3}{(\phi_{1,2} - \phi_{2,1})} \quad (21)$$

Since the magnitudes of  $\phi_1$  and  $\phi_2$  are always equal and  $K_3$  is constant

$$K_1 = K_2 = K$$

Since

$$e^{i\omega t} = \cos \omega t + i \sin \omega t$$

Equation 19 can be written as

$$\alpha = 2K e^{\lambda t} \cos \omega t + K_3$$

or in a more general form

$$\alpha = K_0 e^{\lambda t} \cos (\omega t + \delta) + K_3 \quad (22)$$

where

$$K_0 = 2K$$

Equation 22 is the basic modal which will be used to fit the one-degree-of-freedom data. A physical representation of what Equation 22 means and how it reduces the Tricyclic Theory to a pure pitching motion case is shown in Figure 4. The two arms  $K_1$  and  $K_2$  have been replaced by a single arm of length  $K$  where  $K=K_1+K_2$ . This arm is rotating at a rate  $\omega=\omega_1$  and has an initial orientation of  $\delta=\delta_1$ . The cosine function projects this arm onto the vertical axis of the aeroballistic axis system to give values of  $\theta$ . This "projection" follows the pure pitching of the model as if it would look when observed from the rear.

#### Computation of Aerodynamic Stability Coefficients

To fit Equation 22 to the angular oscillation data the WOBBLE computer program was used. This program fits the theory to short segments of the data in overlapping pieces so that the stability parameters  $\lambda_1$ ,  $\omega_1$  and  $K_1$  are determined as functions of time.

#### Computation of Linear Coefficients

Using the velocity and model parameters (Appendix A) along with  $\lambda_1$ ,  $\omega_1$  and  $K_1$  the pitching moment stability coefficient,  $C_{M_\alpha}$ , and the damping moment stability coefficient,  $(C_{M_q} + C_{M_{\dot{\alpha}}})$ , were computed. Equations 17 and 18 were used to compute these coefficients as functions of time.

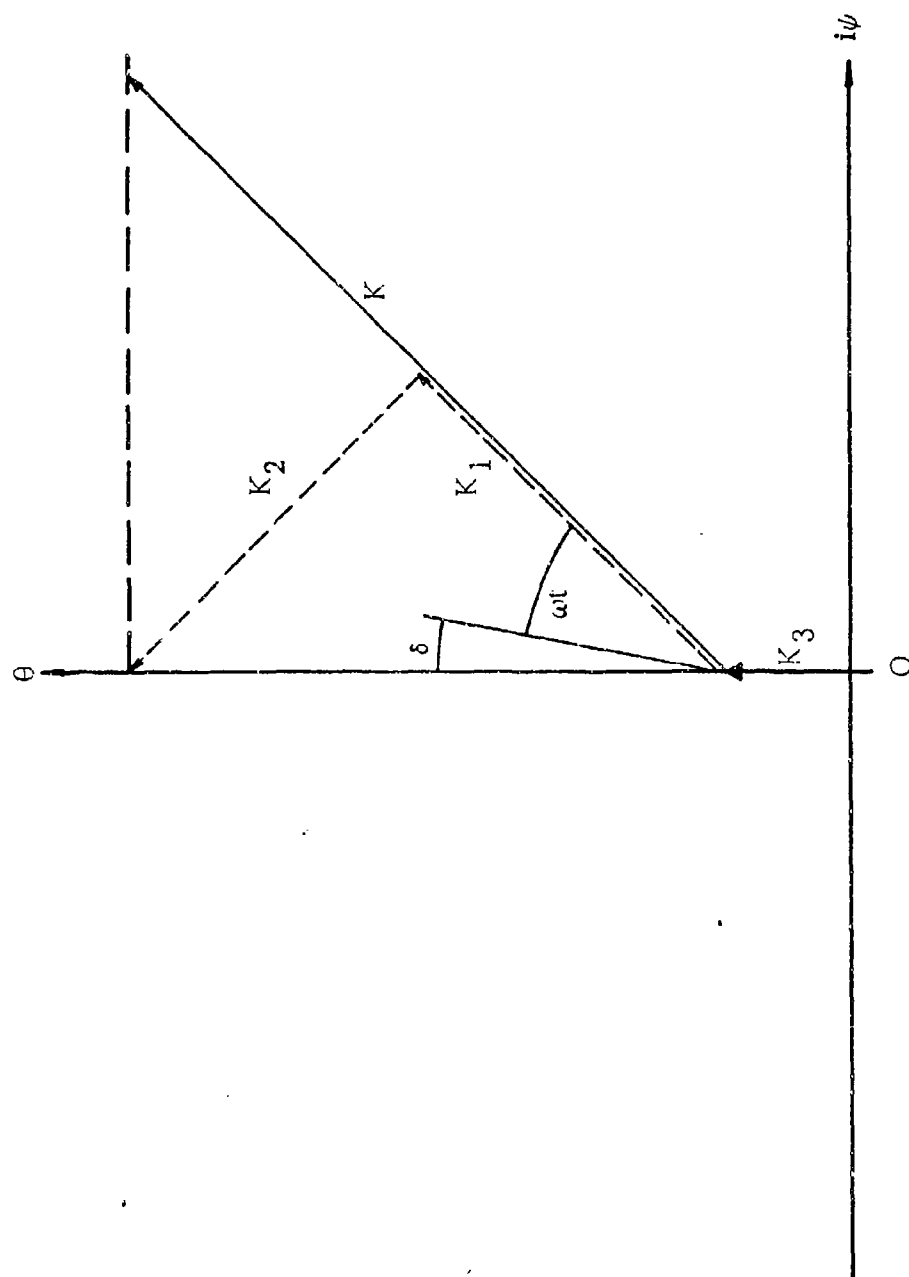


Figure 4. Single-Degree-of-Freedom Motion

## Experimental Technique

Four different configurations were tested, the Ground Point, Olin, Swaged Point, and Tracer. Schematic representations of the model configurations are given in Figures 5, 6, 7, and 8 respectively.

### One-Degree-of-Freedom Wind Tunnel Test Procedures

All of the tests were carried out in the University of Notre Dame's vertical supersonic wind tunnel shown in Figure 9. This wind tunnel features a vertical test section fitted with interchangeable steel and glass walls. A steel wall was used on one side to give maximum support to the model support system and a glass wall was used on the other side to allow observation of the models. The basic idea behind the support system is shown in Figures 10, 11, 12 and 12a.

To mount the model in the tunnel the following system was used. A length of piano wire 0.030" in diameter was inserted through the hole in the glass wall and into a syringe tube. The purpose of the two syringe tubes, one on each side of the model, was to insure that the model would remain in the center of the wind tunnel test section after it was released and allowed to oscillate. After running the wire through the first syringe tube, it was pushed through a small hole 0.040" in diameter drilled perpendicular to the longitudinal axis at the center of gravity of the model. The wire was then pushed through the second syringe tube and guided out of the test section through a hole in the steel wall. The wire was secured outside the wind tunnel test section by a system shown in Figure 11. On



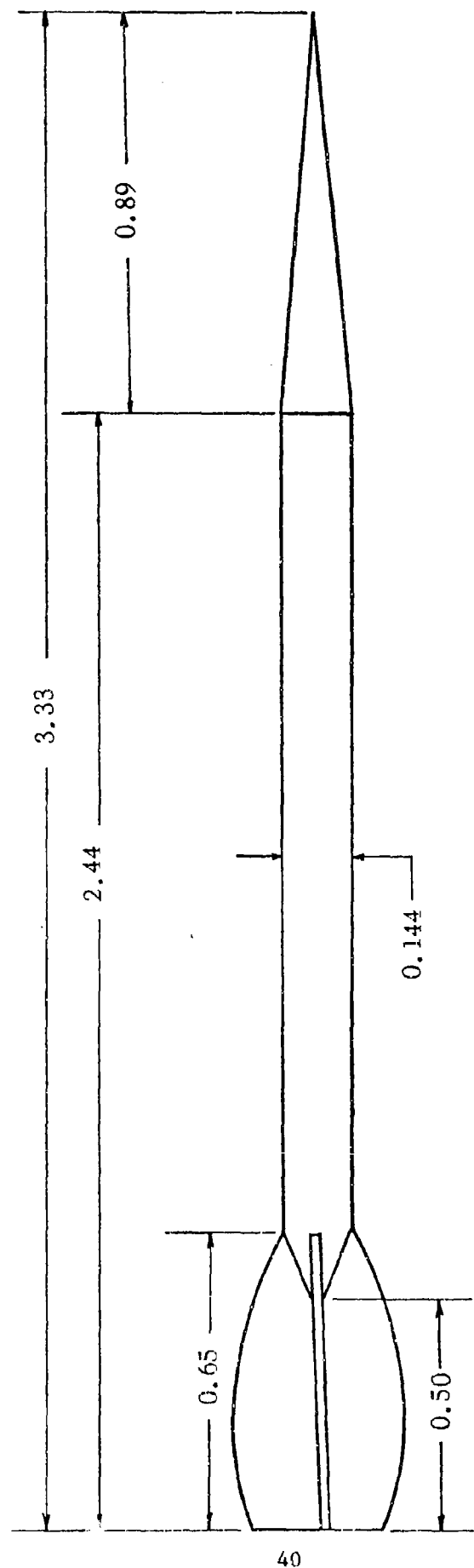


Figure 5. Ground Point Wind Tunnel Model

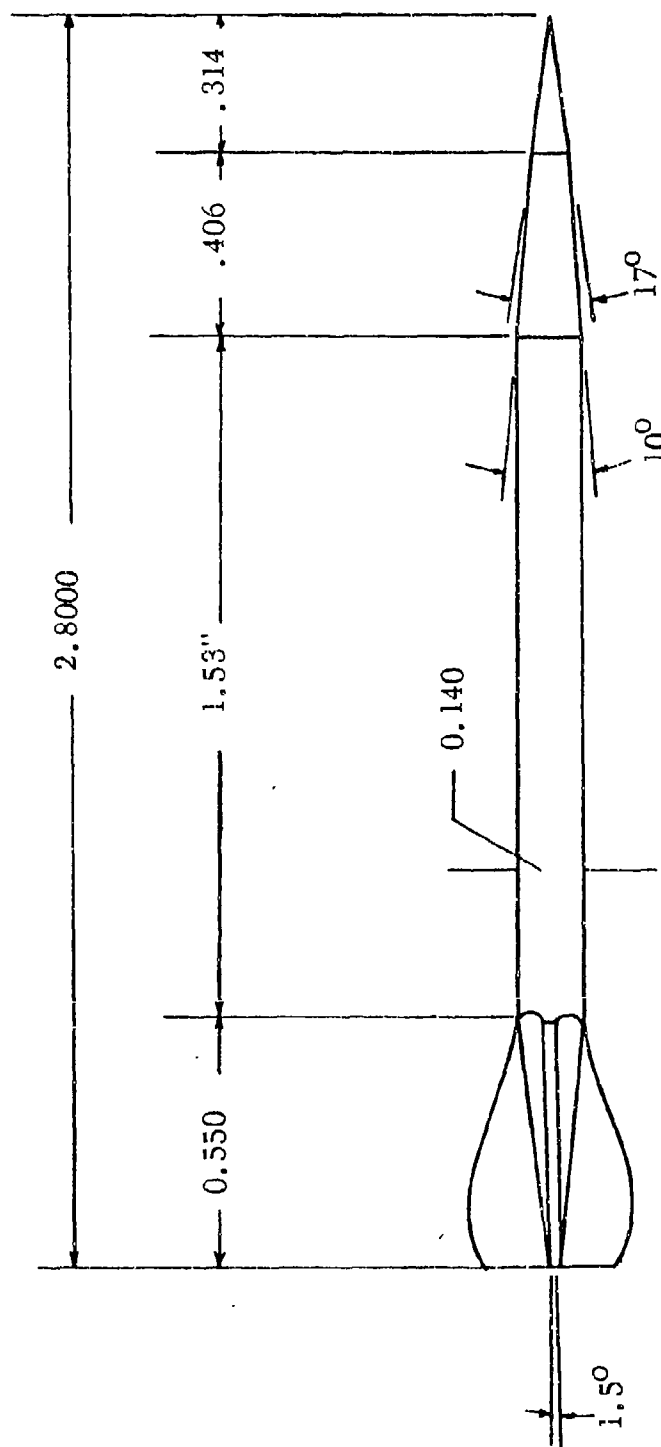


Figure 6. Olin Wind Tunnel Model

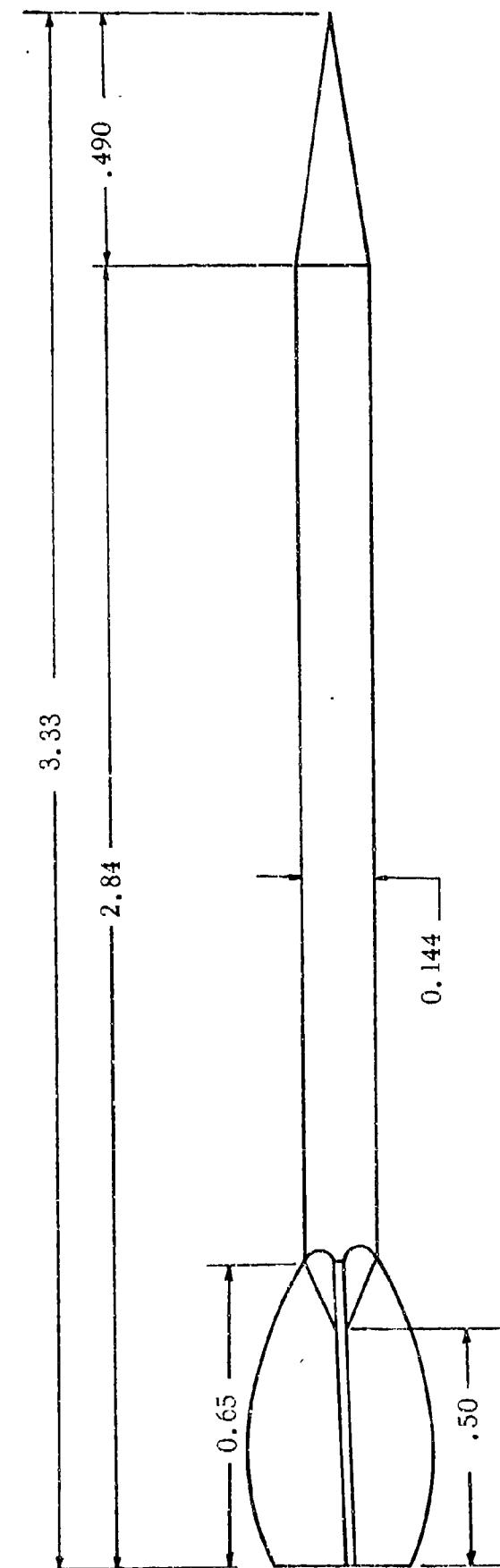


Figure 7. Swaged Point Wind Tunnel Model

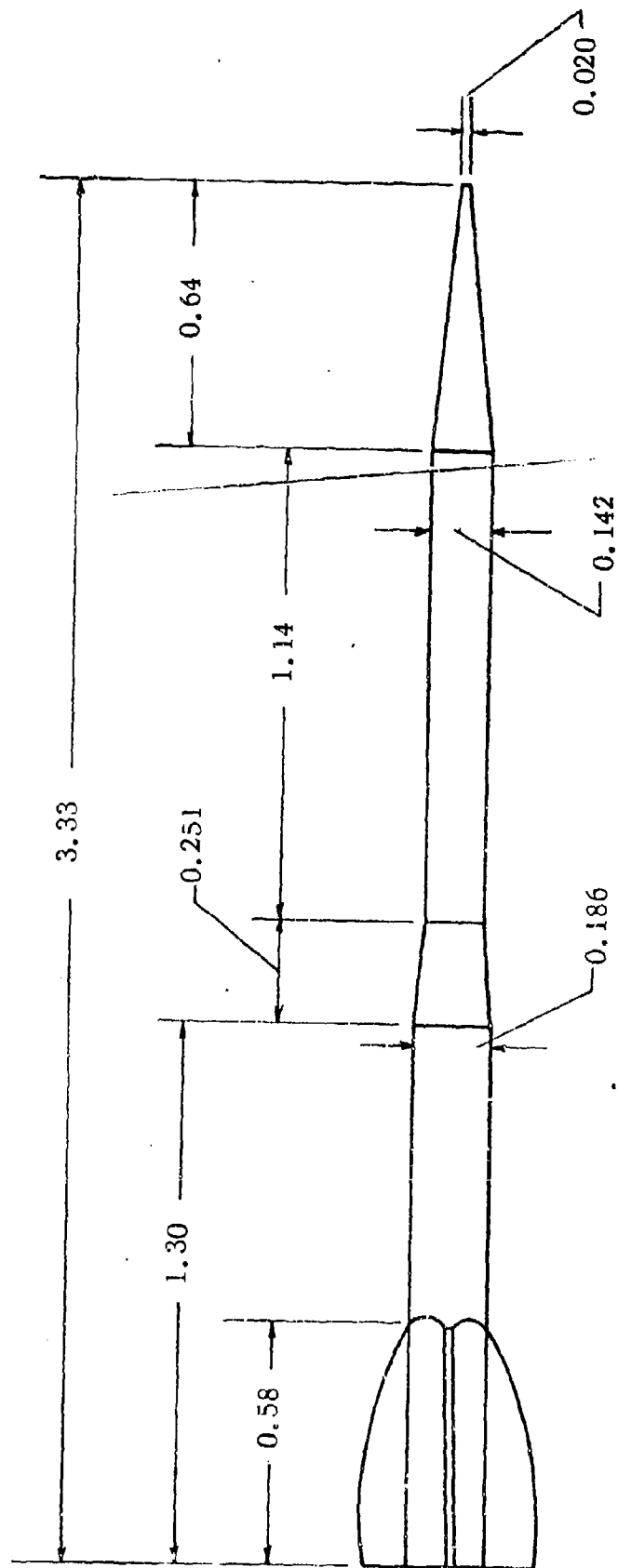


Figure 8. Tracer Wind Tunnel Model

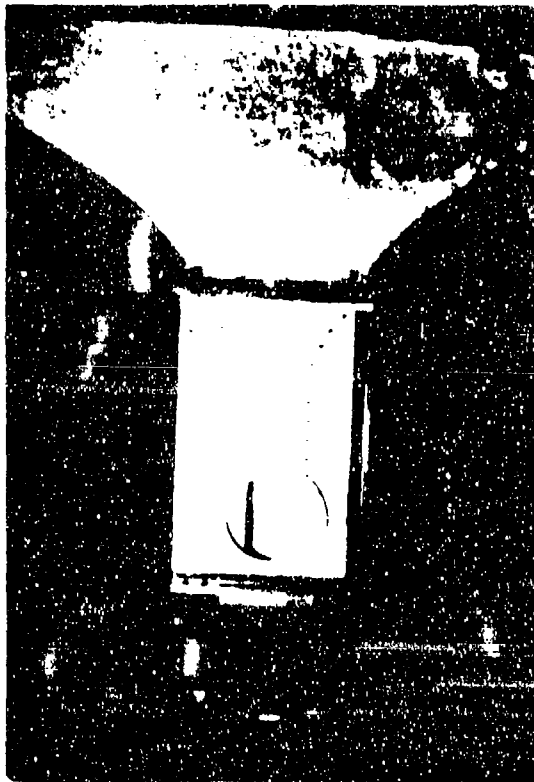


Figure 9. Vertical Supersonic Wind Tunnel

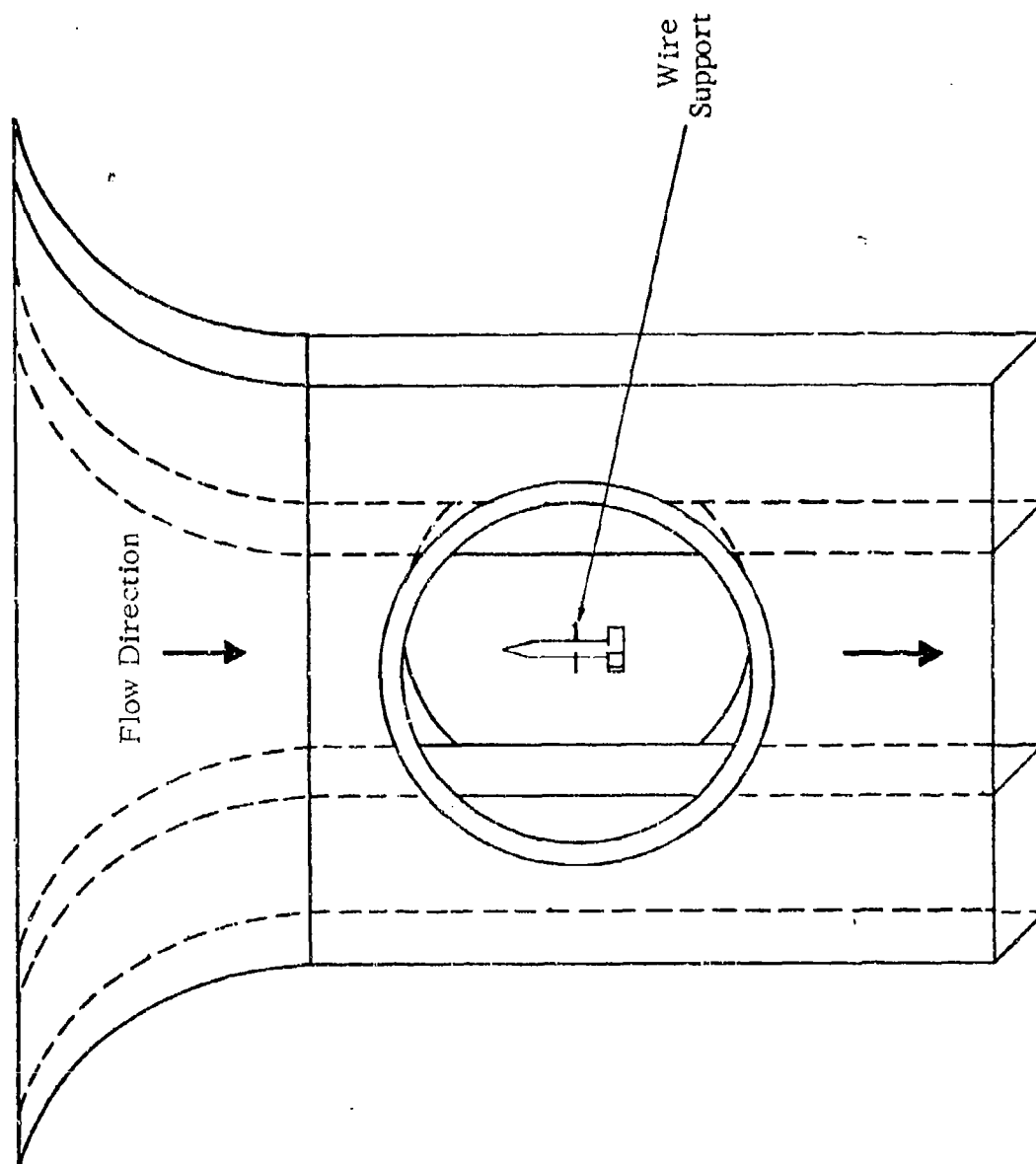


Figure 10. Flechette Mounted in Supersonic Wind Tunnel

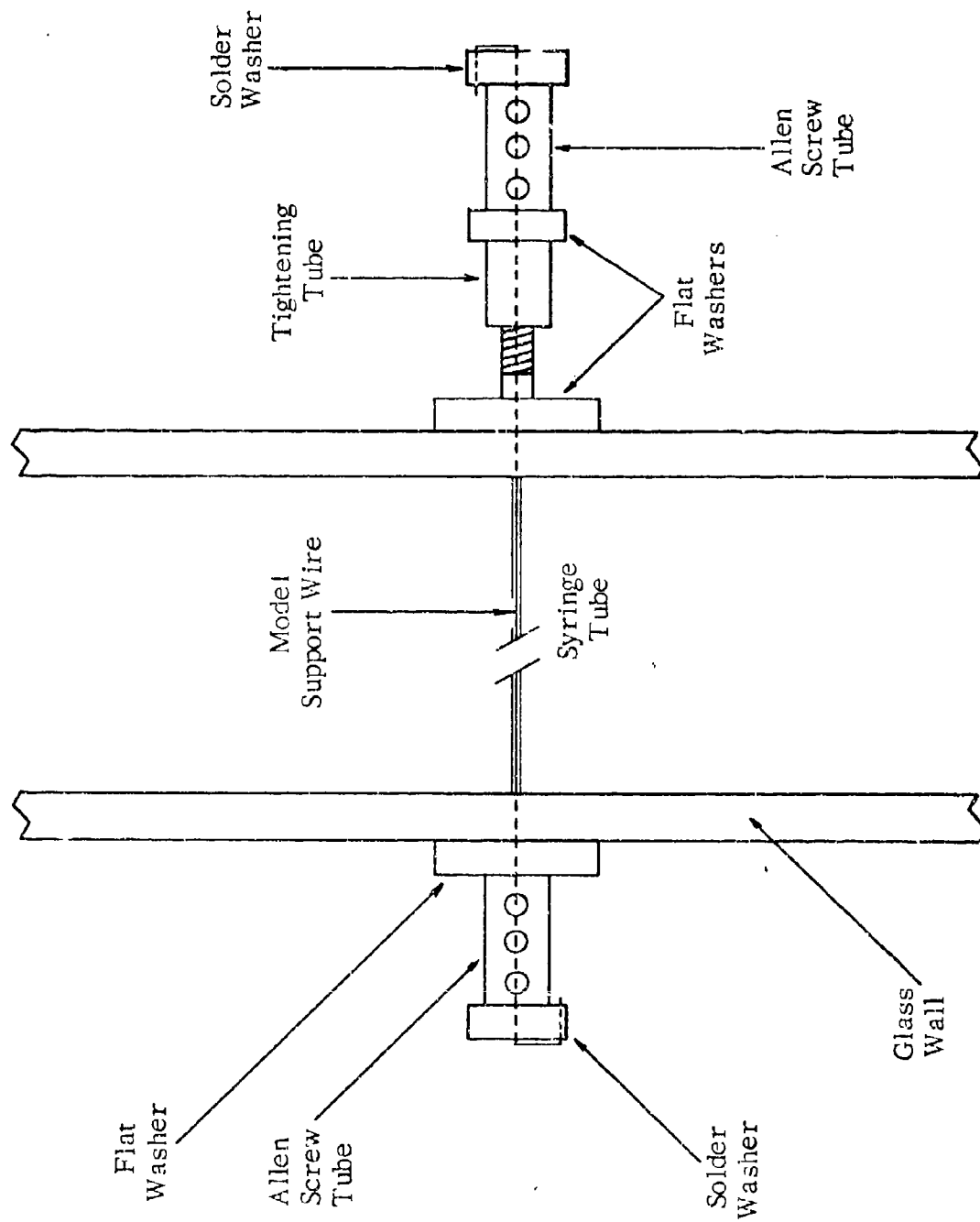


Figure 11. Exterior Support System

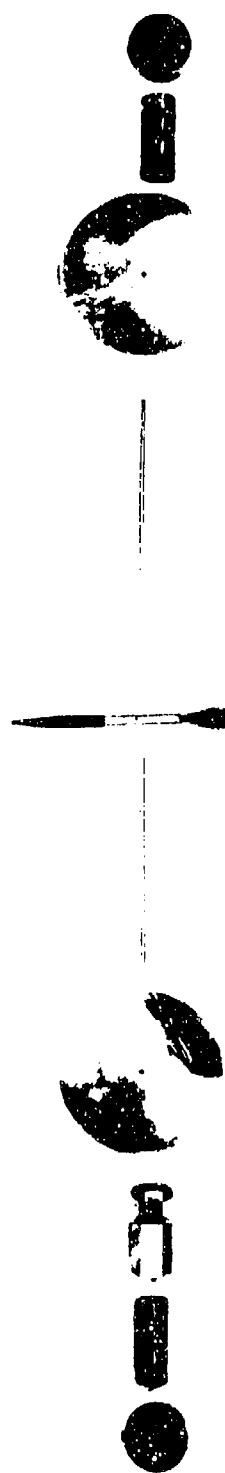


Figure 12. Exterior Support System (Exploded View)



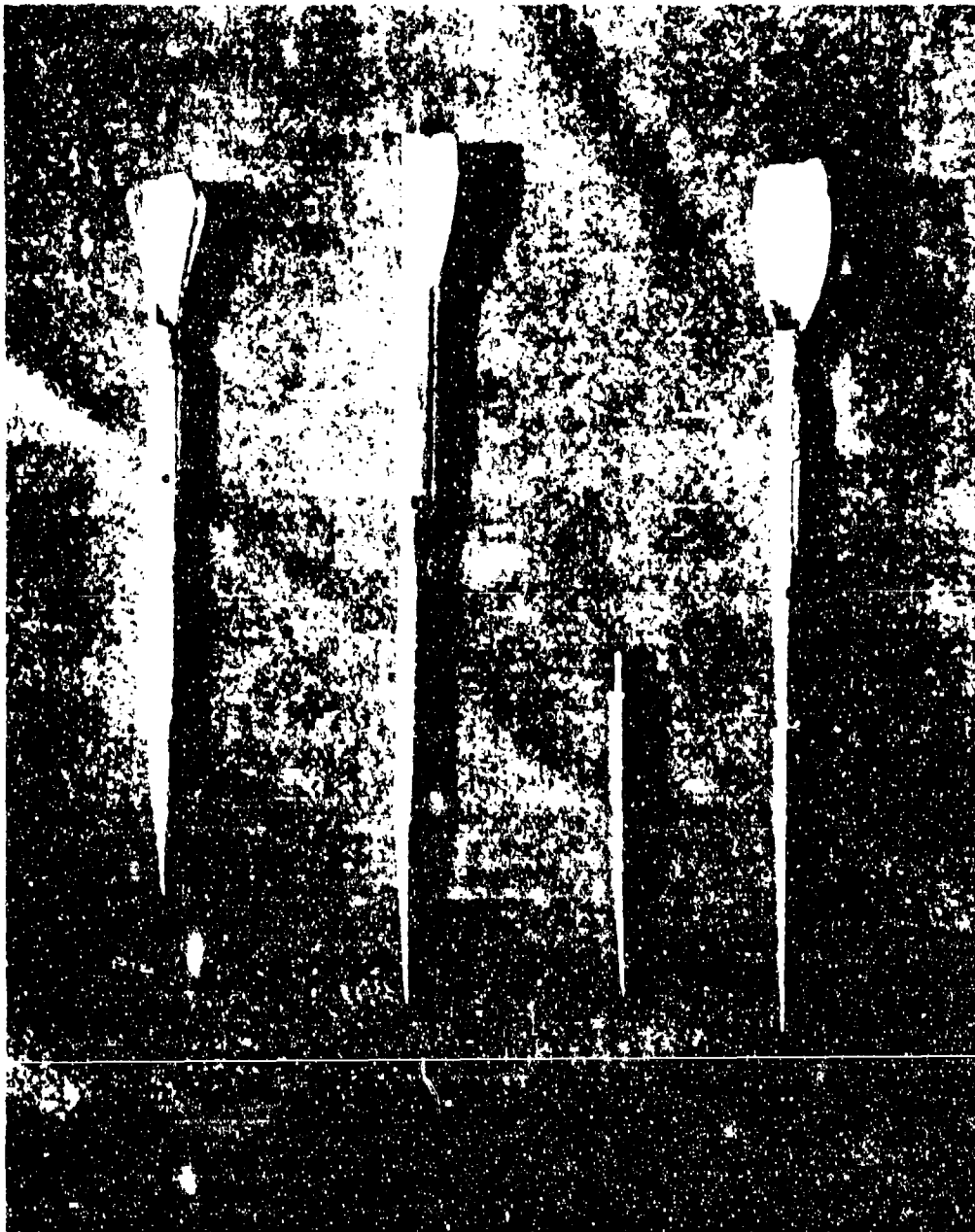


Figure 6. Supersonic Wind Tunnel Models

the glass wall side the wire was put through a hole in a flat washer placed flush against the glass wall. The hole in the washer had a diameter closer in size to the diameter of the wire than the hole in the glass wall. This cut down on the disturbance of the flow caused by the presence of the hole in the wall of the test section. Next, the wire was secured by placing it through an Allen screw tube and a solder washer. An Allen screw tube is a long cylinder with a small diameter hole drilled along its longitudinal axis and three small holes drilled perpendicular to the axis. These holes have been tapped to accommodate Allen screws which can be tightened to clamp down on the piano wire and hold it in place. A solder washer is a short cylinder containing two small diameter holes, one at the center and one near the outer edge. After running the wire through the center hole it can be bent around into the second hole at the outer edge. This hole also has a small hole drilled perpendicular to it and tapped to hold an Allen screw. As in the Allen screw tube, this Allen screw can be tightened down on the support wire to secure it. This system holds the support wire on the glass wall side of the test section.

After running the wire through the steel wall side it was pushed through a flat washer identical to the one on the glass wall side. A tightening tube was placed next in position and the wire was guided through it. A tightening tube is two concentric cylinders which are matched by threading. The length of the tube can be adjusted to the desired size by rotating the outer tube about the inner one. Finally, the

piano wire was secured using an Allen screw tube and a soldier washer. This completed the setting up of the support system. One advantage not already mentioned comes to light at this point. The models could be easily removed and inserted into the test section of the wind tunnel.

After the support system was in place the tension in the wire was adjusted by changing the length of the tightening tube. The tension was set so that the model would not change its vertical position after the tunnel was turned on. The model was then rotated  $180^{\circ}$  and held in place by a retaining mechanism shown in Figure 13. This system consisted of an extendable retainer which was placed around the nose of the model to secure it at its initial angle of attack. The retainer was connected to a release wire which could be manually operated from outside the tunnel. When the release wire was pulled the retainer would slip off the nose of the model and the model would be free to oscillate.

To record the oscillations of the model a Wollensak Fastex high speed motion picture camera was used. The camera was set-up as shown in Figure 14 on the glass wall side of the test section. Two floodlights, one just above the camera position and one above the inlet of the wind tunnel, were used to provide maximum lighting of the model in the test section. The camera was operated at a speed of 3000 frames per second for three seconds with a lens opening of f5.6.

Upon completing all preparations the tunnel was started following the procedure in Appendix B. The retainer was pulled back and the subsequent angular motion of the model was recorded.

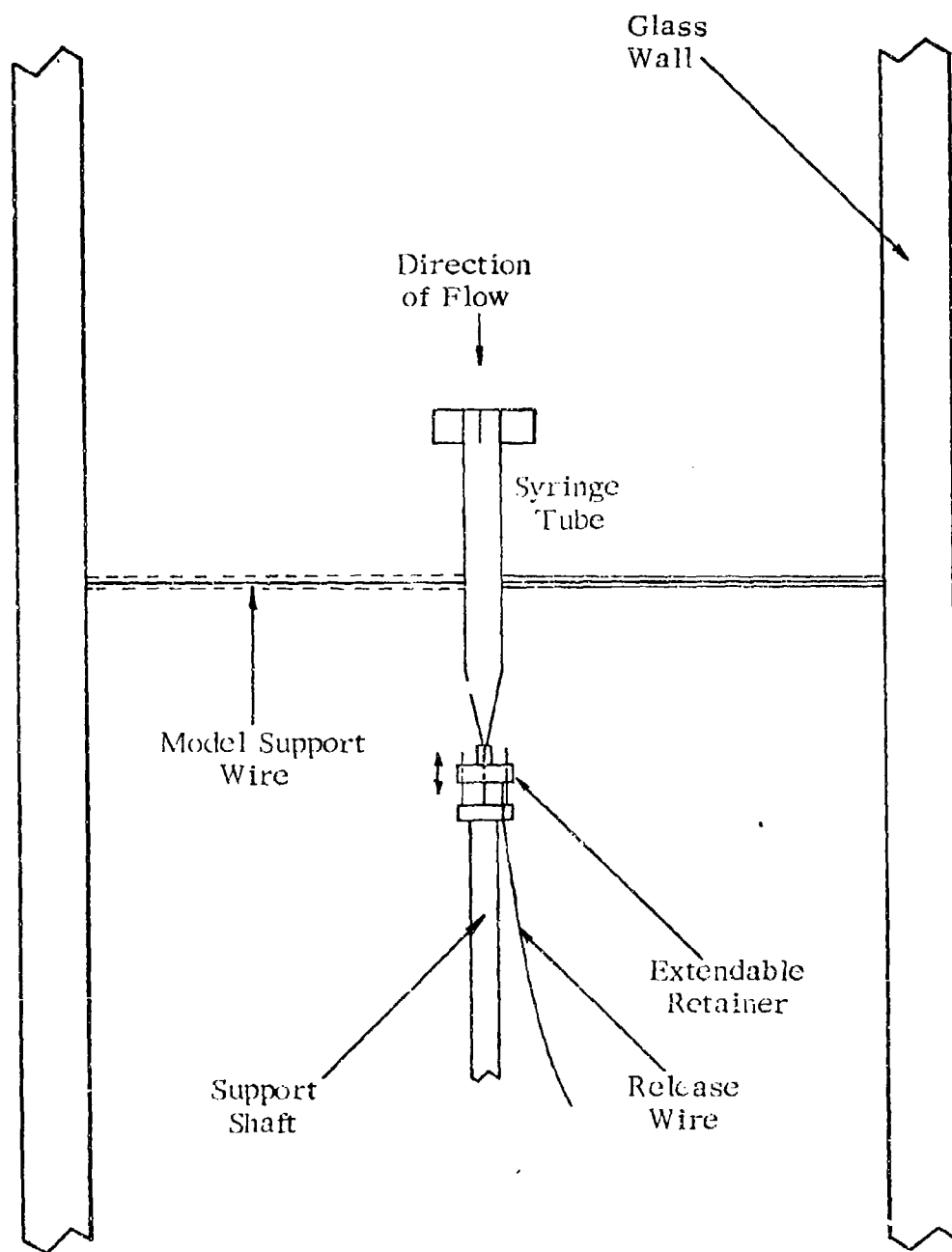


Figure 13. Retaining Mechanism

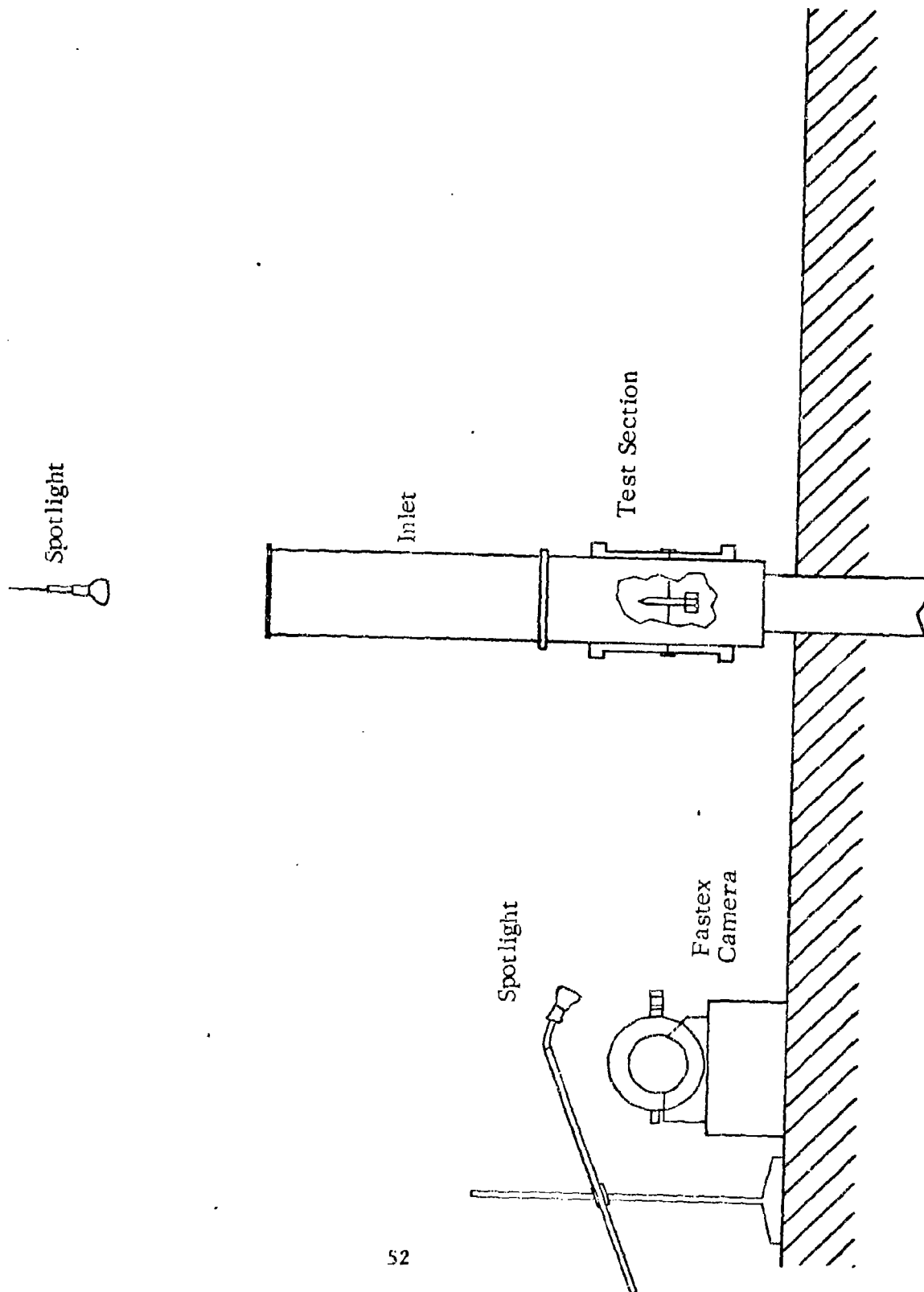


Figure 14. Camera Setup

### One-Degree-of-Freedom Data Reduction Procedure

The one-degree-of-freedom oscillations were converted to numerical values of angle of attack in the following manner. Two reference dots at a known distance apart had been placed on the steel wall in the test section behind the model. These dots were included in each frame of the film record of the angular motions of the model. The dots were placed such that a horizontal line running between them was above the highest point that the model with the largest radius would reach. For each configuration the radius of oscillation, the distance from the pivot point to the nose of the model, was also known. The relative coordinates of the reference dots and the nose of the model were determined from the data film using an optical comparator shown in Figure 15. A computer program called REDUCE, presented in Appendix C, using these coordinates and the known conversion distance between the reference dots was then employed to produce a time history of the angular oscillations of the model. A schematic of the reduction coordinates is presented in Figure 16.

### Velocity Determination Technique

Since all the tests were not conducted on the same day it was necessary to determine the velocity in the wind tunnel on the particular day the test was conducted. A method of measuring the static pressure in the test section was necessary to do this. A system like the one in Figure 17 was used to do this

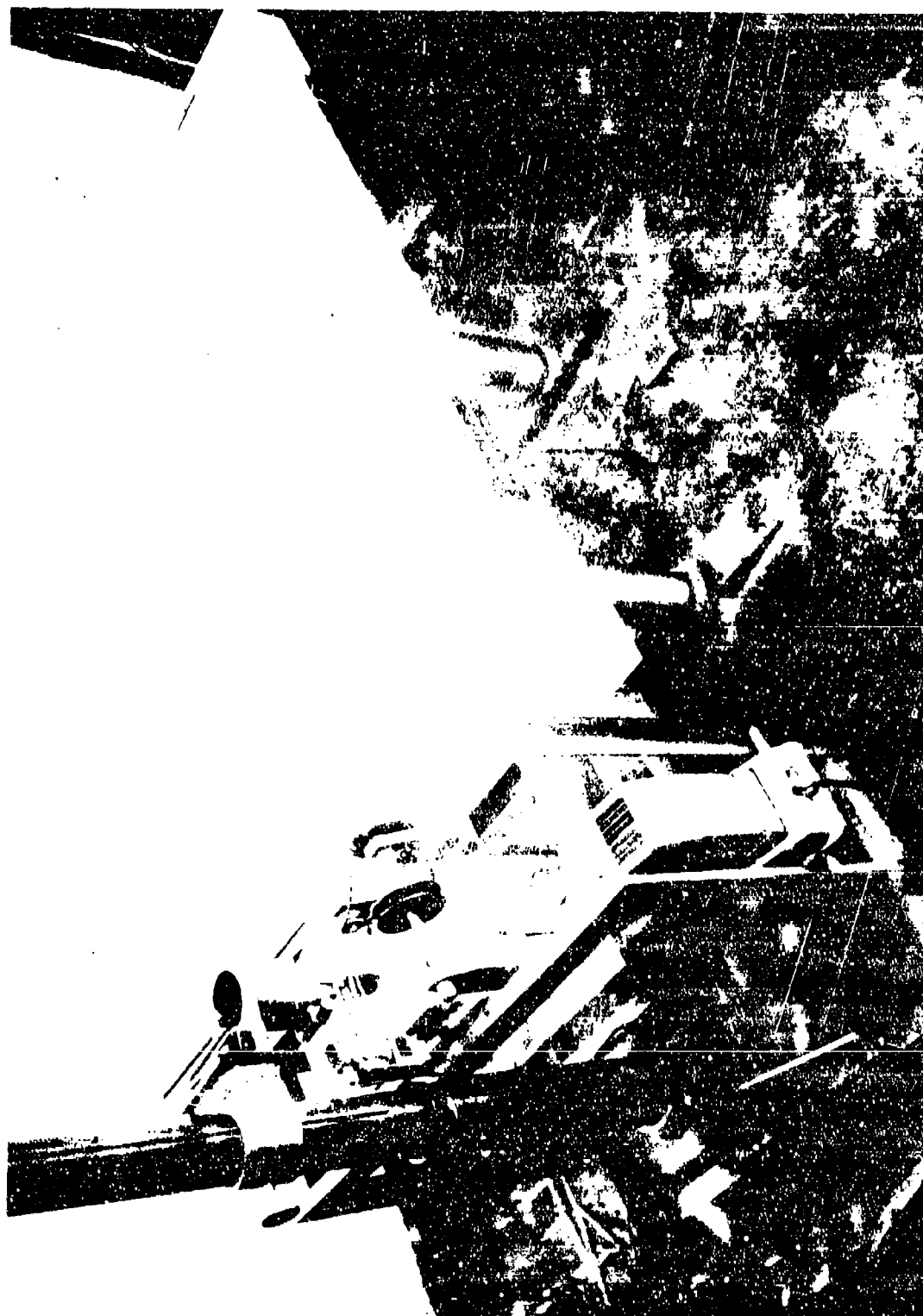
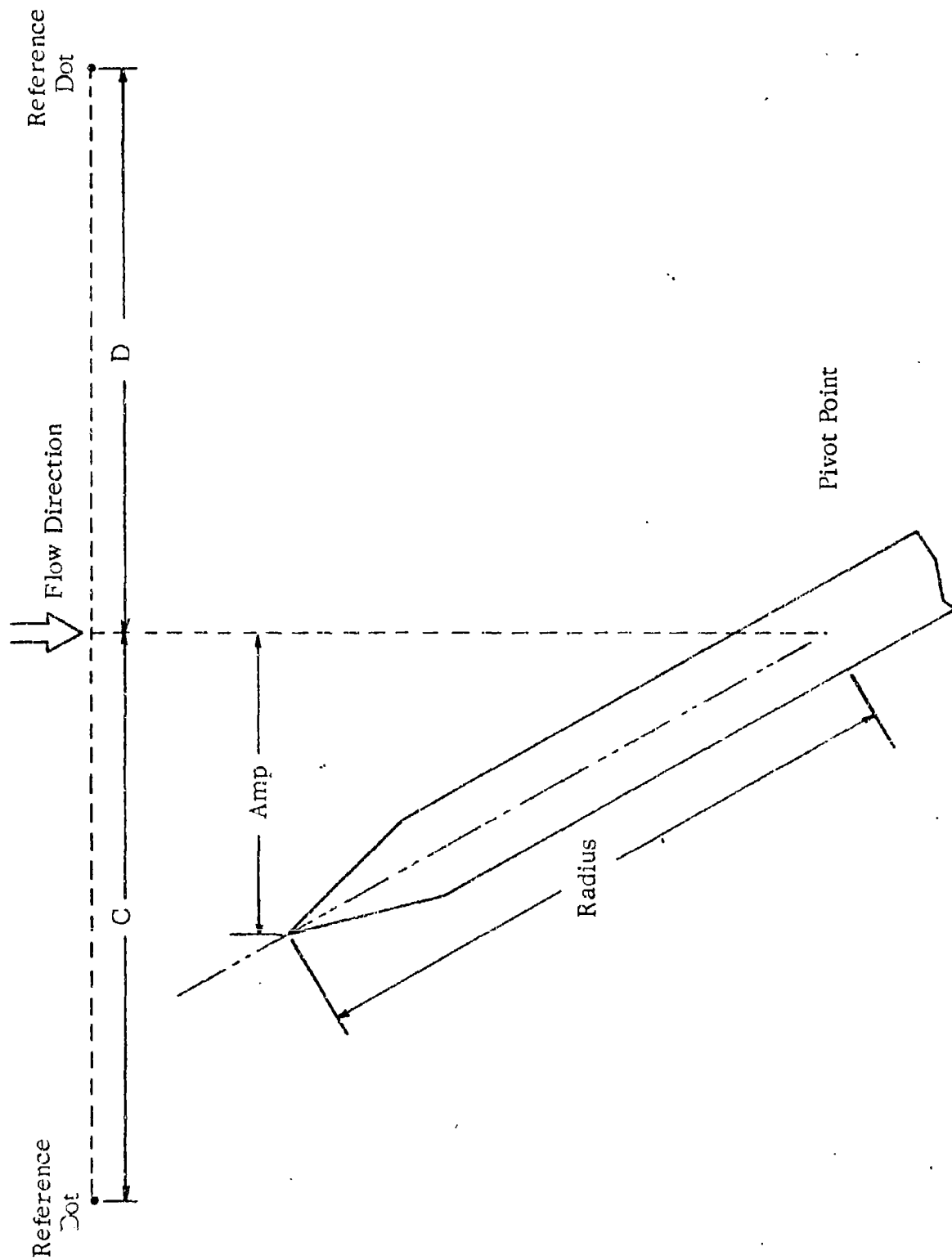


Figure 15. Optical Comparator





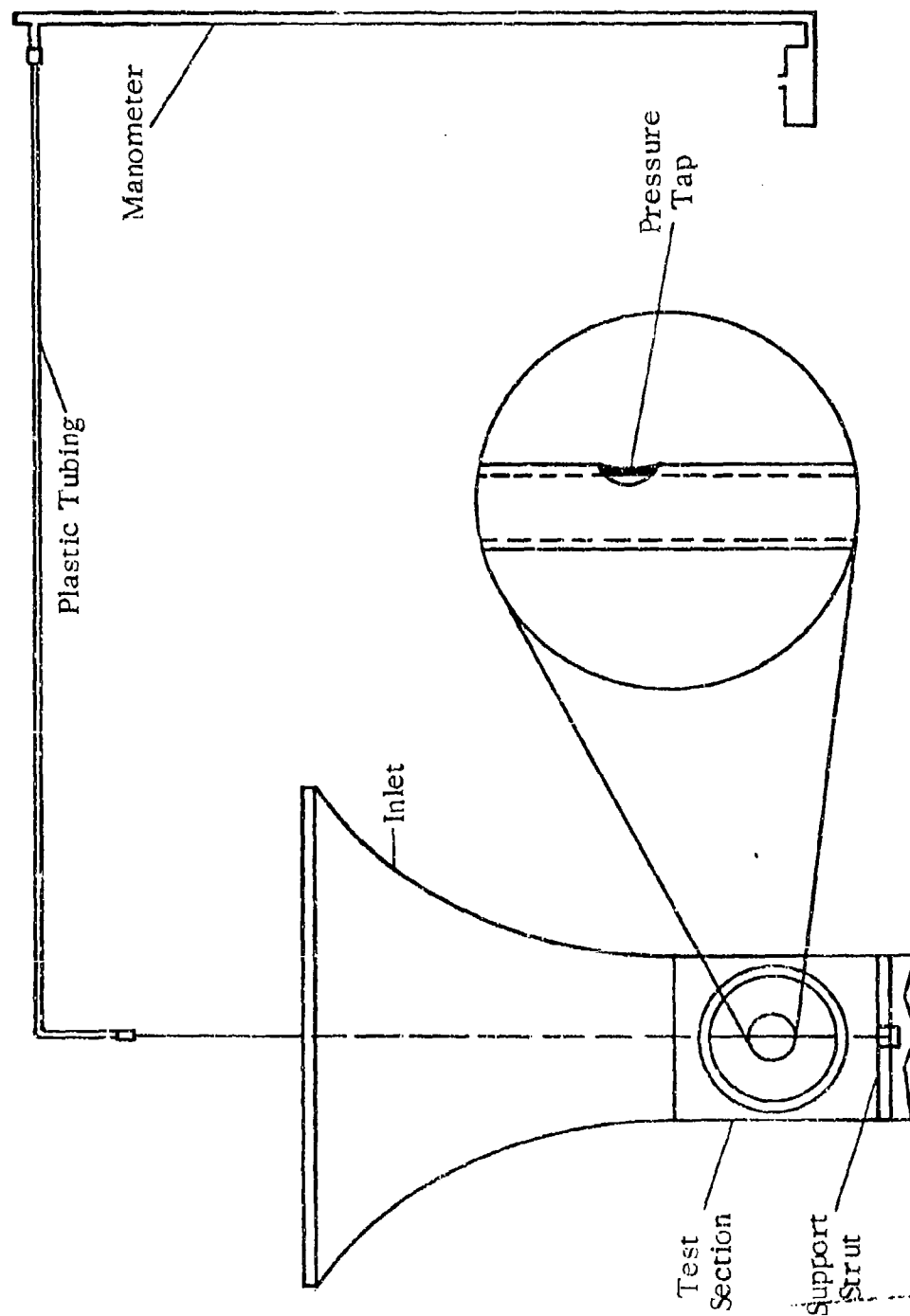


Figure 17. Velocity Measurement Setup

A long thin tube was placed in the inlet of the wind tunnel and lowered until the end reached the support strut just below the test section. This end of the tube was secured to the strut to help maintain the position of the tube near the center of the wind tunnel test section. A small hole had been drilled in the side of the tube to coincide with the position of the model when the tube was in place. The end of the tube in the tunnel was sealed and the open end was connected to a manometer by a length of plastic tubing. This upper end was fastened so as to put tension on the tube and prevent it from moving about in the test section when the pressure measurement was being taken. Any movement of the tube would affect the pressure reading and produce an incorrect value of the velocity.

Before starting the tunnel a tare reading was made on the manometer and the stagnation or total pressure was taken from a barometer. Since the manometer scale did not coincide with that of the barometer the tare reading and barometer reading, which should have been equal had their scales coincided, were different. This difference was a correction factor which would have to be added to the pressure reading taken when the tunnel was on to give the actual static pressure. The tunnel was turned on and the pressure was recorded. Having all of these pressure readings the ratio of static to total pressure could be solved for using the following formula:

$$\frac{p}{P_t} = \frac{P_{\text{read}} + (P_t - P_{\text{tare}})}{P_t}$$

where

$$(P_t - P_{tare}) = \text{correction factor}$$

Once this ratio was known the Mach number could be found in the Isentropic Flow Tables of Reference 8. For the REDUCE computer program it was necessary to put the velocity in units of feet per second from the Mach number. A sample calculation of this is shown in Appendix D.

## ONE-DEGREE-OF-FREEDOM TEST RESULTS

### ~~One Degree-of-Freedom Data Reduction~~

The WOBBLE computer program was used to fit the Aeroballistic Theory to the one-degree-of-freedom angular data obtained from the REDUCE program. The data was fitted in segments of 1.8 cycles and the stability parameters  $K_1$ ,  $K_T$ ,  $\lambda_1$ , and  $\omega_1$  were determined by WOBBLE at a time interval of 0.03 seconds. The stability parameter  $K_T$ , the trim arm, is analogous to the  $K_3$  in the Linear Theory and is due to aerodynamic asymmetries in the configurations. The average percent error of the fitting of the theory to the data for all the tests carried was less than 3%. A representative plot of probable error (P.E.) versus time is given in Figure 18. The stability parameters were obtained from the fits as functions of time. Plots of the stability parameters versus time for all the configurations are presented in Figures 19 through 34.

### One-Degree-of-Freedom Stability Coefficients

The pitching moment and damping moment stability coefficients,  $C_{M_\alpha}$  and  $(C_{M_q} + C_{M_{\dot{\alpha}}})$ , were obtained versus time from the WOBBLE fits. Plots of the mean values of the coefficients per fit versus mean angle of attack per fit are presented in Figures 35 through 42 for all the configurations. These plots given an approximation of how the coefficients vary with angle of attack. Included on these graphs are Ballistic Range Laboratory (BRL) results for the respective configurations and

coefficients. The BRL data was plotted at an angle of attack of  $2^\circ$ .

Figures 43 through 50 are plots of BRL results for the stability coefficients versus Mach number for all the configurations. Mean values of the Notre Dame results for the coefficients at low angles of attack are included on these graphs. The Notre Dame data was plotted at a Mach number of 1.3 which was an average value of all the tests carried out.

An important point which should be brought up at this point is the discrepancy in the definition of the damping moment stability coefficient between the two sets of results. The computations in this investigation were carried out using a factor of  $(\frac{d}{2u})$  in the definition of the damping moment stability coefficient (see Equation 3). The BRL definition used a factor of  $(\frac{d}{u})$  causing the respective computed values of  $(C_{M_q} + C_{M_{\dot{\alpha}}})$  to be off by a factor of two. To account for this and allow the results to be directly compared, the BRL values of  $(C_{M_q} + C_{M_{\dot{\alpha}}})$  were increased by a factor 2 before plotting. This essentially gave all the values presented a uniform definition and allowed the comparisons of the results to be made.

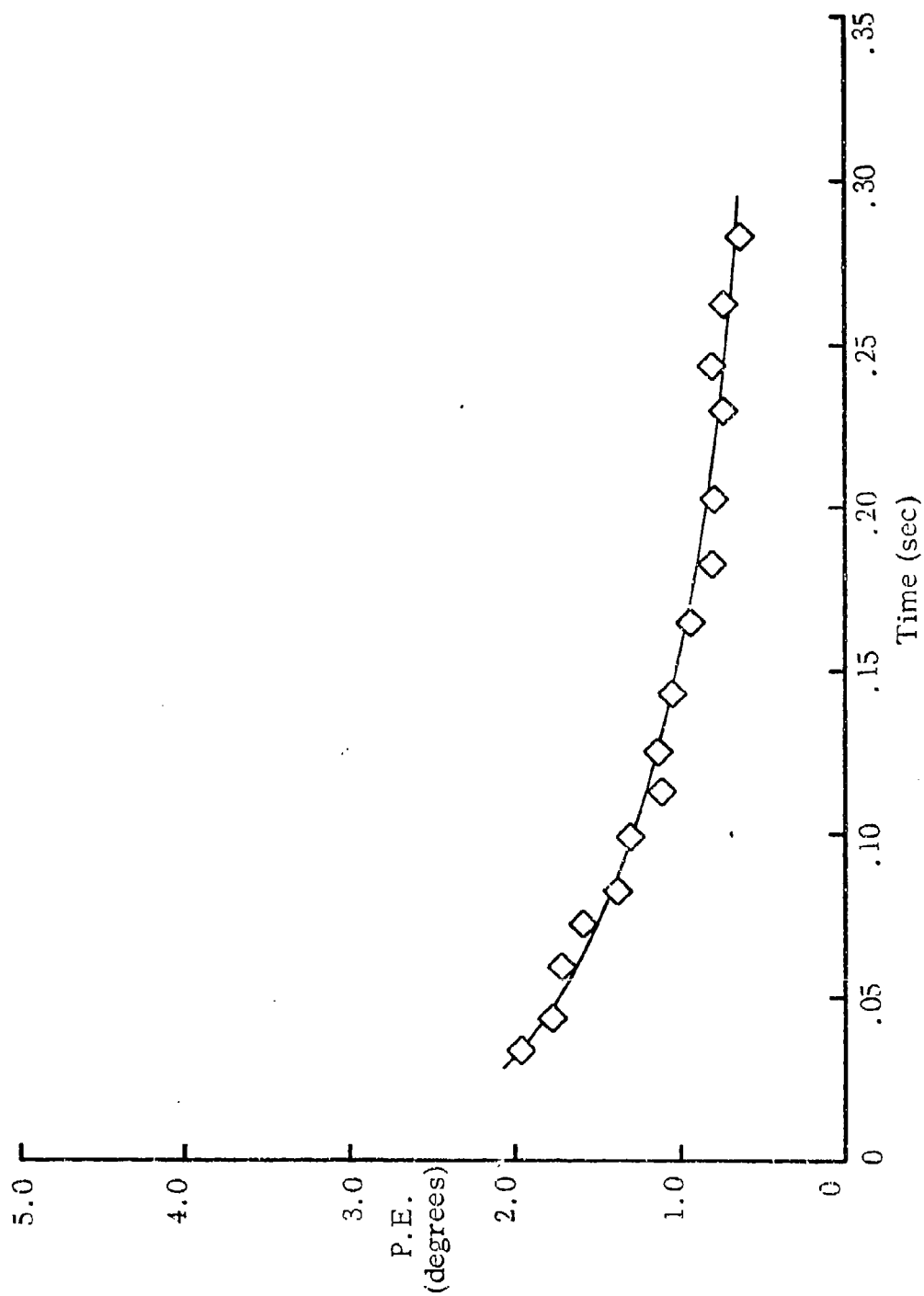


Figure 18. Probable Error versus Time

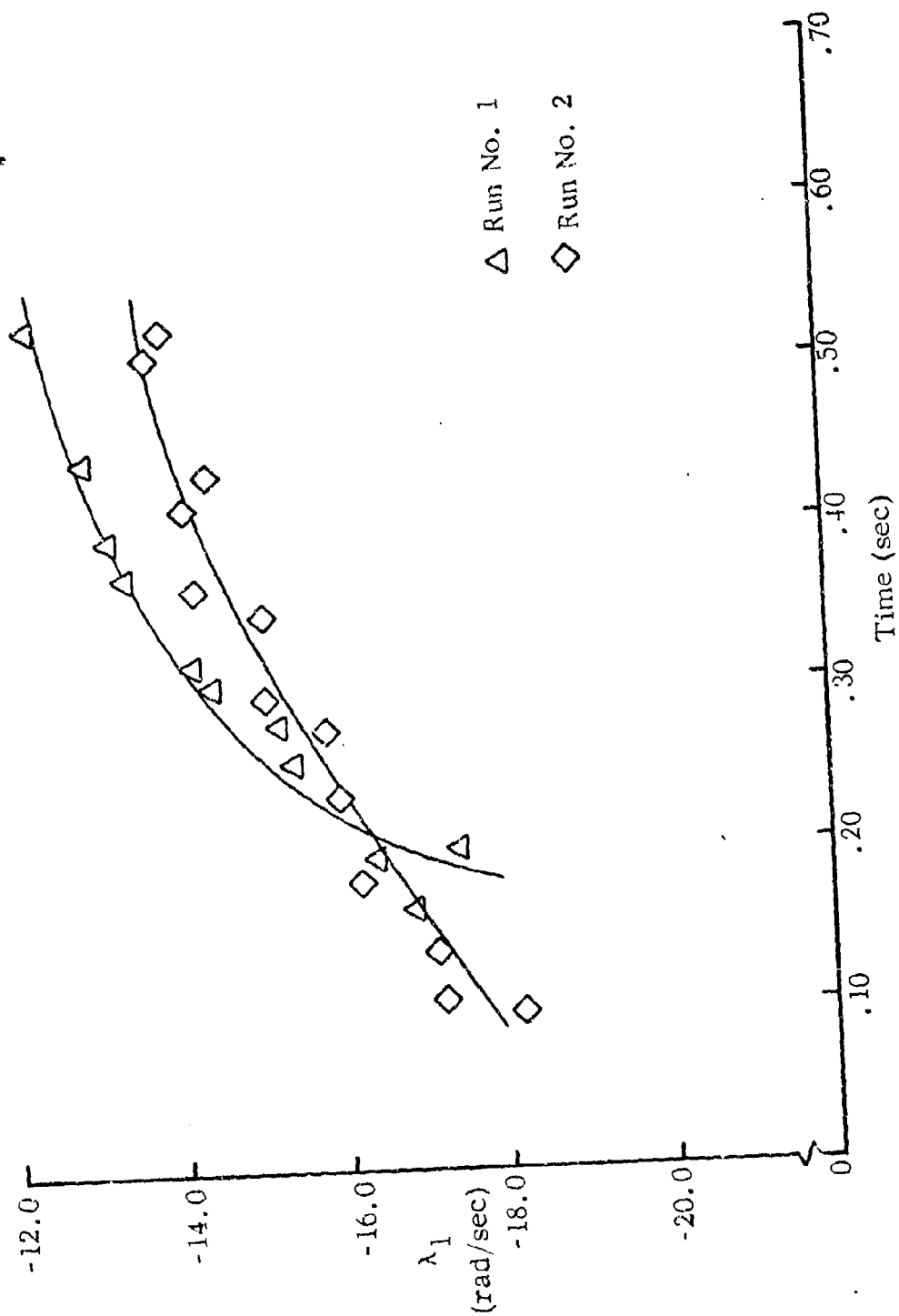


Figure 19.  $\lambda_1$  versus Time (Ground Point)

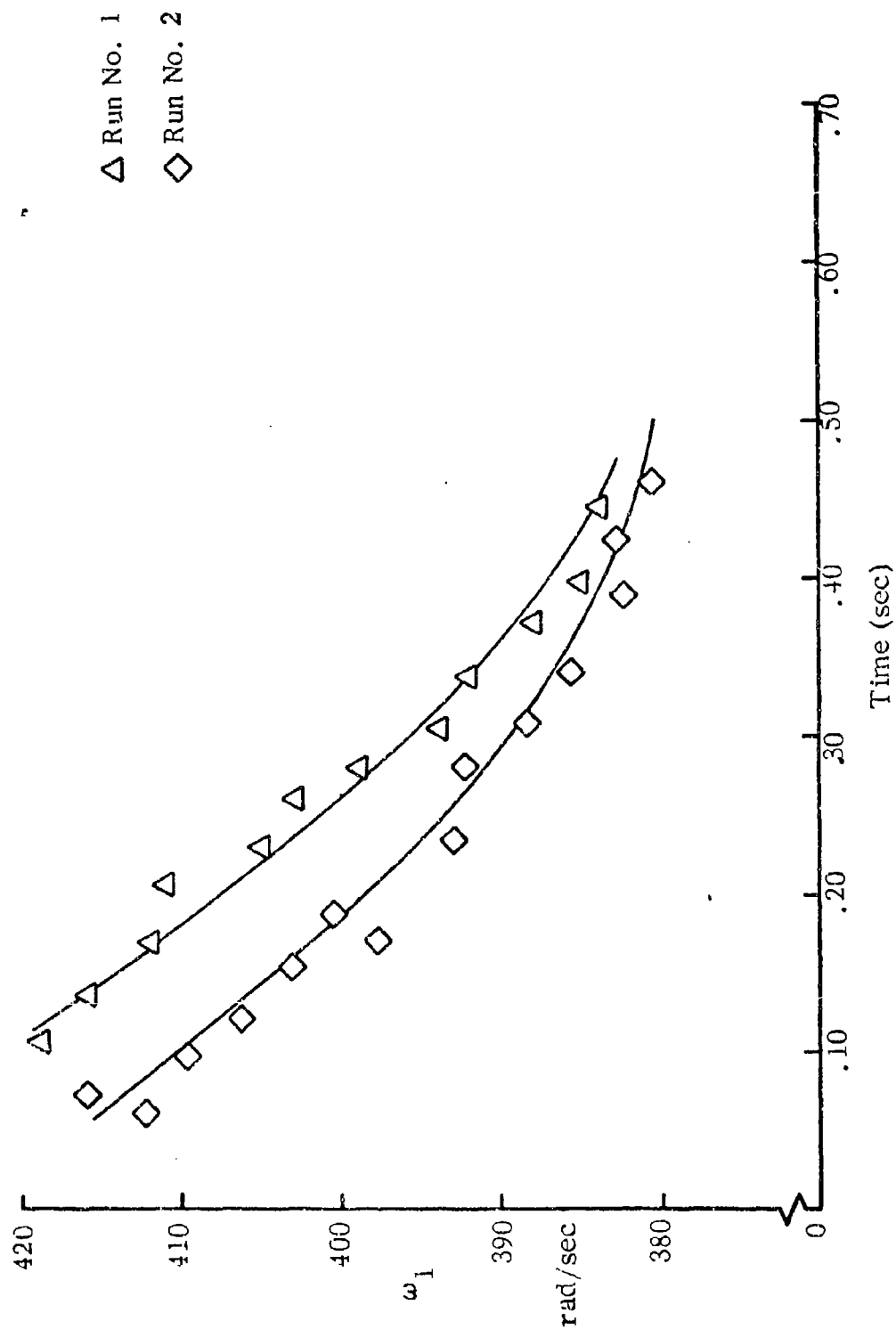


Figure 20.  $\omega_1$  versus Time (Ground Point)



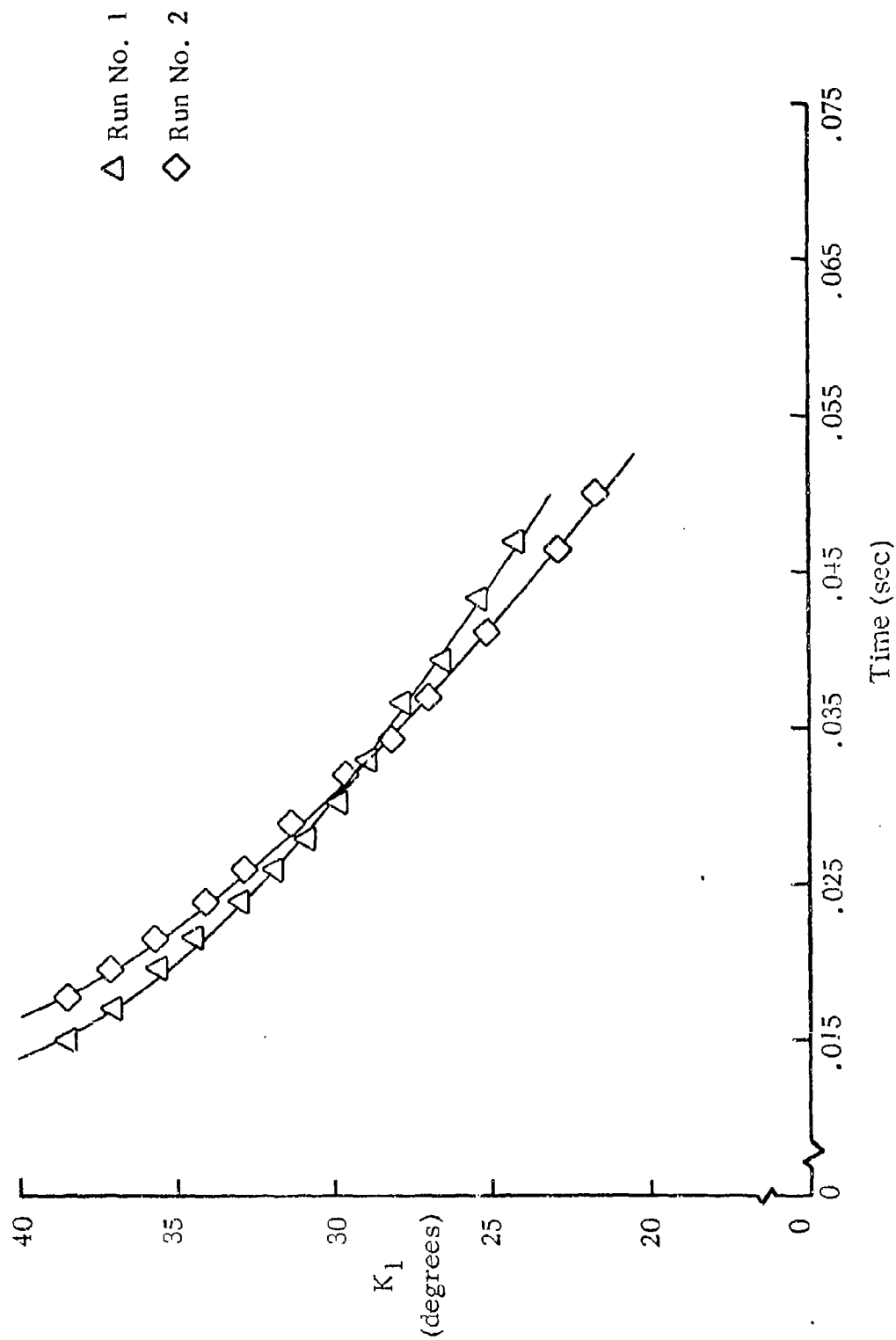


Figure 21.  $K_1$  versus Time (Ground Point)

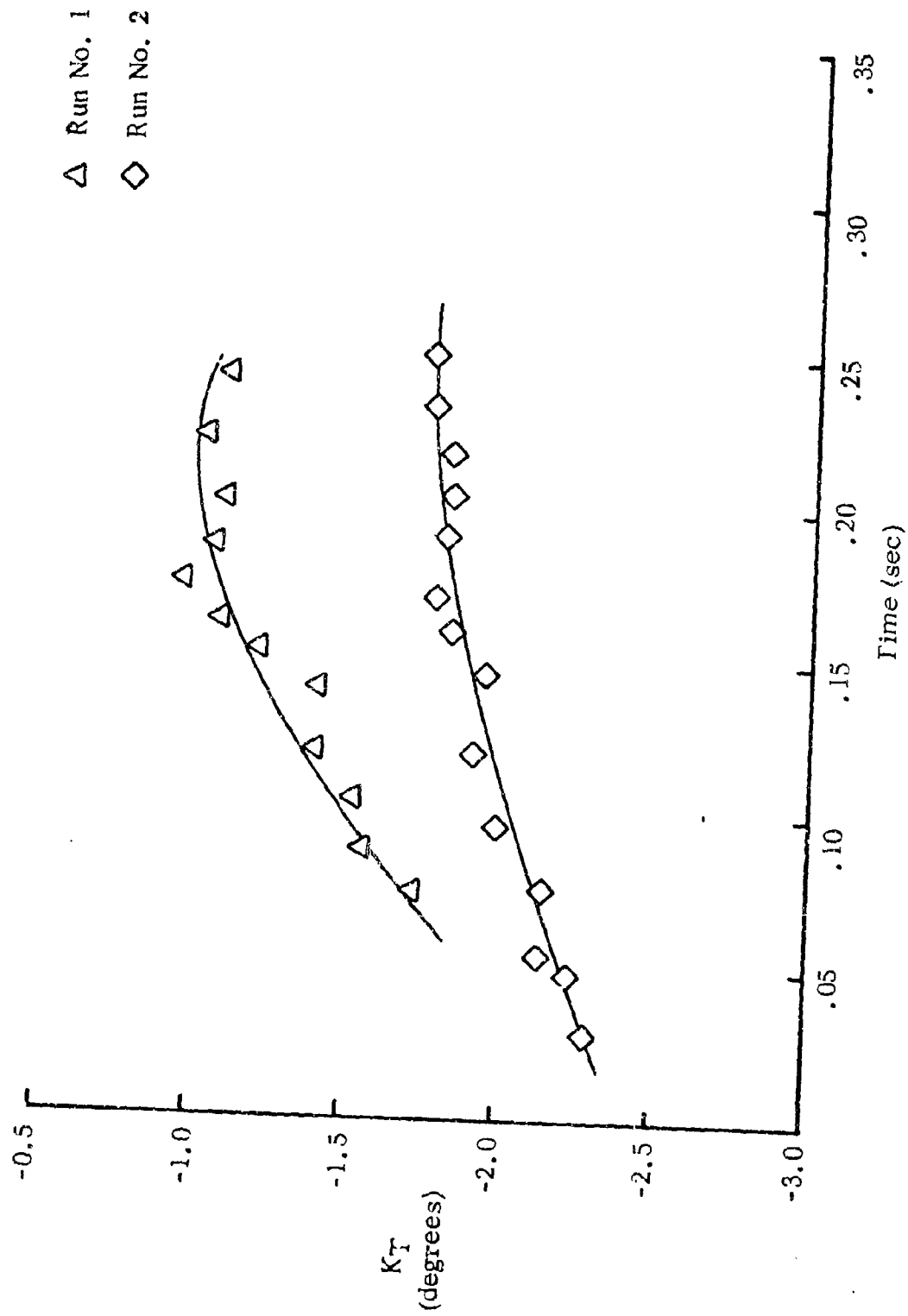


Figure 22.  $K_T$  versus Time (Ground Point)

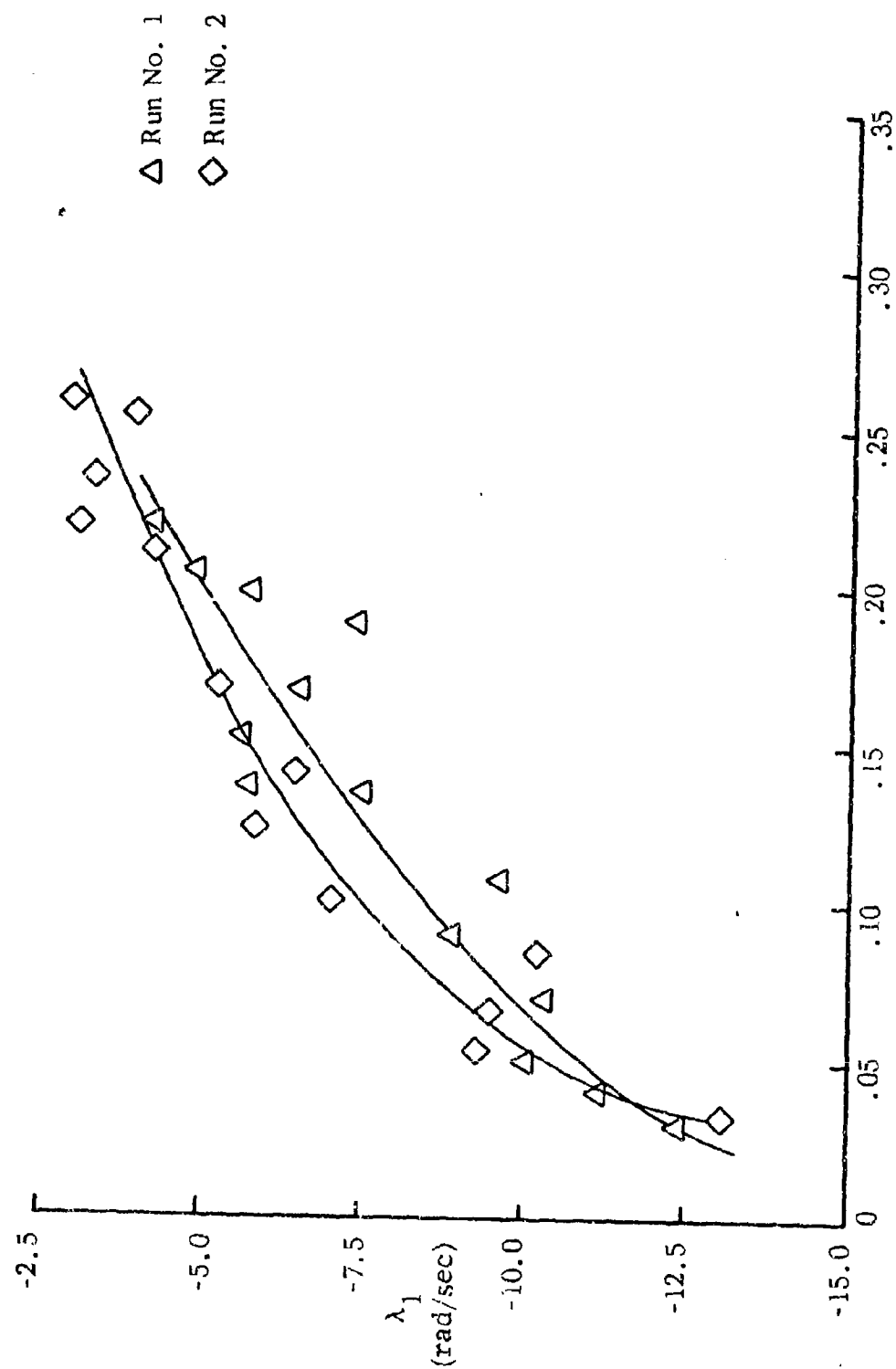


Figure 23.  $\lambda_1$  versus Time (min)

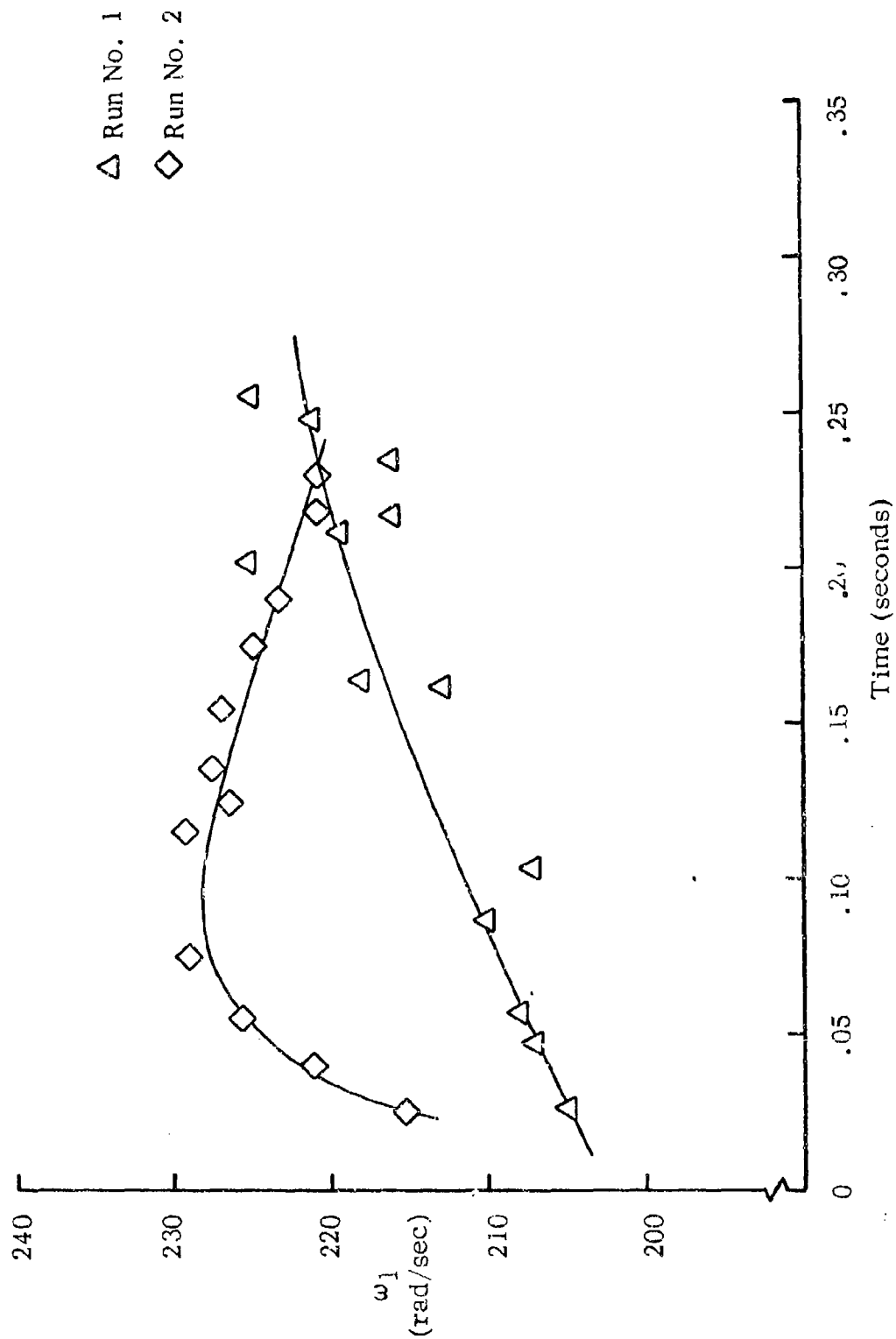


Figure 24.  $\omega_1$  versus Time (Olin)

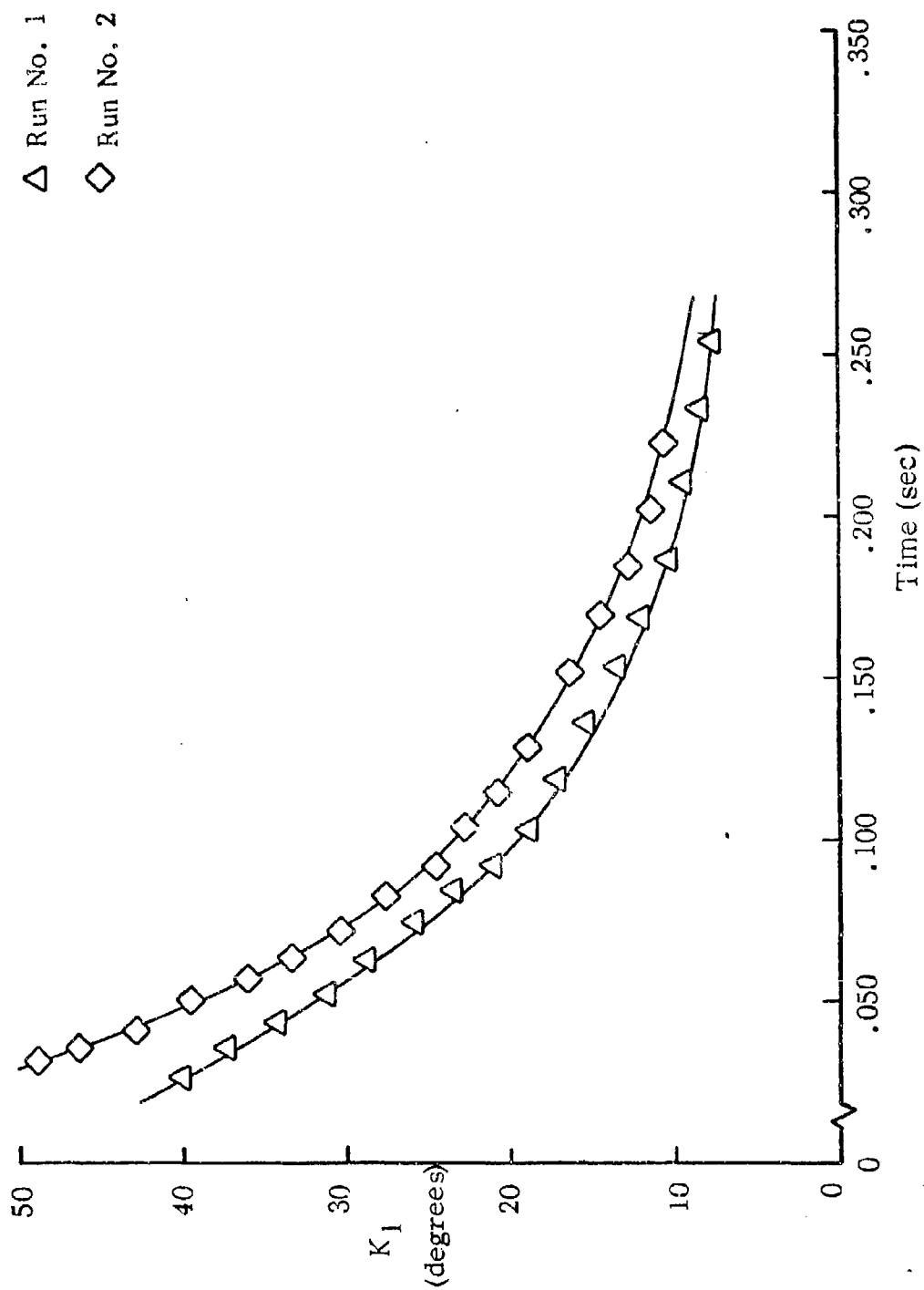


Figure 25.  $K_1$  versus Time (Olin)

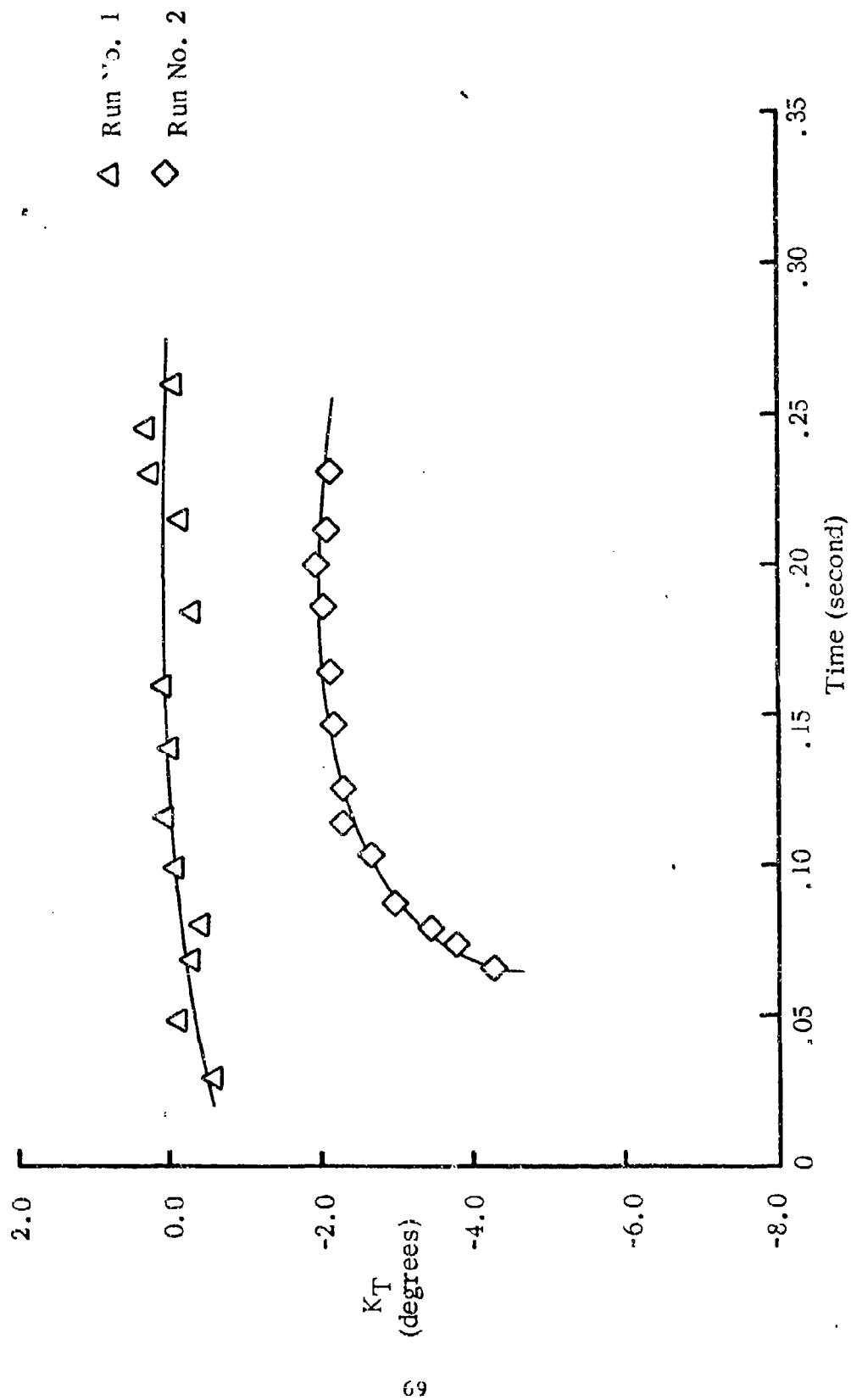


Figure 26.  $K_T$  versus Time (014n)

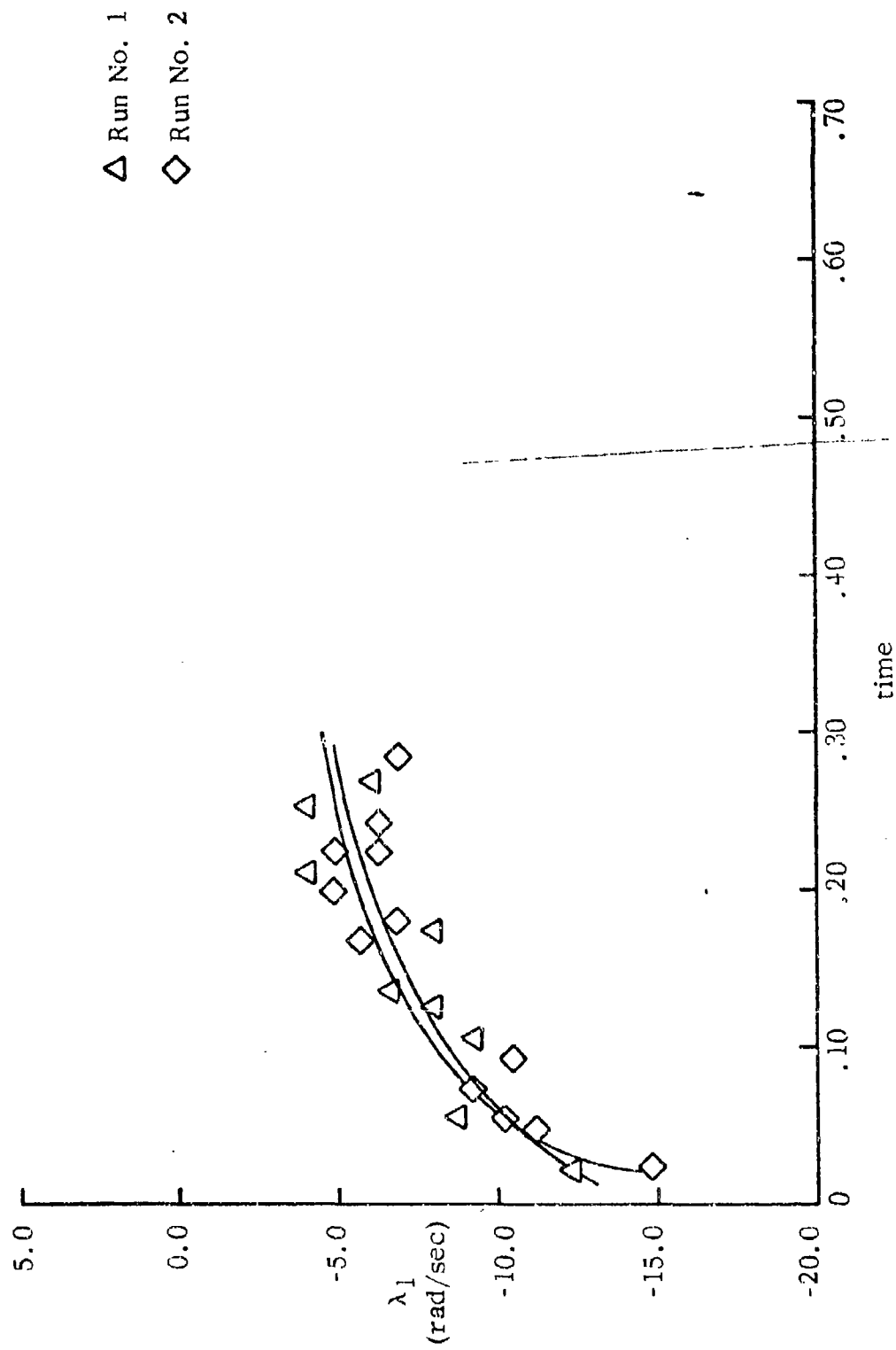


Figure 27.  $\lambda_1$  versus Time (Swaged Point)

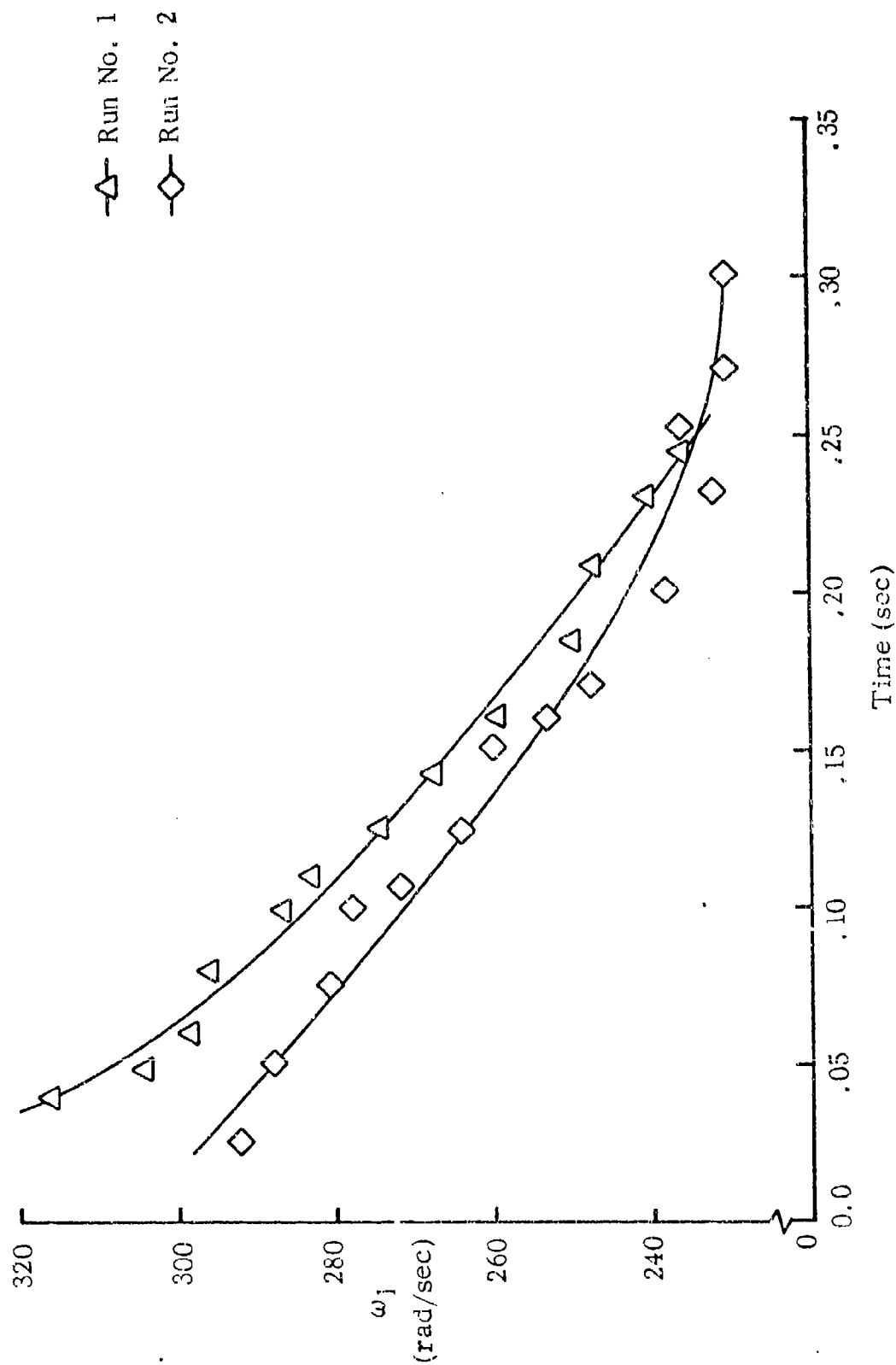


Figure 28.  $\omega_j$  versus Time (Swaged Point)



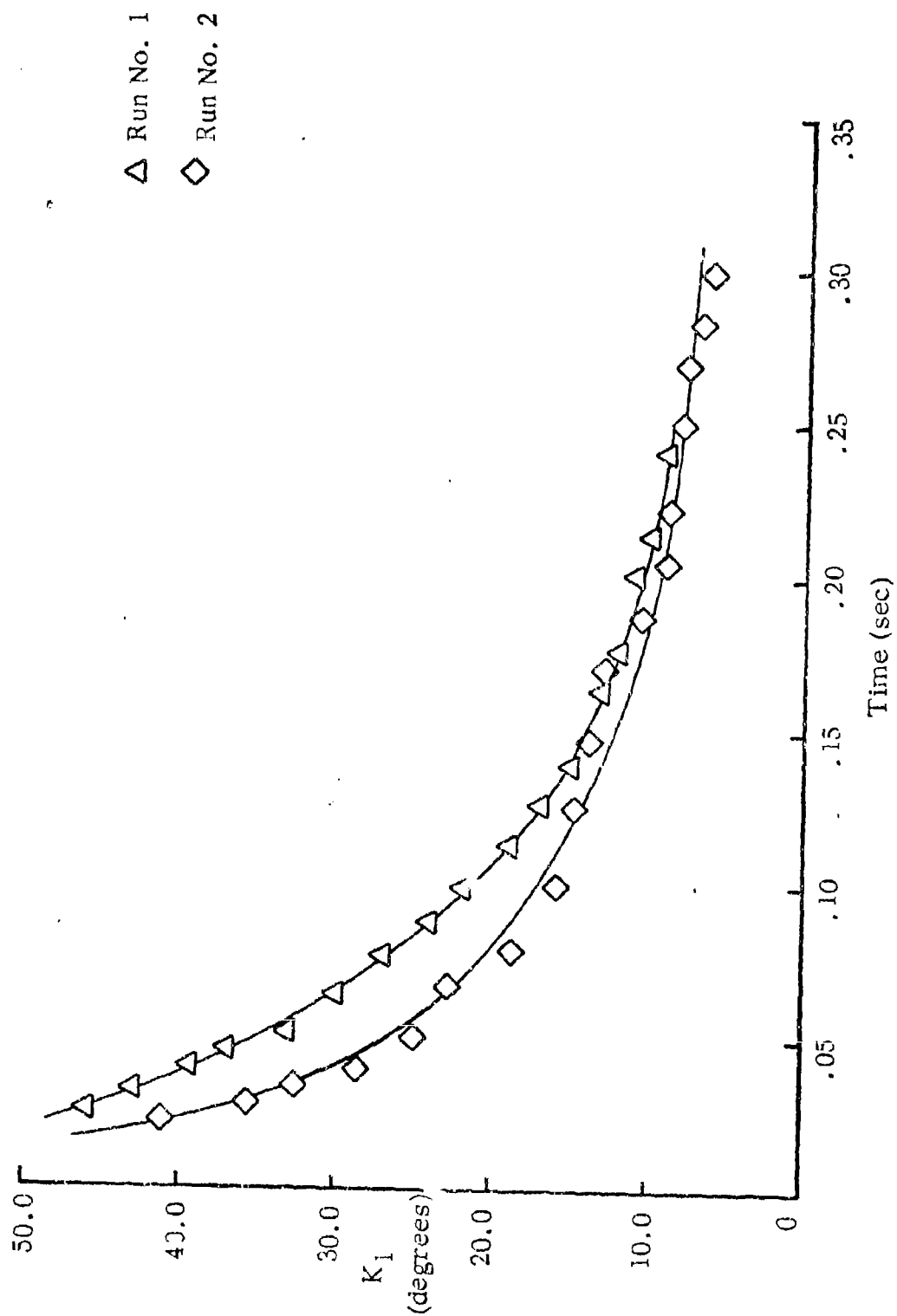


Figure 29.  $K_I$  versus Time (Swaged Point)

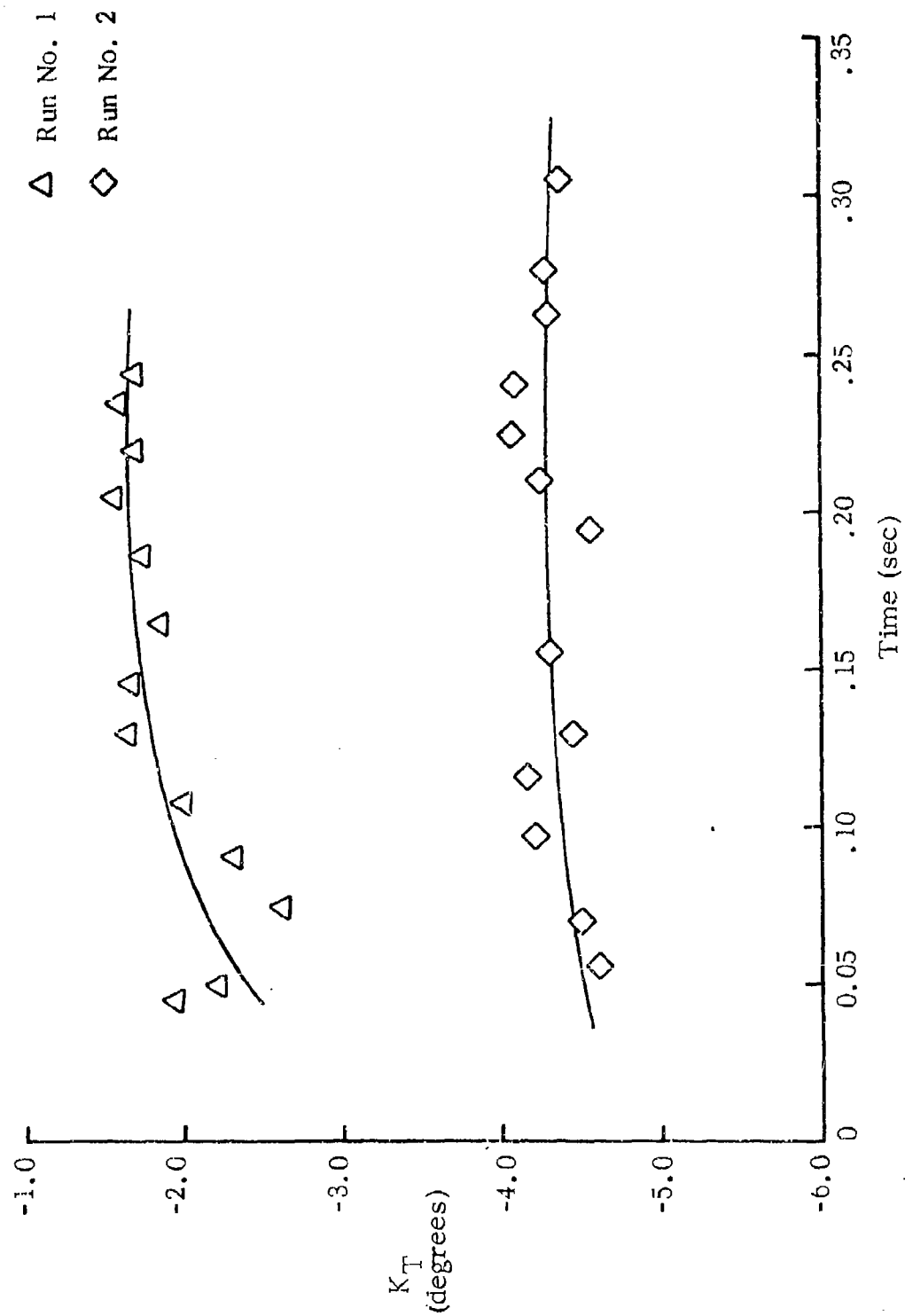


Figure 30.  $K_T$  versus Time (Swaged Point)

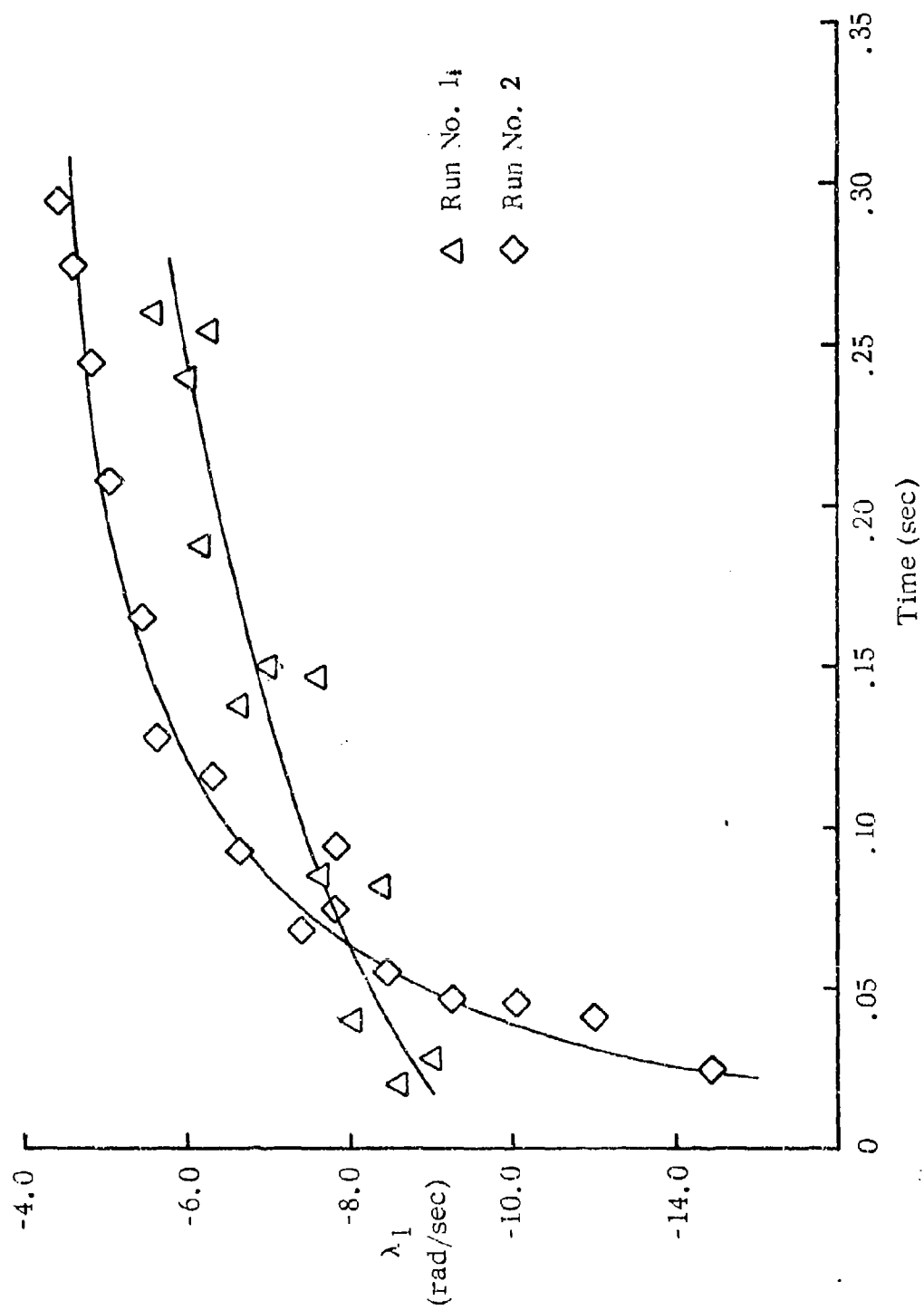


Figure 31.  $\lambda_1$  versus Time (Tracer)

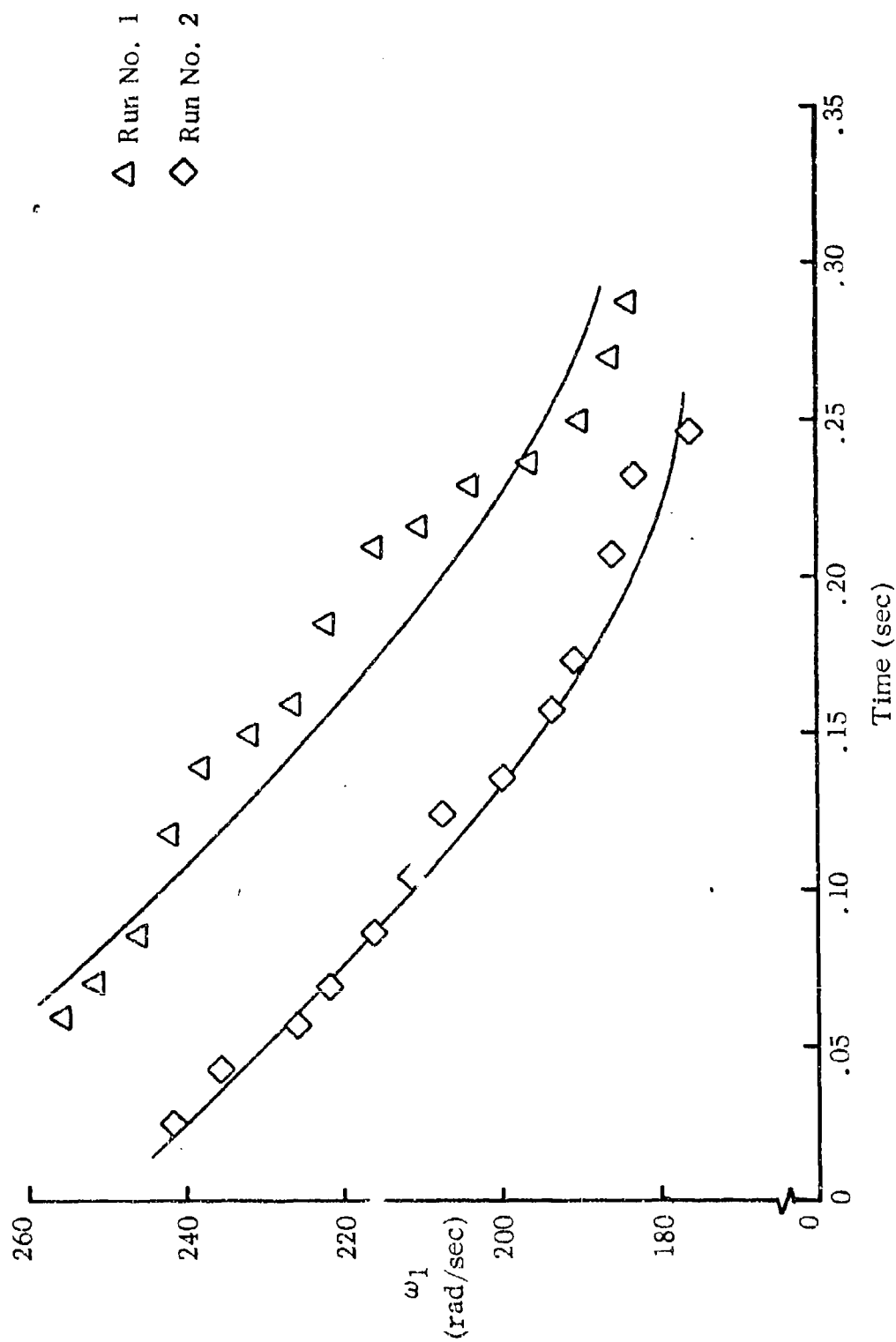


Figure 32.  $\omega_1$  versus Time (Tracer)

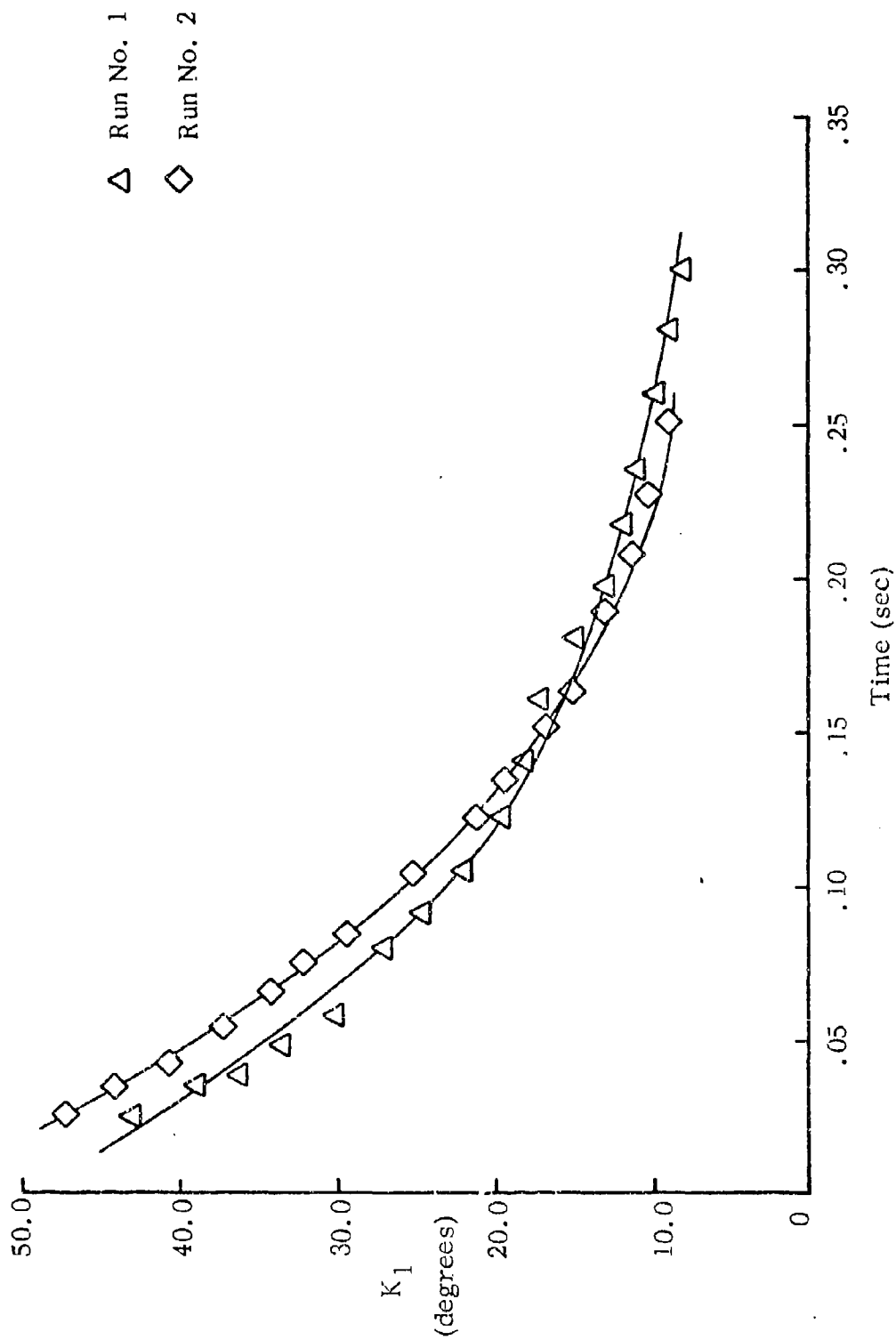


Figure 33.  $K_1$  versus Time (Tracer)

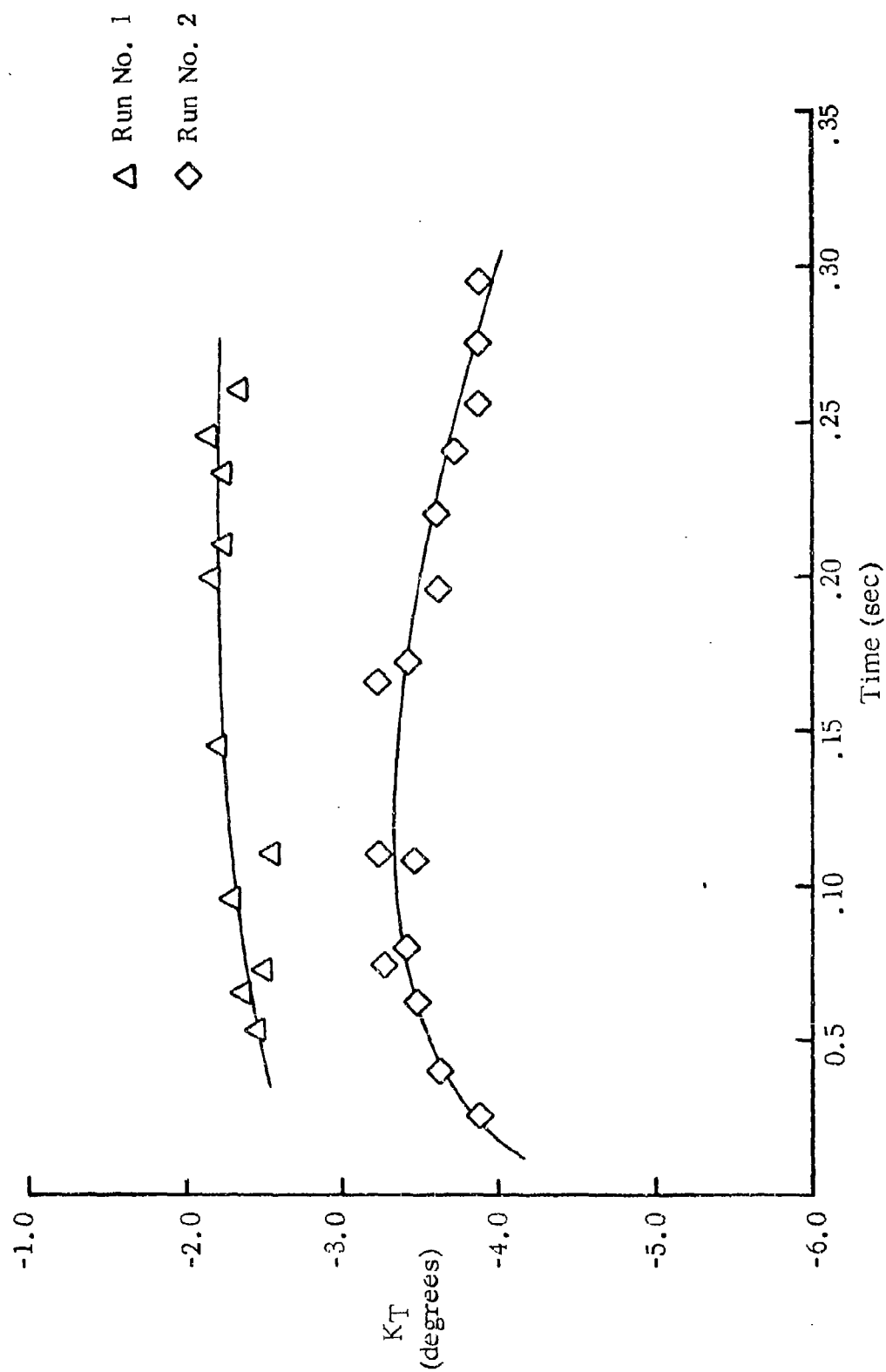


Figure 34.  $K_T$  versus Time (Tracer)

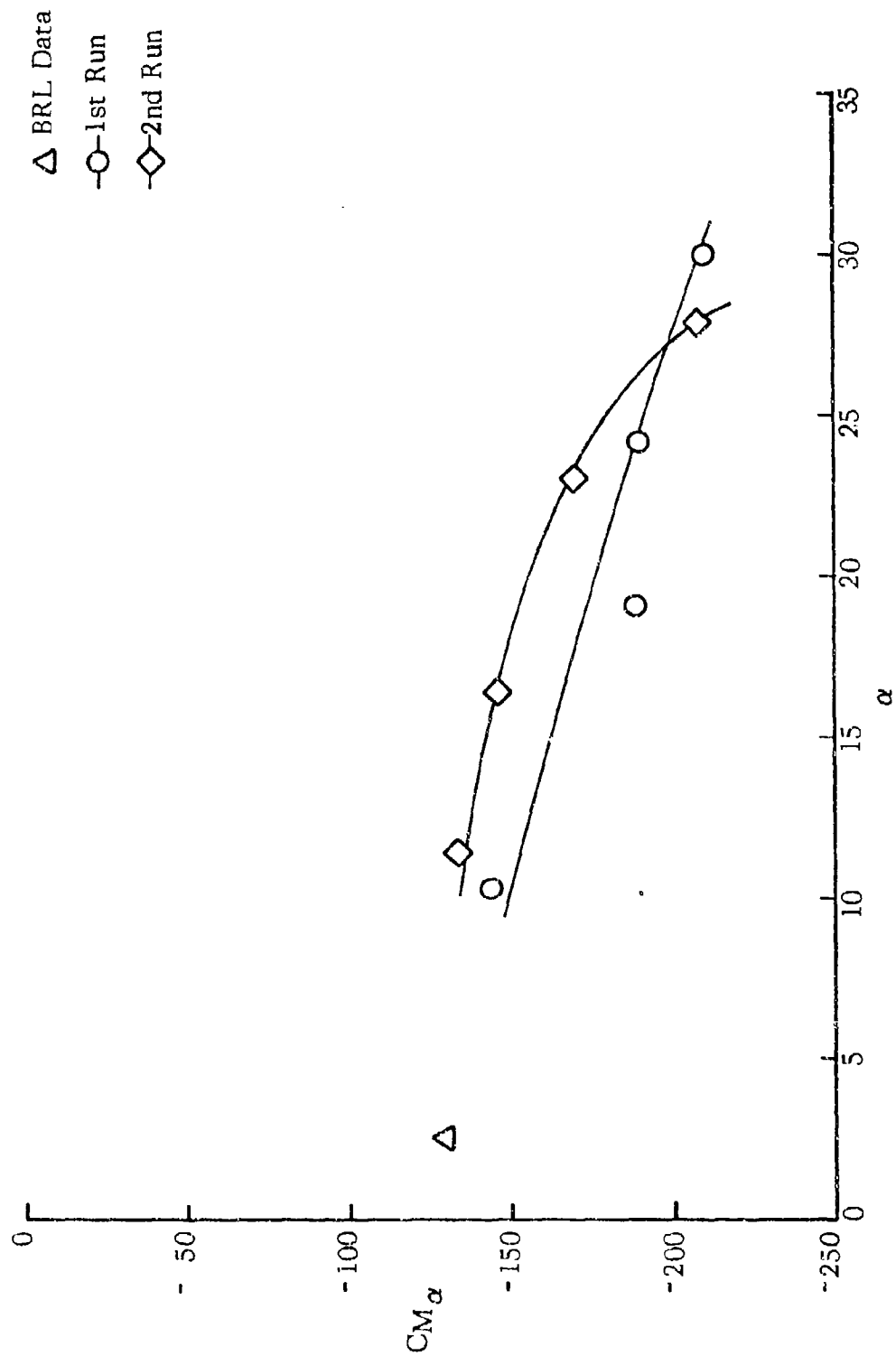


Figure 35.  $CM_\alpha$  vs  $\alpha$  (Ground Point)

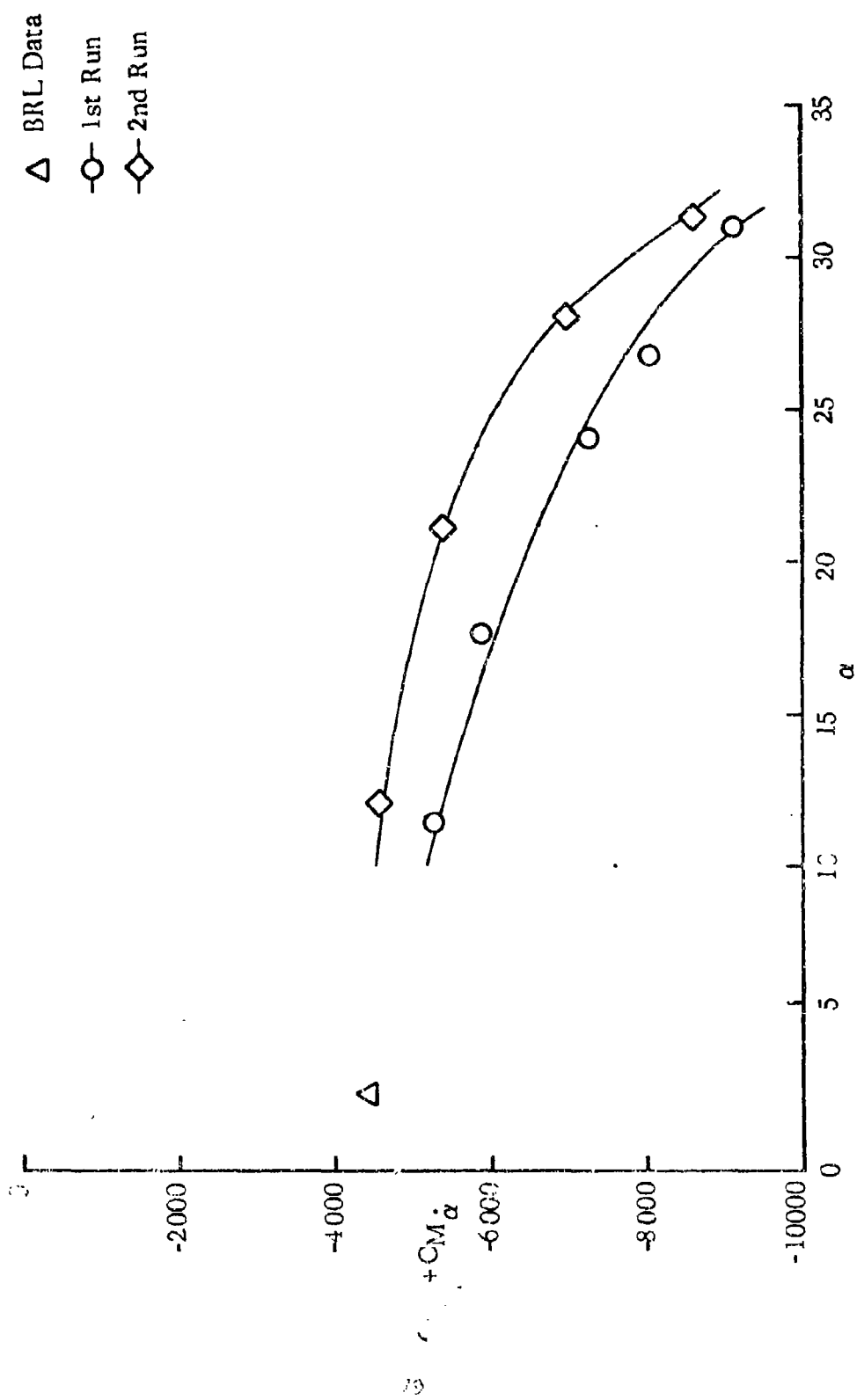


Figure 36.  $C_M + C_M \alpha$  vs  $\alpha$  (G.P.)



$\Delta$  BRL Data  
 $\circ$  Run No. 1  
 $\diamond$  Run No. 2

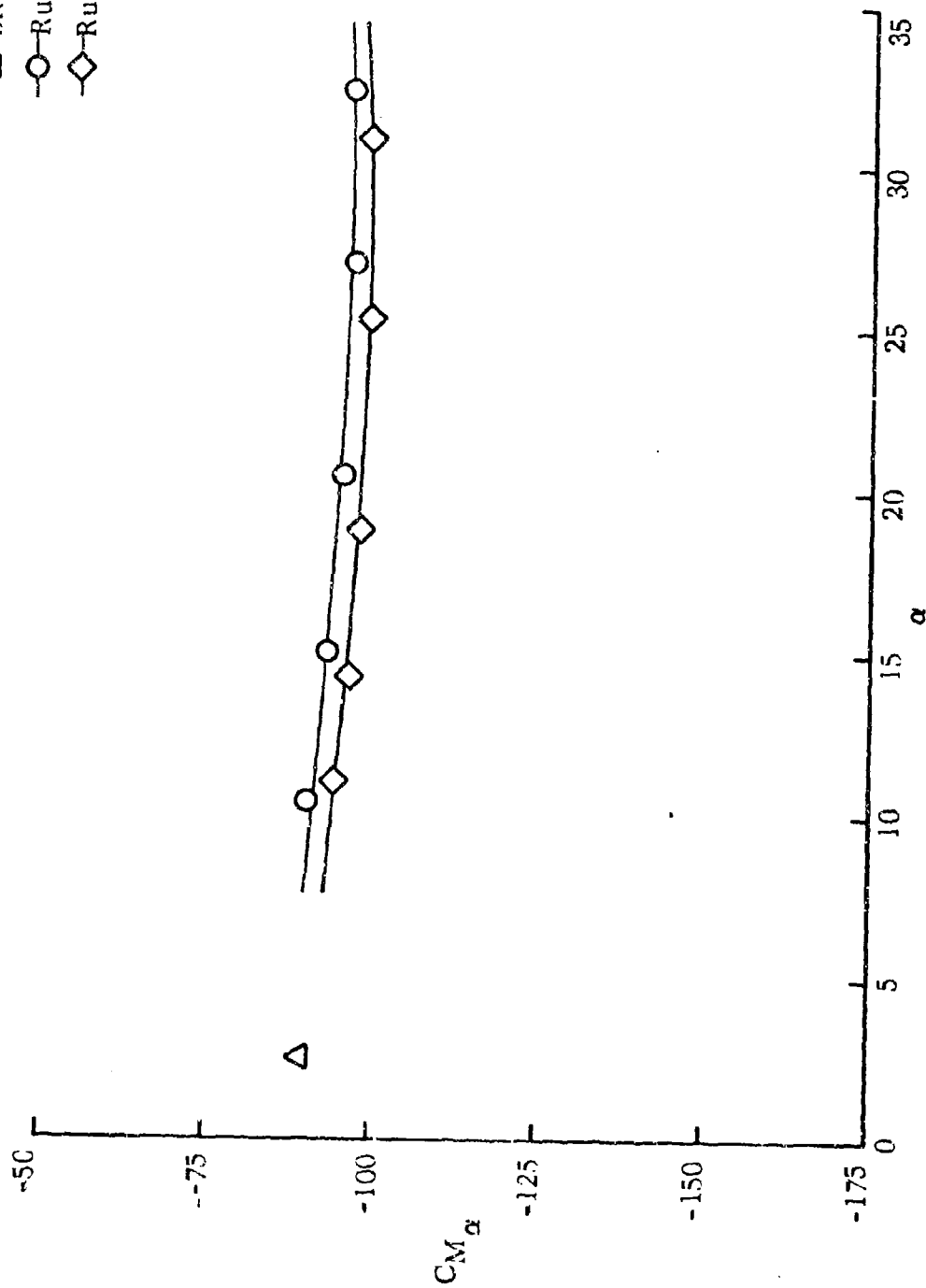


Figure 37.  $C_{M_\alpha}$  vs  $\alpha$  (olin)

$\Delta$  BRL Data  
 $\circ$  Run No. 1  
 $\diamond$  Run No. 2

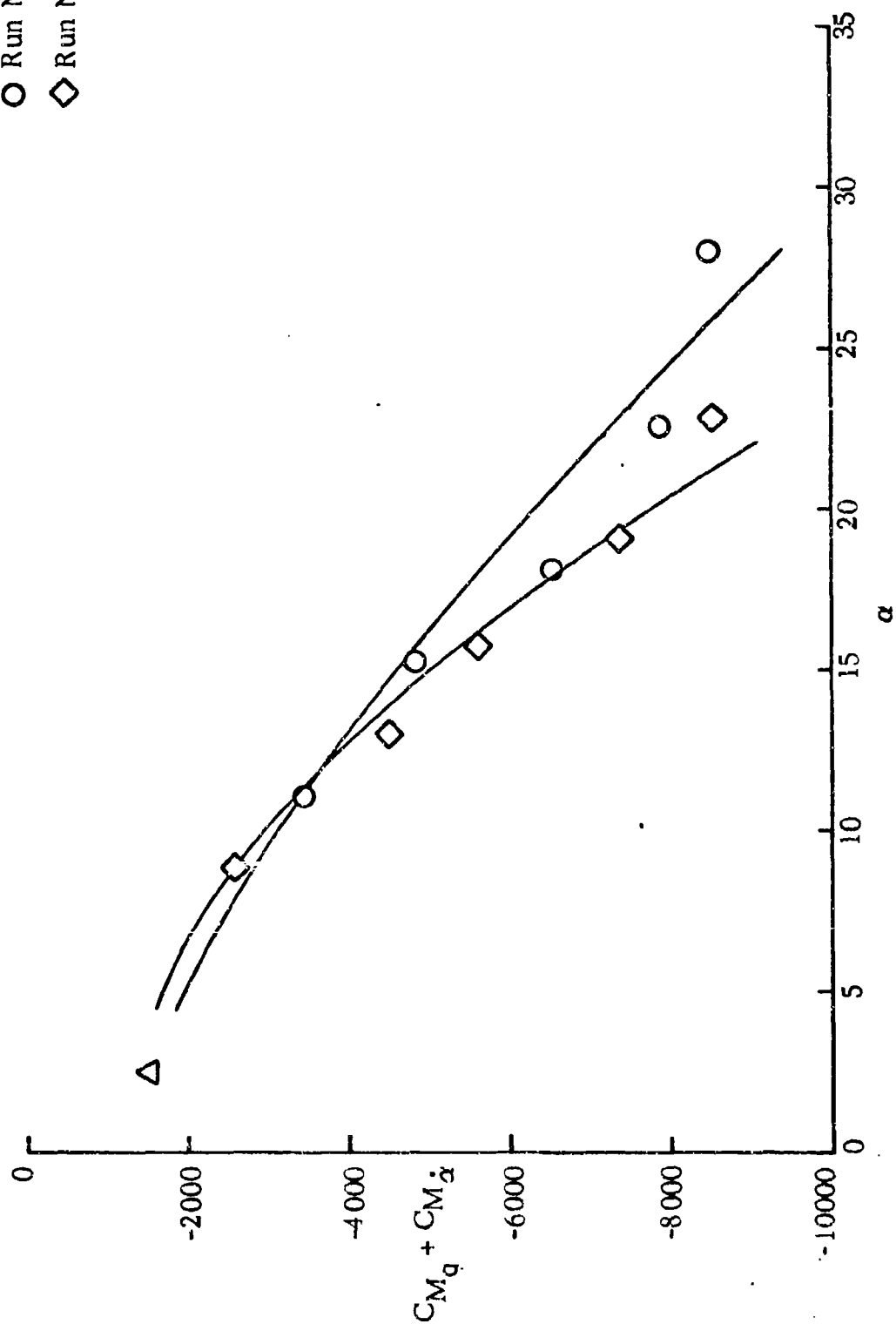


Figure 38.  $C_{M_q} + C_{M_\alpha}$  vs  $\alpha$  (Olin)

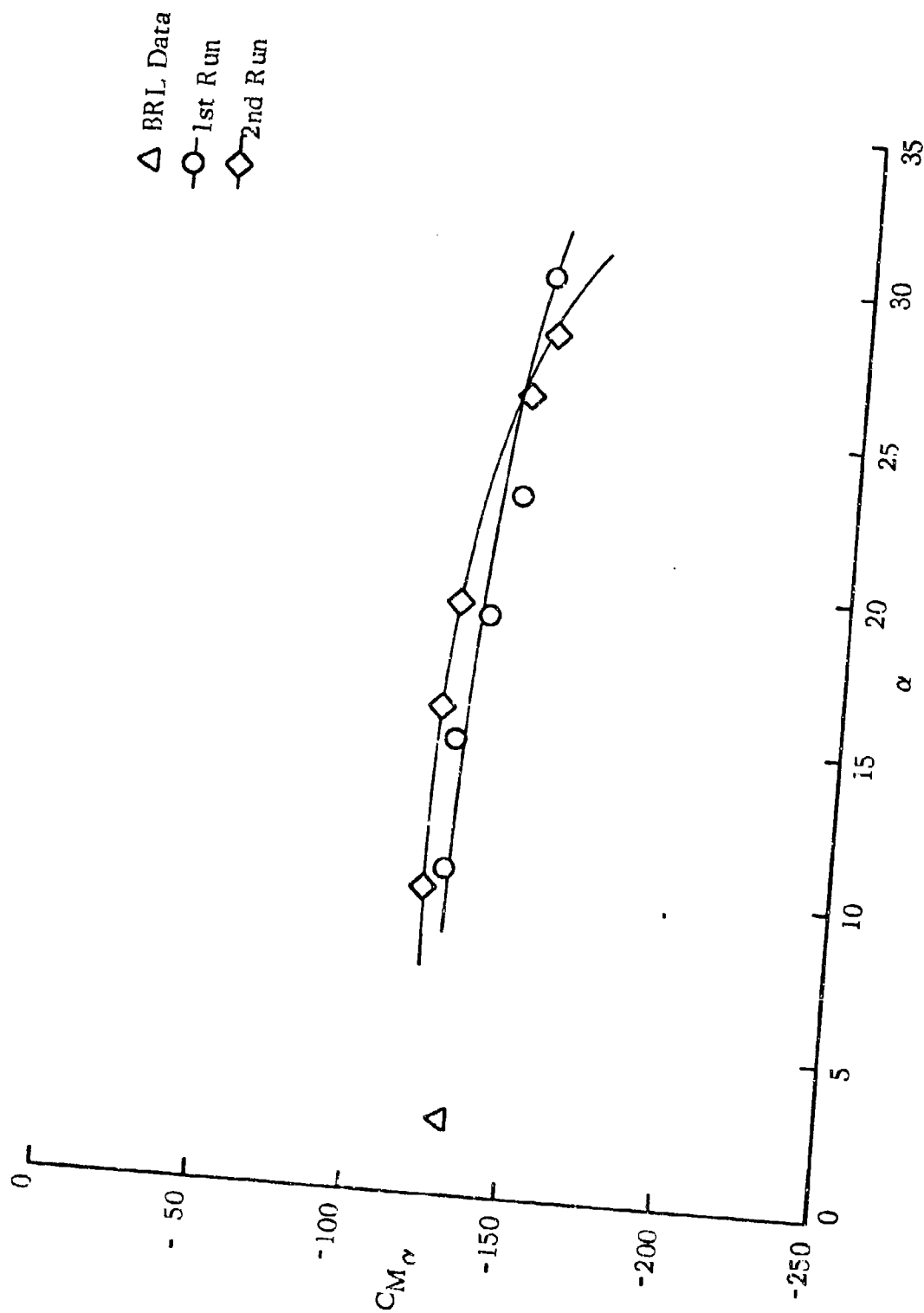


Figure 39.  $C_{M_\alpha}$  vs  $\alpha$  (Swaged Point)

$\Delta$  BRL Data  
 $\circ$  Run No. 1  
 $\diamond$  Run No. 2

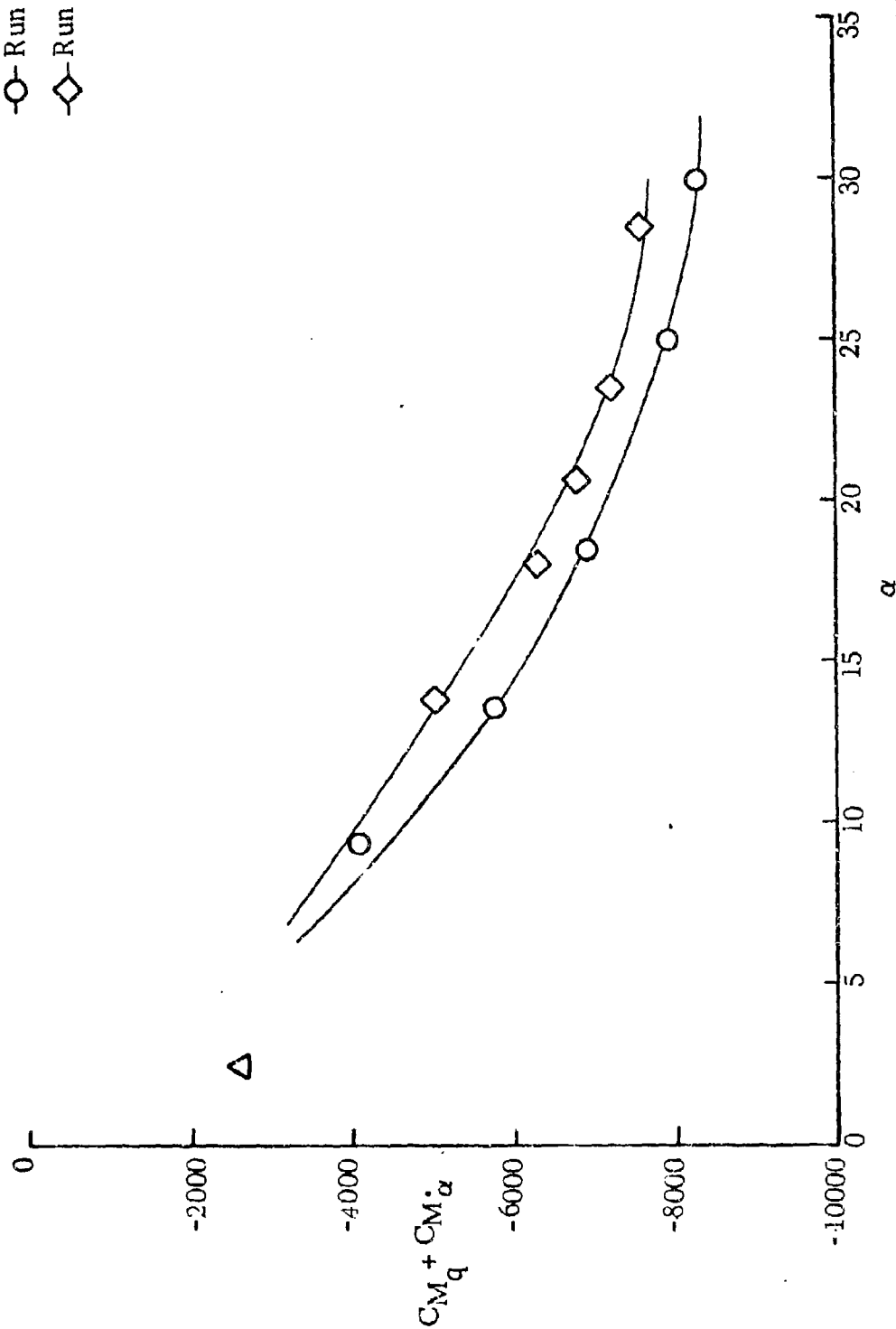


Figure 40.  $C_M + C_{M_\alpha}$  vs  $\alpha$  (Swaged Point)

$\Delta$  BRL Data  
 $\circ$  1st Run  
 $\diamond$  2nd Run

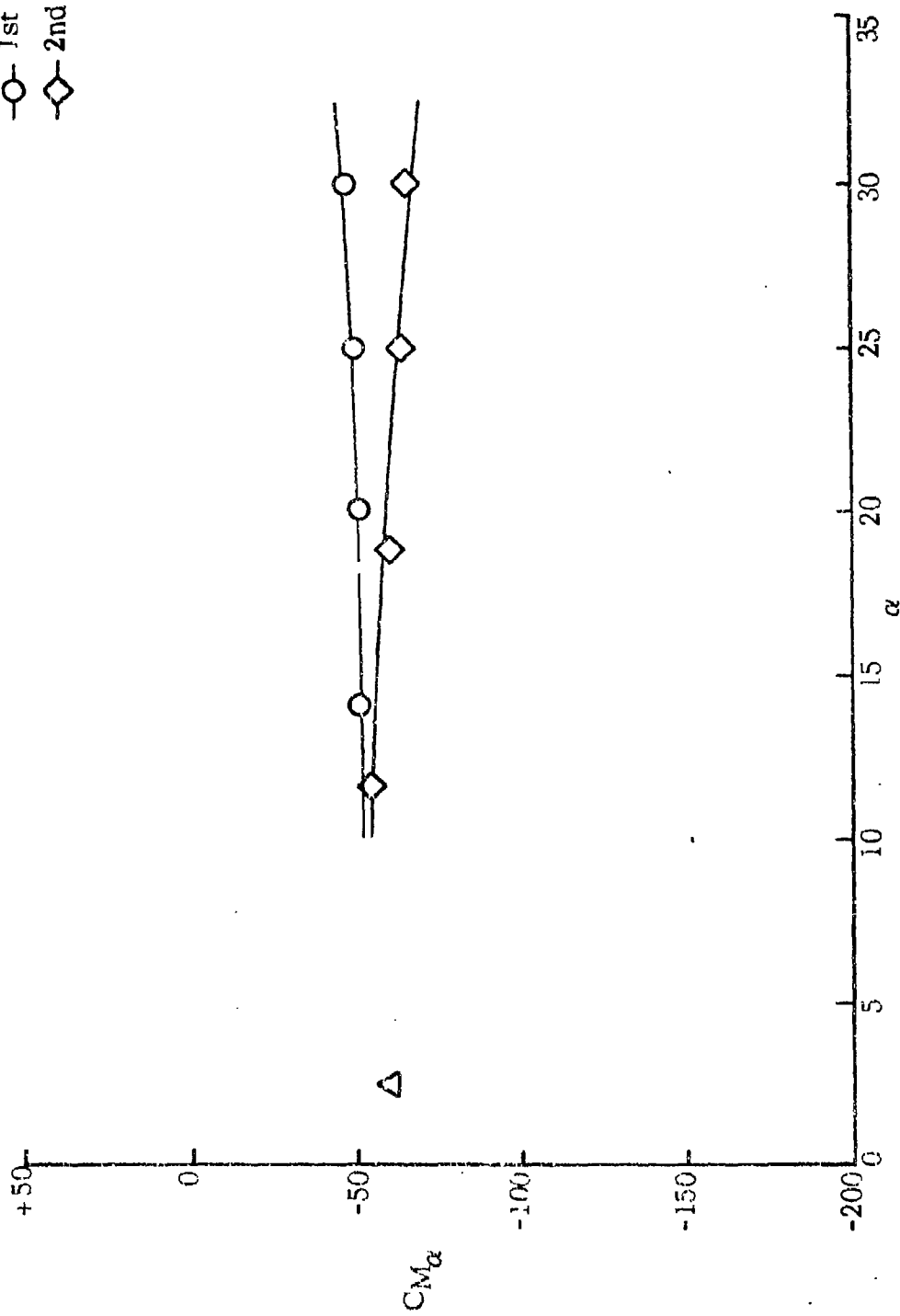


Figure 41.  $C_M$  vs  $\alpha$  (Tracer)

$\Delta$  BRL Data  
 -○- 1st Run  
 -◇- 2nd Run

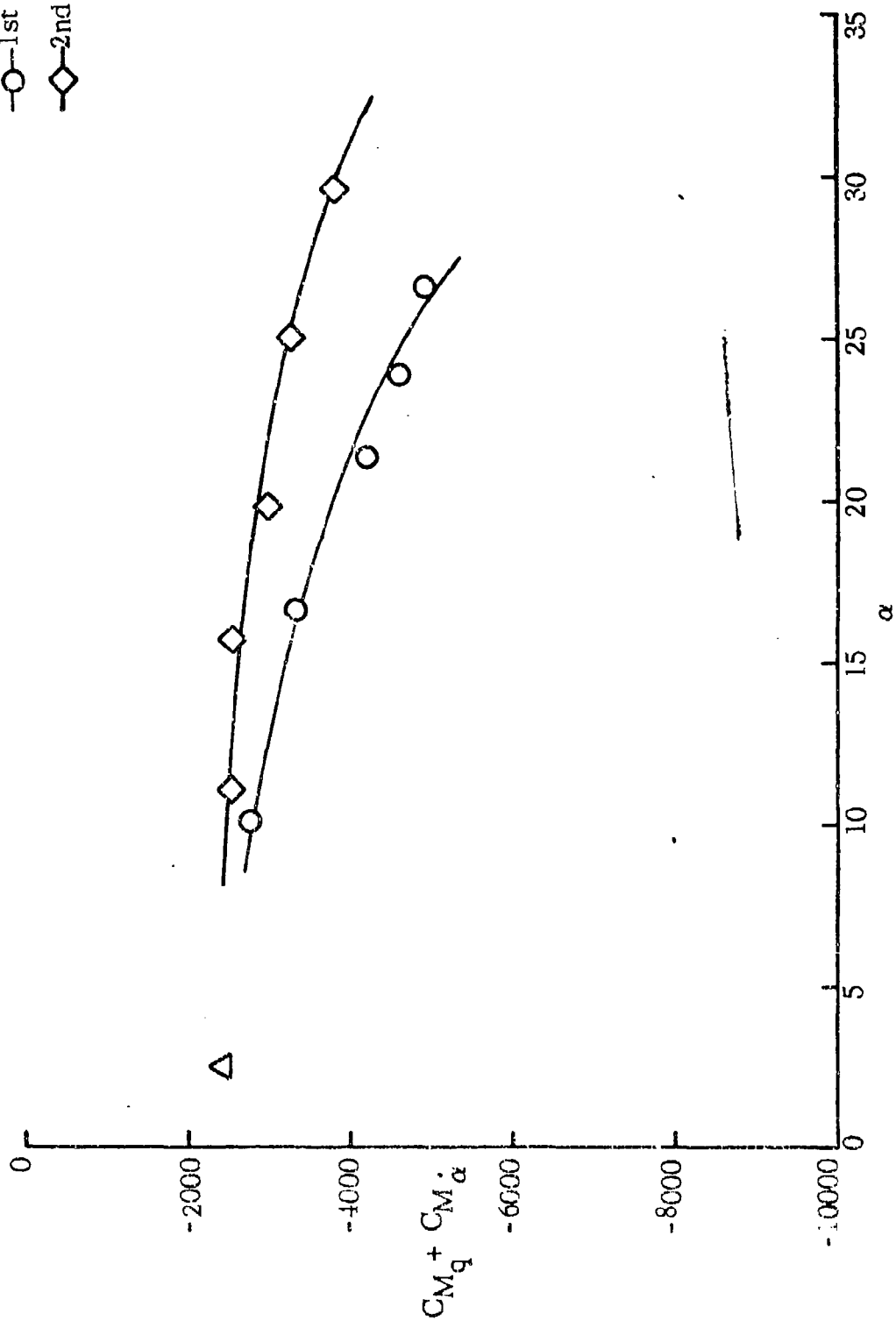


Figure 42.  $C_M + C_{M_\alpha}$  vs  $\alpha$  (Tracer)

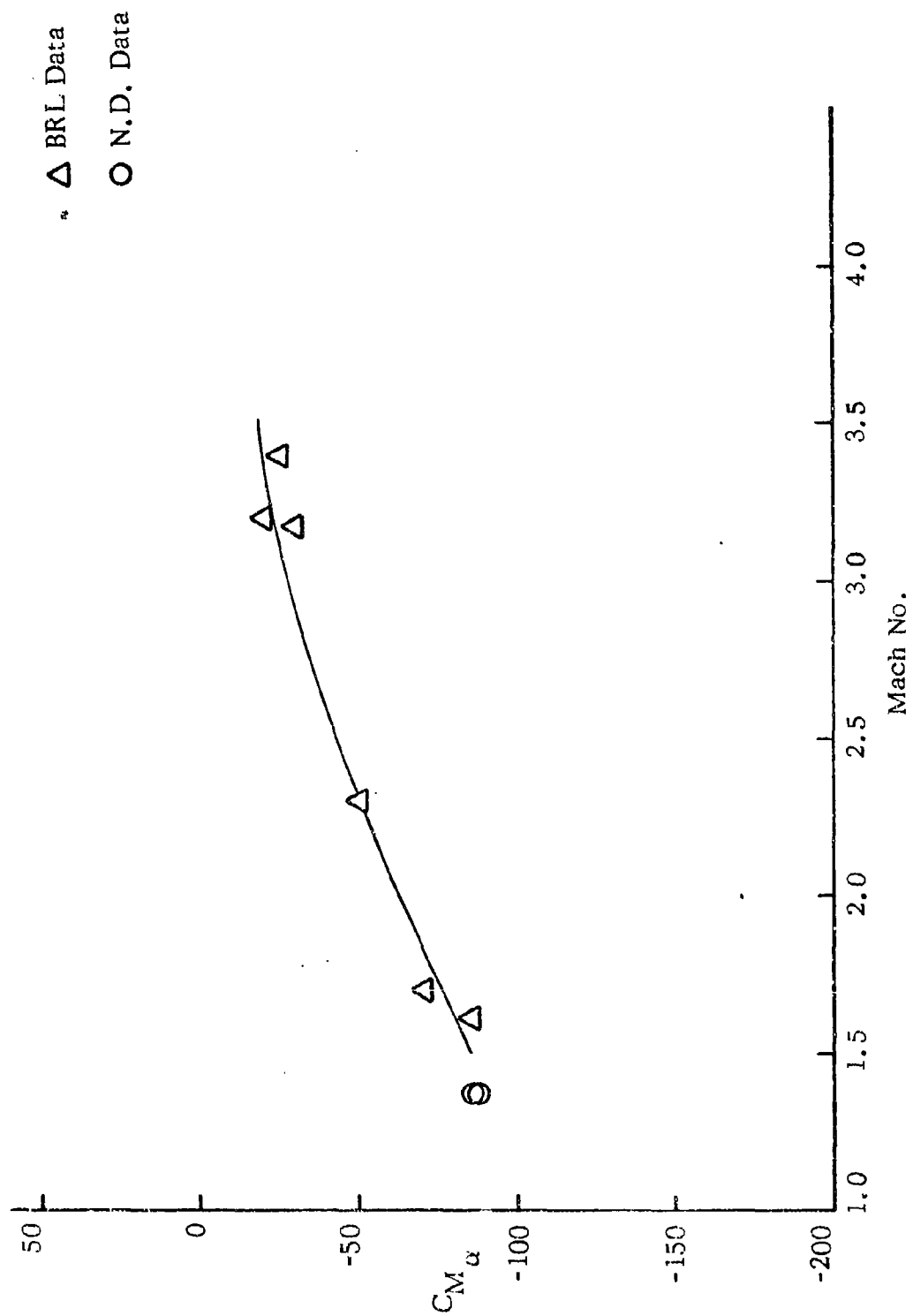


Figure 43.  $C_{M_\alpha}$  vs Mach No. (Olin)

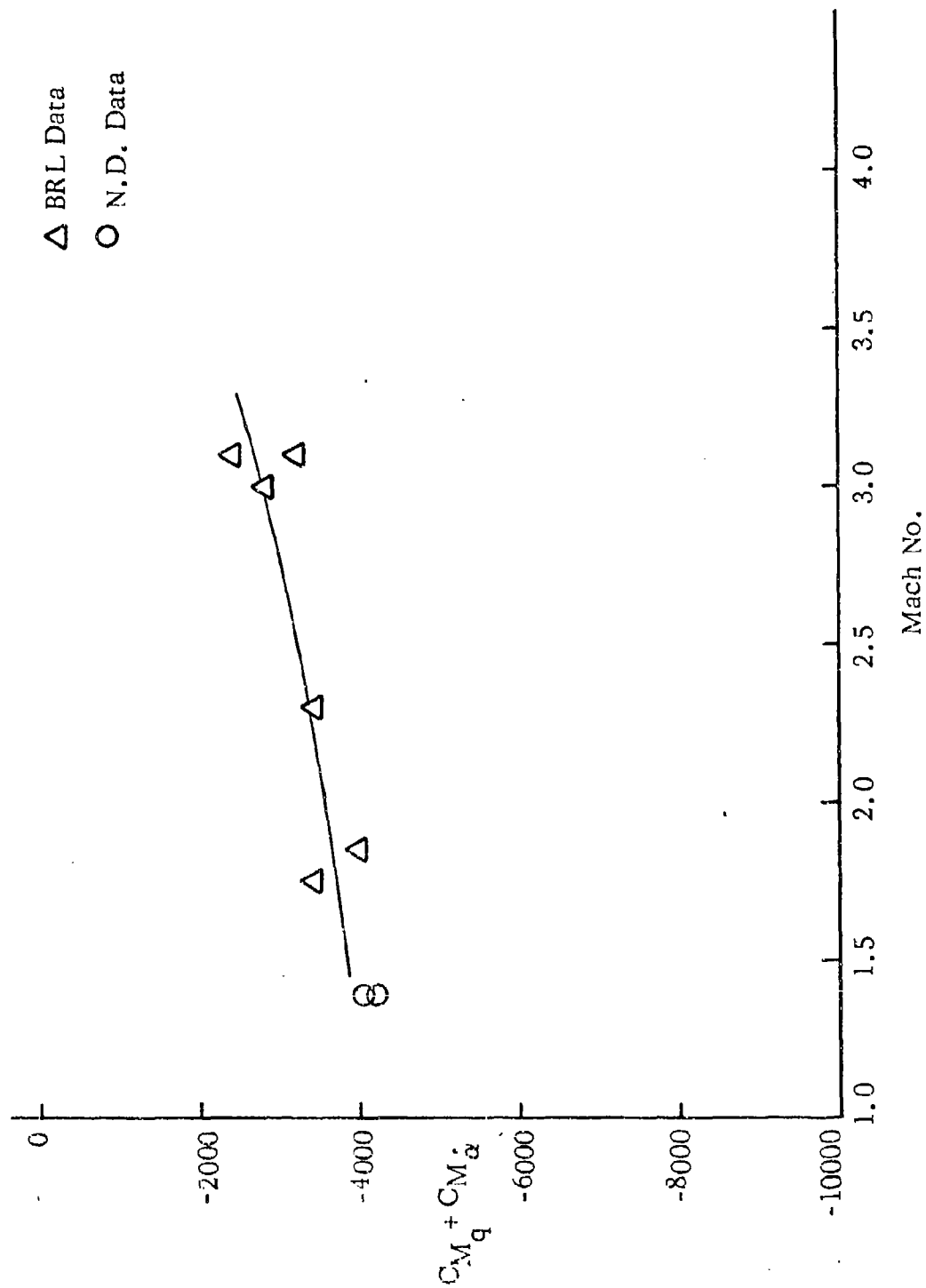


Figure 44.  $(C_{M_q} + C_{M_\alpha})$  vs Mach No. (Ground Point)



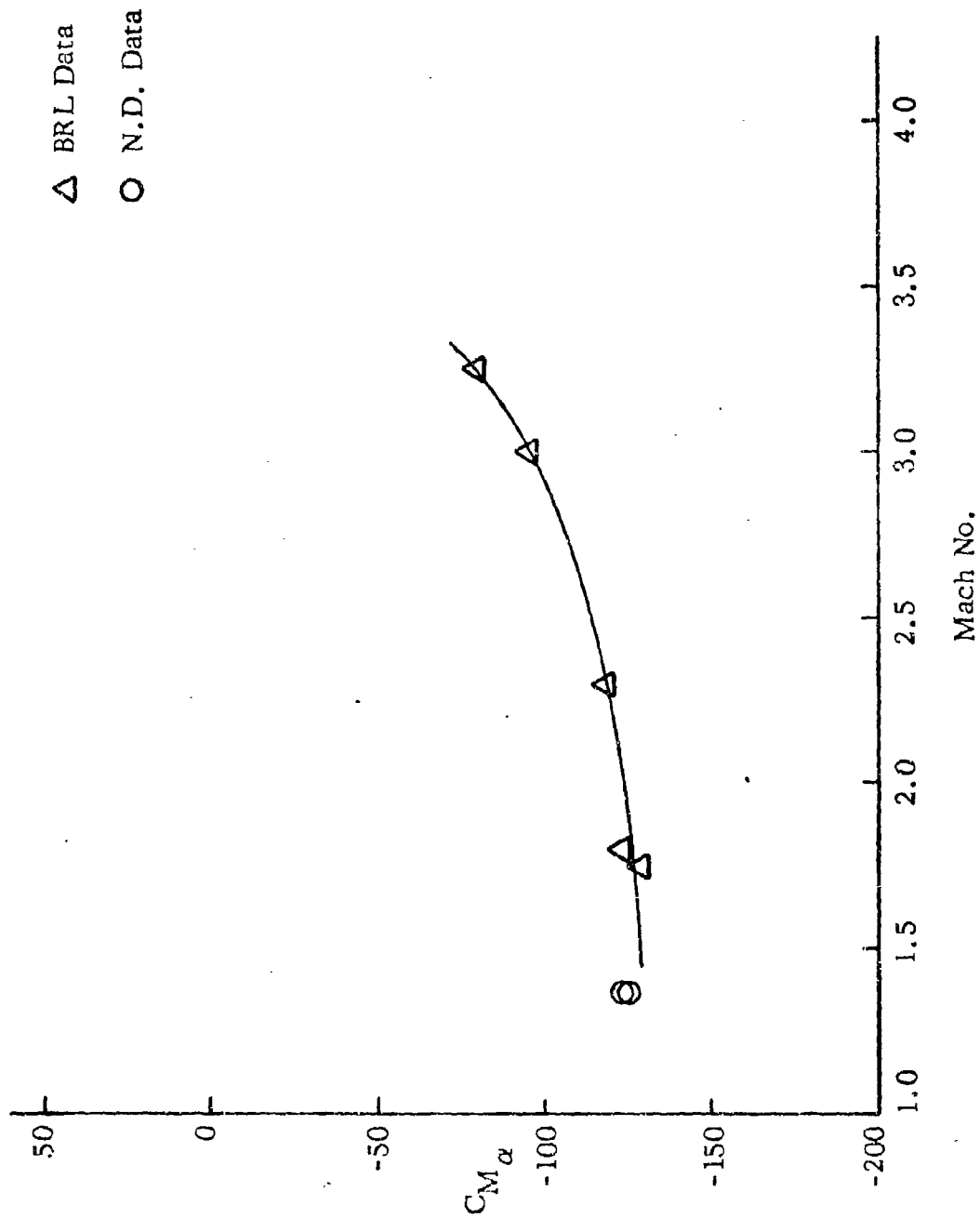


Figure 45.  $C_{M\alpha}$  vs Mach No. (Ground Point)

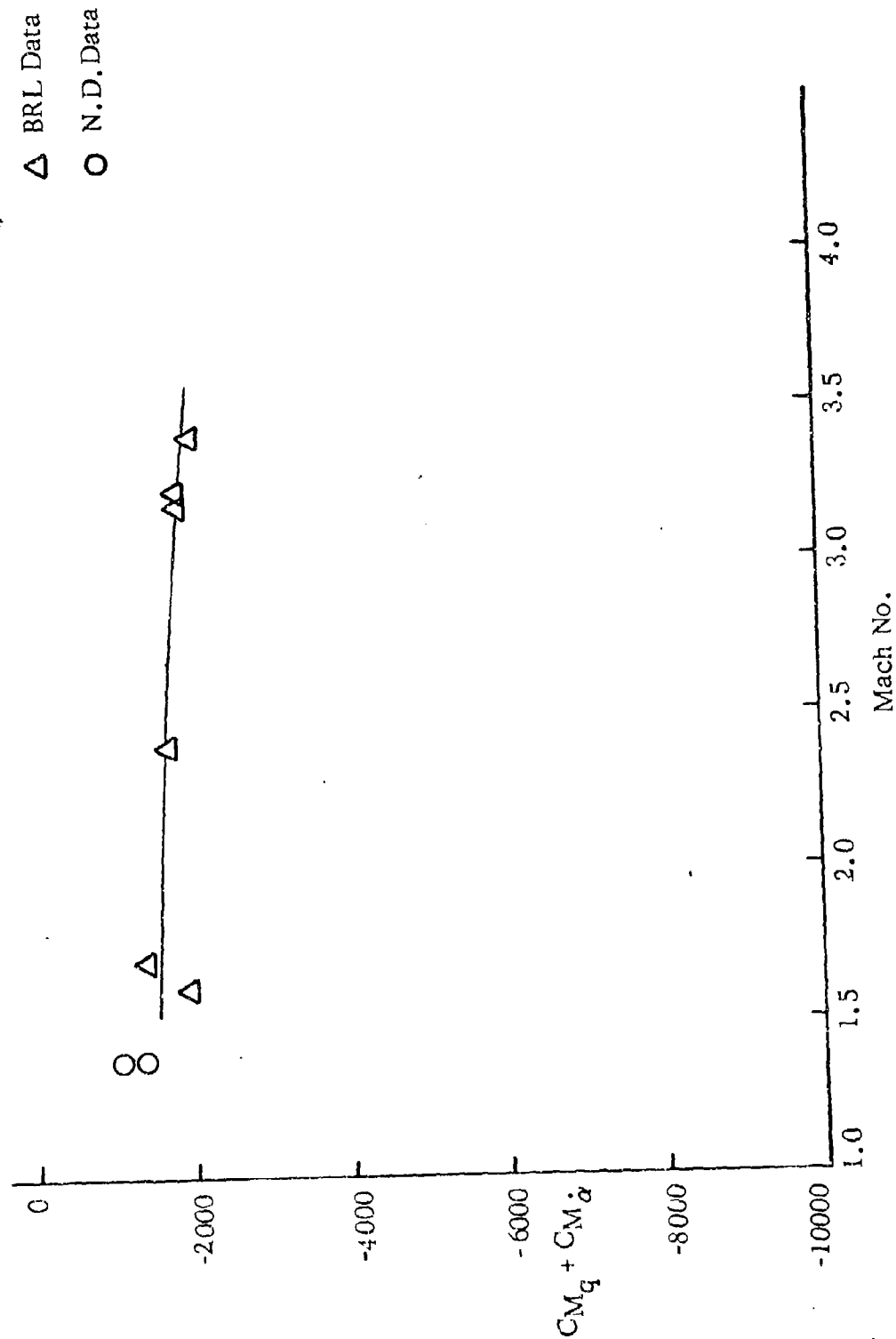


Figure 46.  $CM_q + CM_\alpha$  vs Mach No. (Olin)

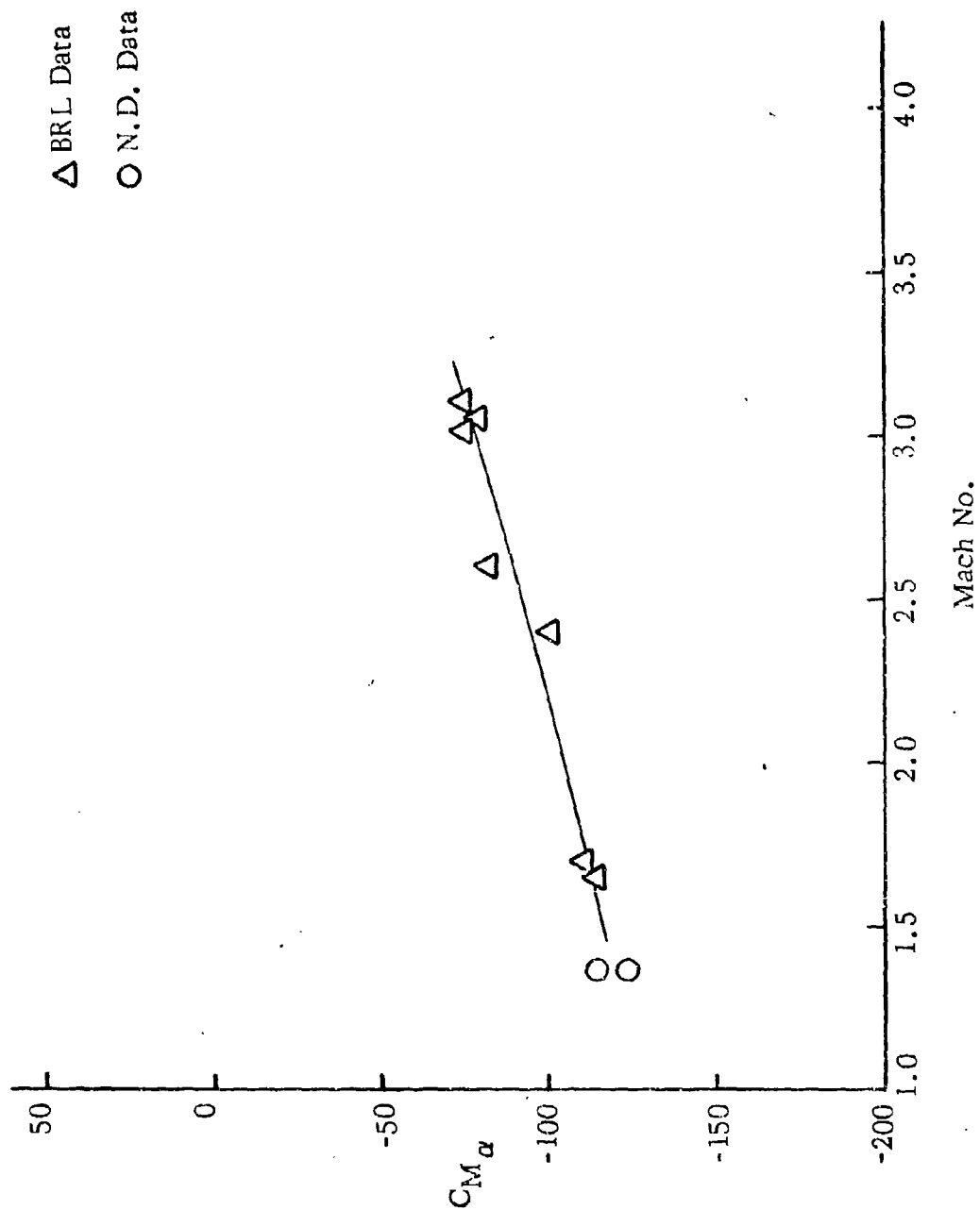


Figure 47.  $C_{M_\alpha}$  vs Mach No. (Swaged Point)

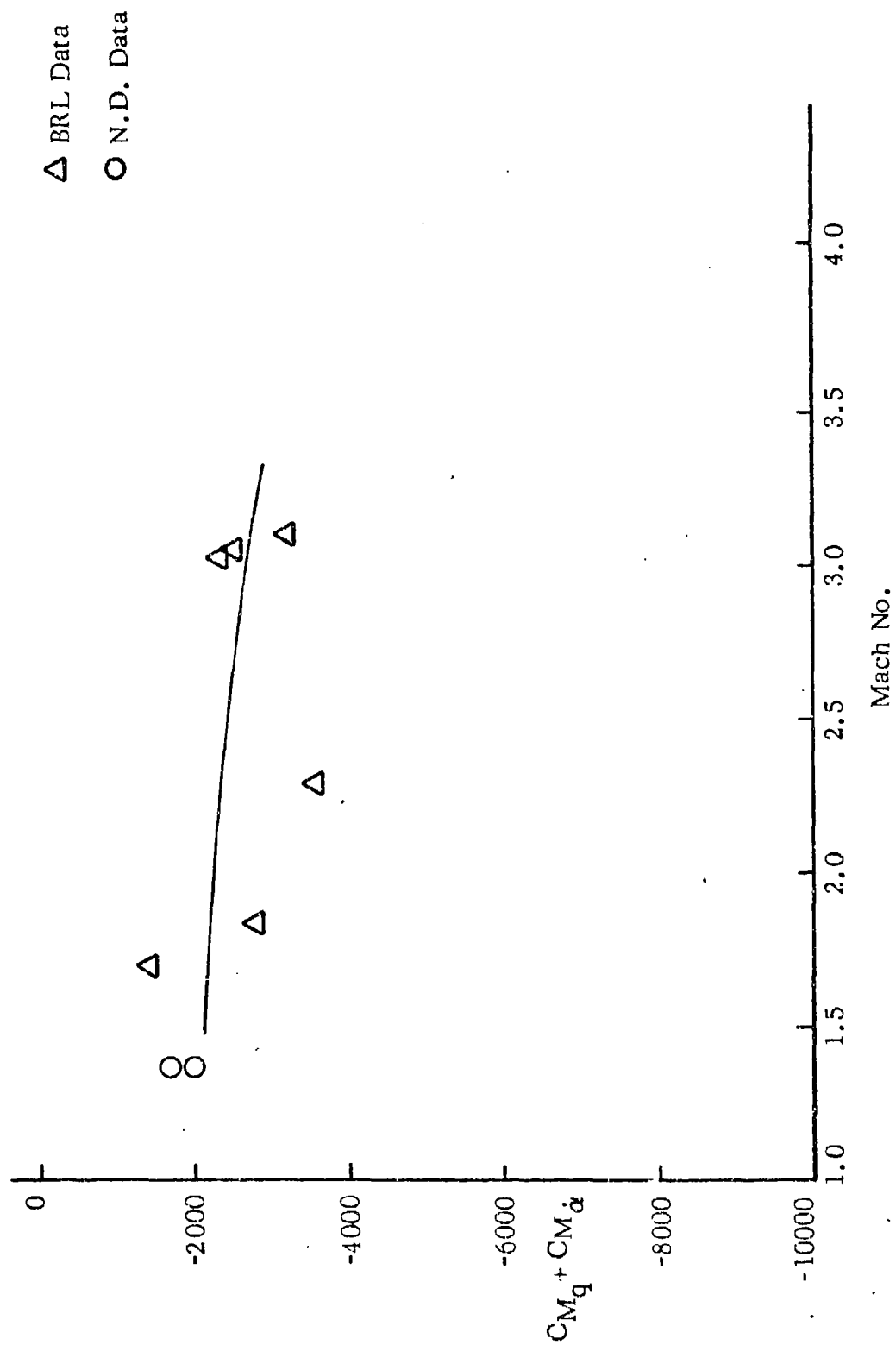


Figure 48.  $(C_{M_q} + C_{M_\alpha})$  vs Mach No. (Swaged Point)

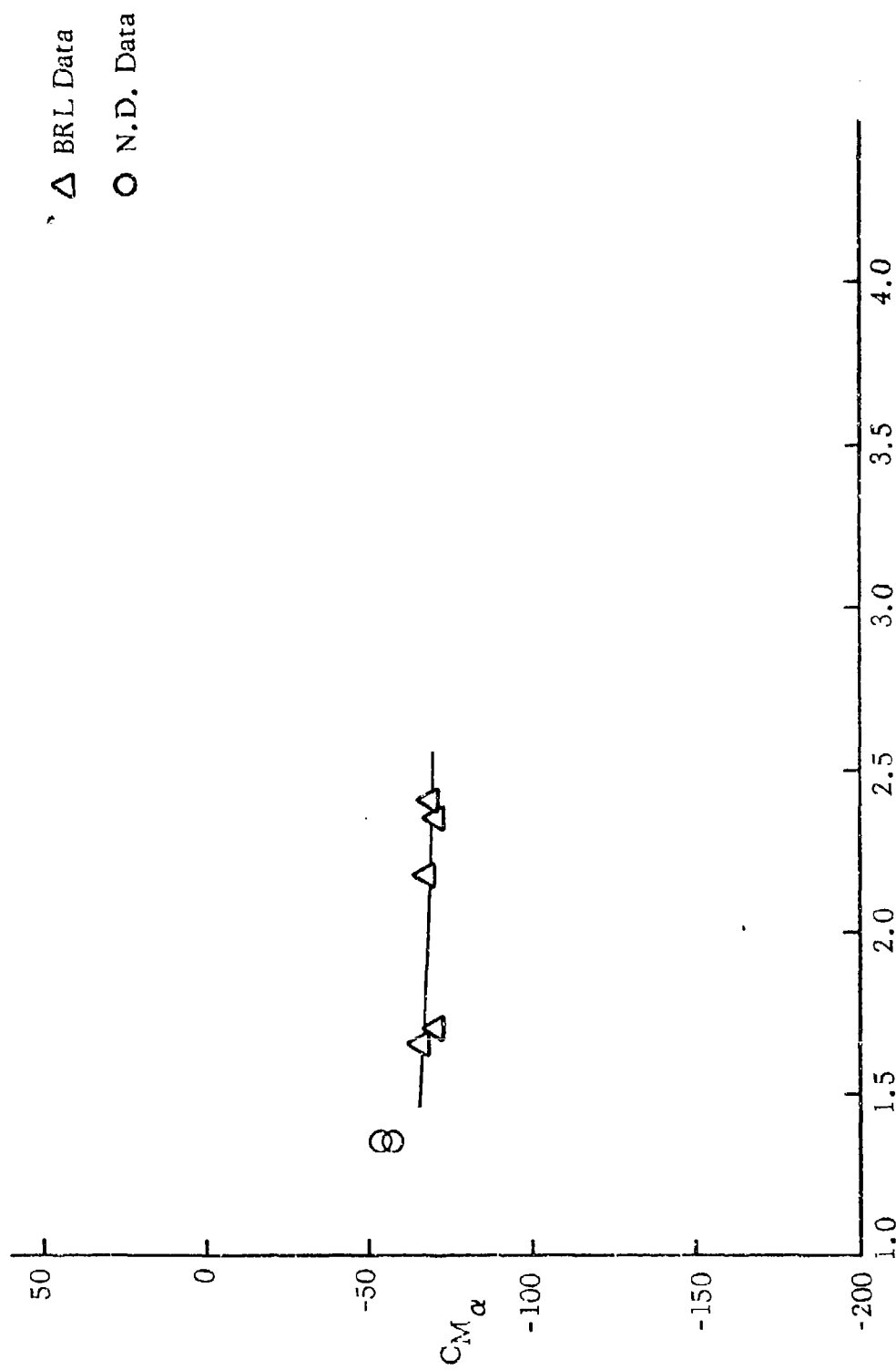


Figure 49.  $C_{M_\alpha}$  vs Mach No. (Tracer)

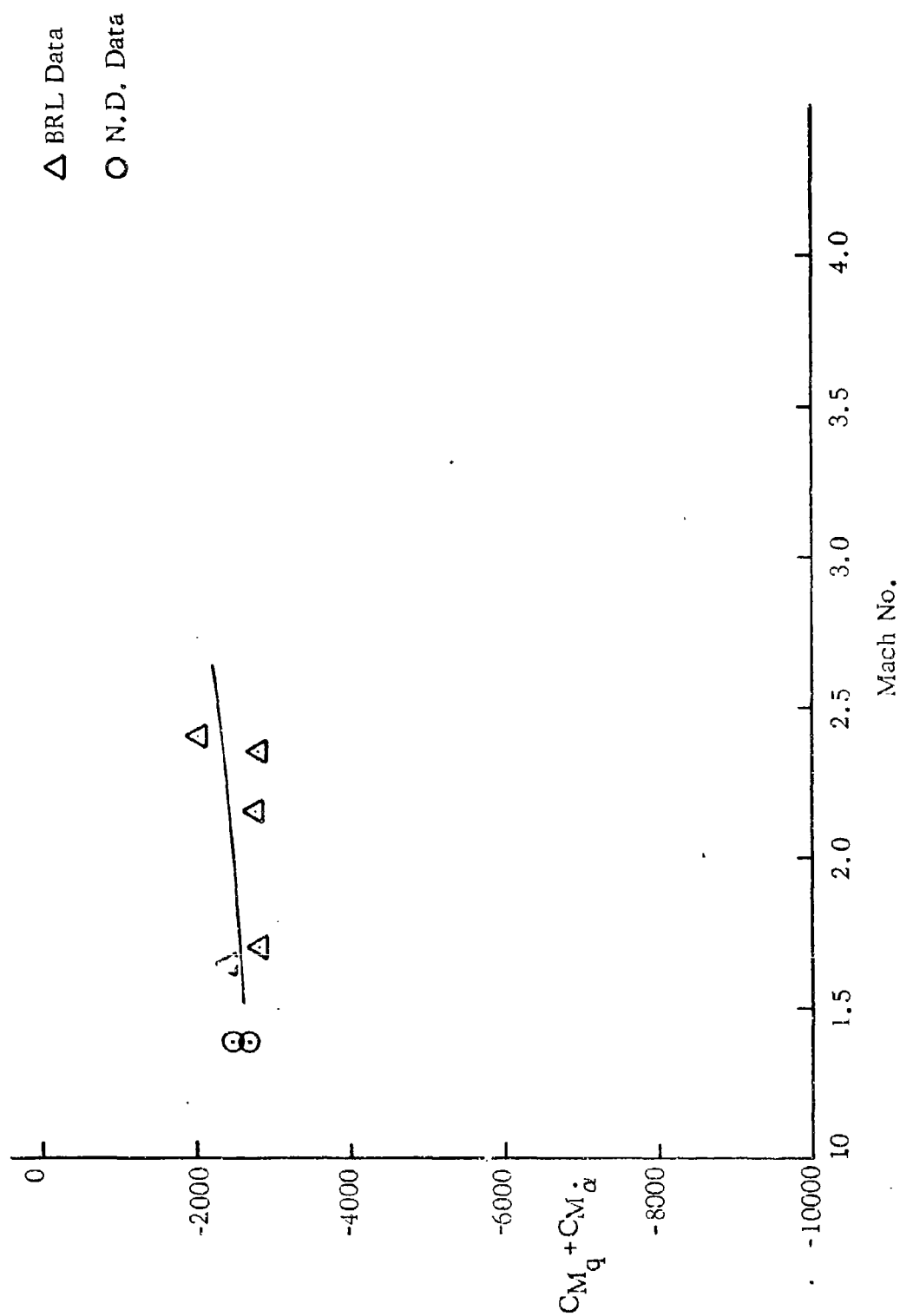


Figure 50.  $(C_{M_q} + C_{M_\alpha})$  vs Mach No. (Tracer)

## CONCLUSIONS

Single-degree-of-freedom dynamic supersonic wind tunnel tests of four flechette configurations has been presented. Linear values of  $C_{M_\alpha}$  and  $(C_{M_q} + C_{M_{\dot{\alpha}}})$  were determined from stability parameters acquired from the data taken during the tests. These values of  $C_{M_{\dot{\alpha}}}$  and  $C_{M_q} + C_{M_{\dot{\alpha}}}$  showed good repeatability and were compared to results from the Ballistics Range Laboratory (BRL) for the same designs at low angles of attack. Over the range of comparison the agreement between the two sets of data was shown to be quite good.

The repeatability of the results was a good indication of the absence of frictional effects and interference effects to the flow which might have been caused by the support system. In Reference 7 it was shown that this excellent one-degree-of-freedom dynamic testing technique can be easily extended to include the determination of nonlinear values of the static pitching and damping stability coefficients. Also, because the model is suspended at its center of gravity, there is no reason why this technique could not be moved into a horizontal supersonic wind tunnel if necessary.

## APPENDIX A

### MODEL PARAMETERS

#### Grount Point

Diameter = .012 ft.  
 $I_y = .000004647 \text{ slugs-ft}^2$   
Mass = .0003647 slugs  
Radius = 1.69 in.

#### Olin

Diameter = .0119 ft.  
Mass = .000303 slugs  
 $I_y = .000007040 \text{ slug-ft}^2$   
Radius = 1.52 in.

#### Tracer

Diameter = .01533 ft.  
Mass = .0004520 slugs  
 $I_y = .0000105570 \text{ slugs-ft}^2$   
Radius = 2.11 in.

#### Swaged Point

Diameter = .012 ft  
Mass = .0003933 slugs  
 $I_y = .000006041 \text{ slugs-ft}^2$   
Radius = 1.69 in.



## APPENDIX B

### SUPERSONIC WIND TUNNEL OPERATING PROCEDURE

#### Starting Procedure

1. Open valve to compressor manifold for wind tunnel to be used - make sure that the other wind tunnels are either shut off or blocked from the manifold.
2. Inform University Power Plant of intention to run compressors.
3. Turn cooling water on (one valve near wall inside laboratory).
4. Turn each compressor shaft to make sure they are free to rotate.
5. Check oil level for each compressor (oil level should be above gear).
6. Check oil pump for each compressor i.e. depress six plungers and observe oil bubbles.
7. Add a few squirts of No. 51 oil to hole in top of shaft bushing.
8. Check mercury manometer tubing in compressor room to make sure it is connected.
9. Turn master power switch on for each compressor.
10. Start one compressor - allow at least one minute after compressor comes up to speed before starting the second compressor and allow another one minute after this compressor comes up to speed before starting third compressor.
11. If mercury manometer reads more than 18 inches, Shut Down Immediately.

### Shut Down Procedure

1. Shut compressors off one at a time at one minute intervals.
2. Turn master power switch off for each compressor.
3. Shut compressor cooling water off.
4. Inform University Power Plant that compressors have been shut off.

## APPENDIX C

### ONE-DEGREE-OF-FREEDOM TEST RESULTS ON R&D FLECHETTES

The model\* was initially disturbed to an angle of attack of approximately  $180^\circ$  and then allowed to oscillate freely. The resulting angular motions were then recorded by a high speed camera technique.

#### One-Degree-of-Freedom Data Reduction

The "Wobble" computer program was used to fit the one-degree-of-freedom Aeroballistic Theory to the angular oscillations obtained from the moving camera technique. This data was fitted in segments of 2.2 cycles with each segment containing approximately 25 points. The stability parameters  $K_1$ ,  $K_T$ ,  $\lambda_1$ ,  $\omega_1$ , were determined by the Wobble program at a time interval of 0.015 seconds. The average percent error of the theory to the data showed an error of less than 3%. A representative plot of probable error of fit vs time is shown in Fig. 1a.

The stability parameters were obtained from the fits as functions of time, representative angular oscillations, probable errors of fit, and stability parameters are presented in Figs. 2 through 6. The resulting stability coefficients versus time are presented in Figs. 7 and 8.

#### One-Degree-of-Freedom Nonlinear Stability Coefficients

To get an indication of the nonlinearity of the stability coefficients

---

\*Figure 1.

(All dimensions in inches)

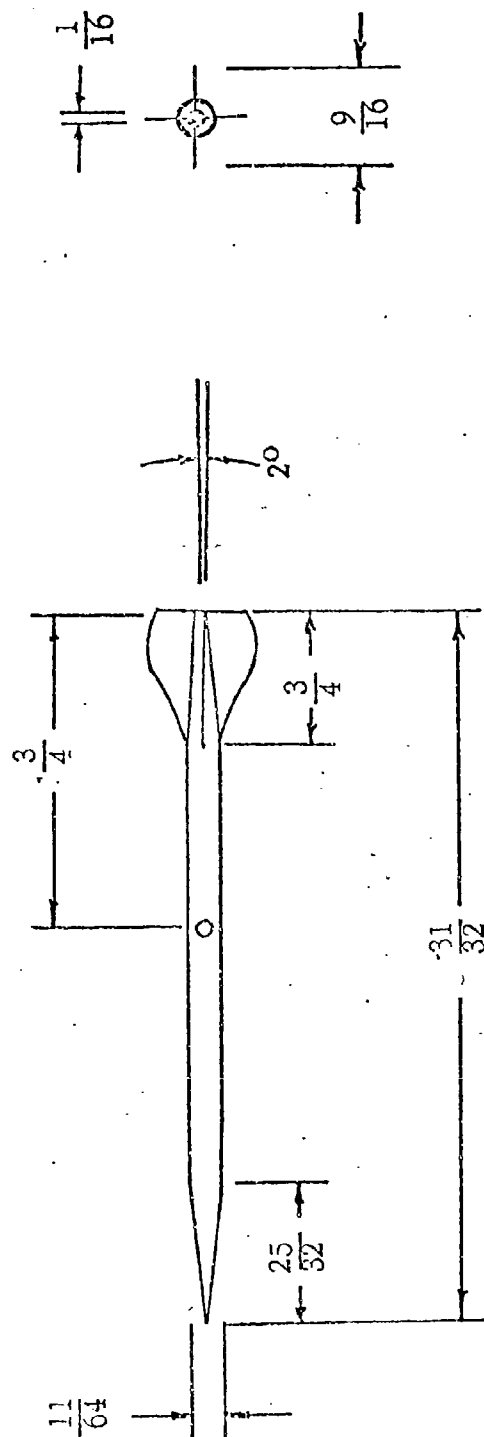


Figure 1. Schematic 1-D Pitch Model

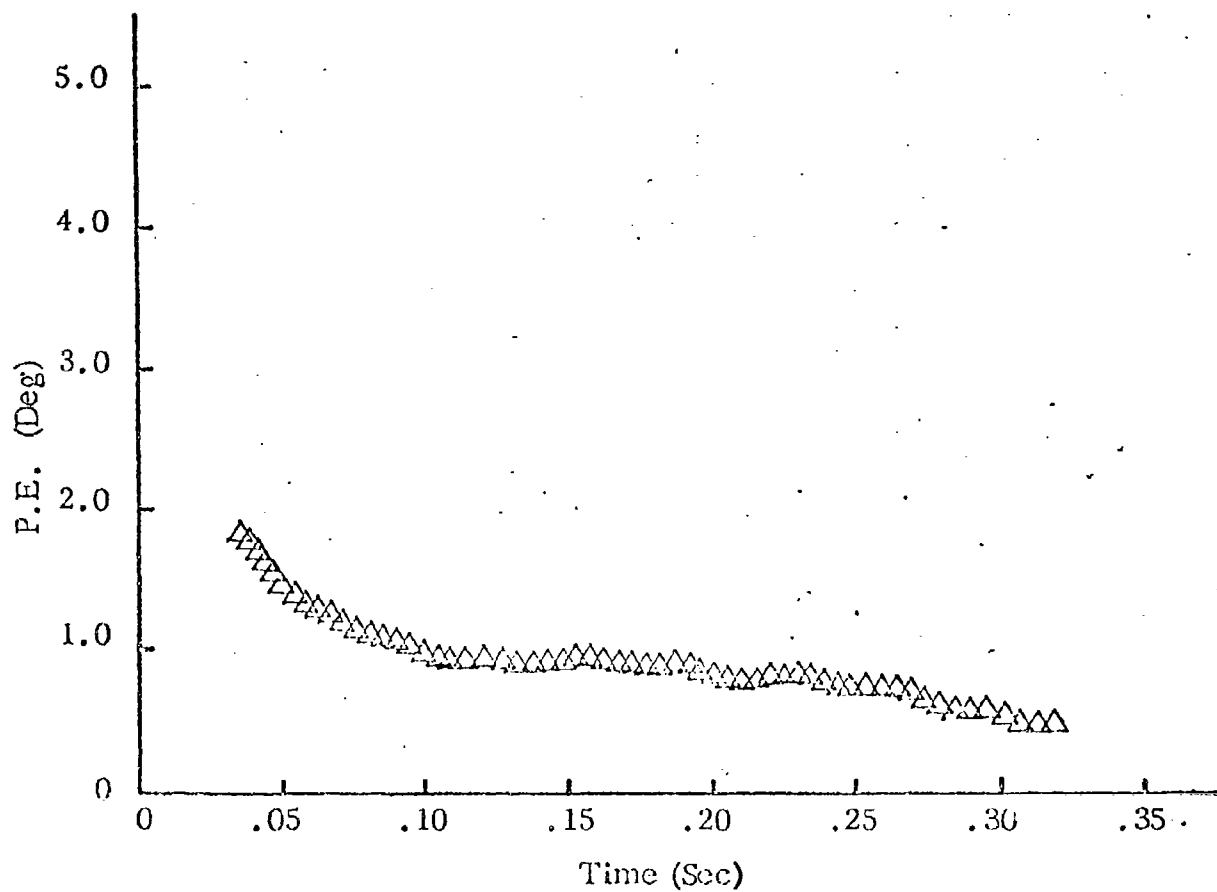


Figure 1a. Probable Error of Fit vs Time

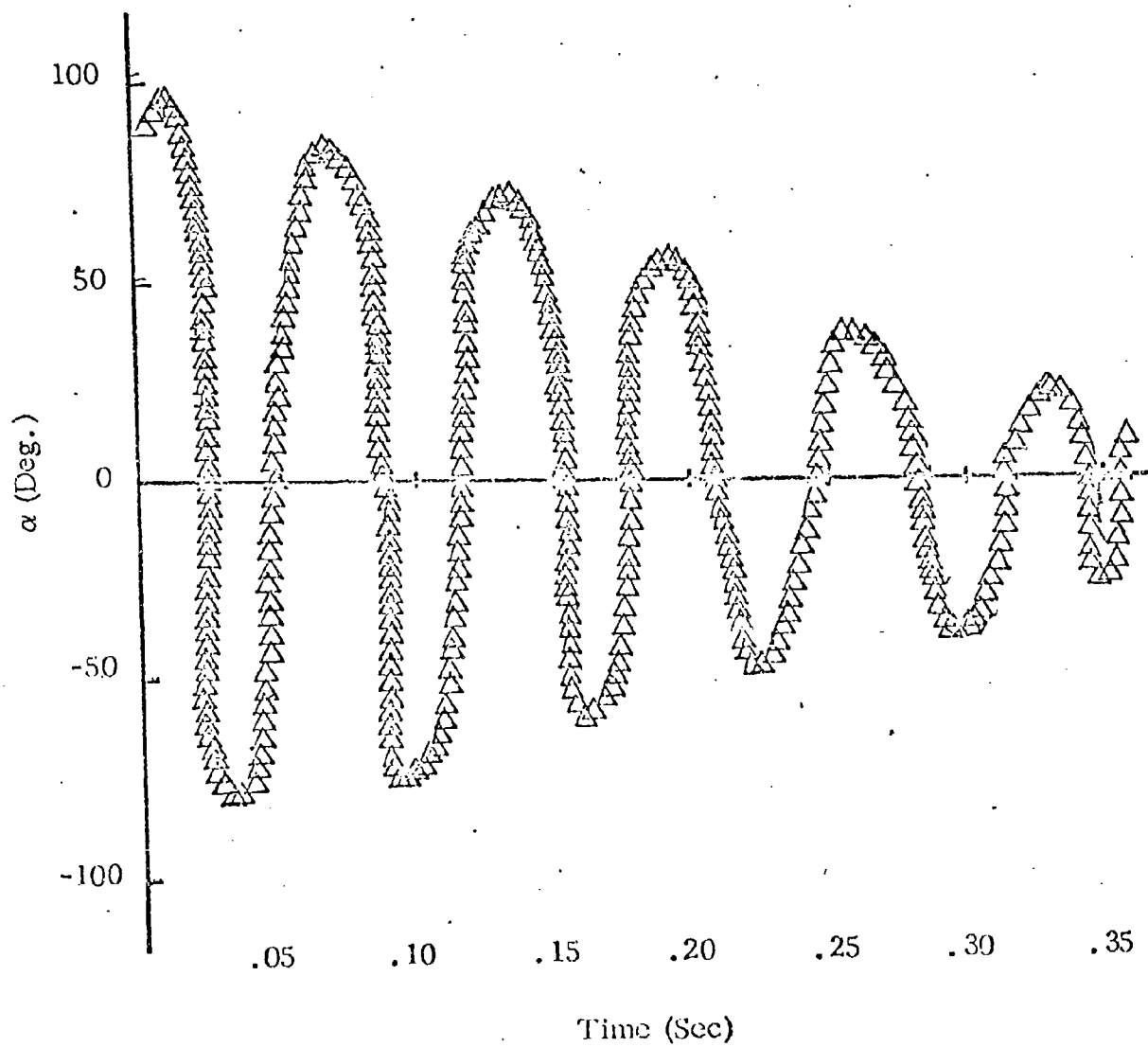


Figure 2. 1-D Oscillatory Motion

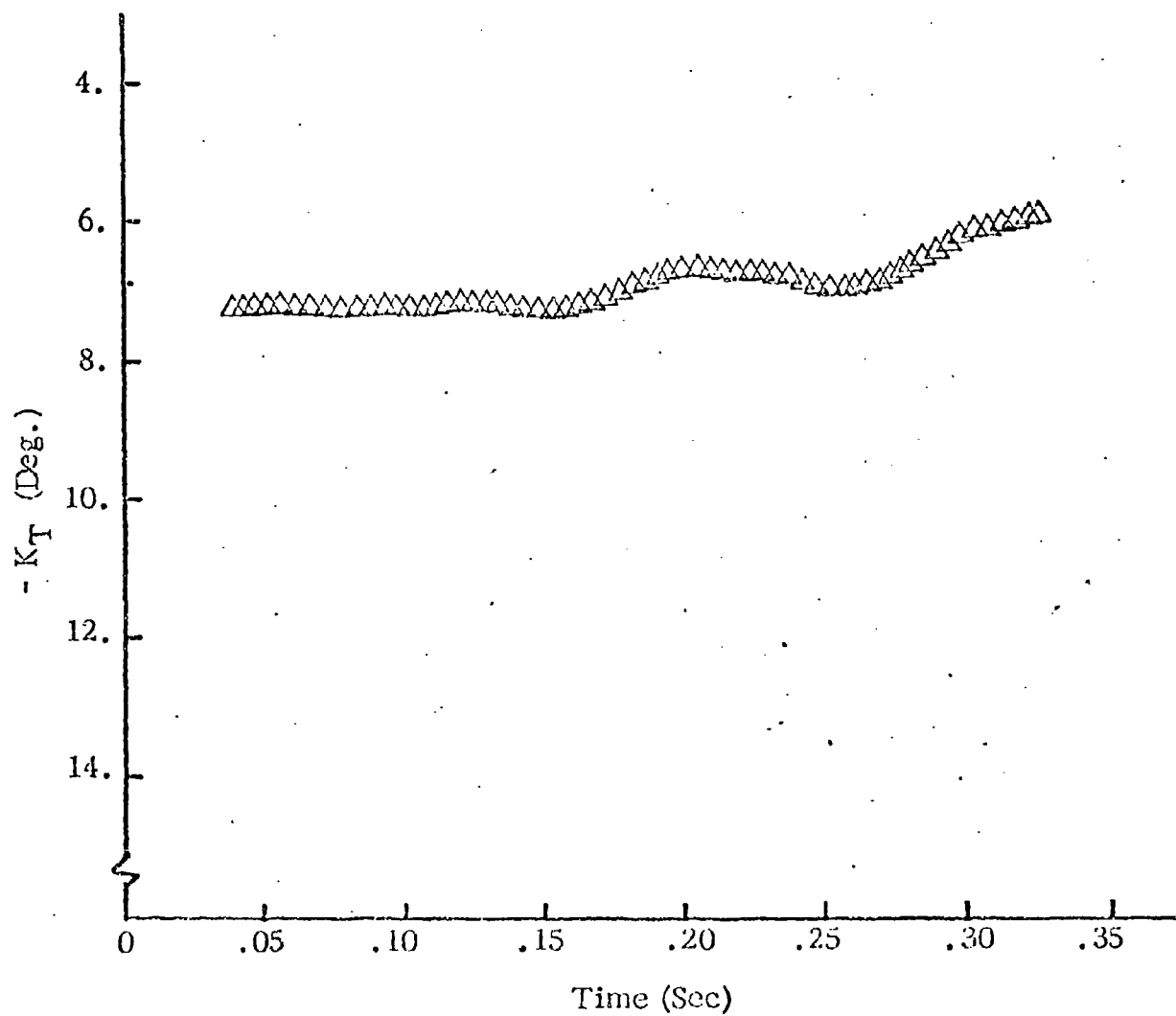


Figure 3. Trim Mode vs Time

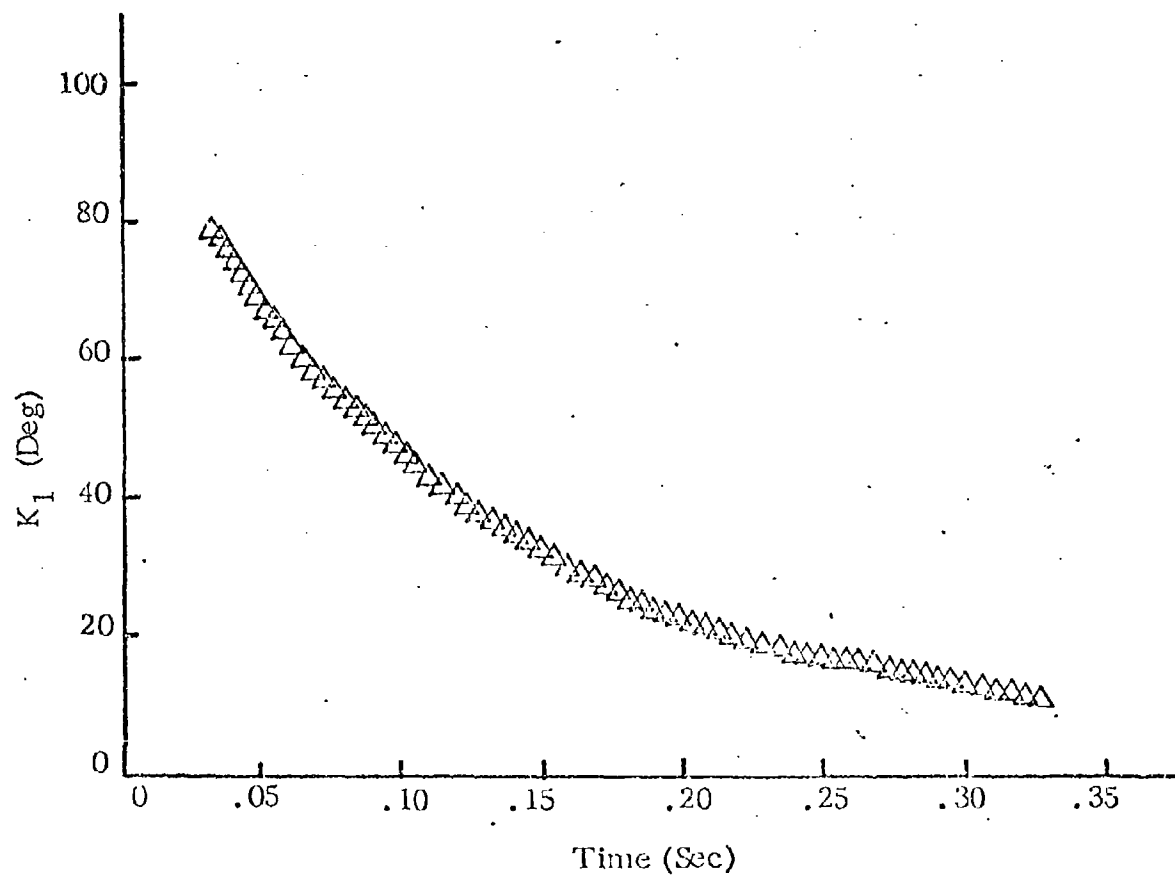


Figure 4.  $K_1$  vs Time



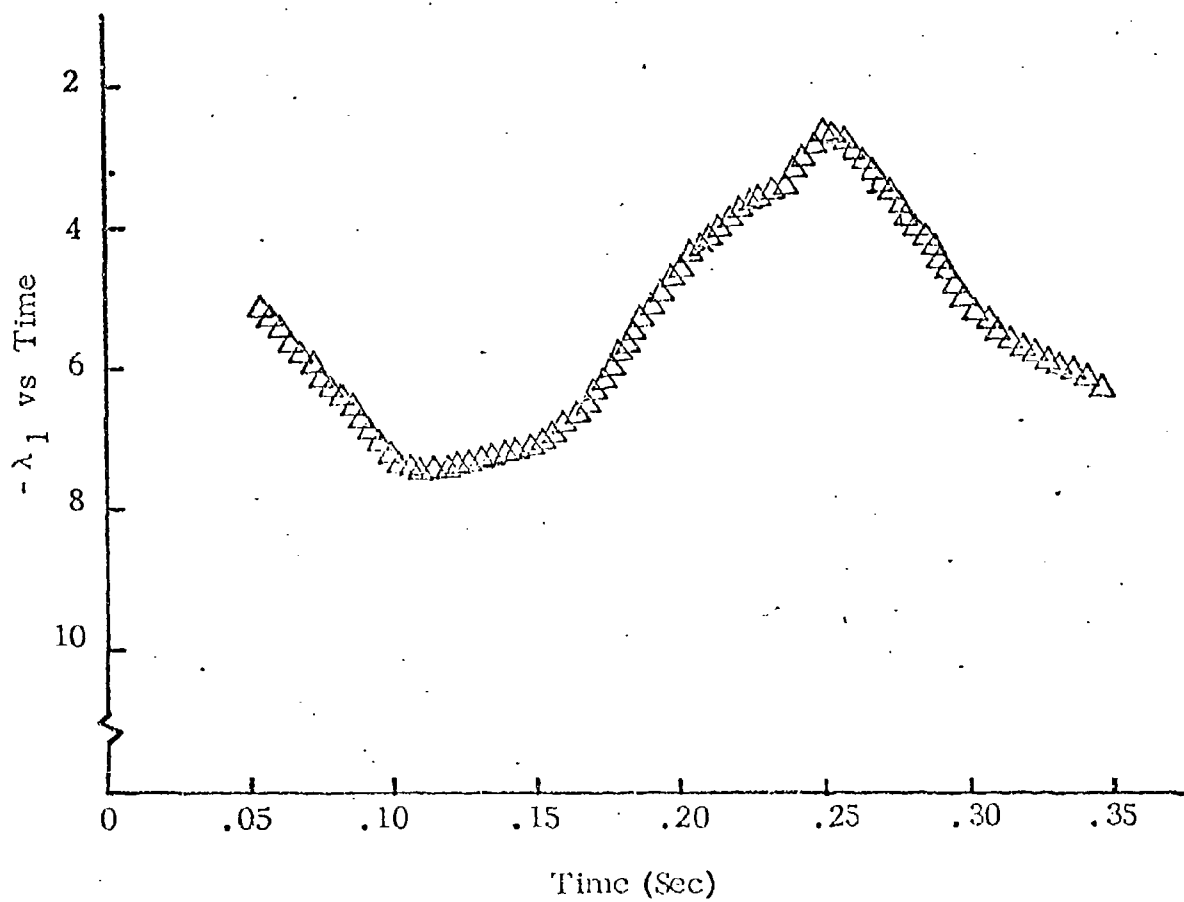


Figure 5.  $\lambda_1$  vs Time

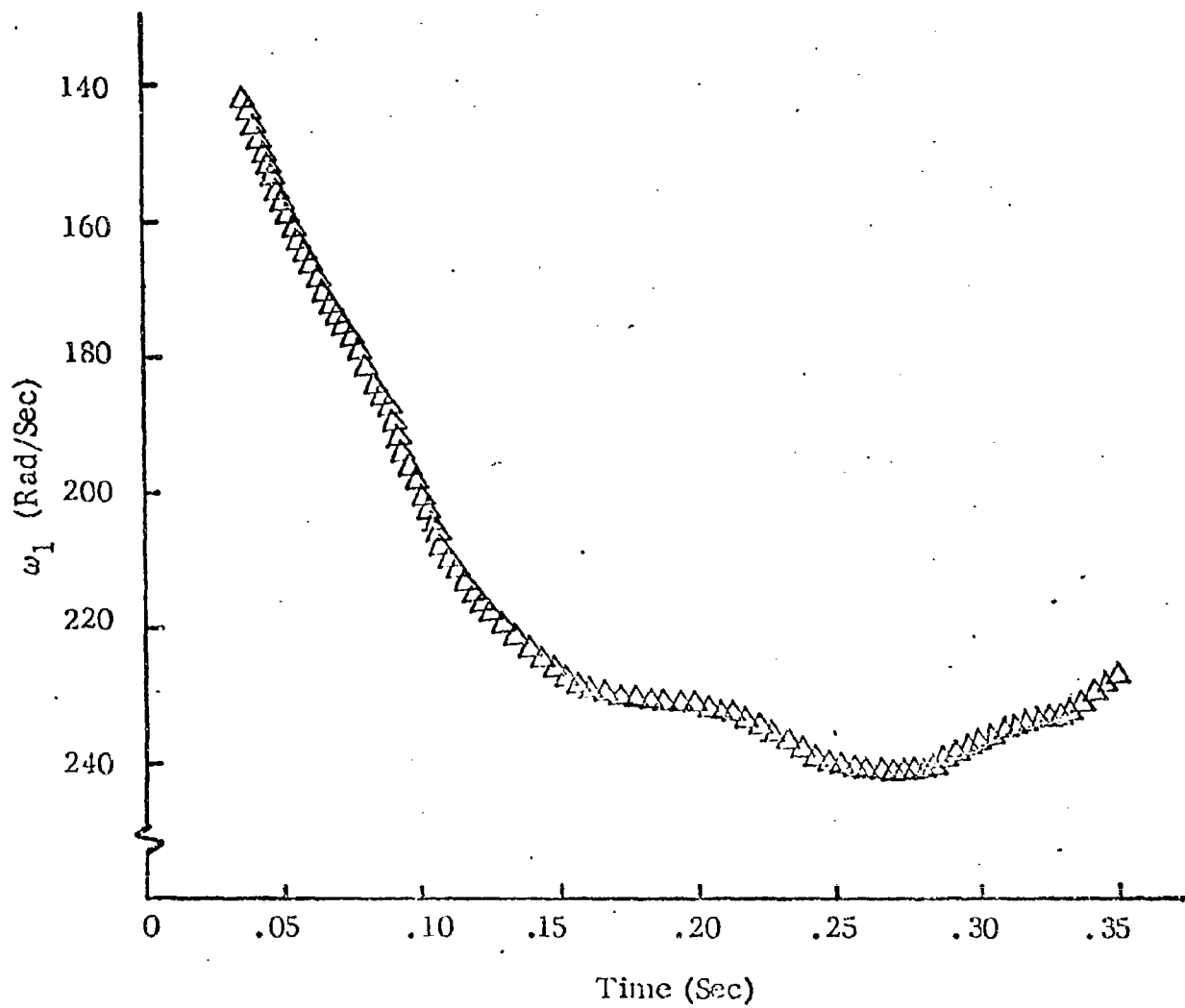


Figure 6.  $\omega_1$  vs Time

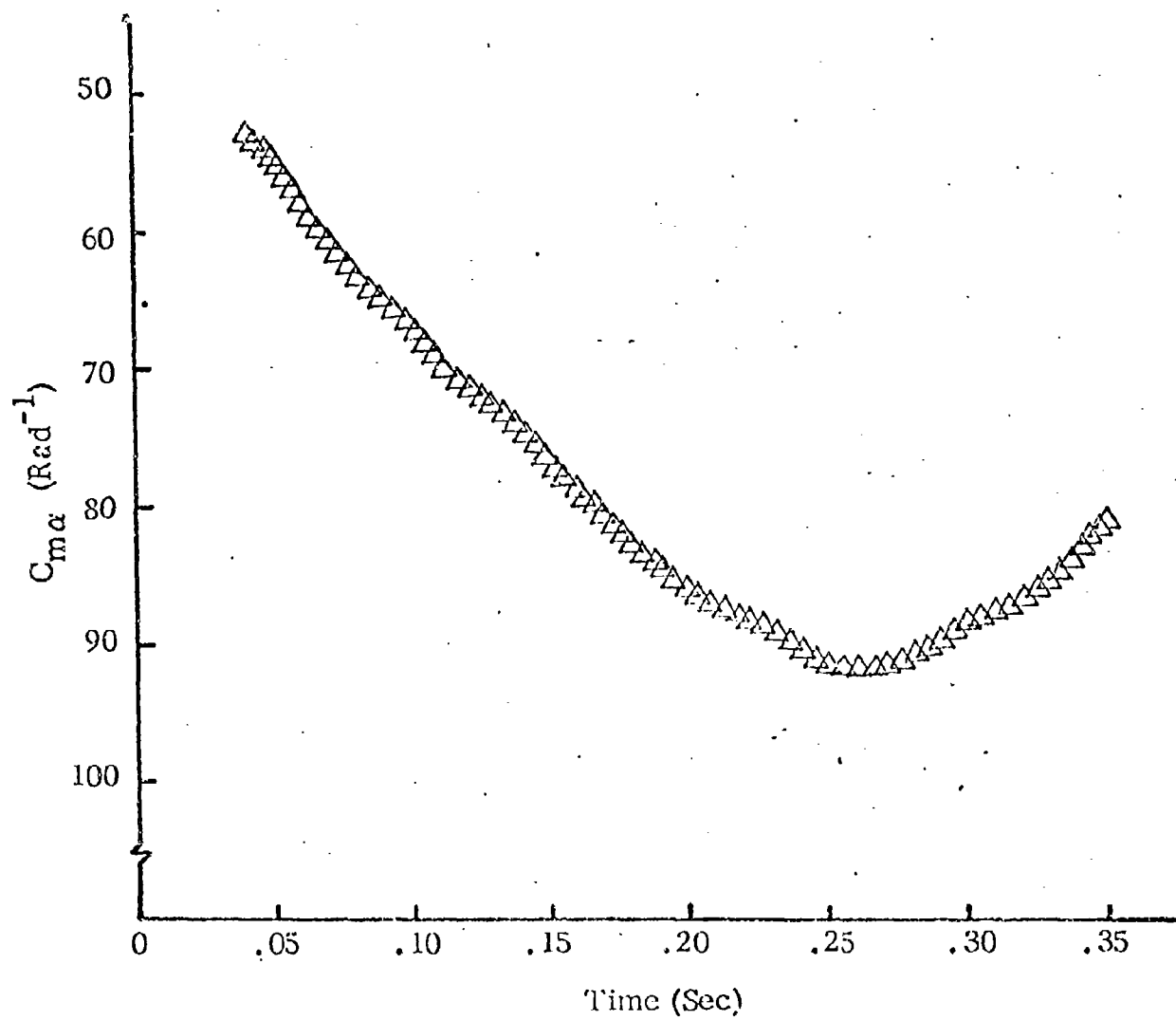


Figure 7.  $C_{m\alpha}$  vs Time

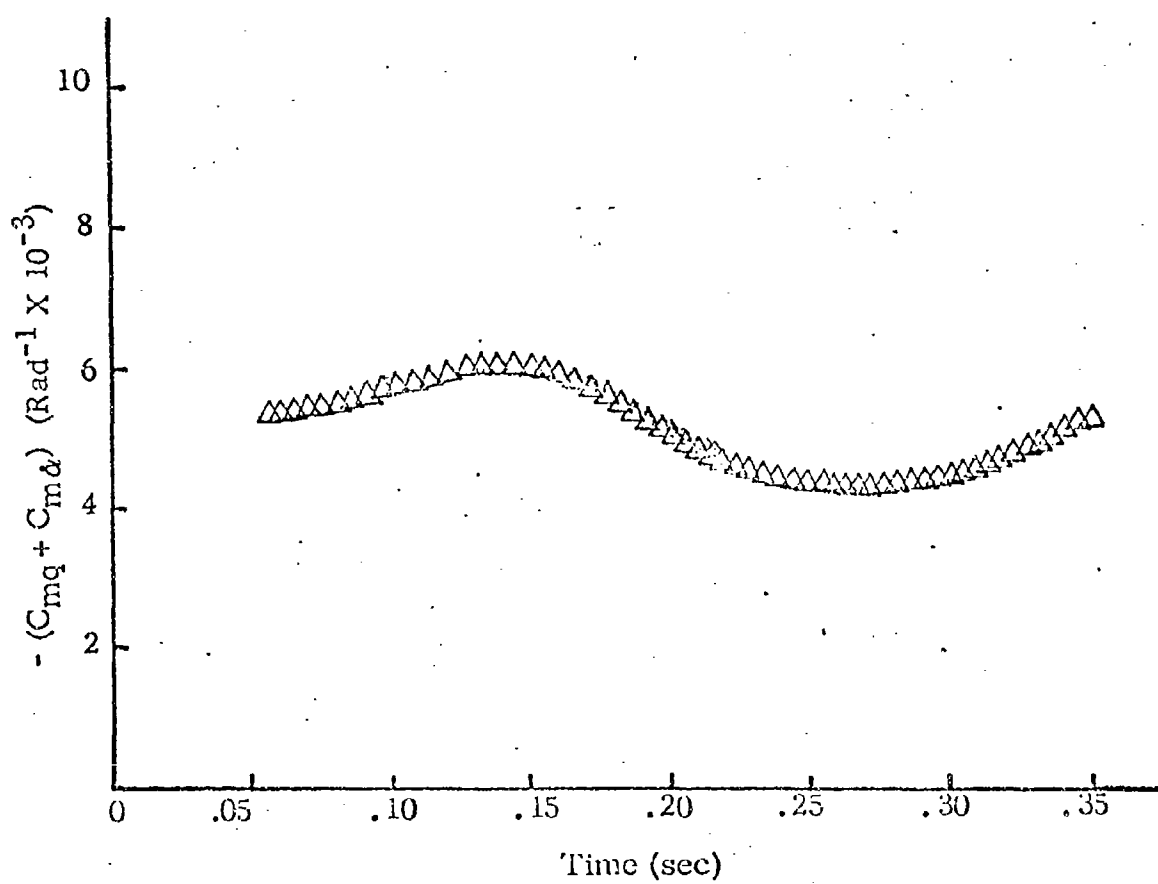


Figure 8.  $(C_{mq} + C_{ma})$  vs Time

$$C_{m\alpha}(\alpha) = C_{m\alpha_0} + C_{m\alpha_2}(\alpha)^2$$

- △ Run 9
- Run 12
- Run 14

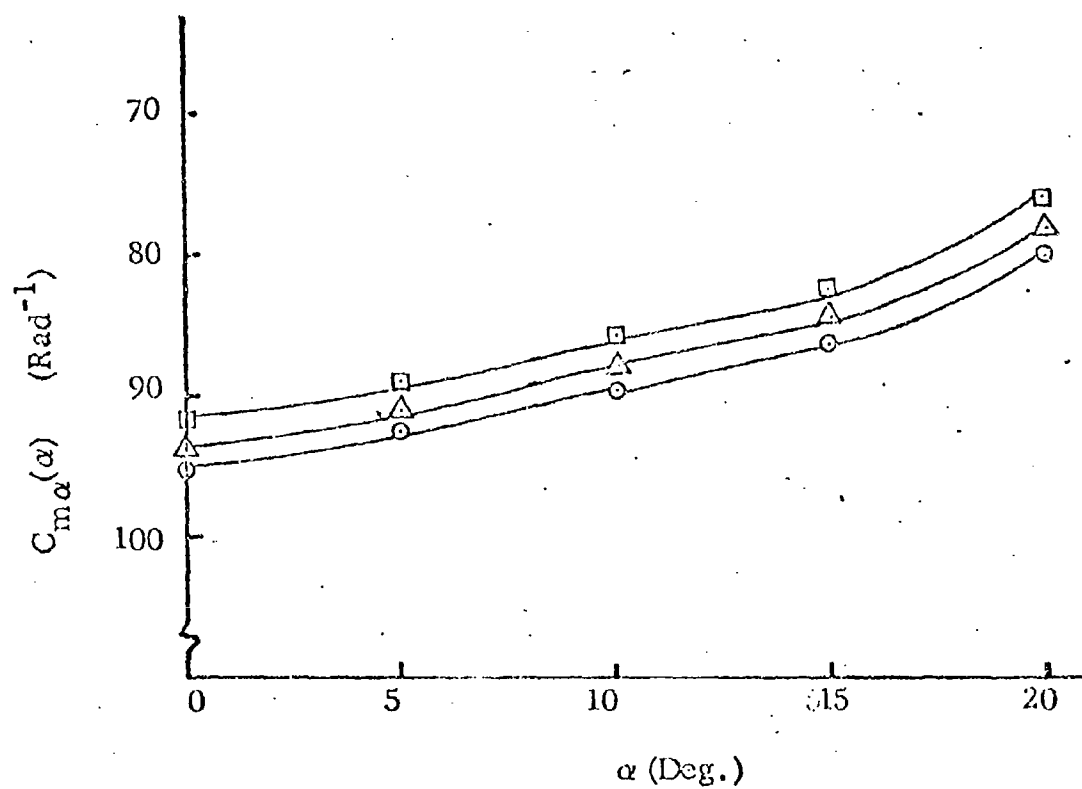


Figure 9.  $C_{m\alpha}(\alpha)$  vs  $\alpha$

$$C_{mq}(\alpha) + C_{m\dot{\alpha}}(\alpha) = (C_{mq} + C_{m\dot{\alpha}})_0 + (C_{mq} + C_{m\dot{\alpha}})_2 (\alpha^2)$$

△ Run 9

○ Run 12

□ Run 14

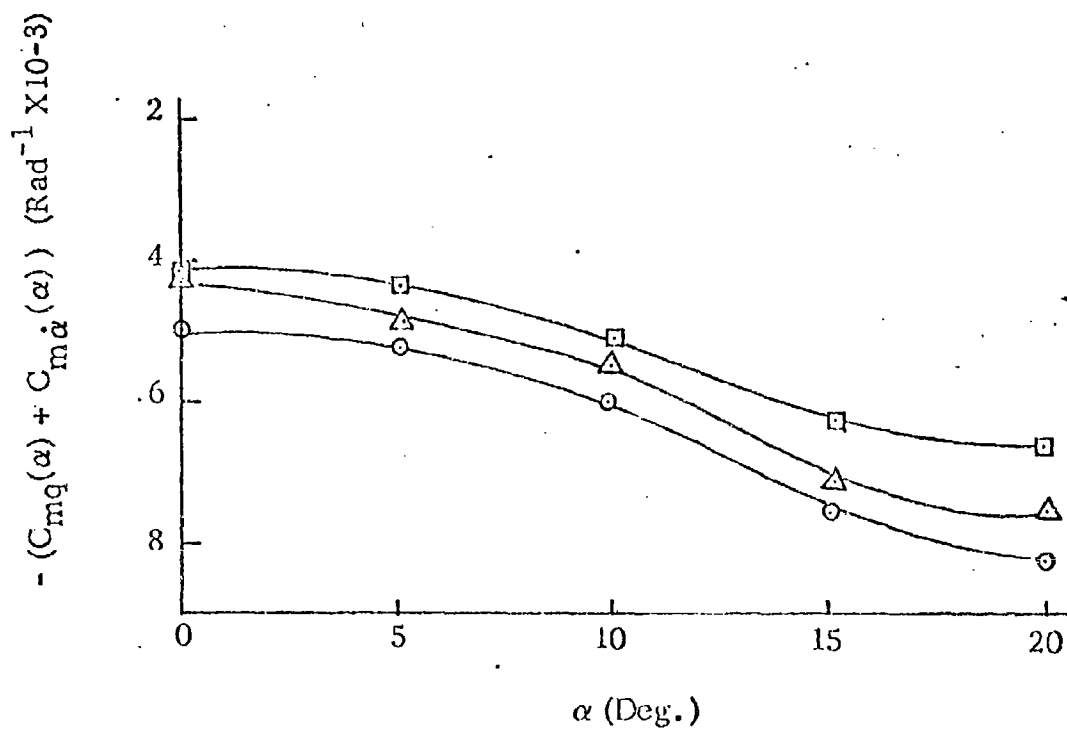


Figure 10.  $(C_{mq}(\alpha) + C_{m\dot{\alpha}}(\alpha))$  vs  $\alpha$

with angle of attack, the one-degree-of-freedom Nonlinear Aeroballistic Theory was employed. Using this nonlinear theory, the stability coefficients were determined as polynomial functions of the angle of attack. Representative plots of runs made are presented in Figs. 9 and 10.

Both  $C_{m\alpha}$ , the pitching moment coefficient and  $C_{mq} + C_{m\dot{\alpha}}$  the damping moment coefficient were found to vary nonlinearly with angle of attack. Both were found to be highly repeatable.  $C_{m\alpha}$  varied no more than 2% about its mean while  $C_{mq} + C_{m\dot{\alpha}}$  varied less than 5% about its mean.

## APPENDIX C

### DISPERSION THEORY OF HIGH FINENESS RATIO, CRUCIFORM FIN BODIES \*

A complete Jump and Dispersion Theory is developed for free flight vehicles. Six-degree-of-freedom computer computations indicates that the theory accurately predicts the jump and dispersion of flechettes.

The initial conditions and dispersion values are established by range test firings. The raw data is fitted by least squares method and put into initial condition form. Initial conditions are applied to the theory and 6-D numerical computations to evaluate dispersion for eight test rounds. The results are compared to test firing target data. The agreement between the theory and test results indicate the data analysis and theory provide an accurate means of predicting dispersion of flechettes. Analysis of the firing data indicates that the initial conditions result from an impulse imparted to the flechette in the muzzle blast. The transverse impulse imparted to the flechette initially must be equal to the angular impulse to obtain zero dispersion. Other disturbances in the blast region such as sabot separation influence the initial conditions and hence dispersion. First maximum yaw theory is discussed and disproved.

---

\*Prepared by Lawrence E. Lijewski.



# TABLE OF CONTENTS

	Page
TABLE OF CONTENTS . . . . .	112
LIST OF TABLES . . . . .	114
LIST OF FIGURES . . . . .	116
LIST OF SYMBOLS . . . . .	122
INTRODUCTION . . . . .	130
DISPERSION THEORY . . . . .	134
High Roll Rate Theory . . . . .	138
Low Roll Rate Theory . . . . .	140
Very Slow Roll Rate Theory . . . . .	142
VALIDATION OF THEORY . . . . .	144
Phase I . . . . .	145
Phase II . . . . .	155
Phase III . . . . .	160
Comparison: High, Low, Very Slow Roll Rate Theories . . . . .	194
Phase IV . . . . .	200
FREE FLIGHT DATA ANALYSIS . . . . .	206
DISPERSION ANALYSIS . . . . .	246
Free Flight vs Theory . . . . .	246
Dispersion Theory vs First Maximum Yaw Hypothesis . . . . .	266

TABLE OF CONTENTS (continued)

	Page
PHYSICAL EVALUATION OF DISPERSION . . . . .	276
CONCLUSIONS . . . . .	282
APPENDIX A-1 . . . . .	285
APPENDIX A-2 . . . . .	295
REFERENCES . . . . .	337

# LIST OF TABLES

Number		Page
I	Theory Validation, Restoring and Damping Moments, Cases 1-9 . . . . .	146
II	Theory Validation, Restoring and Damping Moments, Cases 10-18 . . . . .	147
III	Theory Validation, Restoring and Damping Moments, Cases 19-27 . . . . .	151
IV	Theory Validation, Restoring and Damping Moments, Cases 28-36 . . . . .	152
V	Magnus Coefficients, at Mach 4.5 . . . . .	155
VI	Theory Validation, Magnus, Cases 37-57 . . . . .	157
VII	Theory Validation, Asymmetries, Cases 58-68 . . . . .	162
VIII	Theory Validation, Asymmetries, Cases 69-79 . . . . .	163
IX	Theory Validation, Asymmetries, Cases 80-90 . . . . .	164
X	Theory Validation, Asymmetries, Cases 91-101 . . . . .	172
XI	Theory Validation, Asymmetries, Cases 102-112 . . . . .	173
XII	Theory Validation, Asymmetries, Cases 113-123 . . . . .	174

# LIST OF TABLES (continued)

Number		Page
XIII	Theory Validation, Asymmetries, Cases 124-134 . . . . .	181
XIV	Theory Validation, Asymmetries, Cases 135-145 . . . . .	182
XV	Theory Validation, Asymmetries, Cases 146-156 . . . . .	183
XVI	Theory Validation, Asymmetries, Cases 157-167 . . . . .	191
XVII	Theory Validation, Asymmetries, Cases 168-178 . . . . .	192
XVIII	Theory Validation, Asymmetries, Cases 179-189 . . . . .	193
XIX	Theory Validation, Gravity Cases 190-201 . . . . .	204
XX	Frankford Test Firing Data . . . . .	209
XXI	Aerodynamic Parameters from Least Squares Fit . . . . .	245
XXII	Dispersion Analysis Results . . . . .	247

# LIST OF FIGURES

Number		Page
1	Dispersion: Phase I Cases 10-18. . . . .	148
2	Trajectories, Cases 10-18 . . . . .	149
3	Dispersion: Phase I Cases 28-36 . . . . .	153
4	Trajectories, Cases 28-36 . . . . .	154
5	Dispersion: Phase II Cases 46,47,48,55,56, 57 . . . . .	158
6	Dispersion: Phase II Cases 38,41,44,47, 50,53,56 . . . . .	159
7	Dispersion: Phase III Cases 58-68 . . . . .	166
8	Dispersion: Phase III Cases 69-79 . . . . .	167
9	Dispersion: Phase III Cases 80-90 . . . . .	168
10	Dispersion: Phase III Theory, Cases 58-90 . .	169
11	Trajectory, Case 79 . . . . .	170
12	Dispersion: Phase III Cases 91-101 . . . . .	175
13	Dispersion: Phase III Cases 102-112 . . . . .	176
14	Dispersion: Phase III Cases 113-123 . . . . .	177
15	Dispersion: Phase III Theory, Cases 91-123 .	178
16	Trajectory, Case 101 . . . . .	179
17	Dispersion: Phase III Cases 124-134 . . . . .	185
18	Dispersion: Phase III Cases 135-145 . . . . .	186
19	Dispersion: Phase III Cases 146-156 . . . . .	187
20	Dispersion: Phase III Theory, Cases 124-156 .	188
21	Trajectory, Case 134 . . . . .	189

# LIST OF FIGURES (continued)

Number		Page
22	Dispersion: Phase III Cases 157-167 . . . . .	195
23	Dispersion: Phase III Cases 168-178 . . . . .	196
24	Dispersion: Phase III Cases 179-189 . . . . .	197
25	Dispersion: Phase III Theory, Cases 157-189 .	198
26	Trajectory, Case 189 . . . . .	199
27	Phase III Theory Equations 24, 28, 30 . . . . .	201
28	Phase III Theory Effective Limits . . . . .	202
29	Ground Point Flechette, With and Without Sabot . . . . .	207
30	Free Flight Test Apparatus and Set-Up . . . .	208
31	Raw Translational Data Ground Point - Round 4 . . . . .	210
32	Raw Angular Data Ground Point - Round 4 . .	211
33	Raw Translational Data Ground Point - Round 6 . . . . .	212
34	Raw Angular Data Ground Point - Round 6 . .	213
35	Raw Translational Data Ground Point - Round 7 . . . . .	214
36	Raw Angular Data Ground Point - Round 7 . .	215
37	Raw Translational Data Ground Point - Round 8 . . . . .	216

# LIST OF FIGURES (continued)

Number		Page
38	Raw Angular Data Ground Point - Round 8 . . .	217
39	Raw Translational Data Ground Point - Round 14 . . . . .	218
40	Raw Angular Data Ground Point - Round 14 . . . . .	219
41	Raw Translational Data Ground Point - Round 16 . . . . .	220
42	Raw Angular Data Ground Point - Round 16 . .	221
43	Raw Translational Data Ground Point - Round 17 . . . . .	222
44	Raw Angular Data Ground Point - Round 17 . .	223
45	Raw Translational Data Ground Point - Round 19 . . . . .	224
46	Raw Angular Data Ground Point - Round 19 . .	225
47	Axis Rotation Approximates Pure Pitching Motion . . . . .	227
48	Fitted Translational Data Ground Point - Round 4 . . . . .	229
49	Fitted Angular Data Ground Point - Round 4 . .	230
50	Fitted Translational Data Ground Point - Round 6 . . . . .	231
51	Fitted Angular Data Ground Point - Round 6 . .	232

# LIST OF FIGURES (continued)

Number		Page
52	Fitted Translational Data Ground Point - Round 7 . . . . .	233
53	Fitted Angular Data Ground Point - Round 7 . . . . .	234
54	Fitted Translational Data Ground Point - Round 8 . . . . .	235
55	Fitted Angular Data Ground Point - Round 8 .	236
56	Fitted Translational Data Ground Point - Round 14 . . . . .	237
57	Fitted Angular Data Ground Point - Round 14 . . . . .	238
58	Fitted Translational Data Ground Point - Round 16 . . . . .	239
59	Fitted Angular Data Ground Point - Round 16 . . . . .	240
60	Fitted Translational Data Ground Point - Round 17 . . . . .	241
61	Fitted Angular Data Ground Point - Round 17 . . . . .	242
62	Fitted Translational Data Ground Point - Round 19 . . . . .	243



# LIST OF FIGURES (continued)

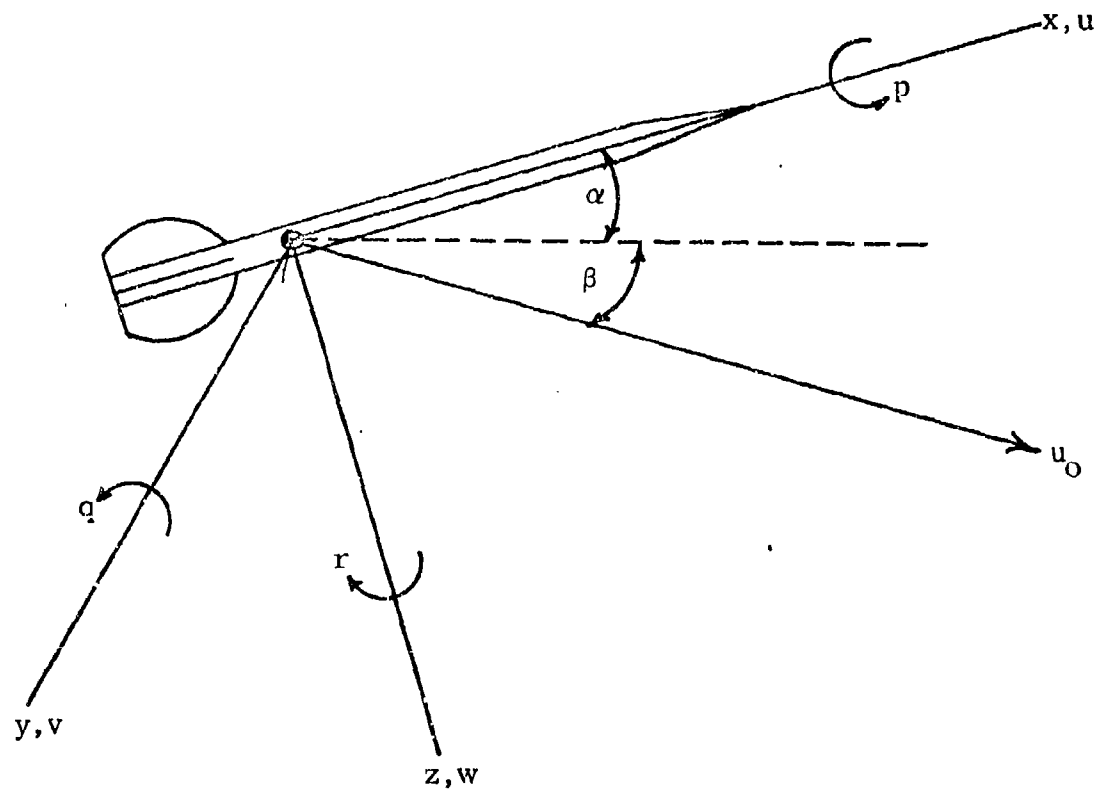
Number		Page
63	Fitted Angular Data Ground Point - Round 19 . .	244
64	Dispersion: Ground Point - Round 4 Test	
	Firing vs Theory, at 50 ft. Downrange . . .	248
65	Dispersion: Ground Point - Round 6 Test	
	Firing vs Theory, at 50 ft. Downrange . . .	249
66	Dispersion: Ground Point - Round 7 Test	
	Firing vs Theory, at 50 ft. Downrange . . .	250
67	Dispersion: Ground Point - Round 8 Test	
	Firing vs Theory, at 50 ft. Downrange . . .	251
68	Dispersion: Ground Point - Round 14 Test	
	Firing vs Theory, at 50 ft. Downrange . . .	252
69	Dispersion: Ground Point - Round 16 Test	
	Firing vs Theory, at 50 ft. Downrange . . .	253
70	Dispersion: Ground Point - Round 17 Test	
	Firing vs Theory, at 50 ft. Downrange . . .	254
71	Dispersion: Ground Point - Round 19 Test	
	Firing vs Theory, at 50 ft. Downrange . . .	255
72	Flight Transition Sequence - Round 4 . . . . .	257
73	Flight Transition Sequence - Round 6 . . . . .	258
74	Flight Transition Sequence - Round 7 . . . . .	259
75	Flight Transition Sequence - Round 8 . . . . .	260

# LIST OF FIGURES (concluded)

Number		Page
76	Flight Transition Sequence - Round 14 . . . .	261
77	Flight Transition Sequence - Round 16 . . . .	262
78	Flight Transition Sequence - Round 17 . . . .	263
79	Flight Transition Sequence - Round 19 . . . .	264
80	Dispersion vs First Maximum Yaw, Frankford Test Firing Results . . . . .	267
81	Dispersion vs First Maximum Yaw, Theory - Initial Conditions, 1 ft. Downrange . . . . .	269
82	Dispersion vs First Maximum Yaw, Theory - Initial Conditions, 3 ft. Downrange . . . . .	270
83	Dispersion vs First Maximum Yaw, Theory - Initial Conditions, 5 ft. Downrange . . . . .	271
84	Jump Angles for Various Initial Conditions . .	273
85	Flechette In-Bore Position . . . . .	277
86	Typical Flechette Blast Region . . . . .	279
87	Muzzle Blast Effects . . . . .	280
88	Supersonic Free Flight, Ground Point Flechette . . . . .	281

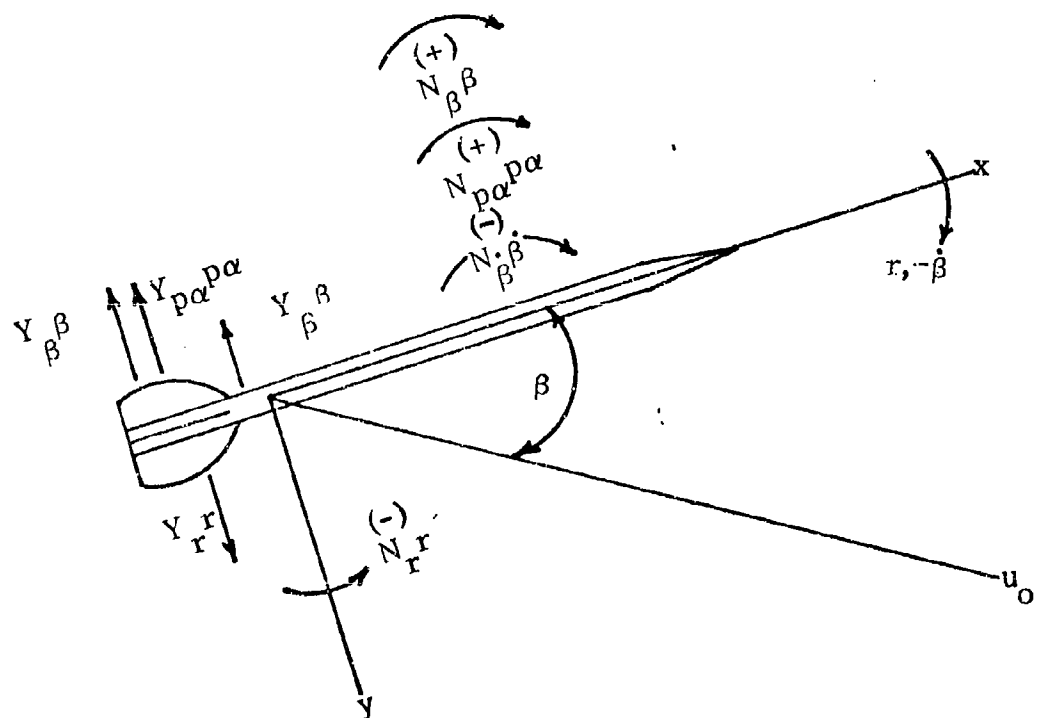
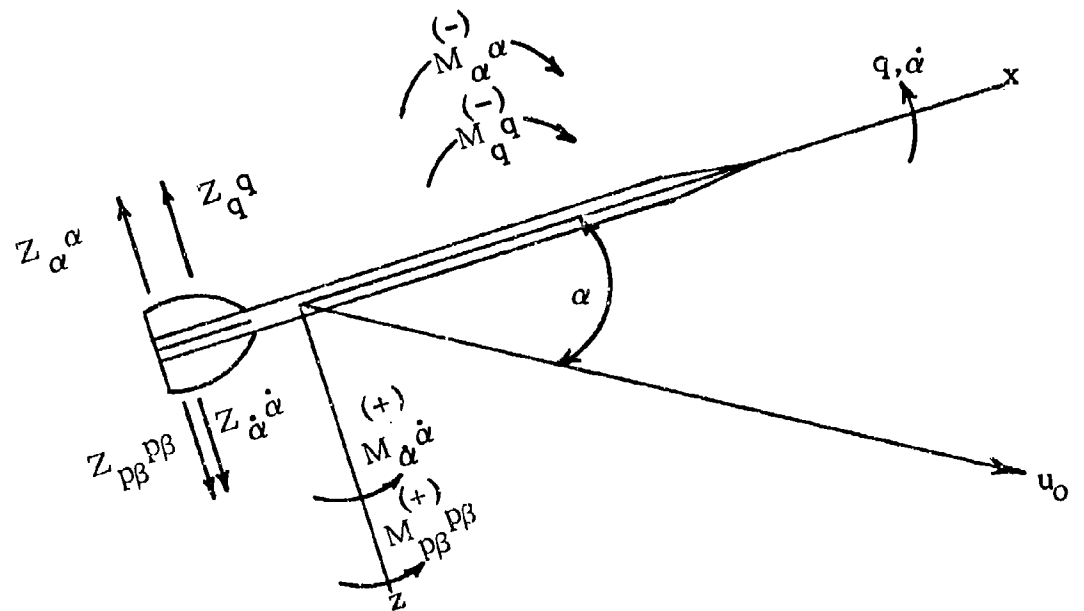
# LIST OF SYMBOLS

## Axis System



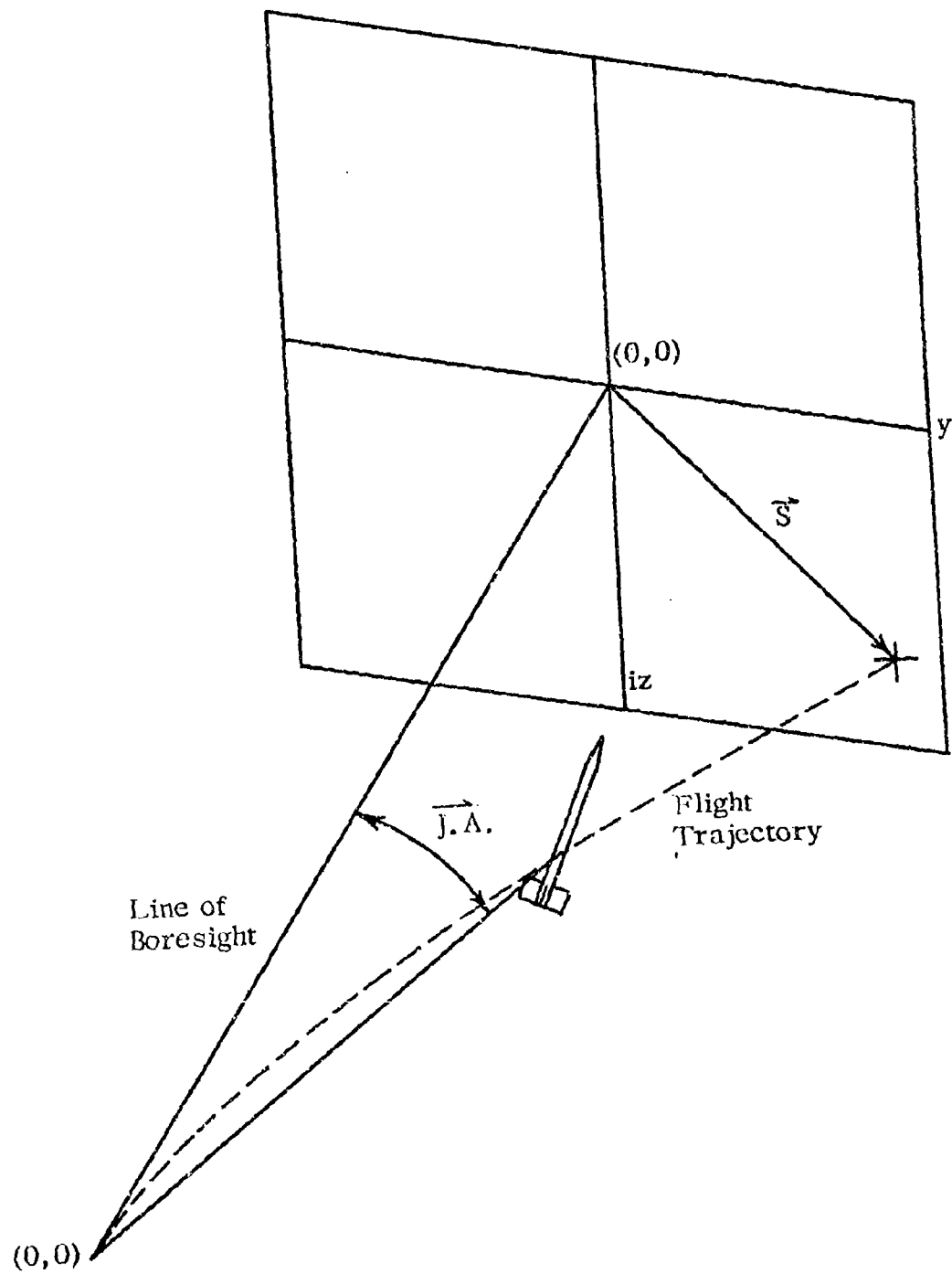
# LIST OF SYMBOLS (continued)

## Force and Moment Systems



# LIST OF SYMBOLS (continued)

Jump Angle



# LIST OF SYMBOLS (continued)

$\overline{\alpha}$  complex angle of attack (degrees or radians)

$$\overline{\alpha} = \beta + i\alpha$$

$\alpha$  pitch angle of attack

$\alpha_0$  initial angle of attack

$\overline{\dot{\alpha}}_0$  initial angular rate (rad/sec)

$$\overline{\dot{\alpha}}_0 = \dot{\beta}_0 + i + \dot{\alpha}_0$$

$\beta$  yaw angle of attack

$C_z$  pitching force coefficients

$$C_z = \frac{Z}{QS}$$

$C_M$  pitching moment coefficients

$$C_M = \frac{M}{QSd}$$

$C_{z\alpha}$  static force stability coefficient (rad<sup>-1</sup>)

$$C_{z\alpha} = \frac{\partial C_z}{\partial \alpha} = \frac{Z_\alpha \alpha}{\alpha QS} = \frac{Y_\beta \beta}{\beta QS}$$

$C_{M\alpha}$  static moment stability coefficient (rad<sup>-1</sup>)

$$C_{M\alpha} = \frac{\partial C_M}{\partial \alpha} = \frac{M_\alpha \alpha}{\alpha QSd} = -\frac{N_\beta \beta}{\beta QSd}$$

$C_{zq}$  damping force stability coefficient (rad<sup>-1</sup>)

$$C_{zq} = \frac{\partial C_z}{\partial \left(\frac{qd}{2u}\right)} = \frac{Z_q q}{\left(\frac{qd}{2u}\right) QS} = -\frac{Y_r r}{\left(\frac{rd}{2u}\right) QS}$$

# LIST OF SYMBOLS (continued)

$C_{Z\dot{\alpha}}$  lag force stability coefficient ( $\text{rad}^{-1}$ )

$$C_{Z\dot{\alpha}} = \frac{\partial C_Z}{\partial \left(\frac{\dot{\alpha}d}{2u}\right)} = \frac{Z_{\dot{\alpha}\dot{\alpha}}}{\left(\frac{\dot{\alpha}d}{2u}\right) QS} = \frac{Y_{\dot{\beta}\dot{\beta}}}{\left(\frac{\dot{\beta}d}{2u}\right) QS}$$

$C_{M_q}$  damping moment stability coefficient ( $\text{rad}^{-1}$ )

$$C_{M_q} = \frac{\partial C_M}{\partial \left(\frac{qd}{2u}\right)} = \frac{M_q q}{\left(\frac{qd}{2u}\right) QSd} = \frac{N_r r}{\left(\frac{rd}{2u}\right) QSd}$$

$C_{M\dot{\alpha}}$  lag moment stability coefficient ( $\text{rad}^{-1}$ )

$$C_{M\dot{\alpha}} = \frac{\partial C_M}{\partial \left(\frac{\dot{\alpha}d}{2u}\right)} = \frac{M_{\dot{\alpha}\dot{\alpha}}}{\left(\frac{\dot{\alpha}d}{2u}\right) QSd} = - \frac{N_{\dot{\beta}\dot{\beta}}}{\left(\frac{\dot{\beta}d}{2u}\right) QSd}$$

$C_{Z_{p\beta}}$  magnus force stability coefficient ( $\text{rad}^{-2}$ )

$$C_{Z_{p\beta}} = \frac{\partial C_Z}{\partial \beta \partial \left(\frac{pd}{2u}\right)} = \frac{Y_{p\alpha} p\alpha}{\left(\frac{pd}{2u}\right) \alpha QS} = \frac{Z_{p\beta} p\beta}{\left(\frac{pd}{2u}\right) \beta QS}$$

$C_{M_{p\beta}}$  magnus moment stability coefficient ( $\text{rad}^{-2}$ )

$$C_{M_{p\beta}} = \frac{\partial C_M}{\partial \beta \partial \left(\frac{pd}{2u}\right)} = \frac{N_{p\alpha} p\alpha}{\left(\frac{pd}{2u}\right) \alpha QSd} = \frac{M_{p\beta} p\beta}{\left(\frac{pd}{2u}\right) \beta QSd}$$

$C_{Z_{\delta_\epsilon}} \vec{\delta_\epsilon}$  aerodynamic asymmetry force, total coefficient

$$C_{Z_{\delta_\epsilon}} \vec{\delta_\epsilon} = C_{Y_r} \delta_r + i C_{Z_\epsilon} \delta_\epsilon$$

$C_{M_{\delta_\epsilon}} \vec{\delta_\epsilon}$  aerodynamic asymmetry moment, total coefficient

$$C_{M_{\delta_\epsilon}} \vec{\delta_\epsilon} = C_{M_{\delta_\epsilon}} \delta_\epsilon + i C_{N_{\delta_r}} \delta_r$$

# LIST OF SYMBOLS (continued)

$d$	flechette body diameter (ft)
$\vec{\delta}_\epsilon$	complex aerodynamic asymmetry vector $\vec{\delta}_\epsilon = \delta_r + i\delta_\epsilon$
$\delta$	phase angle (rad)
$g$	acceleration due to gravity 32.2 ft/sec <sup>2</sup>
$\gamma$	rotation angle between $\alpha, \beta$ axis system and $\alpha', \beta'$ system to approximate pure pitching motion (deg.)
$I_x$	axial moment of inertia (slugs-ft <sup>2</sup> )
$I_y$	transverse moment of inertia (slugs-ft <sup>2</sup> )
$\vec{J.A.}$	jump angle vector (mils)
$\vec{K}_1$	nutation mode amplitude (deg)
$\vec{K}_2$	precession mode amplitude (deg)
$\vec{K}_3, k-T$	trim mode amplitude (deg)
$\vec{K}_4$	yaw of repose amplitude (deg)
$k_{1,2,3,4,5,6}$	dispersion or jump angle amplitude coefficients
$\lambda_{1,2}, \lambda_{N,P}$	damping factors for nutation and precession modes respectively (rad/sec)
$m$	mass of flechette (slugs)
$p$	roll rate (rad/sec)
$p_0$	initial roll rate (rad/sec)
$\vec{q}$	complex angular velocity (rad/sec) $\vec{q} = q + ir$
$q$	pitching angular velocity (rad/sec)



# LIST OF SYMBOLS (continued)

$Q$	dynamic pressure $\frac{\text{slugs}}{\text{ft} \cdot \text{sec}^2}$
	$Q = \frac{1}{2} \rho u^2$
$r$	yawing angular velocity (rad/sec)
$\rho$	density (slugs/ft <sup>3</sup> )
$S$	reference area $S = \frac{\pi d^2}{4}$
$\overline{S}$	complex translation (ft)
	$\overline{S} = y + iz$
$\overline{S}_0$	initial complex translation (ft)
	$\overline{S}_0 = y_0 + iz_0$
$\dot{\overline{S}}_0$	initial complex velocity (ft/sec)
	$\dot{\overline{S}}_0 = \dot{y}_0 + i\dot{z}_0$
$s$	gyroscopic stability factor
$r$	dynamic weight factor
$t$	time (sec)
$u$	axial velocity (ft/sec)
$u_0$	initial axial velocity (ft/sec)
$v, w$	transverse velocities (ft/sec)
$\overline{w}$	complex transverse velocity (ft/sec)
	$\overline{w} = v + iw$

LIST OF SYMBOLS (concluded)

$\omega, \omega_N, \omega_P$  nutation and precession mode frequencies (rad/sec)  
 $x, y, z$  position components

## INTRODUCTION

The accuracy and dispersion of free flight vehicles has been a problem in aerodynamics and ballistics for many years. Until the present time, the primary investigations into causes and effects of jump (the angle between the line of boresight and the line connecting the point of launch with the instantaneous position on the trajectory,) and dispersion have been directed toward projectiles and, in particular, artillery rounds. A full program to investigate jump and dispersion characteristics of low trajectory finned bodies has been lacking and therefore is the subject of this dissertation. The purpose of this analysis is to develop a basic understanding of the parameters causing the jump and dispersion of flechettes. The flechette, being a gun launched finned body, requires a different approach to the problem. The old concept employed in the analysis of the dispersion of artillery rounds is that the dispersion results from initial launch disturbances imparted by the gun to the shell.<sup>1,2</sup> This concept is no longer valid for flechettes since the flechette is a fin missile, sabot launched, and its dispersion must be tied to the disturbances it encounters when clearing the muzzle blast and sabot separation region. In addition, asymmetries are more prevalent in finned bodies than projectiles and a finned body is more apt to be influenced by the blast. These factors must be taken into account by a theory involving finned bodies.

In order to develop this new approach, (1) a theoretical expression for jump and dispersion had to be developed, (2) the theory had to be

validated, (3) free flight test firings had to be undertaken and initial condition data extracted, and (4) the test firing results had to be correlated with the validated theory. The Jump and Dispersion Theory was developed, in general, for both fin and spin stabilized missiles in air. The theory includes the effects of: initial conditions, Magnus, aerodynamic asymmetries, and gravity. In the past, theory development for projectiles included only initial angle of attack and initial angular rate.<sup>1,3</sup> Initial transverse velocity was considered non-existent<sup>4</sup> or negligible. Zaroodny<sup>5</sup> included a linear momentum term to account for any transverse motion of the projectile but attributed it to the gun during recoil. Any transverse impulse imparted to the projectile by the blast was ignored. Other authors, including Sterne<sup>2</sup> attributed the jump only to bore clearance and therefore only included, effectively, the initial angle of attack. Magnus effects were always neglected in previous studies either due to lack of familiarity with the subject or lack of data. In general, all cross-forces, except lift, were neglected mainly for convenience sake. Zaroodny, however, cautioning against wholesale simplifying said "it would seem desirable that our formulas allow us to include these other forces as the experimental information on these forces becomes available." Aerodynamic asymmetries were neglected for projectiles but included in Murphy's work.<sup>6</sup> It was not until Nicolaides<sup>7,8,9</sup> that all four factors affecting dispersion; initial angle of attack, initial angular rate, initial transverse position and velocity, were put into one theory. The work presented here expands the work of Nicolaides to include all parameters affecting dispersion in detail. Three separate

equations comprise the theory to include the complete range of roll rates. Before, only high roll rates were considered; with the study of finned bodies, the roll rate range extends down to zero roll and accurate theories had to be deduced from known aerodynamic equations.

To validate the theory, a six-degree-of-freedom trajectory computer program numerically integrating the equations of motion was utilized.<sup>10, 11, 12</sup>

The validation consisted of four phases. The procedure began with the most basic theory equation and consecutively added terms to validate the entire theory. Initial conditions, magnus, asymmetries and gravity were successively validated with roll rate and velocity varied in each phase.

Before the advent of adequate photographic material, obtaining test data was often difficult. At first, jump target data was taken separate from yaw data. The thinking was that the yaw data was part of the projectile's characteristics and not affecting jump. As photographic methods improved, and theories developed, the data was correlated. The correlation of the data was often a problem. A fit of the motion to a least squares method was difficult. Fowler, Kent, and Hitchcock developed a method that would plot the magnitude of the yaw separately from the orientation and then fit the curves separately. A better method was developed by McShane-Charters-Turetsky approximated the yawing motion to a circle. For projectiles the method has been refined and is an excellent method. However, for finned bodies with not always circular angular motions, a different method of data analysis had to be devised. Utilizing the free flight data taken by test engineers at Frankford Arsenal on a number of flechettes, the least squares method was employed to fit the data pre-

sented here. The nearly planar oscillations of the flechette in the first few feet downrange were fit to a pure pitching motion<sup>13, 14</sup> and the position downrange fit to a third order polynomial. From these results, angle of attack, angular rate and transverse position and velocity were determined for the first few feet downrange. Before, there was some controversy as to whether or not the least squares fit could be extrapolated back to the muzzle. Zaroodny contended that the  $x=0$  position had to be taken out of the blast region to allow the aerodynamic equations to be valid. On the other hand, Kent, Hitchcock, Fowler and Sterne held to the fact that the free flight region began the instant the projectile left the bore. In the analysis of flechettes the position  $x=0$  is taken somewhere downrange after the sabot separation sequence has occurred. This is seen to be 3 to 5 feet downrange and assumed clear of any muzzle blast effects.

The striking shortcoming of previous works is the lack of correlation between test data and valid theory. For the flechette, correlation between the theory and test data was undertaken as well as correlation between test results and first maximum yaw data. Currently, the first maximum yaw theory<sup>15</sup> is held by some to be an accurate method of predicting dispersion. This theory disallows any influence of initial angular rate, transverse position or velocity on dispersion. The dispersion analysis presented here disproves this theory with actual test data. The details of each of these aspects of this program are developed in the following sections.

## DISPERSION THEORY

Dispersion relationships for free flight vehicles are embedded in the trajectory equation of any such aeroballistic body. To evaluate the trajectory equation and thus the dispersion, the linear second-order differential equation of angular motion is a logical starting point.

$$\ddot{\vec{w}} + N_1 \dot{\vec{w}} + N_2 \vec{w} = \vec{N}_3 e^{ipt} + \vec{N}_4 \quad (1)$$

where  $N_1$ ,  $N_2$ ,  $\vec{N}_3$ , and  $\vec{N}_4$  are constants.

$$N_1 = \left[ \frac{Z_w + ipZ_{pv}}{Z_{\dot{w}} - m} \right] + \frac{M_{\dot{w}}}{I_y} \left[ \frac{mu + Z_q}{Z_{\dot{w}} - m} \right] - \left[ \frac{ipI_x}{I_y} + \frac{M_q}{I_y} \right] \quad (2)$$

$$N_2 = \left[ \frac{M_w + ipM_{pv}}{I_y} \right] \left[ \frac{mu + Z_q}{Z_{\dot{w}} - m} \right] - \left[ \frac{Z_w + ipZ_{pv}}{Z_{\dot{w}} - m} \right] \left[ \frac{ipI_x}{I_y} + \frac{M_q}{I_y} \right] \quad (3)$$

$$\vec{N}_3 = \left[ \frac{Z_{\delta_\epsilon} \dot{\delta}_\epsilon}{Z_{\dot{w}} - m} \right] \left[ \frac{M_q}{I_y} + \frac{ipI_x}{I_y} - ip \right] - \frac{M_{\delta_\epsilon} \dot{\delta}_\epsilon}{I_y} \left[ \frac{mu + Z_q}{Z_{\dot{w}} - m} \right] \quad (4)$$

$$\vec{N}_4 = \frac{img}{I_y} \left[ \frac{M_q + ipI_x}{Z_{\dot{w}} - m} \right] \quad (5)$$

In this discussion of dispersion theory, it is assumed that,

- (1) total velocity,  $u_0$ , is constant, equal to  $\dot{u}$  in the theory development.
- (2) all force and moment coefficients dependent on angle of attack are considered to be linear with angle of attack.
- (3) all force and moment coefficients independent of angle of attack are considered to be constant.

- (4) a linear relationship exists between  $x$  (distance down range) and time for the non-drag case.
- (5) roll rate,  $p$ , is considered to be constant.
- (6) products of force and moment derivatives are negligible, except those involving  $Z_{\delta_\epsilon}$  and  $M_{\delta_\epsilon}$ .

Utilizing these assumptions, and the binomial expansion of  $(Z_w - m)^{-1}$ , 2, 3, 4 and 5 become:

$$N_1 \approx - \left[ \frac{Z_w + ipZ_{pv}}{m} \right] - \left[ \frac{M_g + uM_w}{I_y} \right] - \frac{ipI_x}{I_y} \quad (2a)$$

$$N_2 \approx -u \left[ \frac{M_w + ipM_{pv}}{I_y} \right] + \frac{ipI_x}{I_y} \left[ \frac{Z_w + ipZ_{pv}}{m} \right] \quad (3a)$$

$$\vec{N}_3 \approx \frac{ipZ_{\delta_\epsilon} \vec{\delta}_\epsilon}{m} \left[ 1 - \frac{I_x}{I_y} \right] + \frac{uM_{\delta_\epsilon} \vec{\delta}_\epsilon}{I_y} \quad (4a)$$

$$\vec{N}_4 \approx g \left[ \frac{pI_x}{I_y} \right] \quad (5a)$$

The solution to Equation 1 is that of tricyclic motion; that is,

$$\vec{w} = \vec{K}_1 e^{\phi_1 t} + \vec{K}_2 e^{\phi_2 t} + \vec{K}_3 e^{ip\tau} + \vec{K}_4 \quad (6)$$

where the complex coefficients are:

$$\vec{K}_{1,2} = \frac{\vec{w}_0 - (\phi_{2,1}) \vec{w}_0 + \vec{K}_3 (\phi_{2,1} - ip)}{\phi_{1,2} - \phi_{2,1}} \quad (7)$$

$$\vec{K}_3 = \frac{\vec{N}_3}{(ip - \phi_1)(ip - \phi_2)} \quad (8)$$



$$\vec{K}_4 = \frac{\vec{N}_4}{N_2} \quad (9)$$

and

$$\phi_{1,2} = -\frac{N_1}{2} \pm \frac{1}{2} \sqrt{N_1^2 - 4N_2} \quad (10)$$

The trajectory equation for free-flight motion:

$$\vec{\ddot{S}} = (\vec{\ddot{w}} - iu\vec{q}) \quad (11)$$

An expression for  $\vec{q}$  is obtained from the equations of motion

$$\begin{aligned} \vec{q} &= i\vec{w} \left[ \frac{Z_{\dot{w}} - m}{mu + Z_q} \right] + i\vec{w} \left[ \frac{Z_w + ipZ_{pv}}{mu + Z_q} \right] + \left[ \frac{iZ_{\delta\epsilon} \vec{\delta\epsilon}}{mu + Z_q} \right] e^{ipt} - \left[ \frac{mg}{mu + Z_q} \right] \\ \vec{q} &\approx i\vec{w} \left[ 1 - \frac{Z_q + Z_{\dot{w}}}{m} \right] + i\vec{w} \left[ \frac{Z_w + ipZ_{pv}}{mu} \right] + \left[ \frac{iZ_{\delta\epsilon} \vec{\delta\epsilon}}{mu} \right] e^{ipt} - \frac{g}{u} \end{aligned} \quad (12)$$

yielding a solution of the form:

$$\vec{S} = \vec{k}_1 e^{\phi_1 t} + \vec{k}_2 e^{\phi_2 t} + \vec{k}_3 e^{ipt} + \vec{k}_4 t^2 + \vec{k}_5 t + \vec{k}_6 \quad (13)$$

where the entire expression for the solution is:

$$\begin{aligned} \vec{S} &= \vec{K}_1 e^{\phi_1 t} \left[ \frac{1}{\phi_1} \left( \frac{Z_q + uZ_{\dot{w}}}{mu} \right) + \frac{u}{\phi_1^2} \left( \frac{Z_w + ipZ_{pv}}{mu} \right) \right] \\ &+ \vec{K}_2 e^{\phi_2 t} \left[ \frac{1}{\phi_2} \left( \frac{Z_q + uZ_{\dot{w}}}{mu} \right) + \frac{u}{\phi_2^2} \left( \frac{Z_w + ipZ_{pv}}{mu} \right) \right] \\ &+ \left[ \frac{Z_w + ipZ_{pv}}{m} \vec{K}_3 + \frac{Z_{\delta\epsilon} \vec{\delta\epsilon}}{m} \right] \int_0^t \int_0^t e^{ipt} dt dt \\ &+ \left[ \frac{Z_q + uZ_{\dot{w}}}{mu} \right] \vec{K}_3 \int_0^t e^{ipt} + \left[ \frac{\vec{K}_4}{2} \left( \frac{Z_w + ipZ_{pv}}{m} \right) + \frac{ig}{2} \right] t^2 \end{aligned}$$

$$+ t \left[ \vec{S}_0 + \left( \frac{Z_q + uZ_{\dot{w}}}{mu} \right) (\vec{K}_4 - \vec{w}_0) - \left( \frac{Z_w + ipZ_{pv}}{m} \right) \left( \frac{\vec{K}_1}{\phi_1} + \frac{\vec{K}_2}{\phi_2} \right) \right] \quad (14)$$

$$+ \left[ \vec{S}_0 - \left( \frac{Z_q + uZ_{\dot{w}}}{mu} \right) \left( \frac{\vec{K}_1}{\phi_1} + \frac{\vec{K}_2}{\phi_2} \right) - \left( \frac{Z_w + ipZ_{pv}}{m} \right) \left( \frac{\vec{K}_1}{\phi_1^2} + \frac{\vec{K}_2}{\phi_2^2} \right) \right]$$

The term  $\left( \frac{Z_q + uZ_{\dot{w}}}{mu} \right)$  is of an order of magnitude  $10^{-3}$  and thus is neglected from all further discussion. This reduces 14 to:

$$\begin{aligned} \vec{S} = & \vec{K}_1 e^{\phi_1 t} \left[ \frac{u}{\phi_1^2} \left( \frac{Z_w + ipZ_{pv}}{mu} \right) \right] + \vec{K}_2 e^{\phi_2 t} \left[ \frac{u}{\phi_2^2} \left( \frac{Z_w + ipZ_{pv}}{mu} \right) \right] \\ & + \left[ \frac{Z_w + ipZ_{pv}}{m} \vec{K}_3 + \frac{Z_{\delta\epsilon} \vec{\delta\epsilon}}{m} \right] \int_0^t \int_0^t c^{ipt} dt dt + \left[ \frac{\vec{K}_4}{2} \left( \frac{Z_w + ipZ_{pv}}{m} \right) + \frac{ig}{2} \right] t^2 \\ & + t \left[ \vec{S}_0 - \left( \frac{Z_w + ipZ_{pv}}{m} \right) \left( \frac{\vec{K}_1}{\phi_1} + \frac{\vec{K}_2}{\phi_2} \right) \right] + \left[ \vec{S}_0 - \left( \frac{Z_w + ipZ_{pv}}{m} \right) \left( \frac{\vec{K}_1}{\phi_1^2} + \frac{\vec{K}_2}{\phi_2^2} \right) \right] \end{aligned} \quad (15)$$

By further inspection, terms with  $\phi_1^2$  and  $\phi_2^2$  will be negligible since they contain products of force and moment derivatives. Equation 15 becomes:

$$\begin{aligned} \vec{S} = & \left[ \frac{Z_w + ipZ_{pv}}{m} \vec{K}_3 + \frac{Z_{\delta\epsilon} \vec{\delta\epsilon}}{m} \right] \int_0^t \int_0^t c^{ipt} dt dt + \left[ \frac{\vec{K}_4}{2} \left[ \frac{Z_w + ipZ_{pv}}{m} \right] + \frac{ig}{2} \right] t^2 \\ & + t \left[ \vec{S}_0 - \left( \frac{Z_w + ipZ_{pv}}{m} \right) \left( \frac{\vec{K}_1}{\phi_1} + \frac{\vec{K}_2}{\phi_2} \right) \right] + \vec{S}_0 \end{aligned} \quad (16)$$

Equation 16 contains only the significant terms in dispersion theory.

This equation is valid for all values of roll rate.

### High Roll Rate Theory

For roll rates greater than 100 rad/sec, Equation 16 reduces to an approximate solution. Integration of the double integral gives:

$$\int_0^t \int_0^t e^{ipt} dt dt = \frac{e^{ipt}}{(ip)^2} - \frac{t}{ip} - \frac{1}{(ip)^2} \quad (17)$$

For high roll rates, the first and third terms go to zero, leaving only the second term to affect dispersion. Applying this approximation to Equation 16 :

$$\begin{aligned} \vec{S} = & \left[ \frac{\vec{K}_4}{2} \left( \frac{Z_w + ipZ_{pv}}{m} \right) + \frac{ig}{2} \right] t^2 + \left[ \vec{S}_0 - \left( \frac{Z_w + ipZ_{pv}}{m} \right) \left( \frac{\vec{K}_1}{\phi_1} + \frac{\vec{K}_2}{\phi_2} + \frac{\vec{K}_3}{ip} \right) \right. \\ & \left. + \frac{iZ_{\delta\epsilon} \vec{\delta\epsilon}}{mp} \right] t + \vec{S}_0 \end{aligned} \quad (18)$$

where, by applying previous aerodynamic relationships:

$$\left( \frac{\vec{K}_1}{\phi_1} + \frac{\vec{K}_2}{\phi_2} + \frac{\vec{K}_3}{ip} \right) = \left[ \frac{\vec{w}_0 - \vec{w}_0 (\phi_1 + \phi_2)}{-\phi_1 \phi_2} \right] + \left[ \frac{\frac{uM_{\delta\epsilon} \vec{\delta\epsilon}}{I_y} + i \frac{pZ_{\delta\epsilon} \vec{\delta\epsilon}}{m} \left( 1 - \frac{I_x}{I_y} \right)}{(ip) \phi_1 \phi_2} \right] \quad (19)$$

$$\phi_1 + \phi_2 = -N_1$$

$$\phi_1 \phi_2 = N_2$$

$$\vec{K}_4 = -gpI_x \left[ \frac{1}{\left( M_{\alpha} + \frac{p^2 I_x}{mu} Z_{p\beta} \right) + i \left( pM_{p\beta} + \frac{pI_x}{mu} Z_w \right)} \right] \quad (20)$$

Substituting 19 and 20 into 18 and expanding the various terms:

$$\begin{aligned} \vec{S} = & \frac{igt^2}{2} \left[ 1 + \frac{ipI_x}{mud} \left[ \frac{C_{Z\alpha} + i\left(\frac{pd}{2u}\right) C_{Zp\beta}}{\left(C_{M\alpha} + \frac{pI_x}{mud} \frac{pd}{2u} C_{Zp\beta}\right) + i\left(C_{Mp\beta} \frac{pd}{2u} - \frac{pI_x}{mud} C_{Z\alpha}\right)} \right] \right] \\ & + ut \left[ \frac{\vec{S}_0}{u} + - \frac{I_y}{mud} \left[ \frac{C_{Z\alpha} + i\frac{pd}{2u} C_{Zp\beta}}{\left(C_{M\alpha} + \frac{pI_x}{mud} \frac{pd}{2u} C_{Zp\beta}\right) + i\left(C_{Mp\beta} \frac{pd}{2u} - \frac{pI_x}{mud} C_{Z\alpha}\right)} \right] \right. \\ & \left. + i C_{Z\delta\epsilon} \vec{\delta\epsilon} \left[ \frac{\rho u \pi d^2}{8mp} \right] \right] \end{aligned} \quad (21)$$

$$\left[ \vec{\alpha}_0 - \alpha_0 \left( \frac{ipI_x}{I_y} \right) - C_{M\delta\epsilon} \vec{\delta\epsilon} \left( \frac{\rho u^2 \pi d^3}{8pI_y} \right) - C_{Z\delta\epsilon} \vec{\delta\epsilon} \left( 1 - \frac{I_x}{I_y} \right) \frac{\rho u \pi d^2}{8m} \right] + \vec{S}_0$$

Employing assumption 6 ,

$$\begin{aligned} \vec{S} = & \frac{ig}{2} \left( \frac{x}{u} \right)^2 \left[ 1 + \frac{ipI_x}{mud} \Lambda \right] + (x) \left[ \frac{\vec{S}_0}{u} + i C_{Z\delta\epsilon} \vec{\delta\epsilon} \left( \frac{\rho u \pi d^2}{8mp} \right) \right. \\ & - \frac{I_y}{mud} \Lambda \left[ \vec{\alpha}_0 - \alpha_0 \left( \frac{ipI_x}{I_y} \right) - C_{M\delta\epsilon} \vec{\delta\epsilon} \left( \frac{\rho u^2 \pi d^3}{8pI_y} \right) \right. \\ & \left. \left. - C_{Z\delta\epsilon} \vec{\delta\epsilon} \left( 1 - \frac{I_x}{I_y} \right) \frac{\rho u \pi d^2}{8m} \right] \right] + \vec{S}_0 \end{aligned} \quad (22)$$

where

$$A = \frac{C_{Z\alpha} + i\left(\frac{pd}{2u}\right) C_{Zp\beta}}{\left(C_{M\alpha} + \frac{pI_x}{mud} \frac{pd}{2u} C_{Zp\beta}\right) + i\left(C_{Mp\beta} \frac{pd}{2u} - \frac{pI_x}{mud} C_{Z\alpha}\right)}$$

The mil-relation offers a method to define the Jump Angle from Equation 22.

$$\text{Jump Angle} = \frac{\vec{S}}{x} (10^3) \quad (23)$$

$$\begin{aligned} \vec{J.A.} = & \frac{ig}{2} \left( \frac{x}{u^2} \right) (10^3) \left[ 1 + \frac{ipL_x}{mud} A \right] + (10^3) \left[ \frac{\vec{S}_0}{u} + i C_{Z_{\delta_\epsilon}} \vec{\delta_\epsilon} \left( \frac{\rho u \pi d^2}{8 m p} \right) \right. \\ & - \frac{I_y}{mud} A \left[ \vec{\alpha}_0 - \vec{\alpha}_0 \left( \frac{ipL_x}{I_y} \right) - C_{M_{\delta_\epsilon}} \vec{\delta_\epsilon} \left( \frac{\rho u^2 \pi d^3}{8 p I_y} \right) \right. \\ & \left. \left. - C_{Z_{\delta_\epsilon}} \vec{\delta_\epsilon} \left( 1 - \frac{I_x}{I_y} \right) \frac{\rho u \pi d^2}{8 m} \right] \right] + \frac{1000}{x} \vec{S}_0 \end{aligned} \quad (24)$$

Equation 24 gives an approximation for the Jump Angle for high roll rate cases with gravity, at any position  $x$  down range.

#### Low Roll Rate Theory

For roll rates less than 100 rad/sec but having a parameter,  $pt$ , greater than 1, Equation 16 can be reduced to another approximation.

As before, integration of the double integral yields Equation 17

$$\int_0^t \int_0^t e^{ipt} = \frac{e^{ipt}}{(ip)^2} - \frac{t}{ip} - \frac{1}{(ip)^2}$$

For low roll rates all three terms are significant to dispersion.

Equation 16 now becomes:

$$\begin{aligned} \vec{S} = & \left( \frac{Z_w + ipZ_{p\beta}}{m} \vec{K}_3 + \frac{Z_{\delta_\epsilon} \vec{\delta_\epsilon}}{m} \right) (1 - e^{ipt}) \frac{1}{p^2} + \left[ \frac{\vec{K}_4}{2} \left( \frac{Z_w + ipZ_{p\beta}}{m} \right) + \frac{ig}{2} \right] t^2 \\ & + \left[ \vec{S}_0 - \left( \frac{Z_w + ipZ_{p\beta}}{m} \right) \left( \frac{\vec{K}_1}{\phi_1} + \frac{\vec{K}_2}{\phi_2} \right) + \frac{\vec{K}_3}{ip} + \frac{iZ_{\delta_\epsilon} \vec{\delta_\epsilon}}{mp} \right] t + \vec{S}_0 \end{aligned} \quad (25)$$

The  $\vec{K}_3$  arm, or rolling trim vector must be separately examined.

From Equation 8,

$$\vec{K}_3 = \frac{\vec{N}_3}{(ip-\phi_1)(ip-\phi_2)}$$

or

$$\vec{K}_3 = \frac{\vec{N}_3}{(ip)^2 - ip(\phi_1 + \phi_2) + \phi_1\phi_2}$$

Numerical inspection of the three denominator terms indicates that the first two terms can be neglected. Each term is not only less than 1% of the third term but also they're subtracted from one another to make their contribution even more minimal. Thus  $K_3$  is approximated by,

$$\vec{K}_3 = -\frac{I_y}{md} \left[ \frac{ip C_{Z\delta_\epsilon} \vec{\delta_\epsilon} \left(1 - \frac{I_x}{I_y}\right) + i \frac{mud}{I_y} C_{M\delta_\epsilon} \vec{\delta_\epsilon}}{\left[ C_{M\alpha} + \frac{pI_x}{mud} \left(\frac{pd}{2u}\right) C_{Zp\beta} \right] + i \left[ C_{Mp\beta} \left(\frac{pd}{2u}\right) - \left(\frac{pI_x}{mud}\right) C_{Z\alpha} \right]} \right]$$

for low roll rates, the second term in the numerator and the first term in the denominator dominate all other terms and become the only significant terms. Thus,

$$\vec{K}_3 = -\frac{ui C_{M\delta_\epsilon} \vec{\delta_\epsilon}}{C_{M\alpha}} \quad (26)$$

The same approximation holds true for applicable terms in Equation 25, thus reducing the jump angle equation to:

$$\begin{aligned} \vec{J.A.} = & \left\{ \frac{ig}{2} \left( \frac{x}{u^2} \right) + \frac{\rho u^2 \pi d^2}{8mp^2} \left[ C_{Z\delta_\epsilon} \vec{\delta_\epsilon} - i \left( \frac{C_{Z\alpha}}{C_{M\alpha}} \right) C_{M\delta_\epsilon} \vec{\delta_\epsilon} \right] (1 - e^{ipt}) \right. \\ & + \left[ \frac{\vec{S}_0}{u} + i C_{Z\delta_\epsilon} \vec{\delta_\epsilon} \left( \frac{\rho u \pi d^2}{8mp} \right) - \frac{I_y}{mud} A \left[ \vec{\dot{\alpha}}_0 - C_{M\delta_\epsilon} \vec{\delta_\epsilon} \left( \frac{\rho u^2 \pi d^3}{8pI_y} \right) \right. \right. \\ & \left. \left. - C_{Z\delta_\epsilon} \vec{\delta_\epsilon} \left( 1 - \frac{I_x}{I_y} \right) \frac{\rho u \pi d^2}{8m} \right] + \frac{\vec{S}_0}{x} \right\} (10^3) \end{aligned}$$

Combining terms and dropping the negligible second last term,

$$\begin{aligned} \vec{J.A.} = & \left[ \frac{ig}{2} \left( \frac{x}{u^2} \right) + \frac{\rho u^2 \pi d^2}{8m} \left[ C_{Z\delta_\epsilon} \vec{\delta_\epsilon} - i \left( \frac{C_{Z\alpha}}{C_{M\alpha}} \right) C_{M\delta_\epsilon} \vec{\delta_\epsilon} \right] \left[ \frac{1}{p^2 x} + \frac{i}{pu} - \frac{e^{ipt}}{p^2 x} \right] \right. \\ & \left. + \left[ \frac{\vec{S}_0}{u} - \frac{I_y}{mud} \left( \frac{C_{Z\alpha}}{C_{M\alpha}} \right) \vec{\alpha}_0 \right] + \frac{\vec{S}_0}{x} \right] (10^3) \end{aligned} \quad (27)$$

Expanding  $e^{ipt}$  to  $\cos p \left( \frac{x}{u} \right) + i \sin p \left( \frac{x}{u} \right)$ ,

$$\begin{aligned} \vec{J.A.} = & \left\{ \frac{ig}{2} \left( \frac{x}{u^2} \right) + \frac{\rho u^2 \pi d^2}{8mx} \left[ C_{Z\delta_\epsilon} \vec{\delta_\epsilon} - i \left( \frac{C_{Z\alpha}}{C_{M\alpha}} \right) C_{M\delta_\epsilon} \vec{\delta_\epsilon} \right] \left[ \frac{1}{p^2} \left( 1 - \cos p \frac{x}{u} \right) \right. \right. \\ & \left. \left. + \frac{i}{p} \left( \frac{x}{u} - \frac{\sin p \frac{x}{u}}{p} \right) \right] + \left[ \frac{\vec{S}_0}{u} - \frac{I_y}{mud} \left( \frac{C_{Z\alpha}}{C_{M\alpha}} \right) \vec{\alpha}_0 \right] + \frac{\vec{S}_0}{x} \right\} (10^3) \end{aligned} \quad (28)$$

Equation 28 accurately approximates the jump angle for roll rates:

$$p > 100 \text{ rad/sec}$$

$$pt \geq 1.0$$

### Very Slow Roll Rate Theory

For very low roll rates; that is,  $p \geq 0$  and  $pt \leq 1$ , Equation 28 is again applicable.

One approximation is used, however, and that is that  $\cos \left( \frac{px}{u} \right)$  and  $\sin \left( \frac{px}{u} \right)$  are approximated by power series.

$$\begin{aligned} \cos \left( \frac{px}{u} \right) &= 1 - \frac{(px)^2}{2u^2} + \frac{(px)^4}{24u^4} - \frac{(px)^6}{720u^6} + \dots \\ \sin \left( \frac{px}{u} \right) &= \frac{px}{u} - \frac{(px)^3}{6u^3} + \frac{(px)^5}{120u^5} - \frac{(px)^7}{5040u^7} + \dots \end{aligned} \quad (29)$$

Substituting and simplifying,

$$\begin{aligned}
 \vec{J} \cdot \vec{A} = & \left\{ \frac{ig}{2} \left( \frac{x}{u^2} \right) + \frac{\rho \pi d^2 x}{16m} \left[ C_{z\delta_\epsilon} \vec{\delta}_\epsilon - i \left( \frac{C_{z\alpha}}{C_{M\alpha}} \right) C_{M\delta_\epsilon} \vec{\delta}_\epsilon \right] \right\} \left[ \left( 1 - \frac{1}{12} \left( \frac{px}{u} \right)^2 \right. \right. \\
 & \left. \left. + \frac{1}{360} \left( \frac{px}{u} \right)^4 \right) + i \left( \frac{px}{3u} - \frac{1}{60} \left( \frac{px}{u} \right)^3 + \frac{1}{2520} \left( \frac{px}{u} \right)^5 \right) \right] \\
 & + \left[ \frac{\vec{S}_o}{u} - \frac{L_y}{mud} \left( \frac{C_{z\alpha}}{C_{M\alpha}} \right) \vec{a}_o \right] + \frac{\vec{S}_o}{x} \Bigg\} (10^3)
 \end{aligned} \tag{30}$$



## VALIDATION OF THEORY

The theoretical expressions for Jump Angle; Equations 24, 28 and 30; show that the dispersion depends on the initial conditions, aerodynamic coefficients, distance downrange, and mass parameters. Dispersion for this theoretical analysis is defined to be the deviation from the line of fire. By analyzing only one Flechette configuration to validate the theory, the producibility Ground Point, and taking all cases to be evaluated at 1000 feet downrange, then the expression for the Jump Angle can only be affected by the initial conditions and aerodynamic coefficients.

To assure that the three equations for Jump Angle are valid and to show the effects for various initial conditions and aerodynamic coefficients, the expressions for the Jump Angle were evaluated for a series of cases and compared to numerical integration of the six-degree-of-freedom equations of motion, (6-D). A sample case run can be found in Appendix A-2. The series of cases is broken down into various phases of development. Phase I considers various initial conditions but with only the restoring and damping aerodynamic coefficients. This phase validates the use of initial conditions alone. Phase II utilizes a set of constant initial conditions, except for roll rate, and constant restoring and damping coefficients, while varying Magnus coefficients to determine their influence. Phase III brings into consideration all the aerodynamic coefficients to include the configurational asymmetry coefficients. Different coefficients are used by varying the initial velocity and roll

rates are varied to evaluate high, low, and very low roll theories. Phase IV considers the effects of gravity for various initial velocities and roll rates. No configurational asymmetries are used in order to isolate the gravitational influence. Values for all coefficients are found in Appendix A1, as well as other data including mass parameters. Since computations were done at 1000 ft downrange, the Jump Angle in mils is equivalent to the deviation from the line of fire in feet for all presented cases. The axis system used throughout this analysis is illustrated in the list of symbols.

#### Phase I

To validate the effects of initial conditions with restoring and damping coefficients only, 36 cases were evaluated using the high roll rate theory, Equation 24. The cases are divided into 4 sections isolating different initial conditions and their effects.

#### Cases 1-9

The first section shows the effects of roll rate and velocity with zero  $\vec{S}_0$ ,  $\vec{\alpha}_0$  and  $\vec{\dot{\alpha}}_0$

TABLE I  
THEORY VALIDATION, RESTORING AND  
DAMPING MOMENTS, CASES 1-9

C A S E	Initial Conditions					Coefficients			$\overrightarrow{J.A}$ (mils)	
						$C_{Z\alpha}$ $C_{M\alpha}$ $C_{M_q} + C_{M_{\dot{\alpha}}}$	$C_{Zp\beta}$ $C_{M_{p\beta}}$	$C_{YE}$ $C_{ZE}$ $C_{ME}$ $C_{NE}$	6-D	Theory
	$\overrightarrow{S}_0$	$\overrightarrow{\alpha}_0$	$\overrightarrow{\dot{\alpha}}_0$	$p_0$	$u_0$					
1	0	0	0	31416	5000	$\updownarrow$ A1	$\updownarrow$ 0	$\updownarrow$ 0	0 + 0i	J + 0i
2	0	0	0	18850					0 + 0i	0 + 0i
3	0	0	0	6283					0 + 0i	0 + 0i
4	0	0	0	31416	3000				0 + 0i	0 + 0i
5	0	0	0	18850					0 + 0i	0 + 0i
6	0	0	0	6283					0 + 0i	0 + 0i
7	0	0	0	31416	1000				0 + 0i	0 + 0i
8	0	0	0	18850					0 + 0i	0 + 0i
9	0	0	0	6283					0 + 0i	0 + 0i

Table I clearly indicates that no deviation from the line of fire occurs if  $\vec{S}_0$ ,  $\vec{\alpha}_0$ , and  $\vec{\dot{\alpha}}_0$  are set to zero. Roll rate and velocity changes have no effect on the Jump Angle for this particular situation. This is a trivial solution, it being obvious from inspection of Equation 24.

#### Cases 10-18

The second section gives the effects of initial translational velocity,  $\vec{S}_0 = \vec{y} + i\vec{z}$ , with various roll rates and velocities. To assure the solution is correct in three dimensional space, the initial translation velocity is given in both y and iz directions. Equation 24 reduces to:

$$\vec{J.A.} = \frac{1000}{u} \vec{S}_0$$

TABLE II  
THEORY VALIDATION, RESTORING AND  
DAMPING MOMENTS, CASES 10-18

C A S E	Initial Conditions					Coefficients			$\begin{matrix} C_{YE} \\ C_{ZE} \\ C_{ME} \\ C_{NE} \end{matrix}$	$\overrightarrow{J.A.}$ (mils)	
	$\overrightarrow{s}_0$	$\overrightarrow{\alpha}_0$	$\overrightarrow{\dot{\alpha}}_0$	$p_0$	$u_0$	$\begin{matrix} C_{Z\alpha} \\ C_{M\alpha} \end{matrix}$	$C_{Zp\beta}$	$\begin{matrix} C_{Mq} + C_{M\dot{\alpha}} \\ C_{Mp\beta} \end{matrix}$		6-D	Theory
10	$\begin{matrix} 100+ \\ 100i \end{matrix}$	0	0	31416	5000	$\downarrow$         $A1$	$\downarrow$         0	$\downarrow$         0	$\begin{matrix} 20.002 + \\ 20.006 i \end{matrix}$	$\begin{matrix} 20.000 + \\ 20.000 i \end{matrix}$	
11	$\begin{matrix} 100+ \\ 100i \end{matrix}$	0	0	18850					$\begin{matrix} 20.002 + \\ 20.006 i \end{matrix}$	$\begin{matrix} 20.000 + \\ 20.000 i \end{matrix}$	
12	$\begin{matrix} 100+ \\ 100i \end{matrix}$	0	0	6283					$\begin{matrix} 20.002 + \\ 20.006 i \end{matrix}$	$\begin{matrix} 20.000 + \\ 20.000 i \end{matrix}$	
13	$\begin{matrix} 100+ \\ 100i \end{matrix}$	0	0	31416	3000				$\begin{matrix} 33.346 + \\ 33.368 i \end{matrix}$	$\begin{matrix} 33.333 + \\ 33.333 i \end{matrix}$	
14	$\begin{matrix} 100+ \\ 100i \end{matrix}$	0	0	18850					$\begin{matrix} 33.346 + \\ 33.368 i \end{matrix}$	$\begin{matrix} 33.333 + \\ 33.333 i \end{matrix}$	
15	$\begin{matrix} 100+ \\ 100i \end{matrix}$	0	0	6283					$\begin{matrix} 33.346 + \\ 33.368 i \end{matrix}$	$\begin{matrix} 33.333 + \\ 33.333 i \end{matrix}$	
16	$\begin{matrix} 100+ \\ 100i \end{matrix}$	0	0	31416	1000				$\begin{matrix} 100.254 + \\ 100.765 i \end{matrix}$	$\begin{matrix} 100.000 + \\ 100.000 i \end{matrix}$	
17	$\begin{matrix} 100+ \\ 100i \end{matrix}$	0	0	18850					$\begin{matrix} 100.254 + \\ 100.764 i \end{matrix}$	$\begin{matrix} 100.000 + \\ 100.000 i \end{matrix}$	
18	$\begin{matrix} 100+ \\ 100i \end{matrix}$	0	0	6283					$\begin{matrix} 100.257 + \\ 100.765 i \end{matrix}$	$\begin{matrix} 100.000 + \\ 100.000 i \end{matrix}$	

The correlation between the theory and the 6-D integration for Cases 10-18 is excellent as shown in Table II. The Jump Angle is seen to be affected by velocity but not roll rate, as would be expected from the reduced Jump Angle equation. Figure I illustrates the deviation from the line of fire for initial velocities of 5000 ft/sec (Cases 10-12), 3000 ft/sec (Cases 13-15) and 1000 ft/sec (Cases 16-18). Since the theory and 6-D

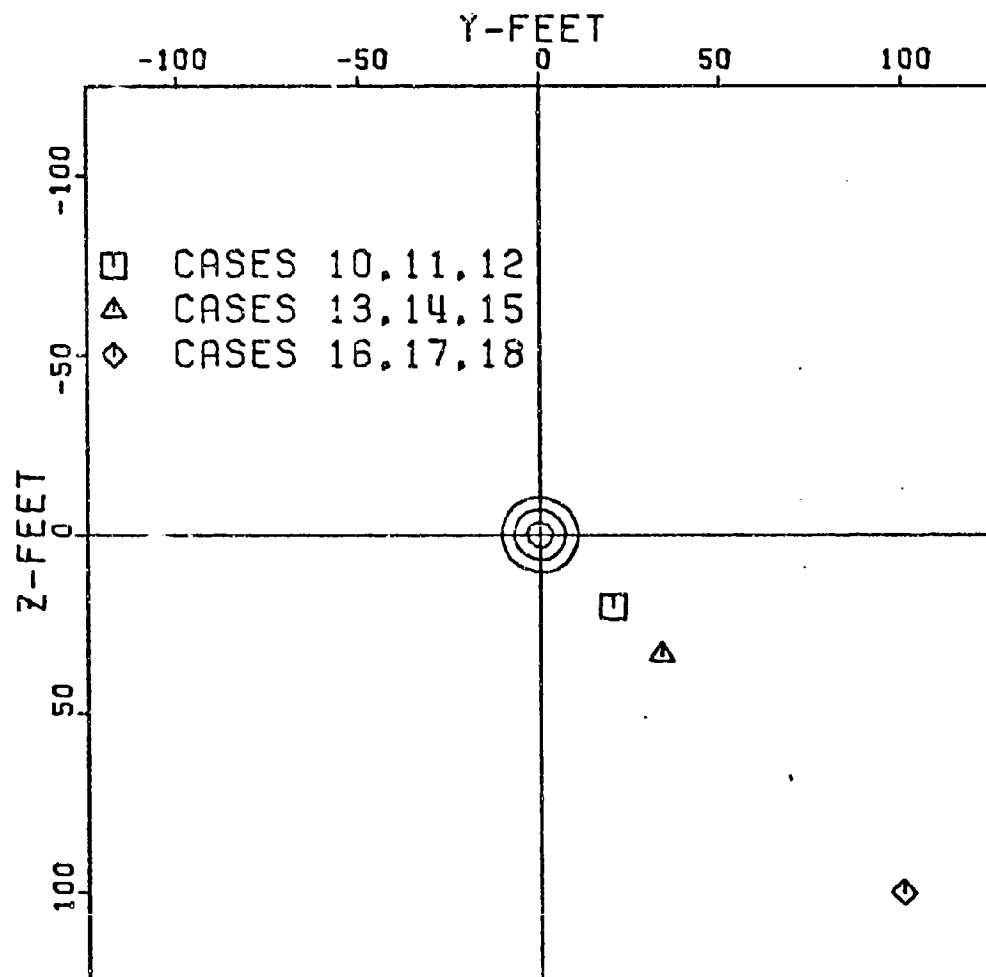


Figure 1. Dispersion: Phase I Cases 10-18

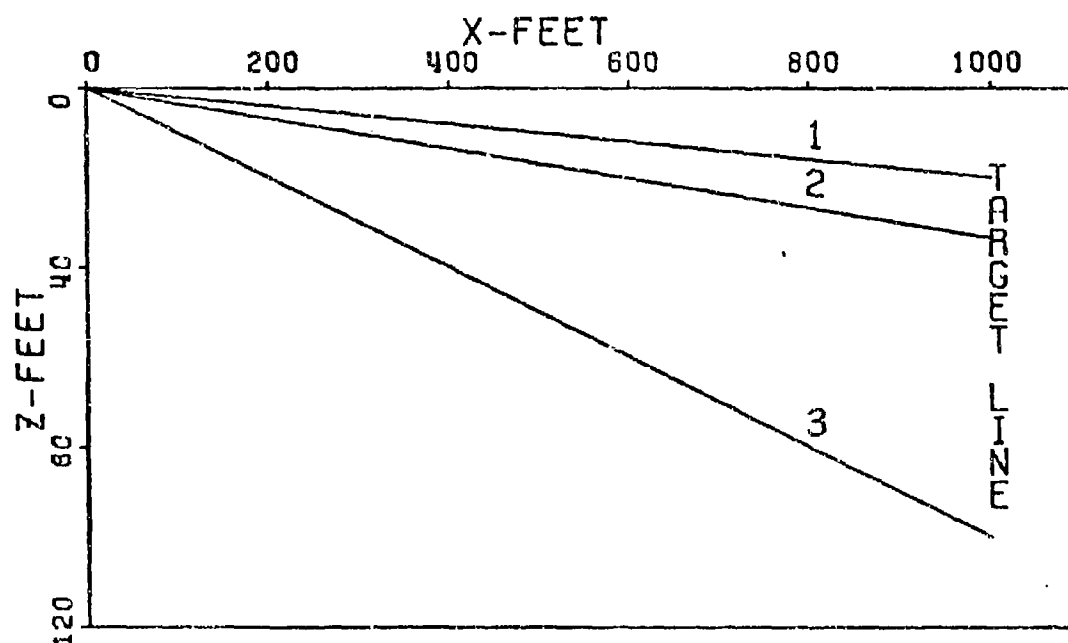
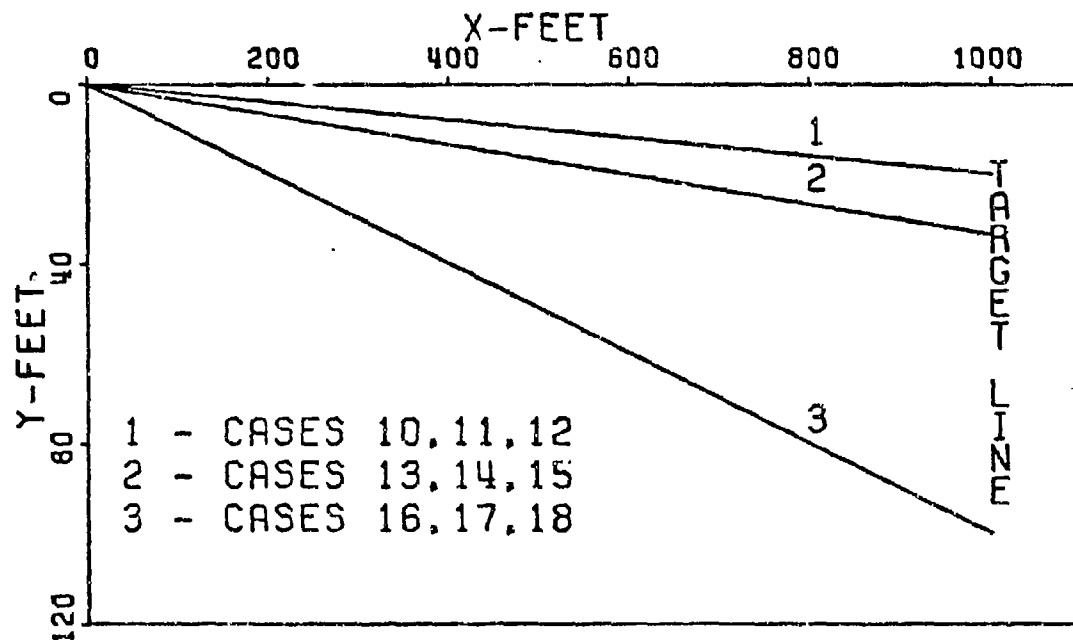


Figure 2. Trajectories, Cases 10-18

are so close, they are plotted as one point. Figure 2 illustrates the trajectory in both the x-y and x-z planes. The deviation from the line of fire is linear with distance downrange in both planes. This would be expected with no gravitational force acting.

#### Cases 19-27

The third section gives the effects of initial angle of attack,  $\vec{\alpha}_0$ , with various roll rates and velocities. Again a complex initial condition is used to validate the theory in three dimensional space. Equation 24 reduces to:

$$\vec{J.A.} = i\vec{\alpha}_0 \left( \frac{pI_x}{mud} \right) \left[ \frac{C_{Z\alpha}}{C_{M\alpha} - i \left( \frac{pI_x}{mud} \right) C_{Z\alpha}} \right] 1000$$

Table III shows the range of error between the 6-D computation and the theory to be 0.036 to 0.040 mils in the y-direction and 0.038 to 0.041 mils in the z-direction. Although the y-direction deviations differ in sign, the error between them is approximately 0.00225 degrees, an extremely small angle. This angle will give an approximate deviation of 0.04 feet from the line of fire at 1000 feet downrange. With the  $\vec{J.A.}$  being so close to zero it can be expected that the signs may differ due to computational errors. The results do show Jump Angle variance with both roll rate and velocity. The largest changes occur as velocity goes to 1000 ft/sec.

TABLE III  
THEORY VALIDATION, RESTORING AND  
DAMPING MOMENTS, CASES 19-27

C A S E	Initial Conditions					Coefficients			$\overline{J}, \overline{A}$ . (mils)	
						$C_{Z\alpha}$ $C_{M\alpha}$ $C_{M_q} + C_{M_{\dot{\alpha}}}$	$C_{Zp\beta}$ $C_{M_{p\beta}}$	$C_{YE}$ $C_{ZE}$ $C_{ME}$ $C_{NE}$	6-D	Theory
	$\overline{\xi}_0$	$\overline{\alpha}_0$	$\overline{\dot{\alpha}}_0$	$p_0$	$u_c$					
19	0	1+i	0	31416	5000	A.1	0	0	0.012+	-0.027
20	0	1+i	0	18850					0.068i	+0.027i
21	0	1+i	0	6283					0.023+	-0.017
22	0	1+i	0	31416	3000				0.058i	+0.017i
23	0	1+i	0	18850					0.034+	-0.006
24	0	1+i	0	6283					0.047i	+0.006i
25	0	1+i	0	31416	1000				0.012+	-0.026
26	0	1+i	0	18850					0.067+	+0.026i
27	0	1+i	0	6283					0.022+	-0.016
									0.056i	+0.016i
									0.033+	-0.005
									0.046i	+0.005i
									-0.037+	-0.073
									0.111i	+0.073i
									-0.008+	-0.044
									0.082i	+0.044i
									0.021+	-0.015
									0.053i	+0.015i

Cases 28-36

The fourth section gives the effects of initial angular rate  $\dot{\bar{\alpha}}_0$ , with varying roll rate and velocity. An angular rate of 250 rad/sec is used in both directions of the complex plane to test validity in three dimensional space. Equation 24 reduces to:



$$\vec{J.A.} = -\vec{\alpha}_0 \left( \frac{I_y}{\text{mud}} \right) \left[ \frac{CZ_\alpha}{C_{M_\alpha} - i \left( \frac{pI_x}{\text{mud}} \right) CZ_\alpha} \right] 1000$$

TABLE IV

THEORY VALIDATION, RESTORING AND  
DAMPING MOMENTS, CASES 28-36

C A S E	Initial Conditions					Coefficients			$\overline{J.A.}$ (mils)	
						$C_{Z\alpha}$ $C_{M\alpha}$ $C_{M_q} + C_{M\dot{\alpha}}$	$C_{Zp\beta}$ $C_{M_{p\beta}}$	$C_{YE}$ $C_{ZE}$ $C_{ME}$ $C_{NE}$	6-D	Theory
	$\vec{s}_0$	$\vec{\alpha}_0$	$\vec{\dot{\alpha}}_0$	$p_0$	$u_0$					
28	0	0	250+ 250i	31416	5000	A1	0	0	-2.027 -2.034i	-2.073 -2.073i
29	0	0	250+ 250i	18850					-2.025 -2.030i	-2.073 -2.073i
30	0	0	250+ 250i	6283					-2.027 -2.029i	-2.073 -2.073i
31	0	0	250+ 250i	31416	3000				-1.961 -1.967i	-1.970 -1.970i
32	0	0	250+ 250i	18850					-1.962 -1.966i	-1.970 -1.970i
33	0	0	250+ 250i	6283					-1.964 -1.964i	-1.970 -1.970i
34	0	0	250+ 250i	31416	1000				-5.238 -5.274i	-5.540 -5.540i
35	0	0	250+ 250i	18850					-5.243 -5.264i	-5.540 -5.540i
36	0	0	250+ 250i	6283					-5.254 -5.260i	-5.540 -5.540i

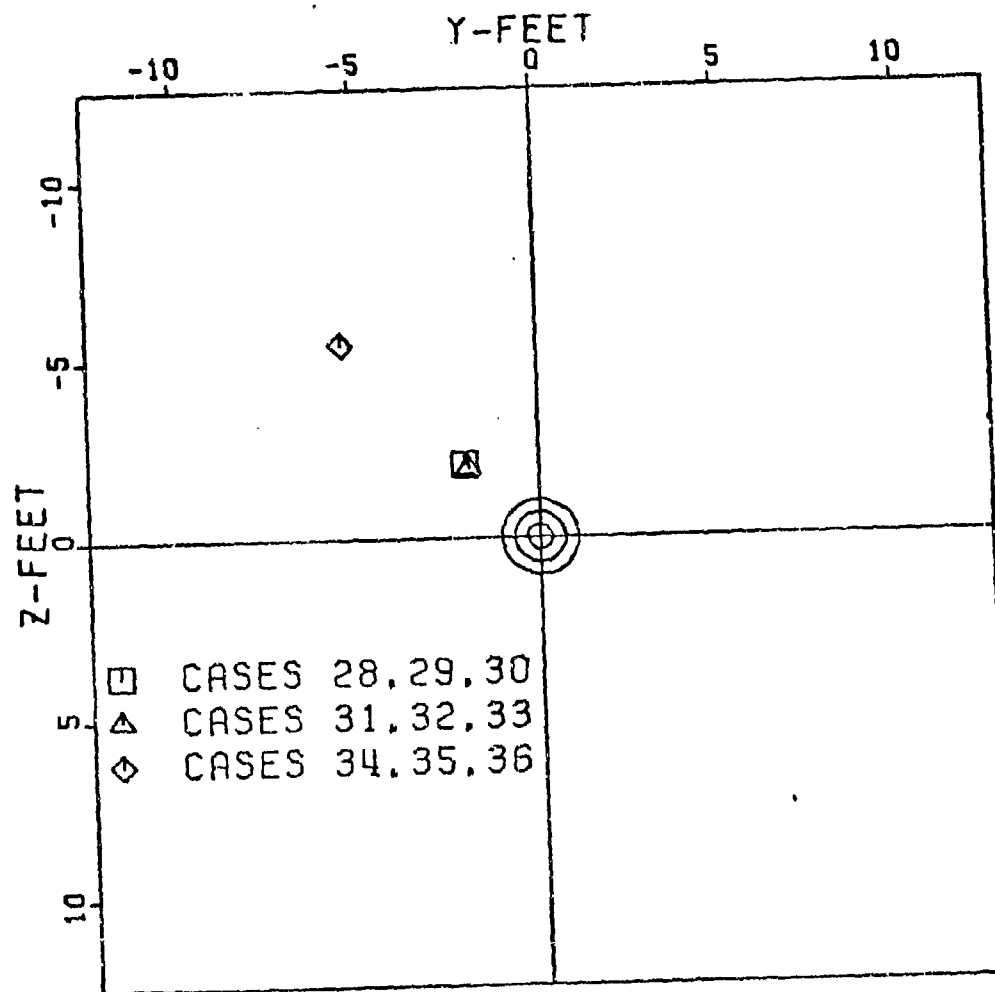


Figure 3. Dispersion: Phase I Cases 28-36

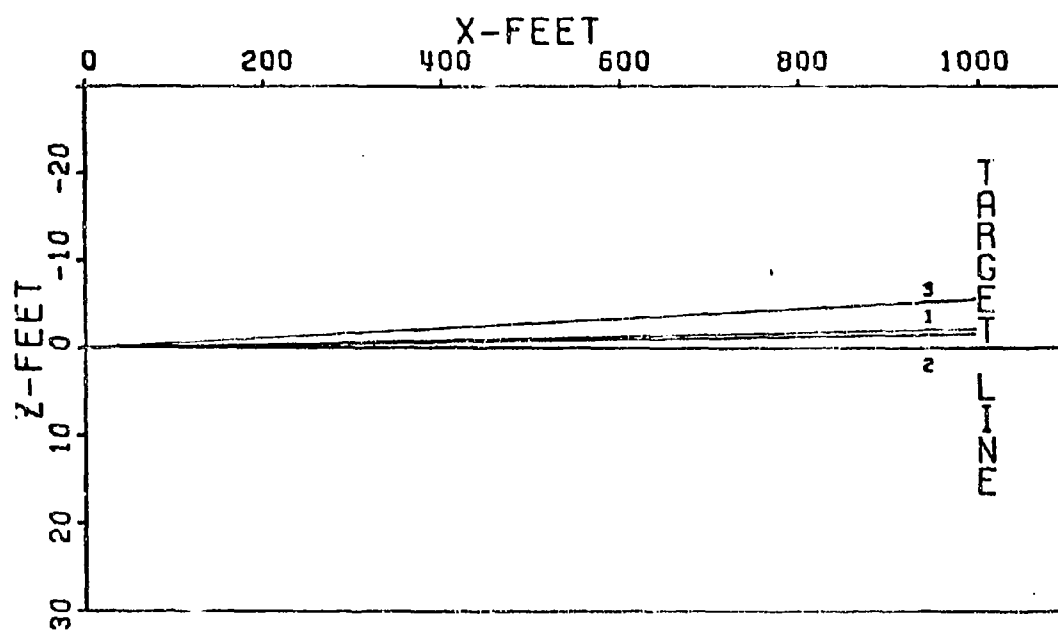
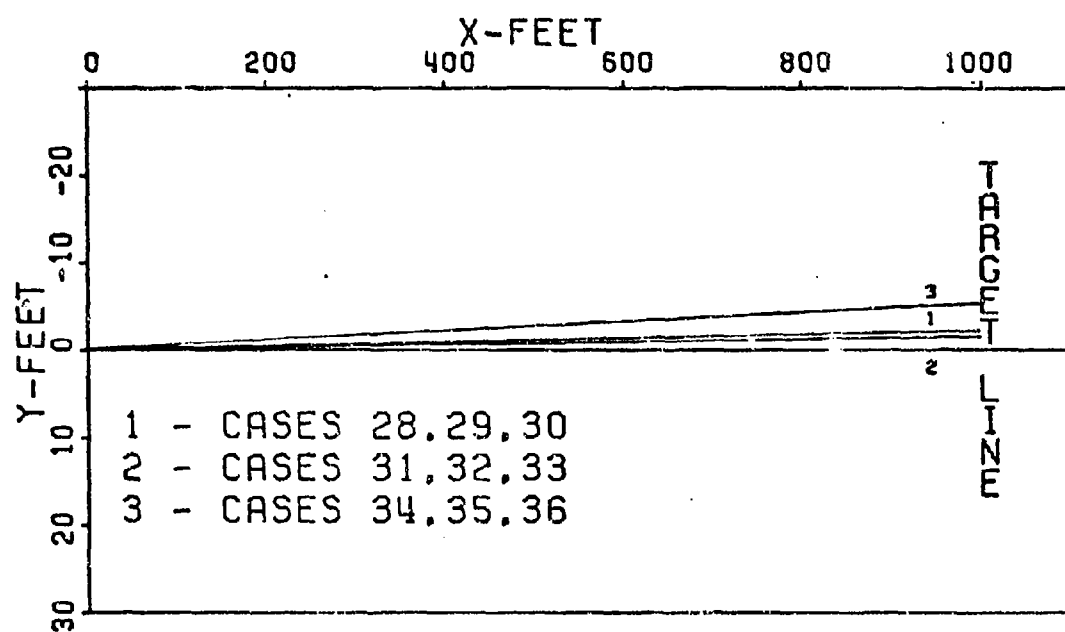


Figure 4. Trajectories, Cases 28-36

Table IV indicates excellent agreement between the theory and 6-D computations. Roll rate is found not to affect the Jump Angle appreciably but velocity does, as would be expected from the reduced Jump Angle equation. Figure 3 shows the dispersion pattern while Figure 4 illustrates the trajectories. Cases 28, 29, and 30 are plotted as one point due to the small difference between them. Cases 31, 32, 33 and 34, 35, and 36 are plotted similarly.

## Phase II

To validate the effect of Magnus Forces and Moments on the dispersion of flechettes, 21 Cases were run varying the initial roll rate and Magnus Coefficients. All other conditions were held constant. The variance of Magnus coefficients with Mach number had to be chosen since no data was available. Arbitrarily, the ratio of  $C_{z_{p\beta}}/C_{M_{p\beta}}$  was chosen to be the same as that of  $C_{z_{\alpha}}/C_{M_{\alpha}}$ . The Magnus Coefficients used are presented as functions of Mach Number in Appendix A1 with only the values at Mach 4.5 tabulated here for identification sake:

TABLE V  
MAGNUS COEFFICIENTS,  
AT MACH 4.5

$C_{z_{p\beta}}$	$C_{M_{p\beta}}$
$\pm 34.8$	$\pm 110.0$
$\pm 31.6$	$\pm 100.0$
$\pm 28.4$	$\pm 90.0$

Equation 24 now becomes:

$$\vec{J.A.} = \left[ \frac{\vec{S}_O}{u} - \frac{I_y}{mud} \left[ \vec{\alpha}_O - i \vec{\alpha}_O \left( \frac{p I_x}{I_y} \right) \right] \right. \\ \left. \left[ \frac{C_{Z_\alpha} + i \left( \frac{pd}{2u} \right) C_{Z_{p\beta}}}{\left( C_{M_\alpha} + \frac{p I_x}{mud} \frac{pd}{2u} C_{Z_{p\beta}} \right) + i \left( C_{M_{p\beta}} \frac{pd}{2u} - \frac{p I_x}{mud} C_{Z_\alpha} \right)} \right] \right] 1000$$

Initial conditions used in this section are consistent with those of other sections to provide a basis for comparison. Three cases of zero Magnus were run, one at each roll rate to provide a standard to judge the influence of Magnus.

The effects of Magnus coefficients on dispersion are minimal as seen in Table VI. The variance between the zero Magnus cases and any other case is found not to be greater than 0.209 mils (or feet at 1000 feet of range). In order to obtain the maximum Magnus effects, the largest possible Magnus coefficients were used. Hence,  $C_{Z_{p\beta}} = 34.8$  and  $C_{M_{p\beta}} = 110.0$  are the largest possible coefficients since cases 40 and 49 become unstable. Table VI indicates the effects (for positive Magnus coefficients)

- (1) increasing horizontal dispersion with increasing p
- (2) decreasing vertical dispersion with increasing p
- (3) increasing horizontal dispersion with increasing Magnus
- (4) decreasing vertical dispersion with increasing Magnus

TABLE VI  
THEORY VALIDATION, MAGNUS, CASES 37-57

C A S E	Magnus Forces & Moments	Roll Rate	$p_o$	$p_o$	$p_c$
			31416 rad/sec	18850 rad/sec	6283 rad/sec
37	$C_{Z_{p\beta}} = 0.0$		(6-D) 17.994+	(6-D) 18.003+	(6-D) 18.013+
38	$C_{M_{p\beta}} = 0.0$		18.042i Theory	18.032i Theory	18.022i Theory
39			17.900+ 17.954i	17.910+ 17.944i	17.921+ 17.933i
40	$C_{Z_{p\beta}} = 34.8$		Unstable	18.141+ 17.903i	18.057+ 17.979i
41	$C_{M_{p\beta}} = 110.0$			17.909+ 17.942i	17.920+ 17.931i
42					
43	$C_{Z_{p\beta}} = 31.6$		18.203+ 17.849i	18.123+ 17.915i	18.053+ 17.982i
44	$C_{M_{p\beta}} = 100.0$		17.899 17.954i	17.909 17.942i	17.920+ 17.931i
45					
46	$C_{Z_{p\beta}} = 28.4$		18.183+ 17.869i	18.114+ 17.925i	18.050+ 17.987i
47	$C_{M_{p\beta}} = 90.0$		17.899 17.954i	17.909 17.942i	17.920+ 17.931i
48					
49	$C_{Z_{p\beta}} = -34.8$		Unstable	17.877+ 18.170i	17.969+ 18.067i
50	$C_{M_{p\beta}} = -110.0$			17.090+ 17.942i	17.920+ 17.931i
51					
52	$C_{Z_{p\beta}} = -31.6$		17.807+ 18.258i	17.888+ 18.158i	17.973+ 18.063i
53	$C_{M_{p\beta}} = -100.0$		17.899+ 17.954i	17.909+ 17.942i	17.920+ 17.931i
54					
55	$C_{Z_{p\beta}} = -28.4$		17.826+ 18.233i	17.900+ 18.144i	17.977+ 18.059i
56	$C_{M_{p\beta}} = -90.0$		17.899+ 17.954i	17.909+ 17.942i	17.820+ 17.931i
57					

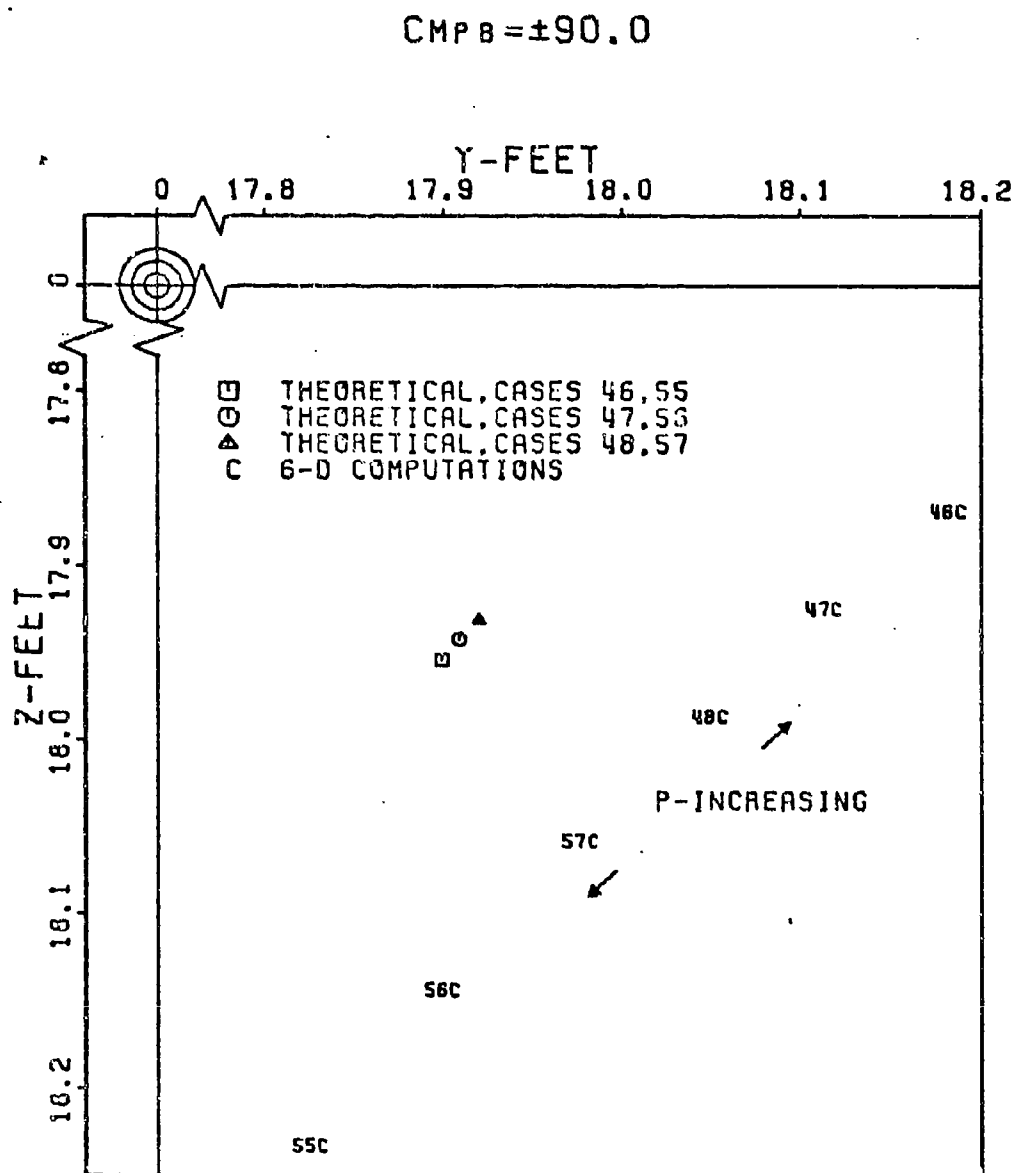


Figure 5. Dispersion: Phase II Cases 46,47,48,55,56,57

$P=18850 \text{ RAD/SEC}$

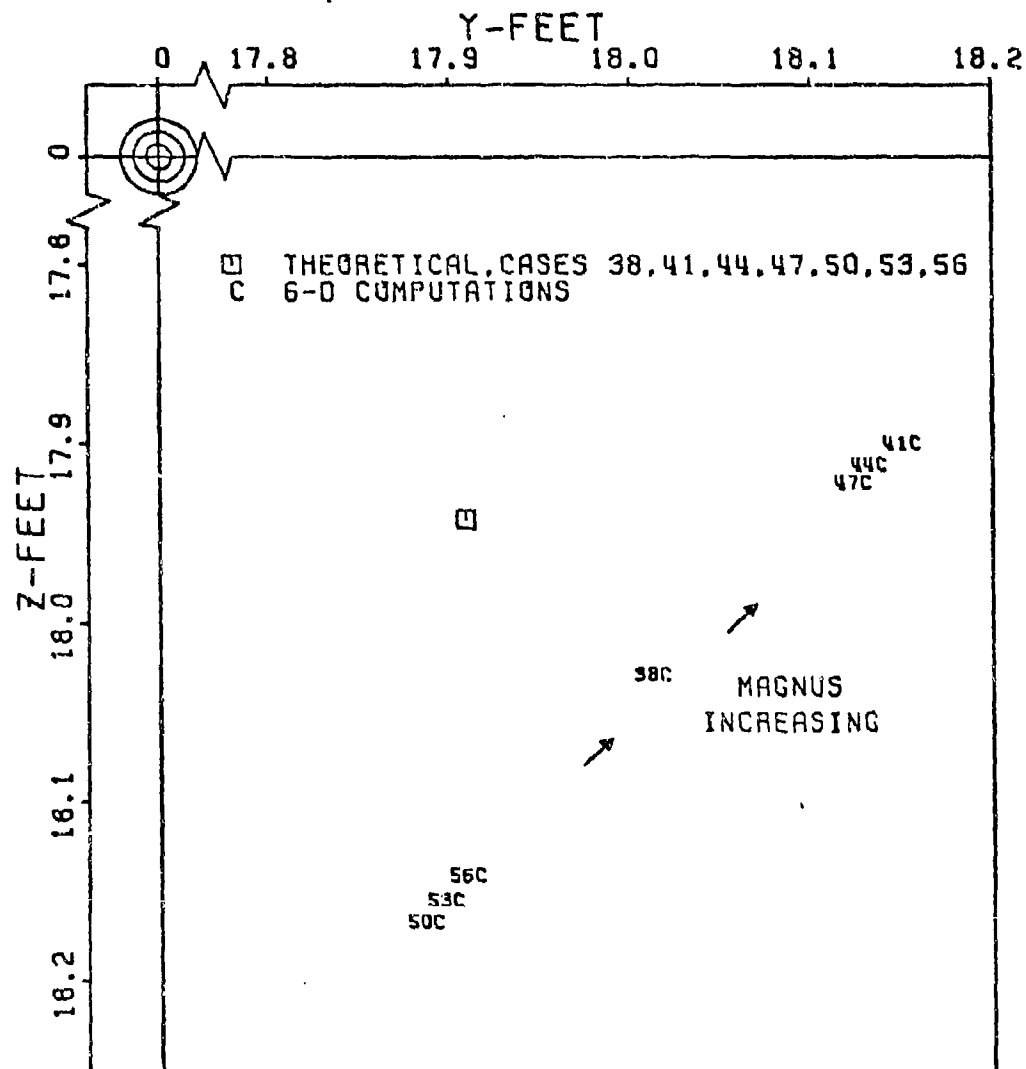


Figure 6. Dispersion: Phase II Cases 38, 41, 44, 47, 50, 53, 56



(for negative Magnus coefficients)

- (5) decreasing horizontal dispersion with increasing  $p$
- (6) increasing vertical dispersion with increasing  $p$
- (7) decreasing horizontal dispersion with decreasing Magnus
- (8) increasing vertical dispersion with decreasing Magnus

For example, Figure 5 illustrates the effects of roll rate for constant Magnus coefficients of  $\pm 90^\circ$  (1,2,5,6 above). Figure 6 illustrates the effects of Magnus for a constant sample roll rate (3,4,7,8 above).

Obviously, when only a 0.209 mil maximum deviation due to Magnus occurs when the situation is geared toward finding the largest effect due to Magnus, smaller deviations due to Magnus would be found in actual situations. It can be concluded that Magnus has no large effect on dispersion although it could be significant if the total dispersion is close to zero.

### Phase III

To validate the effects of aerodynamic asymmetries on dispersion of flechettes, a large number of cases were run varying roll rate, velocity, and initial conditions while holding the asymmetry coefficients constant. The asymmetries coefficients were selected to allow  $1^\circ$  of non-rolling trim to exist while the flechette was in flight. The asymmetry coefficients,  $C_{YE}$ ,  $C_{ZE}$ ,  $C_{ME}$  and  $C_{NE}$  are presented in Appendix A-1 as a function of Mach number. The variance with Mach number was chosen arbitrarily: the ratio of asymmetry force to asymmetry moment identical to the ratio

of  $C_{Z\alpha}$  to  $C_{M\alpha}$ . The wide range of roll rates makes mandatory use of all three dispersion theories. The governing equations are presented as they apply.

#### Cases 58-90

The first set of cases utilizes zero initial disturbances while varying velocity and roll rate. For roll rates of 31416 rad/sec down to 100 rad/sec the High Roll Rate Theory yields the governing equation,

$$\vec{J} \cdot \vec{A} = \frac{\rho u \pi d^2}{8m} \left[ C_{M\delta_\epsilon} \vec{\delta}_\epsilon \left( \frac{A}{p} \right) + C_{Z\delta_\epsilon} \vec{\delta}_\epsilon \left( \frac{I_y - I_x}{mud} A + \frac{i}{p} \right) \right] 1000$$

For roll rates:  $p < 100$  rad/sec and  $pt \geq 1.0$ , the Low Roll Rate Theory takes effect:

$$\vec{J} \cdot \vec{A} = \frac{\rho u^2 \pi d^2}{8mx} \left[ C_{Z\delta_\epsilon} \vec{\delta}_\epsilon - i \left( \frac{C_{Z\alpha}}{C_{M\alpha}} \right) C_{M\delta_\epsilon} \vec{\delta}_\epsilon \right] \left[ \frac{1}{p^2} \left( 1 - \cos \frac{px}{u} \right) + \frac{1}{p} \left( \frac{x}{u} - \frac{1}{p} \sin \frac{px}{u} \right) \right] 1000$$

Finally, the very Slow Roll Rate Theory applies for values of  $pt < 1.0$ :

$$\vec{J} \cdot \vec{A} = \frac{\rho \pi d^2 x}{16m} \left[ C_{Z\delta_\epsilon} \vec{\delta}_\epsilon - i \left( \frac{C_{Z\alpha}}{C_{M\alpha}} \right) C_{M\delta_\epsilon} \vec{\delta}_\epsilon \right] \left[ \left( 1 - \frac{1}{12} \left( \frac{px}{u} \right)^2 + \frac{1}{360} \left( \frac{px}{u} \right)^4 \right) + i \left( \frac{px}{3u} - \frac{1}{60} \left( \frac{px}{u} \right)^3 + \frac{1}{2520} \left( \frac{px}{u} \right)^5 \right) \right] 1000$$

Tables 7, 8, and 9 list Cases 58-90:

TABLE VII  
THEORY VALIDATION, ASYMMETRIES,  
CASES 58-68

C A S E	Initial Conditions					Coefficients			$\vec{J.A.}$ (mils)	
	$\vec{s}_o$	$\vec{\alpha}_o$	$\vec{\dot{\alpha}}_o$	$p_o$	$u_o$	$C_{Z\alpha}$	$C_{Z_{p\beta}}$	$C_{YE}$	6-D	Theory
						$C_{M\alpha}$		$C_{ZE}$		
						$C_{M_q} + C_{M\dot{\alpha}}$	$C_{M_{p\beta}}$	$C_{ME}$ $C_{NE}$		
58	0	0	0	31416	5000	A1	A1	A1	0.018- 0.013i	0.018- 0.014i
59	0	0	0	18850					0.030- 0.027i	0.029- 0.025i
60	0	0	0	6283					0.060- 0.127i	0.064- 0.130i
61	0	0	0	500					0.997- 0.992i	1.013- 1.009i
62	0	0	0	300					1.620- 1.721i	1.688- 1.683i
63	0	0	0	100					4.574- 4.896i	4.675- 4.975i
64	0	0	0	50					8.666- 12.280i	8.780- 12.489i
65	0	0	0	25					20.669- 26.418i	21.150- 26.927i
66	0	0	0	10					-7.973- -62.197i	-8.210- -63.210i
67	0	0	0	5					-29.857- -61.459i	-30.372- -62.353i
68	0	0	0	0					-49.706- -49.706i	-50.427- -50.427i

TABLE VIII  
THEORY VALIDATION, ASYMMETRIES,  
CASES 69-79

C A S E	Initial Conditions					Coefficients			$\bar{J}. \bar{A}.$ (mils)	
						$C_{Z\alpha}$ $C_{M\alpha}$ $C_{M_q} + C_{M_{\dot{\alpha}}}$	$C_{Z_{p\beta}}$ $C_{M_{p\beta}}$	$C_{YE}$ $C_{ZE}$ $C_{ME}$ $C_{NE}$		
	$\bar{S}_0$	$\bar{\alpha}_0$	$\bar{\dot{\alpha}}_0$	$p_0$	$u_0$				6-D	Theory
69	0	0	0	31416	3000	A1	A1	A1	0.008- 0.004i	0.009- 0.004i
70	0	0	0	18850					0.013- 0.008i	0.013- 0.008i
71	0	0	0	6283					0.033- 0.028i	0.034- 0.029i
72	0	0	0	500					0.394- 0.398i	0.401- 0.396i
73	0	0	0	300					0.663- 0.659i	0.666- 0.662i
74	0	0	0	100					1.841- 1.998i	1.994- 1.984i
75	0	0	0	50					3.780- 4.513i	3.411- 4.164i
76	0	0	0	25					5.676- 8.457i	5.721- 8.516i
77	0	0	0	10					9.203- 32.628i	9.217- 32.897i
78	0	0	0	5					-41.029- -41.985i	-42.273i -42.273i
79	0	0	0	0					-33.014 -33.014i	-33.194 -33.194i

TABLE IX  
THEORY VALIDATION, ASYMMETRIES,  
CASES 80-90

C A S E	Initial Conditions					Coefficients			J.A. (mils)	
						$C_{Z\alpha}$ $C_{M\alpha}$ $C_{Mq}+C_{M\dot{\alpha}}$	$C_{Zp\beta}$ $C_{Mp\beta}$	$C_{YE}$ $C_{ZE}$ $C_{ME}$ $C_{NE}$	6-D	Theory
	$\vec{s}_0$	$\vec{\alpha}_0$	$\vec{\dot{\alpha}}_0$	$p_0$	$u_0$					
80	0	0	0	31416	1000	$\Delta 1$	$\Delta 1$	$\Delta 1$	Unstable	
81	0	0	0	18850					Unstable	
82	0	0	0	6283					0.025- 0.010i	0.023- 0.014i
83	0	0	0	500					0.241- 0.229i	0.238- 0.229i
84	0	0	0	300					0.396- 0.380i	0.394- 0.385i
85	0	0	0	100					1.177- 1.160i	1.174- 1.165i
86	0	0	0	50					2.346- 2.329i	2.349- 2.352i
87	0	0	0	25					4.684- 4.672i	4.699- 4.702i
88	0	0	0	10					10.224- 14.447i	10.177- 14.476i
89	0	0	0	5					24.402- 31.013i	24.516- 31.212i
90	0	0	0	0	-58.711 -58.711i	-58.450 -58.450i				

Evident from Tables VII, VIII, IX is the fact that roll rate has tremendous influence on the dispersion of flechettes with aerodynamic asymmetries. Figures 7, 8, and 9 illustrate the dispersion pattern for these cases. The 6-D computations and theory are in very good agreement considering the large deviations involved. It should be noted that the actual flechette with its velocity approaching 5000 ft/sec is affected very little by aerodynamic asymmetries. However, if the flechette were only to roll very slowly, large dispersion ranges in excess of 60 mils could occur. Velocity also has a noticeable effect on dispersion. Figure 10 shows the three theory curves from Figures 7, 8, 9 in composite to illustrate velocity effects. A sample trajectory, Case 79, is shown in Figure 11, illustrating the curved path of flight. This is typical of trajectories involving aerodynamic asymmetries.

### Cases 91-123

To show the relation between the effects on dispersion for initial transverse velocity and aerodynamic asymmetries a second set of cases were run. Roll rate and velocity were varied as in the first set of cases, but  $\vec{S}_0$  was set at  $(100 + 100i)$  ft/sec with  $\vec{\alpha}_0 = 0$  and  $\vec{\dot{\alpha}}_0 = 0$ . Tables X, XI, and XII list the results. For high roll rate cases, Equation 24 becomes:

$$\vec{J.A.} = \left[ \frac{\vec{S}_0}{u} + \frac{\rho u \pi d^2}{8m} \left[ C_{M_{\delta_\epsilon}} \vec{\delta_\epsilon} \left( \frac{\Lambda}{p} \right) + C_{Z_{\delta_\epsilon}} \vec{\delta_\epsilon} \left( \frac{I_y - I_x}{m u d} \Lambda + \frac{i}{p} \right) \right] \right] 1000$$

For low rate cases, Equation 28 becomes:

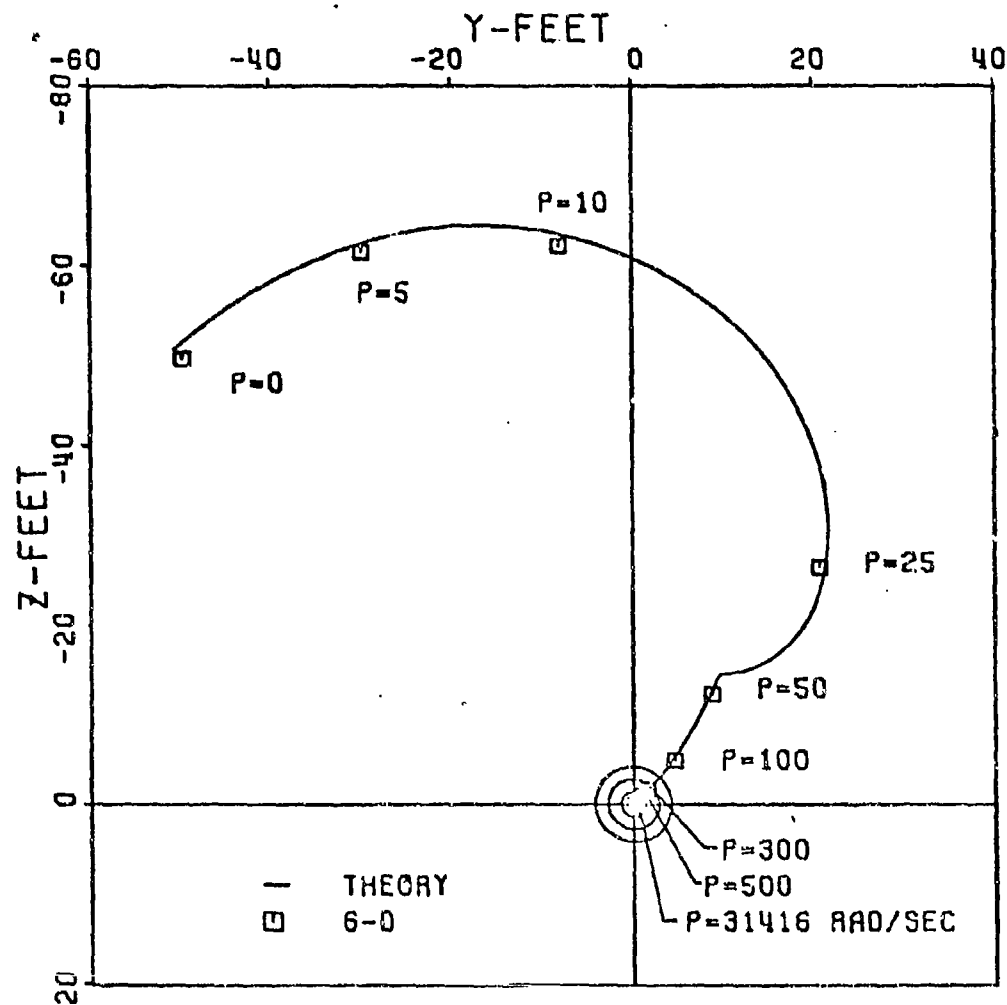


Figure 7. Dispersion: Phase III Cases 58-68

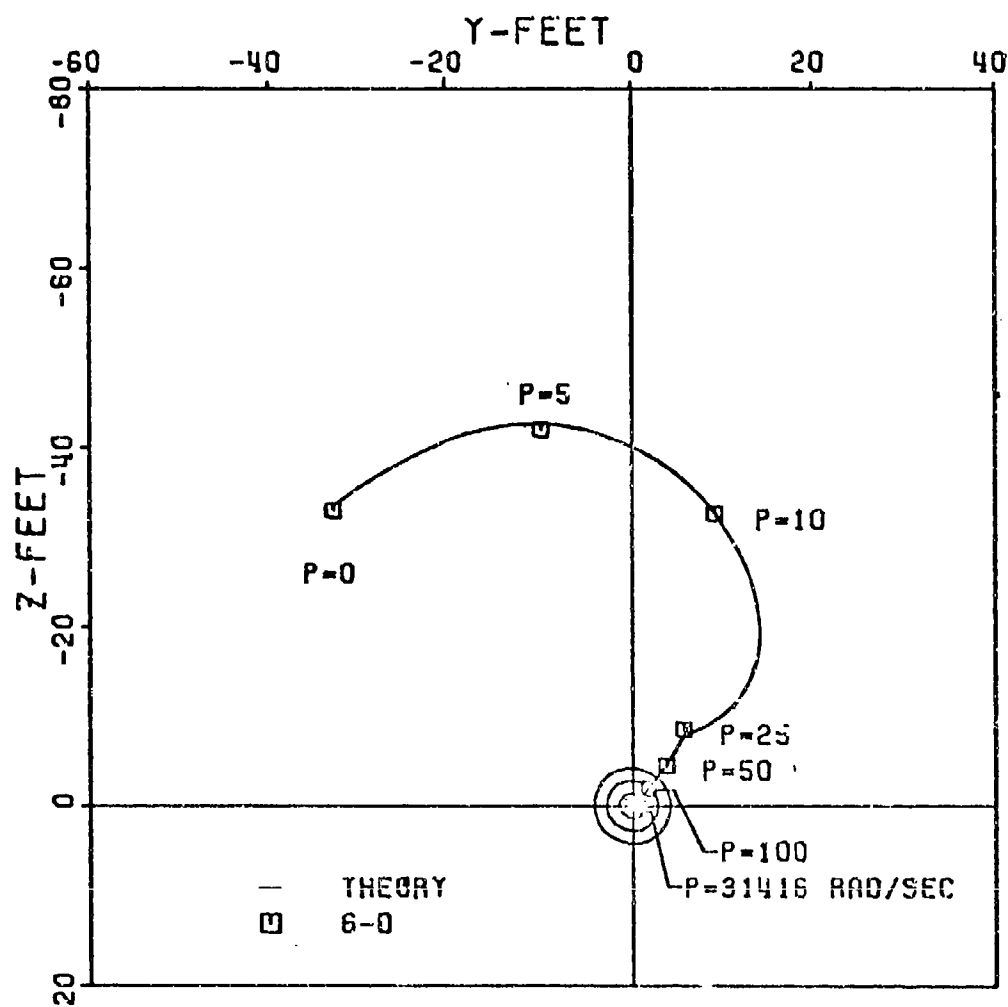


Figure 8. Dispersion: Phase III Cases 69-79



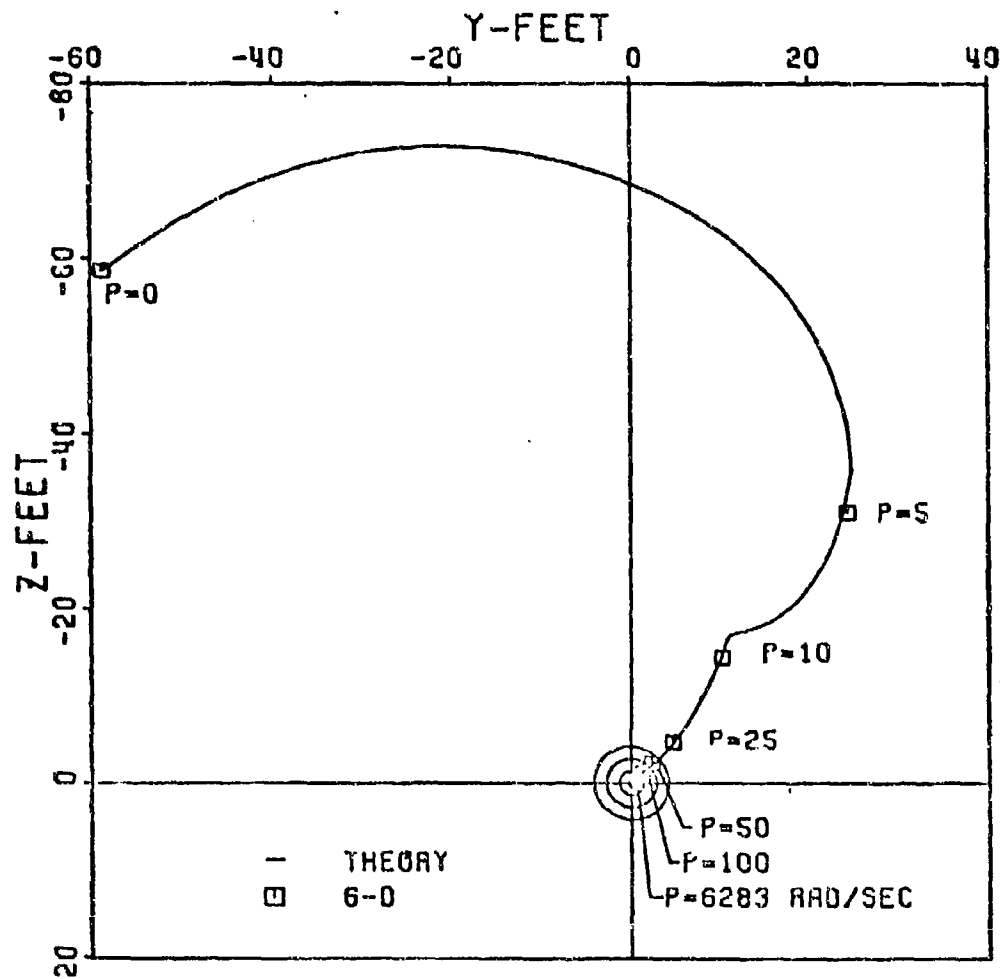


Figure 9. Dispersion: Phase III Cases 80-90

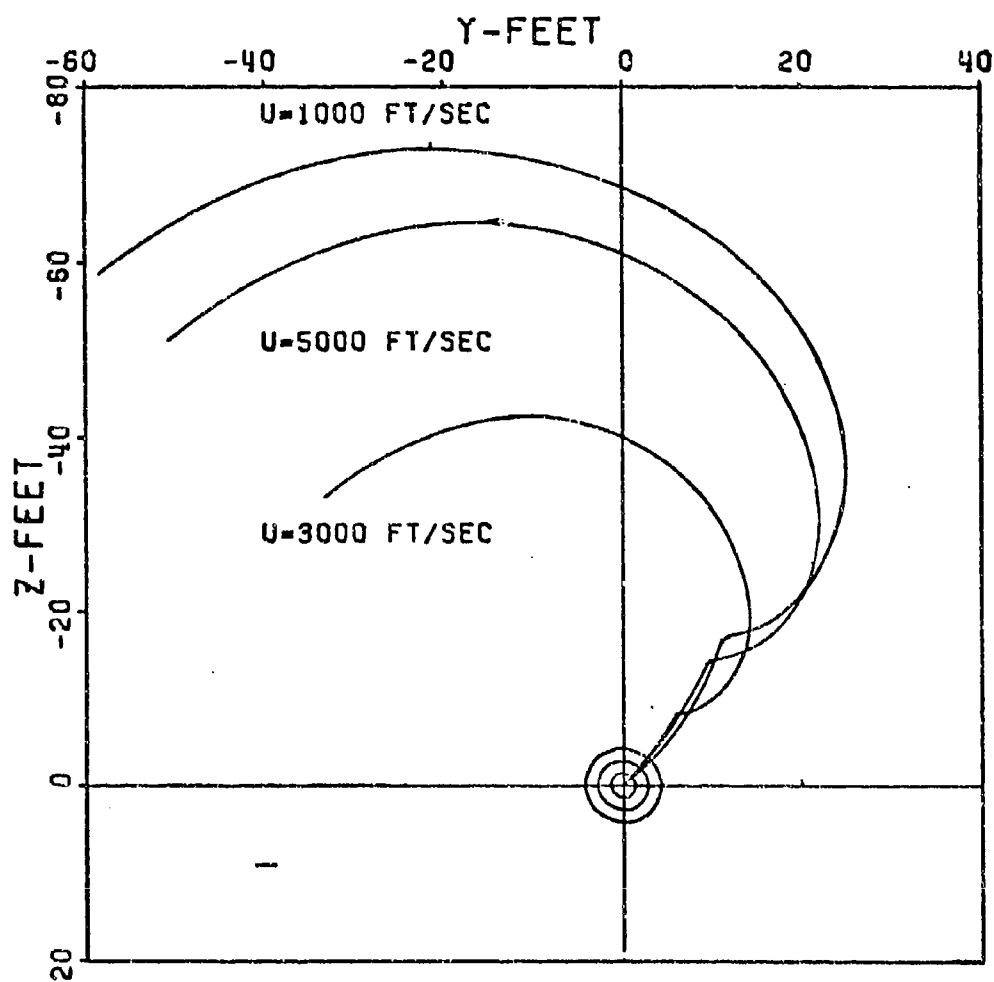


Figure 10. Dispersion: Phase III Theory, Cases 58-90

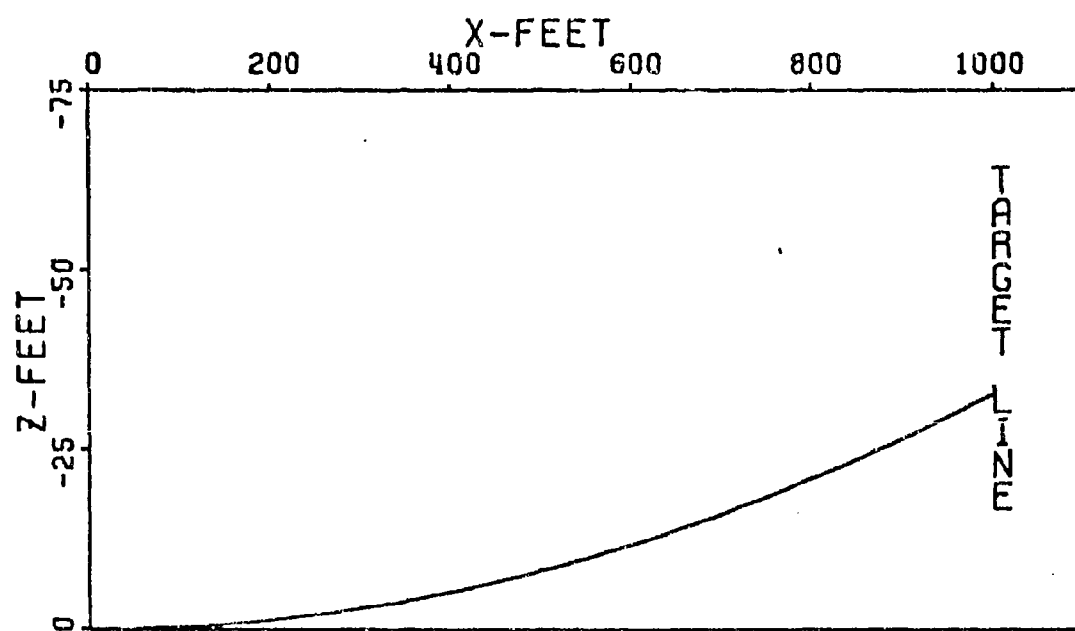
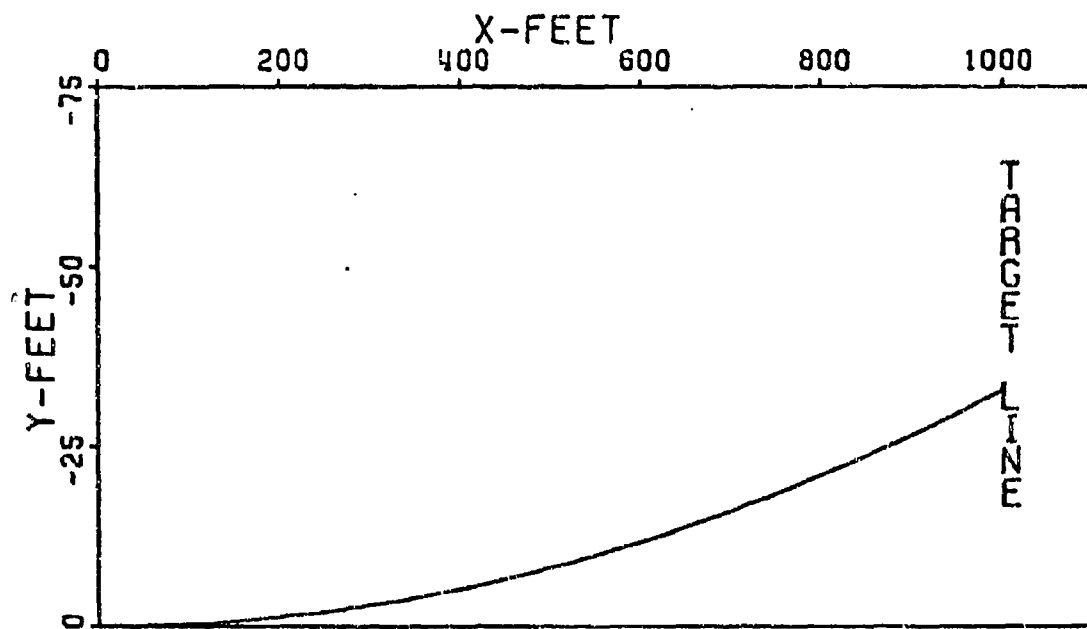


Figure 11. Trajectory, Case 79

$$\vec{J.A.} = \left[ \frac{\vec{S}_0}{u} + \frac{\rho u^2 \pi d^2}{8 m x} \left[ C_{Z_{\delta_\epsilon}} \vec{\delta_\epsilon} - i \left( \frac{C_{Z_\alpha}}{C_{M_\alpha}} \right) C_{M_{\delta_\epsilon}} \vec{\delta_\epsilon} \right] \left[ \frac{1}{p^2} (1 - \cos \frac{px}{u}) + \frac{i}{p} \left( \frac{x}{u} - \frac{1}{p} \sin \frac{px}{u} \right) \right] \right] 1000$$

For very slow roll cases, Equation 30 becomes:

$$\vec{J.A.} = \left[ \frac{\vec{S}_0}{u} + \frac{\rho \pi d^2 x}{16 m} \left[ C_{Z_{\delta_\epsilon}} \vec{\delta_\epsilon} - i \left( \frac{C_{Z_\alpha}}{C_{M_\alpha}} \right) C_{M_{\delta_\epsilon}} \vec{\delta_\epsilon} \right] \left[ \left( 1 - \frac{1}{12} \left( \frac{px}{u} \right)^2 + \frac{1}{360} \left( \frac{px}{u} \right)^4 \right) + i \left( \frac{px}{3u} - \frac{1}{60} \left( \frac{px}{u} \right)^3 + \frac{1}{2520} \left( \frac{px}{u} \right)^5 \right) \right] \right] 1000$$

Comparing Cases 91, 92, 93 in Table X with Cases 10, 11, 12 in Table II and Cases 58, 59, 60 in Table VII it can be concluded that; except for possible computational error, Cases 91, 92 and 93 are the algebraic sum of Cases 10, 11, 12 and 58, 59, 60; that is, for example, Case 91 equals Case 10 plus Case 58. This fact is obviously true of the theory equations and is here shown to be the case for the 6-D computations as well. Similar comparisons can be made with corresponding cases in Tables II, VIII, XI and II, IX, XII. Thus, the effects of aerodynamic asymmetries and those of initial transverse velocity are independent of one another.

Figures 12, 13 and 14 illustrate the Cases 91-123. The curves are of the same form as Figures 7, 8 and 9 but differ with the addition of  $\vec{S}_0$ . Maximum effect of all parameters is desired. Cases 113, 114 and 115 show the limit of parameter combinations by 113 and 114 going unstable. Roll rate effects are again large and velocity effects are larger than in Cases 58-90. Figure 15 shows this to be true and also shows the cases involving

TABLE X  
THEORY VALIDATION, ASYMMETRIES,  
CASES 91-101

C A S E	Initial Conditions					Coefficients			$\vec{J.A.}$ (mils)	
						$C_{Z\alpha}$ $C_{M\alpha}$	$C_{Zp\beta}$	$C_{YE}$ $C_{ZE}$ $C_{ME}$ $C_{NE}$		
	$\vec{S}_0$	$\vec{\alpha}_0$	$\vec{\dot{\alpha}}_0$	$p_0$	$u_0$	$C_{M\dot{q}} + C_{M\dot{\alpha}}$	$C_{M_{p\beta}}$		6-D	Theory
91	$100+$ $100i$	0	0	31416	5000	A1	A1	A1	20.011+	20.018+
92				18850					19.987i	19.986i
93				6283					20.026+	20.029+
94				500					19.972i	19.975i
95				300					20.056+	20.083+
96				100					19.872i	19.922i
97				50					21.004+	21.013+
98				25					19.012i	18.991i
99				10					21.626+	21.688+
100				5					18.286i	18.317i
101				0					24.593+	24.675+
									15.099i	15.025i
									28.702+	28.780+
									7.687i	7.511i
									40.766-	41.150-
									6.492i	6.927i
									11.983-	11.790-
									42.325i	43.210i
									-9.908-	-10.372
									41.503i	-42.353i
									-29.727	-30.427
									-29.743i	-30.427i

TABLE XI  
THEORY VALIDATION, ASYMMETRIES,  
CASES 102-112

C A S E	Initial Conditions					Coefficients			$\vec{J.A.}$ (mils)	
	$\vec{S}_0$	$\vec{\alpha}_0$	$\vec{\ddot{\alpha}}_0$	$p_0$	$u_0$	$C_{Z\alpha}$	$C_{Z,p\beta}$	$C_{YE}$	6-D	Theory
						$C_{M\alpha}$ $C_{Mq} + C_{M\dot{\alpha}}$	$C_{M,p\beta}$	$C_{ZE}$ $C_{ME}$ $C_{NE}$		
102	$100 + 100i$	0	0	31416	3000	A1	A1	A1	33.352+	33.342+
									33.362i	33.329i
103				18850					33.366+	33.345+
									33.364i	33.325i
104				6283					33.388+	33.367+
									33.347i	33.304i
105				500					33.740+	33.734+
									32.964i	32.937i
106				300					34.009+	34.000+
									33.705i	32.761i
107				100					35.188+	35.327+
									31.361i	31.344i
108				50					37.139+	36.744+
									28.850i	29.169i
109				25					39.029+	39.054+
									24.892i	24.817i
110				10					42.575+	42.550+
									0.716i	0.436i
111				5					23.312-	23.159-
									8.612i	8.940i
112				0					0.380+	0.139+
									0.362i	0.139i

TABLE XII  
THEORY VALIDATION, ASYMMETRIES,  
CASES 113-123

C A S E	Initial Conditions					Coefficients			$\vec{J} \cdot \vec{A}$ . (mils)	
	$\vec{S}_0$	$\vec{\alpha}_0$	$\vec{\dot{\alpha}}_0$	$p_0$	$u_0$	$C_{Z\alpha}$	$C_{Zp\beta}$	$C_{YE}$	6-D	Theory
						$C_{M\alpha}$		$C_{ZE}$		
						$C_{M_q} + C_{M_{\dot{\alpha}}}$	$C_{M_{p\beta}}$	$C_{ME}$		
113	↑	↑	↑	31416	↑	↑	↑	↑	Unstable	
114	↑	↑	↑	18850	↑	↑	↑	↑	Unstable	
115	↑	↑	↑	6283	↑	↑	↑	↑	100.351+	100.023+
									100.814i	99.986i
116	↑	↑	↑	500	↑	↑	↑	↑	100.559+	100.238+
									100.587i	99.771i
117	↑	↑	↑	300	↑	↑	↑	↑	100.710+	100.394+
									100.431i	99.615i
118	100+ 100i	0	0	100	1000	A1	A1	A1	101.492+	101.174+
									99.658i	98.835i
119	↑	↑	↑	50	↑	↑	↑	↑	102.668+	102.349+
									98.495i	97.648i
120	↑	↑	↑	25	↑	↑	↑	↑	105.019+	104.699+
									96.164i	95.298i
121	↑	↑	↑	10	↑	↑	↑	↑	110.862+	110.177+
									86.275i	85.524i
122	↑	↑	↑	5	↑	↑	↑	↑	125.216+	124.516+
									69.958i	68.788i
123	↑	↑	↑	0	↑	↑	↑	↑	41.499+	41.550+
									41.413i	41.550i

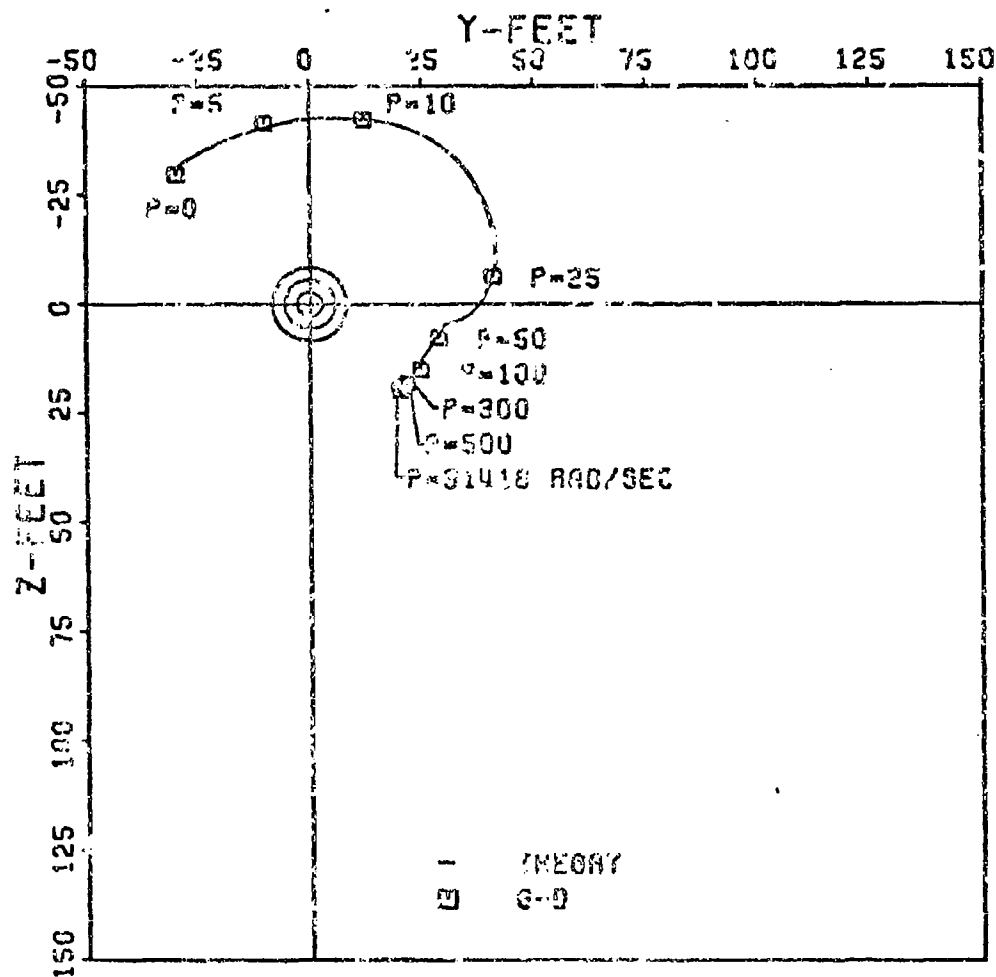


Figure 12. Dispersion: Case III Cases 91-101



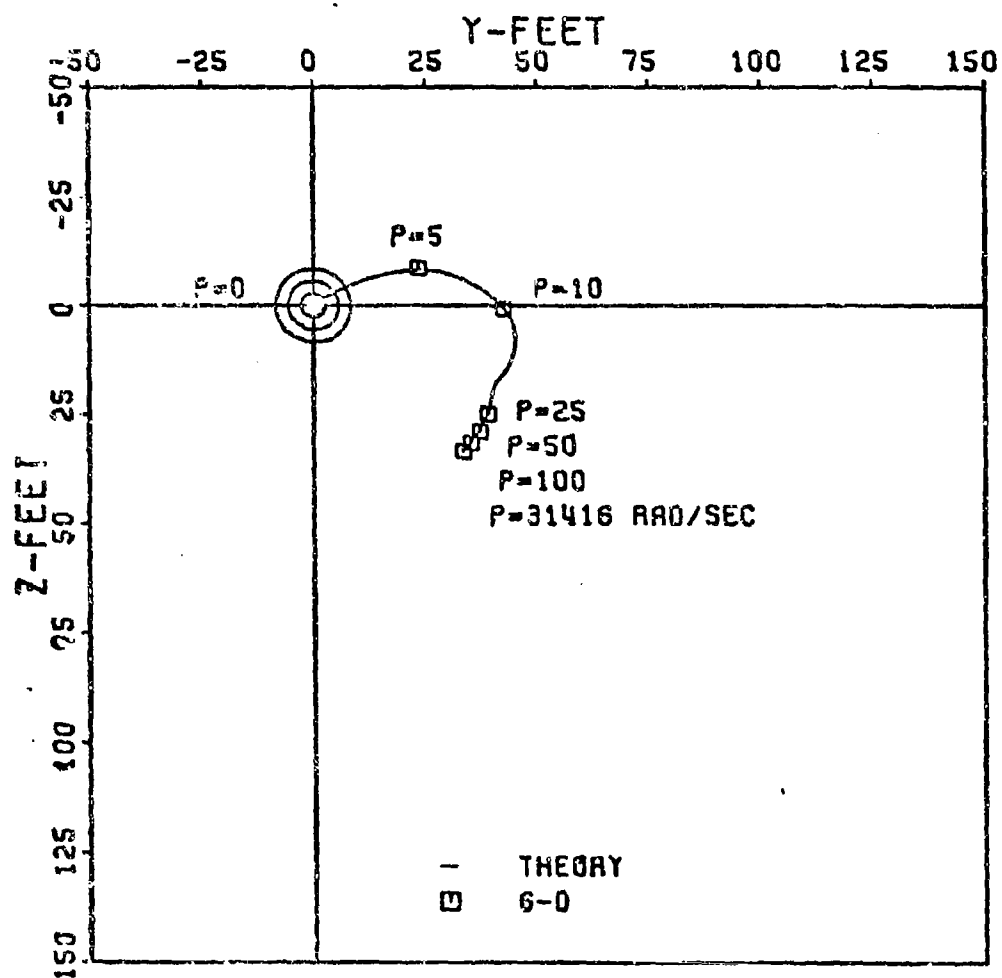


Figure 13. Dispersion: Phase III Cases 102-112

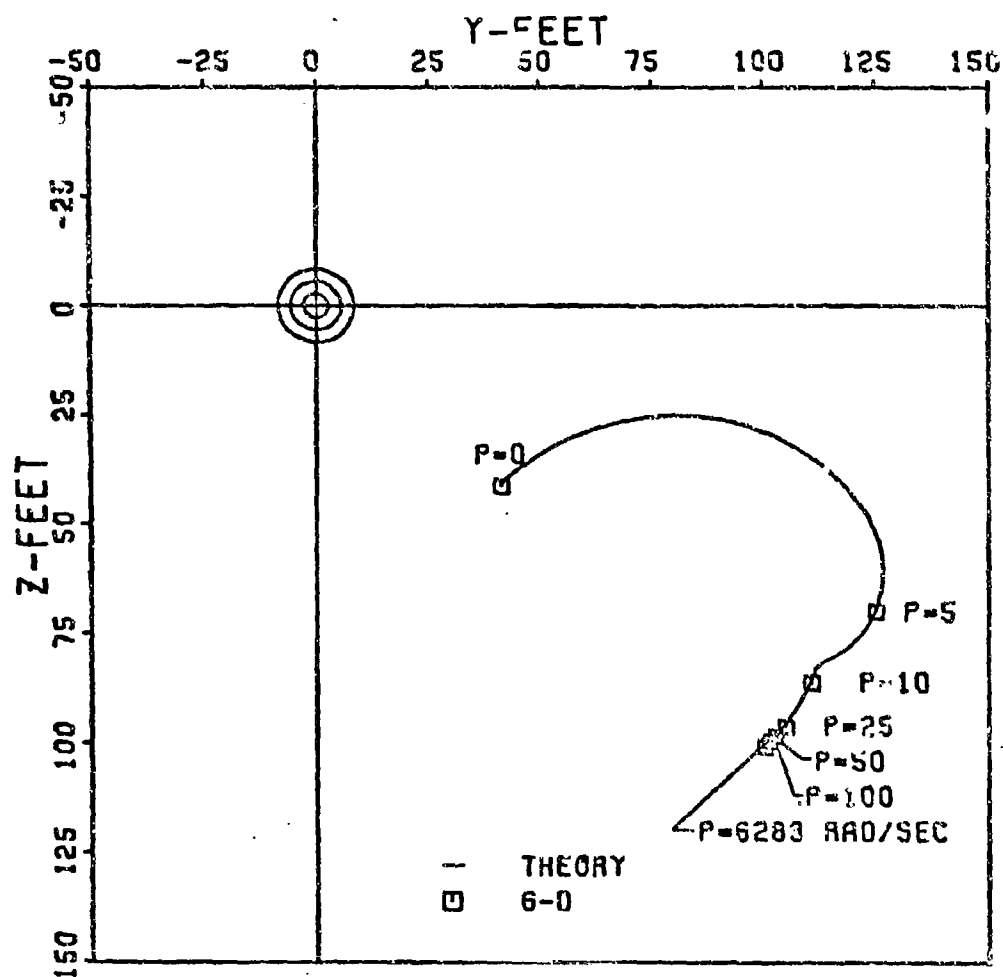


Figure 14. Dispersion: Phase III Cases 113-123

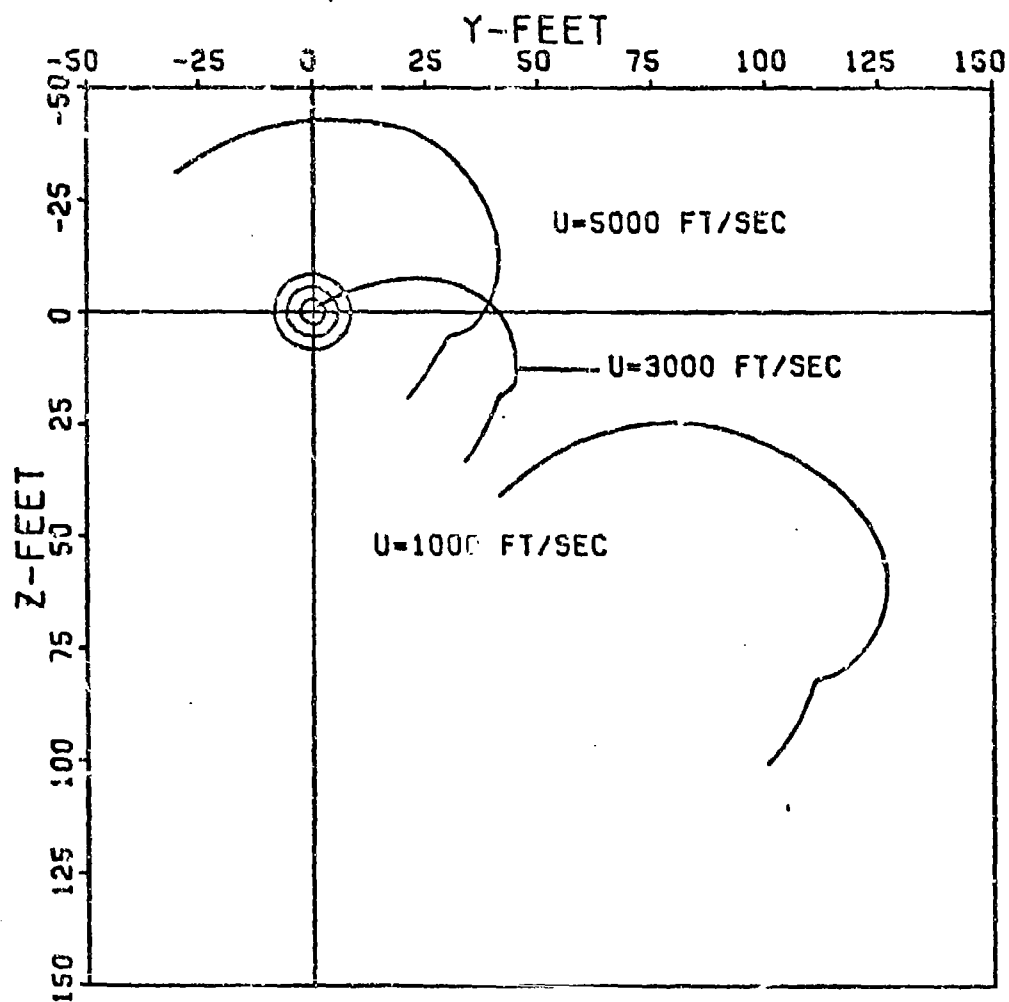


Figure 15. Dispersion: Phase III Theory, Cases 91-123

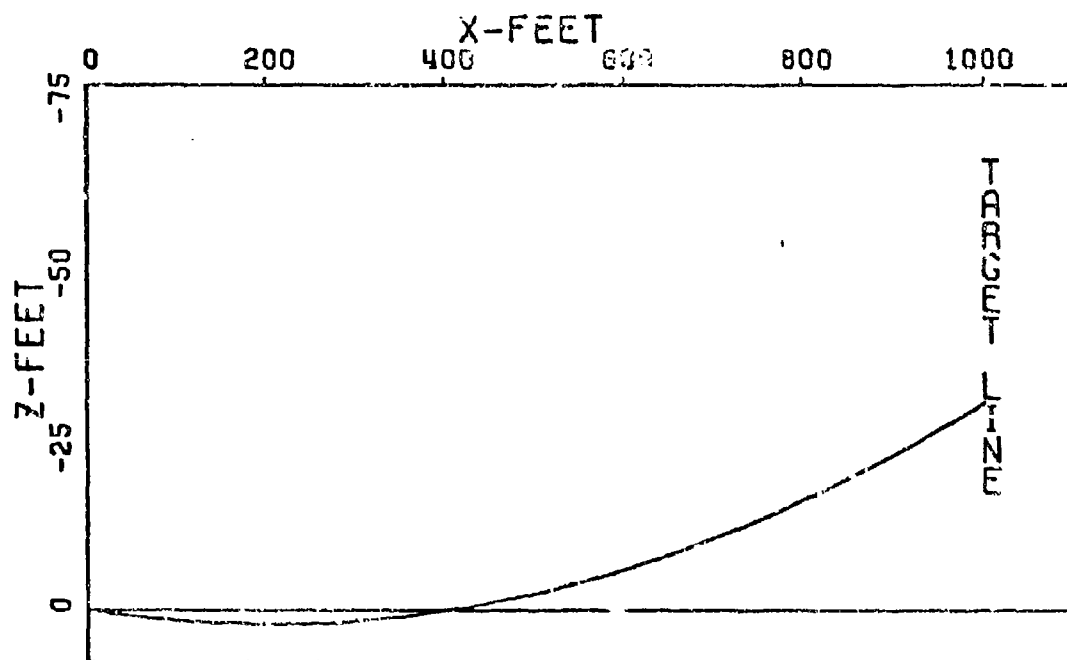
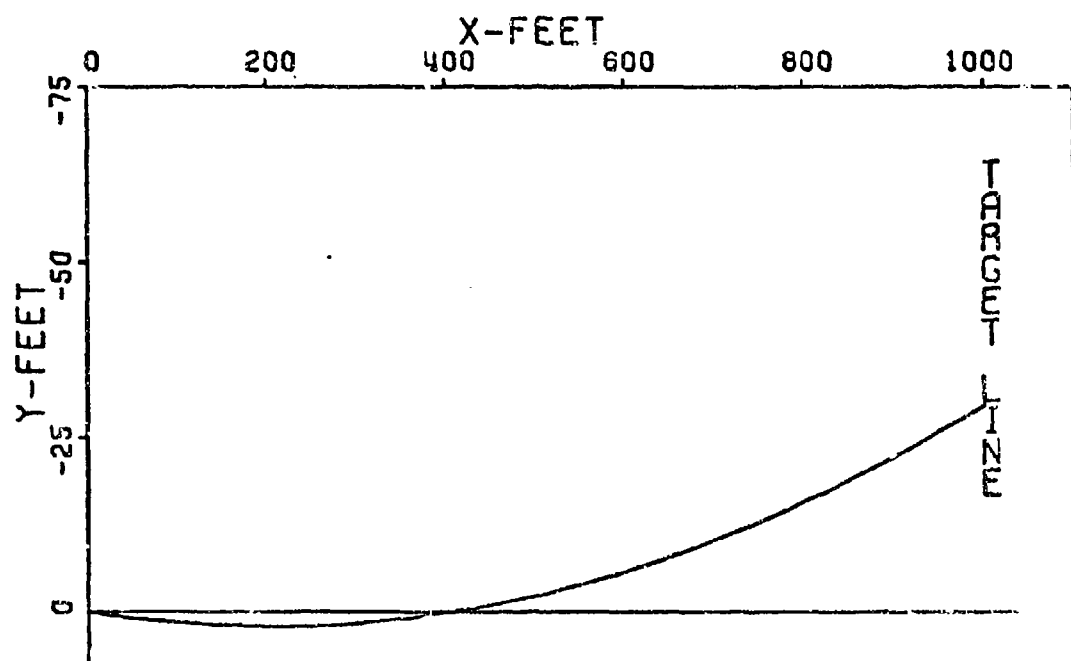


Figure 16. Trajectory, Case 101

$U = 3000$  ft/sec to be ones of smallest dispersion. Such was the case in Figure 10. Figure 16 illustrates a sample trajectory, Case 101.

#### Cases 124-156

To establish the relationship between the effects on dispersion for aerodynamic asymmetries and initial angle of attack, a third set of cases were run. Again roll rate and velocity were varied as done previously but  $\vec{\alpha}_0$  was set at  $(1+i)$  degrees with  $\vec{\beta}_0 = 0$  and  $\vec{\alpha}_0 = 0$ . Tables XIII, XIV, and XV tabulate the results. For all high roll rate cases, Equation 24 reduces to:

$$\vec{J.A.} = \left[ \frac{ipI_x}{mud} A \vec{\alpha}_0 + \frac{\rho u \pi d^2}{8m} \left[ C_{M_{\delta_e}} \vec{\delta}_e \left( \frac{A}{p} \right) + C_{Z_{\delta_e}} \vec{\delta}_e \left( \frac{I_y - I_x}{mud} A + \frac{i}{p} \right) \right] \right] 1000$$

For low roll rate cases, Equation 28 reduces to:

$$\vec{J.A.} = \frac{\rho u^2 \pi d^2}{8m\pi} \left[ C_{Z_{\delta_e}} \vec{\delta}_e - i \left( \frac{C_{Z_{\alpha}}}{C_{M_{\alpha}}} \right) C_{M_{\delta_e}} \vec{\delta}_e \right] \left[ \frac{1}{p^2} (1 - \cos \frac{px}{u}) + \frac{i}{p} \left( \frac{x}{u} - \frac{1}{p} \sin \frac{px}{u} \right) \right] 1000$$

For very low roll rates, Equation 30 reduces to:

$$\vec{J.A.} = \frac{\rho u^2 \pi d^2}{16m} \left[ C_{Z_{\delta_e}} \vec{\delta}_e - i \left( \frac{C_{Z_{\alpha}}}{C_{M_{\alpha}}} \right) C_{M_{\delta_e}} \vec{\delta}_e \right] \left[ \left( 1 - \frac{1}{12} \left( \frac{px}{u} \right)^2 + \frac{1}{360} \left( \frac{px}{u} \right)^4 \right) + i \left( \frac{px}{3u} - \frac{1}{60} \left( \frac{px}{u} \right)^3 + \frac{1}{2520} \left( \frac{px}{u} \right)^5 \right) \right] 1000$$

Only for high roll rates does the  $\vec{\alpha}_0$  term appear.  $\vec{\alpha}_0$  should have no noticeable effect on dispersion for  $p < 100$  rad/sec.

TABLE XIII  
THEORY VALIDATION, ASYMMETRIES,  
CASES 124-134

C A S E	Initial Conditions					Coefficients			$\vec{J.A.}$ (mils)	
	$\vec{S}_0$	$\vec{\alpha}_0$	$\vec{\dot{\alpha}}_0$	$p_0$	$u_0$	$C_{Z\alpha}$	$C_{Z_{p\beta}}$ $C_{M_{p\beta}}$	$C_{YE}$	6-D	Theory
						$C_{M_q} + C_{M_{\dot{\alpha}}}$		$C_{ZE}$ $C_{ME}$ $C_{NE}$		
124	↑	↑	↑	31416	↑	↑	↑	↑	0.028+ 0.052i	0.009- 0.013i
125	↑	↑	↑	18850	↑	↑	↑	↑	0.052+ 0.029i	0.013- 0.009i
126	↑	↑	↑	6283	↑	↑	↑	↑	0.094- 0.080i	0.078- 0.073i
127	↑	↑	↑	500	↑	↑	↑	↑	1.040- 0.954i	1.013- 1.009i
128	↑	↑	↑	300	↑	↑	↑	↑	1.660- 1.680i	1.688- 1.683i
129	0	1+i	0	100	5000	A1	A1	A1	4.628- 4.868i	4.675- 4.975i
130	↑	↑	↑	50	↑	↑	↑	↑	8.732- 12.279i	8.780- 12.489i
131	↑	↑	↑	25	↑	↑	↑	↑	20.784- 26.468i	21.150- 26.927i
132	↑	↑	↑	10	↑	↑	↑	↑	-7.954- 62.367i	-8.210- 63.210i
133	↑	↑	↑	5	↑	↑	↑	↑	-29.912 -61.629i	-30.372 -62.353i
134	↑	↑	↑	0	↑	↑	↑	↑	-49.828 -49.840i	-50.427 -50.427i

TABLE XIV  
THEORY VALIDATION, ASYMMETRIES,  
CASES 135-145

C A S E	Initial Conditions					Coefficients			$\vec{J.A.}$ (mils)	
						$C_{Z\alpha}$ $C_{M\alpha}$ $C_{M_q} + C_{M_{\dot{\alpha}}}$	$C_{Z_{p\beta}}$ $C_{M_{p\beta}}$	$C_{Y\dot{E}}$ $C_{Z\dot{E}}$ $C_{M\dot{E}}$ $C_{N\dot{E}}$	6-D	Theory
	$\vec{S}_0$	$\vec{\alpha}_0$	$\vec{\dot{\alpha}}_0$	$p_0$	$u_0$					
135	$\uparrow$	$\uparrow$	$\uparrow$	31416	$\uparrow$	$\uparrow$	$\uparrow$	$\uparrow$	Unstable	
136				18850					0.035+ 0.046i	-0.003 +0.008i
137				6283					0.066+ 0.017i	0.029- 0.024i
138				500					0.432- 0.357i	0.401- 0.396i
139				300					0.701- 0.618i	0.666- 0.662i
140				100					1.879- 1.958i	1.994- 1.989i
141				50					3.819- 4.473i	3.411- 4.164i
142				25					5.714- 8.416i	5.721- 8.516i
143				10					9.247- 32.586i	9.217- 32.897i
144				5					-9.985- 41.948i	-10.174 -42.273i
145				0					-32.973 -32.981i	-33.194 -33.194i

TABLE XV  
THEORY VALIDATION, ASYMMETRIES,  
CASES 146-156

C A S E	Initial Conditions					Coefficients			$\vec{J.A.}$ (mils)	
						$C_{Z\alpha}$ $C_{M\alpha}$ $C_{M_q} + C_{M_{\dot{\alpha}}}$	$C_{Z_{p\beta}}$ $C_{M_{p\beta}}$	$C_{YE}$ $C_{ZE}$ $C_{ME}$ $C_{NE}$	6-D	Theory
	$\vec{S}_0$	$\vec{\alpha}_0$	$\vec{\dot{\alpha}}_0$	$p_0$	$u_0$					
146	↑	↑	↑	31416	↑	↑	↑	Unstable		
147	↑	↑	↑	18850	↑	↑	↑	Unstable		
148	↑	↑	↑	6283	↑	↑	↑	0.046+ 0.039i	0.008+ 0.001i	
149	↑	↑	↑	500	↑	↑	↑	0.275- 0.188i	0.237- 0.228i	
150	↑	↑	↑	300	↑	↑	↑	0.432- 0.342i	0.393- 0.384i	
151	0	1+i	0	100	1000	A1	A1	A1	1.213- 1.123i	1.174- 1.165i
152	↑	↑	↑	50	↑	↑	↑	↑	2.381- 2.294i	2.349- 2.352i
153	↑	↑	↑	25	↑	↑	↑	↑	4.719- 4.637i	4.699- 4.702i
154	↑	↑	↑	10	↑	↑	↑	↑	10.258- 14.411i	10.177- 14.476i
155	↑	↑	↑	5	↑	↑	↑	↑	24.440- 30.976i	24.516- 31.212i
156	↑	↑	↑	0	↑	↑	↑	↑	-58.669 -58.684i	-58.450 -58.450i



Comparing Cases 124, 125, 126 in Table XIII with Cases 19, 20, 21 in Table III and Cases 58, 59, 60 in Table VII it can be concluded that Cases 124, 125 and 126 are the algebraic sum of Cases 19, 20, 21 and 58, 59, 60; that is, for example, Case 124 equals Case 19 plus Case 58. This is obvious from the reduced theoretical equations for Cases 124-156. It is shown here to be also true for the 6-D computations; allowing for some computational error. Similar comparisons can be made with corresponding cases in Tables III, VIII, XIV and III, IX, XV. Thus the effects of aerodynamic asymmetries and those of initial angle of attack are independent of one another.

Figures 17, 18 and 19 illustrate Cases 124-156. The curves are very similar to those in Figures 7, 8, and 9 with the only difference being the very small  $\vec{\alpha}_0$  contribution in Figures 17, 18, and 19. Cases 135, 146, and 147 result in instabilities, indicating that maximum effect of the various parameters has been accomplished. Effects of roll rate are essentially the same as in Case 58-90 and effects of velocity, Figure 20, the same as in Figure 10. Cases with  $U = 3000$  ft/sec again have the smallest dispersion. Figure 21 shows a typical trajectory, Case 134.

#### Cases 157-189

To validate the relationship between the effects on dispersion for aerodynamic asymmetries and those of initial angular rate, a fourth set of cases were run. As before, roll rate and velocity were varied, but  $\vec{\alpha}_0$  set at  $(250 + 250i)$  rad/sec with  $\vec{S}_0 = 0$  and  $\vec{\alpha}_0 = 0$ . Tables XVI, XVII,

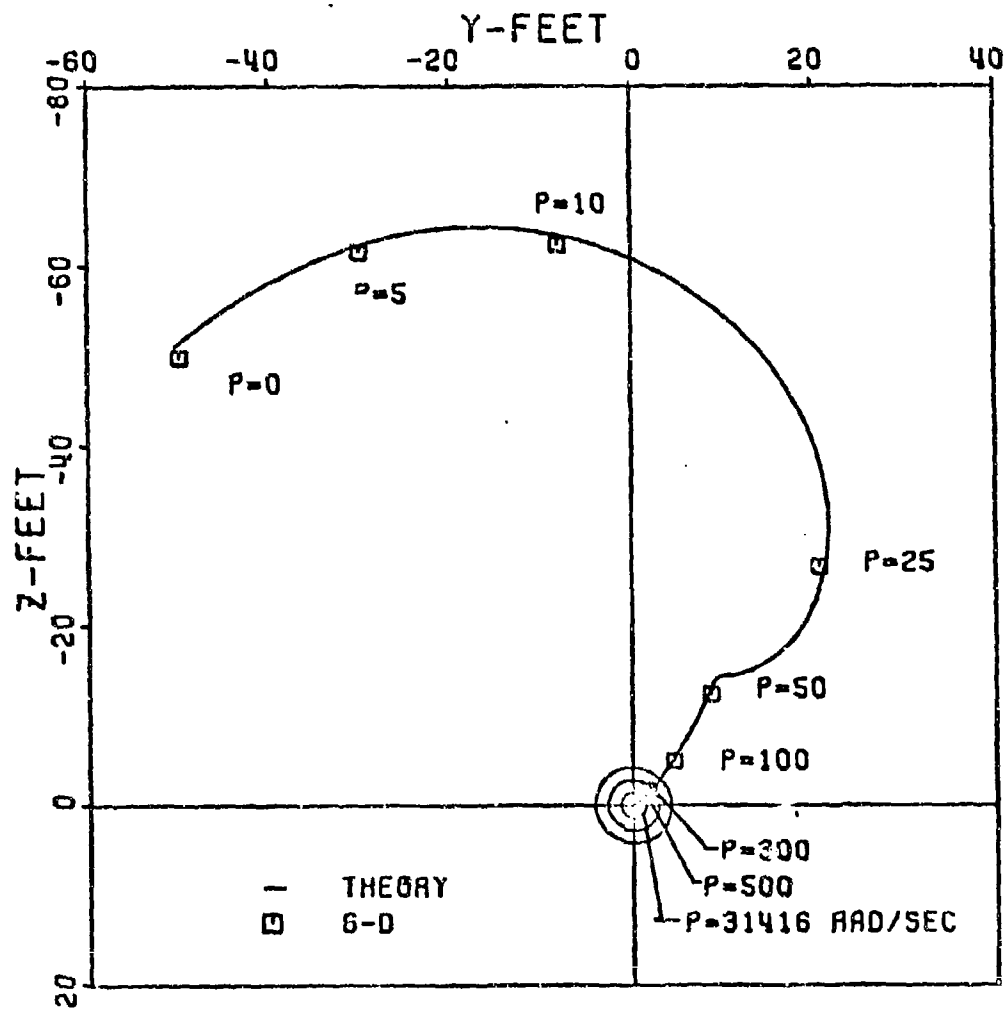


Figure 17. Dispersion: Phase III Cases 124-134

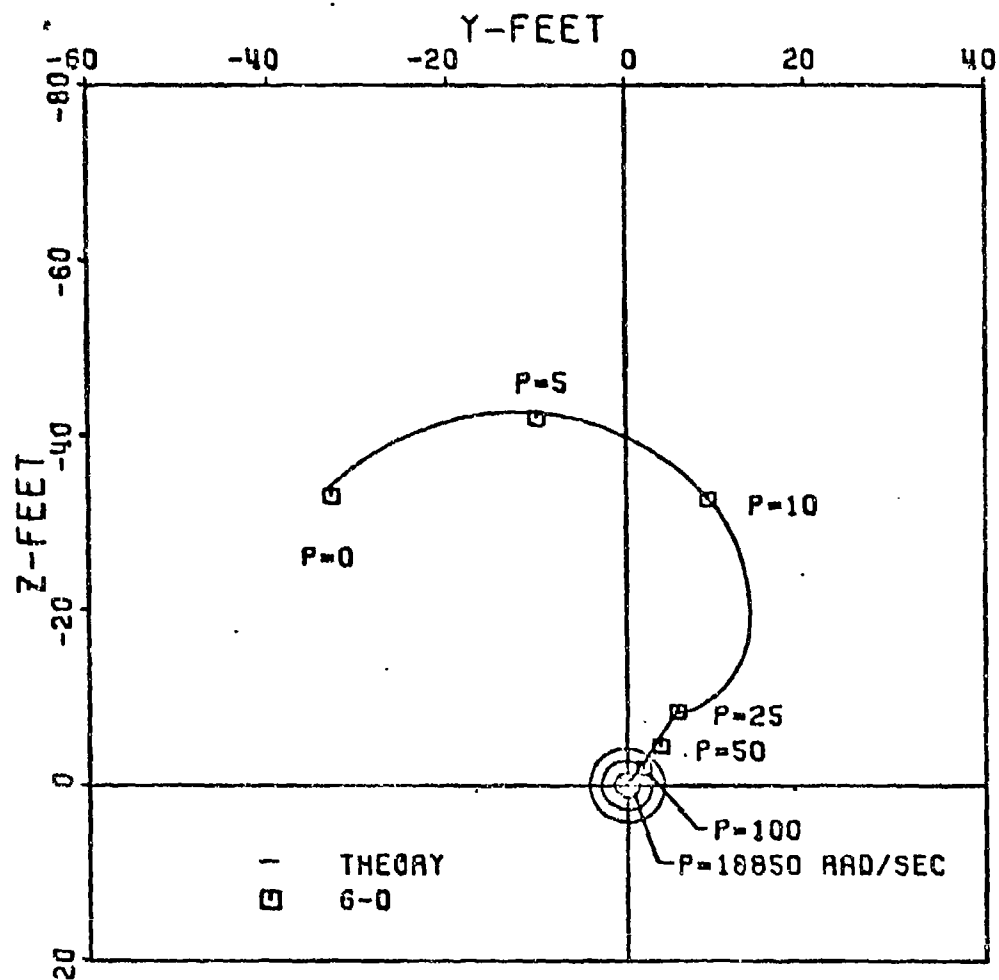


Figure 18. Dispersion: Phase III Cases 135-145

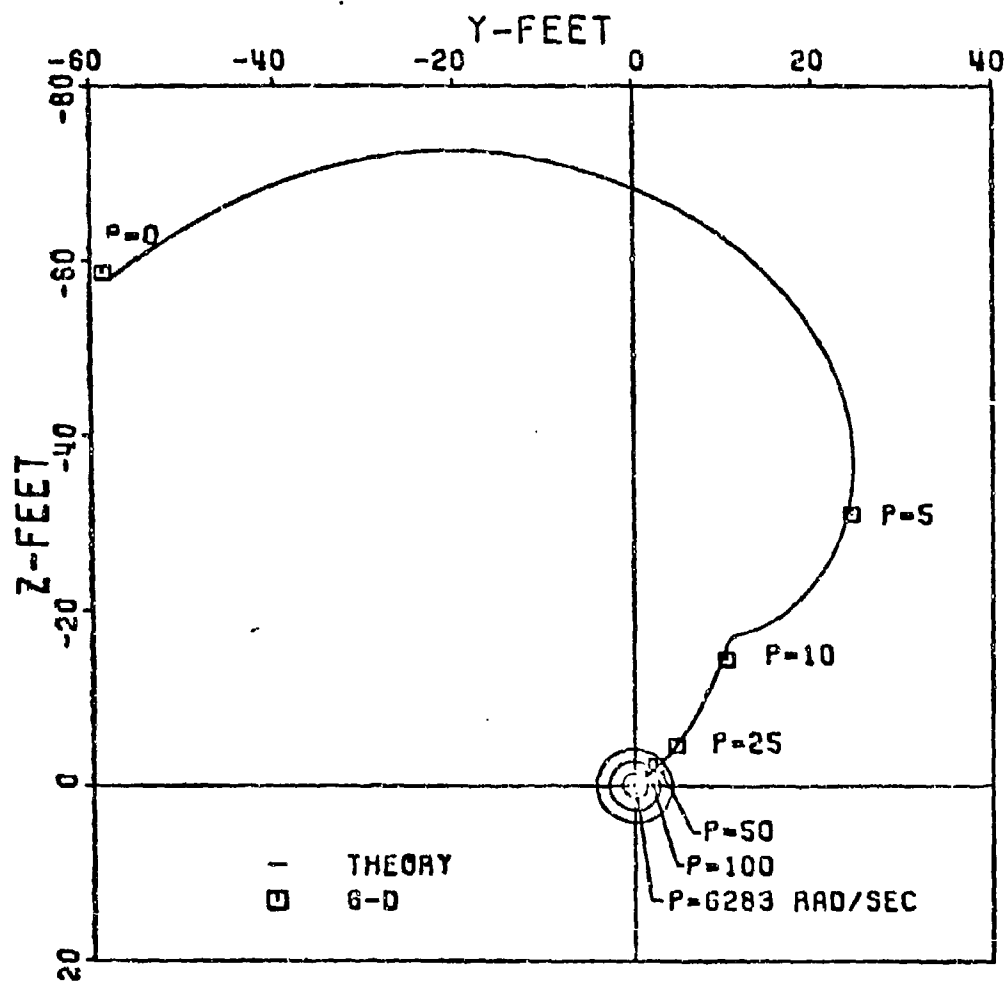


Figure 19. Dispersion: Phase III Cases 146-156

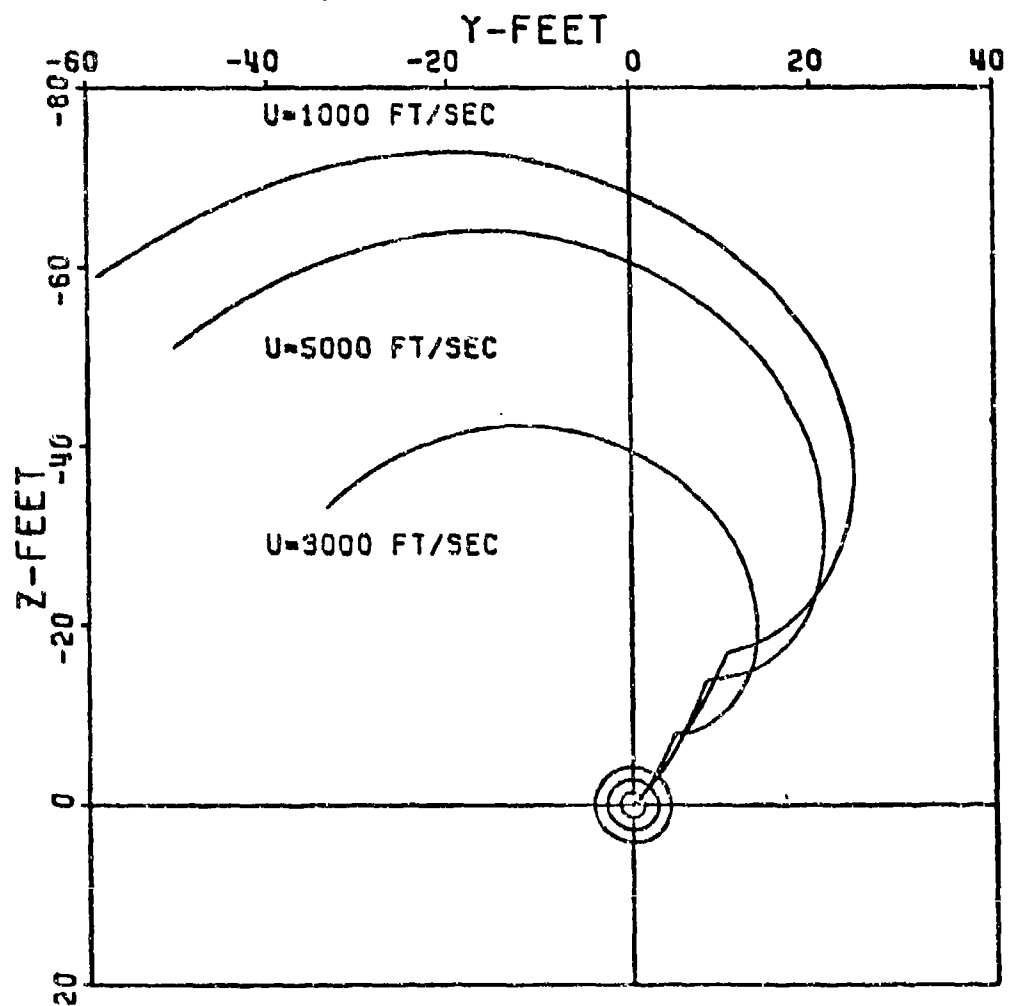


Figure 20. Dispersion: Phase III Theory, Cases 124-156

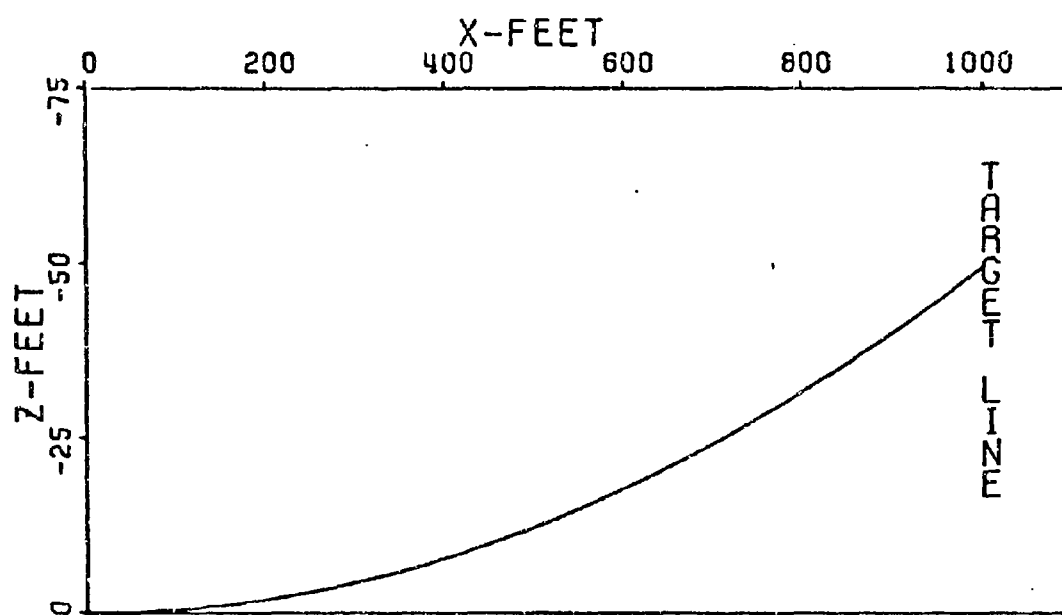
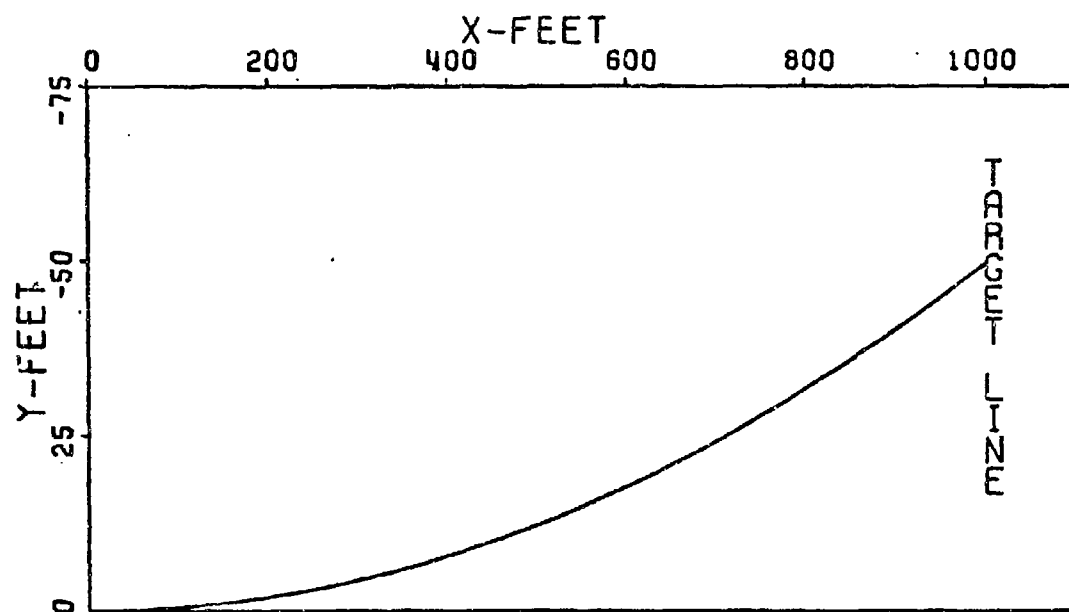


Figure 21. Trajectory, Case 134

XVIII gives the results. For high roll rates, the governing equation becomes:

$$\vec{J} \cdot \vec{\Lambda} = \left[ \frac{\rho u \pi d^2}{8m} \left[ C_{M_{\delta_\epsilon}} \vec{\delta}_\epsilon \left( \frac{\Lambda}{p} \right) + C_{Z_{\delta_\epsilon}} \vec{\delta}_\epsilon \left( \frac{I_y - I_x}{mud} \Lambda + \frac{i}{p} \right) \right] - \frac{I_y}{mud} \Lambda \vec{\alpha}_0 \right] 1000$$

For low roll rates, the governing equation:

$$\vec{J} \cdot \vec{\Lambda} = \left[ \frac{\rho u^2 \pi d^2}{8 m x} \left[ C_{Z_{\delta_\epsilon}} \vec{\delta}_\epsilon - i \left( \frac{C_{Z_\alpha}}{C_{M_\alpha}} \right) C_{M_{\delta_\epsilon}} \vec{\delta}_\epsilon \right] \left[ \left( 1 - \cos \frac{px}{u} \right) + \frac{i}{p} \left( \frac{x}{u} - \frac{1}{p} \sin \frac{px}{u} \right) \right] - \frac{I_y}{mud} \left( \frac{C_{Z_\alpha}}{C_{M_\alpha}} \right) \vec{\alpha}_0 \right] 1000$$

For very slow roll, the governing equation:

$$\vec{J} \cdot \vec{\Lambda} = \left[ \frac{\rho \pi d^2 x}{16m} \left[ C_{Z_{\delta_\epsilon}} \vec{\delta}_\epsilon - i \left( \frac{C_{Z_\alpha}}{C_{M_\alpha}} \right) C_{M_{\delta_\epsilon}} \vec{\delta}_\epsilon \right] \left[ \left( 1 - \frac{1}{12} \left( \frac{px}{u} \right)^2 + \frac{1}{360} \left( \frac{px}{u} \right)^4 \right) + i \left( \frac{px}{3u} - \frac{1}{60} \left( \frac{px}{u} \right)^3 + \frac{1}{2520} \left( \frac{px}{u} \right)^5 \right) \right] - \frac{I_y}{mud} \left( \frac{C_{Z_\alpha}}{C_{M_\alpha}} \right) \vec{\alpha}_0 \right] 1000$$

Comparing Cases 157, 158, 159 in Table XVI with Cases 28, 29, 30 in Table IV and Cases 58, 59, 60 in Table VII, it can be concluded that Cases 157, 158, and 159 are the algebraic sum of Cases 28, 29, 30 and 58, 59, 60; that is, for example, Case 157 equals Case 28 plus Case 58. This is obvious from the reduced theoretical equations for Cases 157-189. Here it is shown to be true for 6-D computations also. Any discrepancy can be attributed to computational error. Similar comparisons can be made with corresponding cases in Table IV, VIII, and XVII. Thus the effects of aerodynamic asymmetries and those of initial angular rate are independent of one another.

TABLE XVI  
THEORY VALIDATION, ASYMMETRIES,  
CASES 157-167

C A S E	Initial Conditions					Coefficients			$\vec{J.A.}$ (mils)	
	$\vec{S}_0$	$\vec{\alpha}_0$	$\vec{\alpha}_0$	$p_0$	$u_0$	$C_{Z\alpha}$ $C_{M\alpha}$	$C_{Zp\beta}$	$C_{YE}$ $C_{ZE}$ $C_{ME}$ $C_{NE}$	6-D	Theory
						$C_{Mq} + C_{M\dot{\alpha}}$	$C_{Mp\beta}$			
157	↑	↑	↑	31416	↑	↑	↑	↑	-1.799 -2.236i	-2.055 -2.087i
158	↑	↑	↑	18850	↑	↑	↑	↑	-1.873 -2.169i	-2.044 -2.098i
159	↑	↑	↑	6283	↑	↑	↑	↑	-1.924 -2.190i	-1.990 -2.151i
160	↑	↑	↑	500	↑	↑	↑	↑	-1.049 -3.000i	-1.060 -3.082i
161	↑	↑	↑	300	↑	↑	↑	↑	-0.419 -3.716i	-0.385 -3.756i
162	0	0	250+ 250i	100	5000	A1	A1	A1	2.457- 6.836i	2.602- 7.048i
163	↑	↑	↑	50	↑	↑	↑	↑	6.576- 14.075i	6.707- 14.562i
164	↑	↑	↑	25	↑	↑	↑	↑	18.366- 27.827i	19.077- 29.000i
165	↑	↑	↑	10	↑	↑	↑	↑	-9.690- 63.387	-10.283 -65.283i
166	↑	↑	↑	5	↑	↑	↑	↑	-31.387 -62.730i	-32.445 -64.426i
167	↑	↑	↑	0	↑	↑	↑	↑	-51.094 -51.094i	-52.500 -52.500i



TABLE XVII  
THEORY VALIDATION, ASYMMETRIES,  
CASES 168-178

C A S E	Initial Conditions					Coefficients			J.A. (mils)								
						$C_{Z\alpha}$ $C_{M\alpha}$ $C_{M_q} + C_{M\dot{\alpha}}$	$C_{Z_{p\beta}}$ $C_{M_{p\beta}}$	$C_{YE}$ $C_{ZE}$ $C_{ME}$ $C_{NE}$	6-D	Theory							
	$\vec{S}_0$	$\vec{\alpha}_0$	$\vec{\dot{\alpha}}_0$	$p_0$	$u_0$												
168	$\downarrow$	$\downarrow$	$\downarrow$	31415	$\downarrow$	$\downarrow$	$\downarrow$	$\downarrow$	Unstable								
169				18850					-1.755 -2.154i	-1.957 -1.978i							
170				6283					-1.866 -2.054i	-1.936 -1.999i							
171				500					-1.572 -2.351i	-1.569 -2.366i							
172				300					-1.308 -2.595i	-1.304 -2.632i							
173				0					0	250+ 250i	100	3000	A1	A1	A1	-0.114 -3.912i	-0.024 -3.959i
174				50					1.873- 6.399i	1.441- 6.134i							
175				25					3.755- 10.393i	3.751- 10.486i							
176				10					7.435- 34.530i	7.247- 34.867i							
177				5					-11.870 -44.054i	-12.144 -44.243i							
178				0					-35.054 -35.053i	-35.164 -35.164i							

TABLE XVIII  
THEORY VALIDATION, ASYMMETRIES,  
CASES 179-189

C. A S E	Initial Conditions					Coefficients			$\vec{J.A.}$ (mils)	
						$C_{Z\alpha}$ $C_{M\alpha}$ $C_{M_q} + C_{M\dot{\alpha}}$	$C_{Zp\beta}$ $C_{Mp\beta}$	$C_{YE}$ $C_{ZE}$ $C_{ME}$ $C_{NE}$	6-D	Theory
	$\vec{s}_0$	$\vec{\alpha}_0$	$\vec{\dot{\alpha}}_0$	$p_0$	$u_0$					
179	0	0	$250 + 250i$	31416	1000	A1	A1	A1	Unstable	
180				18850					Unstable	
181				6283					Unstable	
182				500					-5.015 -5.503i	-5.302 -5.769i
183				300					-4.884 -5.572i	-5.144 -5.925i
184				100					-4.208 -6.135i	-4.366 -6.705i
185				50					-3.056 -7.031i	-3.191 -7.892i
186				25					-0.741 -9.079i	-0.841 -10.242i
187				10					5.244 18.344i	4.637 20.016i
188				5					18.563 33.158i	18.976 36.752i
189				0					-61.894 -61.894i	-63.990 -63.990i

Figures 22, 23 and 24 illustrate Cases 157-189. The curves are similar to those in Figures 7, 8 and 9 but are displaced by the  $\vec{\alpha}_0$  contribution. Cases 168, 179, 180 and 181 indicate that maximum effects of the various parameters has been achieved in other stable cases. The effects of roll rate and velocity follow the same trends as those in Cases 58-90. Figure 25 shows the effects of velocity for Cases 157-189. Cases with  $U = 3000$  ft/sec exhibit the smallest dispersion. A sample trajectory, Case 189, is shown in Figure 26.

### Comparison: High, Low, Very Slow

#### Roll Rate Theories

In Cases 58-189 the High, Low, and Very Slow Roll Rate Theories are validated for various initial conditions and parameters. The theories have been applied for certain ranges in roll rate and roll rate times time (pt.) The range of pt, ( $pt \leq 1.0$ ) are governed by the inherent requirements of power series expansion. However, the ranges of p are arbitrary (to a certain extent) and are based on accuracy of the theories themselves. Each theory approximates the solution very well for a certain range of p and then begins to diverge and become inaccurate. The range of p for which the very slow roll rate theory is accurate is fairly well cut and dried;  $p \geq 0$ ,  $pt \leq 1.0$ . For any  $pt > 1.0$  we must now use the low roll rate theory. The question now arises, how high a roll rate can this theory accommodate? At what value of p must we change to the high roll rate theory? These questions are answered by a plot of sample 6-D computations, Figure 27

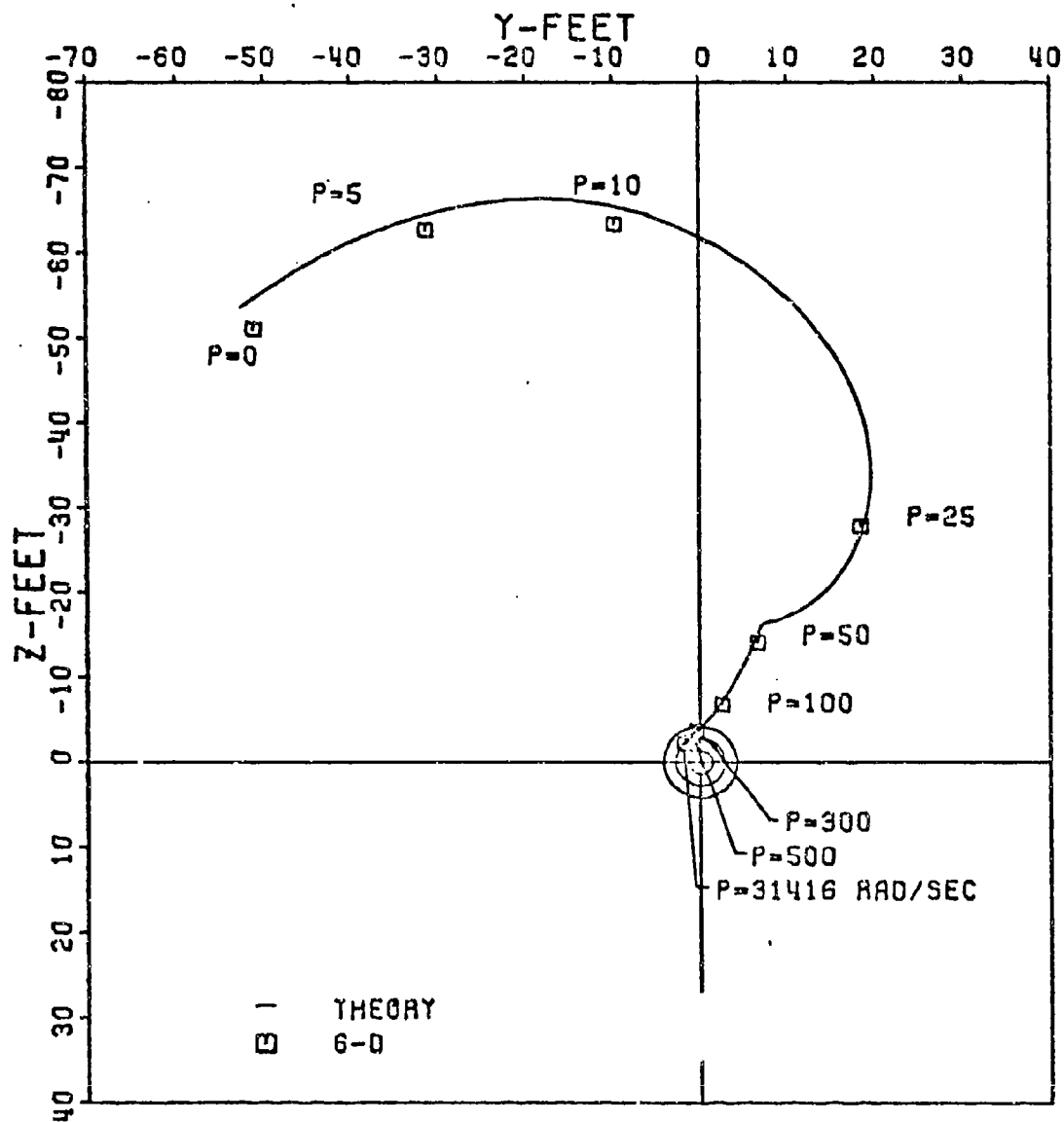


Figure 22. Dispersion: Phase III Cases 157-167

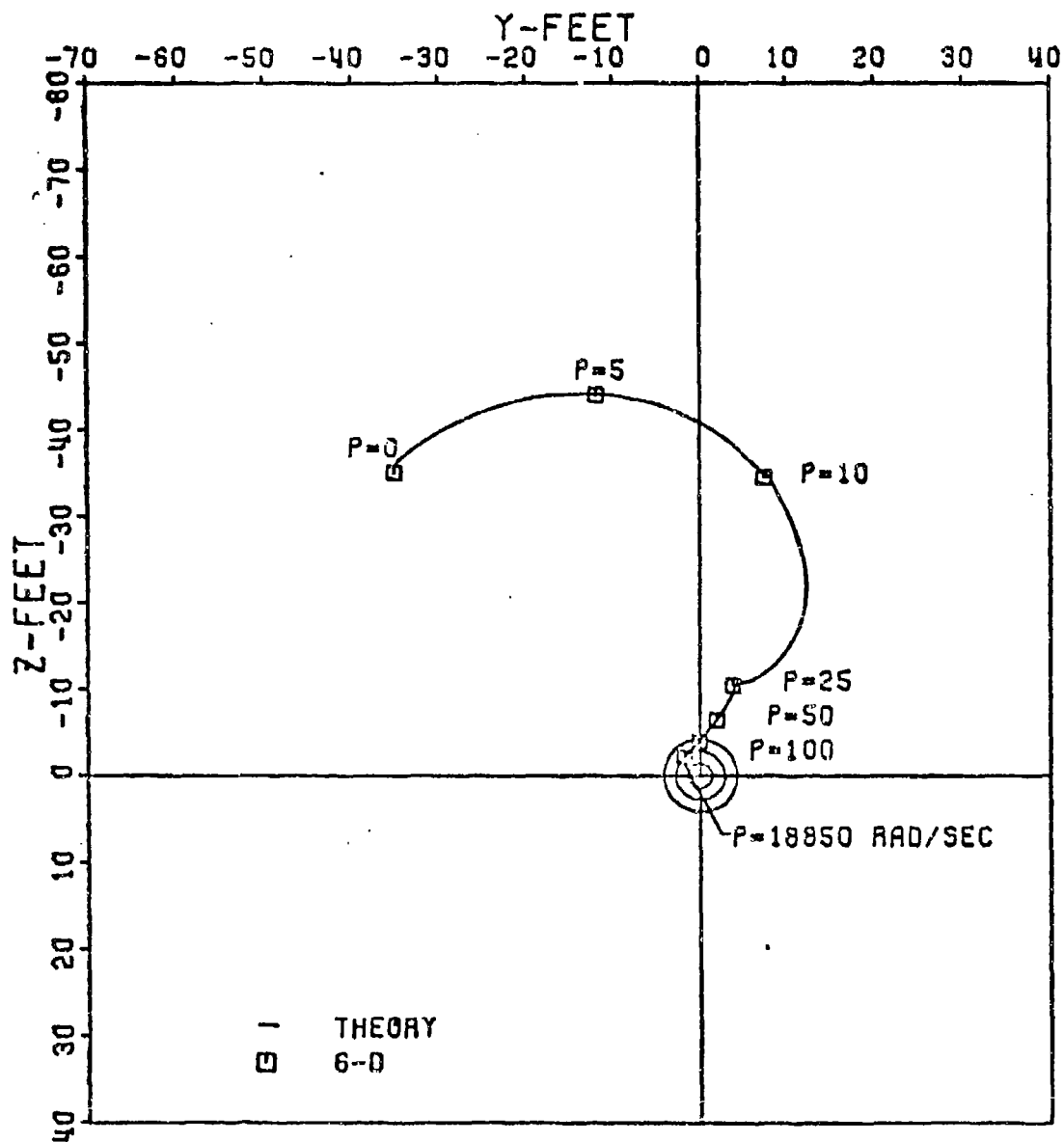


Figure 23. Dispersion: Phase III Cases 168-178

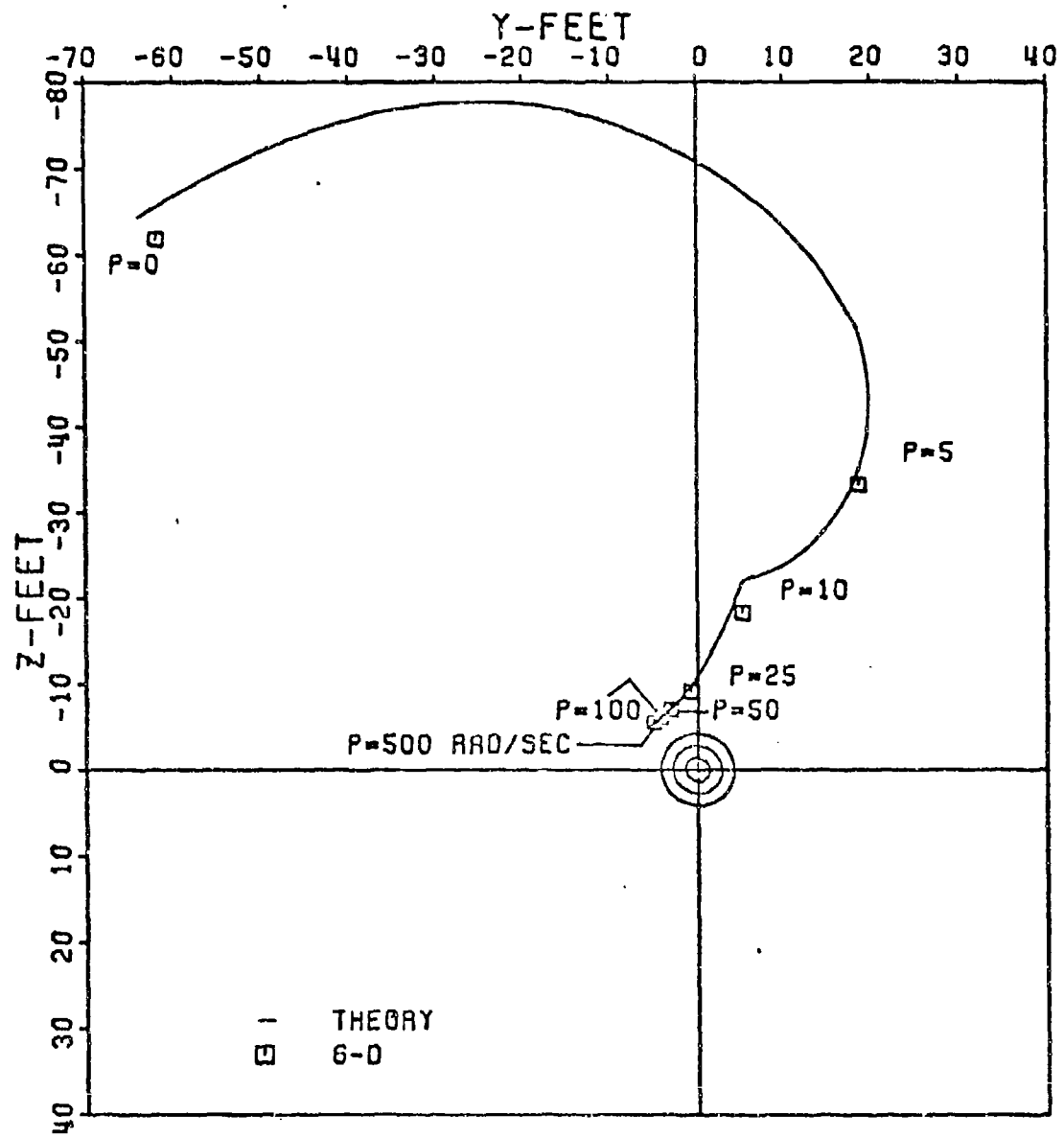


Figure 24. Dispersion: Phase II' Cases 179-189

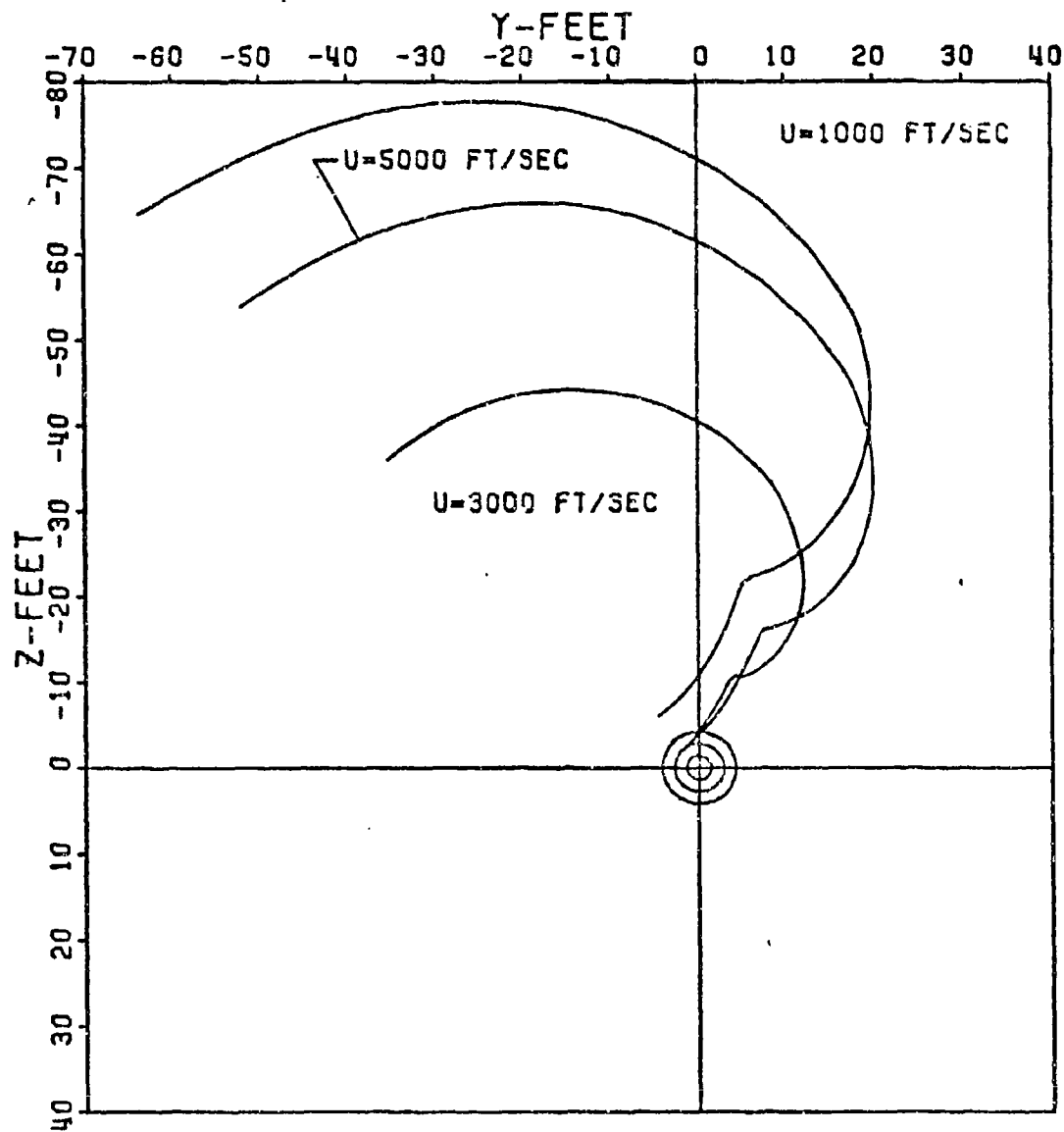


Figure 25. Dispersion: Phase III Theory, Cases 157-189

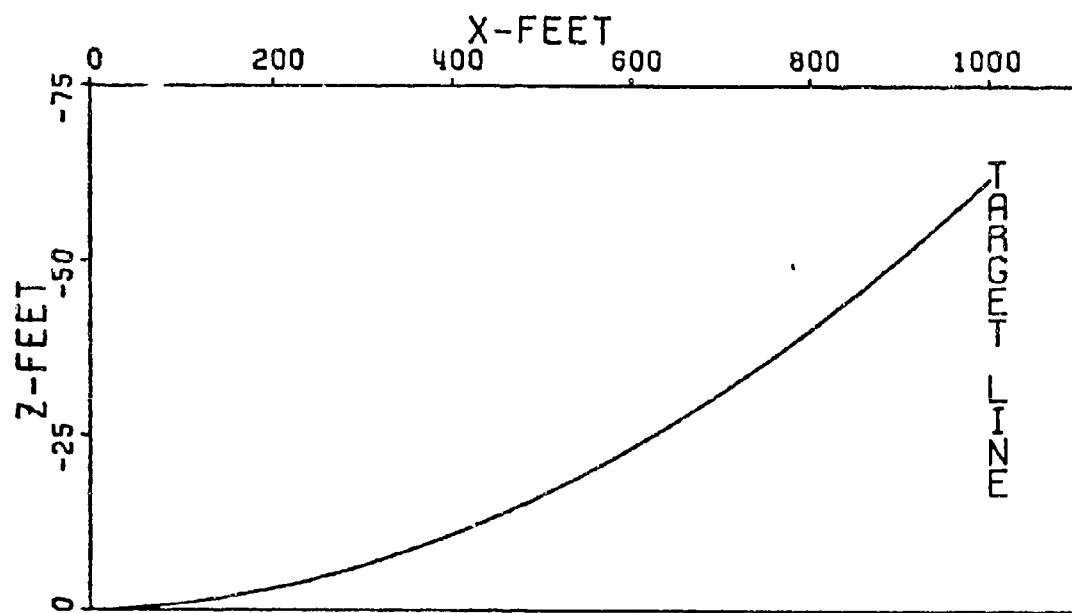
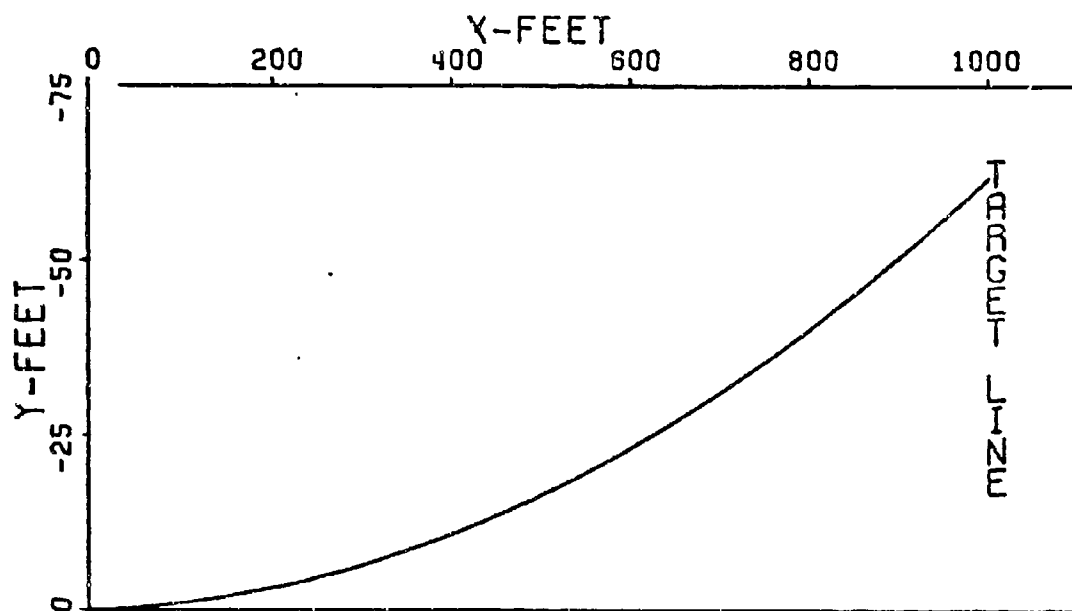


Figure 26. Trajectory, Case 189



and all three theories extended beyond the limits used in the previous validation. The high roll rate theory is a straight line going off to infinity as  $p$  goes to zero. Although the length of the curve in which it is an effective theory is short graphically, the range of roll rates it encompasses is tremendous. Figure 28 illustrates the effective limits of each theory; that is, on the spectrum of possible roll rates it shows where each theory is the most effective. The low roll rate theory handles the largest graphical area but only roll rates less than 100 rad/sec and greater than 5 rad/sec. The upper limit of 100 rad/sec was chosen since here the low roll theory attaches itself to the 6-D results while the high roll theory diverges. The lower limit of 5 rad/sec corresponds to  $pt \leq 1.0$ . Figures 27 and 28 depict Cases 58-68 where  $u_0 = 5000$  ft/sec or  $t = 0.2$  sec. Therefore  $p = 5$  rad/sec corresponds to  $pt = 1.0$ . The very low roll rate theory has the smallest range but is essential in predicting dispersion as the roll rate goes to zero. As  $pt > 1$ , the theory diverges as would be expected from a power series; Equation 29. The sharp turn occurs at  $p \approx 20$  rad/sec or  $pt \approx 4$  for Cases 58-68. Although Cases 58-68 were illustrated here, this analysis of the effective limits of the roll theories was found to be similar for all other cases. For the  $u_0 = 3000$  ft/sec cases the low roll theory limits were  $3.0 < p < 50$  for  $u_0 = 1000$  ft/sec cases:  $1.0 < p < 25.0$ .

#### Phase IV

To validate the effects of gravity on dispersion, a final set of cases were run using the high roll rate theory, Equation 24. Ordinarily, one would think that gravity would only introduce a constant term; one

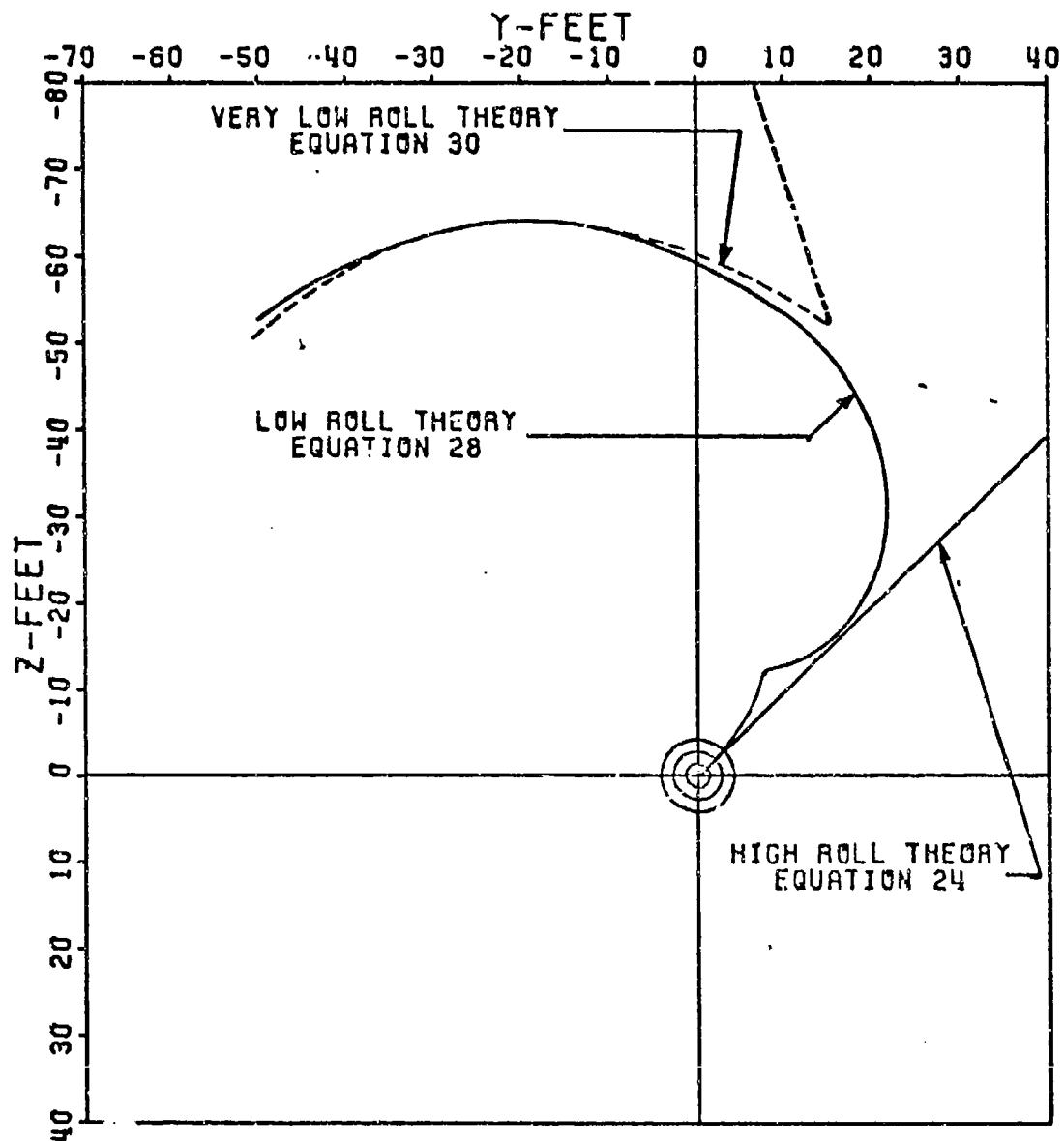


Figure 27. Phase III Theory Equations 24, 28, 30

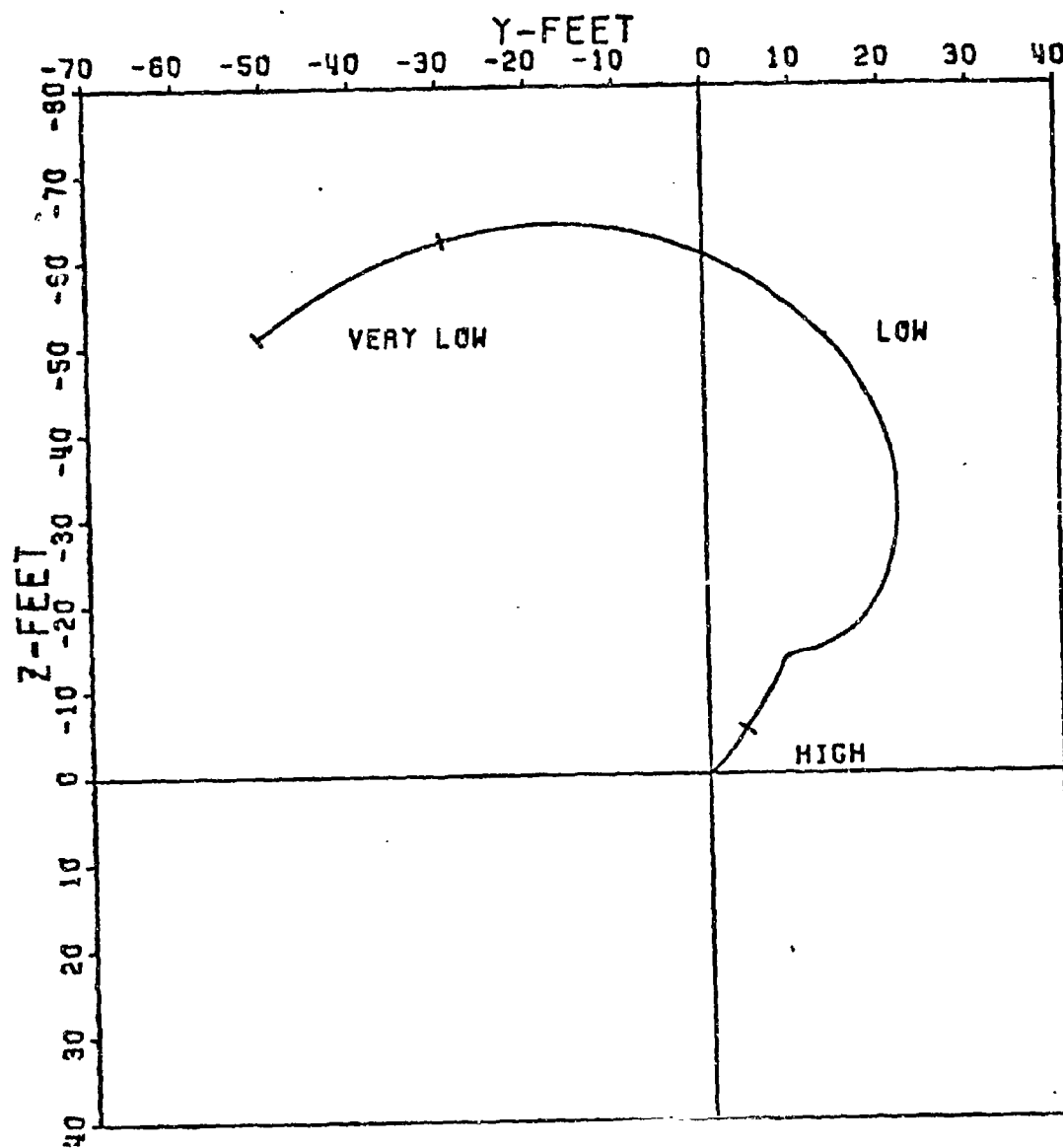


Figure 28. Phase III Theory Effective Limits

that could be factored out. However integration of the equations of motion produce a gravity term dependent upon roll rate. Determination of its validity and consequence is what is important here.  $\vec{S}_0$ ,  $\vec{\alpha}_0$ , and  $\vec{\dot{\alpha}}_0$  were set to zero in order to allow determination of the effects due to roll rate and velocity. The reduced governing equation becomes:

$$\vec{J} \cdot \vec{A} = \frac{ig}{2} \left( \frac{x}{u^2} \right) \left[ 1 + \frac{ipI_x}{mud} A \right] 1000$$

No aerodynamic asymmetries were present and the effects of gravity were assumed independent of effects due to  $\vec{S}_0$ ,  $\vec{\alpha}_0$ ,  $\vec{\dot{\alpha}}_0$ ; a logical assumption. Table XIX lists the results.

Table XIX indicates that the effects due to gravity occur largely in the vertical plane, as would be expected. The transverse contribution is minimal but is affected by both velocity and roll rate. The vertical contribution is only affected by velocity. The unstable cases indicate maximum use of Magnus and thus maximum transverse effects on dispersion. It can be concluded from this brief but thorough treatment that gravity effects dispersion only in the vertical plane (for all practical purposes) and that its contribution is constant with velocity. The roll dependent term,  $\frac{ipI_x}{mud} A$ , has been shown to exist but become negligible for the flechette. This term would possibly become important for projectile dispersion and other missile applications. Projectile motion with gravity is typified by a cocking right of the projectile in flight with a positive  $CM_\alpha$  but negative  $C_{Z_\alpha}$ ; the parameter A would become negative and the entire roll dependent term, positive; that is, cocked to the right, dispersion to

TABLE XIX  
THEORY VALIDATION, GRAVITY  
CASES 190-201

C A S E	Initial Conditions					Coefficients			$\vec{J} \cdot \vec{A}$ . (mils)	
	$\vec{S}_0$	$\vec{\alpha}_0$	$\vec{\dot{\alpha}}_0$	$p_0$	$u_0$	$CZ_\alpha$ $CM_\alpha$ $CM_q + CM_{\dot{\alpha}}$	$CZ_{p\beta}$ $CM_{p\beta}$	$CYE$ $CZE$ $CME$ $CNE$	6-D	Theory
190	↑	↑	↑	31416	5000	↑	↑	↑	-0.001 +0.644i	-0.001 +0.644i
191				18850					-0.001 +0.644i	-0.001 +0.644i
192				6283					-0.001 +0.644i	-0.001 +0.644i
193				0					0.000 +0.644i	0.000 +0.644i
194	0	0	0	31416	3000	A1	A1	0	-0.002 +1.788i	-0.003 +1.789i
195				18850					-0.001 +1.789i	-0.002 +1.789i
196				6283					0.000 +1.788i	-0.001 +1.789i
197				0					0.000 +1.788i	0.000 +1.789i
198	↓	↓	↓	31416	1000	↓	↓	↓	Unstable	
199				18850					Unstable	
200				6283					0.001+ 16.100i	0.001+ 16.100i
201				0					0.000+ 16.100i	0.000+ 16.100i

the right. For a finned missile the opposite would occur due to the agreement in sign between  $C_{M\alpha}$  and  $C_{z\alpha}$ .

## FREE FLIGHT DATA ANALYSIS

In order to analyze actual test firings as to jump and dispersion and correlate them with the validated theory, the initial conditions of each test firing must be obtained and put into the proper form. To obtain raw experimental data, test firings were conducted by the U.S. Army, Frankford Arsenal. The configuration tested was the Producibility Ground Point Flechette, Figure 29. The raw data required was both translational and angular; that is, data was needed to determine position as a function of time and angle of attack of the flechette as a function of time. To accomplish this, Frankford Arsenal devised the test apparatus shown in Figure 30. The gun barrel was mounted on a steel girder and a laser beam was used to obtain the aim point on a target 50 meters down range. At positions, 1, 3, 5, 7, 9, and 11 feet downrange, orthogonal flash x-ray tubes were placed to photograph the flechette as it passed its station. One tube was placed to allow a top view at each station and provide a means of obtaining swerve and yaw data. The other tube allowed a side view at each station to obtain heave and pitch data. At each station reference marks oriented the flechette as to its exact position downrange. This was to allow for any timing error and/or variation in muzzle velocity. The photographs were taken using special soft flash x-ray tubes which permit the photographing of the low density sabot pieces and analyzing the separation in addition to the motion of the flechette.

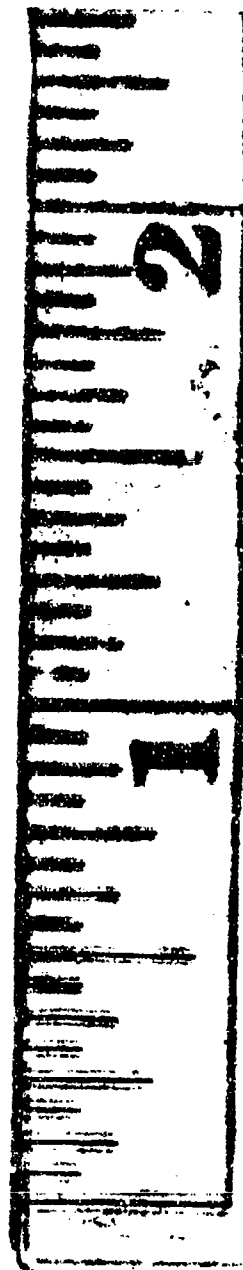


Figure 29. Ground Point Flechette, With and Without Sabot



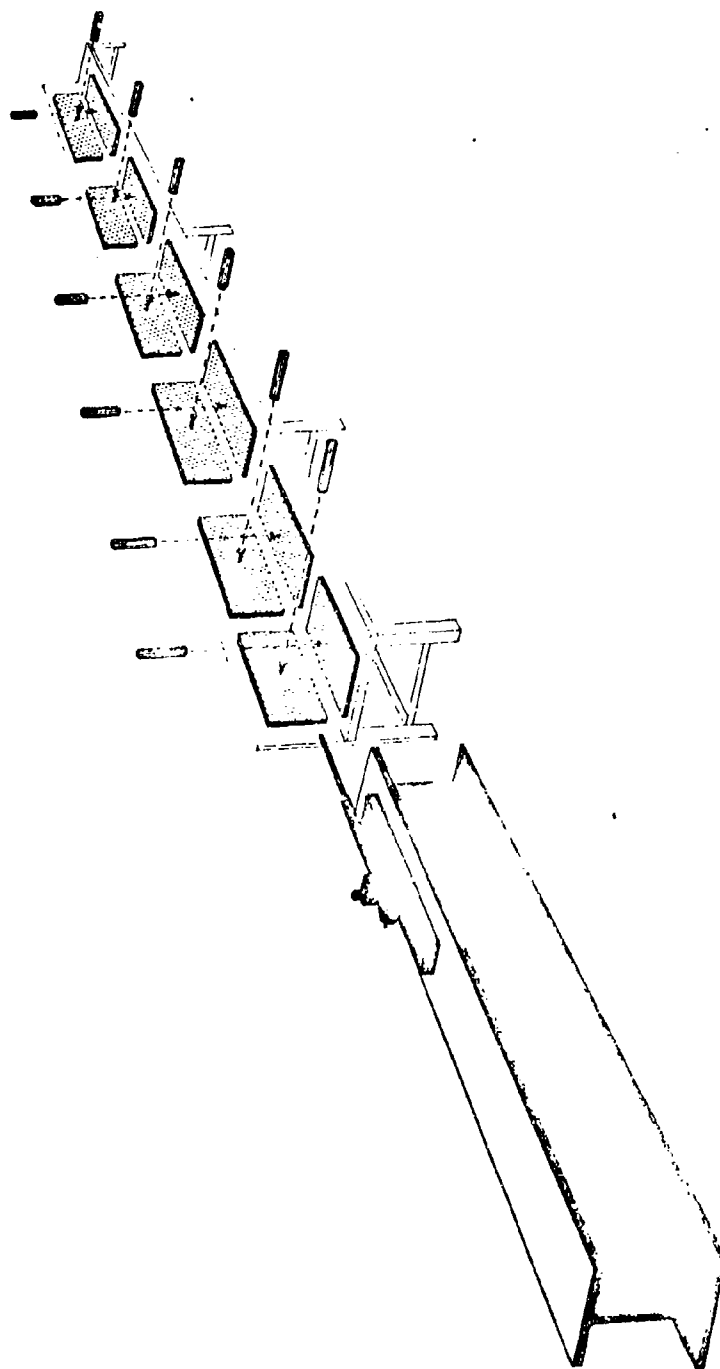


Figure 30. Free Flight Test Apparatus and Set-up

From the battery of test firings of 20 rounds of each type (which included tests of the ground point, and swayed point producibility flechette as well as the R&D version), 8 of the ground point producibility rounds were selected to be analyzed. The eight rounds along with velocity, roll rates and target positions are given in Table XX.

Raw translational and angular data are shown in Figures 31 through 46. The figures illustrate the position and complex angle of attack of the flechette for each station.

TABLE XX  
FRANKFORD TEST FIRING DATA

R O U N D	$u_o$	$p_o$	Target at 50 ft.	
			Y (ft)	iZ (ft)
4	4747	11,454	0.117	-0.038
6	4662	13,201	0.053	-0.010
7	4642	14,219	0.141	-0.004
8	4662	13,000	0.053	0.099
14	4758	13,289	0.053	0.016
16	4753	17,354	0.084	-0.004
17	4677	16,613	0.070	-0.019
19	4679	11,913	0.089	0.059

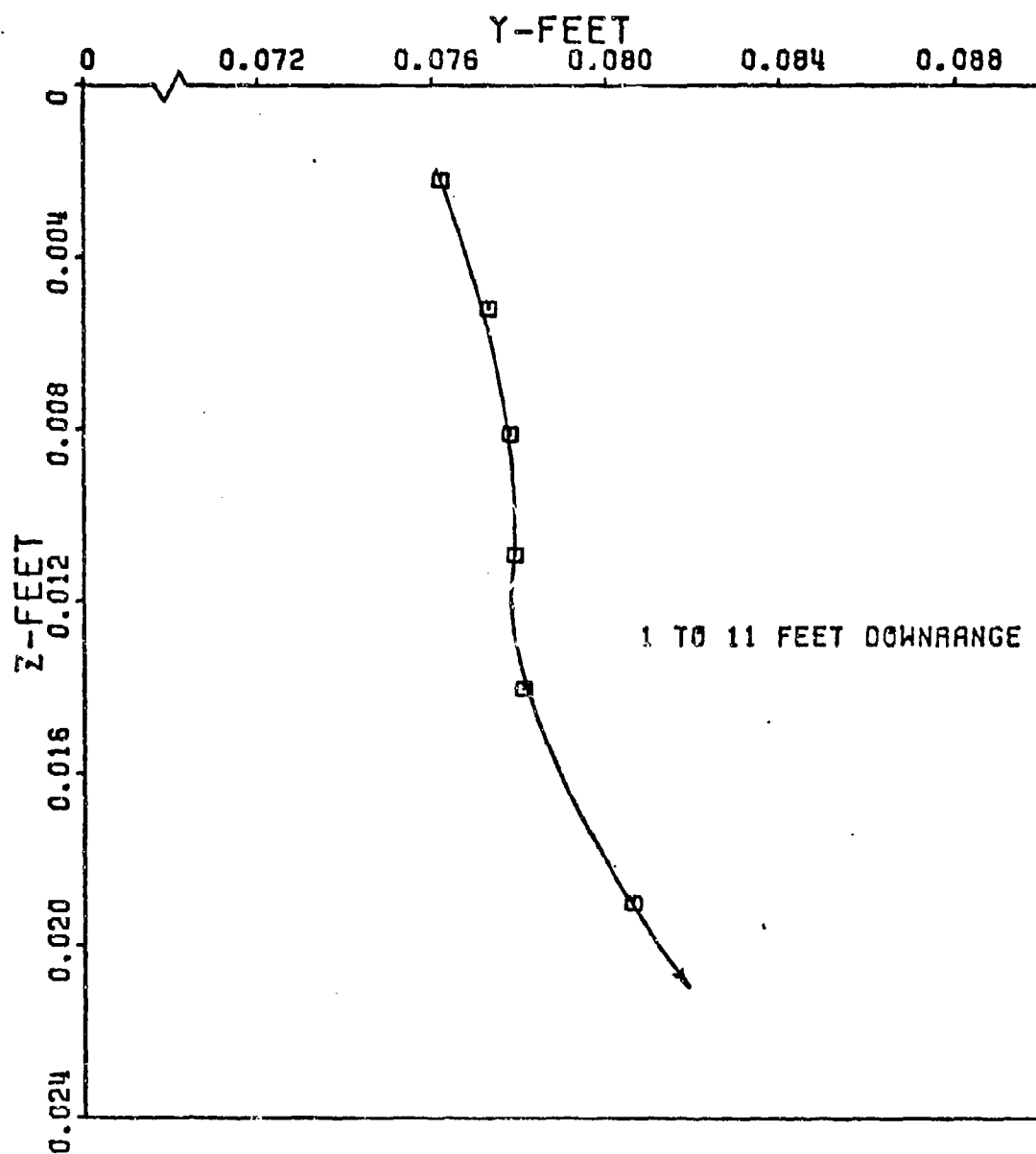


Figure 31. Raw Translational Data Ground Point - Round 4

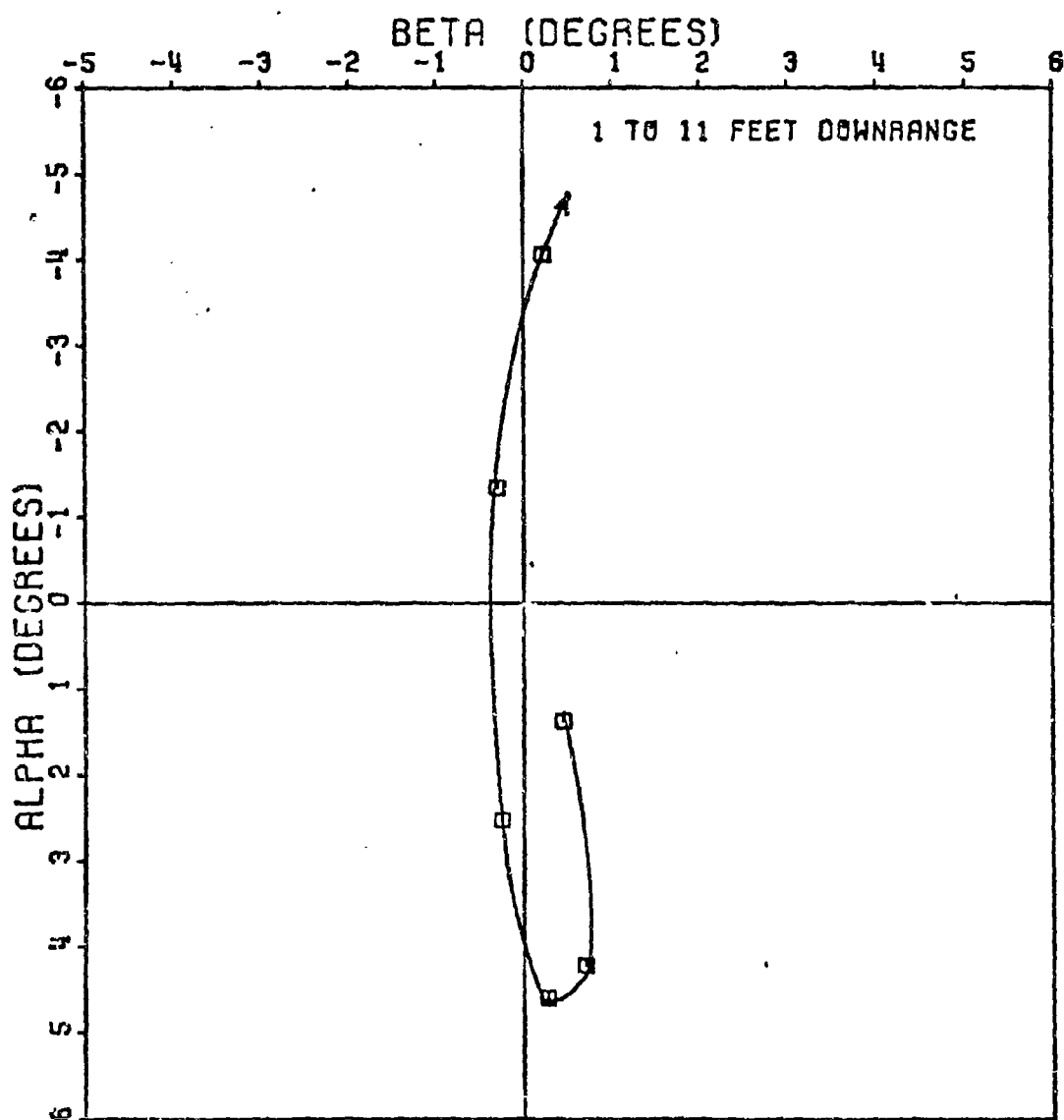


Figure 32. Raw Angular Data Ground Point - Round 4

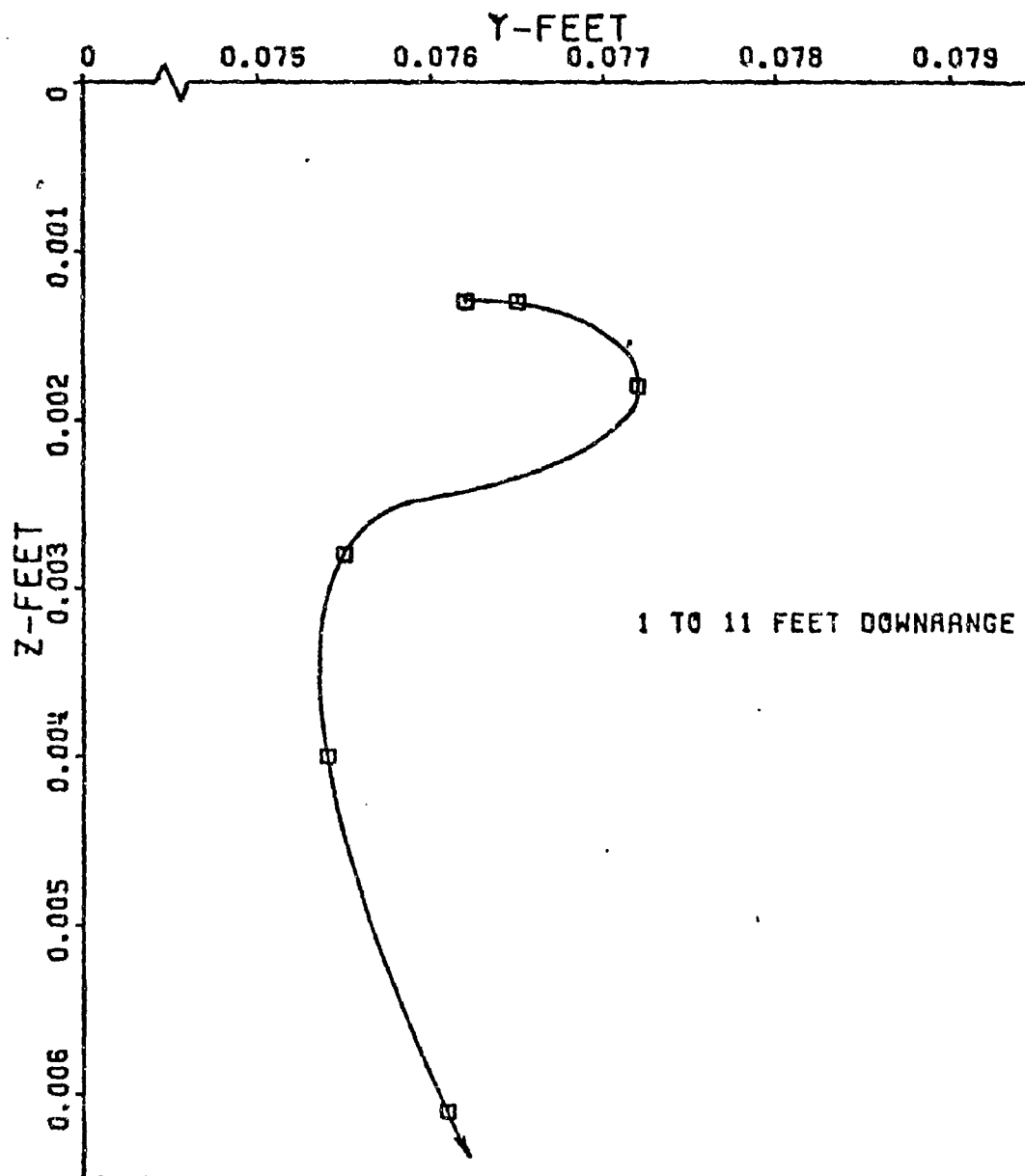


Figure 33. Raw Translational Data Ground Point - Round 6

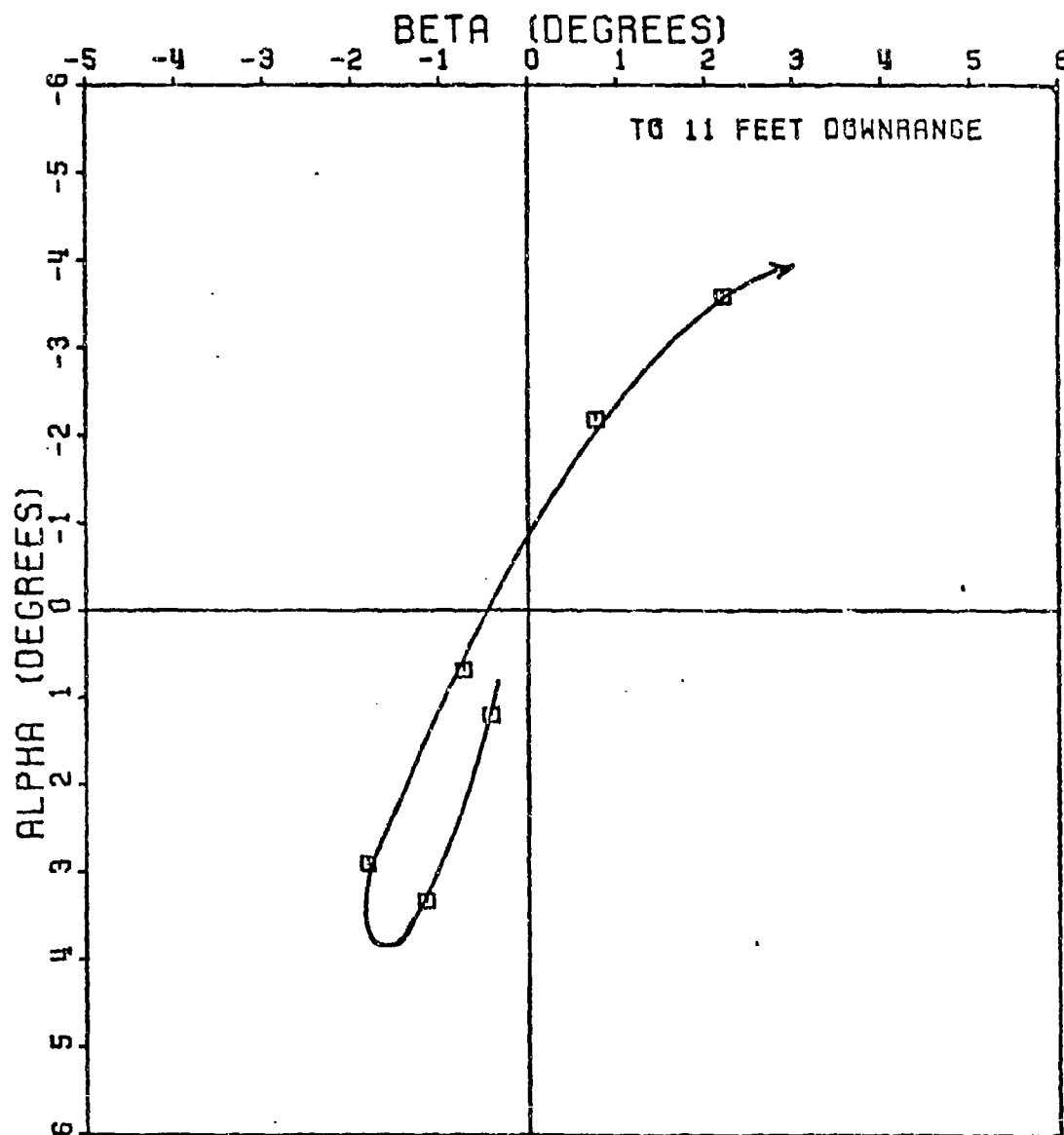


Figure 34. Raw Angular Data Ground Point - Round 6

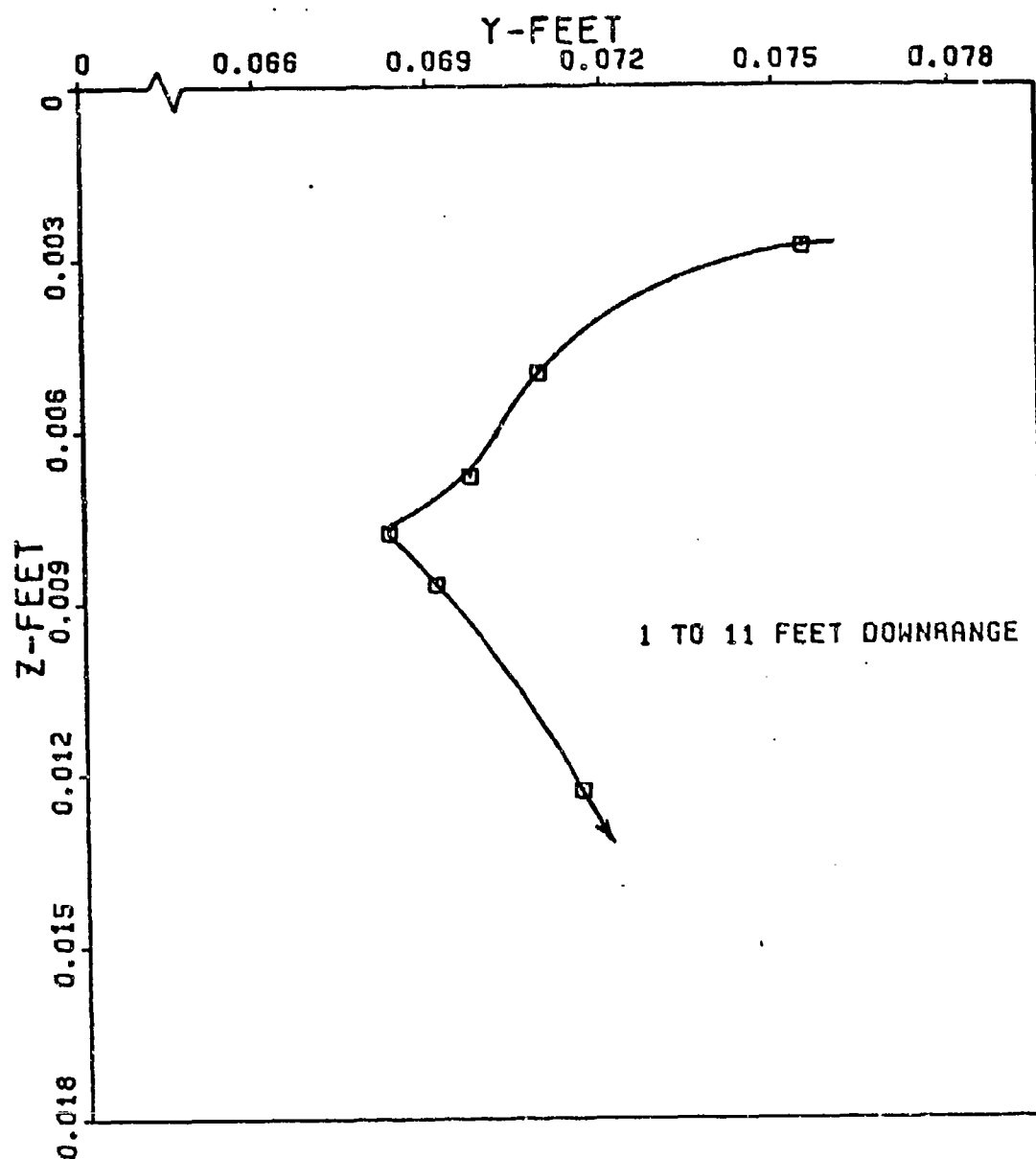


Figure 35. Raw Translational Data Ground Point - Round 7

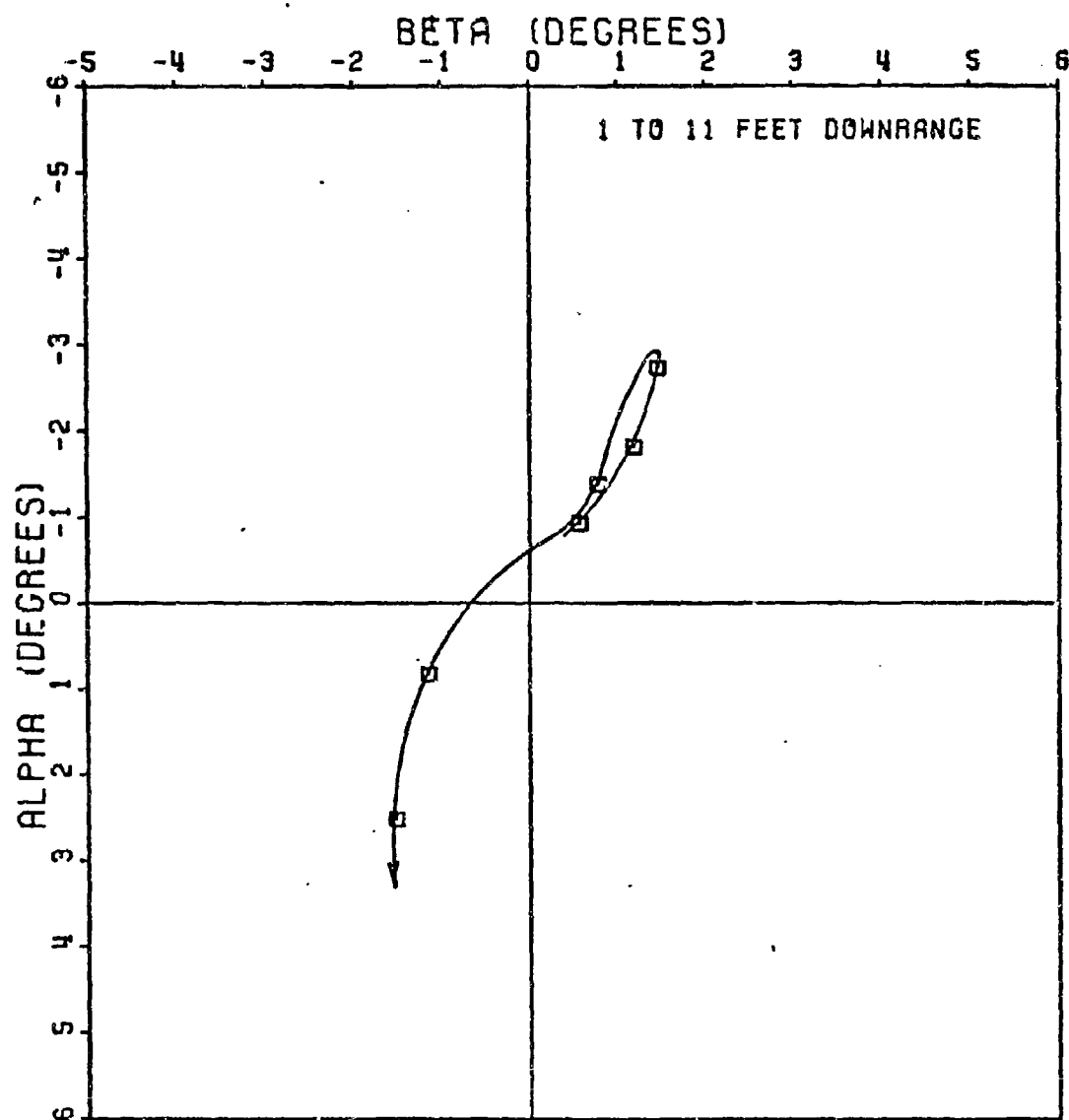


Figure 36. Raw Angular Data Ground Point - Round 7



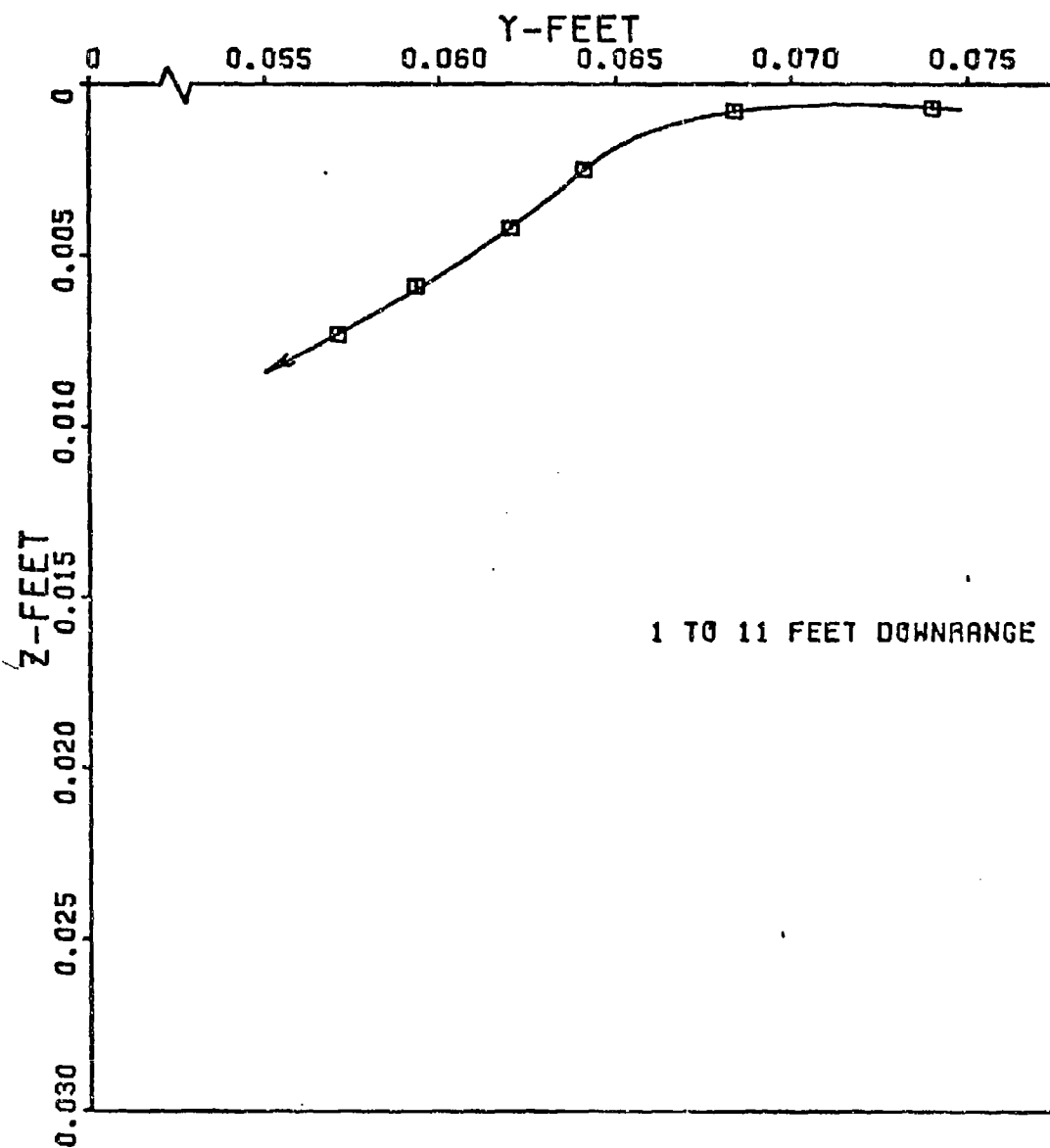


Figure 37. Raw Transitional Data Ground Point - Round 8

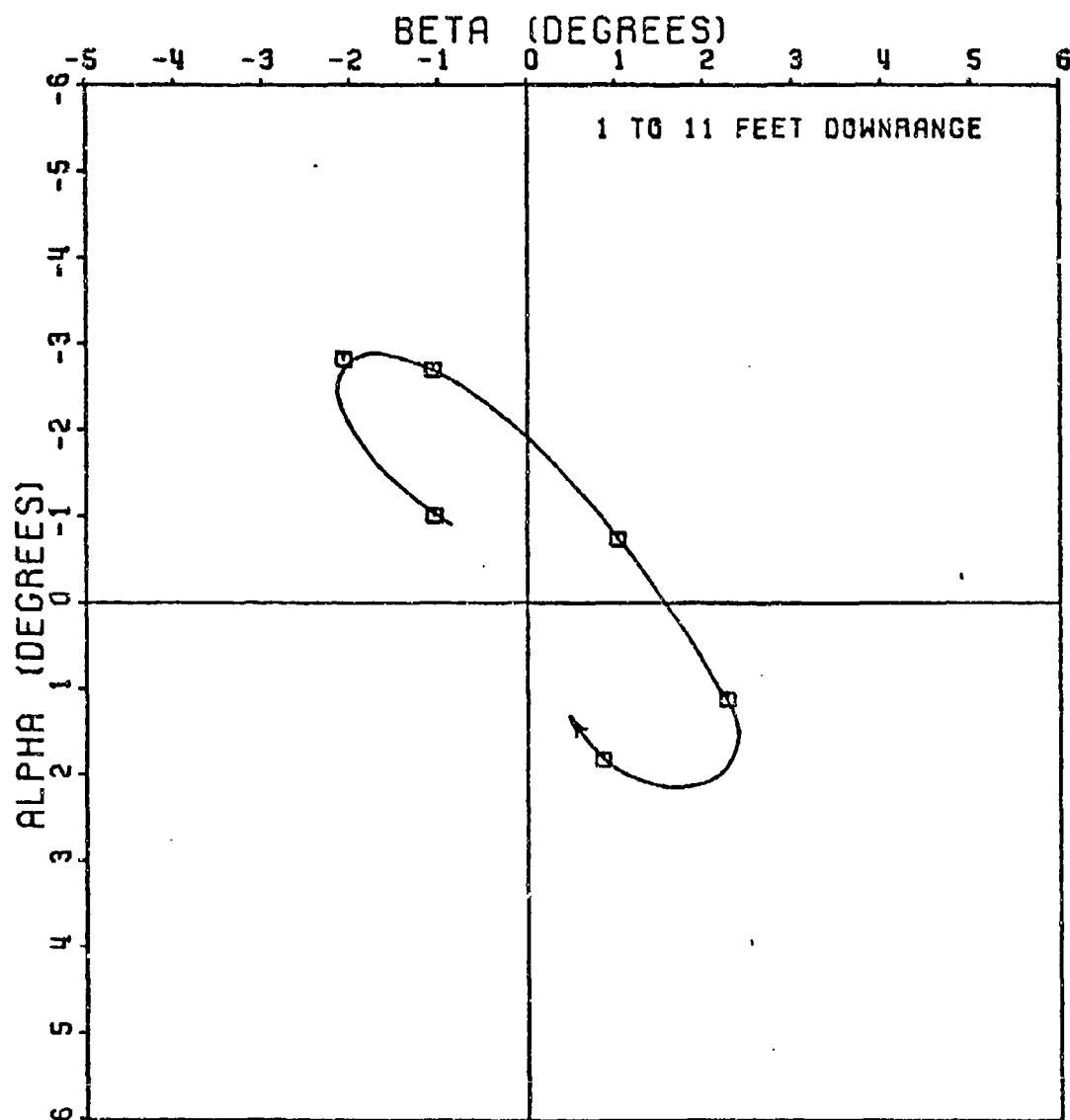


Figure 38. Raw Angular Data Ground Point - Round 8

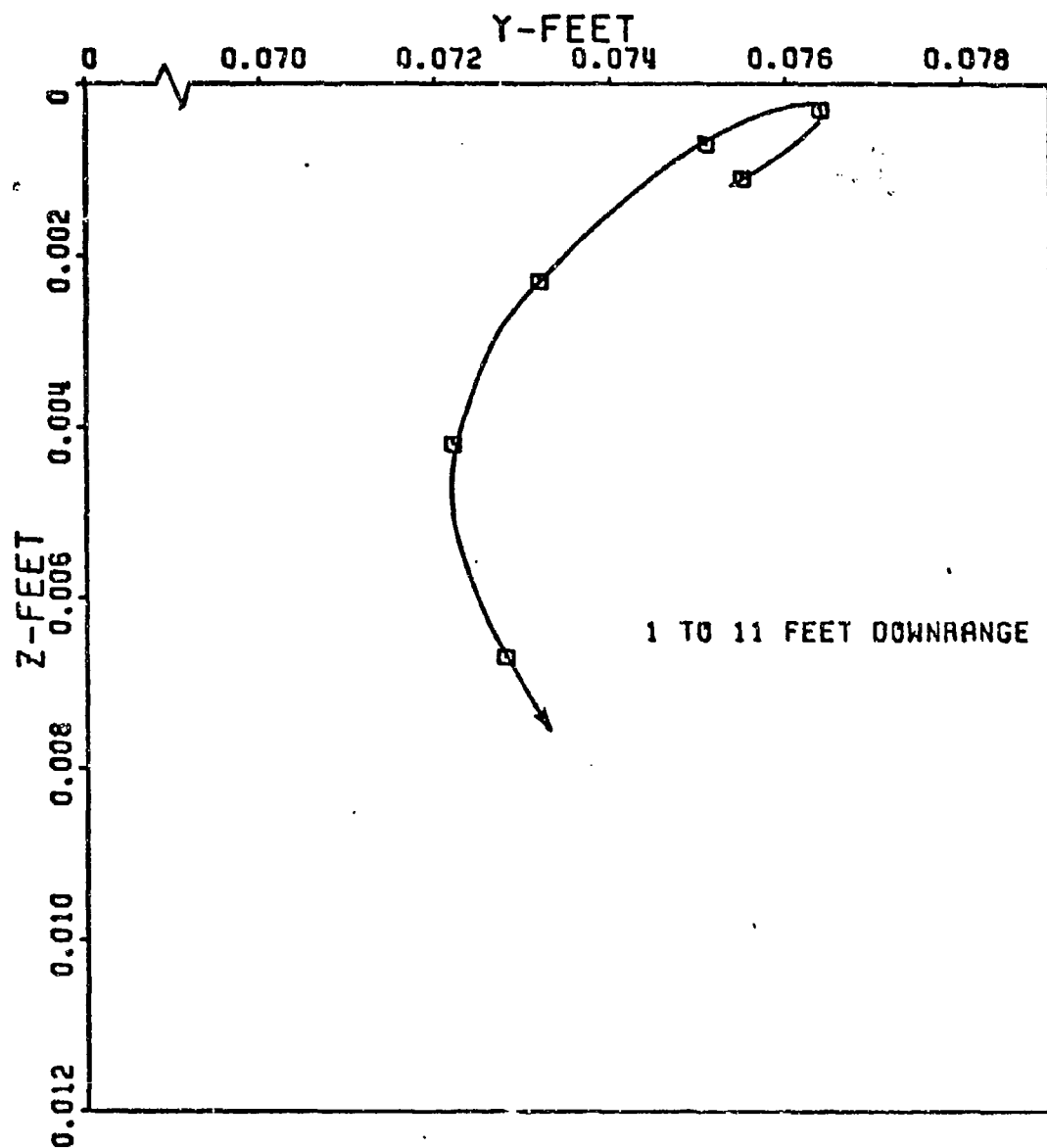


Figure 39. Raw Translational Data Ground Point - Round 14

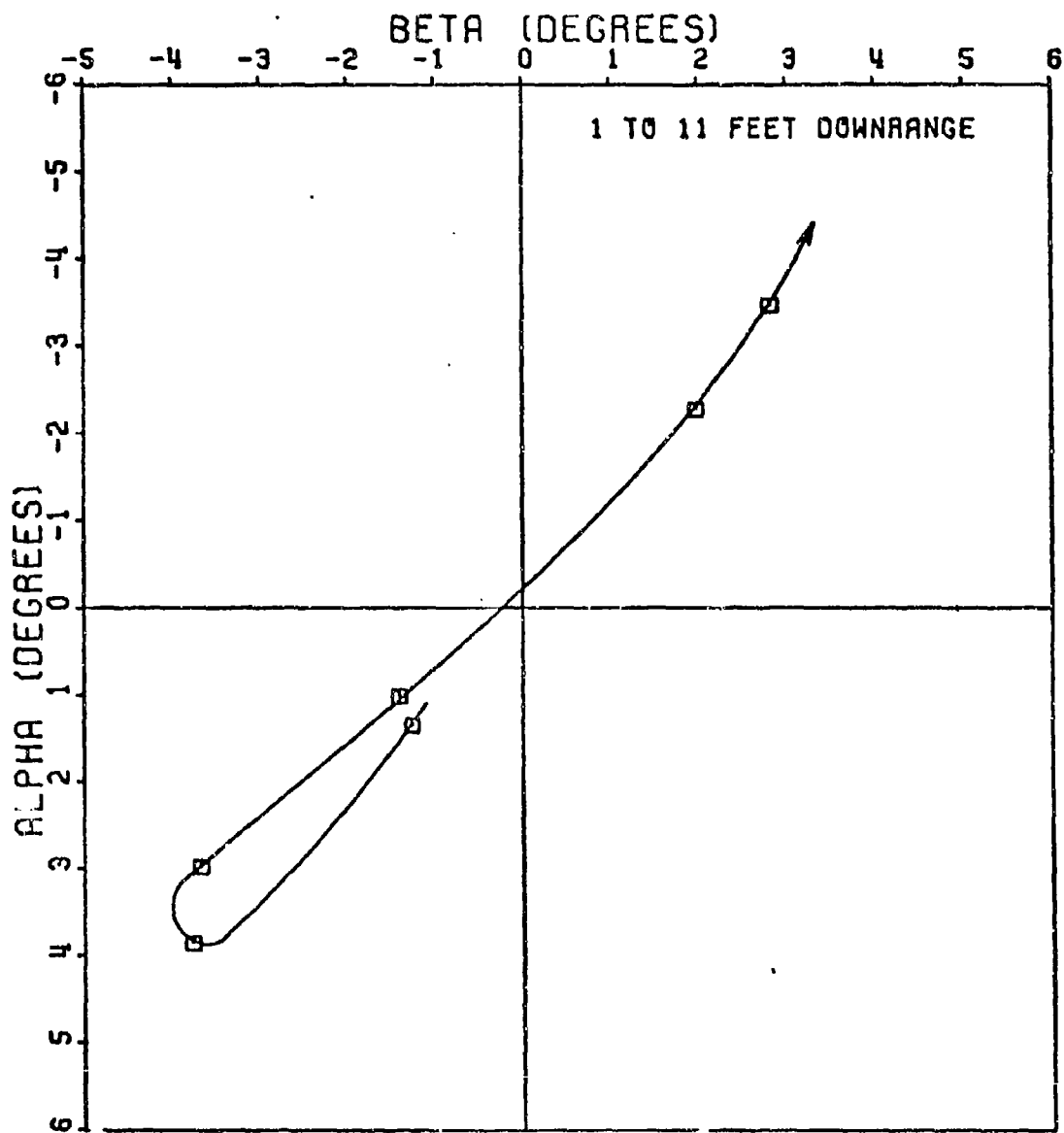


Figure 40. Raw Angular Data Ground Point - Round 14

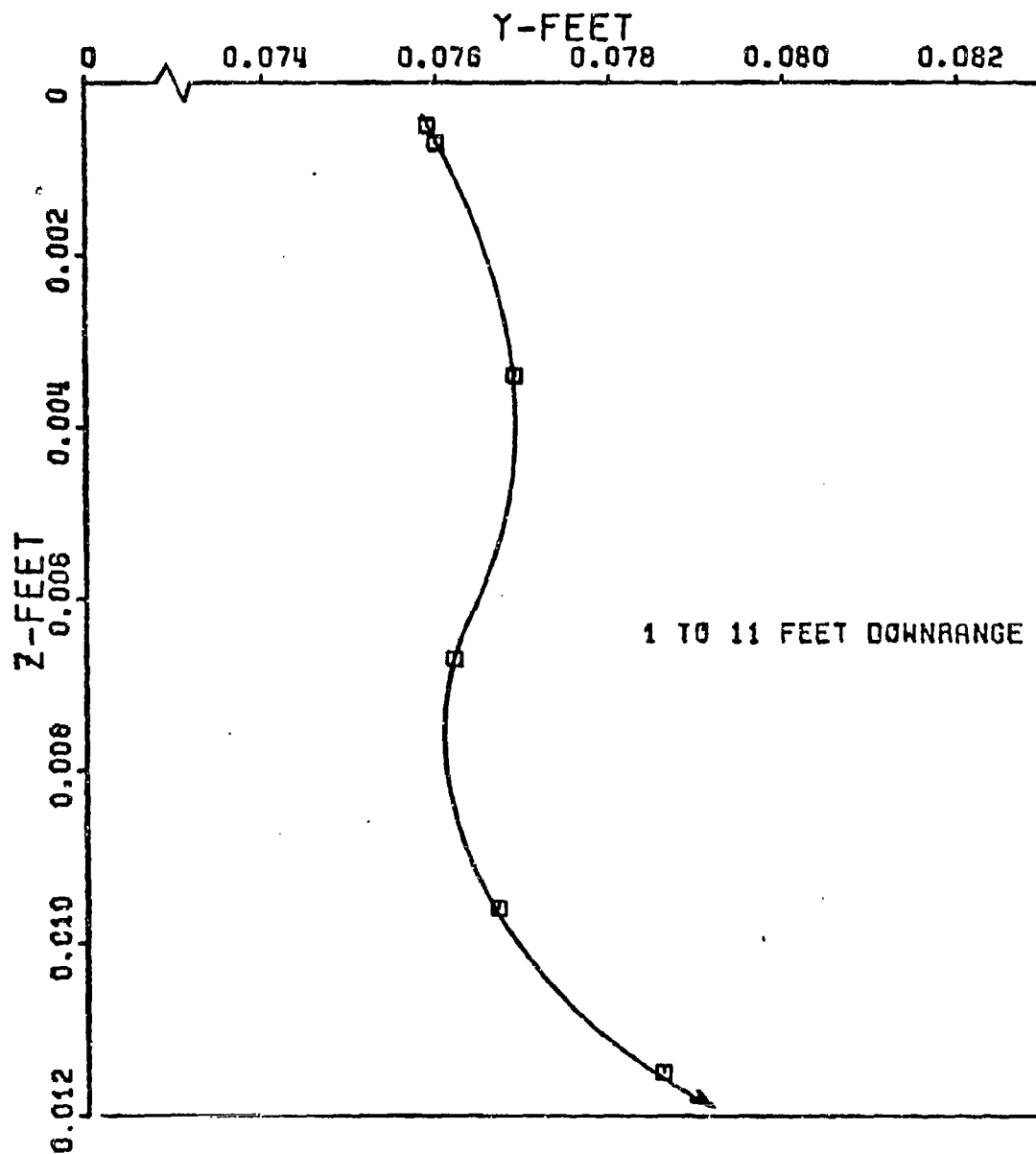


Figure 41. Raw Translational Data Ground Point - Round 16

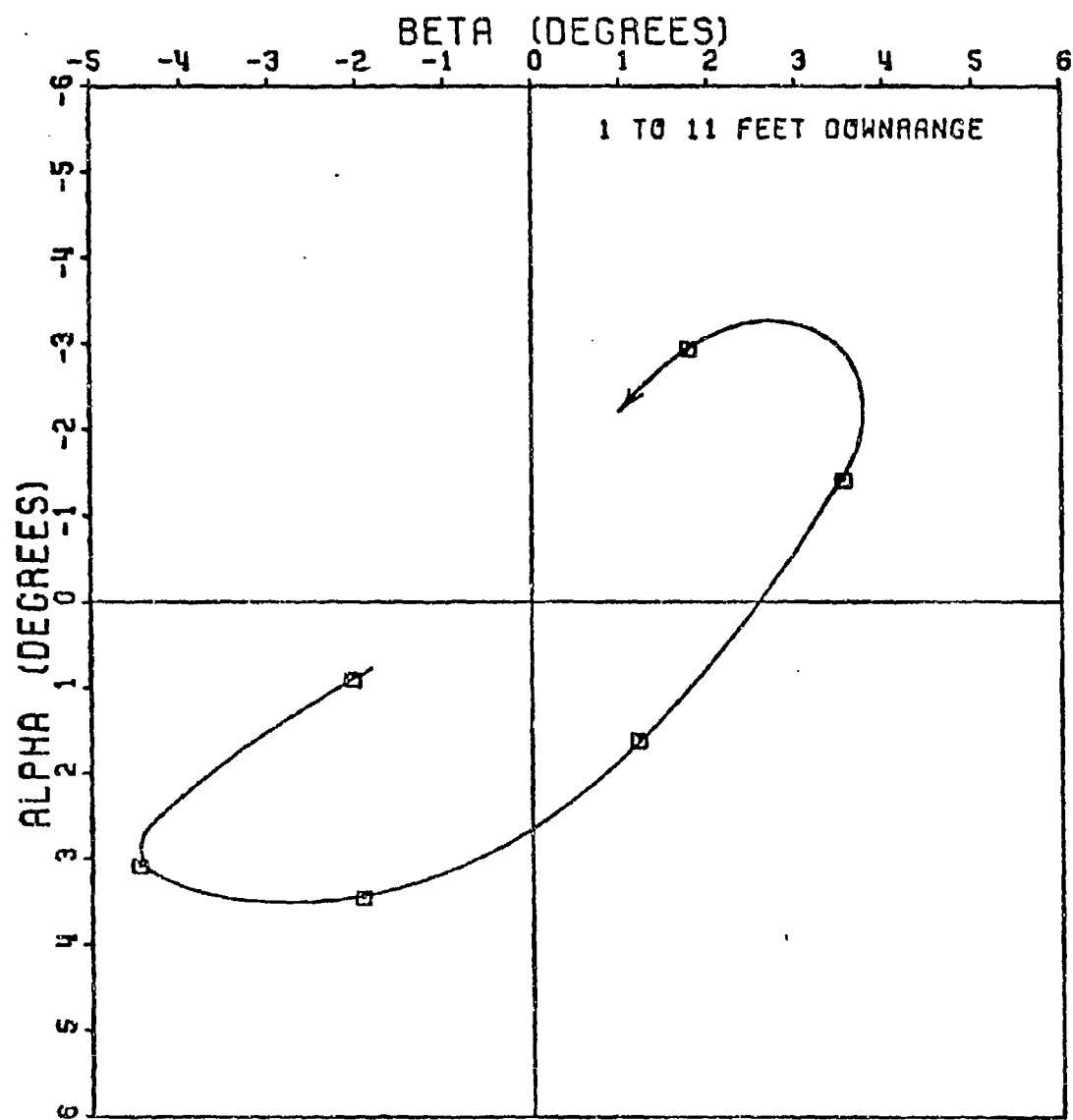


Figure 42. Raw Angular Data Ground Point - Round 16

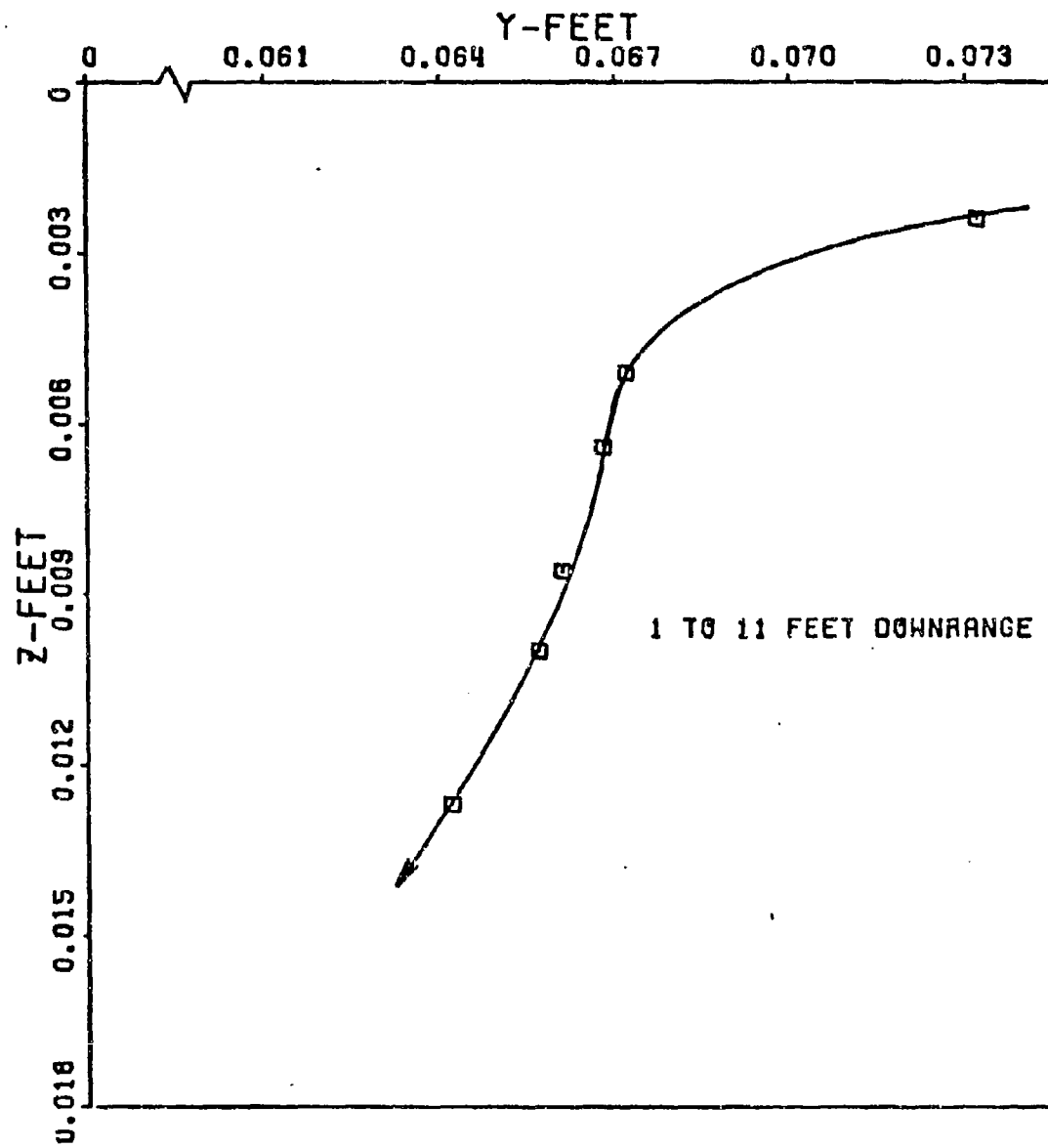


Figure 43. Raw Translational Data Ground Point - Round 17

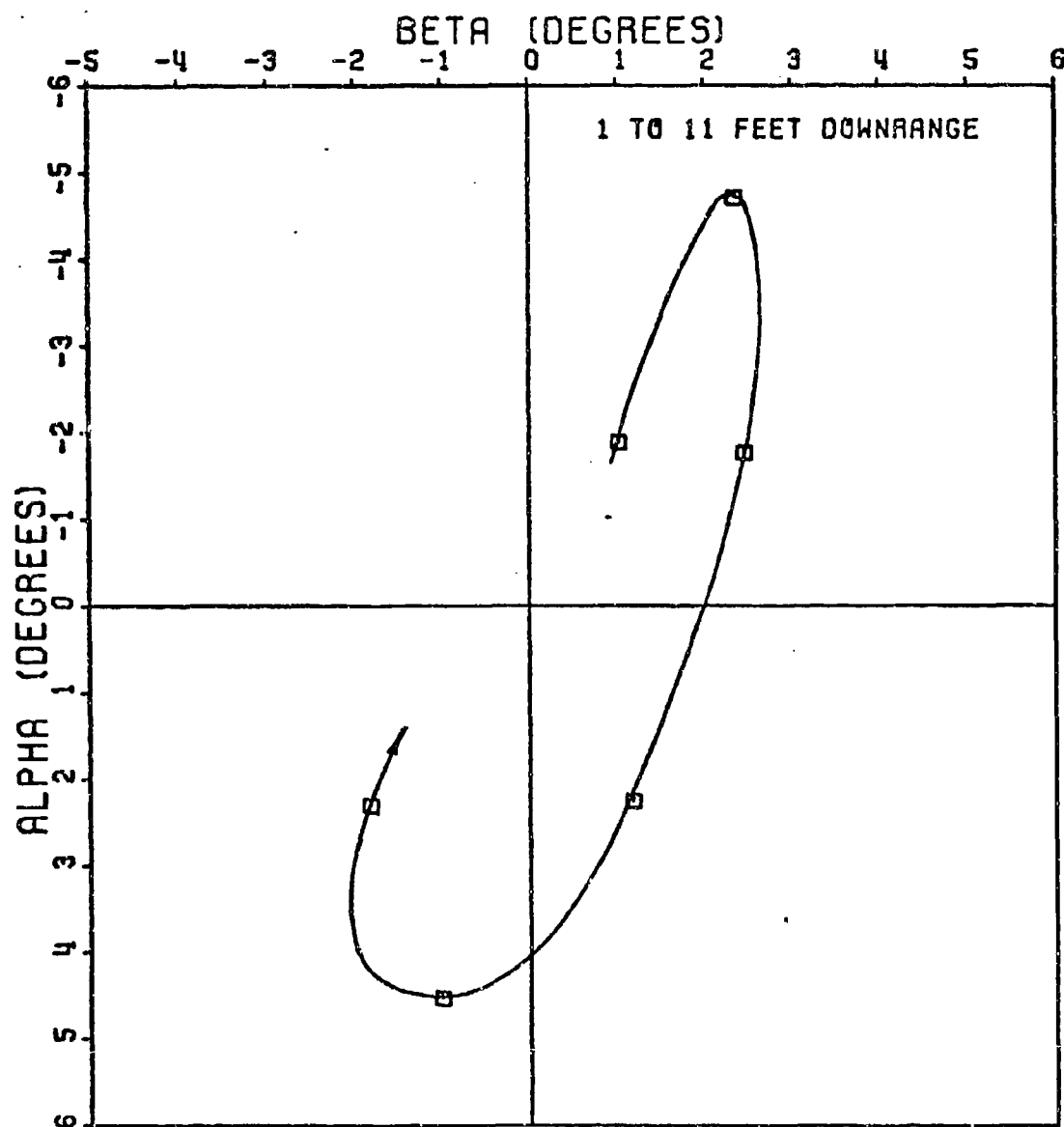


Figure 44. Raw Angular Data Ground Point - Round 17



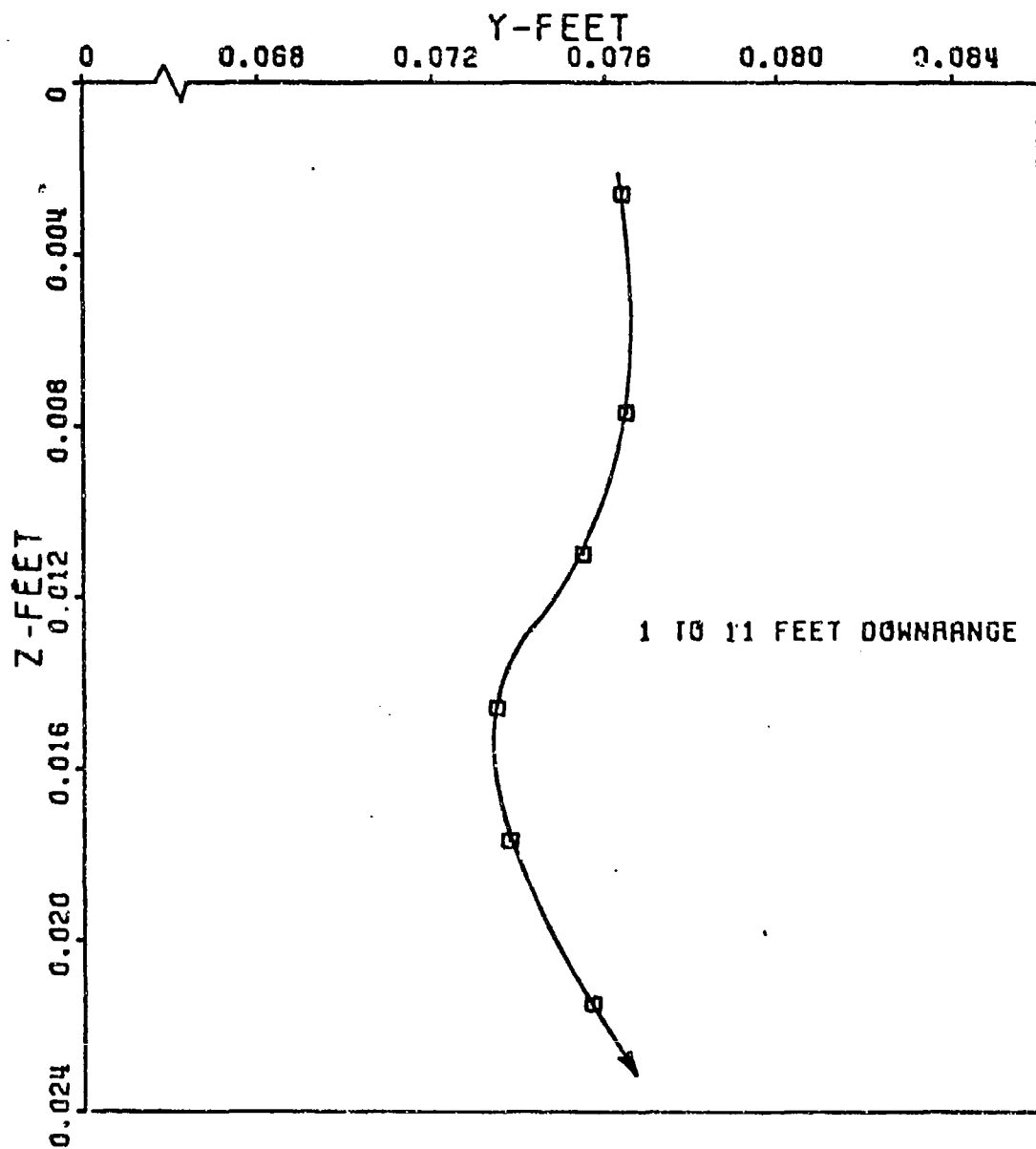


Figure 45. Raw Translational Data Ground Point - Round 19

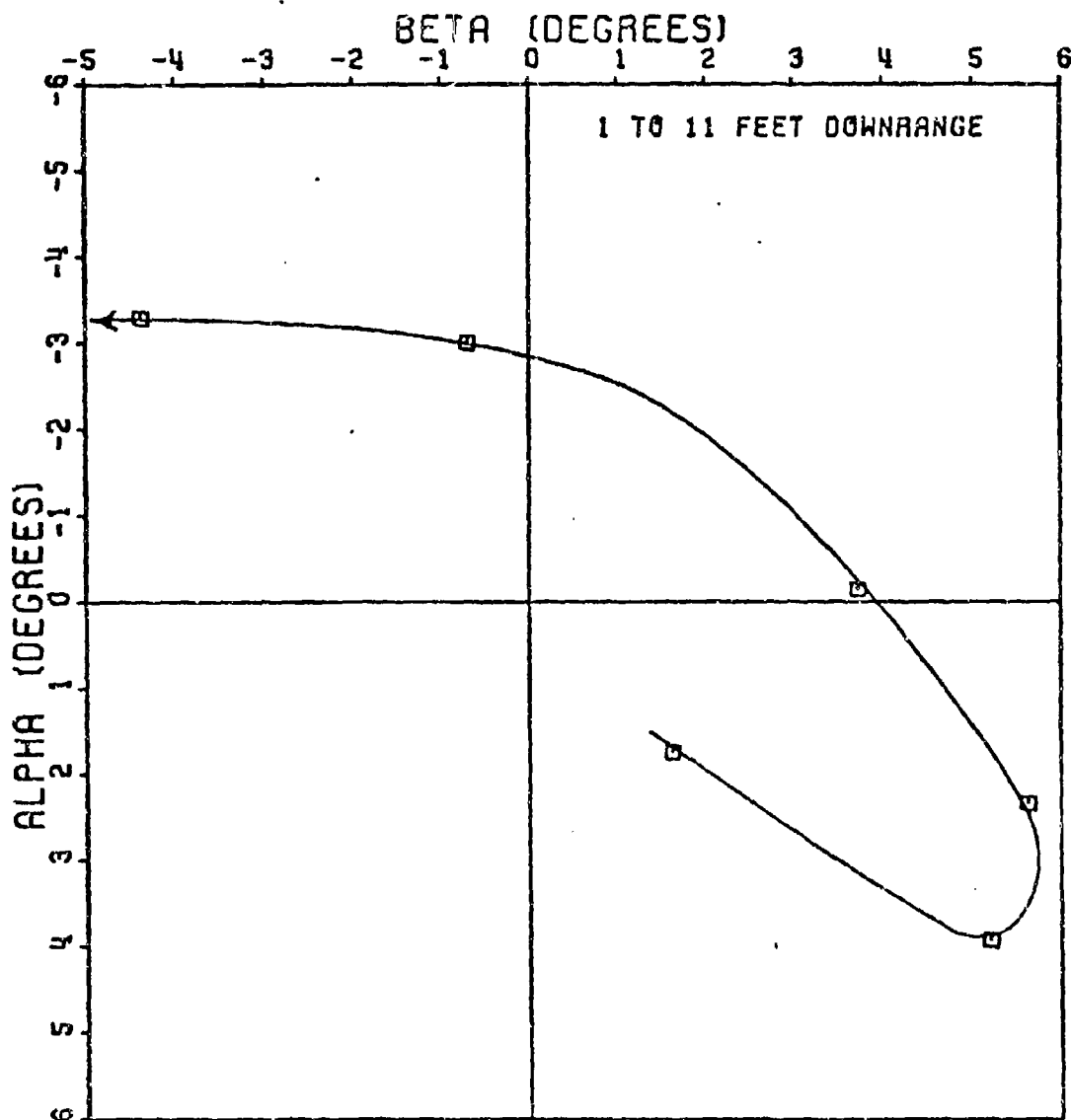


Figure 46. Raw Angular Data Ground Point - Round 19

Once the raw data was obtained, it had to be converted into a form such that initial conditions  $\vec{S}_0$ ,  $\dot{\vec{S}}_0$ ,  $\vec{\alpha}_0$  and  $\dot{\vec{\alpha}}_0$  could be extracted from it. To eventually arrive at values for  $\vec{S}_0$  and  $\dot{\vec{S}}_0$ , the translational parameters, the raw position or translational data had to be approximated by equations. The raw data was fitted to a polynomial equation of third degree by a least squares method. The data in the y-direction was fit separately from that in the z-direction to distinguish between the swerve and heave contributions. With the equations obtained, a simple differentiation yielded equations for the velocities in the y and z directions. The initial conditions  $\vec{S}_0$  and  $\dot{\vec{S}}_0$  are now readily obtainable:

$$\begin{aligned}\vec{S}_0 \text{ (ft)} &= y_0 + iz_0 \\ \dot{\vec{S}}_0 \text{ (ft/sec)} &= \dot{y}_0 + i\dot{z}_0\end{aligned}$$

Obtaining  $\vec{\alpha}_0$  and  $\dot{\vec{\alpha}}_0$  from the raw angular data was more difficult. The traditional way of analyzing any missile motion with pitch, yaw, and roll is by a three-degree-of-freedom least squares fit to the tricyclic motion, Equation 6. However, the availability of only 6 data points made this technique impossible, so another, approximate method, had to be employed. The solution was to approximate the pitching and yawing motion to one-degree-of-freedom while holding the roll rate constant. In order to do this, the  $\beta - \alpha$  axis system had to be rotated to coincide with the more dominant angular mode. Figure 47 illustrates a typical raw angular data plot. Since the angular motion of the flechette tends to approximate an ellipse, the  $\beta - \alpha$  axes are rotated some angle  $\gamma$  to coincide with the

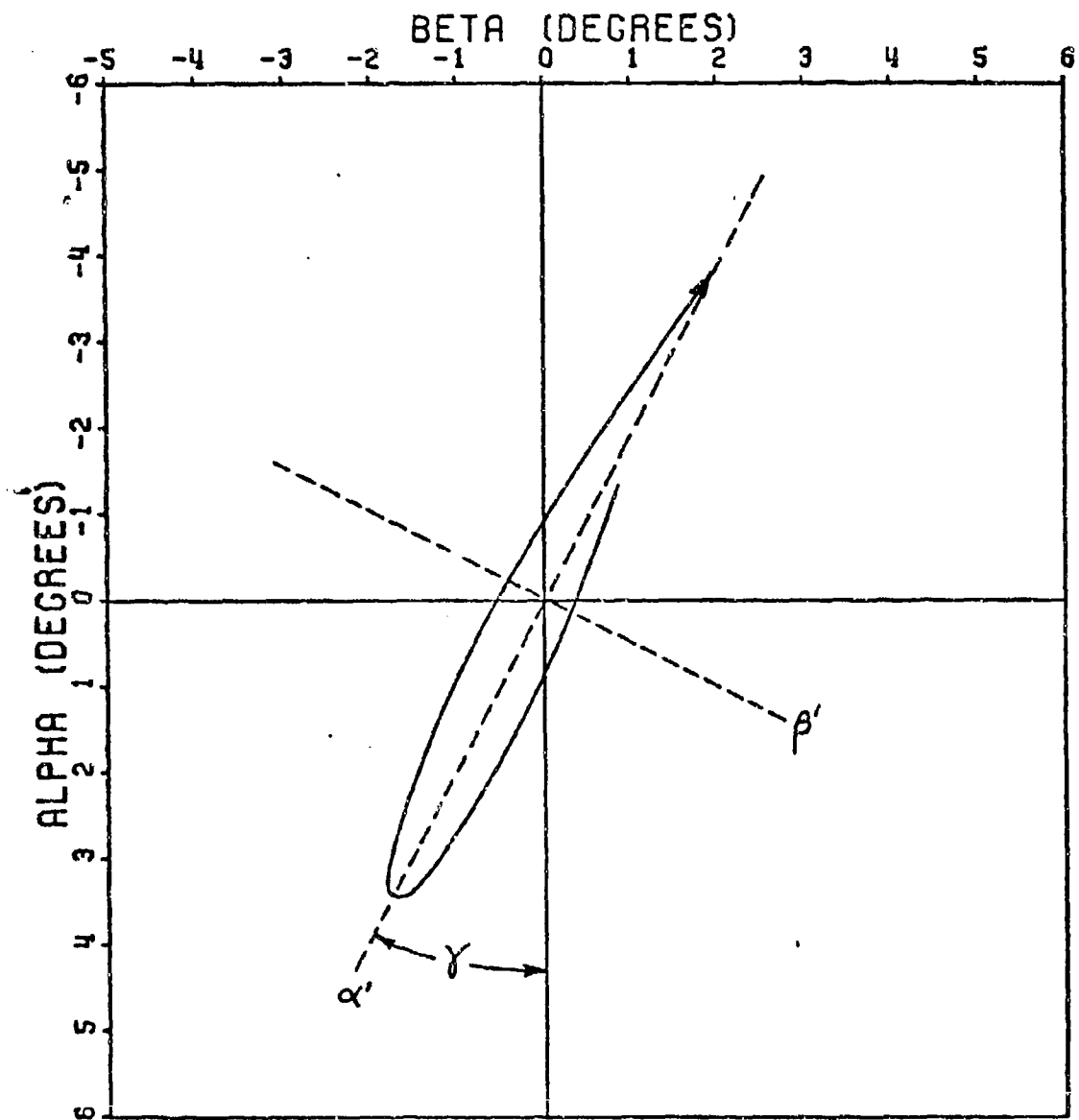


Figure 47. Axis Rotation Approximates Pure Pitching Motion

major and minor axes of the ellipse, as shown. The angular data is retabulated for this new axes system,  $\beta'$ - $\alpha'$ . To fit the data to the one-degree-of-freedom equation:

$$\alpha = K_1 e^{\lambda t} \cos(\omega t + \delta)$$

only the dominant mode can be considered. For example, in Figure 47 the dominant mode occurs along the  $\alpha'$  axis; therefore, only  $\alpha'$  coordinates are utilized in the least squares fit, corresponding  $\beta'$  coordinates are ignored. Table XXI lists the parameters obtained for the eight flechette rounds. Once an equation for  $\alpha'$  is obtained, it represents one dimensional oscillatory motion along the  $\alpha'$  axis. A simple differentiating of the  $\alpha'$  equation yields an equation for  $\dot{\alpha}'$ . The initial conditions  $\vec{\alpha}_0$  and  $\vec{\dot{\alpha}}_0$ , however, are complex whereas  $\alpha'$  and  $\dot{\alpha}'$  are only one dimensional. Therefore, the rotation angle  $\gamma$  is taken into account and the  $\alpha'$  equation is projected back into the  $\beta, \alpha$  axes system:

$$\alpha = \alpha' \cos \gamma$$

$$\dot{\alpha} = \dot{\alpha}' \cos \gamma$$

$$\beta = \alpha' \sin \gamma$$

$$\dot{\beta} = \dot{\alpha}' \sin \gamma$$

Thus the complex initial conditions are approximated.

$$\vec{\alpha}_0 = \beta_0 + i\alpha_0$$

$$\vec{\dot{\alpha}}_0 = \dot{\beta}_0 + i\dot{\alpha}_0$$

Figures 48-63 illustrate the fitted data both translational and angular for the eight rounds. The transitional data includes the pertinent equations.

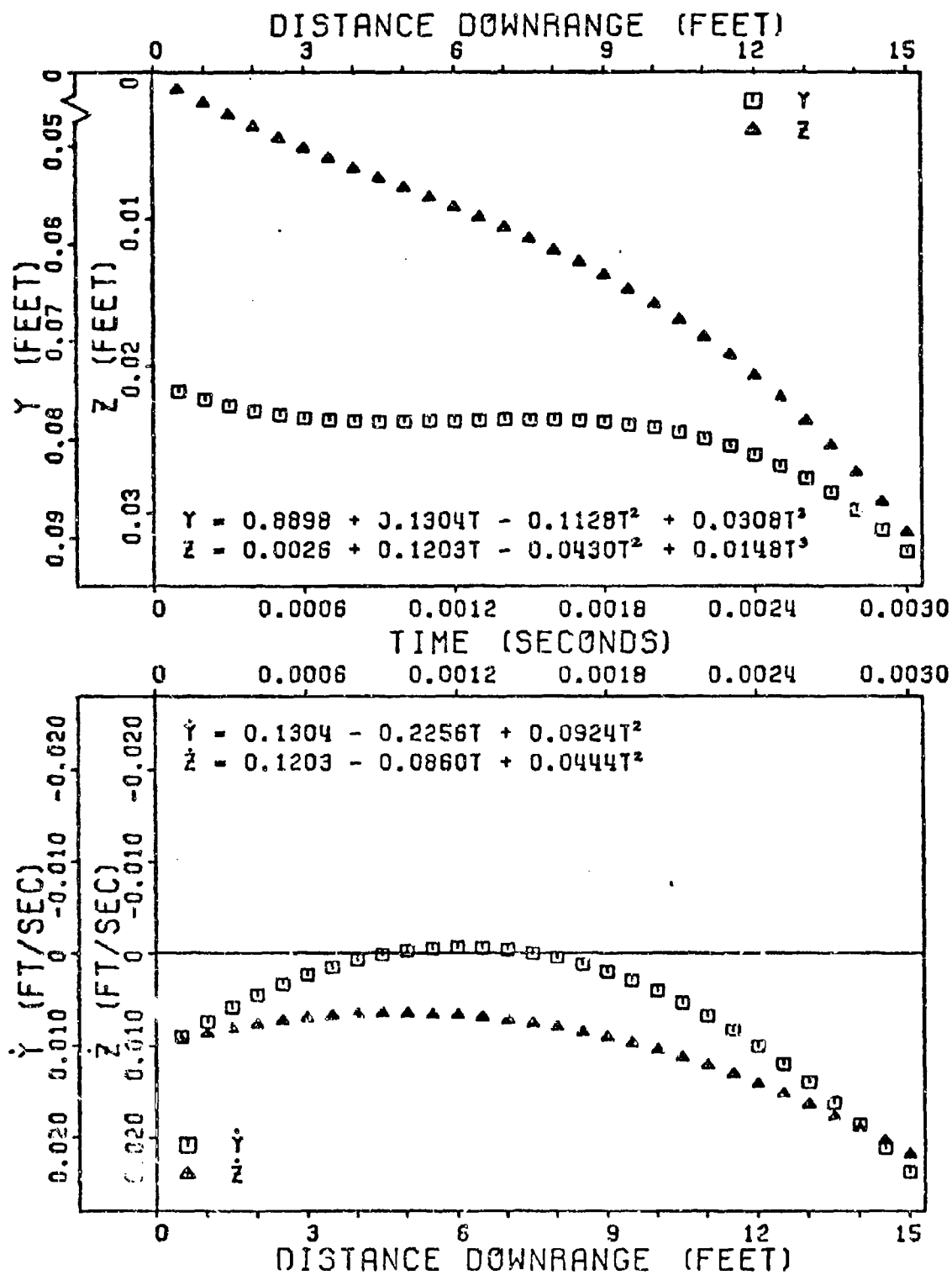


Figure 48. Fitted Translational Data Ground Point - Round 4

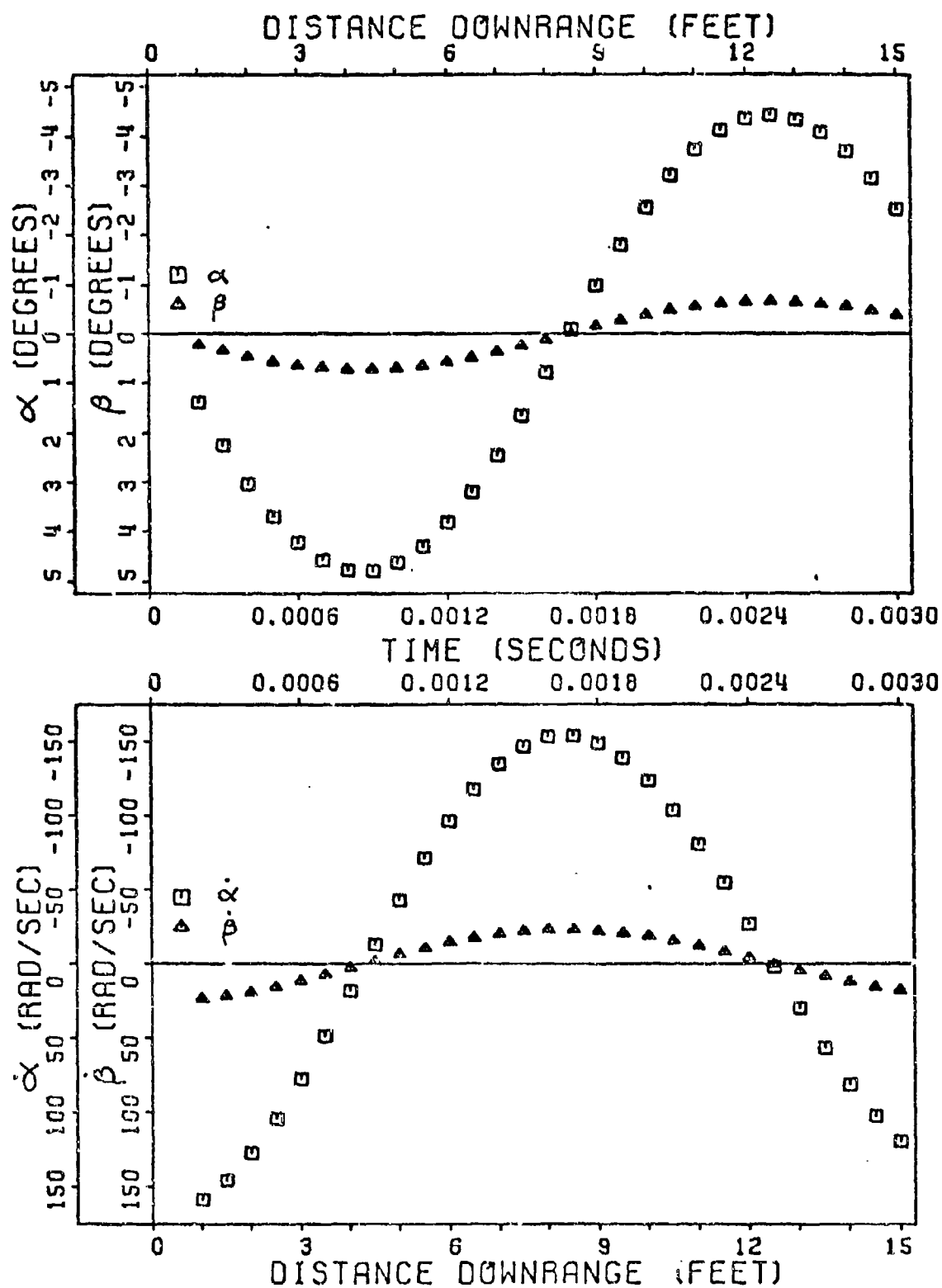


Figure 49. Fitted Angular Data Ground Point - Round 4

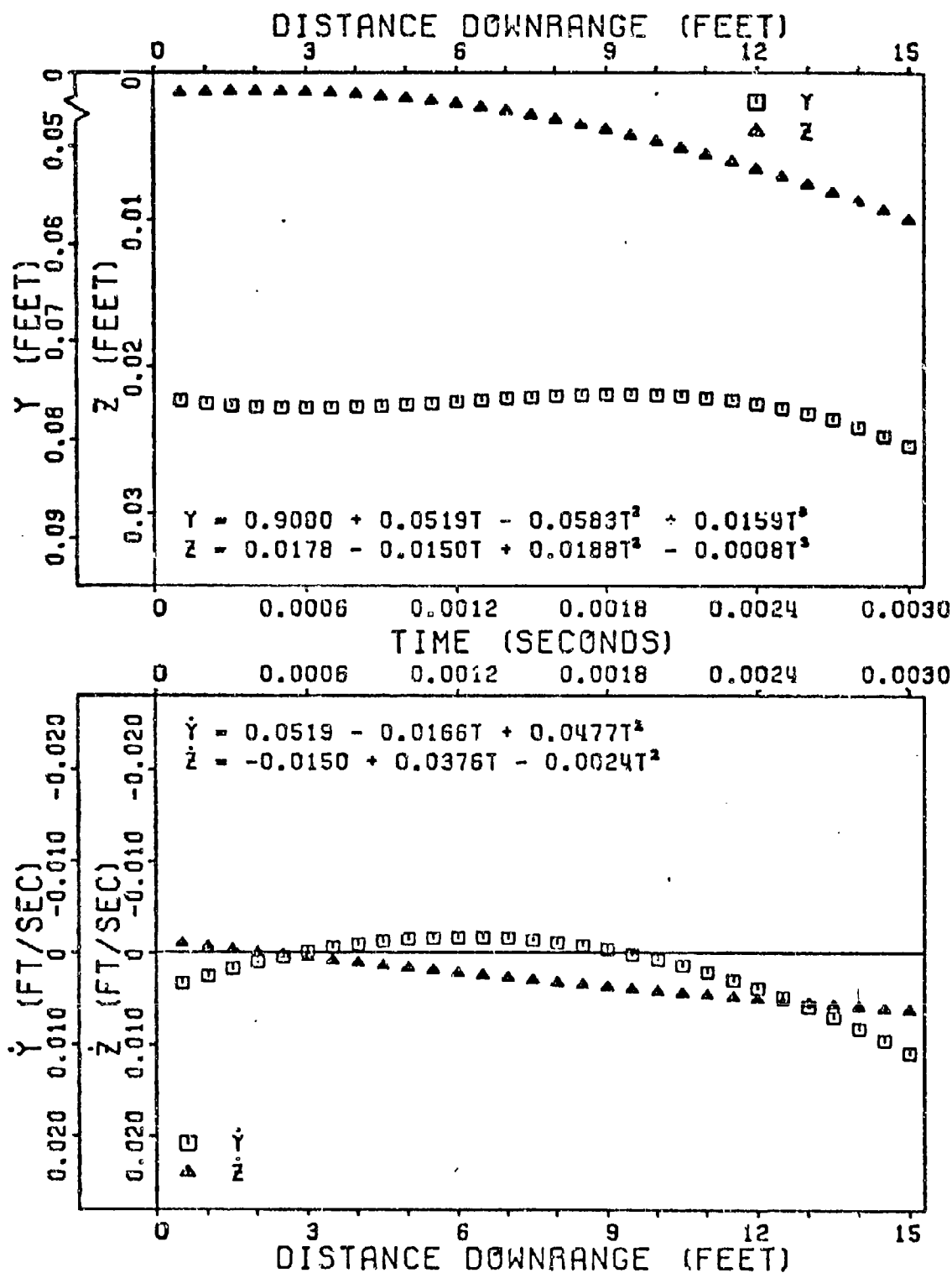


Figure 50. Fitted Translational Data Ground Point - Round 6



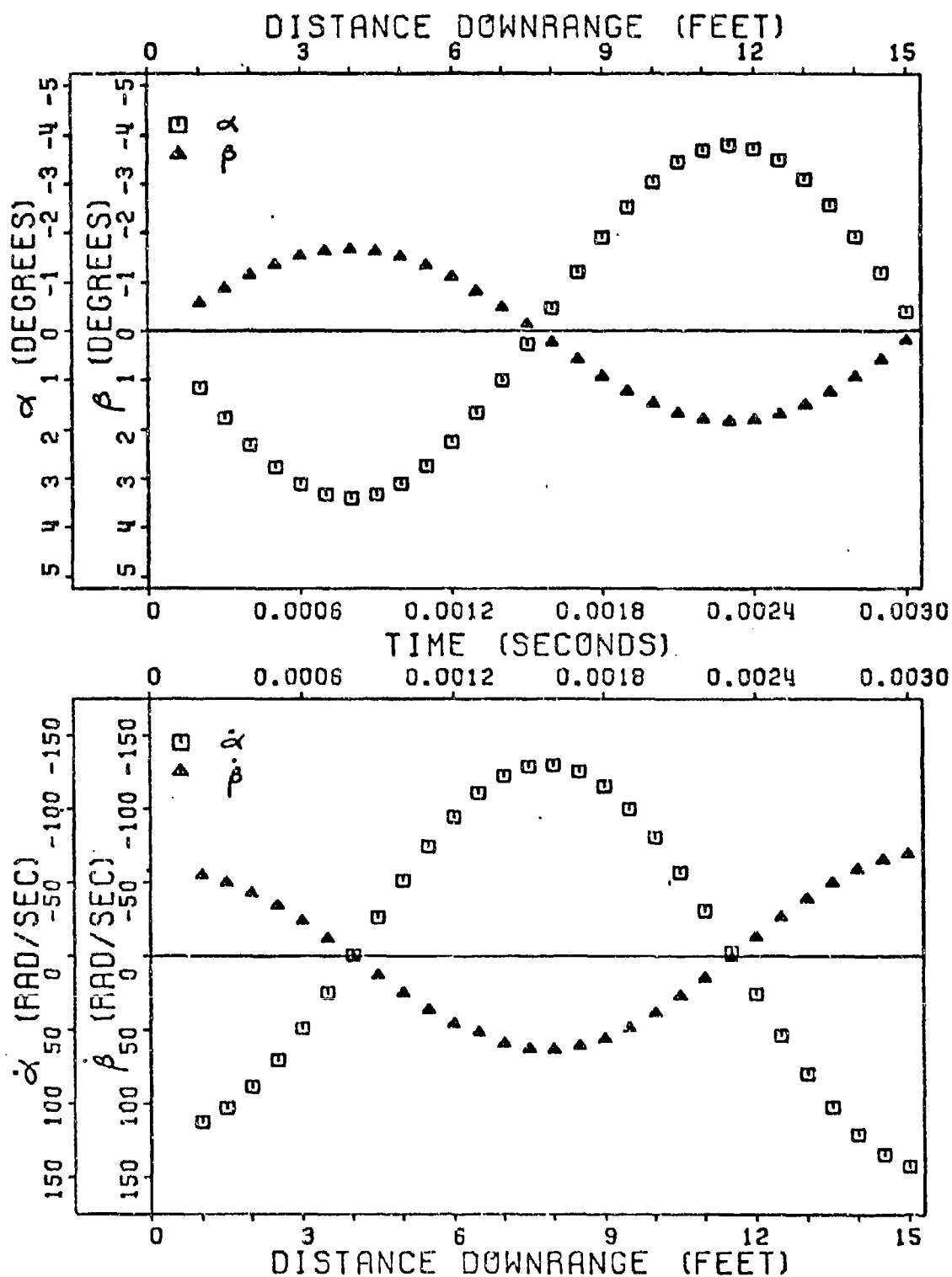


Figure 51. Fitted Angular Data Ground Point - Round 6

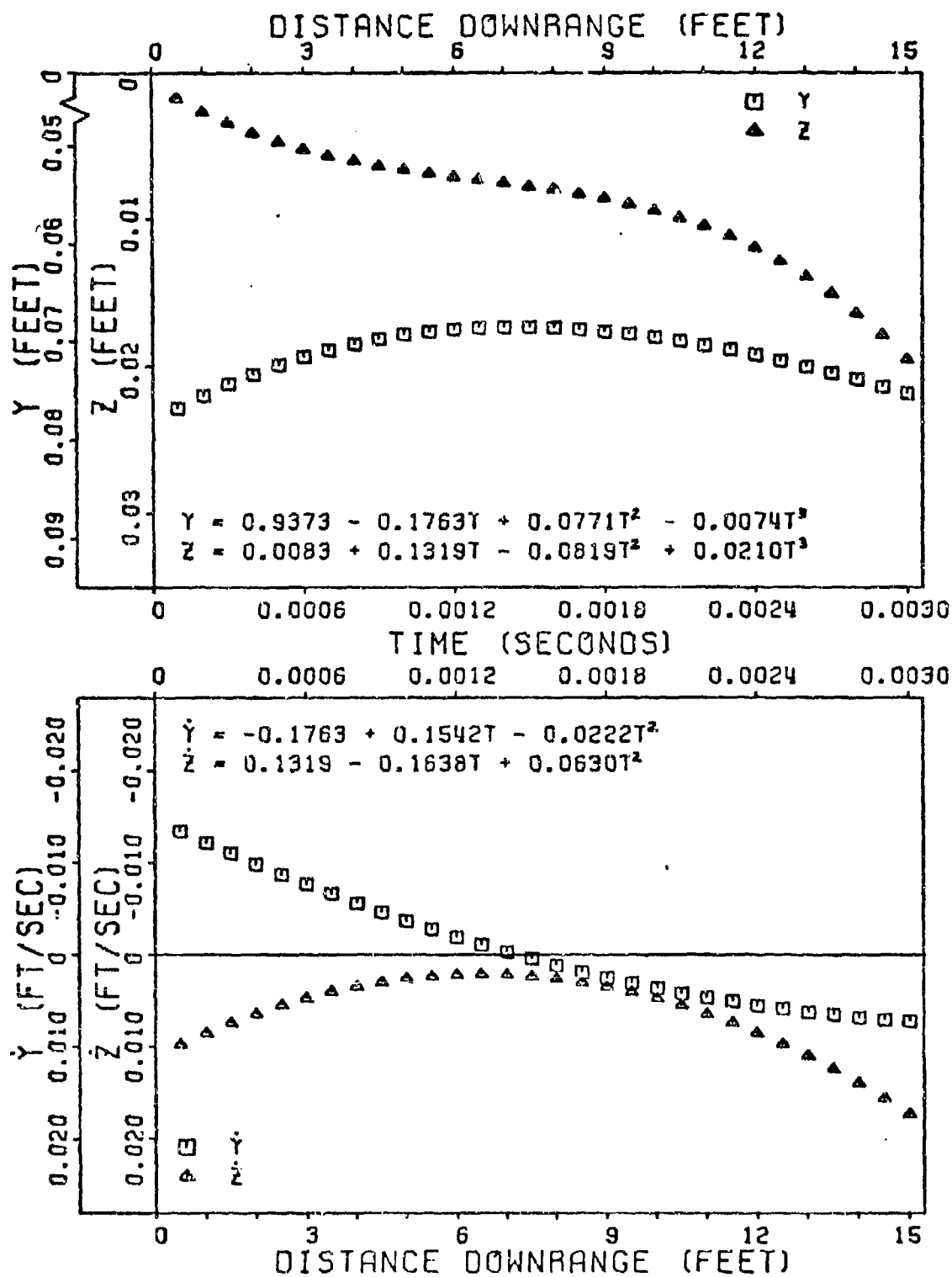


Figure 52. Fitted Translational Data Ground Point - Round 7

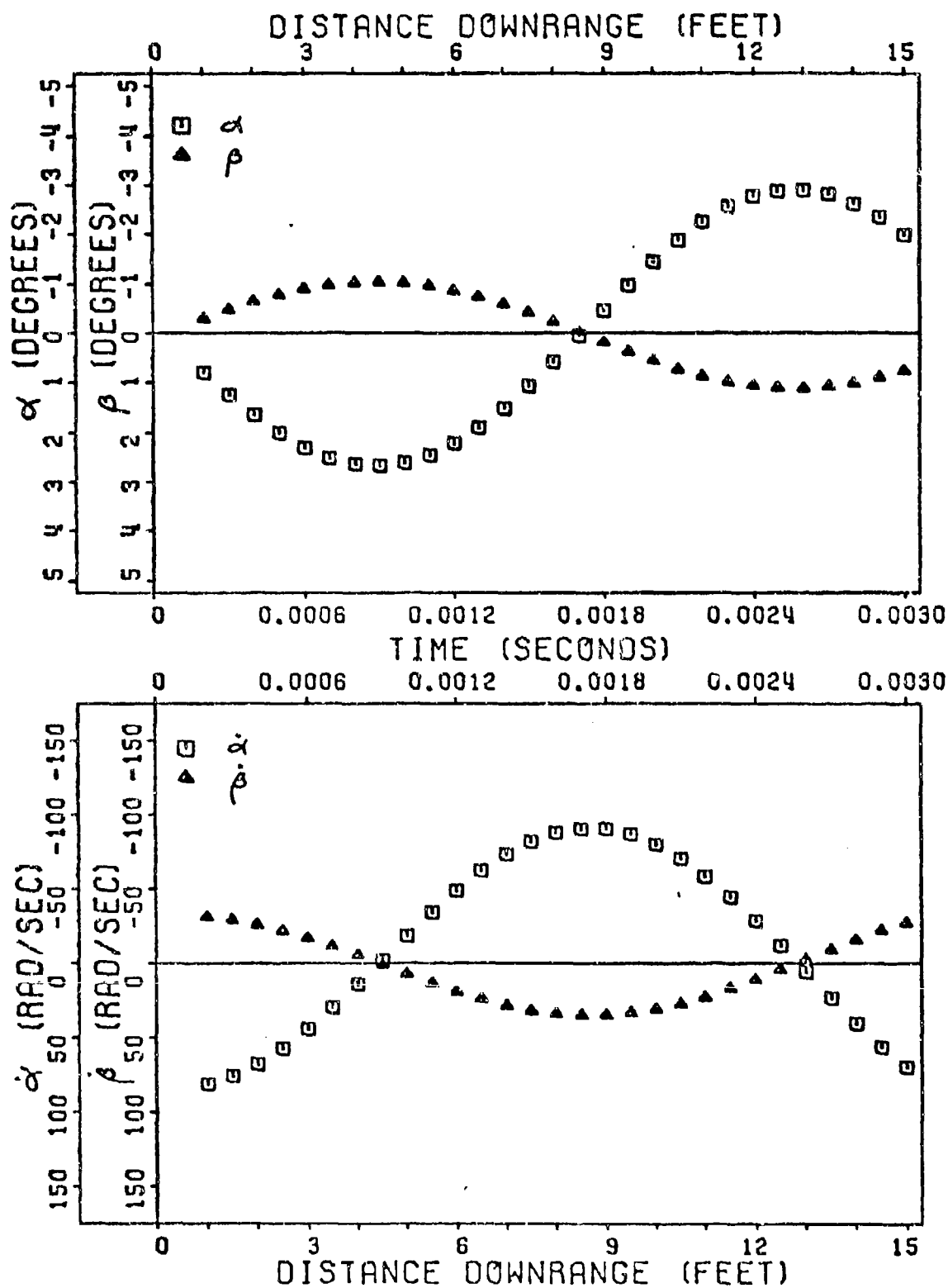


Figure 53. Fitted Angular Data Ground Point - Round 7

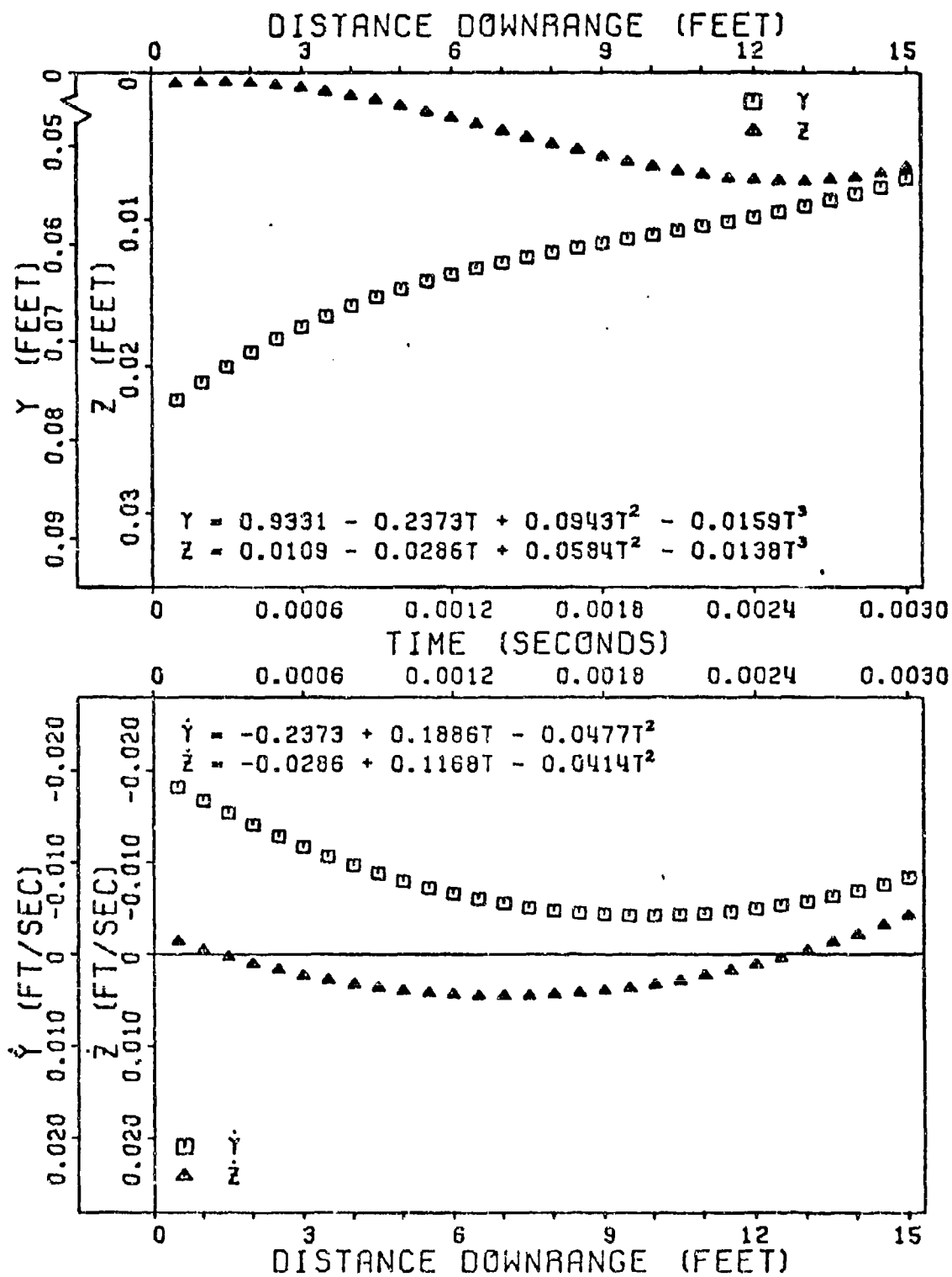


Figure 54. Fitted Translational Data Ground Point - Round 8

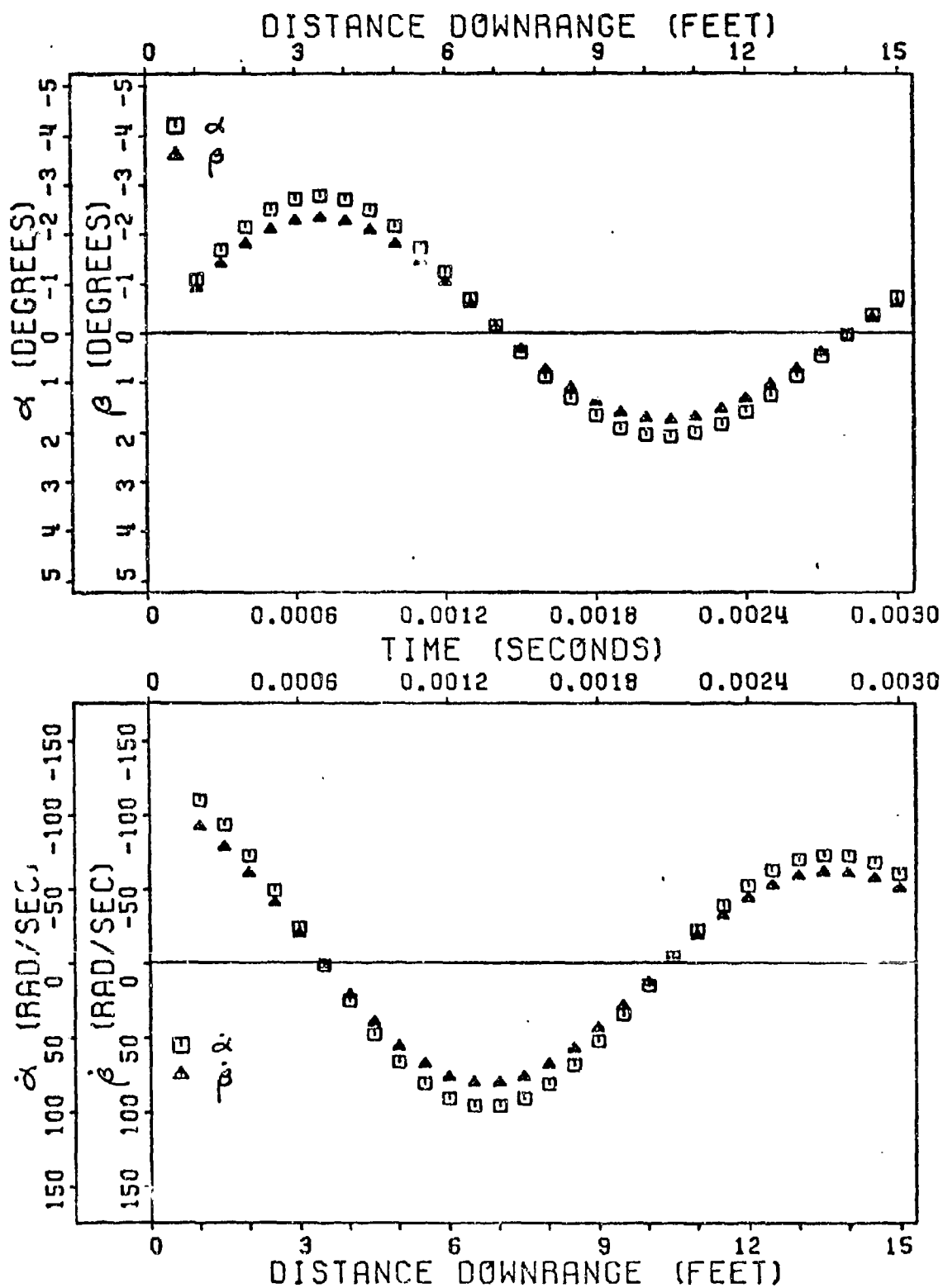


Figure 55. Fitted Angular Data Ground Point -- Round 8

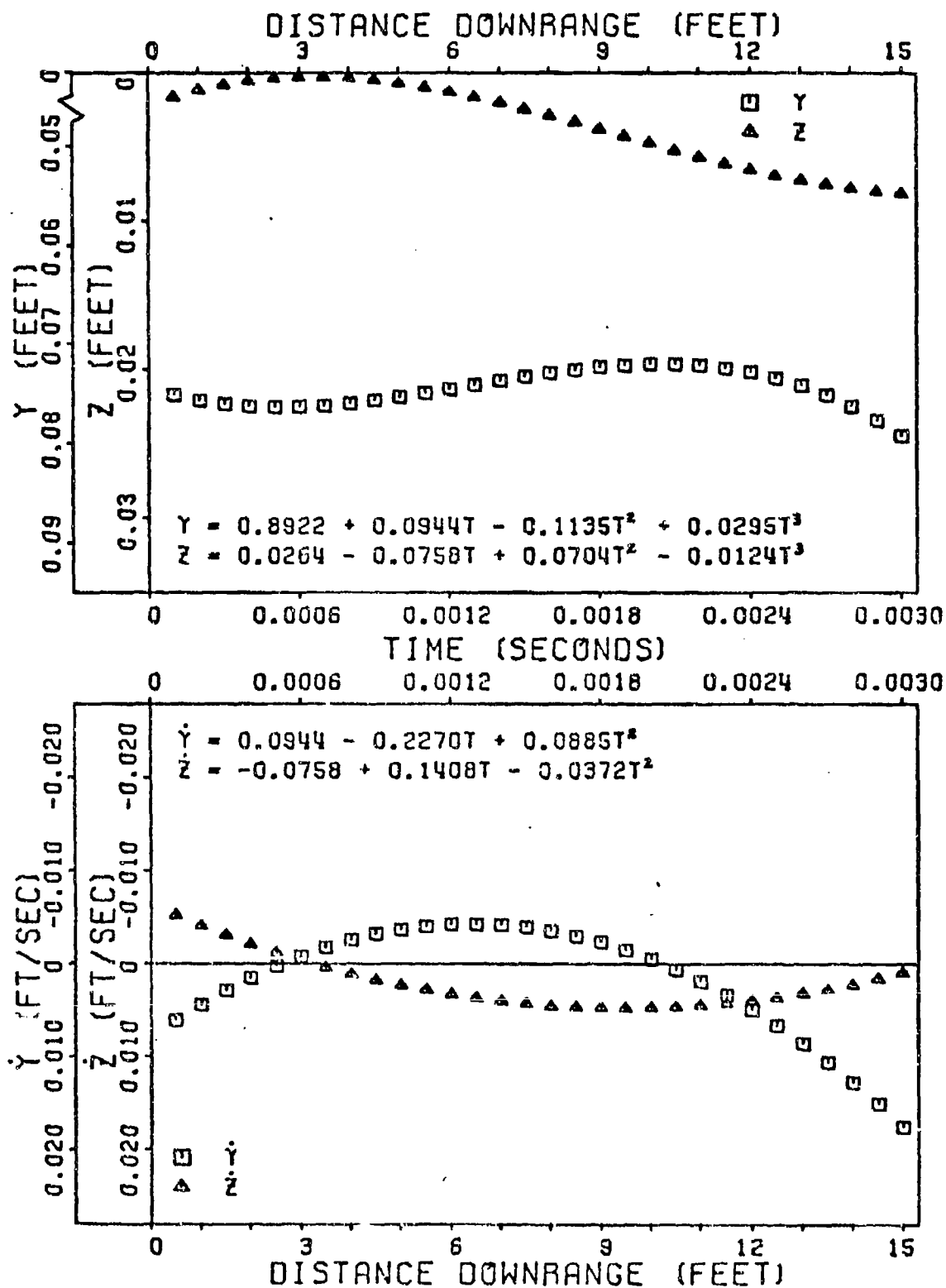


Figure 56. Fitted Translational Data Ground Point - Round 14

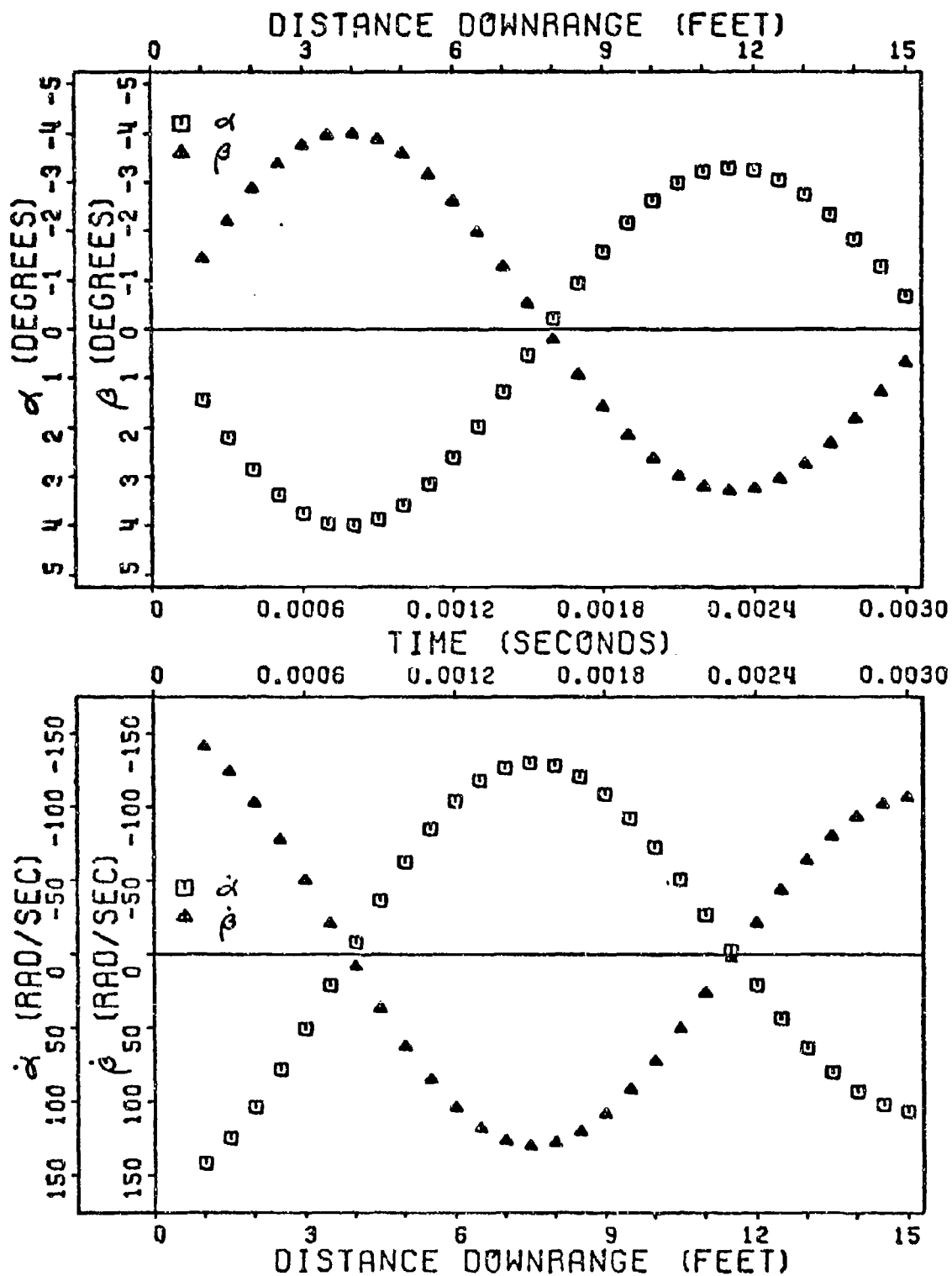


Figure 57. Fitted Angular Data Ground Point - Round 14

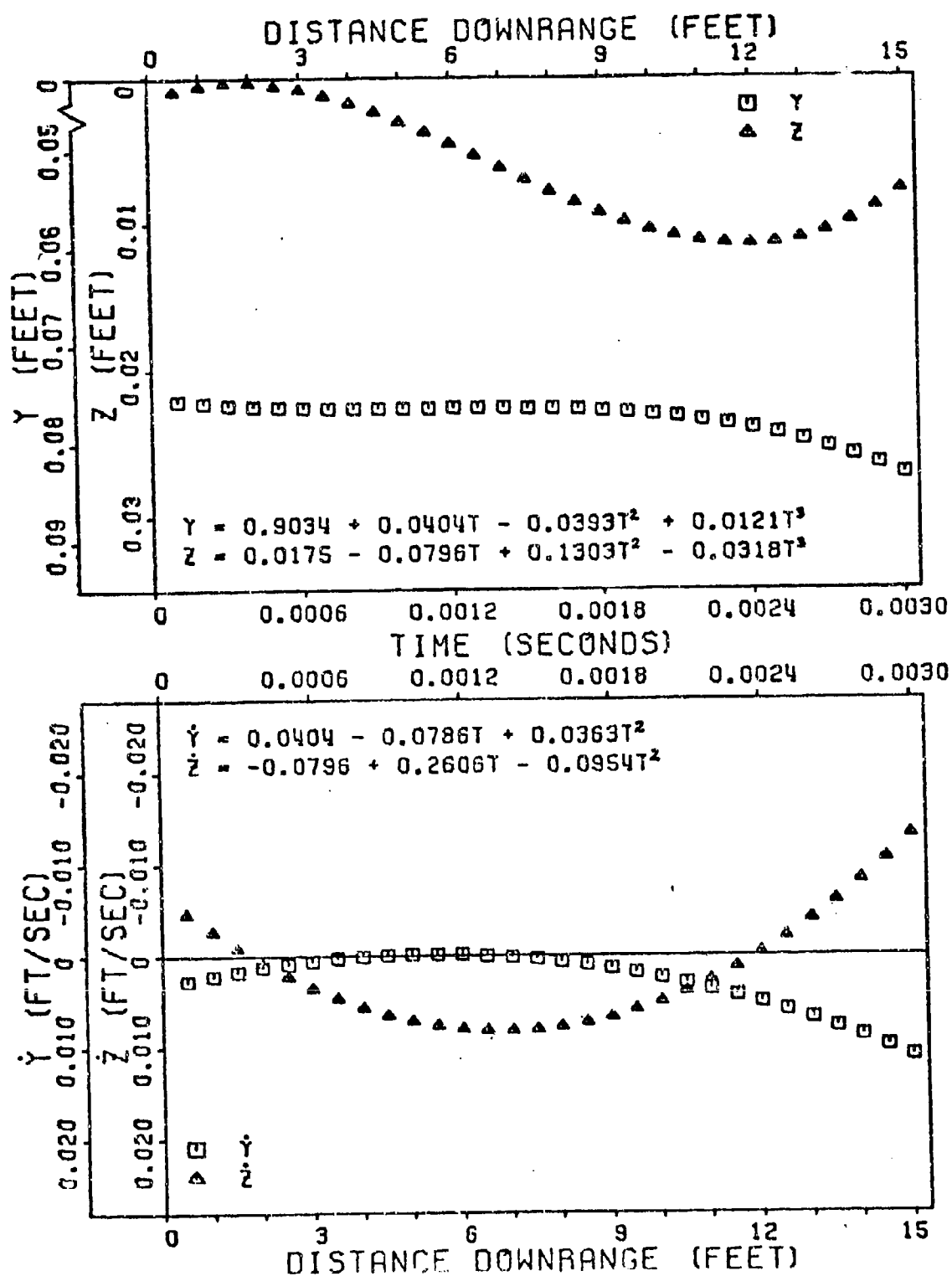


Figure 58. Fitted Translational Data Ground Point - Round 16



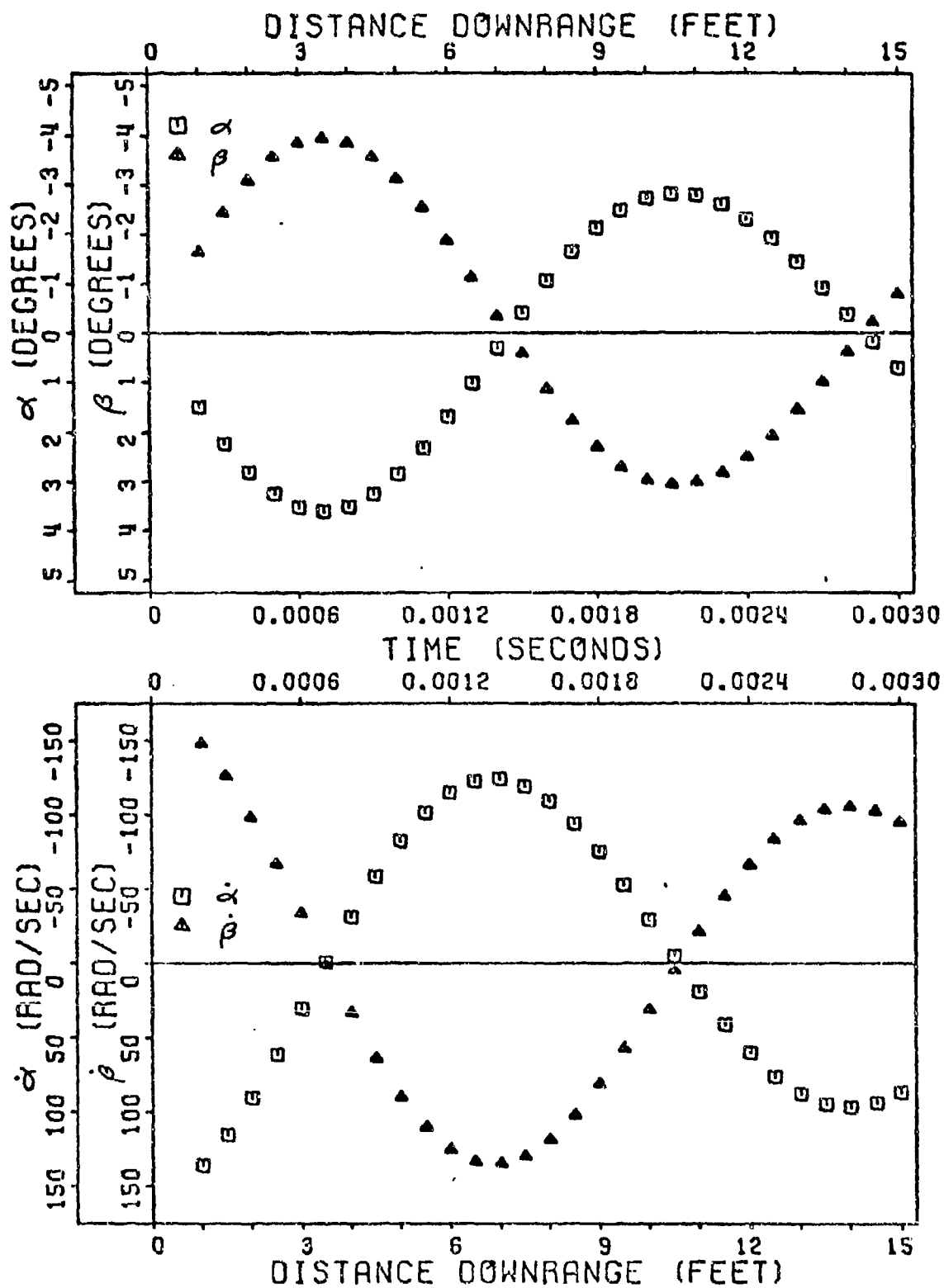


Figure 59. Fitted Angular Data Ground Point - Round 16

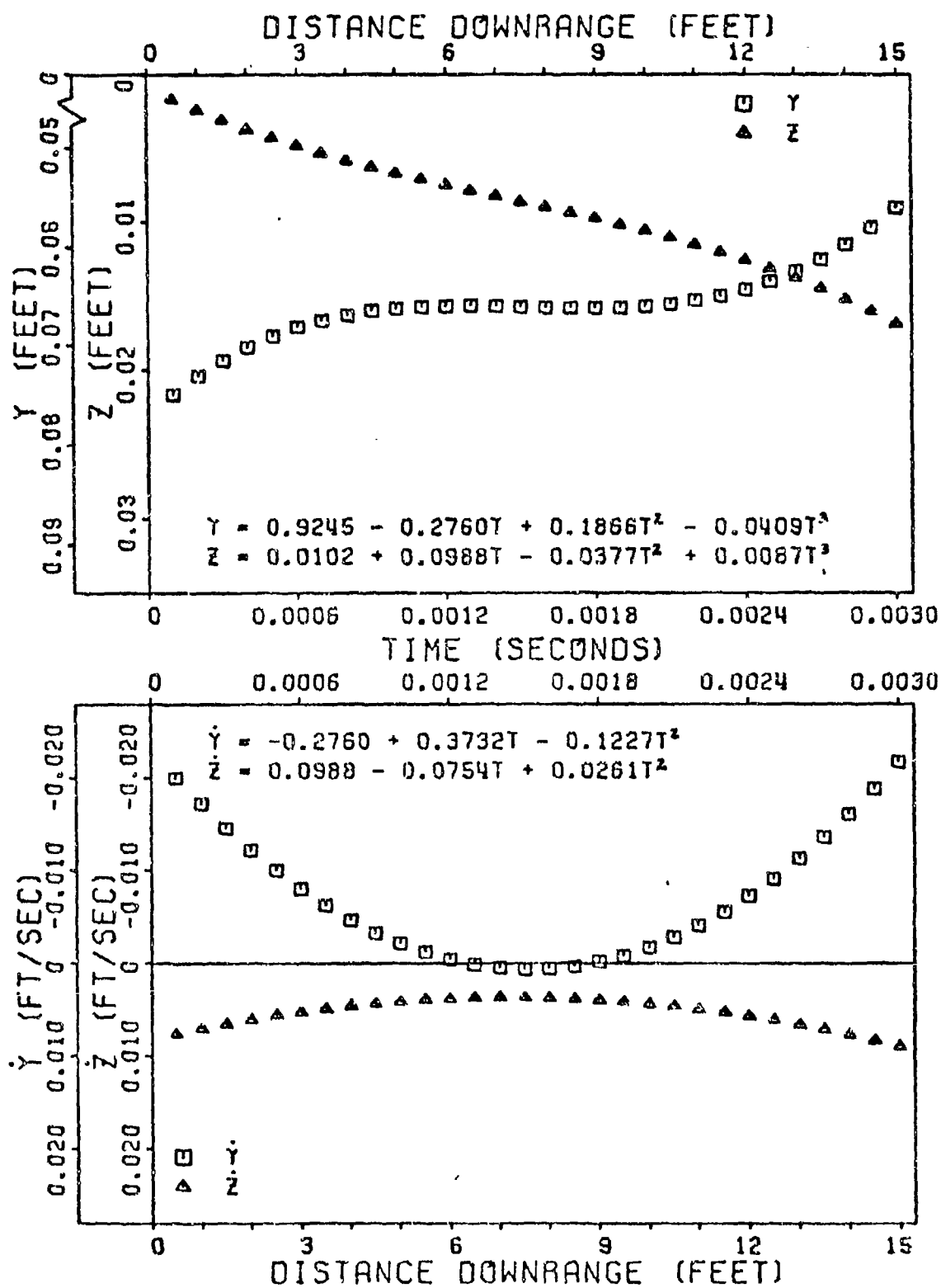


Figure 60. Fitted Translational Data Ground Point - Round 17

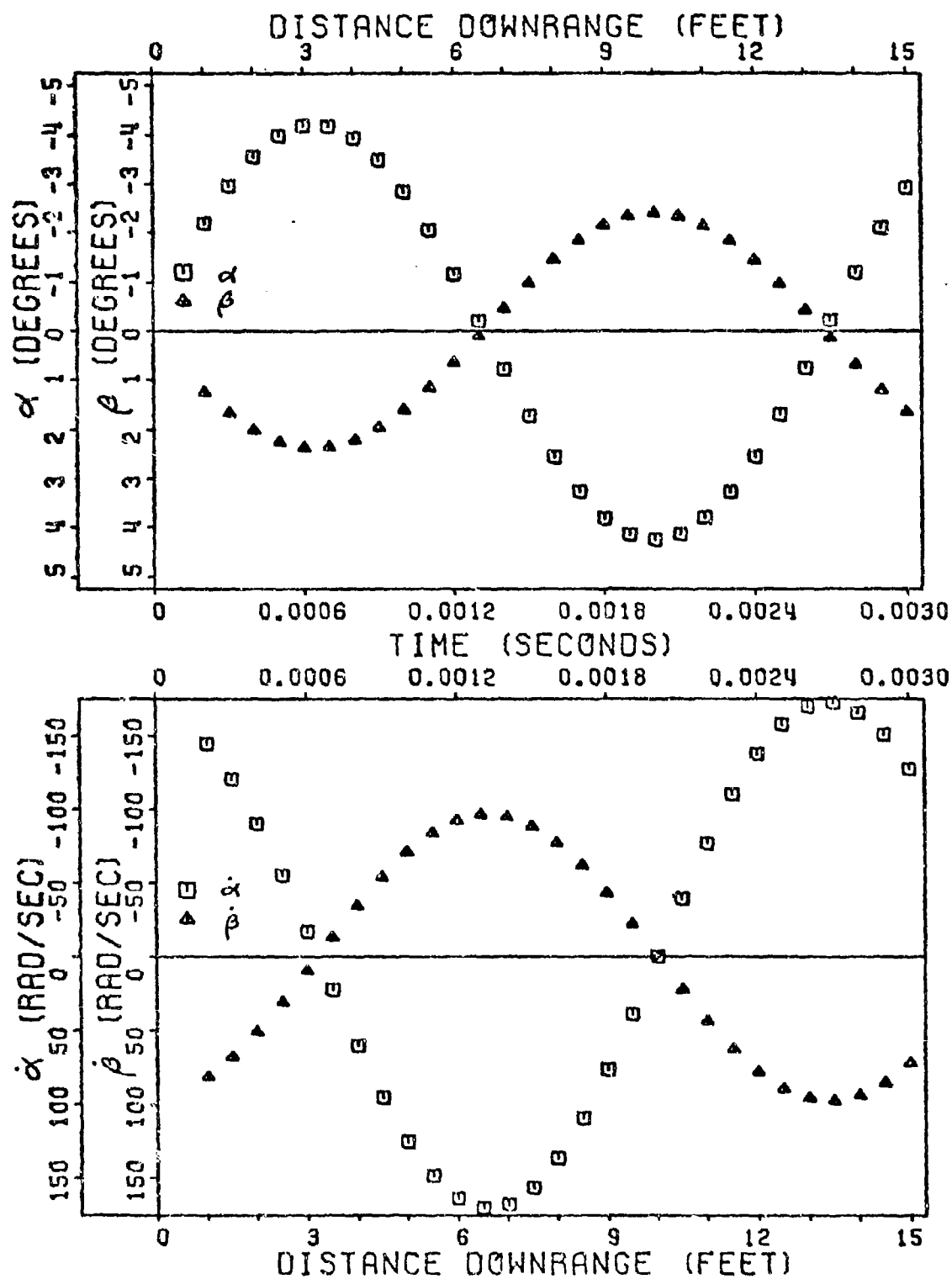


Figure 61. Fitted Angular Data Ground Point - Round 17

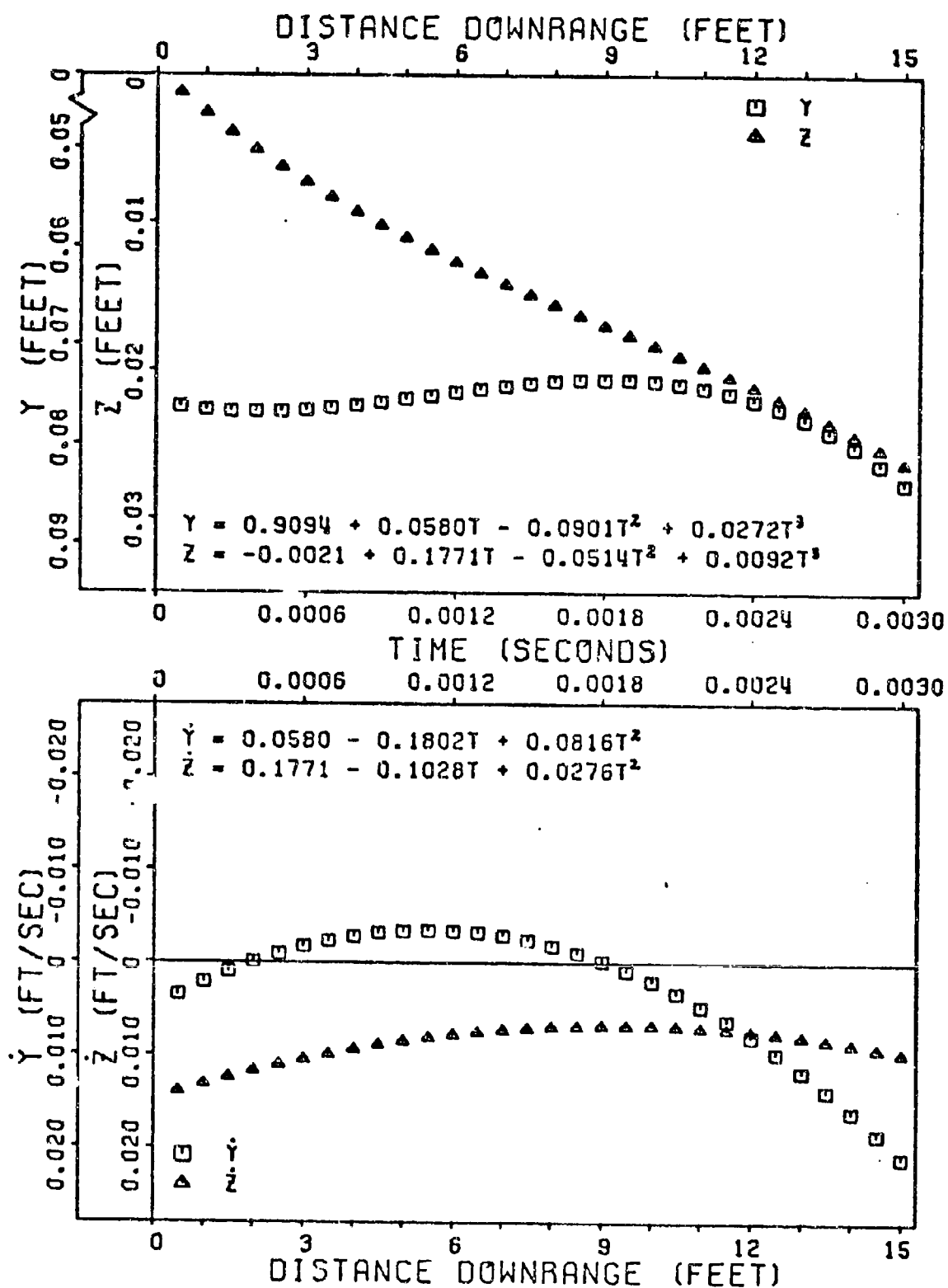


Figure 62. Fitted Translational Data Ground Point - Round 19

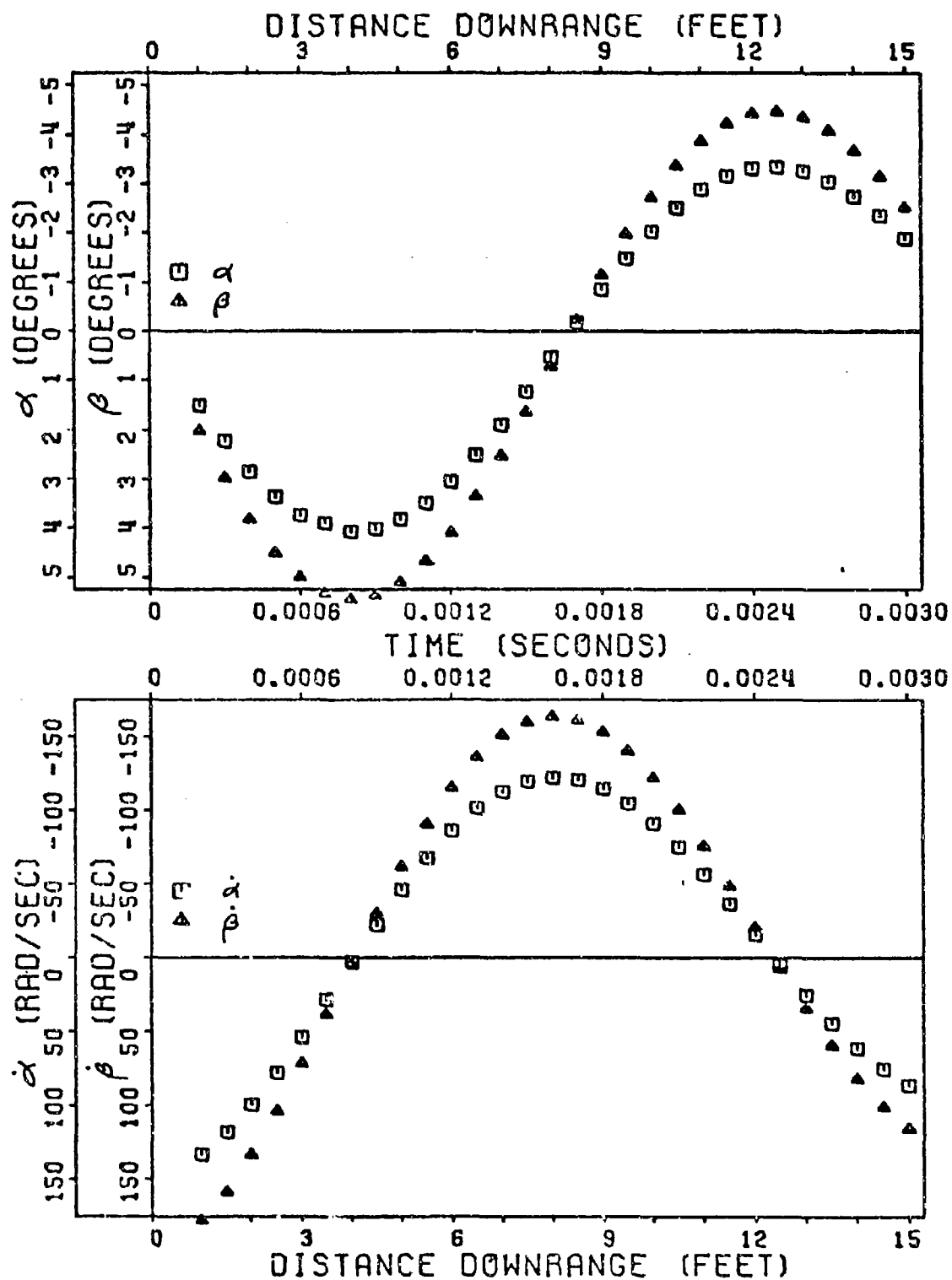


Figure 63. Fitted Angular Data Ground Point - Round 19

TABLE XXI  
AERODYNAMIC PARAMETERS FROM LEAST SQUARES FIT

$R_{UND}$	$K_1$ (degrees)	$\lambda$ (rad/sec)	$\omega$ (rad/sec)	$\delta$ (rad)
4	5.01	-49.48	1921.3	-1.29
6	3.64	68.24	2079.8	-1.21
7	-2.78	46.48	1871.4	-1.26
8	-4.02	-203.19	2267.6	-1.21
14	6.09	-126.37	2042.0	-1.23
16	5.84	-174.7	2211.7	-1.18
17	-4.81	8.53	2314.5	-1.02
19	7.35	-121.62	1889.9	-1.22

$$\alpha = K_1 e^{\lambda t} \cos(\omega t + \delta)$$

$$\dot{\alpha} = K_1 e^{\lambda t} \left[ \lambda \cos(\omega t + \delta) - \omega \sin(\omega t + \delta) \right]$$

## DISPERSION ANALYSIS

### Free Flight vs Theory

Once the initial conditions are determined as in the previous section, they are applied to the theory and compared to the dispersion of each test fired round. To utilize the theory, the fitted data must be chosen for a given time; that is,  $\vec{S}_0$ ,  $\vec{\dot{S}}_0$ ,  $\vec{\alpha}_0$ ,  $\vec{\dot{\alpha}}_0$  must be selected for one given point in time - position downrange. Since the question of what point in time do the initial conditions occur, 3 sets of initial conditions were chosen to correspond with positions 1, 3, 5 feet downrange. This span of position downrange may or may not be sufficient to include the actual time corresponding to the initial conditions for each round. The following analysis will determine each round's effective time for its initial conditions.

For each set of initial conditions, theory and 6-D computations were done and compared to target data for the Frankford test firings. The results are tabulated in Table XXII in mils and plotted in Figures 64-71 in feet; deviation from the time of fire at 50 ft. downrange. The relationship between the deviations in feet and mils at 50 ft. downrange is:

$$\vec{J.A.} \text{ (mils)} = \frac{\vec{S} \text{ (ft)}}{x} (1000)$$

or 
$$\vec{J.A.} \text{ (mils)} = (20) \vec{S} \text{ (ft)}$$

To accurately and concisely analyze the complex and large amount of data in Table XXII, the positions downrange in which the initial conditions were selected must be simultaneously analyzed with the dispersion results at 50 ft downrange. The problem in choosing initial conditions is where they should be taken; at what point downrange. Normally, one would think

TABLE XXII  
DISPERSION ANALYSIS RESULTS

R O U N D	P O S I T I O N (ft)	D O W N R A N G E	Initial Conditions						Frankford Dispersion		Theory Dispersion		6-D Dispersion	
			$u_0$ (ft/sec)	$P_0$ (rad/sec)	$\vec{S}_0$ (ft)	$\vec{S}_0$ (ft/sec)	$\vec{\alpha}_0$ (deg)	$\vec{\alpha}_0$ (rad/sec)	mils	mils	mils	mils	mils	mils
4	1	4747	11454	0.075968+	0.007415+	0.2045+	23.60+	0.002088+	2.333-	0.7501	1.329-	1.861	1.300-	1.703
	3			0.077840+	0.002359+	0.6273+	11.54+	0.0052081			1.3021	1.508	1.1001	1.461
	5			0.078183+	-0.000233+	0.6877+	-6.41	0.0078921			1.413-	1.674	1.380-	1.577
	5			0.0078921	0.0065581	4.61841	-43.041	0.000233+			0.5291	1.508	0.4801	1.461
6	1	4662	13201	0.076348+	0.002541-	-0.5633+	-54.80+	0.0012831	1.050-	0.2001	2.001-	2.213	2.100-	2.293
	3			0.0012951	0.0006311	1.15501	112.481	0.076799+			0.9441	1.753	0.9201	1.796
	5			0.076799+	0.000074+	-1.5239+	-23.78+	0.0012831			1.709-	1.367	1.760-	1.361
	5			0.076458+	-0.001417+	-1.5145+	25.01-	0.0017331			0.3901	1.367	0.3601	1.361
7	1	4642	14219	0.075422+	0.012196+	-0.3073+	-31.50+	0.0066081	2.817-	0.0831	1.777-	1.888	1.820-	1.893
	3			0.0026311	0.0084721	0.79271	81.241	0.071473+			0.6381	1.572	0.5201	1.573
	5			0.071473+	-0.007648+	-0.8928+	-17.09+	0.0052081			1.550-	1.386	1.560-	1.358
	5			0.0052081	0.0046921	2.30271	44.081	0.069225+			0.2631	1.386	0.2001	1.358
8	1	4662	12998	0.074107+	-0.016791-	0.9121	-92.44-	0.0066171	1.067+	1.9831	2.314+	2.527	2.060+	2.225
	3			0.0006171	0.0003751	1.08721	110.171	0.068436+			1.0181	1.596	0.8401	1.621
	5			0.068436+	-0.011776+	-2.2737-	-20.06-	0.0009821			1.577+	0.975	1.600+	1.037
	5			0.0009821	0.0022151	2.70991	23.911	0.064517+			0.2421	0.975	0.2601	1.037
14	1	4756	13289	0.075565+	0.004378-	-1.4392+	-141.45+	0.0011631	1.067+	0.3171	2.727-	2.976	2.620-	2.804
	3			0.0011631	0.0040941	1.43941	141.471	0.076196+			1.1921	1.967	1.0001	1.993
	5			0.076196+	-0.000828-	-3.7492+	-50.31+	0.0002991			1.917-	1.069	1.960+	1.310
	5			0.0002991	0.0003931	3.74971	50.321	0.075217+			0.4421	1.069	0.3601	1.310
16	1	4753	17354	0.075834+	0.002178-	1.6401+	-148.66	0.0005451	1.683-	0.0831	2.790-	3.024	2.740-	2.884
	3			0.0005451	0.0026081	1.50301	136.231	0.076342+			1.1681	1.784	0.9001	1.983
	5			0.076342+	0.000526+	-3.8411+	-33.39+	0.0008151			0.2751	1.037	1.960+	1.093
	5			0.0008151	0.0035351	3.52081	30.601	0.076383+			0.699+	1.037	1.000+	1.093
17	1	4677	16613	0.073036+	-0.017189+	1.2395-	81.70-	0.0030331	1.400-	0.3831	0.767+	1.583	0.880+	1.472
	3			0.0030331	0.0071331	2.85221	82.311	0.073036+			1.3851	1.379	1.180+	1.223
	5			0.073036+	-0.008021+	2.3660-	9.38-	0.0048161			1.342+	2.195	0.3201	1.931
	5			0.0048161	0.0052461	4.18221	16.581	0.066183+			0.3181	2.195	0.5201	1.931
19	1	4679	11913	0.066183+	-0.002125+	1.6065-	-70.94+	0.0066671	1.783+	2.140	1.996-	1.065	0.180-	0.937
	3			0.0066671	0.0041251	2.83971	125.401	0.0764681			0.9151	0.881	0.2001	0.805
	5			0.0764681	0.002102+	2.0237+	178.11+	0.0026111			-0.063-	2.136	1.620+	1.728
	5			0.0026111	0.0131371	1.51141	133.021	0.075375+			1.0631	2.136	0.6001	1.728



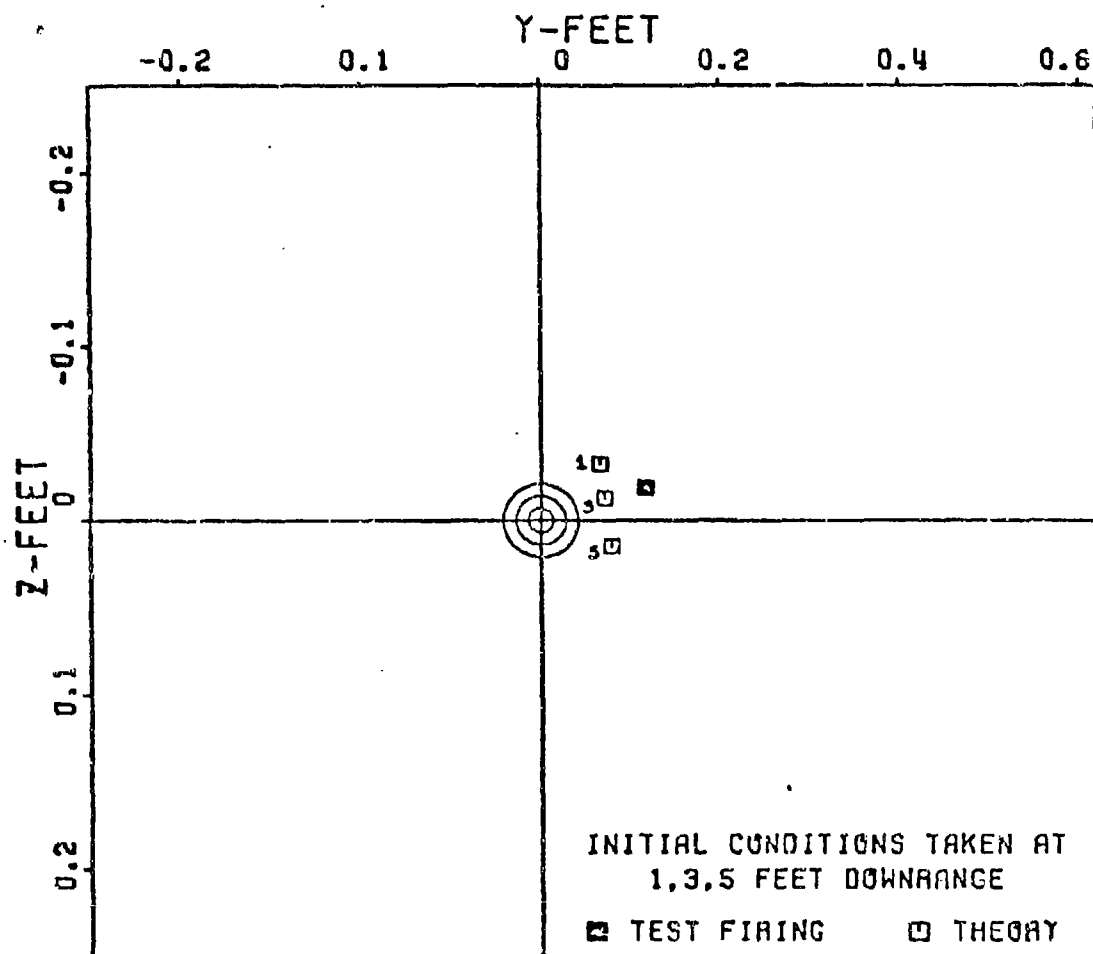


Figure 64. Dispersion: Ground Point - Round 4 Test Firing vs Theory, at 50 ft. Downrange

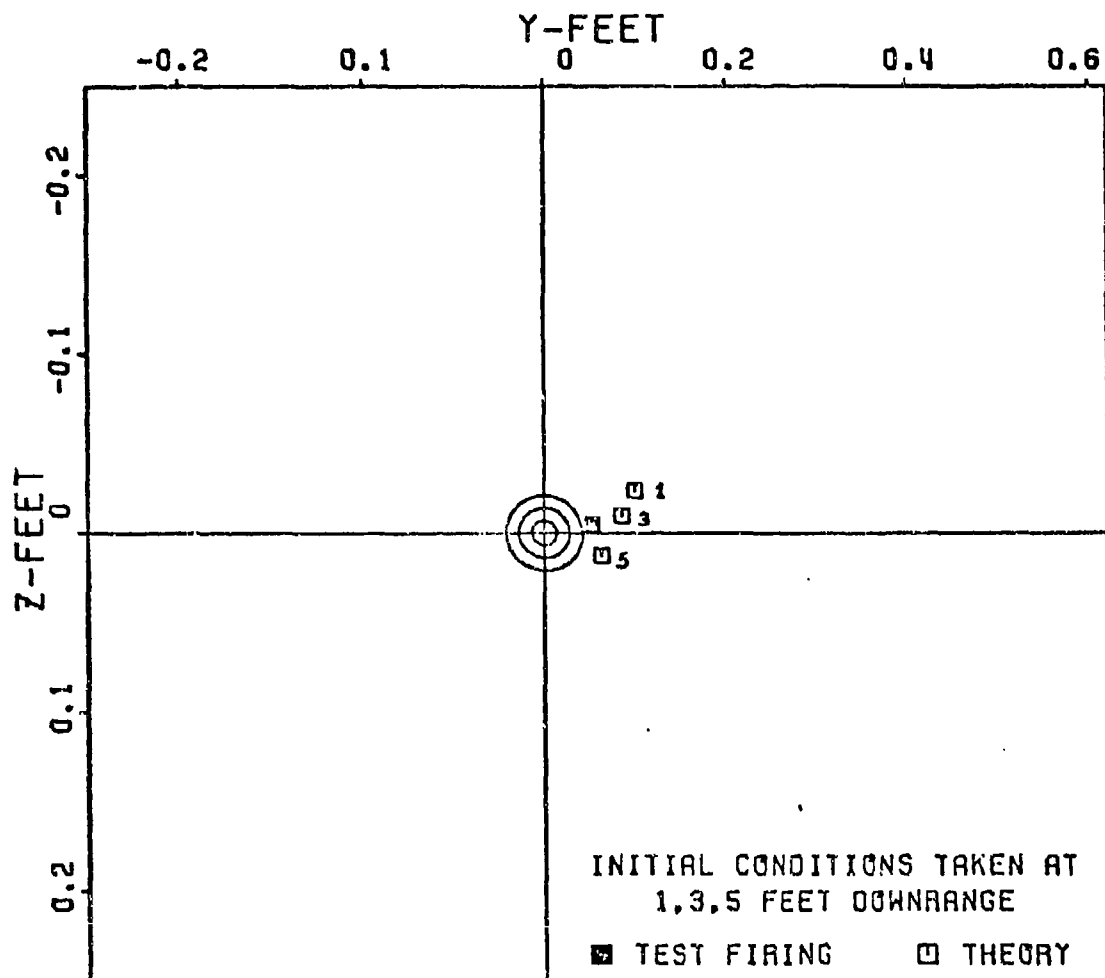


Figure 65. Dispersion: Ground Point - Round 6 Test Firing vs Theory,  
at 50 ft. Downrange

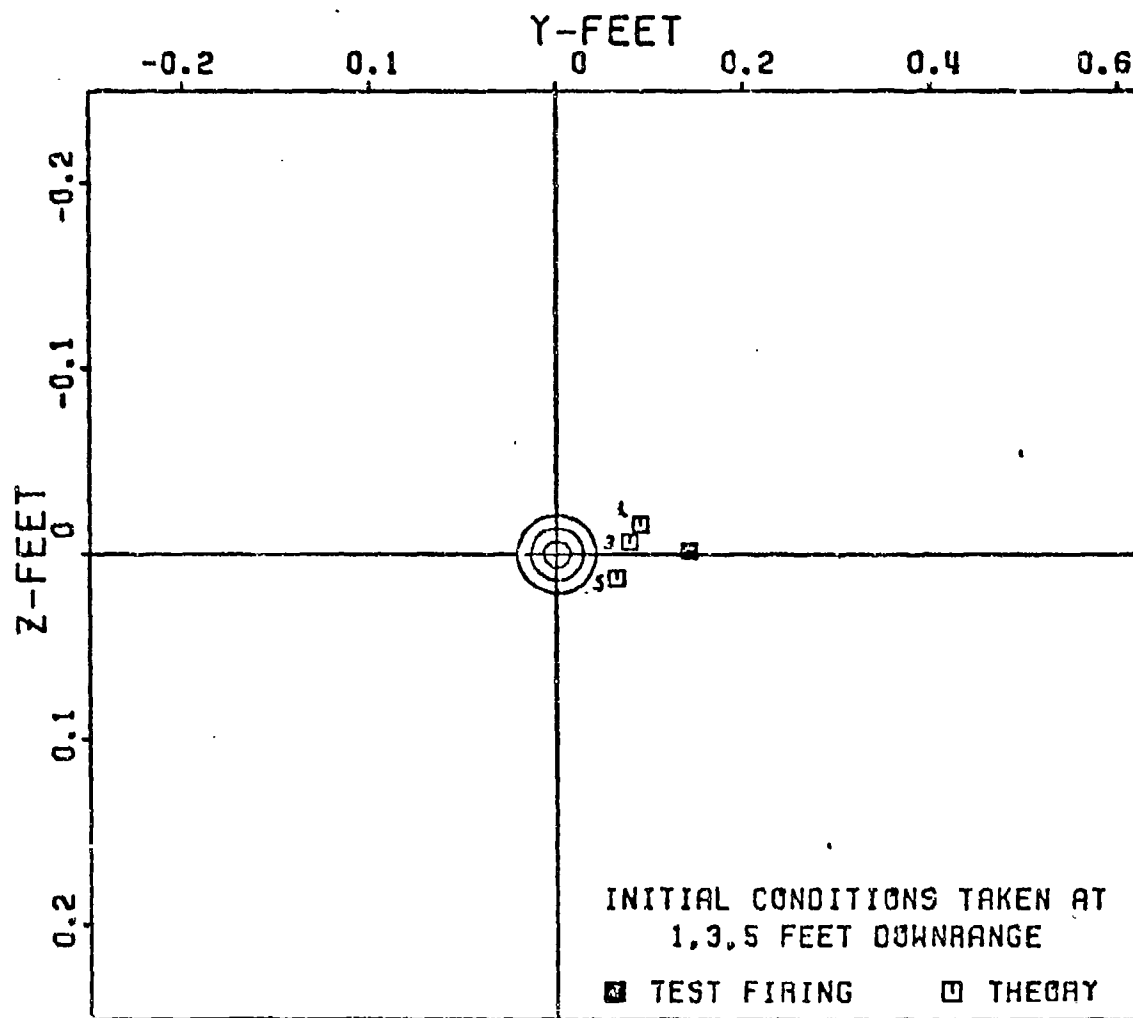


Figure 6. Dispersion: Ground Point - Round 7 Test Firing vs Theory,  
at 50 ft. Downrange

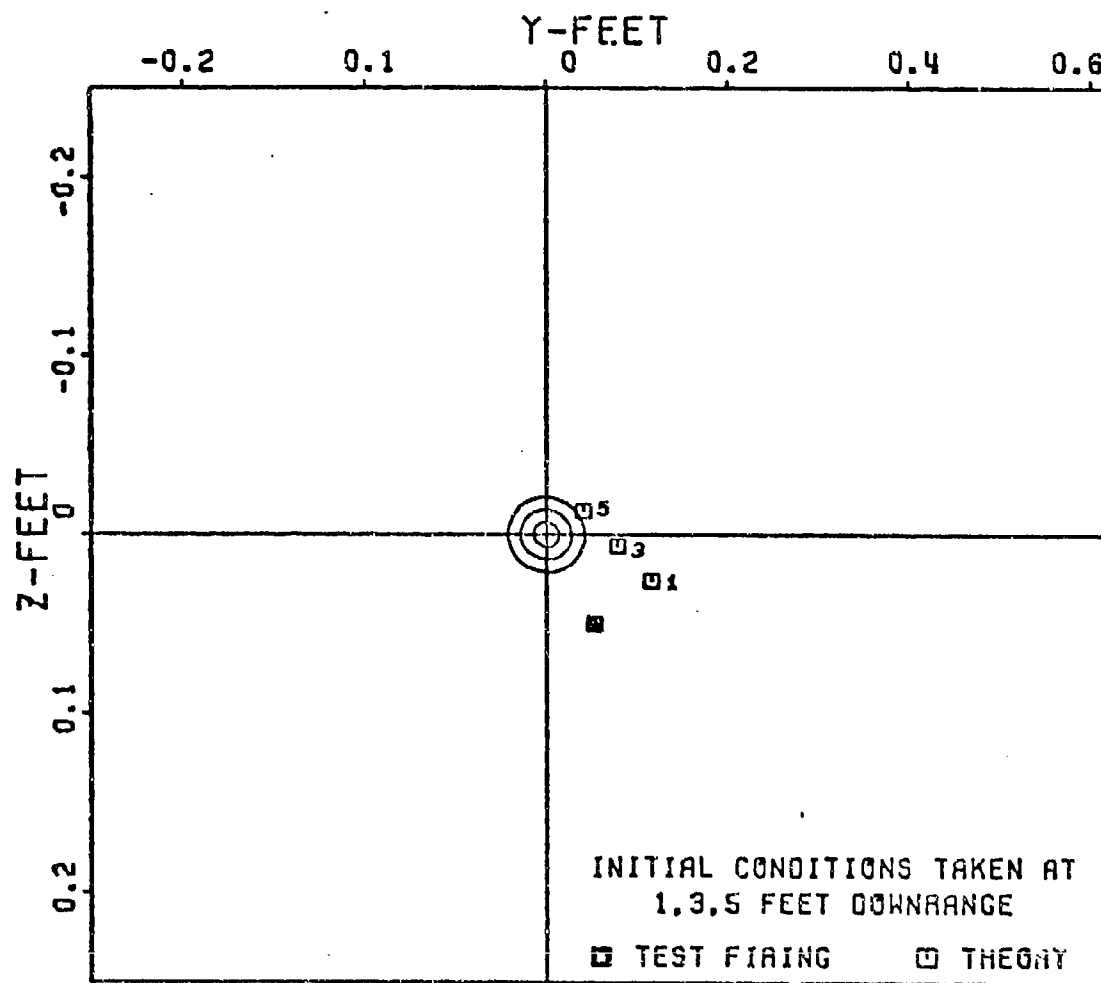


Figure 67. Dispersion: Ground Point - Round 8 Test Firing vs Theory,  
at 50 ft. Downrange

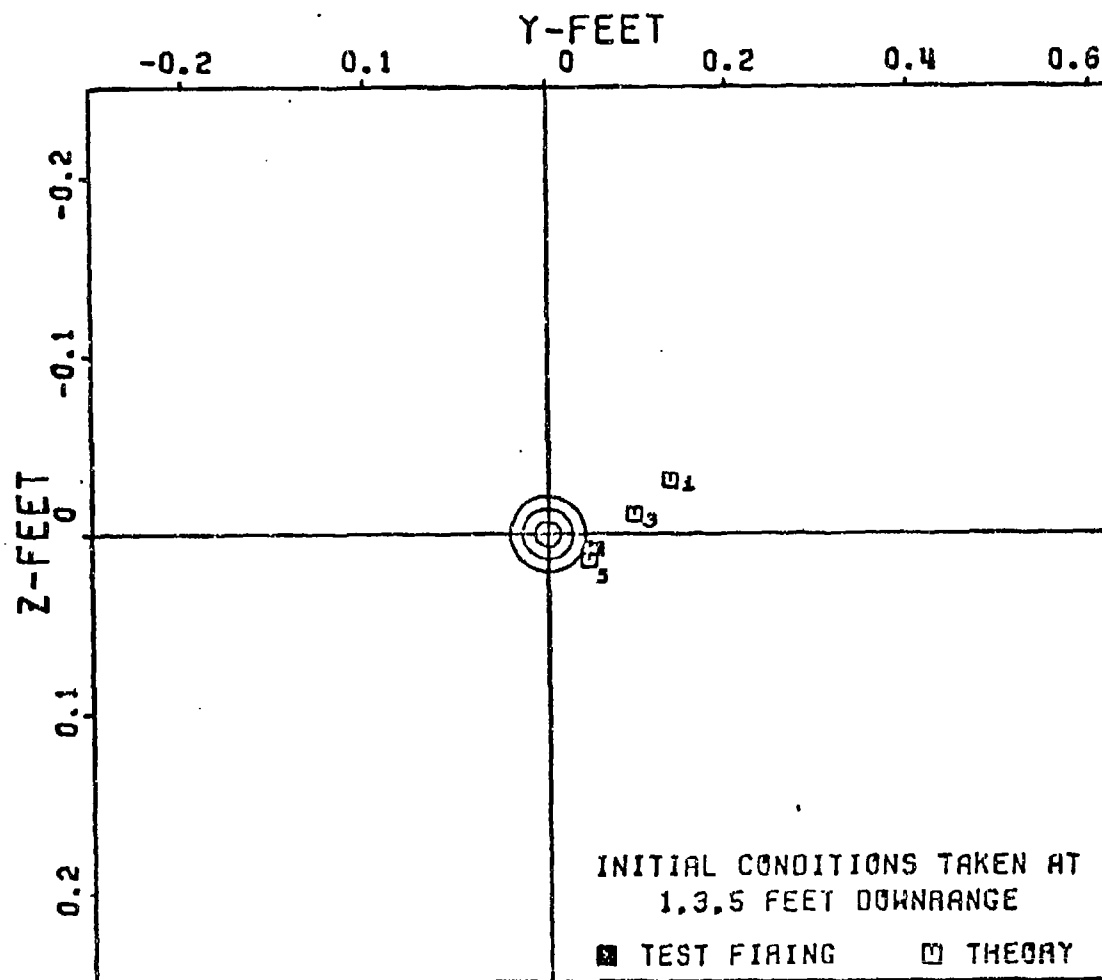


Figure 68. Dispersion: Ground Point - Round 14 Test Firing vs Theory, at 50 ft. Downrange

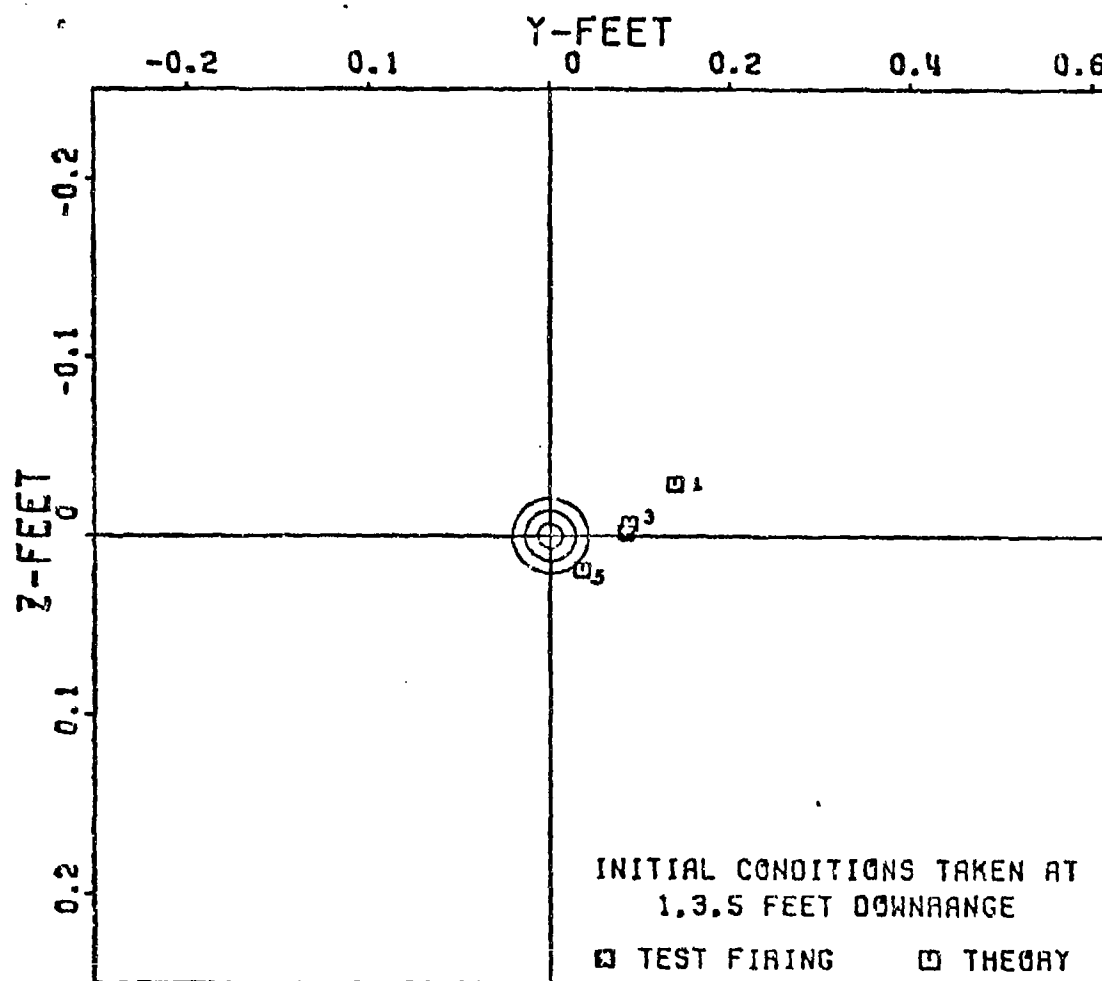


Figure 69. Dispersion: Ground Point - Round 16 Test Firing vs Theory, at 50 ft. Downrange

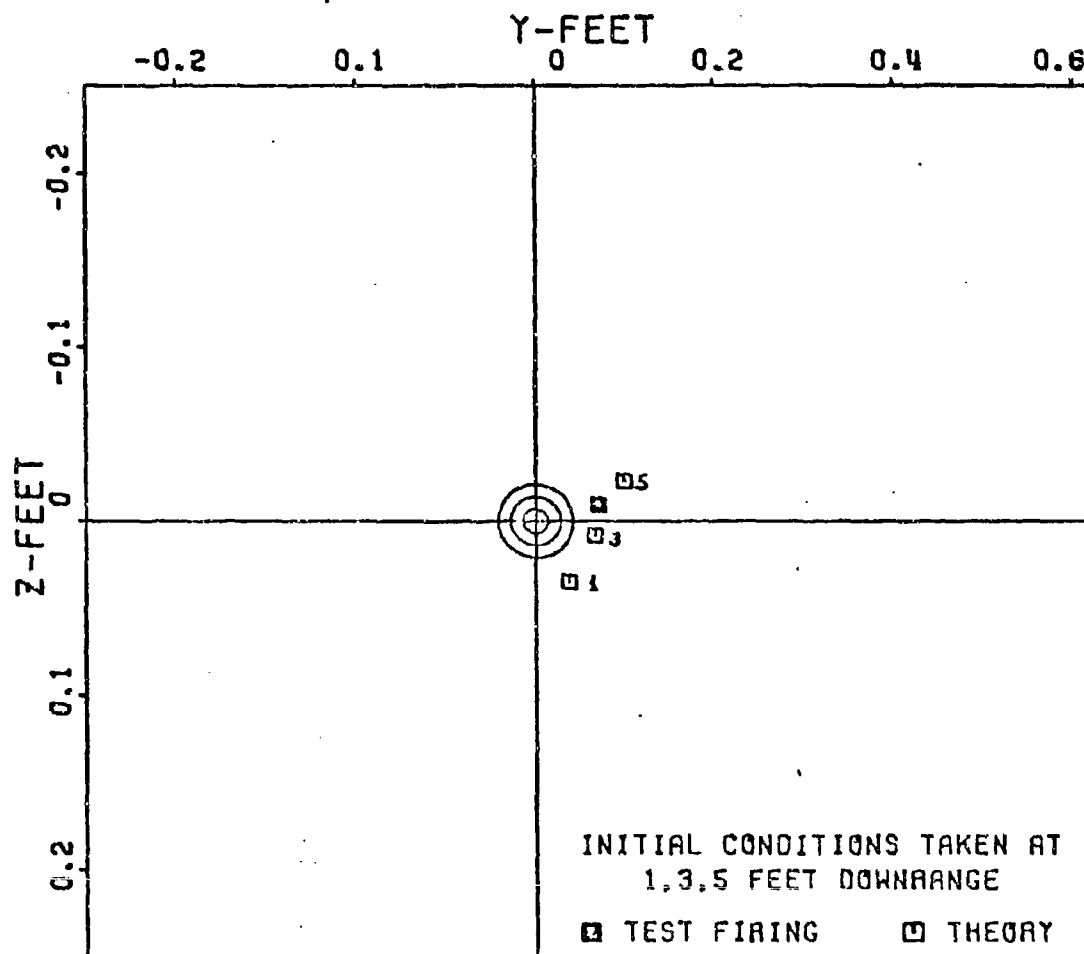


Figure 70. Dispersion: Ground Point - Round 17 Test Firing vs Theory, at 50 ft. Downrange

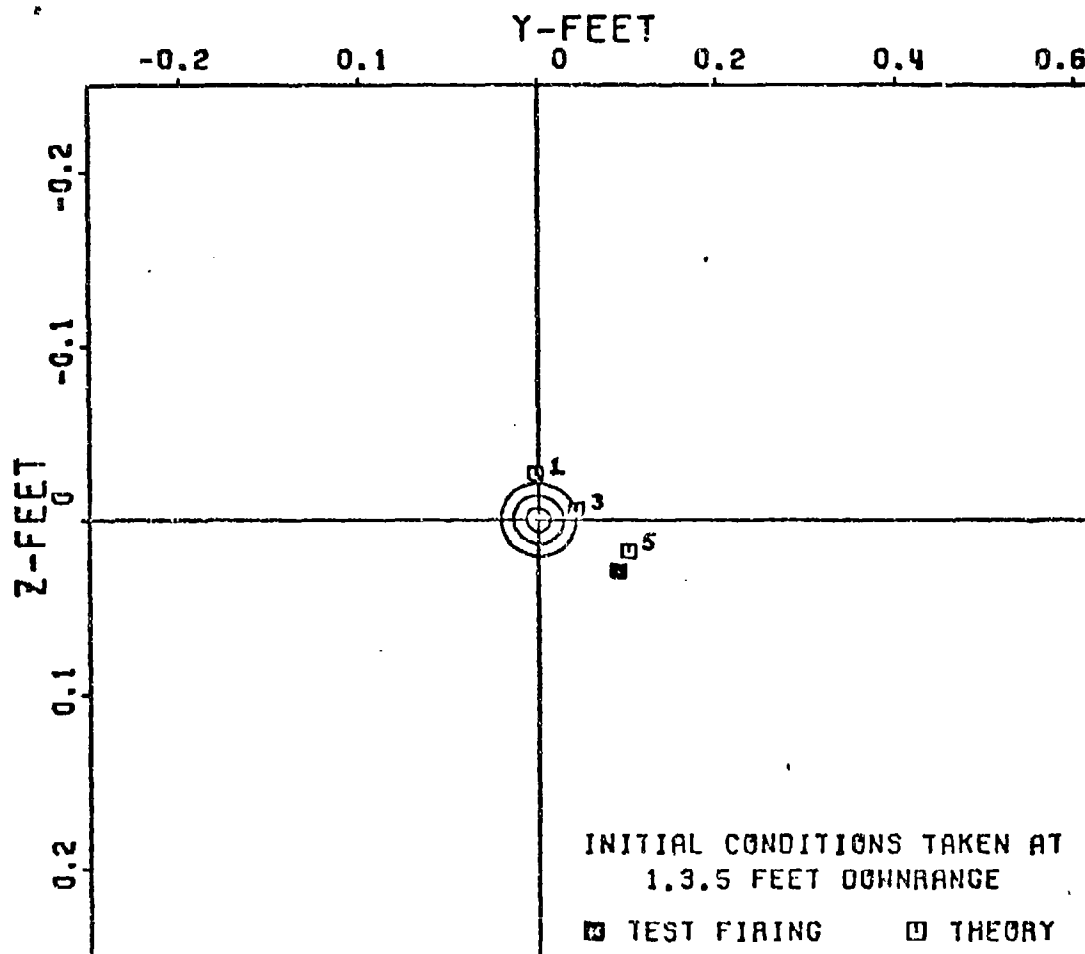


Figure 71. Dispersion: Ground Point - Round 19 Test Firing vs Theory,  
at 50 ft. Downrange



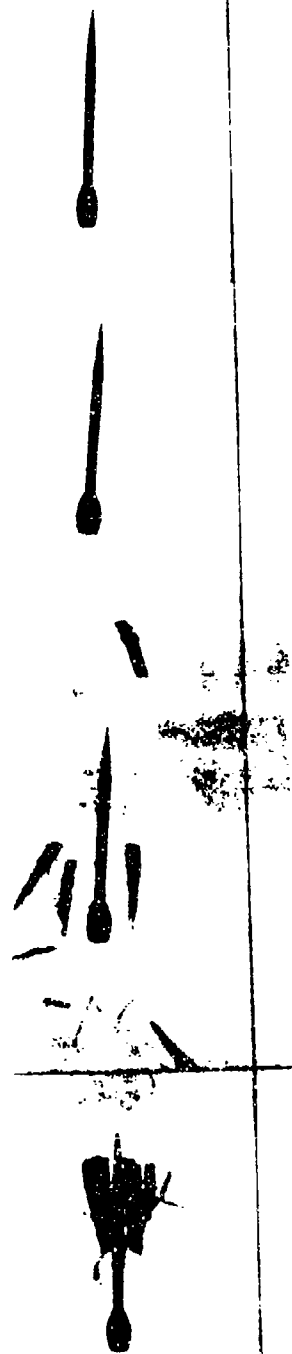
that the initial conditions would occur immediately after leaving the gun barrel. However, the flechette being a finned body needs a sabot configuration to guide it down the barrel, Figure 29. The sabot causes the initial condition location problem since the sabot must separate from the flechette outside of the gun barrel. The exact time and place where this occurs is not constant; varying from round to round. Not only does the sabot separate from the flechette instantaneously different every time, the sabot may not separate cleanly or the same way every time. Interference with the fins after sabot separation can cause disturbances to the flechette and alter the initial conditions. In addition, asymmetric sabot separation can influence the initial conditions. Figures 72-79 illustrate the flight transition sequence for the 8 flechette test rounds. In every sequence the sabot begins to separate, in varying degrees, 1 ft. downrange. At 3 ft. downrange, the sabot is nearly completely separated, but in some cases the sabot particles pose interference problems with the fins. By 5 and 7 ft. downrange the sabot has completely separated and the flechette is in free flight. The correspondence between the flight transition sequence and dispersion results can be seen in each individual round. Figure 64 indicates that the initial conditions for round 4 occur somewhere between 1 and 3 ft. downrange judging by the dispersion of the actual tested round. Figure 72 verifies this fact in that the sabot has separated from the flechette between 1 and 3 ft. downrange. The y-coordinate in the dispersion vector does not

W-0-0



1

SIDE VIEW



7 FT

5 FT

3 FT

1 FT

POSITION CHANGE

Figure 72. Flight Transition Sequence - Round 4

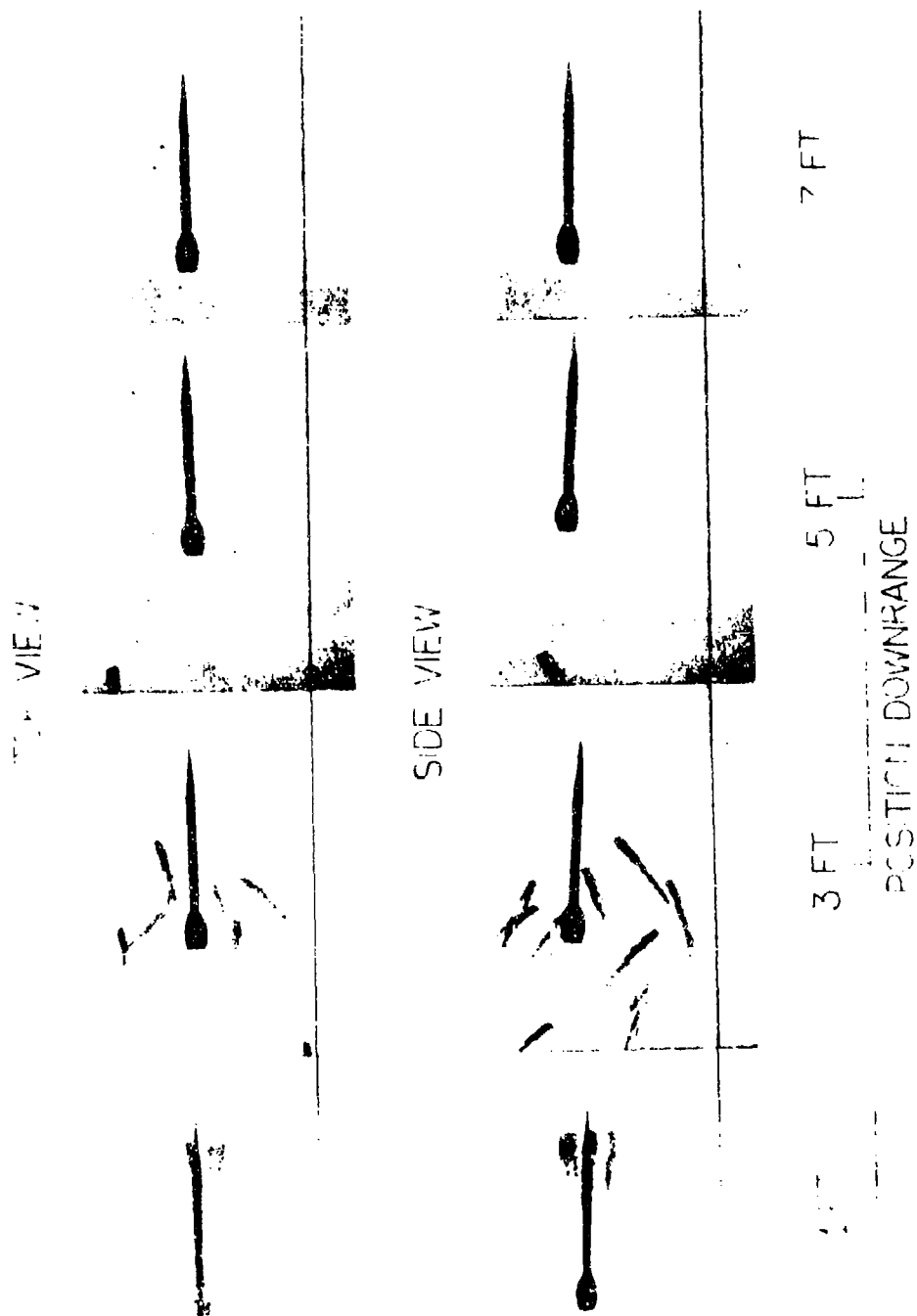


Figure 73. Flight Transition Sequence - Round 6

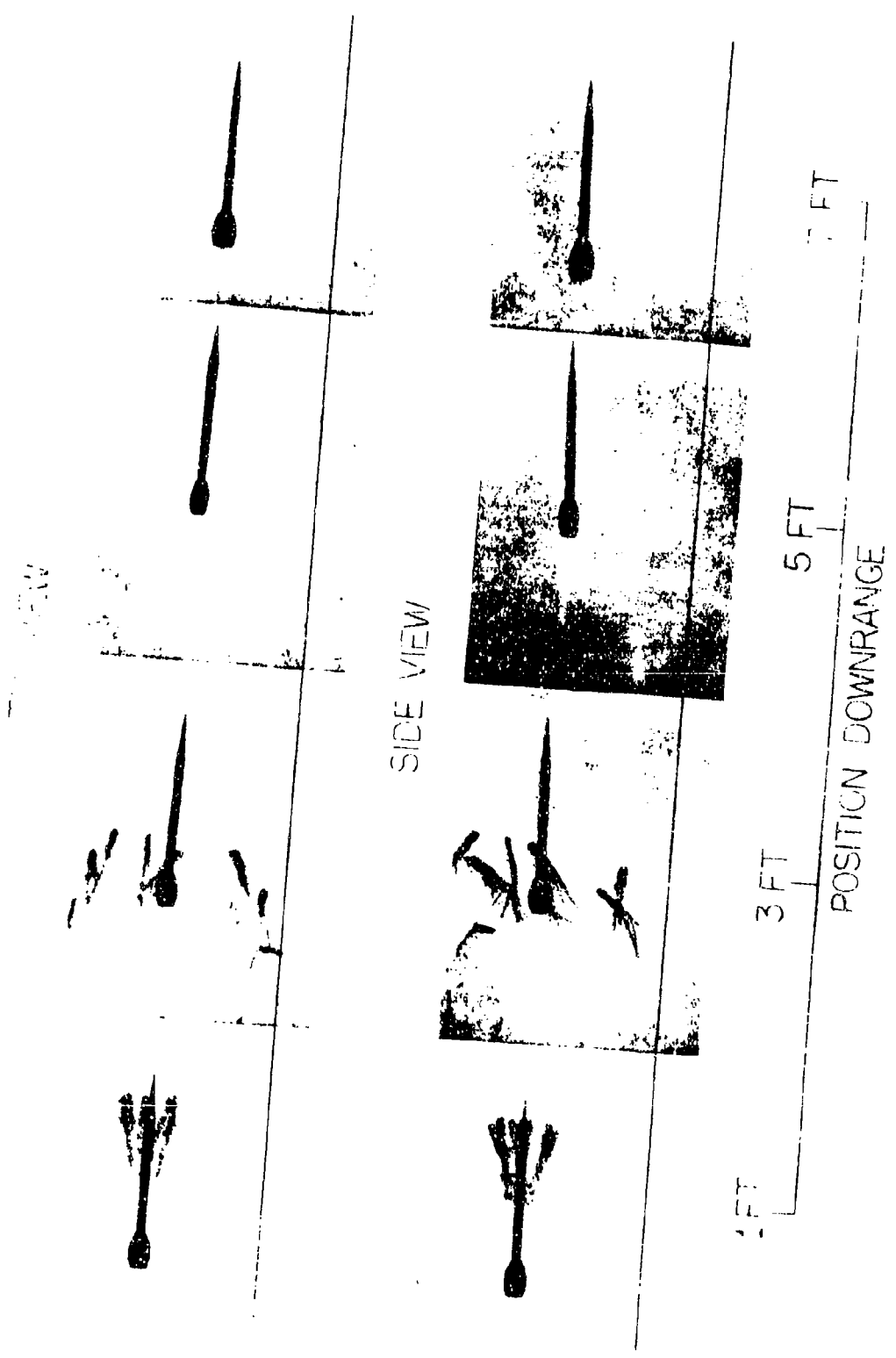
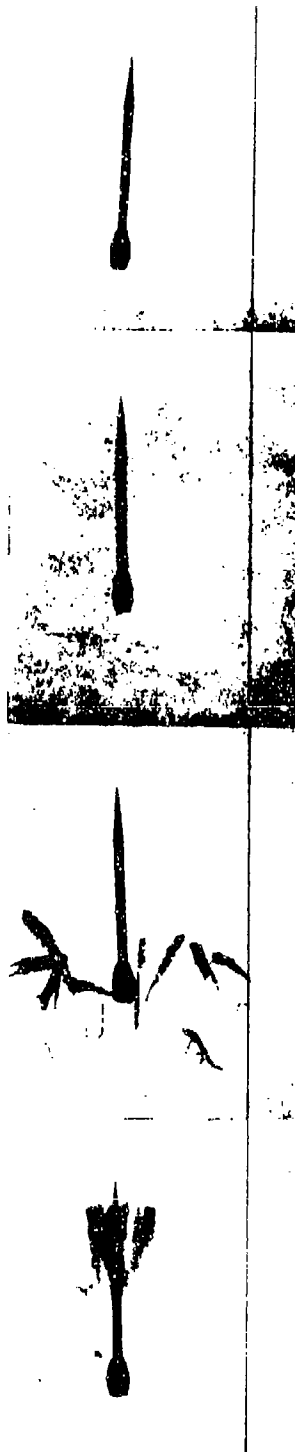


Figure 74. Flight Transition Sequence - Round 7

TCP VIEW



SIDE VIEW

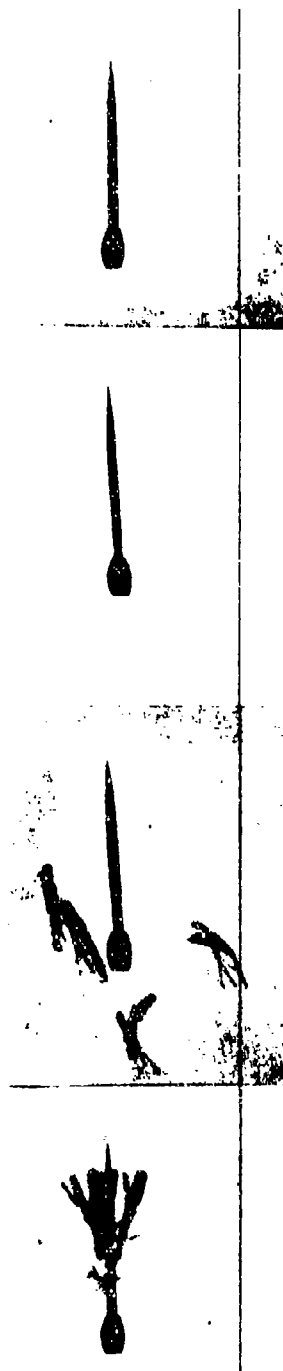


1 FT      3 FT      5 FT      7 FT

POSITION DOWNRANGE

Figure 75. Flight Transition Sequence - Round 8

TCP VIEW



SIDE VIEW



7.5 FT

5 FT

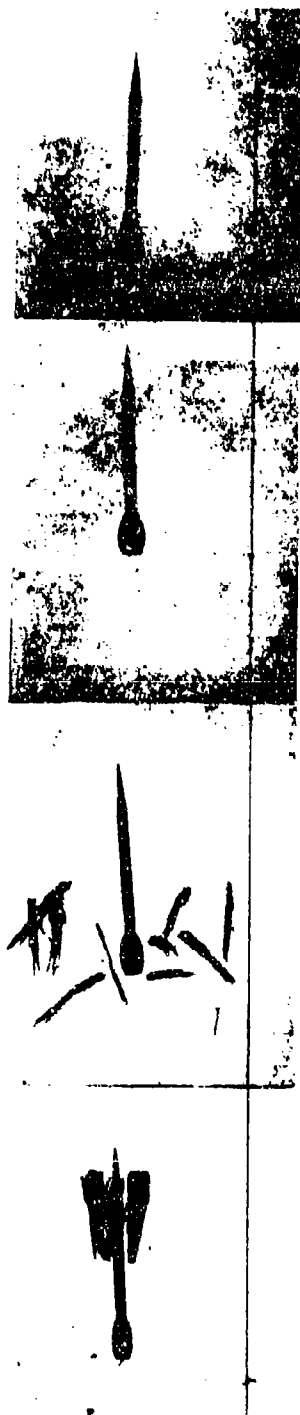
3 FT

1 FT

POSITION DOWNRANGE

Figure 76. Flight Transition Sequence - Round 14

TOP VIEW



SIDE VIEW



1 FT

3 FT

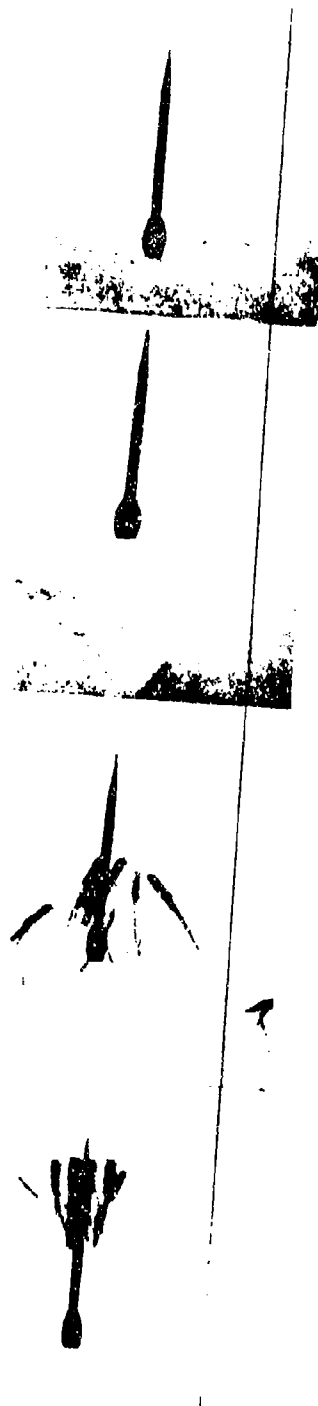
5 FT

7 FT

POSITION DOWNRANGE

Figure 77. Flight Transition Sequence - Round 16

TOP VIEW



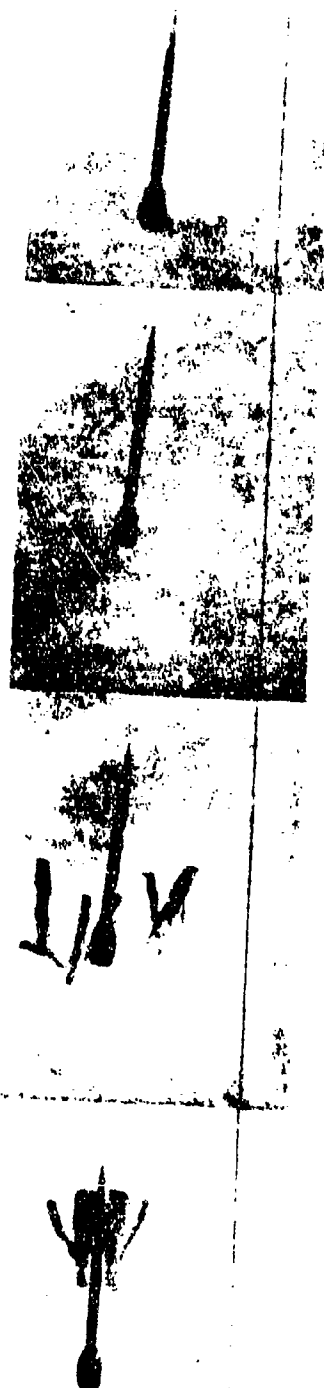
SIDE VIEW



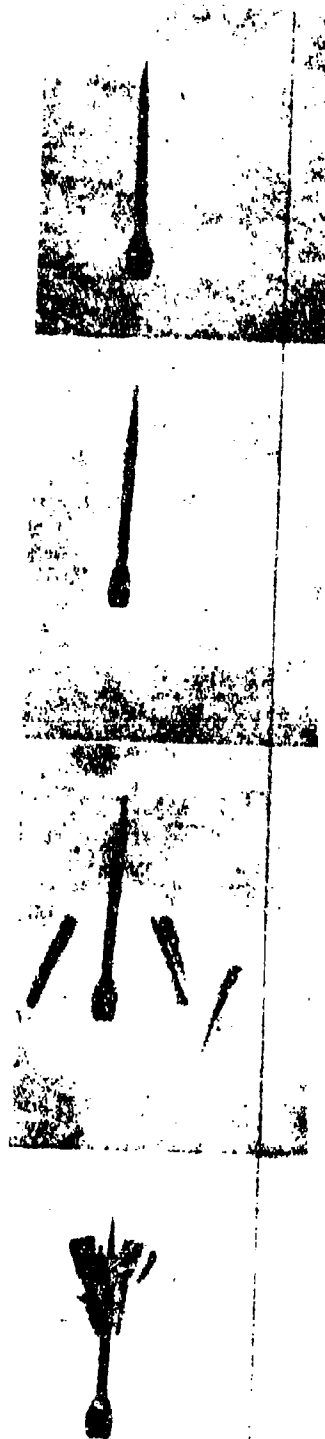
Figure 78. Flight Transition Sequence - Round 17



TOP VIEW



SIDE VIEW



3 FT 5 FT

POSITION CHANGE

Figure 79. Flight Transition Sequence - Round 19

accurately agree with the theory for this case. However, besides computational error other physical factors can influence dispersion. Contributions by fin asymmetries and other configurational asymmetries can be important but are unable to be detected or accounted for. Throughout this analysis this must be kept in mind to partially account for any discrepancy between the actual test firing and the theory and 6-D computations. Figure 65 indicates the initial conditions for round 6 occur between 3 and 5 ft. downrange. Figure 73 verifies this choice showing separation occurring around 3 ft but with sabot particles very close to the fins causing possible interference and delaying the initial conditions location. The initial conditions location for round 7 is difficult to accurately choose since the y-coordinate does not accurately agree, Figure 66. It is safe to say that the initial conditions occur sometime around 3 ft and Figure 74 verifies this choice. The z-coordinate for round 8 is not as accurate as would be desired, Figure 7, but the y-coordinate indicates initial conditions occurring between 3 and 5 ft downrange. Figure 75 agrees with this choice indicated interference with the fins at 3 ft delaying the initial conditions. Initial conditions for round 14 are chosen between 3 and 5 ft. downrange, Figure 68. Figure 76 indicates possible fin interference tending to verify the choice. Figures 69 and 77 indicate and verify the choice of initial conditions in the immediate vicinity of 3 ft downrange for round 16. Possible fin interference at 3 ft downrange, Figure 78, round 17, verifies a choice of initial conditions between 3 and 5 ft, Figure 70. A similar situation occurs for round 19 in Figures 71 and 79. It is often difficult to

choose initial condition positions accurately due to slight discrepancies between theory and test firings. However, the discrepancies are of the order 0.05 ft, which shows up large in Figures 64-71 due to the scale chosen, but is within the error expected from the validation of theory section.

The influence of sabot separation can be readily seen by inspection of Figures 72-79, 1 and 3 ft downrange. In every case, the flechette and sabot are at nearly a zero angle of attack at 1 ft, but has changed angle of attack noticeably by 3 ft downrange. This would indicate that fin interference or asymmetric sabot separation is causing the noticeable effect. It can be concluded that dispersion is dependent upon the initial conditions that the initial conditions are a function of sabot separation and that the theory can predict what the initial conditions are and where they occur.

#### Dispersion Theory vs. First Maximum Yaw Hypothesis

A popular theory to predict the dispersion of flechettes is the First Maximum Yaw Hypothesis. This theory relates the dispersion magnitude to the first maximum yaw magnitude by a nearly linear relationship. Other initial conditions such as angular rate,  $\vec{\alpha}_0$  and translational velocity,  $\vec{S}_0$  are said not to effect dispersion. To disprove this theory and strengthen the position of the theory ascribing to dispersion due to initial conditions  $\vec{S}_0$ ,  $\vec{\alpha}_0$ ,  $\vec{\dot{\alpha}}_0$ , the First Maximum Yaw theory was applied to Frankford Arsenal data. Figure 80 shows a plot of dispersion magnitude vs. first maximum yaw magnitude. Clearly no linear relationship exists between

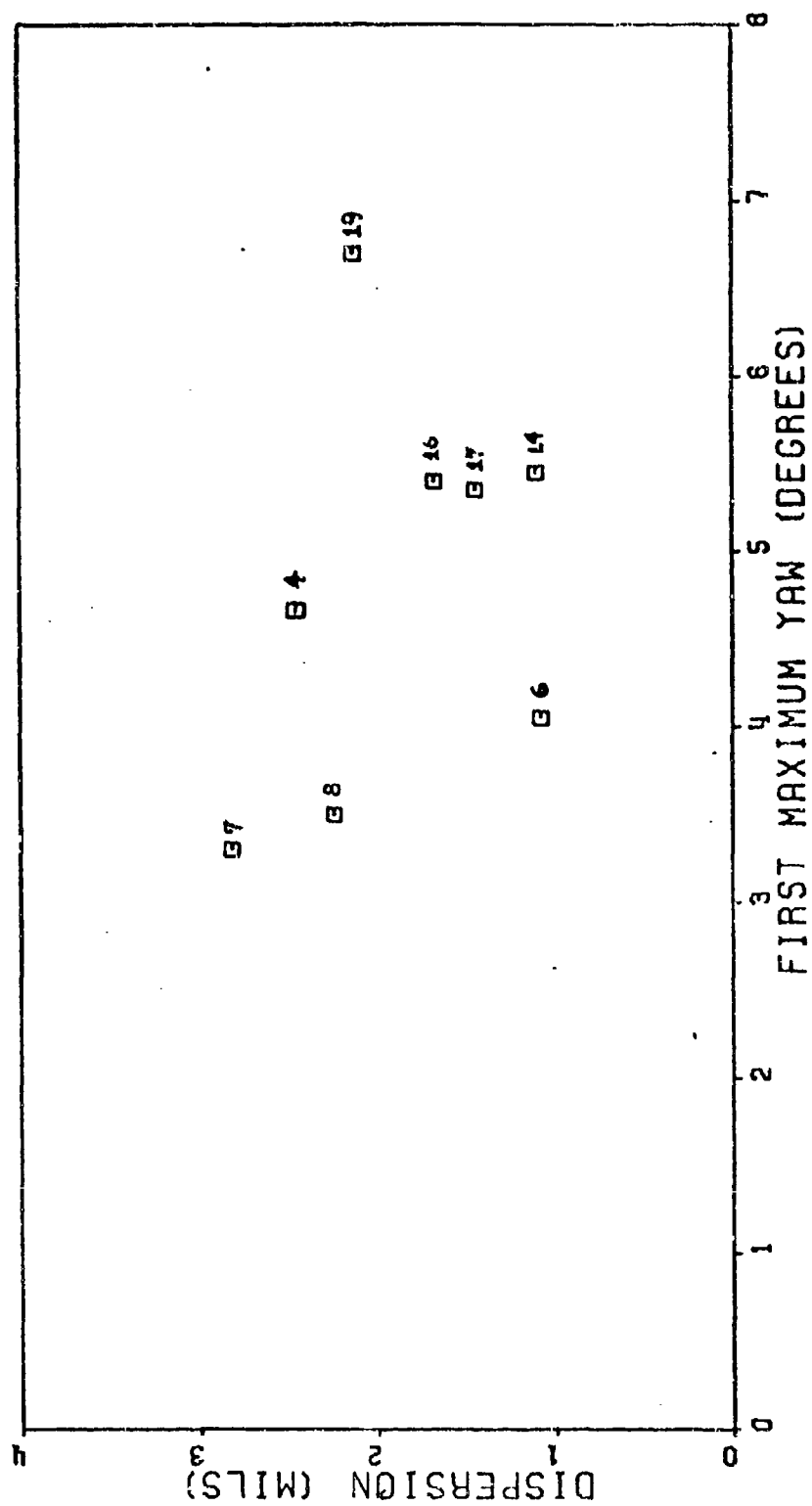


Figure 80. Dispersion vs First Maximum Yaw, Frankford Test Firing Results

dispersion and first maximum yaw. In fact, the plotted data resembles a random shotgun blast. Figures 81, 82 and 83 employ the theory to the first maximum yaw hypothesis. Again the plot substantiates the findings of Figure 80. The disproval of the first maximum yaw hypothesis comes as no surprise since the dispersion theory contradicts it and the 6-D computations, which integrate the actual equations of motion, validated the dispersion theory. Therefore, dispersion could never accurately be predicted by a theory involving only first maximum yaw.

The influence of initial conditions,  $\vec{S}_0$ ,  $\vec{\alpha}_0$ , and  $\vec{\dot{\alpha}}_0$  and dispersion for the actual test firings are expected to be different from that in the validation of theory section because of the different ranges in the initial conditions. For example,  $\vec{S}_0$  in the validation section was  $(100 + 100i)$  ft/sec. In the actual test firings,  $\vec{S}_0$  only ranged as high as 0.017 ft/sec. Of course, the large value was only to validate the theory. Here  $\vec{S}_0$  is very small and its contribution is accordingly smaller. In the reduced equation 24, employed to calculate the theory column in Table XXII,

$$\vec{J.A.}(\text{mils}) = 1000 \left[ \frac{\vec{S}_0}{x} + \frac{\vec{\dot{S}}_0}{u} - \frac{l_y}{mud} A \left( \vec{\alpha}_0 \cdot \vec{\dot{\alpha}}_0 \frac{ipI_x}{I_y} \right) \right]$$

for round 4, 1 ft downrange,

$$1000 \frac{\vec{\dot{S}}_0}{u} = (0.001562 + 0.001841i) \text{ mils}$$

where as,

$$\vec{J.A.} = (1.329 - 1.302i) \text{ mils}$$

Since this is typical of the 8 rounds tested,  $\vec{\dot{S}}_0$  has little effect on dispersion for these rounds.

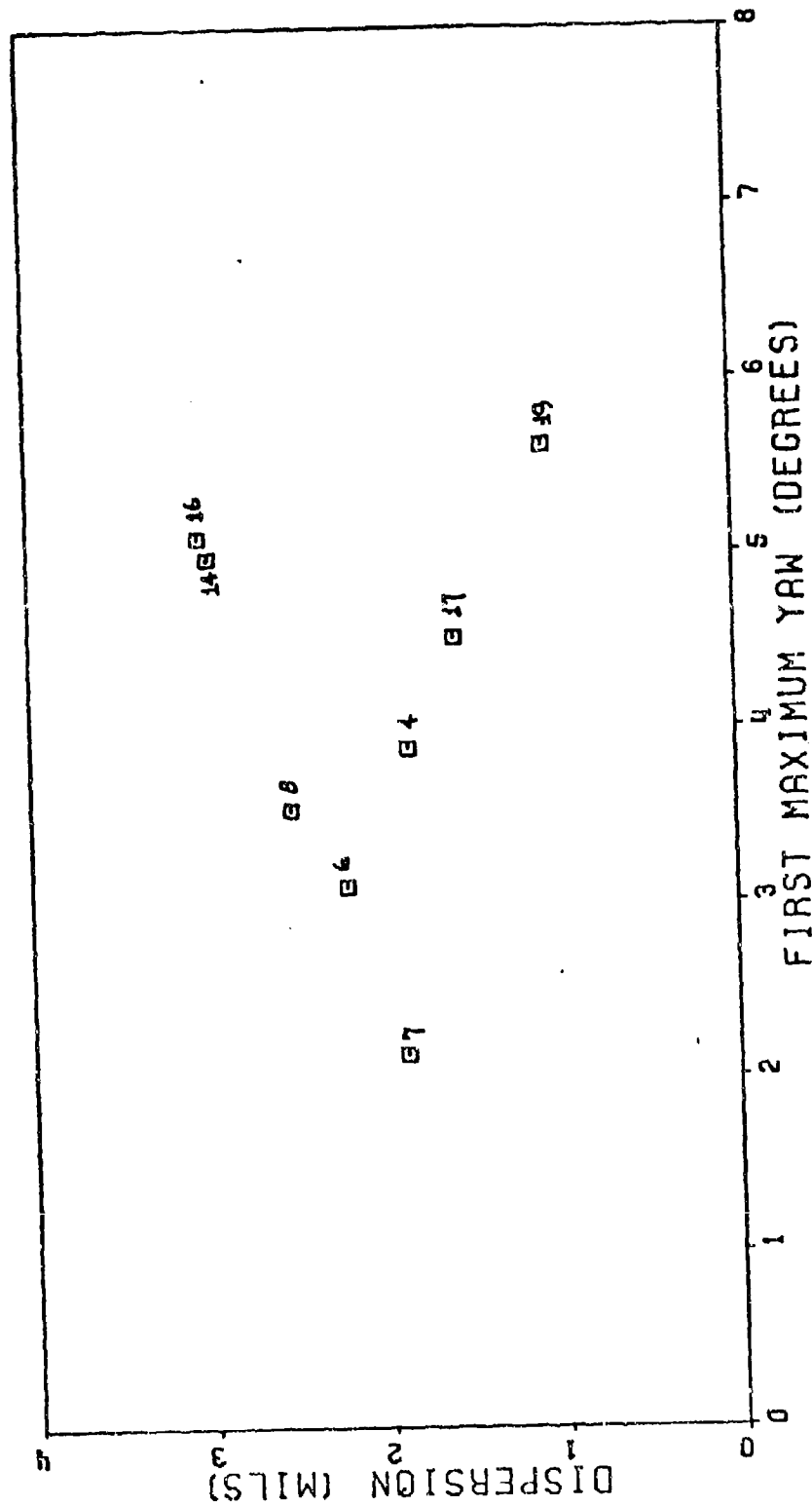


Figure 81. Dispersion vs First Maximum Yaw, Theory - Initial Conditions,  
1 ft Downrange

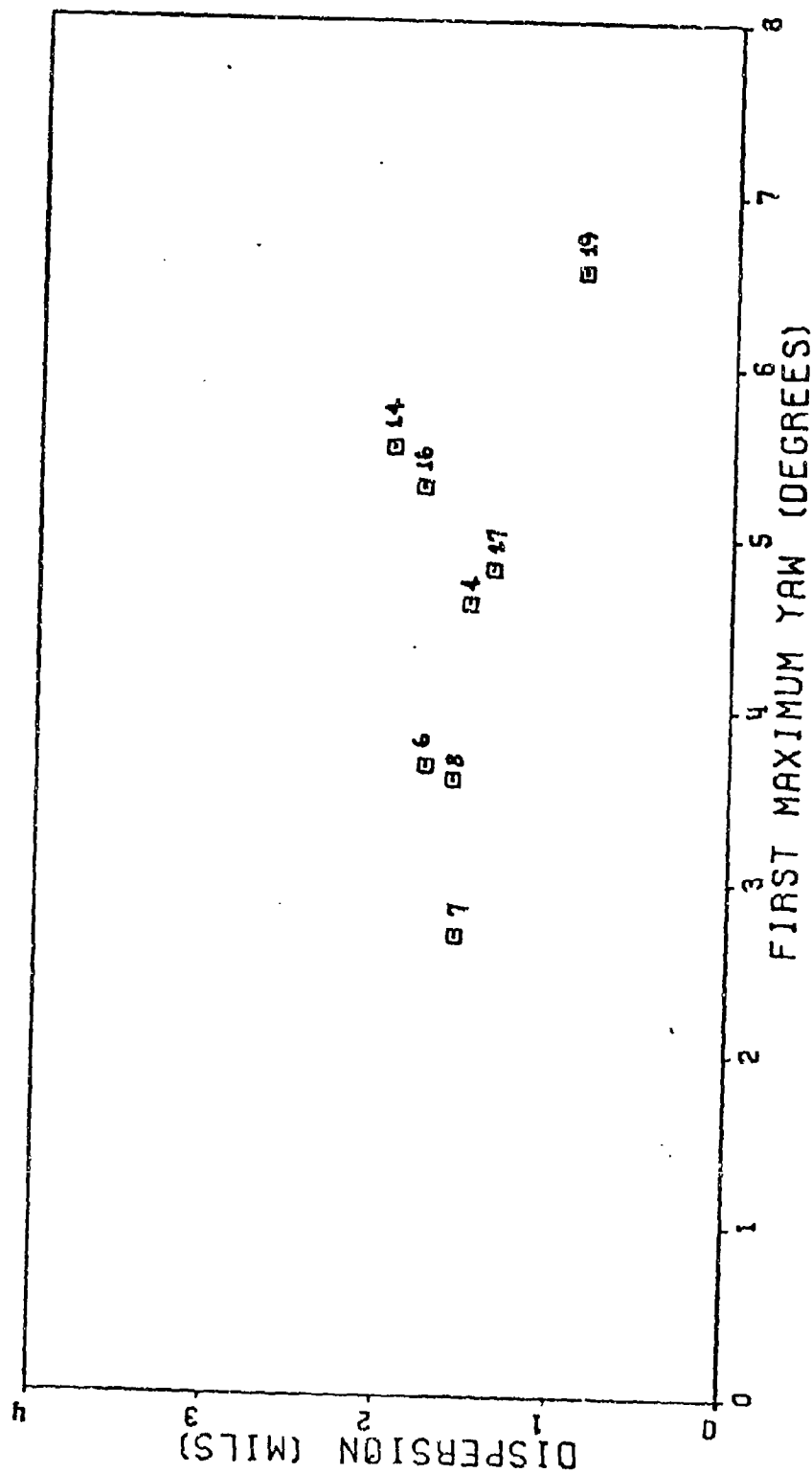


Figure 82. Dispersion vs First Maximum Yaw, Theory - Initial Conditions,  
3 ft. Downrange

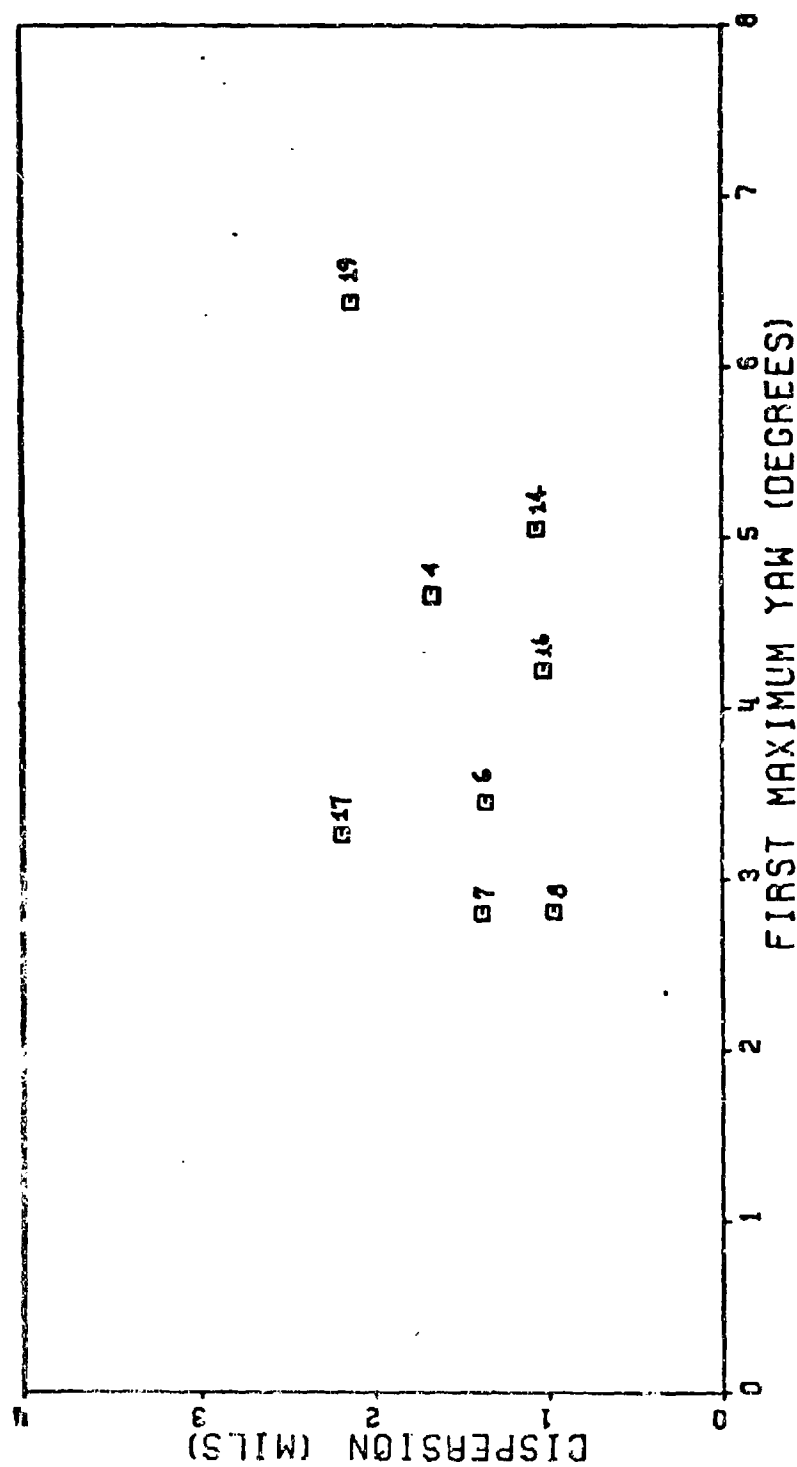


Figure 83. Dispersion vs First Maximum Yaw, Theory - Initial Conditions,  
5 ft. Downrange



Similarly, for this particular case,

$$1000 \frac{\vec{S}_0}{x} = (1.519360 + 0.041760i) \text{ mils}$$

$$1000 \vec{\alpha}_0 \frac{ipL_x A}{\text{mud}} = (-0.01437 + 0.00214i) \text{ mils}$$

$$-1000 \vec{\alpha}_0 \frac{L_y A}{\text{mud}} = (-0.206075 - 1.383672i) \text{ mils}$$

Obviously,  $\vec{S}_0$  and  $\vec{\alpha}_0$  are by far the greatest contributors to dispersion for this case. Inspection of all the other 23 cases in Table XXII agrees with this general pattern.  $\vec{S}_0$  can be nearly eliminated, of course, by accurate setup of the test equipment so that the gun barrel is set exactly at coordinates (0,0). Any  $\vec{S}_0$  then would occur from displacement due to the blast. This leaves the major culprit in dispersion to be  $\vec{\alpha}_0$ . Figure 84 illustrates the dependence of the Jump Angle, and hence dispersion, upon angular rate and angle of attack.

Although  $\vec{\alpha}_0$  contributes the most to the Jump Angle, the combination of  $\vec{S}_0$  and  $\vec{\alpha}_0$  also has a noticeable influence. From the test firings,  $\vec{S}_0$  was found to have a negligible effect on dispersion. Therefore, it is neglected in Figure 84 to simplify the plot. It is evident from Figure 84 that various combinations of  $\vec{\alpha}_0$  and  $\vec{\alpha}_0$  yield zero dispersion. It is possible that large values of  $\vec{\alpha}_0$  and  $\vec{\alpha}_0$  can combine to yield zero dispersion; an impossibility with the first maximum yaw hypothesis. If  $\alpha_0$  and  $\dot{\alpha}_0$  are able to balance to give zero dispersion, then this idea can be expanded to include the entire equation.

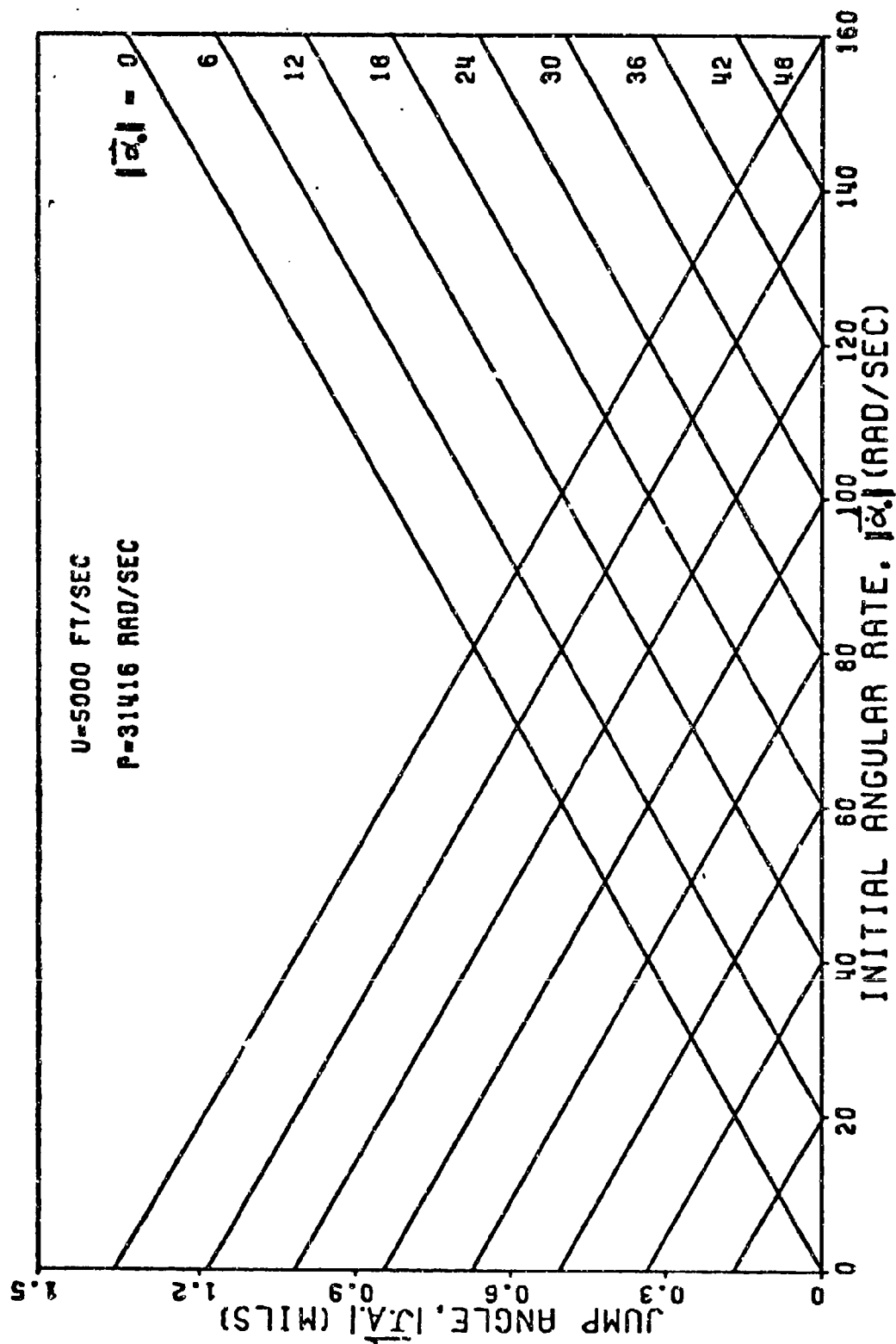


Figure 24. Jump Angles for Various Initial Conditions

The governing equation used throughout this dispersion analysis section is:

$$\vec{J} \cdot \vec{A} = 1000 \left[ \frac{\vec{S}_0}{x} + \frac{\vec{\dot{S}}_0}{u} - \frac{I_y}{mud} A \left( \vec{\alpha}_0 - \vec{\alpha}_0 \frac{ipL_x}{I_y} \right) + \frac{ig}{2} \left( \frac{x}{u^2} \right) \right]$$

Eliminating the constant gravity term,

$$\vec{J} \cdot \vec{A} = 1000 \left[ \frac{\vec{S}_0}{x} + \frac{\vec{\dot{S}}_0}{u} - \frac{I_y}{mud} A \left( \vec{\alpha}_0 - \vec{\alpha}_0 \frac{ipL_x}{I_y} \right) \right]$$

Setting  $\vec{J} \cdot \vec{A}$  to zero, the idea behind Figure 84 is expanded to include  $\vec{S}_0, \vec{\dot{S}}_0$ .

$$\frac{\vec{S}_0}{x} + \frac{\vec{\dot{S}}_0}{u} = \frac{I_y}{mud} A \left( \vec{\alpha}_0 - \vec{\alpha}_0 \frac{ipL_x}{I_y} \right)$$

rearranging

$$m \left[ \vec{S}_0 \left( \frac{u}{x} \right) + \vec{\dot{S}}_0 \right] = \frac{A}{d} (\vec{\alpha}_0 I_y - \vec{\alpha}_0 ipL_x)$$

A dimensional analysis of the equations finds that both sides have units of momentum or impulse. Going one step farther it can be said that to obtain zero dispersion:

initial transverse momentum = initial angular momentum

Therefore it is the imbalance in the initial momentums that causes dispersion. The size of initial conditions can be huge, Figure 84, but if they can combine to balance, zero dispersion results. The way the initial conditions combine, determine the magnitude of the imbalance or dispersion. It should be noted that this dispersion discussed is round to round dispersion and that the inconsistency of the momentum imbalance

8

from round to round causes a dispersion pattern (a set of rounds). The next section will highlight this principle in the evaluation of physical factors affecting dispersion.

## PHYSICAL EVALUATION OF DISPERSION

Initial momentum imbalance has been shown to cause dispersion. Initial conditions determine the magnitude of the imbalance. What causes these initial conditions to occur is the subject of this final section. Initial conditions occur somewhere between zero and five feet downrange to different degrees of magnitude due to various conditions. These conditions are:

1. Fin or body asymmetry
2. In-bore mal-alignment
3. Asymmetric blast
4. Asymmetric sabot separation
5. Sabot-fin interference
6. Fin or body damage

Fin or body asymmetries can cause dispersion magnitudes to range as much or greater than those in the Validation of Theory section for aerodynamic asymmetries. These asymmetries can be overcanted or bent fins, damaged nose cone, or even body deformities. Figure 85 which shows in-bore mal-alignment also shows a slightly bent body, concave downward. In-bore mal-alignment can be attributed to warping and/or the entire flechette at some angle of attack. Clearly, if this flechette were fired, the in-bore angle of attack would produce an  $\vec{\alpha}_0$  outside the gun barrel even before sabot separation. With the flechette at some angle of attack, the blast can cause a large  $\vec{\alpha}_0$  and an  $\vec{S}_0$  and  $\vec{S}_0$ . The blast itself

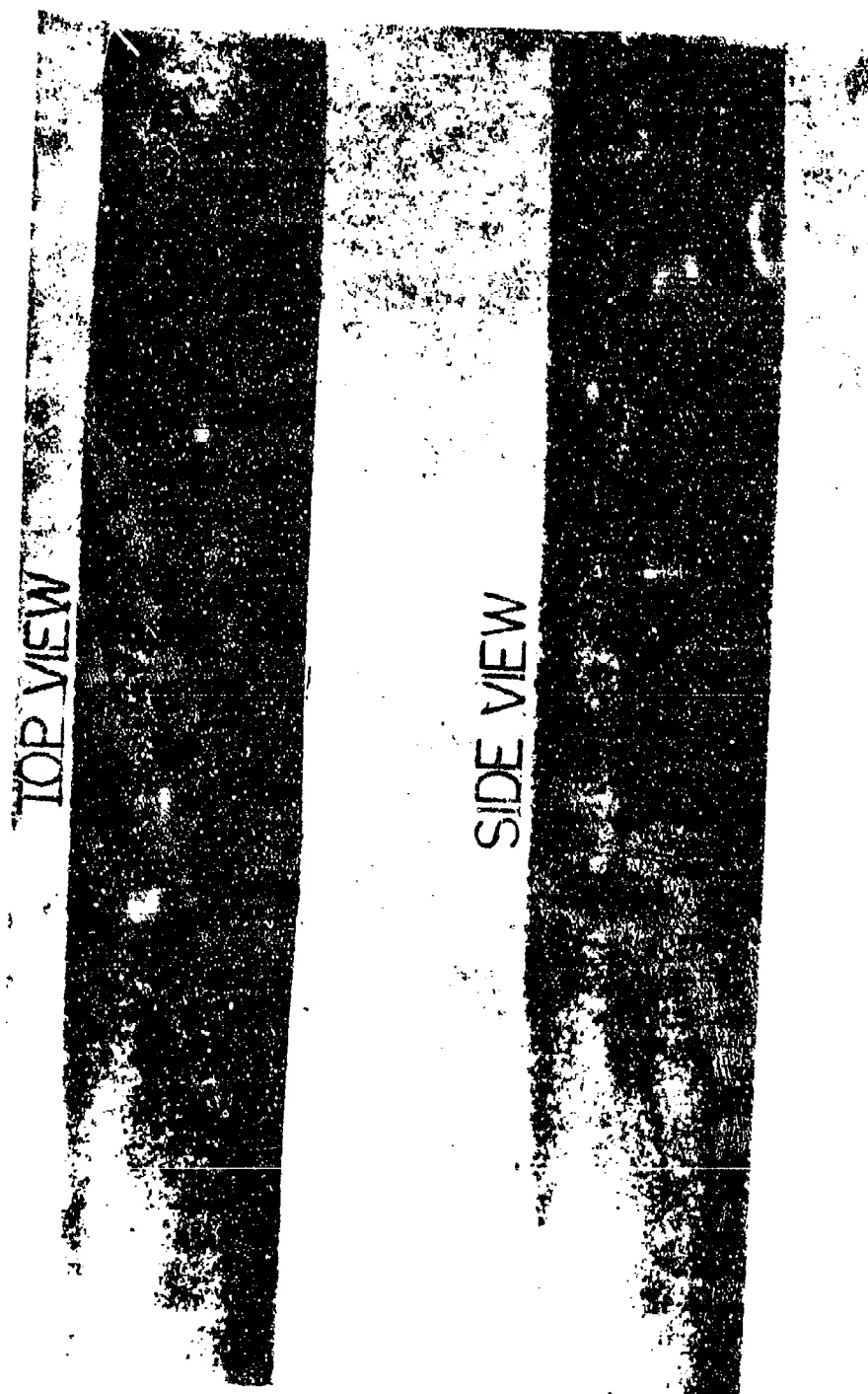


Figure 85. Flechette In-Bore Position

is a chief catalyst in causing the initial conditions. An asymmetric blast can indeed impart influence on the initial conditions, but a symmetric blast can also. Given an initial angle of attack due to some disturbances the symmetric blast can cause significant  $\vec{\alpha}_0$ ,  $\vec{\dot{\alpha}}_0$ ,  $\vec{S}_0$  and  $\vec{\dot{S}}_0$ . Figure 86 shows a typical blast region with the flechette outlined in the picture. The momentum principle discussed in the previous section goes hand-in-hand with this blast region. It is here that the transverse and angular-momentum is imparted to the flechette. Figure 87 illustrates a typical flechette in the blast region. Coming out of the barrel at some angle of attack, the blast catches the flechette and induces some angular rate. At the same time, the flechette is translated laterally giving an  $\vec{S}_0$  and  $\vec{\dot{S}}_0$ . If these contributions cancel each other out; that is, if initial transverse momentum equals initial angular momentum then the dispersion is zero. If they do not cancel, dispersion results. The sketch is highly simplified in that the blast itself is all-engulfing as in Figure 86. Of course, the transition sequence of sabot separation, fin interference, and possible fin damage must not be forgotten. The transition sequence occurs in the blast region, however, and is not considered separate from the blast. When separation occurs, the sabot particles are apt to interfere with the fin section and cause possible damage. Once the sabot has separated and cleared the fins the blast has had its greatest effect and the initial conditions can be determined. After the flechette has moved downrange, it assumes supersonic free flight, Figure 88.

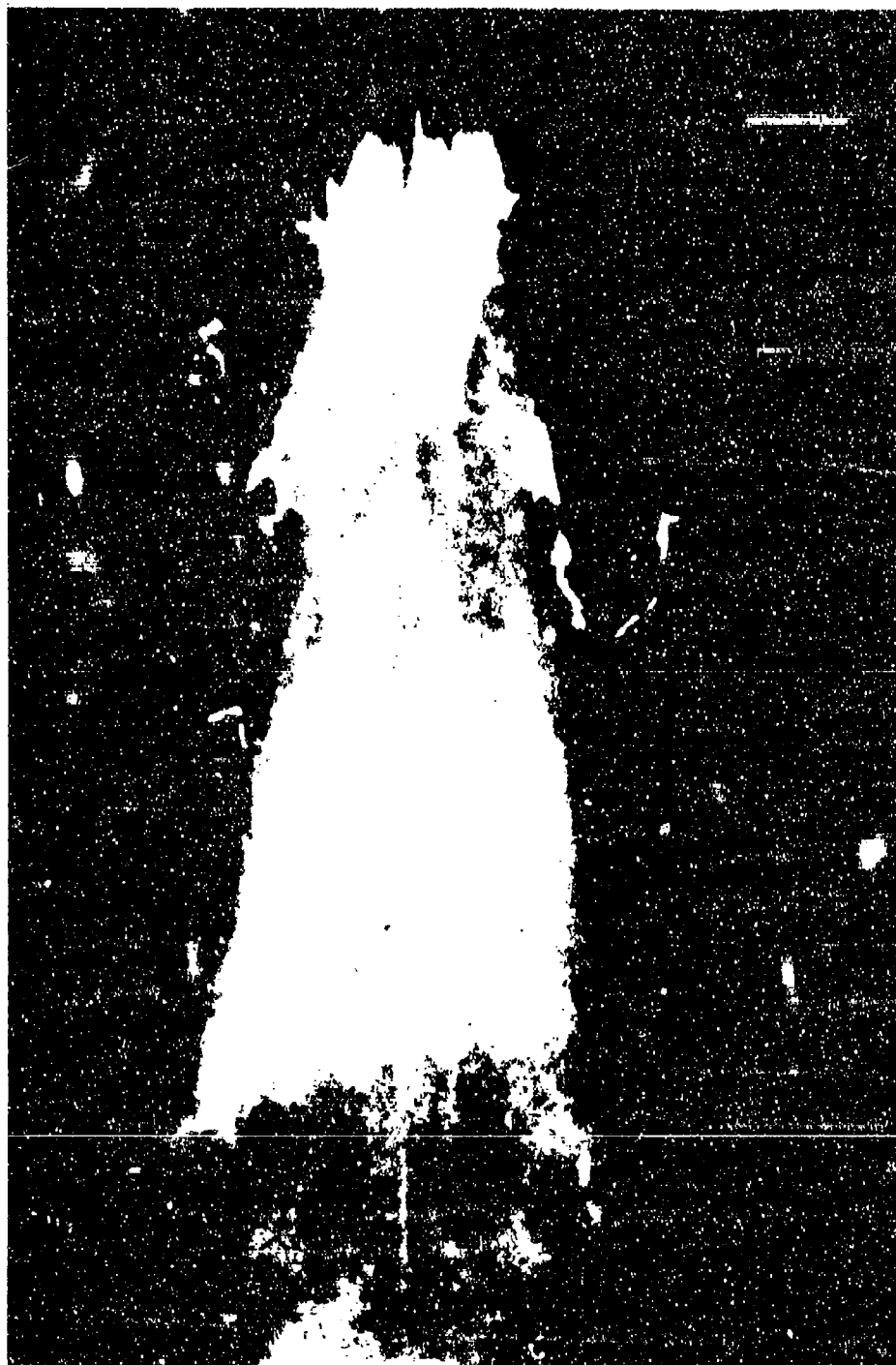


Figure 86. Typical Flechette Blast Region



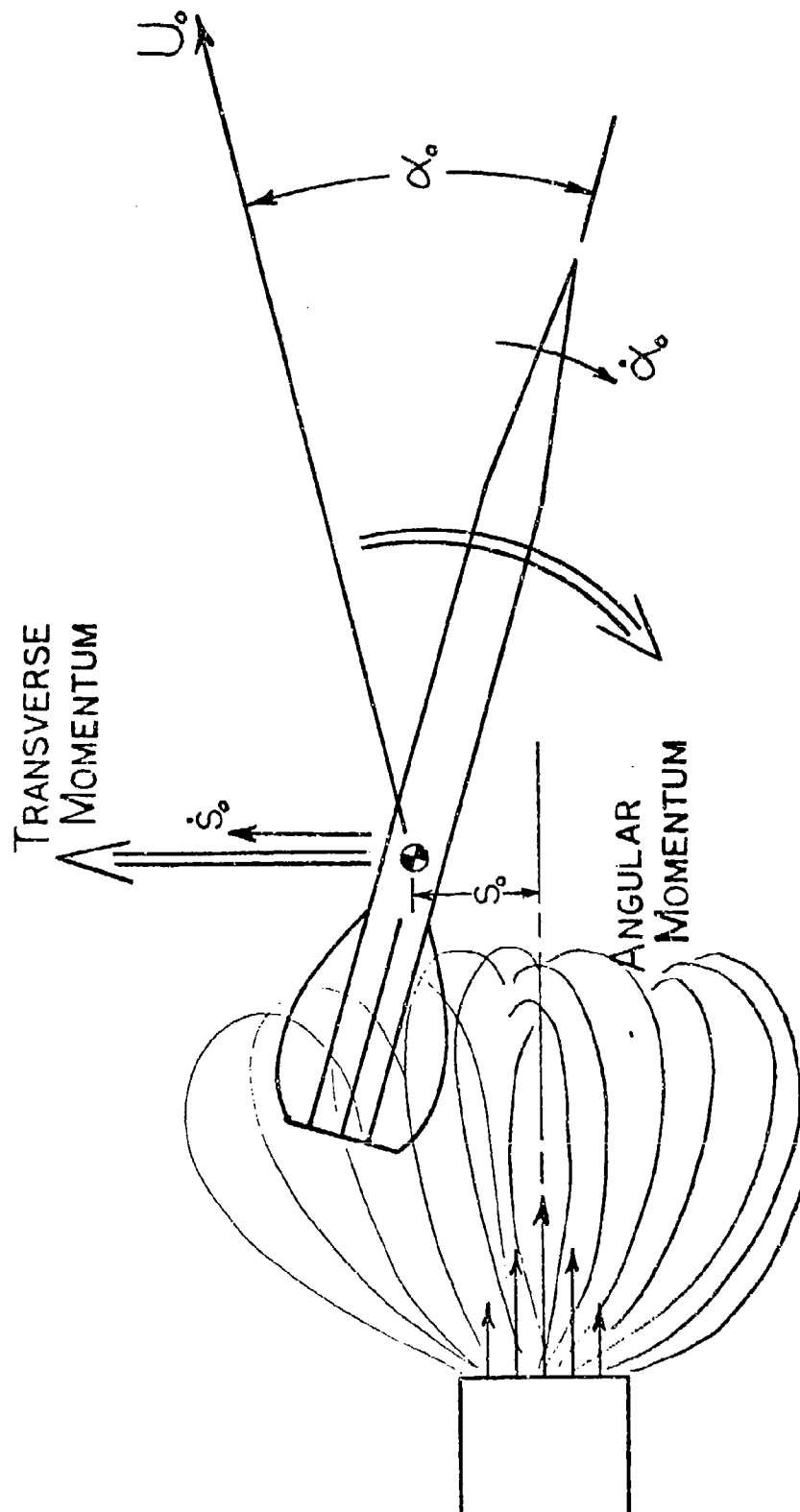


Figure 87. Muzzle Blast Effects

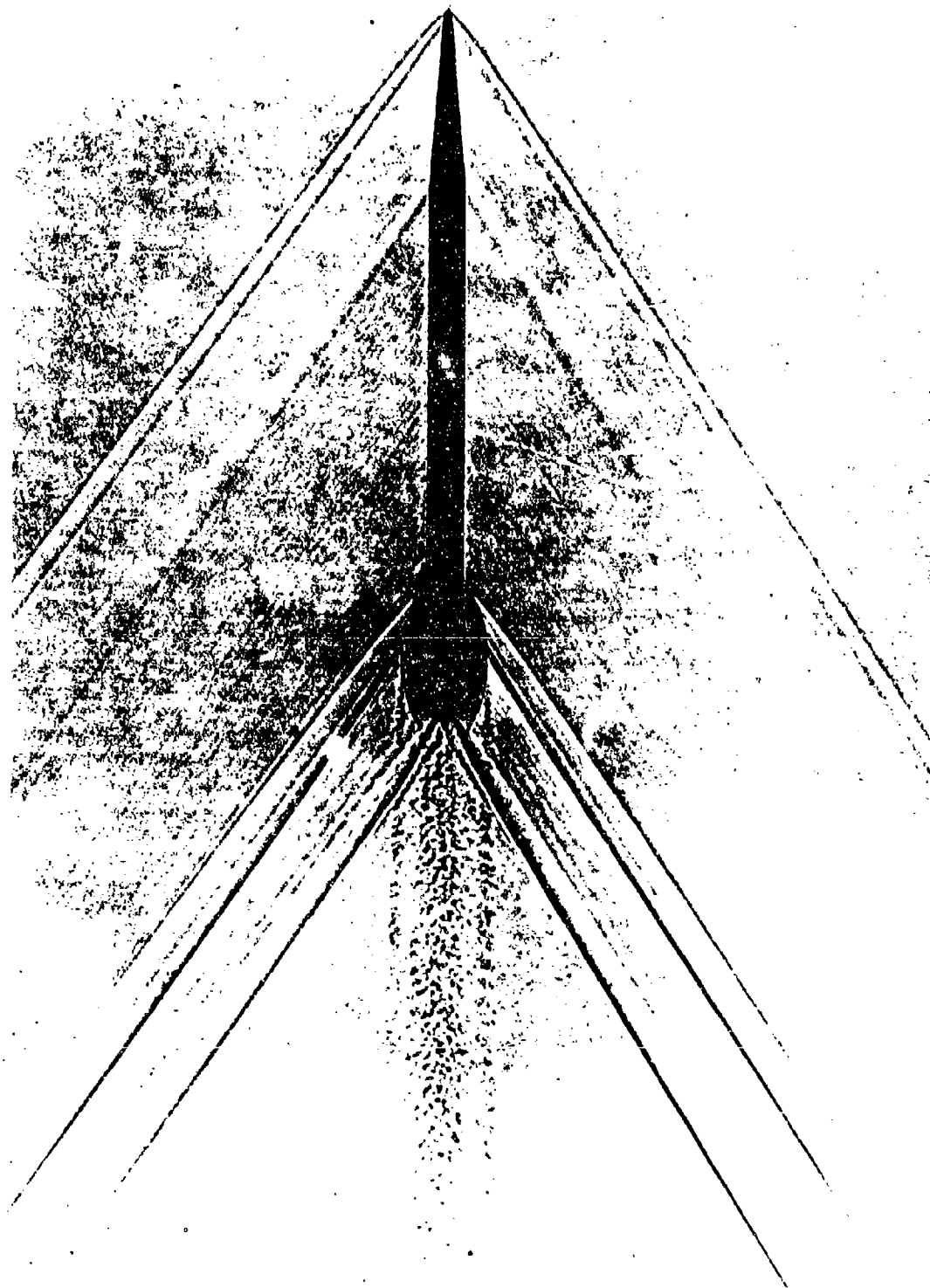


Figure 88. Supersonic Free Flight, Ground Point Flechette

## CONCLUSIONS

A complete Jump and Dispersion Theory has been developed for free flight vehicles. Three governing equations have been determined to accommodate high, low, and very low roll rates. The theories were found to be accurate with six-degree-of-freedom numerical computations of the equations of motion and therefore reliably predict the jump and dispersion of flechettes. The theory validation included 201 case runs in four phases. The first phase validated the theory with respect to restoring and damping moments. The effect of these moments on dispersion was found to depend on the initial conditions. The second phase validated the theory with respect to Magnus forces and moments. The effect of Magnus was found to be very small and not to be of any consequence unless the total dispersion of any given round was of the same order of magnitude as the Magnus effect. Phase three validates the theory with respect to aerodynamic asymmetries and roll rate. All three theories were validated in this phase and found to be quite accurate considering the large dispersions encountered. Aerodynamic asymmetries causing a trim angle of  $1^\circ$  had little effect on the dispersion of flechettes. Slower rolling bodies were shown to have, in general, increasingly larger dispersion values as roll rate decreased. It can be concluded that for free flight vehicles that are prone to aerodynamic asymmetries and fin damage, a high roll rate is essential to lower dispersion and increase accuracy. The fourth phase validates the theory with respect to gravity. The theory indicates a lateral contribution to dispersion from gravity in addition to the obvious vertical contribution.

For the flechette, the lateral contribution was found to be minimal and was neglected in this analysis.

Free flight data was obtained from Frankford Arsenal to correlate with the theory. Angular and translational data was fitted and put into initial condition form. The initial condition data was applied to the theory and compared to target data for the rounds tested. The theory was found to agree favorably in magnitude with the test firings. As a result, the method used to analyze the data can be considered a valid method. Photographs of the test firings were taken to include the flight transition sequence in the blast region. The pictures further verify the analysis method of the initial conditions by allowing agreement between the chosen initial conditions and the position downrange where they were selected.

The evaluation of the free flight dispersion against the theory also disproves the First Maximum Yaw hypothesis. A plot of jump angle vs. first maximum yaw of actual test data produced a shotgun blast pattern with no relationship evident between dispersion and first maximum yaw. In addition, a plot of jump angle versus angular rate for various initial angles of attack indicates an infinite amount of combinations of initial conditions to yield a given jump angle. Thus, zero dispersion has an infinite set of possible initial conditions. It was found for zero dispersion that a unique physical condition holds: to obtain zero dispersion, initial transverse momentum = initial angular momentum. These impulses are imparted to the flechette in the blast region where the body and especially the fins are subject to disturbances. Momentum imbalance is the reason

dispersion occurs. The initial conditions only determine the magnitude of imbalance or dispersion. This dispersion is round to round dispersion. Inconsistency in the imbalance results in a dispersion pattern. The initial conditions were found not to occur until after the sabot separation and the blast has had its greatest effect. The factors causing the existence of initial conditions were found to be not only the blast and sabot separation sequence, but also fin and body asymmetries and bore mal-alignment. In order to decrease dispersion, these physical factors causing initial conditions must be kept at a minimum. The most important aspect would be to protect the fins from asymmetries, damage, and interference from the separating sabot. Initial conditions can never realistically be eliminated but if kept minimal, dispersion is reduced.

## APPENDIX

### A-1

Appendix A1 contains mass parameters and stability coefficients for the Ground Point Flechette. Table A1-1 lists values for mass, diameter, axial and transverse moments of inertia. Figures A1-1 through A1-8 present stability coefficients used in this analysis versus Mach number.  $C_{z\alpha}$ ,  $C_{M\alpha}$ ,  $C_{Mq} + C_{M\dot{\alpha}}$  were provided by Frankford Arsenal.  $C_{z_{p\beta}}$ ,  $C_{M_{p\beta}}$ ,  $C_{YE}$ ,  $C_{ZE}$ ,  $C_{ME}$ ,  $C_{NE}$  were nominal values of the coefficients following the same trends of  $C_{z\alpha}$  and  $C_{M\alpha}$  for Mach number.  $C_{M\alpha}$  and  $C_{Mq}$   $C_{M\dot{\alpha}}$  were verified in the University of Notre Dame supersonic wind tunnel. 16

TABLE A1-1  
FLECHETTE PARAMETERS

mass = 0.000046 slugs

diameter = 0.006 ft.

$I_x$  = 0.000000000217 slugs-ft<sup>2</sup>

$I_y$  = 0.000000036421 slugs-ft<sup>2</sup>

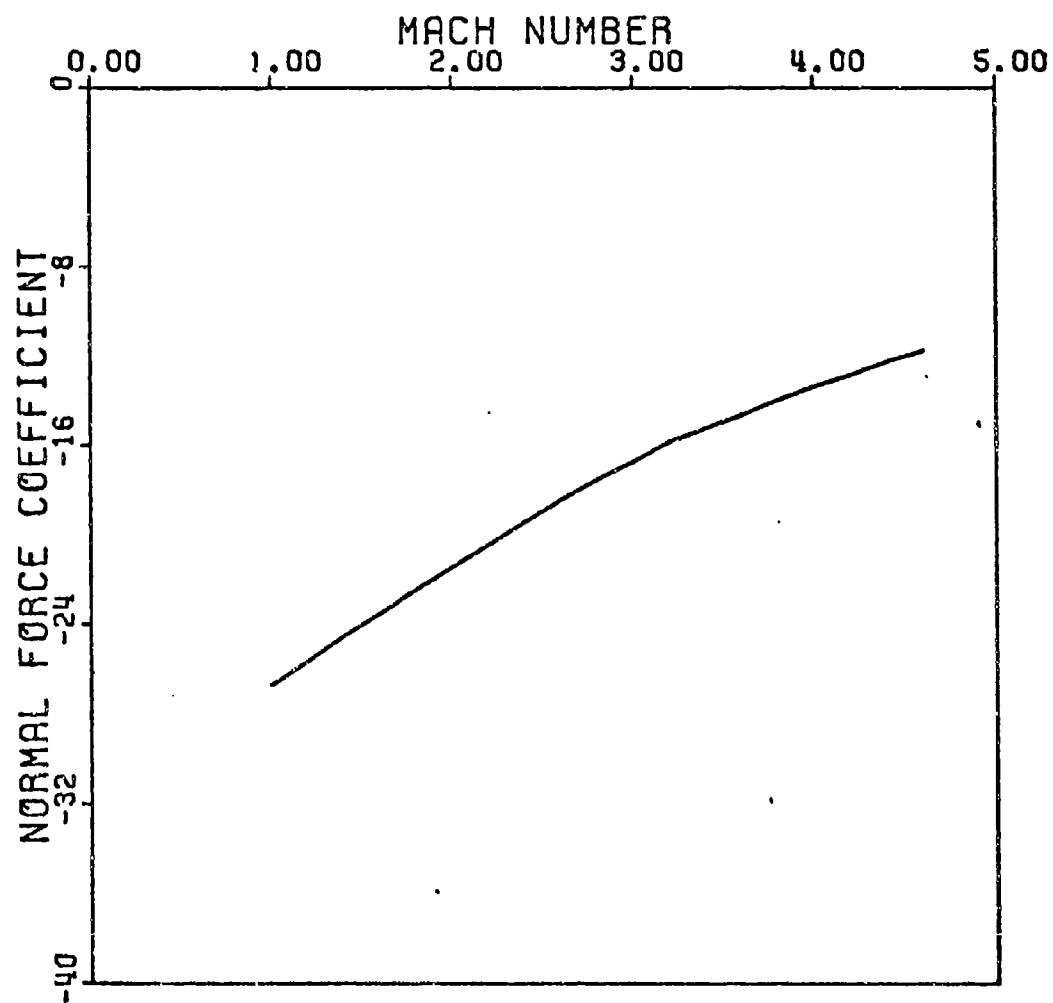


Figure A1-1.  $CZ_\alpha$  vs Mach Number Producibility Ground Point



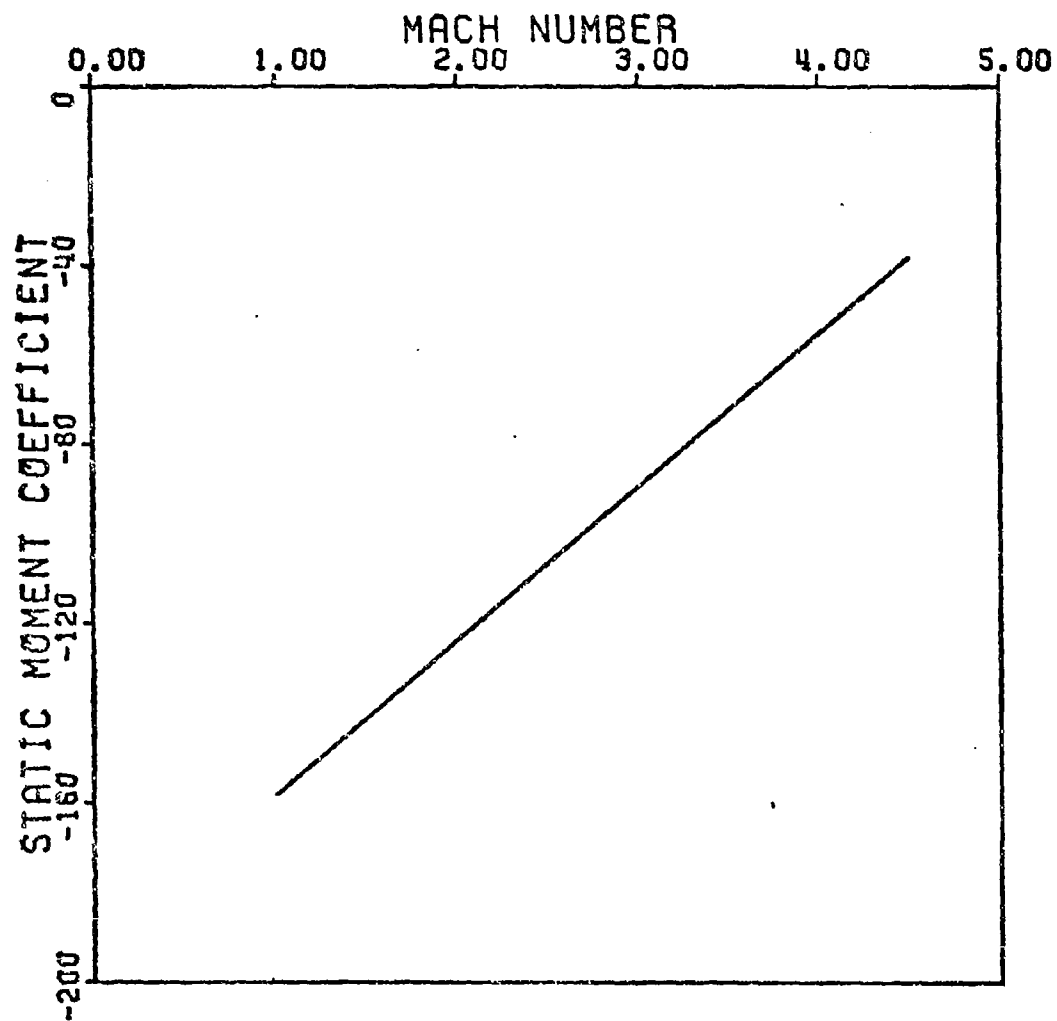


Figure A1-2.  $CM_{\alpha}$  vs Mach Number Producibility Ground Point

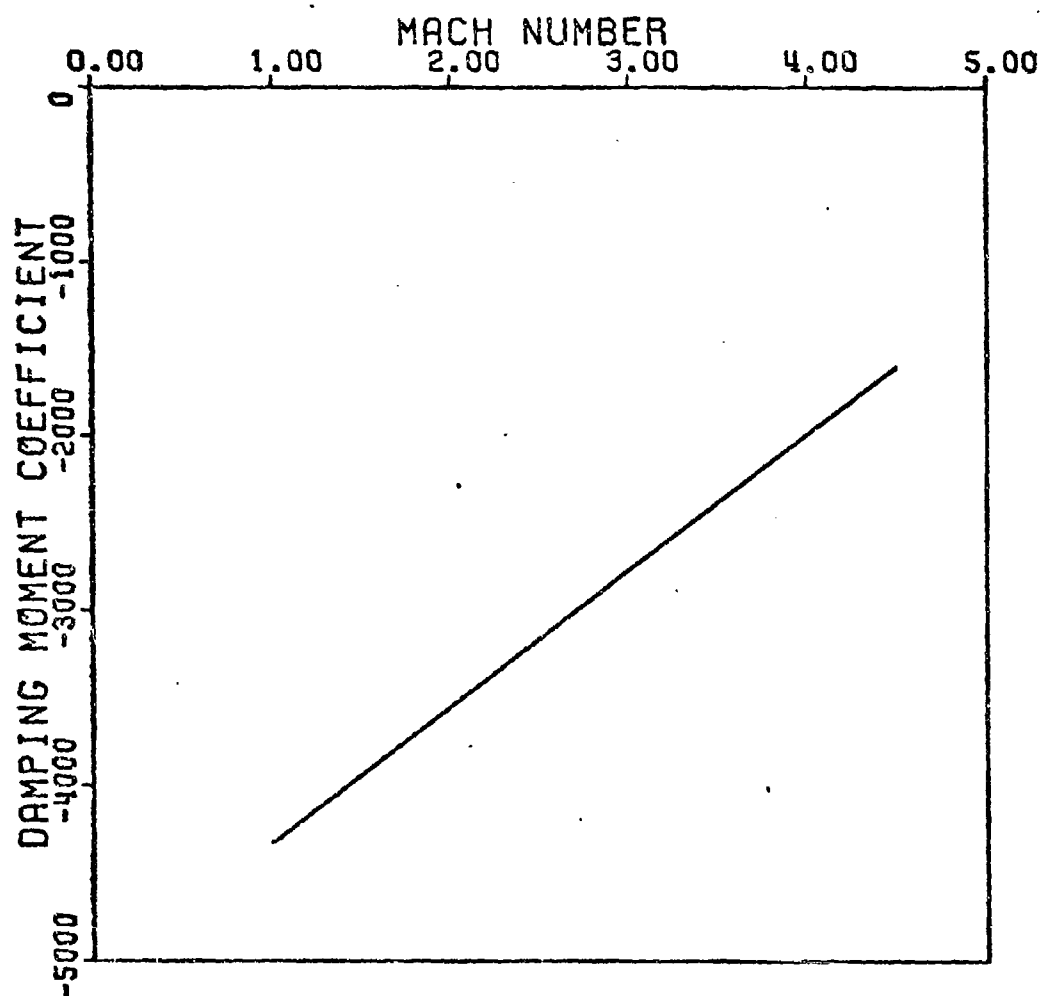


Figure A1-3.  $CM_q + CM_{\dot{\alpha}}$  vs Mach Number Producibility Ground Point

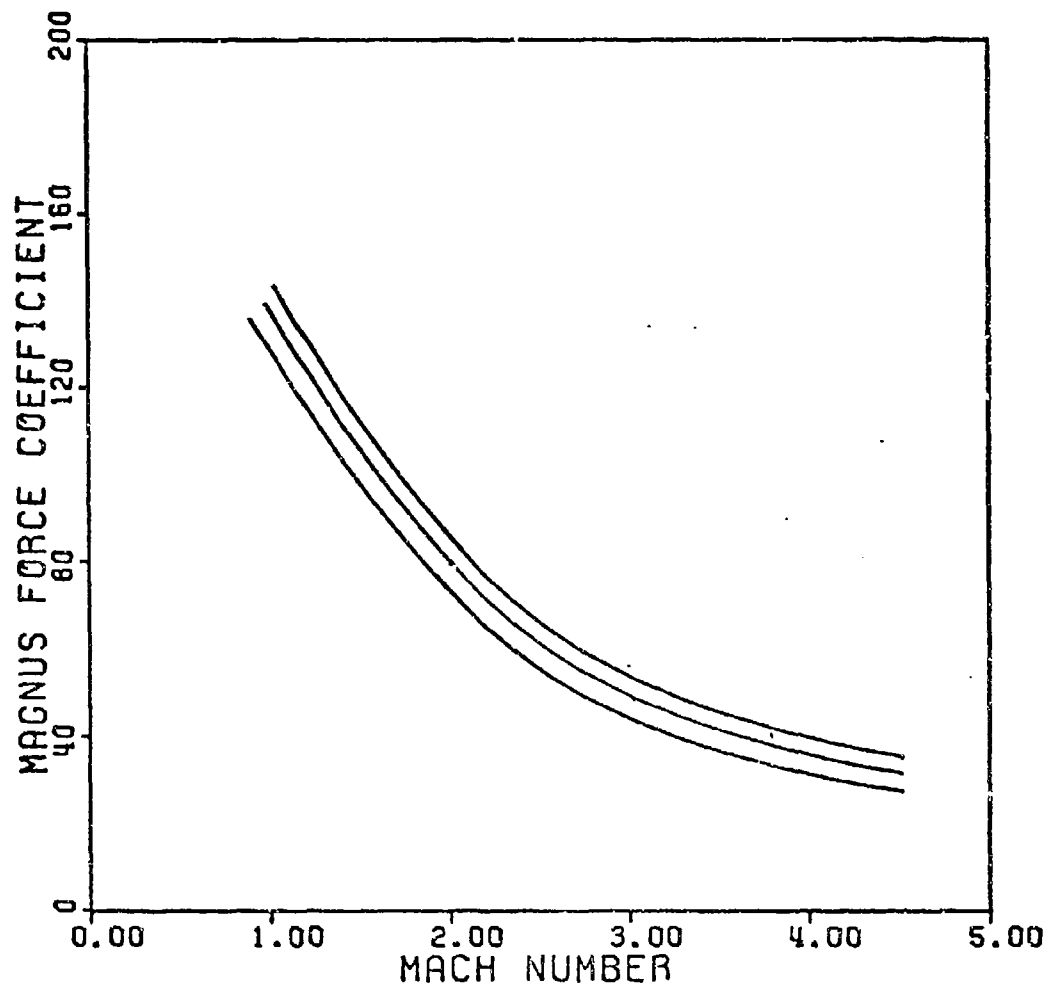


Figure A1-4. CZpb vs Mach Number Producibility Ground Point

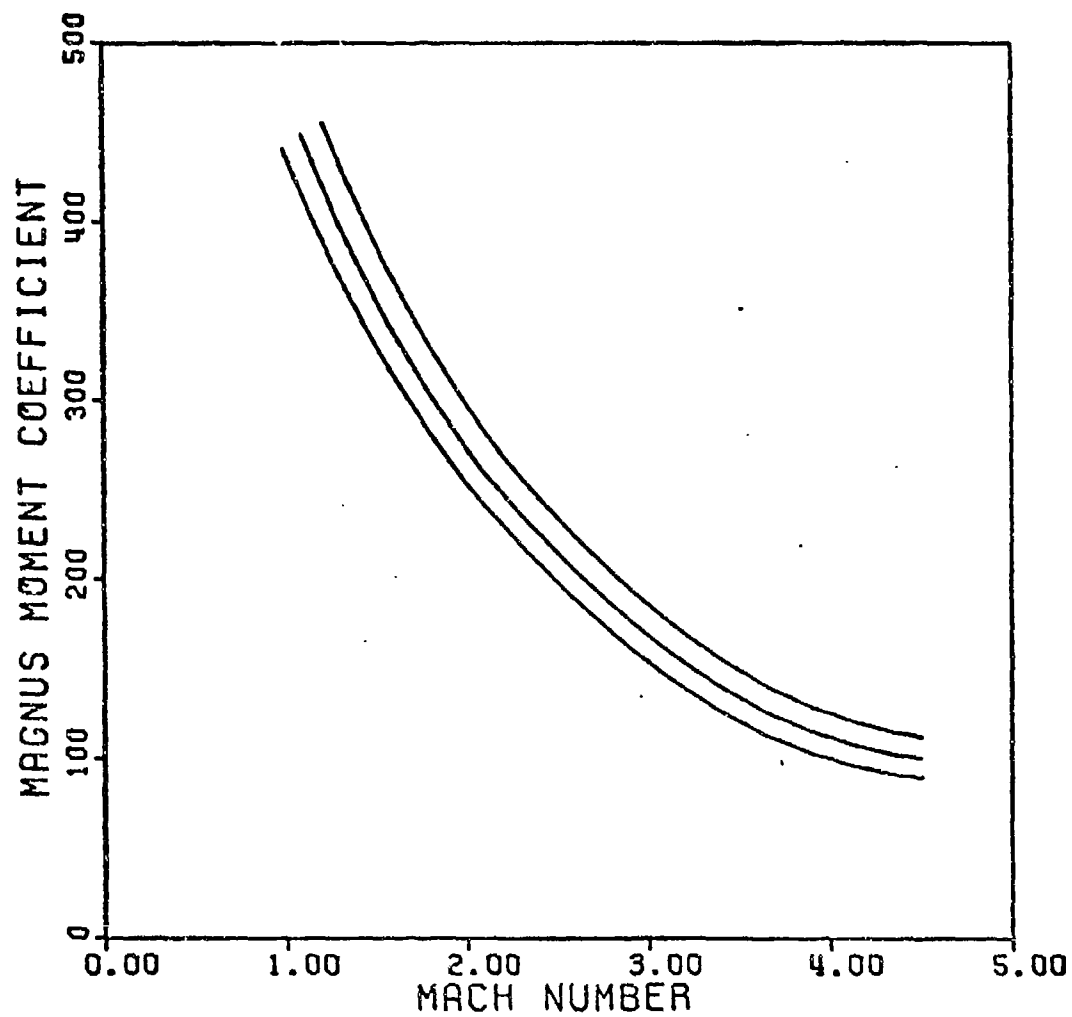


Figure A1-5. CMpb vs Mach Number Producibility Ground Point

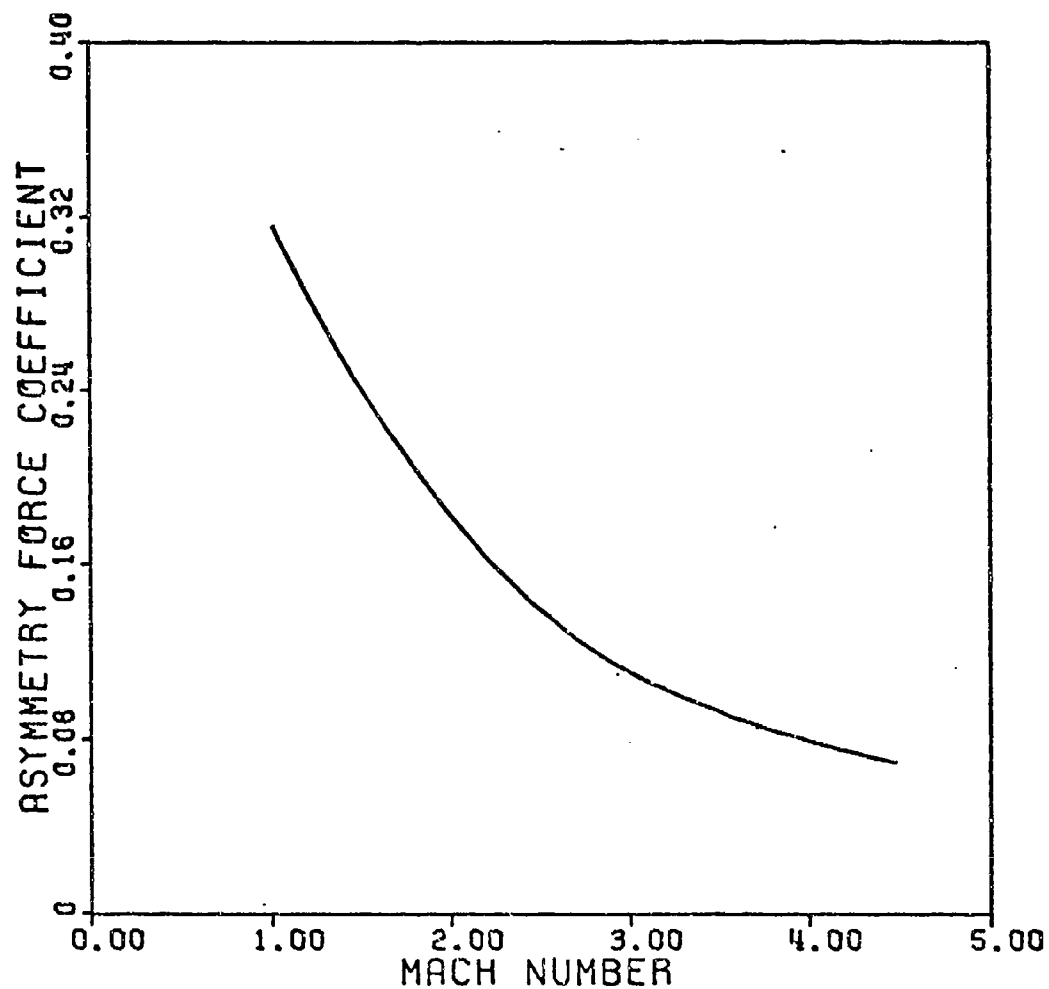


Figure A1-6. CYE, CZE vs Mach Number Producibility Ground Point

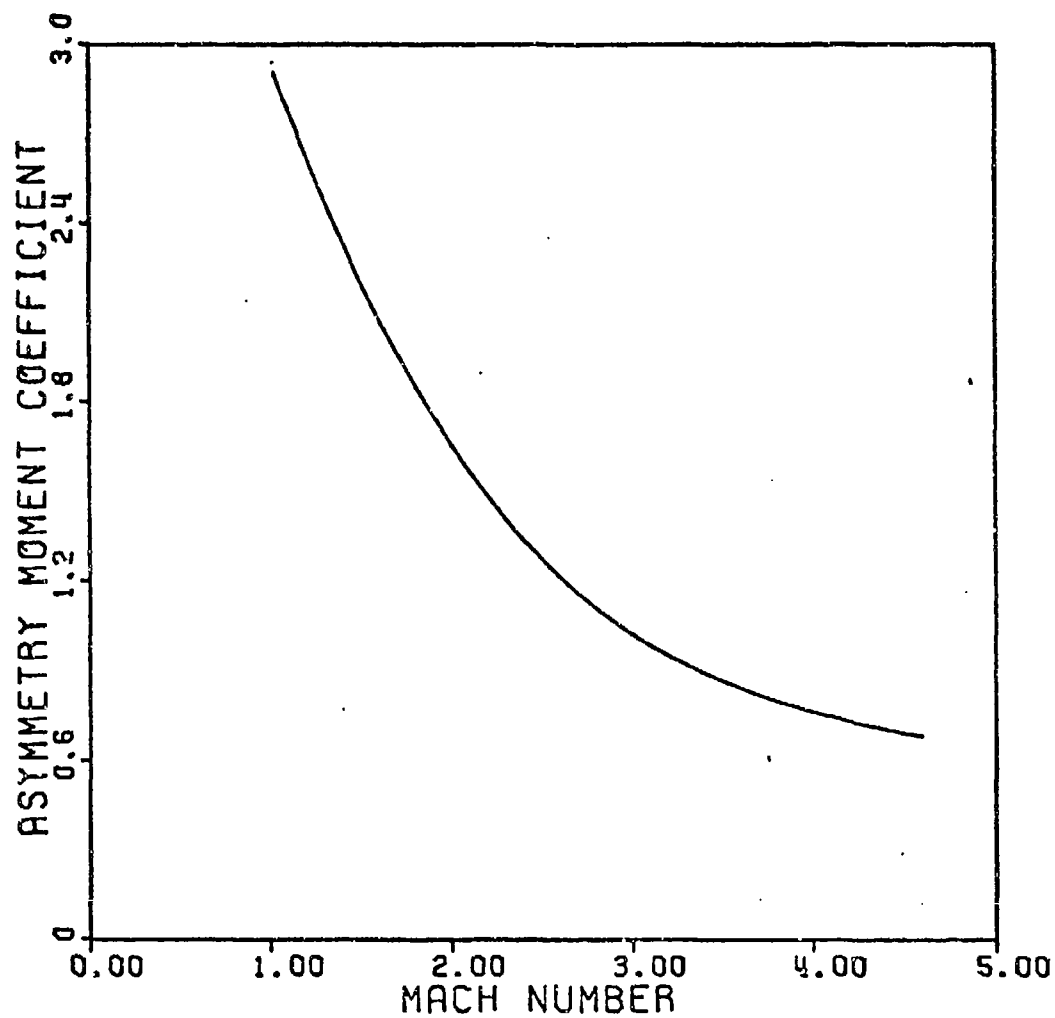


Figure A1-7. CME vs Mach Number Producibility Ground Point

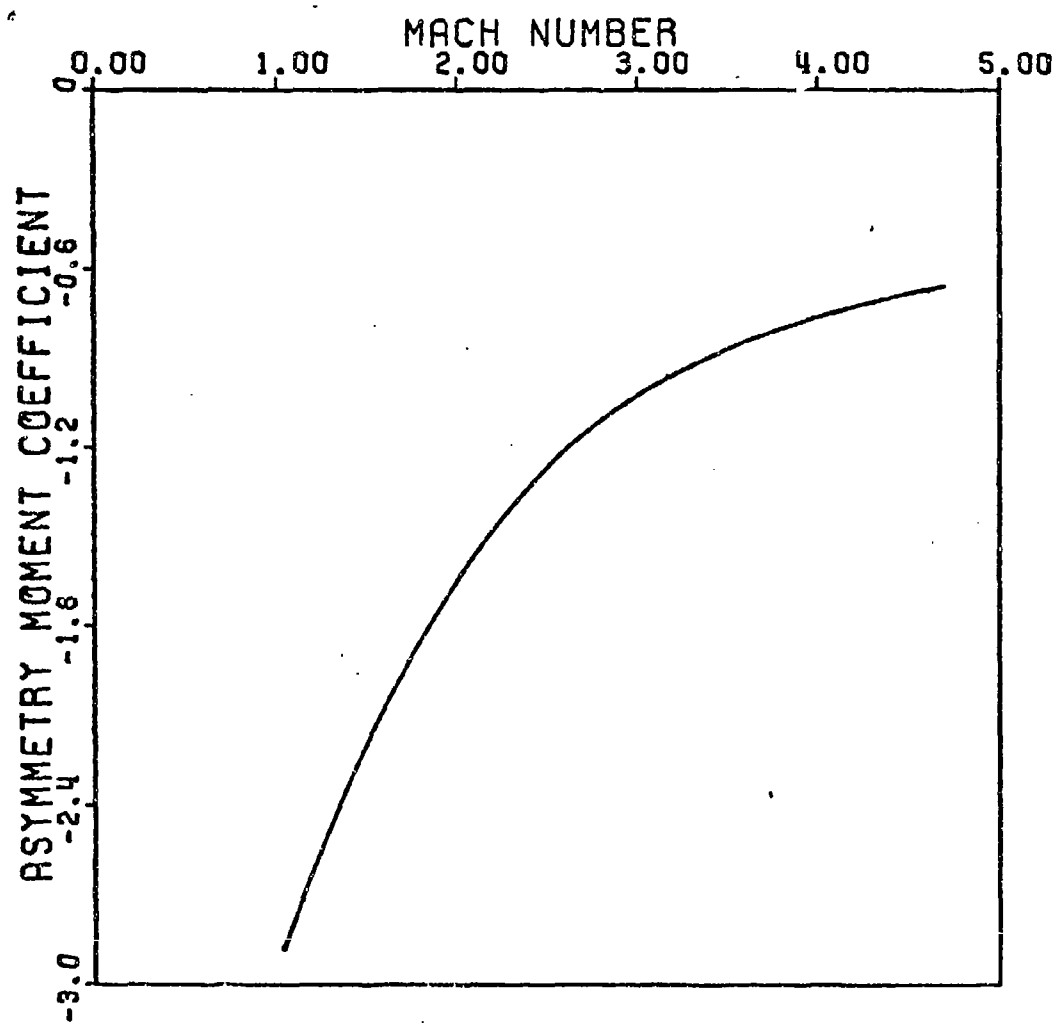


Figure A1-8. CNE vs Mach Number Producibility Ground Point

## APPENDIX

### A-2

Appendix A-2 contains the complete print-out of the results from a typical 6-D computer program run. The results give the time from launch, position coordinates  $x, y, z$ , velocity, roll rate, the magnitude of the complex angle of attack, Mach number, roll orientation angle, angles of pitch and yaw, nutation and precession damping factors, nutation and precession mode frequency rates, the gyroscopic stability factor, dynamic weight factor, and trim angle.

The program is divided into various subroutines to eliminate any superfluous calculations. These subroutines read in aerodynamic coefficients in tabular form as functions of Mach number and angle of attack, initialize the data, and integrate the six-degrees-of-freedom differential equations of motion using a four-step Runge-Kutta scheme to obtain the vehicle trajectory.



FLECHETTE GROUND POINT

PAGE 1

SEC	X	Y	Z	V	P	ALPHA	MACH	PHI	ALPHA	PETA	1-N	1-P	W-V	W-U	5	3AD	P-1
	FT	FT	FT	FT/SEC	RAD/SEC	DEG	DEG	DEG	DEG	DEG	DEG	DEG	DEG	DEG	DEG	DEG	DEG
0.0001	0.50	0.000	0.000	5000.0	500.00	0.0	4.68	0.0	0.0	0.0	55	55	2317	2317	0	0	0
0.0002	1.00	0.000	0.000	5000.0	500.00	0.0	4.68	0.0	1.44	1.44	55	55	2317	2317	0	0	0
0.0003	1.50	0.000	0.000	4999.9	499.99	0.01	4.68	50.64	2.84	2.84	55	55	2317	2317	0	0	0
0.0004	2.00	0.000	0.000	4999.8	499.98	0.02	4.68	51.40	4.14	4.14	55	55	2317	2317	0	0	0
0.0005	2.50	0.000	0.000	4999.7	499.97	0.03	4.68	52.12	5.24	5.24	55	55	2317	2317	0	0	0
0.0006	3.00	0.000	0.000	4999.6	499.96	0.04	4.68	52.76	6.17	6.17	55	55	2317	2317	0	0	0
0.0007	3.50	0.000	0.000	4999.5	499.95	0.05	4.68	53.36	6.97	6.97	55	55	2317	2317	0	0	0
0.0008	4.00	0.000	0.000	4999.4	499.94	0.06	4.68	53.92	7.67	7.67	55	55	2317	2317	0	0	0
0.0009	4.50	0.000	0.000	4999.3	499.93	0.07	4.68	54.44	8.27	8.27	55	55	2317	2317	0	0	0
0.0010	5.00	0.000	0.000	4999.2	499.92	0.08	4.68	54.92	8.79	8.79	55	55	2317	2317	0	0	0
0.0011	5.50	0.000	0.000	4999.1	499.91	0.09	4.68	55.36	9.24	9.24	55	55	2317	2317	0	0	0
0.0012	6.00	0.000	0.000	4999.0	499.90	0.10	4.68	55.76	9.61	9.61	55	55	2317	2317	0	0	0
0.0013	6.50	0.000	0.000	4998.9	499.89	0.11	4.68	56.12	9.91	9.91	55	55	2317	2317	0	0	0
0.0014	7.00	0.000	0.000	4998.8	499.88	0.12	4.68	56.44	10.15	10.15	55	55	2317	2317	0	0	0
0.0015	7.50	0.000	0.000	4998.7	499.87	0.13	4.68	56.72	10.34	10.34	55	55	2317	2317	0	0	0
0.0016	8.00	0.000	0.000	4998.6	499.86	0.14	4.68	56.96	10.49	10.49	55	55	2317	2317	0	0	0
0.0017	8.50	0.000	0.000	4998.5	499.85	0.15	4.68	57.16	10.60	10.60	55	55	2317	2317	0	0	0
0.0018	9.00	0.000	0.000	4998.4	499.84	0.16	4.68	57.32	10.68	10.68	55	55	2317	2317	0	0	0
0.0019	9.50	0.000	0.000	4998.3	499.83	0.17	4.68	57.46	10.73	10.73	55	55	2317	2317	0	0	0
0.0020	10.00	0.000	0.000	4998.2	499.82	0.18	4.68	57.58	10.77	10.77	55	55	2317	2317	0	0	0
0.0021	10.50	0.000	0.000	4998.1	499.81	0.19	4.68	57.68	10.80	10.80	55	55	2317	2317	0	0	0
0.0022	11.00	0.000	0.000	4998.0	499.80	0.20	4.68	57.76	10.82	10.82	55	55	2317	2317	0	0	0
0.0023	11.50	0.000	0.000	4997.9	499.79	0.21	4.68	57.83	10.84	10.84	55	55	2317	2317	0	0	0
0.0024	12.00	0.000	0.000	4997.8	499.78	0.22	4.68	57.89	10.86	10.86	55	55	2317	2317	0	0	0
0.0025	12.50	0.000	0.000	4997.7	499.77	0.23	4.68	57.94	10.88	10.88	55	55	2317	2317	0	0	0
0.0026	13.00	0.000	0.000	4997.6	499.76	0.24	4.68	57.98	10.90	10.90	55	55	2317	2317	0	0	0
0.0027	13.50	0.000	0.000	4997.5	499.75	0.25	4.68	58.01	10.92	10.92	55	55	2317	2317	0	0	0
0.0028	14.00	0.000	0.000	4997.4	499.74	0.26	4.68	58.04	10.94	10.94	55	55	2317	2317	0	0	0
0.0029	14.50	0.000	0.000	4997.3	499.73	0.27	4.68	58.06	10.96	10.96	55	55	2317	2317	0	0	0
0.0030	15.00	0.000	0.000	4997.2	499.72	0.28	4.68	58.08	10.98	10.98	55	55	2317	2317	0	0	0
0.0031	15.50	0.000	0.000	4997.1	499.71	0.29	4.68	58.10	11.00	11.00	55	55	2317	2317	0	0	0
0.0032	16.00	0.000	0.000	4997.0	499.70	0.30	4.68	58.12	11.02	11.02	55	55	2317	2317	0	0	0
0.0033	16.50	0.000	0.000	4996.9	499.69	0.31	4.68	58.14	11.04	11.04	55	55	2317	2317	0	0	0
0.0034	17.00	0.000	0.000	4996.8	499.68	0.32	4.68	58.16	11.06	11.06	55	55	2317	2317	0	0	0
0.0035	17.50	0.000	0.000	4996.7	499.67	0.33	4.68	58.18	11.08	11.08	55	55	2317	2317	0	0	0
0.0036	18.00	0.000	0.000	4996.6	499.66	0.34	4.68	58.20	11.10	11.10	55	55	2317	2317	0	0	0
0.0037	18.50	0.000	0.000	4996.5	499.65	0.35	4.68	58.22	11.12	11.12	55	55	2317	2317	0	0	0
0.0038	19.00	0.000	0.000	4996.4	499.64	0.36	4.68	58.24	11.14	11.14	55	55	2317	2317	0	0	0
0.0039	19.50	0.000	0.000	4996.3	499.63	0.37	4.68	58.26	11.16	11.16	55	55	2317	2317	0	0	0
0.0040	20.00	0.000	0.000	4996.2	499.62	0.38	4.68	58.28	11.18	11.18	55	55	2317	2317	0	0	0
0.0041	20.50	0.000	0.000	4996.1	499.61	0.39	4.68	58.30	11.20	11.20	55	55	2317	2317	0	0	0
0.0042	21.00	0.000	0.000	4996.0	499.60	0.40	4.68	58.32	11.22	11.22	55	55	2317	2317	0	0	0
0.0043	21.50	0.000	0.000	4995.9	499.59	0.41	4.68	58.34	11.24	11.24	55	55	2317	2317	0	0	0
0.0044	22.00	0.000	0.000	4995.8	499.58	0.42	4.68	58.36	11.26	11.26	55	55	2317	2317	0	0	0
0.0045	22.50	0.000	0.000	4995.7	499.57	0.43	4.68	58.38	11.28	11.28	55	55	2317	2317	0	0	0
0.0046	23.00	0.000	0.000	4995.6	499.56	0.44	4.68	58.40	11.30	11.30	55	55	2317	2317	0	0	0
0.0047	23.50	0.000	0.000	4995.5	499.55	0.45	4.68	58.42	11.32	11.32	55	55	2317	2317	0	0	0
0.0048	24.00	0.000	0.000	4995.4	499.54	0.46	4.68	58.44	11.34	11.34	55	55	2317	2317	0	0	0
0.0049	24.50	0.000	0.000	4995.3	499.53	0.47	4.68	58.46	11.36	11.36	55	55	2317	2317	0	0	0
0.0050	25.00	0.000	0.000	4995.2	499.52	0.48	4.68	58.48	11.38	11.38	55	55	2317	2317	0	0	0

## FLECHETTE GROUND POINT

PAGE 2

T SEC	X FT	Y FT	Z FT	V FT/SEC	P RAD/SEC	ALPHA MACH	PHI DEG	ALPHA PER	PETA DEG	L-N 1/SEC	L-P 1/SEC	M-N 1/SEC	S-P 1/SEC	S TAU	P-T DEG
0.0050	24.97	0.089	-0.053	4986.5	500.00	7.32	4.47	16.33	-4.42	-0.34	-0.34	-0.34	-0.34	0	1
0.0051	25.47	0.091	-0.054	4986.2	500.00	6.52	4.47	16.36	-3.62	-0.21	-0.21	-0.21	-0.21	0	1
0.0052	25.97	0.093	-0.053	4986.0	500.00	5.45	4.47	22.73	-3.24	-0.24	-0.24	-0.24	-0.24	0	1
0.0053	26.47	0.094	-0.053	4985.8	500.00	4.17	4.47	22.80	-2.41	-0.11	-0.11	-0.11	-0.11	0	1
0.0054	26.96	0.095	-0.053	4985.6	500.00	2.76	4.47	22.82	-1.48	-0.33	-0.33	-0.33	-0.33	0	1
0.0055	27.46	0.097	-0.052	4985.4	500.00	1.31	4.47	22.82	-0.61	-0.71	-0.71	-0.71	-0.71	0	1
0.0056	27.95	0.097	-0.052	4985.2	500.00	0.67	4.47	19.95	-0.49	-0.19	-0.19	-0.19	-0.19	0	1
0.0057	28.46	0.100	-0.051	4985.0	500.00	1.66	4.47	19.90	1.35	0.33	0.33	0.33	0.33	0	1
0.0058	28.96	0.102	-0.051	4984.7	500.00	2.61	4.47	20.70	2.13	1.23	1.23	1.23	1.23	0	1
0.0059	29.46	0.104	-0.050	4984.5	500.00	3.76	4.47	21.20	2.71	2.67	2.67	2.67	2.67	0	1
0.0060	30.46	0.105	-0.050	4984.3	500.00	4.42	4.47	21.64	3.11	3.09	3.09	3.09	3.09	0	1
0.0061	30.95	0.107	-0.050	4984.1	500.00	4.76	4.47	22.0.12	3.37	3.36	3.36	3.36	3.36	0	1
0.0062	31.45	0.109	-0.050	4983.9	500.00	4.66	4.47	22.3.47	3.31	3.45	3.45	3.45	3.45	0	1
0.0063	31.95	0.111	-0.050	4983.7	500.00	4.49	4.47	22.7.23	3.23	3.26	3.26	3.26	3.26	0	1
0.0064	32.45	0.114	-0.050	4983.5	500.00	3.67	4.47	23.0.42	2.61	2.25	2.25	2.25	2.25	0	1
0.0065	32.95	0.116	-0.051	4983.3	500.00	2.62	4.47	23.3.35	1.55	1.55	1.55	1.55	1.55	0	1
0.0066	33.45	0.119	-0.051	4983.1	500.00	1.67	4.47	24.1.67	1.14	1.14	1.14	1.14	1.14	0	1
0.0067	33.95	0.121	-0.052	4982.9	500.00	0.64	4.47	24.2.76	0.21	0.51	0.51	0.51	0.51	0	1
0.0068	34.45	0.123	-0.052	4982.7	500.00	0.65	4.47	36.24	-0.78	-0.34	-0.34	-0.34	-0.34	0	1
0.0069	34.95	0.126	-0.053	4982.5	500.00	2.20	4.47	53.61	-1.79	-1.28	-1.28	-1.28	-1.28	0	1
0.0070	35.44	0.129	-0.053	4982.3	500.00	3.51	4.47	56.26	-2.74	-2.10	-2.10	-2.10	-2.10	0	1
0.0071	35.94	0.131	-0.054	4982.1	500.00	4.70	4.47	63.15	-3.22	-2.07	-2.07	-2.07	-2.07	0	1
0.0072	36.44	0.133	-0.054	4981.9	500.00	5.66	4.47	65.42	-3.66	-2.46	-2.46	-2.46	-2.46	0	1
0.0073	36.94	0.135	-0.054	4981.7	500.00	6.42	4.47	59.37	-3.72	-1.14	-1.14	-1.14	-1.14	0	1
0.0074	37.44	0.137	-0.053	4981.5	500.00	6.90	4.47	71.97	-5.12	-0.52	-0.52	-0.52	-0.52	0	1
0.0075	37.93	0.139	-0.053	4981.3	500.00	7.36	4.47	74.34	-5.66	-0.48	-0.48	-0.48	-0.48	0	1
0.0076	38.43	0.141	-0.054	4981.1	500.00	6.50	4.47	76.45	-5.39	-0.30	-0.30	-0.30	-0.30	0	1
0.0077	38.93	0.142	-0.054	4980.9	500.00	5.71	4.47	79.13	-6.56	-0.32	-0.32	-0.32	-0.32	0	1
0.0078	39.43	0.143	-0.053	4980.7	500.00	4.75	4.46	79.39	-6.00	-0.54	-0.54	-0.54	-0.54	0	1
0.0079	39.93	0.144	-0.053	4980.5	500.00	3.63	4.46	75.72	-3.23	-1.67	-1.67	-1.67	-1.67	0	1
0.0080	40.43	0.145	-0.052	4980.3	500.00	2.65	4.46	65.41	-2.12	-0.53	-0.53	-0.53	-0.53	0	1
0.0081	40.93	0.146	-0.051	4980.1	500.00	1.69	4.46	72.78	-1.45	-0.32	-0.32	-0.32	-0.32	0	1
0.0082	41.42	0.148	-0.049	4979.9	500.00	1.42	4.46	70.59	-0.53	1.31	1.31	1.31	1.31	0	1
0.0083	41.92	0.146	-0.048	4979.7	500.00	2.26	4.46	32.12	0.51	2.24	2.24	2.24	2.24	0	1
0.0084	42.42	0.149	-0.046	4979.5	500.00	3.24	4.46	31.54	1.05	3.35	3.35	3.35	3.35	0	1
0.0085	42.92	0.150	-0.047	4979.3	500.00	4.18	4.46	32.37	1.63	2.73	2.73	2.73	2.73	0	1
0.0086	43.42	0.151	-0.047	4979.1	500.00	4.74	4.46	31.24	2.14	2.14	2.14	2.14	2.14	0	1
0.0087	43.92	0.152	-0.046	4978.9	500.00	5.12	4.46	31.00	2.31	7.52	7.52	7.52	7.52	0	1
0.0088	44.42	0.153	-0.045	4978.7	500.00	5.22	4.46	31.63	2.44	7.50	7.50	7.50	7.50	0	1
0.0089	44.91	0.154	-0.045	4978.5	500.00	5.08	4.46	32.1.25	2.39	0.21	0.21	0.21	0.21	0	1
0.0090	45.41	0.154	-0.045	4978.3	500.00	4.62	4.46	32.6.63	2.04	1.14	1.14	1.14	1.14	0	1
0.0091	45.91	0.155	-0.045	4978.1	500.00	3.92	4.46	31.9.33	1.57	3.64	3.64	3.64	3.64	0	1
0.0092	46.41	0.157	-0.047	4977.9	500.00	3.14	4.46	33.6.33	0.65	2.00	2.00	2.00	2.00	0	1
0.0093	46.91	0.158	-0.047	4977.7	500.00	2.24	4.46	35.3.44	0.21	2.25	2.25	2.25	2.25	0	1
0.0094	47.40	0.160	-0.047	4977.5	500.00	1.54	4.46	22.59	-0.53	1.44	1.44	1.44	1.44	0	1
0.0095	47.90	0.161	-0.048	4977.3	500.00	1.65	4.46	55.93	-1.31	0.42	0.42	0.42	0.42	0	1
0.0096	48.40	0.163	-0.049	4977.1	500.00	2.37	4.46	102.69	-2.07	-1.17	-1.17	-1.17	-1.17	0	1
0.0097	48.90	0.164	-0.049	4976.9	500.00	2.88	4.46	113.65	-2.71	-0.65	-0.65	-0.65	-0.65	0	1
0.0098	49.40	0.166	-0.050	4976.7	500.00	3.62	4.46	127.75	-3.31	-1.67	-1.67	-1.67	-1.67	0	1
0.0099	49.90	0.167	-0.051	4976.5	500.00	4.62	4.46	127.75	-3.31	-1.67	-1.67	-1.67	-1.67	0	1

FLECHETTE GROUND POINT

PAGE 3

T	X	Y	Z	V	PAW/SEC	ALPHA	MACH	PER	CEG	DATA	1/SEC	1/SEC	W-M	W-P	RAI/SEC	JAU	K-I
SFC	FT	FT	FT	FT/SEC		DEG		SEC		SEC							
0.0100	40.50	0.168	-0.051	4942.8	500.00	4.10	1.16	133.83	3.73	-1.32	-55.	-57.	2325.	-2322.	-0.	0.	1.
0.0101	50.39	0.169	-0.032	4942.7	500.00	4.52	1.44	135.30	3.93	-2.19	-53.	-57.	2325.	-2322.	-0.	0.	1.
0.0102	50.39	0.170	-0.132	4942.5	500.00	4.54	1.44	141.63	4.05	-2.27	-55.	-57.	2325.	-2322.	-0.	0.	1.
0.0103	51.39	0.171	-0.082	4942.1	500.00	4.59	1.46	144.12	3.63	-0.17	-55.	-57.	2325.	-2323.	-0.	0.	1.
0.0104	51.39	0.172	-0.052	4942.3	500.00	4.09	1.45	145.43	3.62	-1.33	-55.	-57.	2325.	-2323.	-0.	0.	1.
0.0105	51.39	0.172	-0.052	4942.2	500.00	3.45	1.46	145.20	3.15	-1.32	-55.	-57.	2325.	-2323.	-0.	0.	1.
0.0106	52.39	0.173	-0.052	4942.1	500.00	2.46	1.44	141.72	2.53	-0.31	-55.	-57.	2325.	-2323.	-0.	0.	1.
0.0107	52.39	0.173	-0.052	4942.1	500.00	1.50	1.46	131.06	1.73	-0.10	-55.	-57.	2325.	-2323.	-0.	0.	1.
0.0108	53.38	0.173	-0.052	4942.1	500.00	1.19	1.46	131.06	0.93	0.53	-55.	-57.	2325.	-2323.	-0.	0.	1.
0.0109	54.38	0.174	-0.052	4942.0	500.00	1.76	1.46	146.62	1.13	1.19	-55.	-57.	2325.	-2323.	-0.	0.	1.
0.0110	54.38	0.174	-0.052	4942.0	500.00	2.39	1.46	146.62	0.71	2.25	-55.	-57.	2325.	-2323.	-0.	0.	1.
0.0111	55.38	0.174	-0.052	4942.0	500.00	3.35	1.46	146.62	1.51	3.02	-55.	-57.	2325.	-2323.	-0.	0.	1.
0.0112	55.38	0.175	-0.052	4941.9	500.00	4.29	1.46	146.62	2.22	3.45	-55.	-57.	2325.	-2323.	-0.	0.	1.
0.0113	56.37	0.175	-0.052	4941.7	500.00	5.06	1.46	146.62	19.57	2.32	-55.	-57.	2325.	-2323.	-0.	0.	1.
0.0114	56.37	0.175	-0.053	4941.6	500.00	5.53	1.46	21.09	3.27	4.53	-55.	-57.	2325.	-2323.	-0.	0.	1.
0.0115	57.37	0.175	-0.053	4941.4	500.00	5.50	1.46	22.71	3.55	4.71	-55.	-57.	2325.	-2323.	-0.	0.	1.
0.0116	57.37	0.177	-0.052	4941.1	500.00	5.57	1.46	21.22	3.55	4.71	-55.	-57.	2325.	-2323.	-0.	0.	1.
0.0117	58.36	0.177	-0.055	4940.9	500.00	5.78	1.46	29.57	3.50	4.53	-55.	-57.	2325.	-2323.	-0.	0.	1.
0.0118	58.36	0.178	-0.056	4940.7	500.00	5.36	1.46	24.50	3.37	4.17	-55.	-57.	2325.	-2323.	-0.	0.	1.
0.0119	59.36	0.180	-0.057	4940.4	500.00	4.73	1.46	31.38	3.57	3.57	-55.	-57.	2325.	-2323.	-0.	0.	1.
0.0120	59.36	0.181	-0.054	4940.1	500.00	3.93	1.46	34.70	2.43	3.16	-55.	-57.	2325.	-2323.	-0.	0.	1.
0.0121	60.36	0.182	-0.053	4940.4	500.00	3.10	1.46	37.59	1.91	2.32	-55.	-57.	2325.	-2323.	-0.	0.	1.
0.0122	60.36	0.183	-0.051	4940.4	500.00	1.89	1.46	40.84	1.23	1.54	-55.	-57.	2325.	-2323.	-0.	0.	1.
0.0123	61.35	0.185	-0.052	4940.3	500.00	0.56	1.46	44.54	0.53	0.74	-55.	-57.	2325.	-2323.	-0.	0.	1.
0.0124	61.35	0.184	-0.054	4940.3	500.00	0.06	1.46	178.32	0.46	-0.19	-55.	-57.	2325.	-2323.	-0.	0.	1.
0.0125	62.35	0.184	-0.055	4940.3	500.00	0.55	1.46	225.53	0.55	-0.70	-55.	-57.	2325.	-2323.	-0.	0.	1.
0.0126	62.35	0.189	-0.057	4940.3	500.00	1.73	1.46	229.21	1.14	-1.29	-55.	-57.	2325.	-2323.	-0.	0.	1.
0.0127	63.35	0.190	-0.054	4940.3	500.00	2.33	1.46	213.39	1.52	-2.70	-55.	-57.	2325.	-2323.	-0.	0.	1.
0.0128	63.35	0.192	-0.055	4940.2	500.00	2.72	1.46	216.51	1.75	-2.09	-55.	-57.	2325.	-2323.	-0.	0.	1.
0.0129	64.34	0.193	-0.051	4940.2	500.00	2.55	1.46	213.64	1.13	-2.24	-55.	-57.	2325.	-2323.	-0.	0.	1.
0.0130	64.34	0.193	-0.052	4940.1	500.00	2.46	1.46	214.77	1.75	-2.24	-55.	-57.	2325.	-2323.	-0.	0.	1.
0.0131	65.34	0.195	-0.073	4940.0	500.00	2.57	1.46	214.77	1.51	-2.17	-55.	-57.	2325.	-2323.	-0.	0.	1.
0.0132	65.34	0.194	-0.071	4940.0	500.00	2.10	1.46	215.70	1.13	-1.76	-55.	-57.	2325.	-2323.	-0.	0.	1.
0.0133	66.33	0.197	-0.073	4940.0	500.00	1.47	1.46	215.47	0.53	-1.33	-55.	-57.	2325.	-2323.	-0.	0.	1.
0.0134	66.33	0.197	-0.073	4940.0	500.00	0.50	1.46	211.83	0.33	-0.40	-55.	-57.	2325.	-2323.	-0.	0.	1.
0.0135	67.33	0.198	-0.074	4940.0	500.00	0.56	1.46	211.83	0.53	-0.21	-55.	-57.	2325.	-2323.	-0.	0.	1.
0.0136	67.33	0.198	-0.077	4940.0	500.00	1.38	1.46	211.83	0.32	0.41	-55.	-57.	2325.	-2323.	-0.	0.	1.
0.0137	68.33	0.201	-0.077	4940.0	500.00	2.25	1.46	211.83	2.01	1.02	-55.	-57.	2325.	-2323.	-0.	0.	1.
0.0138	68.33	0.201	-0.074	4940.0	500.00	3.35	1.46	211.83	2.55	1.50	-55.	-57.	2325.	-2323.	-0.	0.	1.
0.0139	69.32	0.202	-0.074	4940.0	500.00	3.92	1.46	211.83	3.22	2.07	-55.	-57.	2325.	-2323.	-0.	0.	1.
0.0140	69.32	0.203	-0.070	4940.0	500.00	4.47	1.46	211.83	3.56	2.15	-55.	-57.	2325.	-2323.	-0.	0.	1.
0.0141	70.32	0.205	-0.051	4940.0	500.00	4.63	1.46	211.83	4.31	2.57	-55.	-57.	2325.	-2323.	-0.	0.	1.
0.0142	70.32	0.205	-0.052	4940.0	500.00	5.05	1.46	211.83	4.20	2.79	-55.	-57.	2325.	-2323.	-0.	0.	1.
0.0143	71.31	0.207	-0.053	4940.0	500.00	5.35	1.46	211.83	4.21	2.74	-55.	-57.	2325.	-2323.	-0.	0.	1.
0.0144	71.31	0.207	-0.055	4940.0	500.00	4.64	1.46	211.83	4.31	2.53	-55.	-57.	2325.	-2323.	-0.	0.	1.
0.0145	72.31	0.210	-0.055	4940.0	500.00	4.47	1.46	211.83	3.86	2.19	-55.	-57.	2325.	-2323.	-0.	0.	1.
0.0146	72.31	0.212	-0.055	4940.0	500.00	3.54	1.46	211.83	3.47	1.70	-55.	-57.	2325.	-2323.	-0.	0.	1.
0.0147	73.30	0.214	-0.055	4940.0	500.00	3.17	1.46	211.83	2.97	1.12	-55.	-57.	2325.	-2323.	-0.	0.	1.
0.0148	73.30	0.215	-0.051	4940.0	500.00	2.42	1.46	211.83	2.38	0.47	-55.	-57.	2325.	-2323.	-0.	0.	1.
0.0149	74.30	0.218	-0.052	4940.0	500.00	1.76	1.46	211.83	1.74	-0.23	-55.	-57.	2325.	-2323.	-0.	0.	1.

## FLECHETTE GROUND POINT

PAGE 4

T SEC	X FT	Y FT	Z FT	V FT/SEC	P FAR/SEC	ALPHA DEG	MACH	PHI DEG	ALPHA DEG	PET DEG	L-V 1/SEC	L-P 1/SEC	W-P RAC/SEC	S	TAU	K-T DEG
74.80	0.221	-0.034	4976.7	500.00	1.43	4.45	29.30	1.00	-0.04	-35	-57	2327	-2326	-0	0	1
75.30	0.223	-0.054	4978.7	500.00	1.67	4.46	35.37	0.45	-1.01	-33	-57	2327	-2326	-0	0	1
75.79	0.225	-0.087	4979.7	500.00	2.24	4.46	312.94	-0.15	-2.23	-55	-57	2327	-2326	-0	0	1
76.29	0.227	-0.089	4978.6	500.00	2.84	4.45	335.23	0.45	-2.75	-55	-57	2327	-2326	-0	0	1
76.79	0.230	-0.103	4978.6	500.00	3.25	4.45	332.61	-1.07	-3.13	-55	-57	2327	-2326	-0	0	1
77.29	0.232	-0.101	4979.5	500.00	3.72	4.46	337.84	-1.34	-3.46	-55	-57	2327	-2326	-0	0	1
77.79	0.234	-0.102	4978.4	500.00	3.92	4.46	337.93	-1.54	-3.61	-55	-57	2327	-2326	-0	0	1
78.28	0.235	-0.106	4978.3	500.00	3.92	4.46	337.93	-1.54	-3.61	-55	-57	2327	-2326	-0	0	1
78.78	0.238	-0.105	4978.2	500.00	3.75	4.46	330.55	-1.62	-3.27	-55	-57	2327	-2326	-0	0	1
79.28	0.240	-0.105	4978.1	500.00	3.41	4.46	335.52	-1.13	-3.20	-55	-57	2327	-2326	-0	0	1
79.78	0.241	-0.105	4978.0	500.00	2.67	4.46	332.15	-0.34	-2.31	-55	-57	2327	-2326	-0	0	1
80.27	0.243	-0.107	4978.0	500.00	2.39	4.46	1.77	0.41	-2.35	-55	-57	2327	-2326	-0	0	1
80.77	0.245	-0.107	4978.0	500.00	1.92	4.46	17.07	0.43	-1.26	-55	-57	2327	-2326	-0	0	1
81.27	0.247	-0.104	4978.0	500.00	1.60	4.46	42.73	0.43	-1.26	-55	-57	2327	-2326	-0	0	1
81.77	0.245	-0.109	4977.9	500.00	1.32	4.46	77.49	1.11	-0.71	-55	-57	2327	-2326	-0	0	1
82.27	0.240	-0.109	4977.9	500.00	1.61	4.46	105.89	1.59	-0.20	-55	-57	2327	-2326	-0	0	1
82.76	0.252	-0.109	4977.9	500.00	2.03	4.46	123.82	2.01	0.25	-55	-57	2327	-2326	-0	0	1
83.26	0.264	-0.109	4977.9	500.00	2.42	4.46	131.56	2.34	0.42	-55	-57	2327	-2326	-0	0	1
83.76	0.266	-0.113	4977.9	500.00	2.70	4.46	131.56	2.54	0.47	-55	-57	2327	-2326	-0	0	1
84.26	0.268	-0.111	4977.6	500.00	2.84	4.46	143.12	2.55	1.00	-55	-57	2327	-2326	-0	0	1
84.75	0.263	-0.111	4977.7	500.00	2.81	4.46	143.33	2.62	1.01	-55	-57	2327	-2326	-0	0	1
85.25	0.262	-0.112	4977.7	500.00	2.61	4.46	145.93	2.44	0.99	-55	-57	2327	-2326	-0	0	1
85.75	0.265	-0.113	4977.6	500.00	2.27	4.46	145.93	2.17	0.64	-55	-57	2327	-2326	-0	0	1
86.25	0.267	-0.113	4977.6	500.00	1.80	4.46	145.93	1.70	0.29	-55	-57	2327	-2326	-0	0	1
86.74	0.270	-0.116	4977.6	500.00	1.29	4.46	132.77	1.25	-0.14	-55	-57	2327	-2326	-0	0	1
87.24	0.272	-0.115	4977.6	500.00	0.97	4.46	103.43	0.73	-0.54	-55	-57	2327	-2326	-0	0	1
87.74	0.275	-0.116	4977.6	500.00	1.17	4.46	43.77	0.13	-1.17	-55	-57	2327	-2326	-0	0	1
88.24	0.277	-0.117	4977.6	500.00	1.77	4.46	41.56	0.43	-1.70	-55	-57	2327	-2326	-0	0	1
88.74	0.283	-0.117	4977.5	500.00	2.46	4.46	37.17	-0.05	-2.21	-55	-57	2327	-2326	-0	0	1
89.23	0.282	-0.115	4977.5	500.00	3.13	4.46	31.52	-1.03	-2.87	-55	-57	2327	-2326	-0	0	1
89.73	0.285	-0.115	4977.4	500.00	3.71	4.46	31.15	-2.12	-3.64	-55	-57	2327	-2326	-0	0	1
90.23	0.297	-0.116	4977.3	500.00	4.15	4.46	31.95	-2.51	-3.32	-55	-57	2327	-2326	-0	0	1
90.73	0.290	-0.119	4977.2	500.00	4.47	4.46	33.32	-2.79	-3.49	-55	-57	2327	-2326	-0	0	1
91.22	0.284	-0.120	4977.1	500.00	4.56	4.46	34.73	-2.35	-3.33	-55	-57	2327	-2326	-0	0	1
91.72	0.284	-0.120	4977.0	500.00	4.56	4.46	34.55	-2.57	-3.75	-55	-57	2327	-2326	-0	0	1
92.22	0.266	-0.120	4976.9	500.00	4.34	4.46	34.57	-2.31	-3.24	-55	-57	2327	-2326	-0	0	1
92.72	0.268	-0.120	4976.7	500.00	3.89	4.46	40.35	-2.72	-2.33	-55	-57	2327	-2326	-0	0	1
93.21	0.260	-0.119	4976.6	500.00	3.50	4.46	42.13	-2.12	-2.72	-55	-57	2327	-2326	-0	0	1
93.71	0.262	-0.119	4976.5	500.00	2.80	4.46	43.41	-2.30	-2.03	-55	-57	2327	-2326	-0	0	1
94.21	0.263	-0.118	4976.4	500.00	2.21	4.46	44.31	-1.53	-1.60	-55	-57	2327	-2326	-0	0	1
94.71	0.265	-0.118	4976.5	500.00	1.51	4.45	43.11	-1.12	-0.94	-55	-57	2327	-2326	-0	0	1
95.21	0.267	-0.119	4976.5	500.00	0.82	4.46	35.52	-0.73	-0.48	-55	-57	2327	-2326	-0	0	1
95.70	0.268	-0.119	4976.5	500.00	0.33	4.46	37.52	-0.30	0.14	-55	-57	2327	-2326	-0	0	1
96.20	0.261	-0.117	4976.5	500.00	0.62	4.46	275.52	0.08	0.81	-55	-57	2327	-2326	-0	0	1
96.70	0.311	-0.117	4976.5	500.00	1.02	4.46	264.36	0.36	1.30	-55	-57	2327	-2326	-0	0	1
97.20	0.313	-0.117	4976.5	500.00	1.44	4.45	253.91	0.61	1.30	-55	-57	2327	-2326	-0	0	1
97.69	0.315	-0.116	4976.5	500.00	1.82	4.46	235.53	0.73	1.50	-55	-57	2327	-2326	-0	0	1
98.19	0.315	-0.115	4976.4	500.00	1.74	4.47	265.24	0.76	1.52	-55	-57	2327	-2326	-0	0	1
98.69	0.318	-0.116	4976.4	500.00	1.67	4.46	275.24	0.64	1.55	-55	-57	2327	-2326	-0	0	1
99.19	0.320	-0.116	4976.4	500.00	1.48	4.46	253.44	0.43	1.41	-55	-57	2327	-2326	-0	0	1

COPIES AVAILABLE TO ONE DOES NOT  
PERMIT FULLY LEGIBLE PRODUCTION

## FLECHETTE GROUND POINT

PAGE 5

T	X	Y	Z	V	P	ALPHA	MACH	PHI	ALPHA	PCT	L-N	L-P	M-V	M-P	S	JAV	M-T
SEC	FT	FT	FT	FT/SEC	PAD/SEC	SEC	SEC	DEG	DEG	DEG	1/500	1/500	1/500	1/500	1/500	1/500	1/500
0.0200	99.88	0.322	-0.115	4976.4	500.00	1.15	4.45	254.78	0.14	1.18	-55	-57	2324	-2325	-0	0	1
0.0201	100.18	0.325	-0.115	4975.4	500.00	0.91	4.46	271.25	-0.24	0.83	-55	-57	2324	-2325	-0	0	1
0.0202	100.68	0.328	-0.116	4975.4	500.00	0.85	4.46	0.91	-0.57	0.52	-55	-57	2323	-2325	-0	0	1
0.0203	101.18	0.329	-0.116	4975.4	500.00	1.14	4.46	35.16	-1.13	0.13	-55	-57	2323	-2325	-0	0	1
0.0204	101.68	0.329	-0.116	4975.4	500.00	1.42	4.46	54.03	-1.61	-0.26	-55	-57	2323	-2325	-0	0	1
0.0205	102.17	0.331	-0.115	4976.3	500.00	2.15	4.46	64.64	-2.03	-0.24	-55	-57	2323	-2325	-0	0	1
0.0206	102.67	0.333	-0.117	4975.3	500.00	2.65	4.46	72.07	-2.47	-0.39	-55	-57	2324	-2325	-0	0	1
0.0207	103.17	0.335	-0.117	4976.2	500.00	3.09	4.46	81.22	-2.92	-1.25	-55	-57	2324	-2325	-0	0	1
0.0208	103.67	0.335	-0.117	4975.1	500.00	3.40	4.46	94.32	-3.26	-1.54	-55	-57	2324	-2325	-0	0	1
0.0209	104.16	0.338	-0.117	4975.1	500.00	3.66	4.45	95.67	-3.33	-1.53	-55	-57	2324	-2325	-0	0	1
0.0210	104.65	0.340	-0.114	4975.0	500.00	3.58	4.46	98.23	-3.23	-1.62	-55	-57	2323	-2325	-0	0	1
0.0211	105.16	0.342	-0.115	4975.9	500.00	3.37	4.45	89.82	-3.14	-1.21	-55	-57	2323	-2325	-0	0	1
0.0212	105.65	0.343	-0.114	4975.4	500.00	3.06	4.46	80.05	-2.90	-0.91	-55	-57	2323	-2325	-0	0	1
0.0213	106.15	0.346	-0.115	4975.4	500.00	2.62	4.46	65.21	-2.55	-0.53	-55	-57	2323	-2325	-0	0	1
0.0214	106.65	0.346	-0.115	4975.4	500.00	2.17	4.46	75.06	-2.15	-0.10	-55	-57	2323	-2325	-0	0	1
0.0215	107.15	0.345	-0.115	4975.7	500.00	1.76	4.45	60.52	-1.72	0.32	-55	-57	2323	-2325	-0	0	1
0.0216	107.65	0.345	-0.115	4975.7	500.00	1.52	4.46	44.93	-1.24	0.67	-55	-57	2323	-2325	-0	0	1
0.0217	108.14	0.347	-0.114	4975.7	500.00	1.56	4.46	24.29	-0.76	1.36	-55	-57	2323	-2325	-0	0	1
0.0218	108.64	0.347	-0.113	4975.7	500.00	1.94	4.46	7.43	-0.31	1.41	-55	-57	2323	-2325	-0	0	1
0.0219	109.14	0.349	-0.113	4975.7	500.00	2.22	4.46	357.02	0.11	2.21	-55	-57	2323	-2325	-0	0	1
0.0220	109.64	0.349	-0.113	4975.6	500.00	2.59	4.46	353.33	0.45	2.55	-55	-57	2323	-2325	-0	0	1
0.0221	110.13	0.350	-0.113	4975.6	500.00	2.85	4.45	351.70	0.73	2.79	-55	-57	2323	-2325	-0	0	1
0.0222	110.63	0.350	-0.113	4975.6	500.00	3.06	4.45	351.93	0.92	2.95	-55	-57	2323	-2325	-0	0	1
0.0223	111.13	0.351	-0.113	4975.6	500.00	3.16	4.45	353.49	1.01	3.10	-55	-57	2323	-2325	-0	0	1
0.0224	111.63	0.351	-0.113	4975.6	500.00	3.17	4.46	353.16	1.01	2.85	-55	-57	2323	-2325	-0	0	1
0.0225	112.12	0.352	-0.113	4975.6	500.00	2.86	4.46	345.85	0.92	2.81	-55	-57	2323	-2325	-0	0	1
0.0226	112.62	0.353	-0.113	4975.3	500.00	2.59	4.45	6.30	0.74	2.33	-55	-57	2323	-2325	-0	0	1
0.0227	113.12	0.354	-0.114	4975.3	500.00	2.35	4.45	11.42	0.50	2.33	-55	-57	2323	-2325	-0	0	1
0.0228	113.62	0.355	-0.114	4975.2	500.00	2.05	4.45	20.58	0.20	1.95	-55	-57	2323	-2325	-0	0	1
0.0229	114.11	0.355	-0.115	4975.2	500.00	1.58	4.46	33.93	-0.12	1.52	-55	-57	2323	-2325	-0	0	1
0.0230	114.61	0.357	-0.115	4975.2	500.00	1.58	4.46	33.93	-0.12	1.52	-55	-57	2323	-2325	-0	0	1
0.0231	115.11	0.358	-0.116	4975.2	500.00	1.25	4.45	53.29	-0.45	1.29	-55	-57	2323	-2325	-0	0	1
0.0232	115.61	0.359	-0.117	4975.2	500.00	1.17	4.46	75.51	-0.73	0.93	-55	-57	2323	-2325	-0	0	1
0.0233	116.10	0.361	-0.117	4975.2	500.00	1.18	4.46	102.64	-1.07	0.43	-55	-57	2323	-2325	-0	0	1
0.0234	116.60	0.362	-0.119	4975.1	500.00	1.31	4.46	122.12	-1.31	0.20	-55	-57	2323	-2325	-0	0	1
0.0235	117.10	0.362	-0.119	4975.1	500.00	1.48	4.45	134.36	-1.43	-0.32	-55	-57	2323	-2325	-0	0	1
0.0236	117.60	0.363	-0.119	4975.1	500.00	1.62	4.46	172.53	-1.67	-0.16	-55	-57	2323	-2325	-0	0	1
0.0237	118.10	0.364	-0.120	4975.1	500.00	1.58	4.45	172.25	-1.58	-0.22	-55	-57	2323	-2325	-0	0	1
0.0238	118.60	0.365	-0.120	4975.1	500.00	1.58	4.46	145.52	-1.45	-0.12	-55	-57	2323	-2325	-0	0	1
0.0239	119.10	0.366	-0.121	4975.1	500.00	1.32	4.45	145.56	-1.32	-0.03	-55	-57	2323	-2325	-0	0	1
0.0240	119.60	0.366	-0.121	4975.1	500.00	1.24	4.45	145.14	-1.25	0.11	-55	-57	2323	-2325	-0	0	1
0.0241	120.10	0.367	-0.122	4975.0	500.00	0.82	4.46	128.65	-0.73	0.36	-55	-57	2323	-2325	-0	0	1
0.0242	120.60	0.367	-0.122	4975.0	500.00	0.75	4.45	95.69	-0.35	0.45	-55	-57	2323	-2325	-0	0	1
0.0243	121.10	0.369	-0.123	4975.0	500.00	1.00	4.45	62.40	-0.37	0.93	-55	-57	2323	-2325	-0	0	1
0.0244	121.60	0.369	-0.123	4975.0	500.00	1.03	4.45	48.35	-0.51	1.34	-55	-57	2323	-2325	-0	0	1
0.0245	122.10	0.369	-0.124	4975.0	500.00	1.02	4.45	42.57	-0.45	1.37	-55	-57	2323	-2325	-0	0	1
0.0246	122.60	0.370	-0.125	4975.0	500.00	2.41	4.45	80.44	-1.47	1.79	-55	-57	2323	-2325	-0	0	1
0.0247	123.10	0.370	-0.125	4975.9	500.00	2.84	4.46	40.07	-1.75	2.24	-55	-57	2323	-2325	-0	0	1
0.0248	123.60	0.371	-0.126	4975.9	500.00	3.20	4.46	40.51	-2.01	2.64	-55	-57	2323	-2325	-0	0	1
0.0249	124.10	0.372	-0.127	4975.8	500.00	3.46	4.46	41.72	-2.32	2.97	-55	-57	2323	-2325	-0	0	1



## FLECHETTE GROUND POINT

PAGE 7

Y	X	Y	Z	V	P	ALPHA	PHI	ALPHA	PETA	L	L-P	4-P	5	IAU	K-I
SEC	FT	FT	FT	FT/SEC	RAD/SEC	DEG	DEG	DEG	DEG	1/SEC	1/SEC	1/SEC	1/SEC	1/SEC	1/SEC
0.0300	189.43	0.459	-0.190	4973.5	500.00	0.58	4.45	72.45	0.34	0.59	-55.	-57.	2330.-2327.	0.	1.
0.0301	189.93	0.461	-0.191	4973.5	500.00	0.57	4.45	72.45	0.34	0.59	-55.	-57.	2330.-2327.	0.	1.
0.0302	190.43	0.463	-0.191	4973.5	500.00	0.57	4.45	72.45	0.34	0.59	-55.	-57.	2330.-2327.	0.	1.
0.0303	190.93	0.465	-0.191	4973.5	500.00	0.57	4.45	72.45	0.34	0.59	-55.	-57.	2330.-2327.	0.	1.
0.0304	191.42	0.467	-0.192	4973.5	500.00	0.57	4.45	72.45	0.34	0.59	-55.	-57.	2330.-2327.	0.	1.
0.0305	191.92	0.469	-0.192	4973.5	500.00	0.57	4.45	72.45	0.34	0.59	-55.	-57.	2330.-2327.	0.	1.
0.0306	192.42	0.472	-0.192	4973.5	500.00	0.57	4.45	72.45	0.34	0.59	-55.	-57.	2330.-2327.	0.	1.
0.0307	192.91	0.474	-0.192	4973.5	500.00	0.57	4.45	72.45	0.34	0.59	-55.	-57.	2330.-2327.	0.	1.
0.0308	193.41	0.476	-0.193	4973.5	500.00	0.57	4.45	72.45	0.34	0.59	-55.	-57.	2330.-2327.	0.	1.
0.0309	193.91	0.478	-0.193	4973.5	500.00	0.57	4.45	72.45	0.34	0.59	-55.	-57.	2330.-2327.	0.	1.
0.0310	194.40	0.481	-0.193	4973.5	500.00	0.57	4.45	72.45	0.34	0.59	-55.	-57.	2330.-2327.	0.	1.
0.0311	194.90	0.483	-0.194	4973.5	500.00	0.57	4.45	72.45	0.34	0.59	-55.	-57.	2330.-2327.	0.	1.
0.0312	195.40	0.485	-0.194	4973.5	500.00	0.57	4.45	72.45	0.34	0.59	-55.	-57.	2330.-2327.	0.	1.
0.0313	195.90	0.487	-0.194	4973.5	500.00	0.57	4.45	72.45	0.34	0.59	-55.	-57.	2330.-2327.	0.	1.
0.0314	196.39	0.489	-0.194	4973.5	500.00	0.57	4.45	72.45	0.34	0.59	-55.	-57.	2330.-2327.	0.	1.
0.0315	196.89	0.491	-0.194	4973.5	500.00	0.57	4.45	72.45	0.34	0.59	-55.	-57.	2330.-2327.	0.	1.
0.0316	197.39	0.493	-0.194	4973.5	500.00	0.57	4.45	72.45	0.34	0.59	-55.	-57.	2330.-2327.	0.	1.
0.0317	197.88	0.495	-0.194	4973.5	500.00	0.57	4.45	72.45	0.34	0.59	-55.	-57.	2330.-2327.	0.	1.
0.0318	198.38	0.497	-0.194	4973.5	500.00	0.57	4.45	72.45	0.34	0.59	-55.	-57.	2330.-2327.	0.	1.
0.0319	198.88	0.500	-0.194	4973.5	500.00	0.57	4.45	72.45	0.34	0.59	-55.	-57.	2330.-2327.	0.	1.
0.0320	199.38	0.502	-0.194	4973.5	500.00	0.57	4.45	72.45	0.34	0.59	-55.	-57.	2330.-2327.	0.	1.
0.0321	199.88	0.504	-0.194	4973.5	500.00	0.57	4.45	72.45	0.34	0.59	-55.	-57.	2330.-2327.	0.	1.
0.0322	200.37	0.506	-0.194	4973.5	500.00	0.57	4.45	72.45	0.34	0.59	-55.	-57.	2330.-2327.	0.	1.
0.0323	200.87	0.508	-0.194	4973.5	500.00	0.57	4.45	72.45	0.34	0.59	-55.	-57.	2330.-2327.	0.	1.
0.0324	201.36	0.510	-0.193	4973.5	500.00	0.57	4.45	72.45	0.34	0.59	-55.	-57.	2330.-2327.	0.	1.
0.0325	201.85	0.512	-0.193	4973.5	500.00	0.57	4.45	72.45	0.34	0.59	-55.	-57.	2330.-2327.	0.	1.
0.0326	202.36	0.514	-0.192	4973.5	500.00	0.57	4.45	72.45	0.34	0.59	-55.	-57.	2330.-2327.	0.	1.
0.0327	202.86	0.516	-0.192	4973.5	500.00	0.57	4.45	72.45	0.34	0.59	-55.	-57.	2330.-2327.	0.	1.
0.0328	203.36	0.518	-0.191	4973.5	500.00	0.57	4.45	72.45	0.34	0.59	-55.	-57.	2330.-2327.	0.	1.
0.0329	203.85	0.520	-0.191	4973.5	500.00	0.57	4.45	72.45	0.34	0.59	-55.	-57.	2330.-2327.	0.	1.
0.0330	204.35	0.522	-0.191	4973.5	500.00	0.57	4.45	72.45	0.34	0.59	-55.	-57.	2330.-2327.	0.	1.
0.0331	204.85	0.524	-0.191	4973.5	500.00	0.57	4.45	72.45	0.34	0.59	-55.	-57.	2330.-2327.	0.	1.
0.0332	205.35	0.526	-0.190	4973.5	500.00	0.57	4.45	72.45	0.34	0.59	-55.	-57.	2330.-2327.	0.	1.
0.0333	205.84	0.528	-0.190	4973.5	500.00	0.57	4.45	72.45	0.34	0.59	-55.	-57.	2330.-2327.	0.	1.
0.0334	206.34	0.530	-0.190	4973.5	500.00	0.57	4.45	72.45	0.34	0.59	-55.	-57.	2330.-2327.	0.	1.
0.0335	206.84	0.532	-0.190	4973.5	500.00	0.57	4.45	72.45	0.34	0.59	-55.	-57.	2330.-2327.	0.	1.
0.0336	207.33	0.534	-0.190	4973.5	500.00	0.57	4.45	72.45	0.34	0.59	-55.	-57.	2330.-2327.	0.	1.
0.0337	207.83	0.536	-0.190	4973.5	500.00	0.57	4.45	72.45	0.34	0.59	-55.	-57.	2330.-2327.	0.	1.
0.0338	208.33	0.538	-0.190	4973.5	500.00	0.57	4.45	72.45	0.34	0.59	-55.	-57.	2330.-2327.	0.	1.
0.0339	208.83	0.540	-0.190	4973.5	500.00	0.57	4.45	72.45	0.34	0.59	-55.	-57.	2330.-2327.	0.	1.
0.0340	209.32	0.542	-0.190	4973.5	500.00	0.57	4.45	72.45	0.34	0.59	-55.	-57.	2330.-2327.	0.	1.
0.0341	209.82	0.544	-0.190	4973.5	500.00	0.57	4.45	72.45	0.34	0.59	-55.	-57.	2330.-2327.	0.	1.
0.0342	210.32	0.546	-0.190	4973.5	500.00	0.57	4.45	72.45	0.34	0.59	-55.	-57.	2330.-2327.	0.	1.
0.0343	210.82	0.548	-0.190	4973.5	500.00	0.57	4.45	72.45	0.34	0.59	-55.	-57.	2330.-2327.	0.	1.
0.0344	211.31	0.550	-0.190	4973.5	500.00	0.57	4.45	72.45	0.34	0.59	-55.	-57.	2330.-2327.	0.	1.
0.0345	211.81	0.552	-0.190	4973.5	500.00	0.57	4.45	72.45	0.34	0.59	-55.	-57.	2330.-2327.	0.	1.
0.0346	212.31	0.554	-0.190	4973.5	500.00	0.57	4.45	72.45	0.34	0.59	-55.	-57.	2330.-2327.	0.	1.
0.0347	212.80	0.556	-0.190	4973.5	500.00	0.57	4.45	72.45	0.34	0.59	-55.	-57.	2330.-2327.	0.	1.
0.0348	213.30	0.558	-0.190	4973.5	500.00	0.57	4.45	72.45	0.34	0.59	-55.	-57.	2330.-2327.	0.	1.
0.0349	213.80	0.560	-0.189	4973.5	500.00	0.57	4.45	72.45	0.34	0.59	-55.	-57.	2330.-2327.	0.	1.

## FLECHETTE GROUND POINT

PAGE 5

T SEC	X FT	Y FT	Z FT	V FT/SEC	P RAD/SEC	ALPHA MICH	PHI DEG	ALPHA DEG	BETA DEG	L-NA 1/500	L-PR 1/500	M-NA 1/500	M-PR 1/500	S	TAU	K-T CLG
0.0350	174.30	0.541	-0.180	4972.4	500.00	1.49	4.45	68.23	-1.22	0.83	-53	-57	2330	-2327	0	1
0.0351	174.79	0.542	-0.180	4972.4	500.00	1.45	4.45	57.57	-0.54	1.00	-55	-57	2330	-2327	0	1
0.0352	175.29	0.542	-0.180	4972.4	500.00	1.48	4.45	46.54	-0.49	1.32	-55	-57	2330	-2327	0	1
0.0353	175.70	0.543	-0.180	4972.4	500.00	1.60	4.45	35.31	-0.41	1.44	-55	-57	2330	-2327	0	1
0.0354	176.20	0.544	-0.180	4972.4	500.00	1.76	4.45	23.94	-0.15	1.75	-55	-57	2330	-2327	0	1
0.0355	176.78	0.544	-0.180	4972.4	500.00	1.66	4.45	24.74	3.11	1.74	-55	-57	2330	-2327	0	1
0.0356	177.28	0.545	-0.181	4972.5	500.00	2.11	4.45	21.99	0.31	2.03	-55	-57	2330	-2327	0	1
0.0357	177.78	0.546	-0.181	4972.5	500.00	2.24	4.45	23.77	0.69	2.18	-55	-57	2330	-2327	0	1
0.0358	178.27	0.546	-0.181	4972.5	500.00	2.33	4.45	20.76	0.52	2.25	-55	-57	2330	-2327	0	1
0.0359	178.77	0.547	-0.182	4972.5	500.00	2.37	4.45	21.42	0.71	2.26	-55	-57	2330	-2327	0	1
0.0360	179.27	0.548	-0.182	4972.5	500.00	2.35	4.45	21.25	0.75	2.22	-55	-57	2330	-2327	0	1
0.0361	179.77	0.549	-0.183	4972.4	500.00	2.27	4.45	26.53	0.79	2.14	-55	-57	2330	-2327	0	1
0.0362	180.26	0.550	-0.183	4972.4	500.00	2.14	4.45	21.41	0.70	2.32	-55	-57	2330	-2327	0	1
0.0363	180.76	0.551	-0.184	4972.3	500.00	1.97	4.45	21.91	0.83	1.53	-53	-57	2330	-2327	0	1
0.0364	181.26	0.551	-0.185	4972.3	500.00	1.76	4.45	36.08	0.52	1.58	-53	-57	2330	-2327	0	1
0.0365	181.75	0.552	-0.185	4972.3	500.00	1.84	4.45	41.00	0.41	1.60	-55	-57	2330	-2327	0	1
0.0366	182.25	0.553	-0.185	4972.3	500.00	1.32	4.45	45.41	0.23	1.20	-55	-57	2330	-2327	0	1
0.0367	182.75	0.554	-0.187	4972.3	500.00	0.91	4.45	53.61	0.15	1.09	-55	-57	2330	-2327	0	1
0.0368	183.25	0.555	-0.189	4972.3	500.00	0.91	4.45	61.39	0.05	0.91	-55	-57	2330	-2327	0	1
0.0369	183.74	0.556	-0.189	4972.3	500.00	0.76	4.45	69.73	-0.03	0.75	-55	-57	2330	-2327	0	1
0.0370	184.24	0.557	-0.191	4972.3	500.00	0.63	4.45	77.76	-0.03	0.53	-55	-57	2330	-2327	0	1
0.0371	184.74	0.558	-0.191	4972.3	500.00	0.54	4.45	83.41	-0.03	0.53	-55	-57	2330	-2327	0	1
0.0372	185.24	0.559	-0.192	4972.3	500.00	0.40	4.45	89.39	-0.07	0.47	-55	-57	2330	-2327	0	1
0.0373	185.73	0.560	-0.192	4972.3	500.00	0.46	4.45	79.11	0.00	0.47	-55	-57	2330	-2327	0	1
0.0374	186.23	0.560	-0.193	4972.3	500.00	0.46	4.45	69.03	0.11	0.47	-55	-57	2330	-2327	0	1
0.0375	186.73	0.561	-0.194	4972.3	500.00	0.56	4.45	59.00	0.26	0.53	-55	-57	2330	-2327	0	1
0.0376	187.22	0.562	-0.195	4972.3	500.00	0.75	4.45	57.14	0.53	0.61	-55	-57	2330	-2327	0	1
0.0377	187.72	0.563	-0.196	4972.3	500.00	0.95	4.45	49.54	0.66	0.71	-55	-57	2330	-2327	0	1
0.0378	188.22	0.564	-0.197	4972.3	500.00	1.15	4.45	47.16	0.55	0.82	-55	-57	2330	-2327	0	1
0.0379	188.72	0.565	-0.198	4972.3	500.00	1.43	4.45	47.12	1.07	0.86	-55	-57	2330	-2327	0	1
0.0380	189.21	0.566	-0.199	4972.2	500.00	1.67	4.45	47.95	1.31	1.05	-55	-57	2330	-2327	0	1
0.0381	189.71	0.567	-0.200	4972.2	500.00	1.80	4.45	70.31	1.52	1.14	-55	-57	2330	-2327	0	1
0.0382	190.21	0.568	-0.201	4972.2	500.00	2.10	4.45	53.35	1.71	1.22	-55	-57	2330	-2327	0	1
0.0383	190.70	0.569	-0.202	4972.2	500.00	2.24	4.45	51.61	1.87	1.26	-55	-57	2330	-2327	0	1
0.0384	191.20	0.570	-0.202	4972.1	500.00	2.37	4.45	52.20	2.03	1.27	-55	-57	2330	-2327	0	1
0.0385	191.70	0.571	-0.204	4972.1	500.00	2.72	4.45	51.45	2.13	1.25	-53	-57	2330	-2327	0	1
0.0386	192.20	0.572	-0.206	4972.1	500.00	2.62	4.45	55.47	2.12	1.13	-53	-57	2330	-2327	0	1
0.0387	192.69	0.573	-0.207	4972.0	500.00	2.37	4.45	56.13	2.11	1.07	-55	-57	2330	-2327	0	1
0.0388	193.19	0.575	-0.209	4972.0	500.00	2.27	4.45	55.30	2.07	0.93	-55	-57	2330	-2327	0	1
0.0389	193.69	0.575	-0.210	4972.0	500.00	2.12	4.45	53.78	1.93	0.75	-55	-57	2330	-2327	0	1
0.0390	194.19	0.578	-0.211	4972.0	500.00	1.54	4.45	54.34	1.56	0.55	-55	-57	2330	-2327	0	1
0.0391	194.69	0.579	-0.212	4971.9	500.00	1.75	4.45	51.55	1.72	0.33	-55	-57	2330	-2327	0	1
0.0392	195.18	0.581	-0.213	4971.9	500.00	1.56	4.45	47.35	1.55	0.10	-55	-57	2330	-2327	0	1
0.0393	195.68	0.587	-0.215	4971.9	500.00	1.40	4.45	41.22	1.33	-0.13	-55	-57	2330	-2327	0	1
0.0394	196.17	0.594	-0.214	4971.9	500.00	1.27	4.45	33.35	1.23	-0.35	-55	-57	2330	-2327	0	1
0.0395	196.67	0.584	-0.217	4971.9	500.00	1.21	4.45	24.59	1.07	-1.56	-55	-57	2330	-2327	0	1
0.0396	197.17	0.587	-0.219	4971.9	500.00	1.19	4.45	15.38	0.51	-0.74	-55	-57	2330	-2327	0	1
0.0397	197.67	0.589	-0.220	4971.9	500.00	1.21	4.45	11.80	0.81	-0.90	-55	-57	2330	-2327	0	1
0.0398	198.16	0.581	-0.221	4971.9	500.00	1.25	4.45	9.27	0.73	-1.02	-55	-57	2330	-2327	0	1
0.0399	198.65	0.582	-0.223	4971.9	500.00	1.30	4.45	5.03	0.69	-1.11	-55	-57	2330	-2327	0	1



FLUCHETTE GROUND POINT

PAGE 9

T	X	Y	Z	V	P	ALPHA	MACH	RHI	ALPHA	BETA	L-N	L-P	W-N	W-P	S	TAU	K-T
SEC	FT	FT	FT	FT/SEC	RSC/SEC	CEG	CEG	CEG	DEG	DEG	1/SEC	1/SEC	200/SEC	200/SEC			DEG
0.0400	199.16	0.594	-0.224	4971.5	500.00	1.33	4.45	6.11	0.56	-1.16	-55	-57	2330	-2327	-0	0	1
0.0401	199.15	0.595	-0.225	4971.5	500.00	1.33	4.45	6.25	0.57	-1.17	-55	-57	2330	-2327	-0	0	1
0.0402	200.15	0.593	-0.226	4971.5	500.00	1.36	4.45	1.20	0.72	-1.15	-55	-57	2330	-2327	-0	0	1
0.0403	200.65	0.599	-0.227	4971.5	500.00	1.36	4.45	20.69	0.79	-1.11	-55	-57	2330	-2327	-0	0	1
0.0404	201.15	0.591	-0.228	4971.5	500.00	1.37	4.45	28.41	0.90	-1.14	-55	-57	2330	-2327	-0	0	1
0.0405	201.64	0.603	-0.229	4971.5	500.00	1.38	4.45	35.48	0.99	-0.95	-55	-57	2330	-2327	-0	0	1
0.0406	202.14	0.605	-0.230	4971.5	500.00	1.41	4.45	45.55	1.11	-0.97	-55	-57	2330	-2327	-0	0	1
0.0407	202.64	0.607	-0.231	4971.5	500.00	1.44	4.45	53.95	1.22	-0.78	-55	-57	2330	-2327	-0	0	1
0.0408	203.13	0.609	-0.232	4971.5	500.00	1.49	4.45	61.37	1.31	-0.70	-55	-57	2330	-2327	-0	0	1
0.0409	203.63	0.610	-0.233	4971.5	500.00	1.53	4.45	67.77	1.39	-0.64	-55	-57	2330	-2327	-0	0	1
0.0410	204.13	0.612	-0.234	4971.5	500.00	1.56	4.45	72.91	1.45	-0.59	-55	-57	2330	-2327	-0	0	1
0.0411	204.63	0.614	-0.235	4971.5	500.00	1.58	4.45	75.56	1.47	-0.57	-55	-57	2330	-2327	-0	0	1
0.0412	205.12	0.615	-0.236	4971.5	500.00	1.57	4.45	71.04	1.52	-0.58	-55	-57	2330	-2327	-0	0	1
0.0413	205.62	0.619	-0.237	4971.5	500.00	1.54	4.45	72.33	1.41	-0.43	-55	-57	2330	-2327	-0	0	1
0.0414	206.12	0.621	-0.238	4971.5	500.00	1.50	4.45	78.92	1.32	-0.70	-55	-57	2330	-2327	-0	0	1
0.0415	206.61	0.623	-0.239	4971.5	500.00	1.54	4.45	75.13	1.20	-0.78	-55	-57	2330	-2327	-0	0	1
0.0416	207.11	0.627	-0.240	4971.5	500.00	1.57	4.45	74.02	0.87	-1.05	-55	-57	2330	-2327	-0	0	1
0.0417	207.61	0.627	-0.241	4971.5	500.00	1.58	4.45	57.47	0.57	-1.20	-55	-57	2330	-2327	-0	0	1
0.0418	208.11	0.620	-0.241	4971.5	500.00	1.54	4.45	43.74	0.45	-1.36	-55	-57	2330	-2327	-0	0	1
0.0419	208.60	0.632	-0.242	4971.5	500.00	1.43	4.45	43.74	0.45	-1.36	-55	-57	2330	-2327	-0	0	1
0.0420	209.10	0.634	-0.243	4971.5	500.00	1.53	4.45	43.09	0.25	-1.51	-55	-57	2330	-2327	-0	0	1
0.0421	209.60	0.637	-0.244	4971.5	500.00	1.55	4.45	37.83	0.03	-1.55	-55	-57	2330	-2327	-0	0	1
0.0422	210.09	0.649	-0.245	4971.5	500.00	1.76	4.45	26.12	-0.17	-1.77	-55	-57	2330	-2327	-0	0	1
0.0423	210.59	0.641	-0.245	4971.5	500.00	1.91	4.45	31.79	-0.33	-1.93	-55	-57	2330	-2327	-0	0	1
0.0424	211.09	0.643	-0.246	4971.5	500.00	2.02	4.45	30.57	-0.51	-1.93	-55	-57	2330	-2327	-0	0	1
0.0425	211.59	0.646	-0.247	4971.5	500.00	2.06	4.45	30.27	-0.64	-1.99	-55	-57	2330	-2327	-0	0	1
0.0426	212.09	0.649	-0.247	4971.5	500.00	2.13	4.45	30.57	-0.74	-2.10	-55	-57	2330	-2327	-0	0	1
0.0427	212.59	0.650	-0.247	4971.5	500.00	2.18	4.45	31.43	-0.81	-1.98	-55	-57	2330	-2327	-0	0	1
0.0428	213.09	0.652	-0.247	4971.5	500.00	2.26	4.45	33.05	-0.94	-1.92	-55	-57	2330	-2327	-0	0	1
0.0429	213.57	0.655	-0.248	4971.5	500.00	2.02	4.45	36.32	-0.95	-1.72	-55	-57	2330	-2327	-0	0	1
0.0430	214.07	0.657	-0.248	4971.5	500.00	1.50	4.45	34.45	-0.92	-1.72	-55	-57	2330	-2327	-0	0	1
0.0431	214.57	0.659	-0.249	4971.5	500.00	1.74	4.45	35.18	-0.74	-1.58	-55	-57	2330	-2327	-0	0	1
0.0432	215.07	0.661	-0.249	4971.5	500.00	1.50	4.45	41.55	-0.72	-1.53	-55	-57	2330	-2327	-0	0	1
0.0433	215.56	0.663	-0.249	4971.5	500.00	1.53	4.45	44.19	-0.55	-1.29	-55	-57	2330	-2327	-0	0	1
0.0434	216.06	0.665	-0.249	4971.5	500.00	1.74	4.45	44.66	-1.54	-1.17	-55	-57	2330	-2327	-0	0	1
0.0435	216.56	0.667	-0.249	4971.5	500.00	1.80	4.45	45.97	-0.51	-0.97	-55	-57	2330	-2327	-0	0	1
0.0436	217.06	0.669	-0.249	4971.5	500.00	0.88	4.45	50.75	-0.66	-0.63	-55	-57	2330	-2327	-0	0	1
0.0437	217.56	0.671	-0.249	4971.5	500.00	0.83	4.45	51.49	-0.53	-0.71	-55	-57	2330	-2327	-0	0	1
0.0438	218.06	0.673	-0.249	4971.5	500.00	0.74	4.45	51.43	-0.42	-0.52	-55	-57	2330	-2327	-0	0	1
0.0439	218.55	0.675	-0.249	4971.5	500.00	0.59	4.45	49.87	-0.43	-0.34	-55	-57	2330	-2327	-0	0	1
0.0440	219.04	0.677	-0.249	4971.5	500.00	0.58	4.45	47.44	-0.47	-0.49	-55	-57	2330	-2327	-0	0	1
0.0441	219.54	0.679	-0.249	4971.5	500.00	0.72	4.45	44.87	-0.54	-0.47	-55	-57	2330	-2327	-0	0	1
0.0442	220.04	0.681	-0.249	4971.5	500.00	0.70	4.45	43.21	-0.54	-0.47	-55	-57	2330	-2327	-0	0	1
0.0443	220.54	0.683	-0.249	4971.5	500.00	0.70	4.45	43.14	-1.09	-0.53	-55	-57	2330	-2327	-0	0	1
0.0444	221.03	0.685	-0.249	4971.5	500.00	1.04	4.45	44.28	-1.03	-0.57	-55	-57	2330	-2327	-0	0	1
0.0445	221.53	0.687	-0.249	4971.5	500.00	1.15	4.45	45.97	-1.23	-0.63	-55	-57	2330	-2327	-0	0	1
0.0446	222.03	0.689	-0.249	4971.5	500.00	1.35	4.45	45.97	-1.23	-0.63	-55	-57	2330	-2327	-0	0	1
0.0447	222.52	0.691	-0.249	4971.5	500.00	1.52	4.45	47.70	-1.55	-0.59	-55	-57	2330	-2327	-0	0	1
0.0448	223.02	0.693	-0.249	4971.5	500.00	1.57	4.45	49.60	-1.51	-0.72	-55	-57	2330	-2327	-0	0	1
0.0449	223.52	0.695	-0.249	4971.5	500.00	1.91	4.45	51.47	-1.65	-0.75	-55	-57	2330	-2327	-0	0	1

SEC	Y	X	Z	V	P	ALPHA	PHI	ALPHA	BETA	L-N	L-P	M-N	W-P	S	ISU	K-T
SEC	FT	FT	FT	FT/SEC	RAO/SEC	DIG	DEC	DEC	DEC	DEC	DEC	DEC	DEC	DEC	DEC	DEC
0.0450	224.01	0.595	-0.248	4571.2	500.00	1.92	4.45	33.23	1.74	0.75	1.9	57	2331	-2329	0	1
0.0451	224.51	0.699	-0.248	4571.2	500.00	2.00	4.45	34.79	1.68	0.16	55	57	2331	-2329	0	1
0.0452	225.01	0.700	-0.248	4571.2	500.00	2.05	4.45	35.10	1.52	0.12	55	57	2331	-2329	0	1
0.0453	225.51	0.701	-0.248	4571.2	500.00	2.06	4.45	35.16	1.35	0.28	55	57	2331	-2329	0	1
0.0454	226.00	0.703	-0.248	4571.1	500.00	2.04	4.45	35.53	1.24	0.37	55	57	2331	-2329	0	1
0.0455	226.50	0.703	-0.247	4571.1	500.00	1.93	4.45	35.59	1.13	0.45	55	57	2331	-2329	0	1
0.0456	227.00	0.703	-0.247	4571.1	500.00	1.60	4.45	35.70	1.07	0.33	55	57	2331	-2329	0	1
0.0457	227.49	0.707	-0.247	4571.1	500.00	1.79	4.45	35.40	1.02	0.17	55	57	2331	-2329	0	1
0.0458	227.99	0.713	-0.247	4571.1	500.00	1.65	4.45	35.31	1.59	0.11	55	57	2331	-2329	0	1
0.0459	228.49	0.710	-0.246	4571.0	500.00	1.57	4.45	35.36	1.26	0.17	55	57	2331	-2329	0	1
0.0460	228.98	0.711	-0.245	4571.0	500.00	1.47	4.45	35.71	1.13	0.35	55	57	2331	-2329	0	1
0.0461	229.48	0.712	-0.245	4571.0	500.00	1.40	4.45	35.24	1.73	0.32	55	57	2331	-2329	0	1
0.0462	229.98	0.714	-0.245	4571.0	500.00	1.35	4.45	35.45	1.84	0.59	55	57	2331	-2329	0	1
0.0463	230.48	0.715	-0.243	4571.0	500.00	1.36	4.45	35.25	1.34	0.34	55	57	2331	-2329	0	1
0.0464	230.97	0.715	-0.245	4571.1	500.00	1.35	4.45	35.60	1.33	0.37	55	57	2331	-2329	0	1
0.0465	231.47	0.717	-0.245	4571.0	500.00	1.37	4.45	35.57	0.84	1.04	55	57	2331	-2329	0	1
0.0466	231.97	0.719	-0.245	4571.0	500.00	1.40	4.45	35.07	0.77	1.17	55	57	2331	-2329	0	1
0.0467	232.47	0.720	-0.245	4571.0	500.00	1.43	4.45	35.35	0.73	1.23	55	57	2331	-2329	0	1
0.0468	232.96	0.720	-0.245	4571.0	500.00	1.45	4.45	35.43	0.70	1.26	55	57	2331	-2329	0	1
0.0469	233.46	0.721	-0.245	4570.9	500.00	1.45	4.45	35.14	0.70	1.27	55	57	2331	-2329	0	1
0.0470	233.96	0.723	-0.245	4570.9	500.00	1.45	4.45	35.89	0.72	1.26	55	57	2331	-2329	0	1
0.0471	234.45	0.724	-0.245	4570.9	500.00	1.42	4.45	35.52	0.75	1.23	55	57	2331	-2329	0	1
0.0472	234.95	0.725	-0.245	4570.9	500.00	1.43	4.45	35.35	0.70	1.19	55	57	2331	-2329	0	1
0.0473	235.45	0.725	-0.245	4570.9	500.00	1.42	4.45	35.61	0.55	1.14	55	57	2331	-2329	0	1
0.0474	235.94	0.727	-0.245	4570.9	500.00	1.41	4.45	35.31	0.70	1.13	55	57	2331	-2329	0	1
0.0475	236.44	0.728	-0.245	4570.9	500.00	1.40	4.45	35.21	0.75	1.13	55	57	2331	-2329	0	1
0.0476	236.94	0.728	-0.245	4570.9	500.00	1.38	4.45	35.42	0.75	0.94	55	57	2331	-2329	0	1
0.0477	237.44	0.729	-0.245	4570.9	500.00	1.39	4.45	35.67	1.11	0.95	55	57	2331	-2329	0	1
0.0478	237.93	0.730	-0.246	4570.9	500.00	1.37	4.45	35.31	1.01	0.93	55	57	2331	-2329	0	1
0.0479	238.43	0.731	-0.245	4570.9	500.00	1.35	4.45	35.57	0.69	0.93	55	57	2331	-2329	0	1
0.0480	238.93	0.732	-0.245	4570.9	500.00	1.33	4.45	35.43	0.74	0.95	55	57	2331	-2329	0	1
0.0481	239.42	0.733	-0.247	4570.8	500.00	1.31	4.45	35.35	0.68	0.95	55	57	2331	-2329	0	1
0.0482	239.92	0.734	-0.247	4570.8	500.00	1.29	4.45	35.64	0.77	1.36	55	57	2331	-2329	0	1
0.0483	240.42	0.734	-0.247	4570.8	500.00	1.28	4.45	35.53	0.68	1.11	55	57	2331	-2329	0	1
0.0484	240.91	0.735	-0.245	4570.8	500.00	1.26	4.45	35.15	0.90	1.32	55	57	2331	-2329	0	1
0.0485	241.41	0.736	-0.242	4570.8	500.00	1.33	4.45	35.27	0.45	1.32	55	57	2331	-2329	0	1
0.0486	241.91	0.736	-0.242	4570.8	500.00	1.36	4.45	35.41	0.44	1.37	55	57	2331	-2329	0	1
0.0487	242.41	0.737	-0.249	4570.8	500.00	1.47	4.45	35.39	0.11	1.55	55	57	2331	-2329	0	1
0.0488	242.90	0.738	-0.249	4570.1	500.00	1.57	4.45	35.52	0.17	1.55	55	57	2331	-2329	0	1
0.0489	243.40	0.739	-0.250	4570.7	500.00	1.47	4.45	35.15	0.33	1.53	55	57	2331	-2329	0	1
0.0490	243.90	0.739	-0.250	4570.7	500.00	1.75	4.45	35.37	0.59	1.70	55	57	2331	-2329	0	1
0.0491	244.39	0.740	-0.251	4570.7	500.00	1.95	4.45	35.63	0.63	1.74	55	57	2331	-2329	0	1
0.0492	244.89	0.741	-0.252	4570.7	500.00	1.81	4.45	35.11	0.75	1.76	55	57	2331	-2329	0	1
0.0493	245.39	0.741	-0.252	4570.7	500.00	1.65	4.45	35.72	0.76	1.76	55	57	2331	-2329	0	1
0.0494	245.89	0.742	-0.253	4570.7	500.00	1.96	4.45	35.34	0.62	1.73	55	57	2331	-2329	0	1
0.0495	246.38	0.743	-0.254	4570.6	500.00	1.64	4.45	35.56	0.87	1.69	55	57	2331	-2329	0	1
0.0496	246.88	0.744	-0.255	4570.6	500.00	1.60	4.45	35.72	1.00	1.51	55	57	2331	-2329	0	1
0.0497	247.38	0.745	-0.255	4570.6	500.00	1.82	4.45	35.45	1.11	1.52	55	57	2331	-2329	0	1
0.0498	247.87	0.746	-0.257	4570.5	500.00	1.73	4.45	35.13	1.00	1.45	55	57	2331	-2329	0	1
0.0499	248.37	0.747	-0.258	4570.5	500.00	1.62	4.45	35.14	0.98	1.53	55	57	2331	-2329	0	1

# FLECHETTE GROUND POINT

PAGE 11

T SEC	X FT	Y FT	Z FT	V FT/SEC	P RAD/SEC	ALPHA MACH DEG	PHI DEG	ALPHA DEG	BETA DEG	L-N L/SEC	L-P L/SEC	4-N RAD/SEC	W-P RAD/SEC	S JAU	M-T DEG
0.0500	248.87	0.745	-0.250	4870.5	500.00	1.50 4.45	44.05	0.94	1.15	-55	-57	2331-2325	-0	0	0
0.0501	249.36	0.749	-0.250	4870.5	500.00	1.50 4.45	44.05	0.94	1.15	-55	-57	2331-2325	-0	0	0
0.0502	249.86	0.753	-0.251	4870.5	500.00	1.25 4.45	45.02	0.87	0.70	-55	-57	2331-2325	-0	0	0
0.0503	250.36	0.751	-0.252	4870.5	500.00	1.14 4.45	45.83	0.83	0.73	-55	-57	2331-2325	-0	0	0
0.0504	250.86	0.752	-0.253	4870.5	500.00	1.05 4.45	46.04	0.81	0.67	-55	-57	2331-2325	-0	0	0
0.0505	251.35	0.753	-0.254	4870.5	500.00	0.98 4.45	46.81	0.70	0.57	-55	-57	2331-2325	-0	0	0
0.0506	251.85	0.754	-0.255	4870.5	500.00	0.94 4.45	47.51	0.51	0.49	-55	-57	2331-2325	-0	0	0
0.0507	252.35	0.755	-0.256	4870.5	500.00	0.93 4.45	48.31	0.53	0.52	-55	-57	2331-2325	-0	0	0
0.0508	252.84	0.756	-0.257	4870.5	500.00	0.95 4.45	49.37	0.57	0.57	-55	-57	2331-2325	-0	0	0
0.0509	253.34	0.757	-0.258	4870.5	500.00	0.98 4.45	50.73	0.63	0.54	-55	-57	2331-2325	-0	0	0
0.0510	253.84	0.758	-0.259	4870.5	500.00	1.04 4.45	52.23	0.71	0.52	-55	-57	2331-2325	-0	0	0
0.0511	254.33	0.759	-0.271	4870.5	500.00	1.14 4.45	53.81	1.03	0.51	-55	-57	2331-2325	-0	0	0
0.0512	254.83	0.751	-0.272	4870.5	500.00	1.23 4.45	55.41	1.19	0.51	-55	-57	2331-2325	-0	0	0
0.0513	255.33	0.752	-0.273	4870.5	500.00	1.33 4.45	57.11	1.29	0.52	-55	-57	2331-2325	-0	0	0
0.0514	255.83	0.753	-0.274	4870.4	500.00	1.44 4.45	58.81	1.33	0.53	-55	-57	2331-2325	-0	0	0
0.0515	256.32	0.754	-0.275	4870.4	500.00	1.56 4.45	60.51	1.50	0.54	-55	-57	2331-2325	-0	0	0
0.0516	256.82	0.755	-0.277	4870.4	500.00	1.69 4.45	62.31	1.67	0.55	-55	-57	2331-2325	-0	0	0
0.0517	257.32	0.756	-0.278	4870.4	500.00	1.70 4.45	64.11	1.67	0.55	-55	-57	2331-2325	-0	0	0
0.0518	257.81	0.753	-0.279	4870.4	500.00	1.76 4.45	65.91	1.73	0.50	-55	-57	2331-2325	-0	0	0
0.0519	258.31	0.770	-0.270	4870.4	500.00	1.79 4.45	67.71	1.77	0.55	-55	-57	2331-2325	-0	0	0
0.0520	258.80	0.773	-0.272	4870.4	500.00	1.81 4.45	69.51	1.80	0.55	-55	-57	2331-2325	-0	0	0
0.0521	259.30	0.775	-0.285	4870.3	500.00	1.80 4.45	71.31	1.75	0.53	-55	-57	2331-2325	-0	0	0
0.0522	259.80	0.775	-0.285	4870.3	500.00	1.77 4.45	73.11	1.77	0.54	-55	-57	2331-2325	-0	0	0
0.0523	260.30	0.778	-0.287	4870.3	500.00	1.72 4.45	74.91	1.72	0.57	-55	-57	2331-2325	-0	0	0
0.0524	260.79	0.778	-0.287	4870.3	500.00	1.66 4.45	76.71	1.66	0.59	-55	-57	2331-2325	-0	0	0
0.0525	261.29	0.780	-0.288	4870.3	500.00	1.60 4.45	78.51	1.67	0.52	-55	-57	2331-2325	-0	0	0
0.0526	261.79	0.782	-0.288	4870.3	500.00	1.57 4.45	80.31	1.67	0.54	-55	-57	2331-2325	-0	0	0
0.0527	262.28	0.784	-0.290	4870.2	500.00	1.45 4.45	82.11	1.45	0.53	-55	-57	2331-2325	-0	0	0
0.0528	262.78	0.785	-0.292	4870.2	500.00	1.45 4.45	83.91	1.45	0.53	-55	-57	2331-2325	-0	0	0
0.0529	263.28	0.787	-0.291	4870.2	500.00	1.43 4.45	85.71	1.43	0.57	-55	-57	2331-2325	-0	0	0
0.0530	263.78	0.789	-0.294	4870.2	500.00	1.42 4.45	87.51	1.42	0.57	-55	-57	2331-2325	-0	0	0
0.0531	264.27	0.791	-0.295	4870.2	500.00	1.43 4.45	89.31	1.39	0.57	-55	-57	2331-2325	-0	0	0
0.0532	264.77	0.793	-0.296	4870.2	500.00	1.45 4.45	91.11	1.37	0.59	-55	-57	2331-2325	-0	0	0
0.0533	265.27	0.795	-0.297	4870.2	500.00	1.47 4.45	92.91	1.37	0.57	-55	-57	2331-2325	-0	0	0
0.0534	265.76	0.797	-0.298	4870.2	500.00	1.47 4.45	94.71	1.37	0.54	-55	-57	2331-2325	-0	0	0
0.0535	266.26	0.799	-0.299	4870.2	500.00	1.50 4.45	96.51	1.36	0.55	-55	-57	2331-2325	-0	0	0
0.0536	266.76	0.801	-0.300	4870.1	500.00	1.51 4.45	98.31	1.36	0.53	-55	-57	2331-2325	-0	0	0
0.0537	267.25	0.803	-0.311	4870.1	500.00	1.50 4.45	100.11	1.37	0.53	-55	-57	2331-2325	-0	0	0
0.0538	267.75	0.805	-0.302	4870.1	500.00	1.46 4.45	101.91	1.36	0.58	-55	-57	2331-2325	-0	0	0
0.0539	268.25	0.807	-0.303	4870.1	500.00	1.45 4.45	103.71	1.36	0.53	-55	-57	2331-2325	-0	0	0
0.0540	268.75	0.809	-0.304	4870.1	500.00	1.42 4.45	105.51	1.36	0.59	-55	-57	2331-2325	-0	0	0
0.0541	269.24	0.812	-0.305	4870.1	500.00	1.42 4.45	107.31	1.36	0.59	-55	-57	2331-2325	-0	0	0
0.0542	269.74	0.814	-0.306	4870.1	500.00	1.33 4.45	109.11	1.33	0.61	-55	-57	2331-2325	-0	0	0
0.0543	270.23	0.816	-0.307	4870.1	500.00	1.34 4.45	110.91	1.34	0.61	-55	-57	2331-2325	-0	0	0
0.0544	270.73	0.819	-0.307	4870.1	500.00	1.33 4.45	112.71	1.33	0.61	-55	-57	2331-2325	-0	0	0
0.0545	271.23	0.820	-0.308	4870.0	500.00	1.30 4.45	114.51	1.33	0.59	-55	-57	2331-2325	-0	0	0
0.0546	271.72	0.822	-0.309	4870.0	500.00	1.28 4.45	116.31	1.33	0.55	-55	-57	2331-2325	-0	0	0
0.0547	272.22	0.824	-0.309	4870.0	500.00	1.28 4.45	118.11	1.33	0.59	-55	-57	2331-2325	-0	0	0
0.0548	272.72	0.827	-0.310	4870.0	500.00	1.24 4.45	119.91	1.34	0.63	-55	-57	2331-2325	-0	0	0
0.0549	273.22	0.829	-0.310	4870.0	500.00	1.24 4.45	121.71	1.34	0.63	-55	-57	2331-2325	-0	0	0

## FLECHETTE GROUND POINT

PAGE 12

T SEC	X FT	Y FT	Z FT	V FT/SEC	P RAD/SEC	ALPHA DEG	PHI DEG	ALPHA DEG	BETA DEG	1-N 1/SEC	1-P 1/SEC	W-V RAD/SEC	W-P RAD/SEC	S	IAU	X-T DEG
0.0550	273.71	0.331	-0.311	4970.0	500.00	1.27	4.45	57.97	0.75	-1.22	-55	-57	2331-2323	-0	0	1
0.0551	274.21	0.333	-0.311	4970.0	500.00	1.26	4.45	55.36	0.14	-1.26	-55	-57	2331-2323	-0	0	1
0.0552	274.71	0.335	-0.312	4970.0	500.00	1.30	4.45	52.98	0.01	-1.30	-55	-57	2331-2323	-0	0	1
0.0553	275.20	0.338	-0.312	4970.0	500.00	1.36	4.45	49.56	-0.13	-1.35	-55	-57	2331-2323	-0	0	1
0.0554	275.70	0.343	-0.313	4970.0	500.00	1.43	4.45	47.10	-0.27	-1.42	-55	-57	2331-2323	-0	0	1
0.0555	276.20	0.347	-0.313	4970.0	500.00	1.50	4.45	45.72	-0.41	-1.45	-55	-57	2331-2323	-0	0	1
0.0556	276.69	0.349	-0.313	4969.9	500.00	1.55	4.45	43.47	-0.55	-1.48	-55	-57	2331-2323	-0	0	1
0.0557	277.19	0.347	-0.314	4969.9	500.00	1.60	4.45	42.43	-0.67	-1.51	-55	-57	2331-2323	-0	0	1
0.0558	277.69	0.349	-0.314	4969.9	500.00	1.72	4.45	41.86	-0.75	-1.53	-55	-57	2331-2323	-0	0	1
0.0559	278.18	0.351	-0.314	4969.9	500.00	1.77	4.45	41.67	-0.79	-1.53	-55	-57	2331-2323	-0	0	1
0.0560	278.68	0.354	-0.314	4969.9	500.00	1.81	4.45	41.70	-0.79	-1.51	-55	-57	2331-2323	-0	0	1
0.0561	279.18	0.356	-0.315	4969.9	500.00	1.82	4.45	42.14	-1.00	-1.48	-55	-57	2331-2323	-0	0	1
0.0562	279.67	0.358	-0.315	4969.9	500.00	1.81	4.45	42.54	-1.17	-1.43	-55	-57	2331-2323	-0	0	1
0.0563	280.17	0.359	-0.315	4969.9	500.00	1.79	4.45	43.21	-1.15	-1.36	-55	-57	2331-2323	-0	0	1
0.0564	280.67	0.362	-0.315	4969.9	500.00	1.74	4.45	43.75	-1.13	-1.28	-55	-57	2331-2323	-0	0	1
0.0565	281.16	0.364	-0.315	4969.9	500.00	1.68	4.45	44.28	-1.10	-1.19	-55	-57	2331-2323	-0	0	1
0.0566	281.66	0.365	-0.315	4969.9	500.00	1.60	4.45	44.56	-1.13	-1.08	-55	-57	2331-2323	-0	0	1
0.0567	282.16	0.367	-0.315	4969.9	500.00	1.52	4.45	44.77	-1.17	-0.97	-55	-57	2331-2323	-0	0	1
0.0568	282.66	0.369	-0.315	4969.9	500.00	1.44	4.45	44.83	-1.15	-0.89	-55	-57	2331-2323	-0	0	1
0.0569	283.15	0.372	-0.314	4969.7	500.00	1.35	4.45	44.15	-1.13	-0.74	-55	-57	2331-2323	-0	0	1
0.0570	283.65	0.373	-0.314	4969.7	500.00	1.28	4.45	43.35	-1.11	-0.63	-55	-57	2331-2323	-0	0	1
0.0571	284.15	0.375	-0.314	4969.7	500.00	1.21	4.45	42.85	-1.00	-0.52	-55	-57	2331-2323	-0	0	1
0.0572	284.64	0.377	-0.314	4969.7	500.00	1.16	4.45	42.58	-0.94	-0.43	-55	-57	2331-2323	-0	0	1
0.0573	285.14	0.379	-0.314	4969.7	500.00	1.13	4.45	39.73	-1.14	-0.34	-55	-57	2331-2323	-0	0	1
0.0574	285.64	0.381	-0.314	4969.7	500.00	1.12	4.45	35.70	-1.07	-0.25	-55	-57	2331-2323	-0	0	1
0.0575	286.13	0.382	-0.314	4969.7	500.00	1.17	4.45	34.11	-1.11	-0.20	-55	-57	2331-2323	-0	0	1
0.0576	286.63	0.384	-0.313	4969.7	500.00	1.15	4.45	30.37	-1.14	-0.14	-55	-57	2331-2323	-0	0	1
0.0577	287.13	0.386	-0.313	4969.7	500.00	1.16	4.45	32.53	-1.16	-0.10	-55	-57	2331-2323	-0	0	1
0.0578	287.62	0.387	-0.313	4969.7	500.00	1.23	4.45	35.15	-1.23	-0.07	-55	-57	2331-2323	-0	0	1
0.0579	288.12	0.389	-0.313	4969.7	500.00	1.25	4.45	41.52	-1.22	-0.34	-55	-57	2331-2323	-0	0	1
0.0580	288.62	0.391	-0.313	4969.7	500.00	1.35	4.45	43.21	-1.31	-0.02	-55	-57	2331-2323	-0	0	1
0.0581	289.11	0.392	-0.312	4969.7	500.00	1.51	4.45	45.23	-1.41	-0.09	-55	-57	2331-2323	-0	0	1
0.0582	289.61	0.394	-0.312	4969.6	500.00	1.57	4.45	47.40	-1.47	0.02	-55	-57	2331-2323	-0	0	1
0.0583	290.11	0.395	-0.312	4969.6	500.00	1.52	4.45	49.46	-1.52	0.06	-55	-57	2331-2323	-0	0	1
0.0584	290.60	0.397	-0.312	4969.6	500.00	1.57	4.45	51.37	-1.57	0.07	-55	-57	2331-2323	-0	0	1
0.0585	291.10	0.398	-0.312	4969.6	500.00	1.60	4.45	53.33	-1.59	0.10	-55	-57	2331-2323	-0	0	1
0.0586	291.60	0.399	-0.312	4969.6	500.00	1.62	4.45	54.37	-1.42	0.15	-55	-57	2331-2323	-0	0	1
0.0587	292.09	0.399	-0.312	4969.6	500.00	1.53	4.45	55.34	-1.42	0.20	-55	-57	2331-2323	-0	0	1
0.0588	292.59	0.397	-0.311	4969.6	500.00	1.53	4.45	55.86	-1.61	0.27	-55	-57	2331-2323	-0	0	1
0.0589	293.09	0.393	-0.311	4969.5	500.00	1.62	4.45	55.87	-1.69	0.34	-55	-57	2331-2323	-0	0	1
0.0590	293.58	0.394	-0.311	4969.5	500.00	1.66	4.45	55.35	-1.73	0.43	-55	-57	2331-2323	-0	0	1
0.0591	294.08	0.395	-0.311	4969.5	500.00	1.53	4.45	52.57	-1.43	0.63	-55	-57	2331-2323	-0	0	1
0.0592	294.58	0.397	-0.311	4969.5	500.00	1.59	4.45	53.38	-1.31	0.73	-55	-57	2331-2323	-0	0	1
0.0593	295.08	0.399	-0.310	4969.5	500.00	1.48	4.45	47.40	-1.21	0.84	-55	-57	2331-2323	-0	0	1
0.0594	295.57	0.399	-0.310	4969.5	500.00	1.45	4.45	44.97	-1.11	0.95	-55	-57	2331-2323	-0	0	1
0.0595	296.07	0.399	-0.310	4969.5	500.00	1.45	4.45	42.12	-1.01	1.05	-55	-57	2331-2323	-0	0	1
0.0596	296.57	0.399	-0.310	4969.5	500.00	1.46	4.45	39.47	-0.91	1.15	-55	-57	2331-2323	-0	0	1
0.0597	297.05	0.399	-0.310	4969.4	500.00	1.47	4.45	37.22	-0.61	1.23	-55	-57	2331-2323	-0	0	1
0.0598	297.56	0.399	-0.310	4969.4	500.00	1.49	4.45	35.50	-0.71	1.31	-55	-57	2331-2323	-0	0	1
0.0599	298.06	0.399	-0.310	4969.4	500.00	1.49	4.45	35.50	-0.71	1.31	-55	-57	2331-2323	-0	0	1

## FLECHETTE GROUND POINT

PAGE 13

T SEC	X FT	Y FT	Z FT	V FT/SEC	P RAD/SEC	ALPHA DEG	PHI DEG	ALPHA DEG	BETA DEG	I-M 1/SEC	L-P 1/SEC	4-5 RAD/SEC	W-P RAD/SEC	S I40	K-1 C/G
0.0400	298.55	0.314	-0.310	4569.4	500.00	1.51	4.45	34.39	-0.53	1.37	-55.	-57.	2331-2328	-0.	1.
0.0401	299.05	0.915	-0.310	4569.4	500.00	1.52	4.45	33.42	-0.54	1.42	-55.	-57.	2331-2328	-0.	1.
0.0402	299.55	0.915	-0.311	4569.4	500.00	1.53	4.45	34.39	-0.53	1.35	-55.	-57.	2331-2328	-0.	1.
0.0603	300.04	0.917	-0.311	4569.4	500.00	1.53	4.45	34.39	-0.54	1.37	-55.	-57.	2331-2328	-0.	1.
0.0604	300.54	0.918	-0.311	4569.4	500.00	1.53	4.45	34.39	-0.53	1.37	-55.	-57.	2331-2328	-0.	1.
0.0605	301.04	0.919	-0.311	4569.4	500.00	1.52	4.45	34.39	-0.53	1.37	-55.	-57.	2331-2328	-0.	1.
0.0606	301.53	0.919	-0.311	4569.4	500.00	1.54	4.45	34.39	-0.53	1.46	-55.	-57.	2331-2328	-0.	1.
0.0607	302.03	0.920	-0.312	4569.4	500.00	1.57	4.45	41.53	-0.51	1.44	-55.	-57.	2331-2328	-0.	1.
0.0608	302.53	0.921	-0.312	4569.4	500.00	1.54	4.45	44.30	-0.52	1.41	-55.	-57.	2331-2328	-0.	1.
0.0609	303.02	0.922	-0.313	4569.4	500.00	1.41	4.45	46.54	-0.57	1.38	-55.	-57.	2331-2328	-0.	1.
0.0610	303.52	0.923	-0.313	4569.4	500.00	1.37	4.45	43.27	-0.55	1.35	-55.	-57.	2331-2328	-0.	1.
0.0611	304.02	0.923	-0.313	4569.4	500.00	1.34	4.45	41.64	-0.53	1.32	-55.	-57.	2331-2328	-0.	1.
0.0612	304.52	0.924	-0.314	4569.4	500.00	1.33	4.45	42.53	-0.53	1.29	-55.	-57.	2331-2328	-0.	1.
0.0613	305.01	0.925	-0.315	4569.4	500.00	1.26	4.45	53.79	-0.15	1.27	-55.	-57.	2331-2328	-0.	1.
0.0614	305.51	0.926	-0.315	4569.4	500.00	1.26	4.45	54.37	-0.13	1.25	-55.	-57.	2331-2328	-0.	1.
0.0615	306.01	0.927	-0.316	4569.4	500.00	1.24	4.45	54.35	-0.07	1.24	-55.	-57.	2331-2328	-0.	1.
0.0616	306.50	0.927	-0.316	4569.4	500.00	1.24	4.45	53.77	0.05	1.24	-55.	-57.	2331-2328	-0.	1.
0.0617	307.00	0.927	-0.317	4569.4	500.00	1.25	4.45	52.72	0.12	1.24	-55.	-57.	2331-2328	-0.	1.
0.0618	307.50	0.928	-0.318	4569.4	500.00	1.27	4.45	51.35	0.22	1.25	-55.	-57.	2331-2328	-0.	1.
0.0619	307.99	0.930	-0.318	4569.4	500.00	1.30	4.45	49.53	0.32	1.26	-55.	-57.	2331-2328	-0.	1.
0.0620	308.49	0.930	-0.315	4569.4	500.00	1.35	4.45	48.34	0.53	1.28	-55.	-57.	2331-2328	-0.	1.
0.0621	308.99	0.931	-0.320	4569.4	500.00	1.40	4.45	47.02	0.56	1.30	-55.	-57.	2331-2328	-0.	1.
0.0622	309.48	0.932	-0.321	4569.4	500.00	1.46	4.45	45.54	0.55	1.31	-55.	-57.	2331-2328	-0.	1.
0.0623	309.98	0.933	-0.321	4569.4	500.00	1.52	4.45	45.16	0.77	1.31	-55.	-57.	2331-2328	-0.	1.
0.0624	310.48	0.934	-0.322	4569.4	500.00	1.57	4.45	44.44	0.55	1.30	-55.	-57.	2331-2328	-0.	1.
0.0625	311.47	0.935	-0.324	4569.4	500.00	1.67	4.45	43.43	1.15	1.25	-55.	-57.	2331-2328	-0.	1.
0.0626	311.97	0.936	-0.325	4569.4	500.00	1.48	4.45	43.52	1.16	1.25	-55.	-57.	2331-2328	-0.	1.
0.0627	312.46	0.937	-0.326	4569.4	500.00	1.71	4.45	44.35	1.21	1.21	-55.	-57.	2331-2328	-0.	1.
0.0628	312.96	0.938	-0.327	4569.4	500.00	1.71	4.45	45.16	1.26	1.15	-55.	-57.	2331-2328	-0.	1.
0.0629	313.46	0.939	-0.328	4569.4	500.00	1.66	4.45	45.47	1.30	1.17	-55.	-57.	2331-2328	-0.	1.
0.0630	313.96	0.939	-0.329	4569.4	500.00	1.57	4.45	45.72	1.33	1.01	-55.	-57.	2331-2328	-0.	1.
0.0631	314.45	0.940	-0.329	4569.4	500.00	1.63	4.45	45.45	1.35	0.92	-55.	-57.	2331-2328	-0.	1.
0.0632	314.95	0.941	-0.331	4569.4	500.00	1.58	4.45	45.31	1.39	0.93	-55.	-57.	2331-2328	-0.	1.
0.0633	315.45	0.942	-0.332	4569.4	500.00	1.56	4.45	45.31	1.39	0.93	-55.	-57.	2331-2328	-0.	1.
0.0634	315.95	0.943	-0.333	4569.4	500.00	1.57	4.45	45.57	1.34	0.73	-55.	-57.	2331-2328	-0.	1.
0.0635	316.44	0.945	-0.336	4569.4	500.00	1.47	4.45	45.03	1.33	0.62	-55.	-57.	2331-2328	-0.	1.
0.0636	316.94	0.946	-0.335	4569.4	500.00	1.41	4.45	44.34	1.31	0.52	-55.	-57.	2331-2328	-0.	1.
0.0637	317.44	0.947	-0.337	4569.4	500.00	1.36	4.45	43.63	1.26	0.41	-55.	-57.	2331-2328	-0.	1.
0.0638	317.94	0.948	-0.339	4569.4	500.00	1.31	4.45	43.35	1.23	0.31	-55.	-57.	2331-2328	-0.	1.
0.0639	318.43	0.949	-0.340	4569.4	500.00	1.29	4.45	43.22	1.23	0.22	-55.	-57.	2331-2328	-0.	1.
0.0640	318.92	0.951	-0.340	4569.4	500.00	1.27	4.45	43.18	1.23	0.13	-55.	-57.	2331-2328	-0.	1.
0.0641	319.42	0.953	-0.342	4569.4	500.00	1.25	4.45	43.35	1.25	0.05	-55.	-57.	2331-2328	-0.	1.
0.0642	319.92	0.954	-0.343	4569.4	500.00	1.25	4.45	43.88	1.25	0.02	-55.	-57.	2331-2328	-0.	1.
0.0643	320.41	0.955	-0.341	4569.4	500.00	1.26	4.45	43.82	1.25	0.05	-55.	-57.	2331-2328	-0.	1.
0.0644	320.91	0.957	-0.345	4569.4	500.00	1.27	4.45	43.21	1.27	0.15	-55.	-57.	2331-2328	-0.	1.
0.0645	321.41	0.958	-0.347	4569.4	500.00	1.31	4.45	43.04	1.23	0.17	-55.	-57.	2331-2328	-0.	1.
0.0646	321.91	0.960	-0.349	4569.4	500.00	1.34	4.45	43.24	1.37	0.24	-55.	-57.	2331-2328	-0.	1.
0.0647	322.40	0.962	-0.349	4569.4	500.00	1.37	4.45	42.73	1.35	0.22	-55.	-57.	2331-2328	-0.	1.
0.0648	322.90	0.963	-0.350	4569.4	500.00	1.40	4.45	42.42	1.37	0.21	-55.	-57.	2331-2328	-0.	1.
0.0649	323.40	0.965	-0.351	4569.4	500.00	1.40	4.45	42.19	1.39	0.24	-55.	-57.	2331-2328	-0.	1.

## FLECHETTE GROUND POINT

PAGE 11

T SEC	X FT	Y FT	Z FT	V FT/SEC	P RAT/SEC	ALPHA MACH	PHI DEG	ALPHA DEG	BETA DEG	L-N 1/500	L-P 1/500	M-N 1/500	M-P 1/500	S TAU	K-T DEG
0.0650	323.39	0.966	-0.353	4568.9	500.00	1.47 4.45	37.69	1.42	-0.39	-55.	-57.	2332.-2323.	-0.	0.	1.
0.0651	323.89	0.968	-0.354	4568.9	500.00	1.49 4.45	39.62	1.43	-0.42	-53.	-57.	2332.-2323.	-0.	0.	1.
0.0652	324.38	0.970	-0.355	4568.8	500.00	1.51 4.45	41.10	1.44	-0.45	-50.	-57.	2332.-2323.	-0.	0.	1.
0.0653	324.89	0.972	-0.356	4568.8	500.00	1.52 4.45	42.32	1.44	-0.50	-55.	-57.	2332.-2323.	-0.	0.	1.
0.0654	325.38	0.973	-0.357	4568.8	500.00	1.53 4.45	43.21	1.42	-0.55	-56.	-57.	2332.-2323.	-0.	0.	1.
0.0655	325.88	0.975	-0.358	4568.8	500.00	1.53 4.45	43.73	1.42	-0.51	-55.	-57.	2332.-2323.	-0.	0.	1.
0.0656	326.38	0.977	-0.360	4568.8	500.00	1.52 4.45	45.93	1.43	-0.67	-55.	-57.	2332.-2323.	-0.	0.	1.
0.0657	326.87	0.977	-0.361	4568.8	500.00	1.51 4.45	48.49	1.43	-0.74	-55.	-57.	2332.-2323.	-0.	0.	1.
0.0658	327.37	0.981	-0.362	4568.8	500.00	1.49 4.45	52.69	1.43	-0.82	-55.	-57.	2332.-2323.	-0.	0.	1.
0.0659	327.87	0.983	-0.363	4568.8	500.00	1.48 4.45	51.63	1.43	-0.93	-55.	-57.	2332.-2323.	-0.	0.	1.
0.0660	328.36	0.985	-0.364	4568.7	500.00	1.47 4.45	49.91	1.42	-0.97	-55.	-57.	2332.-2323.	-0.	0.	1.
0.0661	328.85	0.987	-0.365	4568.7	500.00	1.46 4.45	48.07	1.41	-1.05	-55.	-57.	2332.-2323.	-0.	0.	1.
0.0662	329.35	0.989	-0.366	4568.7	500.00	1.45 4.45	46.09	1.41	-1.15	-55.	-57.	2332.-2323.	-0.	0.	1.
0.0663	329.85	0.991	-0.367	4568.7	500.00	1.44 4.45	44.11	1.42	-1.21	-55.	-57.	2332.-2323.	-0.	0.	1.
0.0664	330.35	0.993	-0.369	4568.7	500.00	1.43 4.45	42.27	1.42	-1.28	-55.	-57.	2332.-2323.	-0.	0.	1.
0.0665	330.85	0.994	-0.369	4568.7	500.00	1.42 4.45	40.53	1.42	-1.35	-55.	-57.	2332.-2323.	-0.	0.	1.
0.0666	331.34	0.995	-0.371	4568.7	500.00	1.40 4.45	38.44	1.43	-1.43	-55.	-57.	2332.-2323.	-0.	0.	1.
0.0667	331.84	1.000	-0.371	4568.7	500.00	1.38 4.45	36.69	1.43	-1.49	-55.	-57.	2332.-2323.	-0.	0.	1.
0.0668	332.34	1.002	-0.371	4568.7	500.00	1.37 4.45	35.15	1.43	-1.49	-55.	-57.	2332.-2323.	-0.	0.	1.
0.0669	332.83	1.004	-0.372	4568.6	500.00	1.36 4.45	33.12	1.43	-1.51	-55.	-57.	2332.-2323.	-0.	0.	1.
0.0670	333.33	1.006	-0.373	4568.6	500.00	1.35 4.45	31.47	1.42	-1.52	-55.	-57.	2332.-2323.	-0.	0.	1.
0.0671	333.83	1.009	-0.374	4568.6	500.00	1.34 4.45	30.15	1.45	-1.53	-55.	-57.	2332.-2323.	-0.	0.	1.
0.0672	334.32	1.011	-0.375	4568.6	500.00	1.33 4.45	29.12	1.41	-1.52	-55.	-57.	2332.-2323.	-0.	0.	1.
0.0673	334.82	1.013	-0.375	4568.5	500.00	1.31 4.45	27.30	1.41	-1.51	-55.	-57.	2332.-2323.	-0.	0.	1.
0.0674	335.32	1.015	-0.376	4568.5	500.00	1.29 4.45	25.42	1.42	-1.59	-55.	-57.	2332.-2323.	-0.	0.	1.
0.0675	335.82	1.017	-0.376	4568.5	500.00	1.28 4.45	24.42	1.42	-1.59	-55.	-57.	2332.-2323.	-0.	0.	1.
0.0676	336.31	1.020	-0.377	4568.5	500.00	1.27 4.45	23.43	1.42	-1.59	-55.	-57.	2332.-2323.	-0.	0.	1.
0.0677	336.81	1.022	-0.377	4568.5	500.00	1.26 4.45	22.43	1.42	-1.59	-55.	-57.	2332.-2323.	-0.	0.	1.
0.0678	337.31	1.024	-0.377	4568.5	500.00	1.25 4.45	21.43	1.42	-1.59	-55.	-57.	2332.-2323.	-0.	0.	1.
0.0679	337.80	1.026	-0.378	4568.5	500.00	1.24 4.45	20.43	1.42	-1.59	-55.	-57.	2332.-2323.	-0.	0.	1.
0.0680	338.30	1.027	-0.378	4568.5	500.00	1.23 4.45	19.43	1.42	-1.59	-55.	-57.	2332.-2323.	-0.	0.	1.
0.0681	338.80	1.031	-0.379	4568.5	500.00	1.22 4.45	18.43	1.42	-1.59	-55.	-57.	2332.-2323.	-0.	0.	1.
0.0682	339.29	1.033	-0.379	4568.5	500.00	1.21 4.45	17.43	1.42	-1.59	-55.	-57.	2332.-2323.	-0.	0.	1.
0.0683	340.79	1.035	-0.379	4568.5	500.00	1.20 4.45	16.43	1.42	-1.59	-55.	-57.	2332.-2323.	-0.	0.	1.
0.0684	341.28	1.037	-0.379	4568.5	500.00	1.19 4.45	15.43	1.42	-1.59	-55.	-57.	2332.-2323.	-0.	0.	1.
0.0685	341.78	1.041	-0.380	4568.4	500.00	1.18 4.45	14.43	1.42	-1.59	-55.	-57.	2332.-2323.	-0.	0.	1.
0.0686	342.27	1.044	-0.380	4568.4	500.00	1.17 4.45	13.43	1.42	-1.59	-55.	-57.	2332.-2323.	-0.	0.	1.
0.0687	342.77	1.046	-0.380	4568.4	500.00	1.16 4.45	12.43	1.42	-1.59	-55.	-57.	2332.-2323.	-0.	0.	1.
0.0688	343.27	1.048	-0.380	4568.4	500.00	1.15 4.45	11.43	1.42	-1.59	-55.	-57.	2332.-2323.	-0.	0.	1.
0.0689	343.76	1.052	-0.381	4568.4	500.00	1.14 4.45	10.43	1.42	-1.59	-55.	-57.	2332.-2323.	-0.	0.	1.
0.0690	344.26	1.054	-0.381	4568.4	500.00	1.13 4.45	9.43	1.42	-1.59	-55.	-57.	2332.-2323.	-0.	0.	1.
0.0691	344.76	1.056	-0.381	4568.4	500.00	1.12 4.45	8.43	1.42	-1.59	-55.	-57.	2332.-2323.	-0.	0.	1.
0.0692	345.25	1.058	-0.381	4568.4	500.00	1.11 4.45	7.43	1.42	-1.59	-55.	-57.	2332.-2323.	-0.	0.	1.
0.0693	345.75	1.061	-0.381	4568.4	500.00	1.10 4.45	6.43	1.42	-1.59	-55.	-57.	2332.-2323.	-0.	0.	1.
0.0694	346.25	1.063	-0.381	4568.3	500.00	1.09 4.45	5.43	1.42	-1.59	-55.	-57.	2332.-2323.	-0.	0.	1.
0.0695	346.75	1.065	-0.381	4568.3	500.00	1.08 4.45	4.43	1.42	-1.59	-55.	-57.	2332.-2323.	-0.	0.	1.
0.0696	347.24	1.067	-0.381	4568.3	500.00	1.07 4.45	3.43	1.42	-1.59	-55.	-57.	2332.-2323.	-0.	0.	1.
0.0697	347.74	1.069	-0.381	4568.3	500.00	1.06 4.45	2.43	1.42	-1.59	-55.	-57.	2332.-2323.	-0.	0.	1.
0.0698	348.24	1.071	-0.381	4568.3	500.00	1.05 4.45	1.43	1.42	-1.59	-55.	-57.	2332.-2323.	-0.	0.	1.
0.0699	348.74	1.073	-0.381	4568.3	500.00	1.04 4.45	0.43	1.42	-1.59	-55.	-57.	2332.-2323.	-0.	0.	1.

FLECHETTE GROUND POINT

PAGE 13

T SEC	X FT	Y FT	Z FT	V FT/SEC	P PAR/SEC	ALPHA NACH DEG	PRI DEG	ALPHA DEG	BETA DEG	1/SEC 1/SEC	1/SEC 1/SEC	W-F 40/SEC	S 40/SEC	IAU S	M-T DEG
0.0700	349.24	1.049	-0.377	4648.3	500.00	1.55 4.45	46.57	-1.43	0.54	-55	-57	2332-2329	-0	0	1
0.0701	348.71	1.071	-0.377	4648.3	500.00	1.51 4.45	46.18	-1.44	0.54	-55	-57	2332-2329	-0	0	1
0.0702	348.23	1.072	-0.377	4648.3	500.00	1.47 4.45	45.80	-1.43	0.54	-55	-57	2332-2329	-0	0	1
0.0703	347.73	1.074	-0.377	4648.3	500.00	1.44 4.45	45.42	-1.42	0.54	-55	-57	2332-2329	-0	0	1
0.0704	347.22	1.076	-0.377	4648.3	500.00	1.41 4.45	45.04	-1.41	0.54	-55	-57	2332-2329	-0	0	1
0.0705	346.72	1.077	-0.377	4648.3	500.00	1.38 4.45	44.66	-1.40	0.54	-55	-57	2332-2329	-0	0	1
0.0706	346.21	1.078	-0.377	4648.3	500.00	1.35 4.45	44.28	-1.39	0.54	-55	-57	2332-2329	-0	0	1
0.0707	345.71	1.079	-0.377	4648.3	500.00	1.32 4.45	43.90	-1.38	0.54	-55	-57	2332-2329	-0	0	1
0.0708	345.21	1.081	-0.377	4648.3	500.00	1.29 4.45	43.52	-1.37	0.54	-55	-57	2332-2329	-0	0	1
0.0709	344.70	1.082	-0.377	4648.3	500.00	1.26 4.45	43.14	-1.36	0.54	-55	-57	2332-2329	-0	0	1
0.0710	344.20	1.084	-0.377	4648.3	500.00	1.23 4.45	42.76	-1.35	0.54	-55	-57	2332-2329	-0	0	1
0.0711	343.70	1.085	-0.377	4648.3	500.00	1.20 4.45	42.38	-1.34	0.54	-55	-57	2332-2329	-0	0	1
0.0712	343.19	1.087	-0.377	4648.3	500.00	1.17 4.45	42.00	-1.33	0.54	-55	-57	2332-2329	-0	0	1
0.0713	342.69	1.088	-0.377	4648.3	500.00	1.14 4.45	41.62	-1.32	0.54	-55	-57	2332-2329	-0	0	1
0.0714	342.19	1.089	-0.377	4648.3	500.00	1.11 4.45	41.24	-1.31	0.54	-55	-57	2332-2329	-0	0	1
0.0715	341.68	1.091	-0.377	4648.3	500.00	1.08 4.45	40.86	-1.30	0.54	-55	-57	2332-2329	-0	0	1
0.0716	341.18	1.092	-0.377	4648.3	500.00	1.05 4.45	40.48	-1.29	0.54	-55	-57	2332-2329	-0	0	1
0.0717	340.68	1.093	-0.377	4648.3	500.00	1.02 4.45	40.10	-1.28	0.54	-55	-57	2332-2329	-0	0	1
0.0718	340.17	1.094	-0.377	4648.3	500.00	0.99 4.45	39.72	-1.27	0.54	-55	-57	2332-2329	-0	0	1
0.0719	339.67	1.095	-0.377	4648.3	500.00	0.96 4.45	39.34	-1.26	0.54	-55	-57	2332-2329	-0	0	1
0.0720	339.17	1.096	-0.377	4648.3	500.00	0.93 4.45	38.96	-1.25	0.54	-55	-57	2332-2329	-0	0	1
0.0721	338.66	1.097	-0.377	4648.3	500.00	0.90 4.45	38.58	-1.24	0.54	-55	-57	2332-2329	-0	0	1
0.0722	338.15	1.098	-0.377	4648.3	500.00	0.87 4.45	38.20	-1.23	0.54	-55	-57	2332-2329	-0	0	1
0.0723	337.65	1.099	-0.377	4648.3	500.00	0.84 4.45	37.82	-1.22	0.54	-55	-57	2332-2329	-0	0	1
0.0724	337.15	1.100	-0.377	4648.3	500.00	0.81 4.45	37.44	-1.21	0.54	-55	-57	2332-2329	-0	0	1
0.0725	336.65	1.101	-0.377	4648.3	500.00	0.78 4.45	37.06	-1.20	0.54	-55	-57	2332-2329	-0	0	1
0.0726	336.14	1.102	-0.377	4648.3	500.00	0.75 4.45	36.68	-1.19	0.54	-55	-57	2332-2329	-0	0	1
0.0727	335.64	1.103	-0.377	4648.3	500.00	0.72 4.45	36.30	-1.18	0.54	-55	-57	2332-2329	-0	0	1
0.0728	335.14	1.104	-0.377	4648.3	500.00	0.69 4.45	35.92	-1.17	0.54	-55	-57	2332-2329	-0	0	1
0.0729	334.64	1.105	-0.377	4648.3	500.00	0.66 4.45	35.54	-1.16	0.54	-55	-57	2332-2329	-0	0	1
0.0730	334.13	1.106	-0.377	4648.3	500.00	0.63 4.45	35.16	-1.15	0.54	-55	-57	2332-2329	-0	0	1
0.0731	333.63	1.107	-0.377	4648.3	500.00	0.60 4.45	34.78	-1.14	0.54	-55	-57	2332-2329	-0	0	1
0.0732	333.13	1.108	-0.377	4648.3	500.00	0.57 4.45	34.40	-1.13	0.54	-55	-57	2332-2329	-0	0	1
0.0733	332.62	1.109	-0.377	4648.3	500.00	0.54 4.45	34.02	-1.12	0.54	-55	-57	2332-2329	-0	0	1
0.0734	332.12	1.110	-0.377	4648.3	500.00	0.51 4.45	33.64	-1.11	0.54	-55	-57	2332-2329	-0	0	1
0.0735	331.62	1.111	-0.377	4648.3	500.00	0.48 4.45	33.26	-1.10	0.54	-55	-57	2332-2329	-0	0	1
0.0736	331.11	1.112	-0.377	4648.3	500.00	0.45 4.45	32.88	-1.09	0.54	-55	-57	2332-2329	-0	0	1
0.0737	330.61	1.113	-0.377	4648.3	500.00	0.42 4.45	32.50	-1.08	0.54	-55	-57	2332-2329	-0	0	1
0.0738	330.11	1.114	-0.377	4648.3	500.00	0.39 4.45	32.12	-1.07	0.54	-55	-57	2332-2329	-0	0	1
0.0739	329.61	1.115	-0.377	4648.3	500.00	0.36 4.45	31.74	-1.06	0.54	-55	-57	2332-2329	-0	0	1
0.0740	329.11	1.116	-0.377	4648.3	500.00	0.33 4.45	31.36	-1.05	0.54	-55	-57	2332-2329	-0	0	1
0.0741	328.60	1.117	-0.377	4648.3	500.00	0.30 4.45	30.98	-1.04	0.54	-55	-57	2332-2329	-0	0	1
0.0742	328.10	1.118	-0.377	4648.3	500.00	0.27 4.45	30.60	-1.03	0.54	-55	-57	2332-2329	-0	0	1
0.0743	327.59	1.119	-0.377	4648.3	500.00	0.24 4.45	30.22	-1.02	0.54	-55	-57	2332-2329	-0	0	1
0.0744	327.09	1.120	-0.377	4648.3	500.00	0.21 4.45	29.84	-1.01	0.54	-55	-57	2332-2329	-0	0	1
0.0745	326.58	1.121	-0.377	4648.3	500.00	0.18 4.45	29.46	-1.00	0.54	-55	-57	2332-2329	-0	0	1
0.0746	326.08	1.122	-0.377	4648.3	500.00	0.15 4.45	29.08	-0.99	0.54	-55	-57	2332-2329	-0	0	1
0.0747	325.57	1.123	-0.377	4648.3	500.00	0.12 4.45	28.70	-0.98	0.54	-55	-57	2332-2329	-0	0	1
0.0748	325.07	1.124	-0.377	4648.3	500.00	0.09 4.45	28.32	-0.97	0.54	-55	-57	2332-2329	-0	0	1
0.0749	324.57	1.125	-0.377	4648.3	500.00	0.06 4.45	27.94	-0.96	0.54	-55	-57	2332-2329	-0	0	1

## FLECHETTE GROUND POINT

PAGE 16

SEC	T	X	Y	Z	V	P	ALPHA	MACH	PHI	ALPHA	PETA	LOV	1/SEC	1/SEC	PAR/SEC	PAR/SEC	S	TAU	K-T
SEC	FT	FT	FT	FT	FT/SEC	PAR/SEC	DEG	DEG	DEG	DEG	DEG	DEG	DEG	DEG	DEG	DEG	DEG	DEG	DEG
0.0750	373.06	1.121	-0.352	4967.7	500.00	1.31	4.45	47.14	0.70	1.11	-55	-57	2332	-2325	-0	0	0	0	0
0.0751	373.56	1.122	-0.359	4967.7	500.00	1.32	4.45	46.90	0.70	1.11	-55	-57	2332	-2325	-0	0	0	0	0
0.0752	374.06	1.123	-0.365	4967.7	500.00	1.33	4.45	46.65	0.70	1.11	-55	-57	2332	-2325	-0	0	0	0	0
0.0753	374.55	1.124	-0.371	4967.7	500.00	1.34	4.45	46.40	0.70	1.11	-55	-57	2332	-2325	-0	0	0	0	0
0.0754	375.05	1.125	-0.377	4967.7	500.00	1.35	4.45	46.15	0.70	1.11	-55	-57	2332	-2325	-0	0	0	0	0
0.0755	375.55	1.126	-0.383	4967.7	500.00	1.36	4.45	45.90	0.70	1.11	-55	-57	2332	-2325	-0	0	0	0	0
0.0756	376.04	1.127	-0.389	4967.7	500.00	1.37	4.45	45.65	0.70	1.11	-55	-57	2332	-2325	-0	0	0	0	0
0.0757	376.54	1.128	-0.395	4967.7	500.00	1.38	4.45	45.40	0.70	1.11	-55	-57	2332	-2325	-0	0	0	0	0
0.0758	377.04	1.129	-0.401	4967.7	500.00	1.39	4.45	45.15	0.70	1.11	-55	-57	2332	-2325	-0	0	0	0	0
0.0759	377.53	1.130	-0.407	4967.7	500.00	1.40	4.45	44.90	0.70	1.11	-55	-57	2332	-2325	-0	0	0	0	0
0.0760	378.03	1.131	-0.413	4967.7	500.00	1.41	4.45	44.65	0.70	1.11	-55	-57	2332	-2325	-0	0	0	0	0
0.0761	378.53	1.132	-0.419	4967.7	500.00	1.42	4.45	44.40	0.70	1.11	-55	-57	2332	-2325	-0	0	0	0	0
0.0762	379.02	1.133	-0.425	4967.7	500.00	1.43	4.45	44.15	0.70	1.11	-55	-57	2332	-2325	-0	0	0	0	0
0.0763	379.52	1.134	-0.431	4967.7	500.00	1.44	4.45	43.90	0.70	1.11	-55	-57	2332	-2325	-0	0	0	0	0
0.0764	380.02	1.135	-0.437	4967.7	500.00	1.45	4.45	43.65	0.70	1.11	-55	-57	2332	-2325	-0	0	0	0	0
0.0765	380.51	1.136	-0.443	4967.7	500.00	1.46	4.45	43.40	0.70	1.11	-55	-57	2332	-2325	-0	0	0	0	0
0.0766	381.01	1.137	-0.449	4967.7	500.00	1.47	4.45	43.15	0.70	1.11	-55	-57	2332	-2325	-0	0	0	0	0
0.0767	381.51	1.138	-0.455	4967.7	500.00	1.48	4.45	42.90	0.70	1.11	-55	-57	2332	-2325	-0	0	0	0	0
0.0768	382.00	1.139	-0.461	4967.7	500.00	1.49	4.45	42.65	0.70	1.11	-55	-57	2332	-2325	-0	0	0	0	0
0.0769	382.50	1.140	-0.467	4967.7	500.00	1.50	4.45	42.40	0.70	1.11	-55	-57	2332	-2325	-0	0	0	0	0
0.0770	383.00	1.141	-0.473	4967.7	500.00	1.51	4.45	42.15	0.70	1.11	-55	-57	2332	-2325	-0	0	0	0	0
0.0771	383.49	1.142	-0.479	4967.7	500.00	1.52	4.45	41.90	0.70	1.11	-55	-57	2332	-2325	-0	0	0	0	0
0.0772	383.99	1.143	-0.485	4967.7	500.00	1.53	4.45	41.65	0.70	1.11	-55	-57	2332	-2325	-0	0	0	0	0
0.0773	384.49	1.144	-0.491	4967.7	500.00	1.54	4.45	41.40	0.70	1.11	-55	-57	2332	-2325	-0	0	0	0	0
0.0774	384.98	1.145	-0.497	4967.7	500.00	1.55	4.45	41.15	0.70	1.11	-55	-57	2332	-2325	-0	0	0	0	0
0.0775	385.48	1.146	-0.503	4967.7	500.00	1.56	4.45	40.90	0.70	1.11	-55	-57	2332	-2325	-0	0	0	0	0
0.0776	385.98	1.147	-0.509	4967.7	500.00	1.57	4.45	40.65	0.70	1.11	-55	-57	2332	-2325	-0	0	0	0	0
0.0777	386.47	1.148	-0.515	4967.7	500.00	1.58	4.45	40.40	0.70	1.11	-55	-57	2332	-2325	-0	0	0	0	0
0.0778	386.97	1.149	-0.521	4967.7	500.00	1.59	4.45	40.15	0.70	1.11	-55	-57	2332	-2325	-0	0	0	0	0
0.0779	387.47	1.150	-0.527	4967.7	500.00	1.60	4.45	39.90	0.70	1.11	-55	-57	2332	-2325	-0	0	0	0	0
0.0780	387.96	1.151	-0.533	4967.7	500.00	1.61	4.45	39.65	0.70	1.11	-55	-57	2332	-2325	-0	0	0	0	0
0.0781	388.45	1.152	-0.539	4967.7	500.00	1.62	4.45	39.40	0.70	1.11	-55	-57	2332	-2325	-0	0	0	0	0
0.0782	388.95	1.153	-0.545	4967.7	500.00	1.63	4.45	39.15	0.70	1.11	-55	-57	2332	-2325	-0	0	0	0	0
0.0783	389.44	1.154	-0.551	4967.7	500.00	1.64	4.45	38.90	0.70	1.11	-55	-57	2332	-2325	-0	0	0	0	0
0.0784	389.94	1.155	-0.557	4967.7	500.00	1.65	4.45	38.65	0.70	1.11	-55	-57	2332	-2325	-0	0	0	0	0
0.0785	390.44	1.156	-0.563	4967.7	500.00	1.66	4.45	38.40	0.70	1.11	-55	-57	2332	-2325	-0	0	0	0	0
0.0786	390.94	1.157	-0.569	4967.7	500.00	1.67	4.45	38.15	0.70	1.11	-55	-57	2332	-2325	-0	0	0	0	0
0.0787	391.44	1.158	-0.575	4967.7	500.00	1.68	4.45	37.90	0.70	1.11	-55	-57	2332	-2325	-0	0	0	0	0
0.0788	391.93	1.159	-0.581	4967.7	500.00	1.69	4.45	37.65	0.70	1.11	-55	-57	2332	-2325	-0	0	0	0	0
0.0789	392.43	1.160	-0.587	4967.7	500.00	1.70	4.45	37.40	0.70	1.11	-55	-57	2332	-2325	-0	0	0	0	0
0.0790	392.93	1.161	-0.593	4967.7	500.00	1.71	4.45	37.15	0.70	1.11	-55	-57	2332	-2325	-0	0	0	0	0
0.0791	393.42	1.162	-0.599	4967.7	500.00	1.72	4.45	36.90	0.70	1.11	-55	-57	2332	-2325	-0	0	0	0	0
0.0792	393.92	1.163	-0.605	4967.7	500.00	1.73	4.45	36.65	0.70	1.11	-55	-57	2332	-2325	-0	0	0	0	0
0.0793	394.42	1.164	-0.611	4967.7	500.00	1.74	4.45	36.40	0.70	1.11	-55	-57	2332	-2325	-0	0	0	0	0
0.0794	394.91	1.165	-0.617	4967.7	500.00	1.75	4.45	36.15	0.70	1.11	-55	-57	2332	-2325	-0	0	0	0	0
0.0795	395.41	1.166	-0.623	4967.7	500.00	1.76	4.45	35.90	0.70	1.11	-55	-57	2332	-2325	-0	0	0	0	0
0.0796	395.91	1.167	-0.629	4967.7	500.00	1.77	4.45	35.65	0.70	1.11	-55	-57	2332	-2325	-0	0	0	0	0
0.0797	396.40	1.168	-0.635	4967.7	500.00	1.78	4.45	35.40	0.70	1.11	-55	-57	2332	-2325	-0	0	0	0	0
0.0798	396.90	1.169	-0.641	4967.7	500.00	1.79	4.45	35.15	0.70	1.11	-55	-57	2332	-2325	-0	0	0	0	0
0.0799	397.40	1.170	-0.647	4967.7	500.00	1.80	4.45	34.90	0.70	1.11	-55	-57	2332	-2325	-0	0	0	0	0

COPY AVAILABLE TO ALL  
311 PERMIT FULLY LEGIBLE PRODUCTION



FLECHETTE GROUND POINT

PAGE 17

Y	X	Z	V	P	ALPHA	MACH	PHI	ALPHA	BETA	W	W-P	S	IAU	E-T
SEC	FT	FT	FT/SEC	KNOTS	DEG	DEG	DEG	DEG	DEG	W-P	W-P	S	IAU	E-T
0.0800	307.89	1.203	4957.2	500.00	1.46	7.45	43.64	0.02	-1.49	-55	-57	2332-2330	-0	0
0.0801	308.39	1.206	4967.2	500.00	1.50	7.45	43.23	-0.05	-1.50	-55	-57	2332-2330	-0	0
0.0802	308.89	1.208	4977.2	500.00	1.51	7.45	42.79	-0.15	-1.50	-55	-57	2332-2330	-0	0
0.0803	309.39	1.211	4987.2	500.00	1.51	7.45	42.34	-0.32	-1.50	-55	-57	2332-2330	-0	0
0.0804	309.89	1.212	4997.2	500.00	1.52	7.45	41.88	-0.57	-1.49	-55	-57	2332-2330	-0	0
0.0805	310.39	1.215	5007.2	500.00	1.52	7.45	41.41	-0.87	-1.47	-55	-57	2332-2330	-0	0
0.0806	310.89	1.217	5017.2	500.00	1.51	7.45	40.92	-1.20	-1.45	-55	-57	2332-2330	-0	0
0.0807	311.39	1.221	5027.2	500.00	1.50	7.45	40.42	-1.55	-1.42	-55	-57	2332-2330	-0	0
0.0808	311.89	1.223	5037.2	500.00	1.49	7.45	39.91	-1.90	-1.39	-55	-57	2332-2330	-0	0
0.0809	312.39	1.225	5047.2	500.00	1.47	7.45	39.39	-2.25	-1.34	-55	-57	2332-2330	-0	0
0.0810	312.89	1.227	5057.2	500.00	1.45	7.45	38.86	-2.59	-1.30	-55	-57	2332-2330	-0	0
0.0811	313.39	1.229	5067.2	500.00	1.43	7.45	38.33	-2.92	-1.25	-55	-57	2332-2330	-0	0
0.0812	313.89	1.230	5077.2	500.00	1.41	7.45	37.79	-3.24	-1.20	-55	-57	2332-2330	-0	0
0.0813	314.39	1.232	5087.2	500.00	1.39	7.45	37.24	-3.55	-1.15	-55	-57	2332-2330	-0	0
0.0814	314.89	1.233	5097.2	500.00	1.37	7.45	36.69	-3.85	-1.10	-55	-57	2332-2330	-0	0
0.0815	315.39	1.234	5107.2	500.00	1.35	7.45	36.14	-4.14	-1.05	-55	-57	2332-2330	-0	0
0.0816	315.89	1.235	5117.2	500.00	1.33	7.45	35.59	-4.42	-1.00	-55	-57	2332-2330	-0	0
0.0817	316.39	1.236	5127.2	500.00	1.31	7.45	35.04	-4.69	-0.95	-55	-57	2332-2330	-0	0
0.0818	316.89	1.237	5137.2	500.00	1.29	7.45	34.49	-4.95	-0.90	-55	-57	2332-2330	-0	0
0.0819	317.39	1.238	5147.2	500.00	1.27	7.45	33.94	-5.20	-0.85	-55	-57	2332-2330	-0	0
0.0820	317.89	1.239	5157.2	500.00	1.25	7.45	33.39	-5.44	-0.80	-55	-57	2332-2330	-0	0
0.0821	318.39	1.240	5167.2	500.00	1.23	7.45	32.84	-5.67	-0.75	-55	-57	2332-2330	-0	0
0.0822	318.89	1.241	5177.2	500.00	1.21	7.45	32.29	-5.89	-0.70	-55	-57	2332-2330	-0	0
0.0823	319.39	1.242	5187.2	500.00	1.19	7.45	31.74	-6.10	-0.65	-55	-57	2332-2330	-0	0
0.0824	319.89	1.243	5197.2	500.00	1.17	7.45	31.19	-6.30	-0.60	-55	-57	2332-2330	-0	0
0.0825	320.39	1.244	5207.2	500.00	1.15	7.45	30.64	-6.49	-0.55	-55	-57	2332-2330	-0	0
0.0826	320.89	1.245	5217.2	500.00	1.13	7.45	30.09	-6.67	-0.50	-55	-57	2332-2330	-0	0
0.0827	321.39	1.246	5227.2	500.00	1.11	7.45	29.54	-6.84	-0.45	-55	-57	2332-2330	-0	0
0.0828	321.89	1.247	5237.2	500.00	1.09	7.45	28.99	-7.00	-0.40	-55	-57	2332-2330	-0	0
0.0829	322.39	1.248	5247.2	500.00	1.07	7.45	28.44	-7.15	-0.35	-55	-57	2332-2330	-0	0
0.0830	322.89	1.249	5257.2	500.00	1.05	7.45	27.89	-7.29	-0.30	-55	-57	2332-2330	-0	0
0.0831	323.39	1.250	5267.2	500.00	1.03	7.45	27.34	-7.42	-0.25	-55	-57	2332-2330	-0	0
0.0832	323.89	1.251	5277.2	500.00	1.01	7.45	26.79	-7.54	-0.20	-55	-57	2332-2330	-0	0
0.0833	324.39	1.252	5287.2	500.00	0.99	7.45	26.24	-7.65	-0.15	-55	-57	2332-2330	-0	0
0.0834	324.89	1.253	5297.2	500.00	0.97	7.45	25.69	-7.75	-0.10	-55	-57	2332-2330	-0	0
0.0835	325.39	1.254	5307.2	500.00	0.95	7.45	25.14	-7.84	-0.05	-55	-57	2332-2330	-0	0
0.0836	325.89	1.255	5317.2	500.00	0.93	7.45	24.59	-7.92	0.00	-55	-57	2332-2330	-0	0
0.0837	326.39	1.256	5327.2	500.00	0.91	7.45	24.04	-8.00	0.05	-55	-57	2332-2330	-0	0
0.0838	326.89	1.257	5337.2	500.00	0.89	7.45	23.49	-8.07	0.10	-55	-57	2332-2330	-0	0
0.0839	327.39	1.258	5347.2	500.00	0.87	7.45	22.94	-8.13	0.15	-55	-57	2332-2330	-0	0
0.0840	327.89	1.259	5357.2	500.00	0.85	7.45	22.39	-8.18	0.20	-55	-57	2332-2330	-0	0
0.0841	328.39	1.260	5367.2	500.00	0.83	7.45	21.84	-8.22	0.25	-55	-57	2332-2330	-0	0
0.0842	328.89	1.261	5377.2	500.00	0.81	7.45	21.29	-8.25	0.30	-55	-57	2332-2330	-0	0
0.0843	329.39	1.262	5387.2	500.00	0.79	7.45	20.74	-8.27	0.35	-55	-57	2332-2330	-0	0
0.0844	329.89	1.263	5397.2	500.00	0.77	7.45	20.19	-8.28	0.40	-55	-57	2332-2330	-0	0
0.0845	330.39	1.264	5407.2	500.00	0.75	7.45	19.64	-8.28	0.45	-55	-57	2332-2330	-0	0
0.0846	330.89	1.265	5417.2	500.00	0.73	7.45	19.09	-8.27	0.50	-55	-57	2332-2330	-0	0
0.0847	331.39	1.266	5427.2	500.00	0.71	7.45	18.54	-8.25	0.55	-55	-57	2332-2330	-0	0
0.0848	331.89	1.267	5437.2	500.00	0.69	7.45	17.99	-8.22	0.60	-55	-57	2332-2330	-0	0
0.0849	332.39	1.268	5447.2	500.00	0.67	7.45	17.44	-8.18	0.65	-55	-57	2332-2330	-0	0
0.0850	332.89	1.269	5457.2	500.00	0.65	7.45	16.89	-8.13	0.70	-55	-57	2332-2330	-0	0
0.0851	333.39	1.270	5467.2	500.00	0.63	7.45	16.34	-8.07	0.75	-55	-57	2332-2330	-0	0
0.0852	333.89	1.271	5477.2	500.00	0.61	7.45	15.79	-8.00	0.80	-55	-57	2332-2330	-0	0
0.0853	334.39	1.272	5487.2	500.00	0.59	7.45	15.24	-7.92	0.85	-55	-57	2332-2330	-0	0
0.0854	334.89	1.273	5497.2	500.00	0.57	7.45	14.69	-7.84	0.90	-55	-57	2332-2330	-0	0
0.0855	335.39	1.274	5507.2	500.00	0.55	7.45	14.14	-7.75	0.95	-55	-57	2332-2330	-0	0
0.0856	335.89	1.275	5517.2	500.00	0.53	7.45	13.59	-7.65	1.00	-55	-57	2332-2330	-0	0
0.0857	336.39	1.276	5527.2	500.00	0.51	7.45	13.04	-7.54	1.05	-55	-57	2332-2330	-0	0
0.0858	336.89	1.277	5537.2	500.00	0.49	7.45	12.49	-7.42	1.10	-55	-57	2332-2330	-0	0
0.0859	337.39	1.278	5547.2	500.00	0.47	7.45	11.94	-7.29	1.15	-55	-57	2332-2330	-0	0
0.0860	337.89	1.279	5557.2	500.00	0.45	7.45	11.39	-7.15	1.20	-55	-57	2332-2330	-0	0
0.0861	338.39	1.280	5567.2	500.00	0.43	7.45	10.84	-7.00	1.25	-55	-57	2332-2330	-0	0
0.0862	338.89	1.281	5577.2	500.00	0.41	7.45	10.29	-6.84	1.30	-55	-57	2332-2330	-0	0
0.0863	339.39	1.282	5587.2	500.00	0.39	7.45	9.74	-6.67	1.35	-55	-57	2332-2330	-0	0
0.0864	339.89	1.283	5597.2	500.00	0.37	7.45	9.19	-6.49	1.40	-55	-57	2332-2330	-0	0
0.0865	340.39	1.284	5607.2	500.00	0.35	7.45	8.64	-6.30	1.45	-55	-57	2332-2330	-0	0
0.0866	340.89	1.285	5617.2	500.00	0.33	7.45	8.09	-6.10	1.50	-55	-57	2332-2330	-0	0
0.0867	341.39	1.286	5627.2	500.00	0.31	7.45	7.54	-5.89	1.55	-55	-57	2332-2330	-0	0
0.0868	341.89	1.287	5637.2	500.00	0.29	7.45	6.99	-5.67	1.60	-55	-57	2332-2330	-0	0
0.0869	342.39	1.288	5647.2	500.00	0.27	7.45	6.44	-5.44	1.65	-55	-57	2332-2330	-0	0
0.0870	342.89	1.289	5657.2	500.00	0.25	7.45	5.89	-5.20	1.70	-55	-57	2332-2330	-0	0
0.0871	343.39	1.290	5667.2	500.00	0.23	7.45	5.34	-4.95	1.75	-55	-57	2332-2330	-0	0
0.0872	343.89	1.291	5677.2	500.00	0.21	7.45	4.79	-4.69	1.80	-55	-57	2332-2330	-0	0
0.0873	344.39	1.292	5687.2	500.00	0.19	7.45	4.24	-4.42	1.85	-55	-57	2332-2330	-0	0
0.0874	344.89	1.293	5697.2	500.00	0.17	7.45	3.69	-4.14	1.90	-55	-57	2332-2330	-0	0
0.0875	345.39	1.294	5707.2	500.00	0.15	7.45	3.14	-3.85	1.95	-55	-57	2332-2330	-0	0
0.0876	345.89	1.295	5717.2	500.00	0.13	7.45	2.59	-3.55	2.00	-55	-57	2332-2330	-0	0
0.0877	346.39	1.296	5727.2	500.00	0.11	7.45	2.04	-3.24	2.05	-55	-57	2332-2330	-0	0
0.0878	346.89	1.297	5737.2	500.00	0.09	7.45	1.49	-2.92	2.10	-55	-57	2332-2330	-0	0
0.0879	347.39	1.298	5747.2	500.00	0.07	7.45	0.94	-2.59	2.15	-55	-57	2332-2330	-0	0
0.0880	347.89	1.299	5757.2	500.00	0.05	7.45	0.39	-2.25	2.20	-55	-57	2332-2330	-0	0
0.0881	348.39	1.300	5767.2	500.00	0.03	7.45	-0.16	-1.90	2.25	-55	-57	2332-2330	-0	0
0.0882	348.89	1.301	5777.2	500.00	0.01	7.45	-0.71	-1.55	2.30	-55	-57	2332-2330	-0	0
0.0883	349.39	1.302	5787.2	500.0										

## FLECHETTE GROUND POINT

PAGE 13

T SEC	X FT	Y FT	Z FT	V FT/SEC	P RAD/SEC	ALPHA DEG	MACH	PRI DEG	ALPHA DEG	FTS SEC	L IN	L-P 1/500	M-N 1/500	S YTD	M-T 1/50
0.0850	423.72	1.238	-0.441	4868.6	500.00	1.47	4.45	44.76	-0.30	1.12	-58	-57	2333--2330	-0	0
0.0851	423.22	1.239	-0.441	4868.6	500.00	1.47	4.45	45.45	-0.65	1.12	-58	-57	2333--2330	-0	0
0.0852	423.72	1.239	-0.441	4868.6	500.00	1.43	4.45	46.15	-0.81	1.14	-58	-57	2333--2330	-0	0
0.0853	424.21	1.241	-0.441	4868.6	500.00	1.43	4.45	46.83	-0.76	1.21	-58	-57	2333--2330	-0	0
0.0854	424.71	1.242	-0.442	4868.6	500.00	1.43	4.45	47.37	-0.71	1.24	-58	-57	2333--2330	-0	0
0.0855	425.21	1.242	-0.442	4868.6	500.00	1.42	4.45	47.82	-0.66	1.26	-58	-57	2333--2330	-0	0
0.0856	425.70	1.243	-0.442	4868.6	500.00	1.42	4.45	48.12	-0.63	1.29	-58	-57	2333--2330	-0	0
0.0857	426.20	1.244	-0.443	4868.6	500.00	1.42	4.45	48.39	-0.61	1.31	-58	-57	2333--2330	-0	0
0.0858	426.70	1.245	-0.443	4868.6	500.00	1.42	4.45	48.62	-0.60	1.34	-58	-57	2333--2330	-0	0
0.0859	427.19	1.246	-0.443	4868.6	500.00	1.42	4.45	48.82	-0.59	1.36	-58	-57	2333--2330	-0	0
0.0860	427.69	1.247	-0.443	4868.6	500.00	1.42	4.45	49.02	-0.58	1.38	-58	-57	2333--2330	-0	0
0.0861	428.19	1.248	-0.444	4868.6	500.00	1.42	4.45	49.24	-0.57	1.40	-58	-57	2333--2330	-0	0
0.0862	428.69	1.249	-0.444	4868.6	500.00	1.42	4.45	49.45	-0.56	1.43	-58	-57	2333--2330	-0	0
0.0863	429.19	1.250	-0.445	4868.6	500.00	1.42	4.45	49.65	-0.55	1.45	-58	-57	2333--2330	-0	0
0.0864	429.69	1.251	-0.445	4868.6	500.00	1.42	4.45	49.85	-0.54	1.47	-58	-57	2333--2330	-0	0
0.0865	430.19	1.252	-0.446	4868.6	500.00	1.42	4.45	50.05	-0.53	1.49	-58	-57	2333--2330	-0	0
0.0866	430.69	1.253	-0.446	4868.6	500.00	1.42	4.45	50.25	-0.52	1.51	-58	-57	2333--2330	-0	0
0.0867	431.19	1.254	-0.447	4868.6	500.00	1.42	4.45	50.45	-0.51	1.53	-58	-57	2333--2330	-0	0
0.0868	431.69	1.255	-0.447	4868.6	500.00	1.42	4.45	50.65	-0.50	1.55	-58	-57	2333--2330	-0	0
0.0869	432.19	1.256	-0.448	4868.6	500.00	1.42	4.45	50.85	-0.49	1.57	-58	-57	2333--2330	-0	0
0.0870	432.69	1.257	-0.448	4868.6	500.00	1.42	4.45	51.05	-0.48	1.59	-58	-57	2333--2330	-0	0
0.0871	433.19	1.258	-0.449	4868.6	500.00	1.42	4.45	51.25	-0.47	1.61	-58	-57	2333--2330	-0	0
0.0872	433.69	1.259	-0.449	4868.6	500.00	1.42	4.45	51.45	-0.46	1.63	-58	-57	2333--2330	-0	0
0.0873	434.19	1.260	-0.450	4868.6	500.00	1.42	4.45	51.65	-0.45	1.65	-58	-57	2333--2330	-0	0
0.0874	434.69	1.261	-0.451	4868.6	500.00	1.42	4.45	51.85	-0.44	1.67	-58	-57	2333--2330	-0	0
0.0875	435.19	1.262	-0.452	4868.6	500.00	1.42	4.45	52.05	-0.43	1.69	-58	-57	2333--2330	-0	0
0.0876	435.69	1.263	-0.453	4868.6	500.00	1.42	4.45	52.25	-0.42	1.71	-58	-57	2333--2330	-0	0
0.0877	436.19	1.264	-0.454	4868.6	500.00	1.42	4.45	52.45	-0.41	1.73	-58	-57	2333--2330	-0	0
0.0878	436.69	1.265	-0.455	4868.6	500.00	1.42	4.45	52.65	-0.40	1.75	-58	-57	2333--2330	-0	0
0.0879	437.19	1.266	-0.456	4868.6	500.00	1.42	4.45	52.85	-0.39	1.77	-58	-57	2333--2330	-0	0
0.0880	437.69	1.267	-0.457	4868.6	500.00	1.42	4.45	53.05	-0.38	1.79	-58	-57	2333--2330	-0	0
0.0881	438.19	1.268	-0.458	4868.6	500.00	1.42	4.45	53.25	-0.37	1.81	-58	-57	2333--2330	-0	0
0.0882	438.69	1.269	-0.459	4868.6	500.00	1.42	4.45	53.45	-0.36	1.83	-58	-57	2333--2330	-0	0
0.0883	439.19	1.270	-0.460	4868.6	500.00	1.42	4.45	53.65	-0.35	1.85	-58	-57	2333--2330	-0	0
0.0884	439.69	1.271	-0.461	4868.6	500.00	1.42	4.45	53.85	-0.34	1.87	-58	-57	2333--2330	-0	0
0.0885	440.19	1.272	-0.462	4868.6	500.00	1.42	4.45	54.05	-0.33	1.89	-58	-57	2333--2330	-0	0
0.0886	440.69	1.273	-0.463	4868.6	500.00	1.42	4.45	54.25	-0.32	1.91	-58	-57	2333--2330	-0	0
0.0887	441.19	1.274	-0.464	4868.6	500.00	1.42	4.45	54.45	-0.31	1.93	-58	-57	2333--2330	-0	0
0.0888	441.69	1.275	-0.465	4868.6	500.00	1.42	4.45	54.65	-0.30	1.95	-58	-57	2333--2330	-0	0
0.0889	442.19	1.276	-0.466	4868.6	500.00	1.42	4.45	54.85	-0.29	1.97	-58	-57	2333--2330	-0	0
0.0890	442.69	1.277	-0.467	4868.6	500.00	1.42	4.45	55.05	-0.28	1.99	-58	-57	2333--2330	-0	0
0.0891	443.19	1.278	-0.468	4868.6	500.00	1.42	4.45	55.25	-0.27	2.01	-58	-57	2333--2330	-0	0
0.0892	443.69	1.279	-0.469	4868.6	500.00	1.42	4.45	55.45	-0.26	2.03	-58	-57	2333--2330	-0	0
0.0893	444.19	1.280	-0.470	4868.6	500.00	1.42	4.45	55.65	-0.25	2.05	-58	-57	2333--2330	-0	0
0.0894	444.69	1.281	-0.471	4868.6	500.00	1.42	4.45	55.85	-0.24	2.07	-58	-57	2333--2330	-0	0
0.0895	445.19	1.282	-0.472	4868.6	500.00	1.42	4.45	56.05	-0.23	2.09	-58	-57	2333--2330	-0	0
0.0896	445.69	1.283	-0.473	4868.6	500.00	1.42	4.45	56.25	-0.22	2.11	-58	-57	2333--2330	-0	0
0.0897	446.19	1.284	-0.474	4868.6	500.00	1.42	4.45	56.45	-0.21	2.13	-58	-57	2333--2330	-0	0
0.0898	446.69	1.285	-0.475	4868.6	500.00	1.42	4.45	56.65	-0.20	2.15	-58	-57	2333--2330	-0	0
0.0899	447.19	1.286	-0.476	4868.6	500.00	1.42	4.45	56.85	-0.19	2.17	-58	-57	2333--2330	-0	0

## FLECHETTE GROUND POINT

PAGE 18

I	SEC	X	Y	Z	V	P	ALPHA	MACH	ORI	ALPHA	ETA	L-N	L-P	W-1	W-P	S	RAU	K-J
0.0000	447.55	1.339	-0.432	0.0000	4965.1	500.00	1.48	4.45	47.07	1.44	-0.31	-55	-57	2333	-2330	-0	0	1
0.0001	448.05	1.341	-0.433	0.0000	4965.1	500.00	1.47	4.45	46.91	1.42	-0.34	-55	-57	2333	-2330	-0	0	1
0.0002	448.55	1.342	-0.434	0.0000	4965.1	500.00	1.46	4.45	46.75	1.40	-0.36	-55	-57	2333	-2330	-0	0	1
0.0003	449.04	1.344	-0.435	0.0000	4965.1	500.00	1.45	4.45	46.59	1.38	-0.38	-55	-57	2333	-2330	-0	0	1
0.0004	449.54	1.346	-0.437	0.0000	4965.1	500.00	1.44	4.45	46.43	1.36	-0.40	-55	-57	2333	-2330	-0	0	1
0.0005	450.03	1.348	-0.438	0.0000	4965.1	500.00	1.43	4.45	46.27	1.34	-0.42	-55	-57	2333	-2330	-0	0	1
0.0006	450.53	1.350	-0.439	0.0000	4965.1	500.00	1.42	4.45	46.11	1.32	-0.44	-55	-57	2333	-2330	-0	0	1
0.0007	451.03	1.351	-0.439	0.0000	4965.1	500.00	1.41	4.45	45.95	1.30	-0.46	-55	-57	2333	-2330	-0	0	1
0.0008	451.52	1.353	-0.439	0.0000	4965.1	500.00	1.40	4.45	45.79	1.28	-0.48	-55	-57	2333	-2330	-0	0	1
0.0009	452.02	1.355	-0.439	0.0000	4965.1	500.00	1.39	4.45	45.63	1.26	-0.50	-55	-57	2333	-2330	-0	0	1
0.0010	452.52	1.357	-0.439	0.0000	4965.1	500.00	1.38	4.45	45.47	1.24	-0.52	-55	-57	2333	-2330	-0	0	1
0.0011	453.01	1.359	-0.439	0.0000	4965.1	500.00	1.37	4.45	45.31	1.22	-0.54	-55	-57	2333	-2330	-0	0	1
0.0012	453.51	1.361	-0.439	0.0000	4965.1	500.00	1.36	4.45	45.15	1.20	-0.56	-55	-57	2333	-2330	-0	0	1
0.0013	454.01	1.363	-0.439	0.0000	4965.1	500.00	1.35	4.45	45.00	1.18	-0.58	-55	-57	2333	-2330	-0	0	1
0.0014	454.50	1.365	-0.439	0.0000	4965.1	500.00	1.34	4.45	44.84	1.16	-0.60	-55	-57	2333	-2330	-0	0	1
0.0015	455.00	1.367	-0.439	0.0000	4965.1	500.00	1.33	4.45	44.68	1.14	-0.62	-55	-57	2333	-2330	-0	0	1
0.0016	455.49	1.369	-0.439	0.0000	4965.1	500.00	1.32	4.45	44.52	1.12	-0.64	-55	-57	2333	-2330	-0	0	1
0.0017	455.99	1.371	-0.439	0.0000	4965.1	500.00	1.31	4.45	44.36	1.10	-0.66	-55	-57	2333	-2330	-0	0	1
0.0018	456.48	1.373	-0.439	0.0000	4965.1	500.00	1.30	4.45	44.20	1.08	-0.68	-55	-57	2333	-2330	-0	0	1
0.0019	456.98	1.375	-0.439	0.0000	4965.1	500.00	1.29	4.45	44.04	1.06	-0.70	-55	-57	2333	-2330	-0	0	1
0.0020	457.48	1.377	-0.439	0.0000	4965.1	500.00	1.28	4.45	43.88	1.04	-0.72	-55	-57	2333	-2330	-0	0	1
0.0021	457.98	1.379	-0.439	0.0000	4965.1	500.00	1.27	4.45	43.72	1.02	-0.74	-55	-57	2333	-2330	-0	0	1
0.0022	458.48	1.381	-0.439	0.0000	4965.1	500.00	1.26	4.45	43.56	1.00	-0.76	-55	-57	2333	-2330	-0	0	1
0.0023	458.97	1.383	-0.439	0.0000	4965.1	500.00	1.25	4.45	43.40	0.98	-0.78	-55	-57	2333	-2330	-0	0	1
0.0024	459.47	1.385	-0.439	0.0000	4965.1	500.00	1.24	4.45	43.24	0.96	-0.80	-55	-57	2333	-2330	-0	0	1
0.0025	459.96	1.387	-0.439	0.0000	4965.1	500.00	1.23	4.45	43.08	0.94	-0.82	-55	-57	2333	-2330	-0	0	1
0.0026	460.46	1.389	-0.439	0.0000	4965.1	500.00	1.22	4.45	42.92	0.92	-0.84	-55	-57	2333	-2330	-0	0	1
0.0027	460.95	1.391	-0.439	0.0000	4965.1	500.00	1.21	4.45	42.76	0.90	-0.86	-55	-57	2333	-2330	-0	0	1
0.0028	461.45	1.393	-0.439	0.0000	4965.1	500.00	1.20	4.45	42.60	0.88	-0.88	-55	-57	2333	-2330	-0	0	1
0.0029	461.95	1.395	-0.439	0.0000	4965.1	500.00	1.19	4.45	42.44	0.86	-0.90	-55	-57	2333	-2330	-0	0	1
0.0030	462.45	1.397	-0.439	0.0000	4965.1	500.00	1.18	4.45	42.28	0.84	-0.92	-55	-57	2333	-2330	-0	0	1
0.0031	462.94	1.399	-0.439	0.0000	4965.1	500.00	1.17	4.45	42.12	0.82	-0.94	-55	-57	2333	-2330	-0	0	1
0.0032	463.44	1.401	-0.439	0.0000	4965.1	500.00	1.16	4.45	41.96	0.80	-0.96	-55	-57	2333	-2330	-0	0	1
0.0033	463.94	1.403	-0.439	0.0000	4965.1	500.00	1.15	4.45	41.80	0.78	-0.98	-55	-57	2333	-2330	-0	0	1
0.0034	464.43	1.405	-0.439	0.0000	4965.1	500.00	1.14	4.45	41.64	0.76	-1.00	-55	-57	2333	-2330	-0	0	1
0.0035	464.93	1.407	-0.439	0.0000	4965.1	500.00	1.13	4.45	41.48	0.74	-1.02	-55	-57	2333	-2330	-0	0	1
0.0036	465.43	1.409	-0.439	0.0000	4965.1	500.00	1.12	4.45	41.32	0.72	-1.04	-55	-57	2333	-2330	-0	0	1
0.0037	465.92	1.411	-0.439	0.0000	4965.1	500.00	1.11	4.45	41.16	0.70	-1.06	-55	-57	2333	-2330	-0	0	1
0.0038	466.42	1.413	-0.439	0.0000	4965.1	500.00	1.10	4.45	41.00	0.68	-1.08	-55	-57	2333	-2330	-0	0	1
0.0039	466.91	1.415	-0.439	0.0000	4965.1	500.00	1.09	4.45	40.84	0.66	-1.10	-55	-57	2333	-2330	-0	0	1
0.0040	467.41	1.417	-0.439	0.0000	4965.1	500.00	1.08	4.45	40.68	0.64	-1.12	-55	-57	2333	-2330	-0	0	1
0.0041	467.91	1.419	-0.439	0.0000	4965.1	500.00	1.07	4.45	40.52	0.62	-1.14	-55	-57	2333	-2330	-0	0	1
0.0042	468.40	1.421	-0.439	0.0000	4965.1	500.00	1.06	4.45	40.36	0.60	-1.16	-55	-57	2333	-2330	-0	0	1
0.0043	468.90	1.423	-0.439	0.0000	4965.1	500.00	1.05	4.45	40.20	0.58	-1.18	-55	-57	2333	-2330	-0	0	1
0.0044	469.40	1.425	-0.439	0.0000	4965.1	500.00	1.04	4.45	40.04	0.56	-1.20	-55	-57	2333	-2330	-0	0	1
0.0045	469.89	1.427	-0.439	0.0000	4965.1	500.00	1.03	4.45	39.88	0.54	-1.22	-55	-57	2333	-2330	-0	0	1
0.0046	470.39	1.429	-0.439	0.0000	4965.1	500.00	1.02	4.45	39.72	0.52	-1.24	-55	-57	2333	-2330	-0	0	1
0.0047	470.88	1.431	-0.439	0.0000	4965.1	500.00	1.01	4.45	39.56	0.50	-1.26	-55	-57	2333	-2330	-0	0	1
0.0048	471.38	1.433	-0.439	0.0000	4965.1	500.00	1.00	4.45	39.40	0.48	-1.28	-55	-57	2333	-2330	-0	0	1
0.0049	471.88	1.435	-0.439	0.0000	4965.1	500.00	0.99	4.45	39.24	0.46	-1.30	-55	-57	2333	-2330	-0	0	1

FLECHETTE GROUND POINT

PAGE 20

T	X	Y	Z	V	P	ALPHA	MACH	PHI	ALPHA	BETA	L-N	L-P	M-N	M-P	S	TAU	K-T
SEC	FT	FT	FT	FT/SEC	FT/SEC	DEG	DEG	DEG	DEG	DEG	1/SEC	1/SEC	1/SEC	1/SEC	1/SEC	1/SEC	1/SEC
0.0950	472.37	1.461	-0.510	4955.5	500.00	1.00	4.45	74.90	1.410	-0.53	-53	-57	2333-2330	-0	0	0	1
0.0951	472.87	1.443	-0.510	4955.5	500.00	1.00	4.45	74.90	1.410	-0.53	-53	-57	2333-2330	-0	0	0	1
0.0952	473.37	1.425	-0.510	4955.5	500.00	1.00	4.45	74.90	1.410	-0.53	-53	-57	2333-2330	-0	0	0	1
0.0953	473.86	1.406	-0.510	4955.5	500.00	1.00	4.45	74.90	1.410	-0.53	-53	-57	2333-2330	-0	0	0	1
0.0954	474.35	1.388	-0.509	4955.5	500.00	1.00	4.45	74.90	1.410	-0.53	-53	-57	2333-2330	-0	0	0	1
0.0955	474.85	1.369	-0.509	4955.5	500.00	1.00	4.45	74.90	1.410	-0.53	-53	-57	2333-2330	-0	0	0	1
0.0956	475.35	1.351	-0.509	4955.5	500.00	1.00	4.45	74.90	1.410	-0.53	-53	-57	2333-2330	-0	0	0	1
0.0957	475.85	1.332	-0.509	4955.5	500.00	1.00	4.45	74.90	1.410	-0.53	-53	-57	2333-2330	-0	0	0	1
0.0958	476.34	1.314	-0.509	4955.5	500.00	1.00	4.45	74.90	1.410	-0.53	-53	-57	2333-2330	-0	0	0	1
0.0959	476.84	1.295	-0.509	4955.5	500.00	1.00	4.45	74.90	1.410	-0.53	-53	-57	2333-2330	-0	0	0	1
0.0960	477.34	1.277	-0.509	4955.5	500.00	1.00	4.45	74.90	1.410	-0.53	-53	-57	2333-2330	-0	0	0	1
0.0961	477.83	1.258	-0.509	4955.5	500.00	1.00	4.45	74.90	1.410	-0.53	-53	-57	2333-2330	-0	0	0	1
0.0962	478.33	1.239	-0.509	4955.5	500.00	1.00	4.45	74.90	1.410	-0.53	-53	-57	2333-2330	-0	0	0	1
0.0963	478.83	1.220	-0.509	4955.5	500.00	1.00	4.45	74.90	1.410	-0.53	-53	-57	2333-2330	-0	0	0	1
0.0964	479.32	1.201	-0.509	4955.5	500.00	1.00	4.45	74.90	1.410	-0.53	-53	-57	2333-2330	-0	0	0	1
0.0965	479.82	1.182	-0.509	4955.5	500.00	1.00	4.45	74.90	1.410	-0.53	-53	-57	2333-2330	-0	0	0	1
0.0966	480.31	1.163	-0.509	4955.5	500.00	1.00	4.45	74.90	1.410	-0.53	-53	-57	2333-2330	-0	0	0	1
0.0967	480.81	1.144	-0.509	4955.5	500.00	1.00	4.45	74.90	1.410	-0.53	-53	-57	2333-2330	-0	0	0	1
0.0968	481.31	1.125	-0.509	4955.5	500.00	1.00	4.45	74.90	1.410	-0.53	-53	-57	2333-2330	-0	0	0	1
0.0969	481.80	1.106	-0.509	4955.5	500.00	1.00	4.45	74.90	1.410	-0.53	-53	-57	2333-2330	-0	0	0	1
0.0970	482.30	1.087	-0.509	4955.5	500.00	1.00	4.45	74.90	1.410	-0.53	-53	-57	2333-2330	-0	0	0	1
0.0971	482.80	1.068	-0.509	4955.5	500.00	1.00	4.45	74.90	1.410	-0.53	-53	-57	2333-2330	-0	0	0	1
0.0972	483.29	1.049	-0.509	4955.5	500.00	1.00	4.45	74.90	1.410	-0.53	-53	-57	2333-2330	-0	0	0	1
0.0973	483.79	1.030	-0.509	4955.5	500.00	1.00	4.45	74.90	1.410	-0.53	-53	-57	2333-2330	-0	0	0	1
0.0974	484.28	1.011	-0.509	4955.5	500.00	1.00	4.45	74.90	1.410	-0.53	-53	-57	2333-2330	-0	0	0	1
0.0975	484.78	0.992	-0.509	4955.5	500.00	1.00	4.45	74.90	1.410	-0.53	-53	-57	2333-2330	-0	0	0	1
0.0976	485.28	0.973	-0.509	4955.5	500.00	1.00	4.45	74.90	1.410	-0.53	-53	-57	2333-2330	-0	0	0	1
0.0977	485.77	0.954	-0.509	4955.5	500.00	1.00	4.45	74.90	1.410	-0.53	-53	-57	2333-2330	-0	0	0	1
0.0978	486.27	0.935	-0.509	4955.5	500.00	1.00	4.45	74.90	1.410	-0.53	-53	-57	2333-2330	-0	0	0	1
0.0979	486.77	0.916	-0.509	4955.5	500.00	1.00	4.45	74.90	1.410	-0.53	-53	-57	2333-2330	-0	0	0	1
0.0980	487.26	0.897	-0.509	4955.5	500.00	1.00	4.45	74.90	1.410	-0.53	-53	-57	2333-2330	-0	0	0	1
0.0981	487.75	0.878	-0.509	4955.5	500.00	1.00	4.45	74.90	1.410	-0.53	-53	-57	2333-2330	-0	0	0	1
0.0982	488.25	0.859	-0.509	4955.5	500.00	1.00	4.45	74.90	1.410	-0.53	-53	-57	2333-2330	-0	0	0	1
0.0983	488.75	0.840	-0.509	4955.5	500.00	1.00	4.45	74.90	1.410	-0.53	-53	-57	2333-2330	-0	0	0	1
0.0984	489.25	0.821	-0.509	4955.5	500.00	1.00	4.45	74.90	1.410	-0.53	-53	-57	2333-2330	-0	0	0	1
0.0985	489.75	0.802	-0.509	4955.5	500.00	1.00	4.45	74.90	1.410	-0.53	-53	-57	2333-2330	-0	0	0	1
0.0986	490.25	0.783	-0.509	4955.5	500.00	1.00	4.45	74.90	1.410	-0.53	-53	-57	2333-2330	-0	0	0	1
0.0987	490.75	0.764	-0.509	4955.5	500.00	1.00	4.45	74.90	1.410	-0.53	-53	-57	2333-2330	-0	0	0	1
0.0988	491.25	0.745	-0.509	4955.5	500.00	1.00	4.45	74.90	1.410	-0.53	-53	-57	2333-2330	-0	0	0	1
0.0989	491.75	0.726	-0.509	4955.5	500.00	1.00	4.45	74.90	1.410	-0.53	-53	-57	2333-2330	-0	0	0	1
0.0990	492.25	0.707	-0.509	4955.5	500.00	1.00	4.45	74.90	1.410	-0.53	-53	-57	2333-2330	-0	0	0	1
0.0991	492.75	0.688	-0.509	4955.5	500.00	1.00	4.45	74.90	1.410	-0.53	-53	-57	2333-2330	-0	0	0	1
0.0992	493.25	0.669	-0.509	4955.5	500.00	1.00	4.45	74.90	1.410	-0.53	-53	-57	2333-2330	-0	0	0	1
0.0993	493.75	0.650	-0.509	4955.5	500.00	1.00	4.45	74.90	1.410	-0.53	-53	-57	2333-2330	-0	0	0	1
0.0994	494.25	0.631	-0.509	4955.5	500.00	1.00	4.45	74.90	1.410	-0.53	-53	-57	2333-2330	-0	0	0	1
0.0995	494.75	0.612	-0.509	4955.5	500.00	1.00	4.45	74.90	1.410	-0.53	-53	-57	2333-2330	-0	0	0	1
0.0996	495.25	0.593	-0.509	4955.5	500.00	1.00	4.45	74.90	1.410	-0.53	-53	-57	2333-2330	-0	0	0	1
0.0997	495.75	0.574	-0.509	4955.5	500.00	1.00	4.45	74.90	1.410	-0.53	-53	-57	2333-2330	-0	0	0	1
0.0998	496.25	0.555	-0.509	4955.5	500.00	1.00	4.45	74.90	1.410	-0.53	-53	-57	2333-2330	-0	0	0	1
0.0999	496.75	0.536	-0.509	4955.5	500.00	1.00	4.45	74.90	1.410	-0.53	-53	-57	2333-2330	-0	0	0	1

## FLECHETTE GROUND PGT

PAGE 21

T SEC	X FT	Y C	Z FT	V FT/SEC	P RAT/SEC	ALPHA CRG	OH1 REC	ALPHA REC	SETS DEG	L-N L/SEC	L-P L/SEC	M-N L/SEC	K-T DEG	TAU	S	L-P RAT/SEC
0.1000	467.02	1.465	-0.510	4765.0	500.00	1.45	4.45	45.52	0.73	1.25	-55	-57	2333	-2333	-1	0
0.1001	467.06	1.466	-0.510	4765.0	500.00	1.45	4.45	45.52	0.69	1.21	-55	-57	2333	-2333	-1	0
0.1002	467.10	1.467	-0.521	4765.0	500.00	1.45	4.45	45.35	0.65	1.18	-55	-57	2333	-2333	-1	0
0.1003	467.14	1.468	-0.521	4765.0	500.00	1.45	4.45	45.35	0.61	1.14	-55	-57	2333	-2333	-1	0
0.1004	467.18	1.469	-0.522	4765.0	500.00	1.47	4.45	45.23	0.57	1.10	-55	-57	2333	-2333	-1	0
0.1005	467.22	1.469	-0.522	4765.0	500.00	1.47	4.45	45.23	0.53	1.06	-55	-57	2333	-2333	-1	0
0.1006	467.26	1.469	-0.523	4765.0	500.00	1.47	4.45	45.35	0.49	1.02	-55	-57	2333	-2333	-1	0
0.1007	467.30	1.469	-0.523	4765.0	500.00	1.47	4.45	45.35	0.45	0.98	-55	-57	2333	-2333	-1	0
0.1008	467.34	1.469	-0.523	4765.0	500.00	1.47	4.45	45.35	0.41	0.94	-55	-57	2333	-2333	-1	0
0.1009	467.38	1.469	-0.523	4765.0	500.00	1.47	4.45	45.35	0.37	0.90	-55	-57	2333	-2333	-1	0
0.1010	467.42	1.469	-0.523	4765.0	500.00	1.47	4.45	45.35	0.33	0.86	-55	-57	2333	-2333	-1	0
0.1011	467.46	1.469	-0.523	4765.0	500.00	1.47	4.45	45.35	0.29	0.82	-55	-57	2333	-2333	-1	0
0.1012	467.50	1.469	-0.523	4765.0	500.00	1.47	4.45	45.35	0.25	0.78	-55	-57	2333	-2333	-1	0
0.1013	467.54	1.469	-0.523	4765.0	500.00	1.47	4.45	45.35	0.21	0.74	-55	-57	2333	-2333	-1	0
0.1014	467.58	1.469	-0.523	4765.0	500.00	1.47	4.45	45.35	0.17	0.70	-55	-57	2333	-2333	-1	0
0.1015	467.62	1.469	-0.523	4765.0	500.00	1.47	4.45	45.35	0.13	0.66	-55	-57	2333	-2333	-1	0
0.1016	467.66	1.469	-0.523	4765.0	500.00	1.47	4.45	45.35	0.09	0.62	-55	-57	2333	-2333	-1	0
0.1017	467.70	1.469	-0.523	4765.0	500.00	1.47	4.45	45.35	0.05	0.58	-55	-57	2333	-2333	-1	0
0.1018	467.74	1.469	-0.523	4765.0	500.00	1.47	4.45	45.35	0.01	0.54	-55	-57	2333	-2333	-1	0
0.1019	467.78	1.469	-0.523	4765.0	500.00	1.47	4.45	45.35	0.00	0.50	-55	-57	2333	-2333	-1	0
0.1020	467.82	1.469	-0.523	4765.0	500.00	1.47	4.45	45.35	0.00	0.46	-55	-57	2333	-2333	-1	0
0.1021	467.86	1.469	-0.523	4765.0	500.00	1.47	4.45	45.35	0.00	0.42	-55	-57	2333	-2333	-1	0
0.1022	467.90	1.469	-0.523	4765.0	500.00	1.47	4.45	45.35	0.00	0.38	-55	-57	2333	-2333	-1	0
0.1023	467.94	1.469	-0.523	4765.0	500.00	1.47	4.45	45.35	0.00	0.34	-55	-57	2333	-2333	-1	0
0.1024	467.98	1.469	-0.523	4765.0	500.00	1.47	4.45	45.35	0.00	0.30	-55	-57	2333	-2333	-1	0
0.1025	468.02	1.469	-0.523	4765.0	500.00	1.47	4.45	45.35	0.00	0.26	-55	-57	2333	-2333	-1	0
0.1026	468.06	1.469	-0.523	4765.0	500.00	1.47	4.45	45.35	0.00	0.22	-55	-57	2333	-2333	-1	0
0.1027	468.10	1.469	-0.523	4765.0	500.00	1.47	4.45	45.35	0.00	0.18	-55	-57	2333	-2333	-1	0
0.1028	468.14	1.469	-0.523	4765.0	500.00	1.47	4.45	45.35	0.00	0.14	-55	-57	2333	-2333	-1	0
0.1029	468.18	1.469	-0.523	4765.0	500.00	1.47	4.45	45.35	0.00	0.10	-55	-57	2333	-2333	-1	0
0.1030	468.22	1.469	-0.523	4765.0	500.00	1.47	4.45	45.35	0.00	0.06	-55	-57	2333	-2333	-1	0
0.1031	468.26	1.469	-0.523	4765.0	500.00	1.47	4.45	45.35	0.00	0.02	-55	-57	2333	-2333	-1	0
0.1032	468.30	1.469	-0.523	4765.0	500.00	1.47	4.45	45.35	0.00	0.00	-55	-57	2333	-2333	-1	0
0.1033	468.34	1.469	-0.523	4765.0	500.00	1.47	4.45	45.35	0.00	0.00	-55	-57	2333	-2333	-1	0
0.1034	468.38	1.469	-0.523	4765.0	500.00	1.47	4.45	45.35	0.00	0.00	-55	-57	2333	-2333	-1	0
0.1035	468.42	1.469	-0.523	4765.0	500.00	1.47	4.45	45.35	0.00	0.00	-55	-57	2333	-2333	-1	0
0.1036	468.46	1.469	-0.523	4765.0	500.00	1.47	4.45	45.35	0.00	0.00	-55	-57	2333	-2333	-1	0
0.1037	468.50	1.469	-0.523	4765.0	500.00	1.47	4.45	45.35	0.00	0.00	-55	-57	2333	-2333	-1	0
0.1038	468.54	1.469	-0.523	4765.0	500.00	1.47	4.45	45.35	0.00	0.00	-55	-57	2333	-2333	-1	0
0.1039	468.58	1.469	-0.523	4765.0	500.00	1.47	4.45	45.35	0.00	0.00	-55	-57	2333	-2333	-1	0
0.1040	468.62	1.469	-0.523	4765.0	500.00	1.47	4.45	45.35	0.00	0.00	-55	-57	2333	-2333	-1	0
0.1041	468.66	1.469	-0.523	4765.0	500.00	1.47	4.45	45.35	0.00	0.00	-55	-57	2333	-2333	-1	0
0.1042	468.70	1.469	-0.523	4765.0	500.00	1.47	4.45	45.35	0.00	0.00	-55	-57	2333	-2333	-1	0
0.1043	468.74	1.469	-0.523	4765.0	500.00	1.47	4.45	45.35	0.00	0.00	-55	-57	2333	-2333	-1	0
0.1044	468.78	1.469	-0.523	4765.0	500.00	1.47	4.45	45.35	0.00	0.00	-55	-57	2333	-2333	-1	0
0.1045	468.82	1.469	-0.523	4765.0	500.00	1.47	4.45	45.35	0.00	0.00	-55	-57	2333	-2333	-1	0
0.1046	468.86	1.469	-0.523	4765.0	500.00	1.47	4.45	45.35	0.00	0.00	-55	-57	2333	-2333	-1	0
0.1047	468.90	1.469	-0.523	4765.0	500.00	1.47	4.45	45.35	0.00	0.00	-55	-57	2333	-2333	-1	0
0.1048	468.94	1.469	-0.523	4765.0	500.00	1.47	4.45	45.35	0.00	0.00	-55	-57	2333	-2333	-1	0
0.1049	468.98	1.469	-0.523	4765.0	500.00	1.47	4.45	45.35	0.00	0.00	-55	-57	2333	-2333	-1	0

## FLECHETTE GROUND POINT

PAGE 22

Y	X	Y	Z	V	P	ALPHA	MACH	PMT	ALPHA	FEY	L-4	L-5	M-4	M-5	S	TAU	M-T
SEC	FT	FT	FT	FT/SEC	PAQ/SEC	DEG	DEG	DEG	DEG	DEG	1/500	1/500	1/500	1/500	1/500	1/500	DEG
0.1050	523.01	1.575	-0.571	4564.5	500.00	1.75	4.45	45.87	0.14	-1.74	-55	-57	2333	-2331	-0	0	1
0.1051	522.50	1.577	-0.571	4564.5	500.00	1.75	4.45	45.87	0.14	-1.74	-55	-57	2333	-2331	-0	0	1
0.1052	522.00	1.580	-0.572	4564.4	500.00	1.74	4.45	45.87	0.14	-1.74	-55	-57	2333	-2331	-0	0	1
0.1053	521.50	1.582	-0.572	4564.4	500.00	1.74	4.45	45.87	0.14	-1.74	-55	-57	2333	-2331	-0	0	1
0.1054	521.00	1.584	-0.573	4564.4	500.00	1.73	4.45	45.86	0.13	-1.73	-55	-57	2333	-2331	-0	0	1
0.1055	520.49	1.586	-0.573	4564.4	500.00	1.73	4.45	45.86	0.13	-1.73	-55	-57	2333	-2331	-0	0	1
0.1056	520.99	1.588	-0.573	4564.4	500.00	1.73	4.45	45.86	0.13	-1.73	-55	-57	2333	-2331	-0	0	1
0.1057	520.48	1.591	-0.574	4564.4	500.00	1.72	4.45	45.85	0.13	-1.72	-55	-57	2333	-2331	-0	0	1
0.1058	520.98	1.593	-0.574	4564.4	500.00	1.72	4.45	45.85	0.13	-1.72	-55	-57	2333	-2331	-0	0	1
0.1059	520.47	1.595	-0.575	4564.4	500.00	1.72	4.45	45.85	0.13	-1.72	-55	-57	2333	-2331	-0	0	1
0.1060	520.97	1.597	-0.575	4564.4	500.00	1.72	4.45	45.85	0.13	-1.72	-55	-57	2333	-2331	-0	0	1
0.1061	520.47	1.599	-0.575	4564.4	500.00	1.72	4.45	45.85	0.13	-1.72	-55	-57	2333	-2331	-0	0	1
0.1062	520.96	1.601	-0.575	4564.4	500.00	1.72	4.45	45.85	0.13	-1.72	-55	-57	2333	-2331	-0	0	1
0.1063	520.45	1.604	-0.576	4564.3	500.00	1.72	4.45	45.84	0.13	-1.72	-55	-57	2333	-2331	-0	0	1
0.1064	520.95	1.606	-0.576	4564.3	500.00	1.72	4.45	45.84	0.13	-1.72	-55	-57	2333	-2331	-0	0	1
0.1065	520.45	1.608	-0.576	4564.3	500.00	1.72	4.45	45.84	0.13	-1.72	-55	-57	2333	-2331	-0	0	1
0.1066	520.95	1.610	-0.576	4564.3	500.00	1.72	4.45	45.84	0.13	-1.72	-55	-57	2333	-2331	-0	0	1
0.1067	520.44	1.612	-0.576	4564.3	500.00	1.72	4.45	45.84	0.13	-1.72	-55	-57	2333	-2331	-0	0	1
0.1068	520.94	1.614	-0.576	4564.3	500.00	1.72	4.45	45.84	0.13	-1.72	-55	-57	2333	-2331	-0	0	1
0.1069	520.44	1.616	-0.576	4564.3	500.00	1.72	4.45	45.84	0.13	-1.72	-55	-57	2333	-2331	-0	0	1
0.1070	520.93	1.618	-0.576	4564.3	500.00	1.72	4.45	45.84	0.13	-1.72	-55	-57	2333	-2331	-0	0	1
0.1071	520.43	1.620	-0.576	4564.3	500.00	1.72	4.45	45.84	0.13	-1.72	-55	-57	2333	-2331	-0	0	1
0.1072	520.93	1.622	-0.576	4564.3	500.00	1.72	4.45	45.84	0.13	-1.72	-55	-57	2333	-2331	-0	0	1
0.1073	520.42	1.624	-0.576	4564.3	500.00	1.72	4.45	45.84	0.13	-1.72	-55	-57	2333	-2331	-0	0	1
0.1074	520.92	1.626	-0.576	4564.3	500.00	1.72	4.45	45.84	0.13	-1.72	-55	-57	2333	-2331	-0	0	1
0.1075	520.42	1.628	-0.576	4564.3	500.00	1.72	4.45	45.84	0.13	-1.72	-55	-57	2333	-2331	-0	0	1
0.1076	520.91	1.630	-0.576	4564.3	500.00	1.72	4.45	45.84	0.13	-1.72	-55	-57	2333	-2331	-0	0	1
0.1077	520.41	1.632	-0.576	4564.3	500.00	1.72	4.45	45.84	0.13	-1.72	-55	-57	2333	-2331	-0	0	1
0.1078	520.90	1.634	-0.576	4564.3	500.00	1.72	4.45	45.84	0.13	-1.72	-55	-57	2333	-2331	-0	0	1
0.1079	520.40	1.636	-0.576	4564.3	500.00	1.72	4.45	45.84	0.13	-1.72	-55	-57	2333	-2331	-0	0	1
0.1080	520.90	1.638	-0.576	4564.3	500.00	1.72	4.45	45.84	0.13	-1.72	-55	-57	2333	-2331	-0	0	1
0.1081	520.39	1.640	-0.576	4564.3	500.00	1.72	4.45	45.84	0.13	-1.72	-55	-57	2333	-2331	-0	0	1
0.1082	520.39	1.642	-0.576	4564.3	500.00	1.72	4.45	45.84	0.13	-1.72	-55	-57	2333	-2331	-0	0	1
0.1083	520.38	1.644	-0.576	4564.3	500.00	1.72	4.45	45.84	0.13	-1.72	-55	-57	2333	-2331	-0	0	1
0.1084	520.38	1.646	-0.576	4564.3	500.00	1.72	4.45	45.84	0.13	-1.72	-55	-57	2333	-2331	-0	0	1
0.1085	520.37	1.648	-0.576	4564.3	500.00	1.72	4.45	45.84	0.13	-1.72	-55	-57	2333	-2331	-0	0	1
0.1086	520.37	1.650	-0.576	4564.3	500.00	1.72	4.45	45.84	0.13	-1.72	-55	-57	2333	-2331	-0	0	1
0.1087	520.36	1.652	-0.576	4564.3	500.00	1.72	4.45	45.84	0.13	-1.72	-55	-57	2333	-2331	-0	0	1
0.1088	520.36	1.654	-0.576	4564.3	500.00	1.72	4.45	45.84	0.13	-1.72	-55	-57	2333	-2331	-0	0	1
0.1089	520.35	1.656	-0.576	4564.3	500.00	1.72	4.45	45.84	0.13	-1.72	-55	-57	2333	-2331	-0	0	1
0.1090	520.35	1.658	-0.576	4564.3	500.00	1.72	4.45	45.84	0.13	-1.72	-55	-57	2333	-2331	-0	0	1
0.1091	520.34	1.660	-0.576	4564.3	500.00	1.72	4.45	45.84	0.13	-1.72	-55	-57	2333	-2331	-0	0	1
0.1092	520.34	1.662	-0.576	4564.3	500.00	1.72	4.45	45.84	0.13	-1.72	-55	-57	2333	-2331	-0	0	1
0.1093	520.33	1.664	-0.576	4564.3	500.00	1.72	4.45	45.84	0.13	-1.72	-55	-57	2333	-2331	-0	0	1
0.1094	520.33	1.666	-0.576	4564.3	500.00	1.72	4.45	45.84	0.13	-1.72	-55	-57	2333	-2331	-0	0	1
0.1095	520.32	1.668	-0.576	4564.3	500.00	1.72	4.45	45.84	0.13	-1.72	-55	-57	2333	-2331	-0	0	1
0.1096	520.32	1.670	-0.576	4564.3	500.00	1.72	4.45	45.84	0.13	-1.72	-55	-57	2333	-2331	-0	0	1
0.1097	520.31	1.672	-0.576	4564.3	500.00	1.72	4.45	45.84	0.13	-1.72	-55	-57	2333	-2331	-0	0	1
0.1098	520.31	1.674	-0.576	4564.3	500.00	1.72	4.45	45.84	0.13	-1.72	-55	-57	2333	-2331	-0	0	1
0.1099	520.30	1.676	-0.576	4564.3	500.00	1.72	4.45	45.84	0.13	-1.72	-55	-57	2333	-2331	-0	0	1
0.1100	520.30	1.678	-0.576	4564.3	500.00	1.72	4.45	45.84	0.13	-1.72	-55	-57	2333	-2331	-0	0	1







FLECHETTE GROUND POINT

PAGE 25

T SEC	X FT	Y FT	Z FT	V FT/SEC	P RAD/SEC	ALPHA DEG	MACH	PHI DEG	ALPHA DEG	BUT4 UGS	L-N 175C	L-P 175C	W-P 175C	S RAD/SEC	U DEG
0.1200	556.44	1.813	-0.541	4952.9	500.00	1.44	4.45	45.51	-1.29	-0.54	-55	-57	2336	-2331	0
0.1201	556.94	1.915	-0.541	4952.8	500.00	1.44	4.45	45.53	-1.32	-0.53	-55	-57	2336	-2331	0
0.1202	557.44	1.917	-0.541	4952.8	500.00	1.44	4.45	45.55	-1.35	-0.51	-55	-57	2336	-2331	0
0.1203	557.93	1.810	-0.540	4952.8	500.00	1.44	4.45	45.58	-1.37	-0.44	-55	-57	2336	-2331	0
0.1204	558.43	1.820	-0.540	4952.8	500.00	1.44	4.45	45.61	-1.39	-0.36	-55	-57	2336	-2331	0
0.1205	558.92	1.822	-0.540	4952.8	500.00	1.44	4.45	45.64	-1.41	-0.24	-55	-57	2336	-2331	0
0.1206	559.42	1.824	-0.540	4952.8	500.00	1.45	4.45	45.67	-1.43	-0.24	-55	-57	2336	-2331	0
0.1207	559.92	1.825	-0.541	4952.8	500.00	1.45	4.45	45.70	-1.44	-0.17	-55	-57	2336	-2331	0
0.1208	600.41	1.827	-0.537	4952.7	500.00	1.45	4.45	45.71	-1.46	-0.09	-55	-57	2336	-2331	0
0.1209	600.91	1.828	-0.536	4952.7	500.00	1.45	4.45	45.71	-1.45	-0.02	-55	-57	2336	-2331	0
0.1210	601.41	1.830	-0.536	4952.7	500.00	1.45	4.45	45.70	-1.45	0.05	-55	-57	2336	-2331	0
0.1211	601.90	1.831	-0.535	4952.7	500.00	1.45	4.45	45.67	-1.44	0.12	-55	-57	2336	-2331	0
0.1212	602.40	1.833	-0.535	4952.7	500.00	1.44	4.45	45.63	-1.43	0.21	-55	-57	2336	-2331	0
0.1213	602.89	1.836	-0.534	4952.7	500.00	1.44	4.45	45.58	-1.42	0.27	-55	-57	2336	-2331	0
0.1214	603.39	1.838	-0.533	4952.7	500.00	1.44	4.45	45.51	-1.40	0.36	-55	-57	2336	-2331	0
0.1215	603.89	1.837	-0.533	4952.7	500.00	1.44	4.45	45.44	-1.38	0.41	-55	-57	2336	-2331	0
0.1216	604.38	1.838	-0.533	4952.7	500.00	1.44	4.45	45.37	-1.34	0.46	-55	-57	2336	-2331	0
0.1217	604.88	1.839	-0.534	4952.6	500.00	1.44	4.45	45.30	-1.33	0.55	-55	-57	2336	-2331	0
0.1218	605.37	1.841	-0.533	4952.5	500.00	1.44	4.45	45.23	-1.30	0.62	-55	-57	2336	-2331	0
0.1219	605.87	1.843	-0.537	4952.5	500.00	1.44	4.45	45.16	-1.26	0.68	-55	-57	2336	-2331	0
0.1220	606.37	1.844	-0.537	4952.5	500.00	1.44	4.45	45.12	-1.19	0.71	-55	-57	2336	-2331	0
0.1221	606.85	1.845	-0.537	4952.5	500.00	1.44	4.45	45.12	-1.15	0.75	-55	-57	2336	-2331	0
0.1222	607.36	1.845	-0.537	4952.5	500.00	1.44	4.45	45.14	-1.10	0.82	-55	-57	2336	-2331	0
0.1223	607.85	1.847	-0.537	4952.5	500.00	1.44	4.45	45.17	-1.05	0.87	-55	-57	2336	-2331	0
0.1224	608.35	1.847	-0.537	4952.4	500.00	1.44	4.45	45.23	-1.11	1.02	-55	-57	2336	-2331	0
0.1225	608.85	1.848	-0.537	4952.4	500.00	1.44	4.45	45.33	-1.11	1.17	-55	-57	2336	-2331	0
0.1226	609.34	1.850	-0.537	4952.5	500.00	1.44	4.45	45.43	-1.12	1.32	-55	-57	2336	-2331	0
0.1227	609.84	1.850	-0.537	4952.5	500.00	1.44	4.45	45.53	-1.15	1.46	-55	-57	2336	-2331	0
0.1228	610.33	1.851	-0.537	4952.5	500.00	1.44	4.45	45.63	-1.16	1.60	-55	-57	2336	-2331	0
0.1229	610.83	1.851	-0.537	4952.5	500.00	1.44	4.45	45.73	-1.17	1.74	-55	-57	2336	-2331	0
0.1230	611.33	1.852	-0.537	4952.5	500.00	1.44	4.45	45.83	-1.17	1.87	-55	-57	2336	-2331	0
0.1231	611.82	1.853	-0.531	4952.5	500.00	1.44	4.44	45.79	-1.07	1.93	-55	-57	2336	-2331	0
0.1232	612.32	1.854	-0.534	4952.5	500.00	1.44	4.44	45.75	-0.96	1.93	-55	-57	2336	-2331	0
0.1233	612.82	1.855	-0.533	4952.5	500.00	1.44	4.44	45.69	-0.92	1.93	-55	-57	2336	-2331	0
0.1234	613.31	1.855	-0.533	4952.4	500.00	1.44	4.44	45.62	-0.84	1.93	-55	-57	2336	-2331	0
0.1235	613.81	1.856	-0.533	4952.4	500.00	1.44	4.44	45.53	-0.81	1.93	-55	-57	2336	-2331	0
0.1236	614.30	1.857	-0.533	4952.4	500.00	1.44	4.44	45.42	-0.81	1.93	-55	-57	2336	-2331	0
0.1237	614.80	1.858	-0.533	4952.4	500.00	1.44	4.44	45.37	-0.77	1.93	-55	-57	2336	-2331	0
0.1238	615.30	1.859	-0.540	4952.4	500.00	1.44	4.44	45.37	-0.77	1.93	-55	-57	2336	-2331	0
0.1239	615.79	1.860	-0.540	4952.4	500.00	1.44	4.44	45.39	-0.72	1.93	-55	-57	2336	-2331	0
0.1240	616.29	1.860	-0.541	4952.4	500.00	1.44	4.44	45.32	-0.65	1.94	-55	-57	2336	-2331	0
0.1241	616.78	1.861	-0.541	4952.4	500.00	1.44	4.44	45.33	-0.61	1.94	-55	-57	2336	-2331	0
0.1242	617.28	1.862	-0.542	4952.4	500.00	1.44	4.44	45.34	-0.51	1.94	-55	-57	2336	-2331	0
0.1243	617.78	1.863	-0.542	4952.4	500.00	1.44	4.44	45.39	-0.46	1.93	-55	-57	2336	-2331	0
0.1244	618.27	1.863	-0.543	4952.3	500.00	1.44	4.44	45.35	-0.32	1.91	-55	-57	2336	-2331	0
0.1245	618.77	1.864	-0.544	4952.3	500.00	1.44	4.44	45.32	-0.30	1.93	-55	-57	2336	-2331	0
0.1246	619.26	1.865	-0.544	4952.3	500.00	1.44	4.44	45.31	-0.26	1.93	-55	-57	2336	-2331	0
0.1247	619.76	1.866	-0.544	4952.3	500.00	1.44	4.44	45.31	-0.26	1.93	-55	-57	2336	-2331	0
0.1248	620.25	1.867	-0.546	4952.3	500.00	1.45	4.44	45.31	-0.53	1.95	-55	-57	2336	-2331	0
0.1249	620.75	1.867	-0.547	4952.3	500.00	1.45	4.44	45.31	-0.50	1.92	-55	-57	2336	-2331	0

Page 26

T	X	Y	Z	V	D	ALPHA		DELTA	L-B	I-B	W-B	V-B	K-B
SEC		FT	FT	FT/SEC	FT/SEC	DEG	SEC	DEG	REF	1/SEC	1/SEC	1/SEC	1/SEC
0.1250	621.25	1.348	-0.647	4982.3	500.00	1.65	4.44	45.33	0.74	1.29	53	-57	2335
0.1251	621.75	1.849	-0.643	4982.3	500.00	1.64	4.44	45.33	0.72	1.25	53	-57	2335
0.1252	622.24	1.870	-0.640	4982.2	500.00	1.64	4.44	45.33	0.74	1.21	53	-57	2335
0.1253	622.74	1.871	-0.630	4982.2	500.00	1.64	4.44	45.33	0.74	1.17	53	-57	2335
0.1254	623.24	1.872	-0.551	4982.2	500.00	1.64	4.44	45.33	0.72	1.13	53	-57	2335
0.1255	623.73	1.873	-0.552	4982.2	500.00	1.64	4.44	45.33	0.72	1.09	53	-57	2335
0.1256	624.23	1.874	-0.553	4982.2	500.00	1.64	4.44	45.33	0.72	1.05	53	-57	2335
0.1257	624.72	1.875	-0.455	4982.2	500.00	1.64	4.44	45.33	0.72	1.01	53	-57	2335
0.1258	625.22	1.876	-0.455	4982.2	500.00	1.64	4.44	45.33	0.72	0.97	53	-57	2335
0.1259	625.71	1.877	-0.456	4982.2	500.00	1.64	4.44	45.33	0.72	0.93	53	-57	2335
0.1260	626.21	1.878	-0.457	4982.2	500.00	1.64	4.44	45.33	0.72	0.89	53	-57	2335
0.1261	626.71	1.879	-0.458	4982.2	500.00	1.64	4.44	45.33	0.72	0.85	53	-57	2335
0.1262	627.20	1.880	-0.459	4982.2	500.00	1.64	4.44	45.33	0.72	0.81	53	-57	2335
0.1263	627.70	1.881	-0.460	4982.2	500.00	1.64	4.44	45.33	0.72	0.77	53	-57	2335
0.1264	628.19	1.882	-0.461	4982.1	500.00	1.64	4.44	45.33	0.72	0.73	53	-57	2335
0.1265	628.69	1.883	-0.462	4982.1	500.00	1.64	4.44	45.33	0.72	0.69	53	-57	2335
0.1266	629.19	1.884	-0.463	4982.1	500.00	1.64	4.44	45.33	0.72	0.65	53	-57	2335
0.1267	629.68	1.885	-0.464	4982.1	500.00	1.64	4.44	45.33	0.72	0.61	53	-57	2335
0.1268	630.18	1.886	-0.465	4982.1	500.00	1.64	4.44	45.33	0.72	0.57	53	-57	2335
0.1269	630.67	1.887	-0.466	4982.1	500.00	1.64	4.44	45.33	0.72	0.53	53	-57	2335
0.1270	631.17	1.888	-0.467	4982.1	500.00	1.64	4.44	45.33	0.72	0.49	53	-57	2335
0.1271	631.67	1.889	-0.468	4982.1	500.00	1.64	4.44	45.33	0.72	0.45	53	-57	2335
0.1272	632.16	1.890	-0.469	4982.0	500.00	1.64	4.44	45.33	0.72	0.41	53	-57	2335
0.1273	632.65	1.891	-0.470	4982.0	500.00	1.64	4.44	45.33	0.72	0.37	53	-57	2335
0.1274	633.15	1.892	-0.471	4982.0	500.00	1.64	4.44	45.33	0.72	0.33	53	-57	2335
0.1275	633.65	1.893	-0.472	4982.0	500.00	1.64	4.44	45.33	0.72	0.29	53	-57	2335
0.1276	634.15	1.894	-0.473	4982.0	500.00	1.64	4.44	45.33	0.72	0.25	53	-57	2335
0.1277	634.64	1.895	-0.474	4982.0	500.00	1.64	4.44	45.33	0.72	0.21	53	-57	2335
0.1278	635.14	1.896	-0.475	4982.0	500.00	1.64	4.44	45.33	0.72	0.17	53	-57	2335
0.1279	635.64	1.897	-0.476	4982.0	500.00	1.64	4.44	45.33	0.72	0.13	53	-57	2335
0.1280	636.13	1.898	-0.477	4982.0	500.00	1.64	4.44	45.33	0.72	0.09	53	-57	2335
0.1281	636.63	1.899	-0.478	4981.9	500.00	1.64	4.44	45.33	0.72	0.05	53	-57	2335
0.1282	637.12	1.900	-0.479	4981.9	500.00	1.64	4.44	45.33	0.72	0.01	53	-57	2335
0.1283	637.62	1.901	-0.480	4981.9	500.00	1.64	4.44	45.33	0.72	0.00	53	-57	2335
0.1284	638.12	1.902	-0.481	4981.9	500.00	1.64	4.44	45.33	0.72	0.00	53	-57	2335
0.1285	638.61	1.903	-0.482	4981.9	500.00	1.64	4.44	45.33	0.72	0.00	53	-57	2335
0.1286	639.11	1.904	-0.483	4981.9	500.00	1.64	4.44	45.33	0.72	0.00	53	-57	2335
0.1287	639.60	1.905	-0.484	4981.9	500.00	1.64	4.44	45.33	0.72	0.00	53	-57	2335
0.1288	640.10	1.906	-0.485	4981.9	500.00	1.64	4.44	45.33	0.72	0.00	53	-57	2335
0.1289	640.60	1.907	-0.486	4981.9	500.00	1.64	4.44	45.33	0.72	0.00	53	-57	2335
0.1290	641.09	1.908	-0.487	4981.9	500.00	1.64	4.44	45.33	0.72	0.00	53	-57	2335
0.1291	641.59	1.909	-0.488	4981.9	500.00	1.64	4.44	45.33	0.72	0.00	53	-57	2335
0.1292	642.08	1.910	-0.489	4981.9	500.00	1.64	4.44	45.33	0.72	0.00	53	-57	2335
0.1293	642.58	1.911	-0.490	4981.9	500.00	1.64	4.44	45.33	0.72	0.00	53	-57	2335
0.1294	643.08	1.912	-0.491	4981.9	500.00	1.64	4.44	45.33	0.72	0.00	53	-57	2335
0.1295	643.57	1.913	-0.492	4981.9	500.00	1.64	4.44	45.33	0.72	0.00	53	-57	2335
0.1296	644.07	1.914	-0.493	4981.9	500.00	1.64	4.44	45.33	0.72	0.00	53	-57	2335
0.1297	644.57	1.915	-0.494	4981.9	500.00	1.64	4.44	45.33	0.72	0.00	53	-57	2335
0.1298	645.06	1.916	-0.495	4981.9	500.00	1.64	4.44	45.33	0.72	0.00	53	-57	2335
0.1299	645.56	1.917	-0.496	4981.9	500.00	1.64	4.44	45.33	0.72	0.00	53	-57	2335

## FLECHETTE GROUND POINT

PAGE 27

Y SEC	X FT	Y FT	Z FT	V FT/SEC	P CM/SEC	ALPHA DEG	PHI DEG	ALPHA DEG	PETA DEG	L-N 1/SEC	L-P 1/SEC	4-N 1/SEC	4-P 1/SEC	TAU	K-2
0.1300	645.05	1.947	-0.701	4951.7	500.00	1.44	4.44	45.52	0.25	-1.41	-52.	-37.	2335.-2332.	0.	1.
0.1301	646.55	1.949	-0.701	4951.7	500.00	1.44	4.44	45.57	0.19	-1.42	-52.	-37.	2335.-2332.	0.	1.
0.1302	647.05	1.951	-0.702	4951.7	500.00	1.43	4.44	45.70	0.11	-1.43	-55.	-37.	2335.-2332.	0.	1.
0.1303	647.54	1.953	-0.702	4951.7	500.00	1.43	4.44	45.69	0.34	-1.43	-55.	-37.	2335.-2332.	0.	1.
0.1304	648.04	1.955	-0.703	4951.7	500.00	1.43	4.44	45.55	0.34	-1.43	-55.	-37.	2335.-2332.	0.	1.
0.1305	648.53	1.958	-0.703	4951.7	500.00	1.44	4.44	45.45	0.11	-1.43	-55.	-37.	2335.-2332.	0.	1.
0.1306	649.03	1.960	-0.704	4951.7	500.00	1.44	4.44	45.52	0.17	-1.42	-55.	-37.	2335.-2332.	0.	1.
0.1307	649.53	1.962	-0.704	4951.6	500.00	1.44	4.44	45.52	0.22	-1.41	-55.	-37.	2335.-2332.	0.	1.
0.1308	650.02	1.964	-0.705	4951.6	500.00	1.44	4.44	45.55	0.12	-1.40	-55.	-37.	2335.-2332.	0.	1.
0.1309	650.52	1.967	-0.705	4951.6	500.00	1.44	4.44	45.51	0.37	-1.40	-55.	-37.	2335.-2332.	0.	1.
0.1310	651.01	1.969	-0.706	4951.6	500.00	1.44	4.44	45.45	0.53	-1.39	-55.	-37.	2335.-2332.	0.	1.
0.1311	651.51	1.971	-0.706	4951.5	500.00	1.47	4.44	45.45	0.53	-1.39	-55.	-37.	2335.-2332.	0.	1.
0.1312	652.01	1.973	-0.705	4951.6	500.00	1.44	4.44	45.43	0.50	-1.31	-55.	-37.	2335.-2332.	0.	1.
0.1313	652.50	1.975	-0.706	4951.6	500.00	1.44	4.44	45.41	0.57	-1.29	-55.	-37.	2335.-2332.	0.	1.
0.1314	653.00	1.977	-0.706	4951.6	500.00	1.44	4.44	45.41	0.73	-1.29	-55.	-37.	2335.-2332.	0.	1.
0.1315	653.50	1.979	-0.706	4951.6	500.00	1.44	4.44	45.41	0.73	-1.21	-55.	-37.	2335.-2332.	0.	1.
0.1316	653.99	1.981	-0.706	4951.6	500.00	1.44	4.44	45.41	0.85	-1.17	-55.	-37.	2335.-2332.	0.	1.
0.1317	654.48	1.984	-0.707	4951.6	500.00	1.44	4.44	45.42	0.81	-1.12	-55.	-37.	2335.-2332.	0.	1.
0.1318	654.98	1.986	-0.707	4951.6	500.00	1.44	4.44	45.43	0.75	-1.09	-55.	-37.	2335.-2332.	0.	1.
0.1319	655.46	1.988	-0.707	4951.6	500.00	1.44	4.44	45.44	0.81	-1.03	-55.	-37.	2335.-2332.	0.	1.
0.1320	655.94	1.990	-0.707	4951.6	500.00	1.44	4.44	45.45	0.85	-0.97	-55.	-37.	2335.-2332.	0.	1.
0.1321	656.42	1.992	-0.707	4951.6	500.00	1.44	4.44	45.45	0.85	-0.92	-55.	-37.	2335.-2332.	0.	1.
0.1322	656.90	1.994	-0.707	4951.6	500.00	1.44	4.44	45.45	0.85	-0.85	-55.	-37.	2335.-2332.	0.	1.
0.1323	657.38	1.995	-0.706	4951.5	500.00	1.44	4.44	45.46	0.85	-0.85	-55.	-37.	2335.-2332.	0.	1.
0.1324	657.86	1.997	-0.706	4951.5	500.00	1.44	4.44	45.45	0.85	-0.75	-55.	-37.	2335.-2332.	0.	1.
0.1325	658.34	1.999	-0.705	4951.5	500.00	1.43	4.44	45.45	0.85	-0.64	-55.	-37.	2335.-2332.	0.	1.
0.1326	658.82	2.001	-0.706	4951.5	500.00	1.43	4.44	45.45	0.85	-0.51	-55.	-37.	2335.-2332.	0.	1.
0.1327	659.30	2.003	-0.705	4951.5	500.00	1.43	4.44	45.43	0.85	-0.55	-55.	-37.	2335.-2332.	0.	1.
0.1328	659.78	2.005	-0.705	4951.4	500.00	1.43	4.44	45.43	0.85	-0.49	-55.	-37.	2335.-2332.	0.	1.
0.1329	660.26	2.006	-0.705	4951.4	500.00	1.43	4.44	45.42	0.85	-0.41	-55.	-37.	2335.-2332.	0.	1.
0.1330	660.74	2.008	-0.705	4951.4	500.00	1.43	4.44	45.42	0.85	-0.34	-55.	-37.	2335.-2332.	0.	1.
0.1331	661.22	2.010	-0.705	4951.4	500.00	1.43	4.44	45.42	0.85	-0.27	-55.	-37.	2335.-2332.	0.	1.
0.1332	661.70	2.013	-0.705	4951.4	500.00	1.43	4.44	45.42	0.85	-0.20	-55.	-37.	2335.-2332.	0.	1.
0.1333	662.18	2.015	-0.705	4951.4	500.00	1.43	4.44	45.42	0.85	-0.13	-55.	-37.	2335.-2332.	0.	1.
0.1334	662.66	2.016	-0.705	4951.4	500.00	1.44	4.44	45.42	0.85	-0.06	-55.	-37.	2335.-2332.	0.	1.
0.1335	663.14	2.016	-0.705	4951.4	500.00	1.44	4.44	45.41	0.85	0.01	-55.	-37.	2335.-2332.	0.	1.
0.1336	663.62	2.017	-0.705	4951.4	500.00	1.44	4.44	45.41	0.85	0.08	-55.	-37.	2335.-2332.	0.	1.
0.1337	664.10	2.017	-0.704	4951.3	500.00	1.44	4.44	45.41	0.85	0.15	-55.	-37.	2335.-2332.	0.	1.
0.1338	664.58	2.017	-0.704	4951.3	500.00	1.44	4.44	45.41	0.85	0.22	-55.	-37.	2335.-2332.	0.	1.
0.1339	665.06	2.020	-0.704	4951.3	500.00	1.44	4.44	45.41	0.85	0.29	-55.	-37.	2335.-2332.	0.	1.
0.1340	665.54	2.021	-0.704	4951.3	500.00	1.44	4.44	45.42	0.85	0.36	-55.	-37.	2335.-2332.	0.	1.
0.1341	666.02	2.024	-0.703	4951.3	500.00	1.44	4.44	45.42	0.85	0.43	-55.	-37.	2335.-2332.	0.	1.
0.1342	666.50	2.025	-0.703	4951.3	500.00	1.44	4.44	45.43	0.85	0.50	-55.	-37.	2335.-2332.	0.	1.
0.1343	666.98	2.027	-0.703	4951.3	500.00	1.44	4.44	45.43	0.85	0.57	-55.	-37.	2335.-2332.	0.	1.
0.1344	667.46	2.028	-0.703	4951.3	500.00	1.44	4.44	45.45	0.85	0.63	-55.	-37.	2335.-2332.	0.	1.
0.1345	667.94	2.029	-0.703	4951.2	500.00	1.44	4.44	45.43	0.85	0.70	-55.	-37.	2335.-2332.	0.	1.
0.1346	668.42	2.030	-0.703	4951.2	500.00	1.44	4.44	45.41	0.85	0.76	-55.	-37.	2335.-2332.	0.	1.
0.1347	668.90	2.031	-0.703	4951.2	500.00	1.44	4.44	45.43	0.85	0.82	-55.	-37.	2335.-2332.	0.	1.
0.1348	669.38	2.032	-0.702	4951.2	500.00	1.44	4.44	45.43	0.85	0.88	-55.	-37.	2335.-2332.	0.	1.
0.1349	669.86	2.033	-0.702	4951.2	500.00	1.44	4.44	45.43	0.85	0.94	-55.	-37.	2335.-2332.	0.	1.

## FLECHETTE GROUND POINT

PAGE 25

T SEC	X FT	Y FT	Z FT	V FT/SEC	P RAD/SEC	ALPHA MACH	PHI DEG	ALPHA DEG	PSTZ DEG	L-N 1/SEC	L-P 1/SEC	M-N 1/SEC	S 1/SEC	TQU	M-T DEG
0.1350	670.25	2.034	-0.702	461.2	500.00	1.44 4.44	45.46	1.04	0.99	-55	-57	2335-2332	0	0	1
0.1351	671.35	2.035	-0.702	461.2	500.00	1.44 4.44	45.42	1.04	1.04	-55	-57	2335-2332	0	0	1
0.1352	671.85	2.036	-0.702	461.2	500.00	1.44 4.44	45.39	1.04	1.04	-55	-57	2335-2332	0	0	1
0.1353	672.35	2.037	-0.702	461.1	500.00	1.44 4.44	45.35	1.04	1.14	-55	-57	2335-2332	0	0	1
0.1354	672.84	2.038	-0.703	461.1	500.00	1.44 4.44	45.32	1.04	1.13	-55	-57	2335-2332	0	0	1
0.1355	673.34	2.039	-0.703	461.1	500.00	1.44 4.44	45.31	1.04	1.22	-55	-57	2335-2332	0	0	1
0.1356	673.83	2.040	-0.703	461.1	500.00	1.44 4.44	45.30	1.04	1.26	-55	-57	2335-2332	0	0	1
0.1357	674.33	2.041	-0.703	461.1	500.00	1.44 4.44	45.31	1.04	1.25	-55	-57	2335-2332	0	0	1
0.1358	674.83	2.041	-0.703	461.1	500.00	1.44 4.44	45.32	1.04	1.32	-55	-57	2335-2332	0	0	1
0.1359	675.32	2.042	-0.703	461.1	500.00	1.44 4.44	45.34	1.04	1.35	-55	-57	2335-2332	0	0	1
0.1360	675.82	2.043	-0.703	461.1	500.00	1.44 4.44	45.37	1.04	1.37	-55	-57	2335-2332	0	0	1
0.1361	676.32	2.044	-0.703	461.1	500.00	1.44 4.44	45.41	1.04	1.37	-55	-57	2335-2332	0	0	1
0.1362	676.81	2.045	-0.704	461.1	500.00	1.44 4.44	45.44	1.04	1.41	-55	-57	2335-2332	0	0	1
0.1363	677.31	2.045	-0.705	461.1	500.00	1.44 4.44	45.47	1.04	1.42	-55	-57	2335-2332	0	0	1
0.1364	677.80	2.046	-0.705	461.1	500.00	1.44 4.44	45.51	1.04	1.43	-55	-57	2335-2332	0	0	1
0.1365	678.30	2.047	-0.704	461.1	500.00	1.44 4.44	45.55	1.04	1.43	-55	-57	2335-2332	0	0	1
0.1366	678.80	2.048	-0.704	461.1	500.00	1.44 4.44	45.58	1.04	1.43	-55	-57	2335-2332	0	0	1
0.1367	679.29	2.049	-0.704	461.1	500.00	1.44 4.44	45.61	1.04	1.43	-55	-57	2335-2332	0	0	1
0.1368	679.78	2.049	-0.707	461.1	500.00	1.44 4.44	45.61	1.04	1.43	-55	-57	2335-2332	0	0	1
0.1369	680.28	2.050	-0.708	461.1	500.00	1.44 4.44	45.61	1.04	1.43	-55	-57	2335-2332	0	0	1
0.1370	680.78	2.051	-0.708	461.1	500.00	1.44 4.44	45.61	1.04	1.43	-55	-57	2335-2332	0	0	1
0.1371	681.27	2.052	-0.709	461.1	500.00	1.44 4.44	45.61	1.04	1.43	-55	-57	2335-2332	0	0	1
0.1372	681.77	2.052	-0.710	461.1	500.00	1.44 4.44	45.61	1.04	1.43	-55	-57	2335-2332	0	0	1
0.1373	682.27	2.053	-0.711	461.1	500.00	1.44 4.44	45.61	1.04	1.43	-55	-57	2335-2332	0	0	1
0.1374	682.75	2.054	-0.711	461.1	500.00	1.44 4.44	45.61	1.04	1.43	-55	-57	2335-2332	0	0	1
0.1375	683.26	2.055	-0.712	461.1	500.00	1.44 4.44	45.61	1.04	1.43	-55	-57	2335-2332	0	0	1
0.1376	683.75	2.056	-0.713	461.1	500.00	1.44 4.44	45.61	1.04	1.43	-55	-57	2335-2332	0	0	1
0.1377	684.25	2.056	-0.714	461.1	500.00	1.44 4.44	45.61	1.04	1.43	-55	-57	2335-2332	0	0	1
0.1378	684.75	2.057	-0.715	461.1	500.00	1.44 4.44	45.61	1.04	1.43	-55	-57	2335-2332	0	0	1
0.1379	685.24	2.058	-0.716	461.1	500.00	1.44 4.44	45.61	1.04	1.43	-55	-57	2335-2332	0	0	1
0.1380	685.74	2.059	-0.717	461.1	500.00	1.44 4.44	45.61	1.04	1.43	-55	-57	2335-2332	0	0	1
0.1381	686.21	2.060	-0.718	461.1	500.00	1.44 4.44	45.61	1.04	1.43	-55	-57	2335-2332	0	0	1
0.1382	686.71	2.061	-0.719	461.1	500.00	1.44 4.44	45.61	1.04	1.43	-55	-57	2335-2332	0	0	1
0.1383	687.21	2.062	-0.720	461.1	500.00	1.44 4.44	45.61	1.04	1.43	-55	-57	2335-2332	0	0	1
0.1384	687.72	2.063	-0.721	461.1	500.00	1.44 4.44	45.61	1.04	1.43	-55	-57	2335-2332	0	0	1
0.1385	688.22	2.064	-0.722	461.1	500.00	1.44 4.44	45.61	1.04	1.43	-55	-57	2335-2332	0	0	1
0.1386	688.71	2.065	-0.723	461.1	500.00	1.44 4.44	45.61	1.04	1.43	-55	-57	2335-2332	0	0	1
0.1387	689.21	2.066	-0.724	461.1	500.00	1.44 4.44	45.61	1.04	1.43	-55	-57	2335-2332	0	0	1
0.1388	689.71	2.067	-0.725	461.1	500.00	1.44 4.44	45.61	1.04	1.43	-55	-57	2335-2332	0	0	1
0.1389	690.20	2.068	-0.726	461.1	500.00	1.44 4.44	45.61	1.04	1.43	-55	-57	2335-2332	0	0	1
0.1390	690.70	2.069	-0.727	461.1	500.00	1.44 4.44	45.61	1.04	1.43	-55	-57	2335-2332	0	0	1
0.1391	691.19	2.070	-0.728	461.1	500.00	1.44 4.44	45.61	1.04	1.43	-55	-57	2335-2332	0	0	1
0.1392	691.69	2.071	-0.729	461.1	500.00	1.44 4.44	45.61	1.04	1.43	-55	-57	2335-2332	0	0	1
0.1393	692.18	2.072	-0.730	461.1	500.00	1.44 4.44	45.61	1.04	1.43	-55	-57	2335-2332	0	0	1
0.1394	692.68	2.073	-0.731	461.1	500.00	1.44 4.44	45.61	1.04	1.43	-55	-57	2335-2332	0	0	1
0.1395	693.18	2.074	-0.732	461.1	500.00	1.44 4.44	45.61	1.04	1.43	-55	-57	2335-2332	0	0	1
0.1396	693.67	2.075	-0.733	461.1	500.00	1.44 4.44	45.61	1.04	1.43	-55	-57	2335-2332	0	0	1
0.1397	694.17	2.076	-0.734	461.1	500.00	1.44 4.44	45.61	1.04	1.43	-55	-57	2335-2332	0	0	1
0.1398	694.65	2.077	-0.735	461.1	500.00	1.44 4.44	45.61	1.04	1.43	-55	-57	2335-2332	0	0	1
0.1399	695.16	2.078	-0.736	461.1	500.00	1.44 4.44	45.61	1.04	1.43	-55	-57	2335-2332	0	0	1

## FLECHETTE GROUND POINT

PAGE 29

T SEC	X FT	Y FT	Z FT	V FT/SEC	P RAD/SEC	ALPHA MACH	PHI DEG	ALPHA SEC	BETA SEC	WGS 1/SEC	L-N 1/SEC	L-P 1/SEC	M-N 1/SEC	M-L 1/SEC	JAW	K-I
0.1470	595.66	2.084	-0.770	4850.4	500.00	1.44 4.4	45.43	1.43	-0.17	-55	-57	2335-2332	-0	0	0	1
0.1401	695.15	2.035	-0.741	4840.6	500.00	1.42 4.4	45.45	1.42	-0.24	-55	-57	2335-2332	-0	0	0	1
0.1407	695.45	2.037	-0.752	4850.6	500.00	1.43 4.4	45.47	1.43	-0.31	-55	-57	2335-2332	-0	0	0	1
0.1403	697.14	2.030	-0.767	4860.6	500.00	1.44 4.4	45.49	1.37	-0.38	-55	-57	2335-2332	-0	0	0	1
0.1434	597.55	2.020	-0.785	4860.5	500.00	1.44 4.4	45.51	1.37	-0.45	-55	-57	2335-2332	-0	0	0	1
0.1405	595.13	2.022	-0.784	4861.4	500.00	1.44 4.4	45.44	1.34	-0.52	-55	-57	2335-2332	-0	0	0	1
0.1436	595.63	2.014	-0.747	4860.5	500.00	1.43 4.4	45.35	1.32	-0.52	-55	-57	2335-2332	-0	0	0	1
0.1407	695.13	2.015	-0.744	4860.5	500.00	1.44 4.4	45.44	1.29	-0.65	-55	-57	2335-2332	-0	0	0	1
0.1418	432.62	2.027	-0.759	4850.5	500.00	1.45 4.4	45.43	1.25	-0.71	-55	-57	2335-2332	-0	0	0	1
0.1409	700.17	2.065	-0.751	4860.5	500.00	1.44 4.4	45.41	1.21	-0.77	-55	-57	2335-2332	-0	0	0	1
0.1410	700.41	2.131	-0.752	4850.3	500.00	1.44 4.4	45.41	1.17	-0.83	-55	-57	2335-2332	-0	0	0	1
0.1411	701.11	2.103	-0.753	4850.6	500.00	1.44 4.4	45.41	1.13	-0.87	-55	-57	2335-2332	-0	0	0	1
0.1412	701.41	2.105	-0.754	4860.5	500.00	1.44 4.4	45.40	1.09	-0.94	-55	-57	2335-2332	-0	0	0	1
0.1413	702.10	2.137	-0.755	4840.5	500.00	1.44 4.4	45.54	1.04	-1.00	-55	-57	2335-2332	-0	0	0	1
0.1414	702.40	2.135	-0.756	4850.5	500.00	1.44 4.4	45.55	0.92	-1.03	-55	-57	2335-2332	-0	0	0	1
0.1415	703.09	2.111	-0.757	4860.5	500.00	1.44 4.4	45.54	0.83	-1.10	-55	-57	2335-2332	-0	0	0	1
0.1416	703.59	2.113	-0.758	4850.4	500.00	1.44 4.4	45.61	0.87	-1.14	-55	-57	2335-2332	-0	0	0	1
0.1417	704.08	2.115	-0.759	4860.4	500.00	1.44 4.4	45.43	0.82	-1.19	-55	-57	2335-2332	-0	0	0	1
0.1418	705.53	2.117	-0.761	4860.4	500.00	1.44 4.4	45.45	0.75	-1.22	-55	-57	2335-2332	-0	0	0	1
0.1419	705.08	2.115	-0.761	4860.4	500.00	1.44 4.4	45.42	0.69	-1.25	-55	-57	2335-2332	-0	0	0	1
0.1420	705.57	2.121	-0.762	4860.4	500.00	1.44 4.4	45.40	0.53	-1.29	-55	-57	2335-2332	-0	0	0	1
0.1421	706.07	2.124	-0.763	4860.4	500.00	1.44 4.4	45.33	0.36	-1.32	-55	-57	2335-2332	-0	0	0	1
0.1422	705.56	2.126	-0.763	4850.4	500.00	1.44 4.4	45.37	0.43	-1.35	-55	-57	2335-2332	-0	0	0	1
0.1423	707.04	2.128	-0.764	4860.4	500.00	1.44 4.4	45.37	0.43	-1.37	-55	-57	2335-2332	-0	0	0	1
0.1424	707.55	2.130	-0.765	4860.4	500.00	1.44 4.4	45.37	0.36	-1.39	-55	-57	2335-2332	-0	0	0	1
0.1425	708.05	2.132	-0.766	4860.3	500.00	1.44 4.4	45.37	0.29	-1.41	-55	-57	2335-2332	-0	0	0	1
0.1426	708.55	2.135	-0.767	4860.3	500.00	1.44 4.4	45.30	0.22	-1.42	-55	-57	2335-2332	-0	0	0	1
0.1427	709.04	2.137	-0.767	4860.3	500.00	1.44 4.4	45.30	0.16	-1.43	-55	-57	2335-2332	-0	0	0	1
0.1428	709.54	2.139	-0.767	4860.3	500.00	1.44 4.4	45.43	0.07	-1.44	-55	-57	2335-2332	-0	0	0	1
0.1429	710.04	2.141	-0.769	4860.3	500.00	1.44 4.4	45.43	0.00	-1.44	-55	-57	2335-2332	-0	0	0	1
0.1430	710.53	2.143	-0.768	4860.3	500.00	1.44 4.4	45.47	-0.07	-1.44	-55	-57	2335-2332	-0	0	0	1
0.1431	711.03	2.146	-0.768	4860.3	500.00	1.44 4.4	45.43	-0.14	-1.43	-55	-57	2335-2332	-0	0	0	1
0.1432	711.52	2.148	-0.769	4860.2	500.00	1.44 4.4	45.51	-0.21	-1.42	-55	-57	2335-2332	-0	0	0	1
0.1433	712.02	2.150	-0.770	4860.2	500.00	1.44 4.4	45.53	-0.29	-1.41	-55	-57	2335-2332	-0	0	0	1
0.1434	712.51	2.152	-0.770	4860.2	500.00	1.44 4.4	45.50	-0.35	-1.39	-55	-57	2335-2332	-0	0	0	1
0.1435	713.01	2.154	-0.771	4860.2	500.00	1.44 4.4	45.55	-0.42	-1.37	-55	-57	2335-2332	-0	0	0	1
0.1436	713.51	2.157	-0.771	4860.2	500.00	1.44 4.4	45.55	-0.49	-1.35	-55	-57	2335-2332	-0	0	0	1
0.1437	714.00	2.159	-0.771	4860.2	500.00	1.43 4.4	45.55	-0.55	-1.32	-55	-57	2335-2332	-0	0	0	1
0.1438	714.50	2.161	-0.771	4860.2	500.00	1.43 4.4	45.55	-0.62	-1.29	-55	-57	2335-2332	-0	0	0	1
0.1439	715.00	2.163	-0.771	4860.2	500.00	1.43 4.4	45.50	-0.69	-1.26	-55	-57	2335-2332	-0	0	0	1
0.1440	715.50	2.165	-0.772	4860.2	500.00	1.44 4.4	45.53	-0.75	-1.24	-55	-57	2335-2332	-0	0	0	1
0.1441	716.00	2.167	-0.772	4860.2	500.00	1.44 4.4	45.50	-0.81	-1.21	-55	-57	2335-2332	-0	0	0	1
0.1442	716.50	2.169	-0.772	4860.1	500.00	1.44 4.4	45.51	-0.87	-1.19	-55	-57	2335-2332	-0	0	0	1
0.1443	716.99	2.171	-0.772	4860.1	500.00	1.44 4.4	45.51	-0.92	-1.17	-55	-57	2335-2332	-0	0	0	1
0.1444	717.47	2.173	-0.772	4860.1	500.00	1.44 4.4	45.50	-0.95	-1.15	-55	-57	2335-2332	-0	0	0	1
0.1445	717.97	2.175	-0.772	4860.1	500.00	1.44 4.4	45.49	-1.00	-1.13	-55	-57	2335-2332	-0	0	0	1
0.1446	718.46	2.177	-0.772	4860.1	500.00	1.44 4.4	45.46	-1.03	-1.10	-55	-57	2335-2332	-0	0	0	1
0.1447	718.94	2.179	-0.772	4860.1	500.00	1.44 4.4	45.47	-1.02	-1.07	-55	-57	2335-2332	-0	0	0	1
0.1448	719.44	2.181	-0.772	4860.1	500.00	1.44 4.4	45.46	-1.07	-1.04	-55	-57	2335-2332	-0	0	0	1
0.1449	719.94	2.183	-0.772	4860.1	500.00	1.44 4.4	45.47	-1.07	-1.06	-55	-57	2335-2332	-0	0	0	1

FLECHETTE GROUND POINT

PAGE 30

SEC	X	Y	Z	V	ALPHA	PHI	ALPHA	DELTA	L-N	L-P	W-P	IAU	P-T
	FT	FT	FT	FT/SEC	DEG	DEG	DEG	DEG	1/SEC	1/SEC	1/SEC		
0.1450	720.45	2.185	-0.772	4960.3	1.44	4.4	45.49	-1.29	-0.72	-55	-57	0	0
0.1451	720.94	2.187	-0.771	4960.3	1.44	4.4	45.49	-1.29	-0.72	-55	-57	0	0
0.1452	721.44	2.189	-0.771	4960.3	1.44	4.4	45.49	-1.29	-0.72	-55	-57	0	0
0.1453	721.94	2.190	-0.771	4960.3	1.44	4.4	45.49	-1.29	-0.72	-55	-57	0	0
0.1454	722.44	2.192	-0.771	4960.3	1.44	4.4	45.49	-1.29	-0.72	-55	-57	0	0
0.1455	722.94	2.194	-0.771	4960.3	1.44	4.4	45.49	-1.29	-0.72	-55	-57	0	0
0.1456	723.44	2.196	-0.771	4960.3	1.44	4.4	45.49	-1.29	-0.72	-55	-57	0	0
0.1457	723.94	2.198	-0.771	4960.3	1.44	4.4	45.49	-1.29	-0.72	-55	-57	0	0
0.1458	724.44	2.200	-0.771	4960.3	1.44	4.4	45.49	-1.29	-0.72	-55	-57	0	0
0.1459	724.94	2.202	-0.771	4960.3	1.44	4.4	45.49	-1.29	-0.72	-55	-57	0	0
0.1460	725.44	2.204	-0.771	4960.3	1.44	4.4	45.49	-1.29	-0.72	-55	-57	0	0
0.1461	725.94	2.206	-0.771	4960.3	1.44	4.4	45.49	-1.29	-0.72	-55	-57	0	0
0.1462	726.44	2.208	-0.771	4960.3	1.44	4.4	45.49	-1.29	-0.72	-55	-57	0	0
0.1463	726.94	2.210	-0.771	4960.3	1.44	4.4	45.49	-1.29	-0.72	-55	-57	0	0
0.1464	727.44	2.212	-0.771	4960.3	1.44	4.4	45.49	-1.29	-0.72	-55	-57	0	0
0.1465	727.94	2.214	-0.771	4960.3	1.44	4.4	45.49	-1.29	-0.72	-55	-57	0	0
0.1466	728.44	2.216	-0.771	4960.3	1.44	4.4	45.49	-1.29	-0.72	-55	-57	0	0
0.1467	728.94	2.218	-0.771	4960.3	1.44	4.4	45.49	-1.29	-0.72	-55	-57	0	0
0.1468	729.44	2.220	-0.771	4960.3	1.44	4.4	45.49	-1.29	-0.72	-55	-57	0	0
0.1469	729.94	2.222	-0.771	4960.3	1.44	4.4	45.49	-1.29	-0.72	-55	-57	0	0
0.1470	730.44	2.224	-0.771	4960.3	1.44	4.4	45.49	-1.29	-0.72	-55	-57	0	0
0.1471	730.94	2.226	-0.771	4960.3	1.44	4.4	45.49	-1.29	-0.72	-55	-57	0	0
0.1472	731.44	2.228	-0.771	4960.3	1.44	4.4	45.49	-1.29	-0.72	-55	-57	0	0
0.1473	731.94	2.230	-0.771	4960.3	1.44	4.4	45.49	-1.29	-0.72	-55	-57	0	0
0.1474	732.44	2.232	-0.771	4960.3	1.44	4.4	45.49	-1.29	-0.72	-55	-57	0	0
0.1475	732.94	2.234	-0.771	4960.3	1.44	4.4	45.49	-1.29	-0.72	-55	-57	0	0
0.1476	733.44	2.236	-0.771	4960.3	1.44	4.4	45.49	-1.29	-0.72	-55	-57	0	0
0.1477	733.94	2.238	-0.771	4960.3	1.44	4.4	45.49	-1.29	-0.72	-55	-57	0	0
0.1478	734.44	2.240	-0.771	4960.3	1.44	4.4	45.49	-1.29	-0.72	-55	-57	0	0
0.1479	734.94	2.242	-0.771	4960.3	1.44	4.4	45.49	-1.29	-0.72	-55	-57	0	0
0.1480	735.44	2.244	-0.771	4960.3	1.44	4.4	45.49	-1.29	-0.72	-55	-57	0	0
0.1481	735.94	2.246	-0.771	4960.3	1.44	4.4	45.49	-1.29	-0.72	-55	-57	0	0
0.1482	736.44	2.248	-0.771	4960.3	1.44	4.4	45.49	-1.29	-0.72	-55	-57	0	0
0.1483	736.94	2.250	-0.771	4960.3	1.44	4.4	45.49	-1.29	-0.72	-55	-57	0	0
0.1484	737.44	2.252	-0.771	4960.3	1.44	4.4	45.49	-1.29	-0.72	-55	-57	0	0
0.1485	737.94	2.254	-0.771	4960.3	1.44	4.4	45.49	-1.29	-0.72	-55	-57	0	0
0.1486	738.44	2.256	-0.771	4960.3	1.44	4.4	45.49	-1.29	-0.72	-55	-57	0	0
0.1487	738.94	2.258	-0.771	4960.3	1.44	4.4	45.49	-1.29	-0.72	-55	-57	0	0
0.1488	739.44	2.260	-0.771	4960.3	1.44	4.4	45.49	-1.29	-0.72	-55	-57	0	0
0.1489	739.94	2.262	-0.771	4960.3	1.44	4.4	45.49	-1.29	-0.72	-55	-57	0	0
0.1490	740.44	2.264	-0.771	4960.3	1.44	4.4	45.49	-1.29	-0.72	-55	-57	0	0
0.1491	740.94	2.266	-0.771	4960.3	1.44	4.4	45.49	-1.29	-0.72	-55	-57	0	0
0.1492	741.44	2.268	-0.771	4960.3	1.44	4.4	45.49	-1.29	-0.72	-55	-57	0	0
0.1493	741.94	2.270	-0.771	4960.3	1.44	4.4	45.49	-1.29	-0.72	-55	-57	0	0
0.1494	742.44	2.272	-0.771	4960.3	1.44	4.4	45.49	-1.29	-0.72	-55	-57	0	0
0.1495	742.94	2.274	-0.771	4960.3	1.44	4.4	45.49	-1.29	-0.72	-55	-57	0	0
0.1496	743.44	2.276	-0.771	4960.3	1.44	4.4	45.49	-1.29	-0.72	-55	-57	0	0
0.1497	743.94	2.278	-0.771	4960.3	1.44	4.4	45.49	-1.29	-0.72	-55	-57	0	0
0.1498	744.44	2.280	-0.771	4960.3	1.44	4.4	45.49	-1.29	-0.72	-55	-57	0	0
0.1499	744.94	2.282	-0.771	4960.3	1.44	4.4	45.49	-1.29	-0.72	-55	-57	0	0

T	X	Y	Z	V	P	ALPHA	MACH	PHI	ALPHA	BETA	L-V	L-P	4-V	W-U	S	LAU	K-T
SEC	FT	FT	FT	FT/SEC	SEC	DEG	DEG	DEG	DEG	DEG	WSEC	WSEC	4-V	W-U	S	LAU	K-T
0.1500	745.24	2.241	-0.777	4957.9	500.00	1.64	4.44	45.50	0.87	1.32	55	-57	233.6	-233.6	0	0	0
0.1501	745.74	2.242	-0.778	4958.0	500.00	1.64	4.44	45.51	0.83	1.29	55	-57	233.6	-233.6	0	0	0
0.1502	746.23	2.243	-0.779	4958.1	500.00	1.63	4.44	45.51	0.79	1.25	55	-57	233.6	-233.6	0	0	0
0.1503	746.73	2.244	-0.779	4958.2	500.00	1.63	4.44	45.52	0.76	1.22	55	-57	233.6	-233.6	0	0	0
0.1504	747.22	2.245	-0.780	4958.4	500.00	1.63	4.44	45.52	0.72	1.18	55	-57	233.6	-233.6	0	0	0
0.1505	747.72	2.246	-0.781	4958.6	500.00	1.63	4.44	45.51	0.68	1.15	55	-57	233.6	-233.6	0	0	0
0.1506	748.22	2.246	-0.782	4958.8	500.00	1.63	4.44	45.51	0.63	1.07	55	-57	233.6	-233.6	0	0	0
0.1507	748.71	2.247	-0.783	4959.0	500.00	1.63	4.44	45.51	0.59	1.03	55	-57	233.6	-233.6	0	0	0
0.1508	749.21	2.248	-0.784	4959.2	500.00	1.64	4.44	45.50	0.55	0.99	55	-57	233.6	-233.6	0	0	0
0.1509	749.70	2.249	-0.785	4959.4	500.00	1.64	4.44	45.50	0.51	0.95	55	-57	233.6	-233.6	0	0	0
0.1510	750.20	2.250	-0.785	4959.6	500.00	1.64	4.44	45.50	0.48	0.93	55	-57	233.6	-233.6	0	0	0
0.1511	750.69	2.251	-0.786	4959.8	500.00	1.64	4.44	45.50	0.44	0.89	55	-57	233.6	-233.6	0	0	0
0.1512	751.19	2.253	-0.789	4959.9	500.00	1.64	4.44	45.50	0.41	0.87	55	-57	233.6	-233.6	0	0	0
0.1513	751.69	2.254	-0.790	4960.0	500.00	1.64	4.44	45.50	0.37	0.84	55	-57	233.6	-233.6	0	0	0
0.1514	752.18	2.256	-0.791	4960.2	500.00	1.64	4.44	45.50	0.33	0.80	55	-57	233.6	-233.6	0	0	0
0.1515	752.69	2.258	-0.792	4960.3	500.00	1.64	4.44	45.50	0.29	0.77	55	-57	233.6	-233.6	0	0	0
0.1516	753.17	2.257	-0.793	4960.4	500.00	1.64	4.44	45.50	0.25	0.73	55	-57	233.6	-233.6	0	0	0
0.1517	753.67	2.259	-0.795	4960.6	500.00	1.64	4.44	45.51	0.21	0.69	55	-57	233.6	-233.6	0	0	0
0.1518	754.17	2.260	-0.795	4960.7	500.00	1.64	4.44	45.51	0.17	0.65	55	-57	233.6	-233.6	0	0	0
0.1519	754.65	2.261	-0.797	4960.9	500.00	1.64	4.44	45.51	0.14	0.61	55	-57	233.6	-233.6	0	0	0
0.1520	755.16	2.262	-0.799	4961.0	500.00	1.64	4.44	45.50	0.10	0.57	55	-57	233.6	-233.6	0	0	0
0.1521	755.65	2.264	-0.799	4961.2	500.00	1.64	4.44	45.50	0.06	0.53	55	-57	233.6	-233.6	0	0	0
0.1522	756.15	2.265	-0.801	4961.2	500.00	1.64	4.44	45.51	0.02	0.49	55	-57	233.6	-233.6	0	0	0

PERMANENT FULLY LICENSE PRODUCTION

[illegible]



## FLECHETTE GROUND POINT

T SEC	X FT	Y FT	Z FT	V FT/SEC	P RAD/SEC	ALPHA MACH DEG	PHI DEG	ALPHA DEG	BETA DEG	L 1/SEC	L-2 1/SEC	M-1 1/SEC	M-2 1/SEC	S 1/SEC	M-1 1/SEC	M-2 1/SEC
0.1500	794.82	2.407	-0.333	4956.3	500.00	1.44	4.44	45.44	1.13	0.82	55	57	2336	-2333	0	0
0.1501	795.82	2.408	-0.333	4956.3	500.00	1.44	4.44	45.44	1.03	0.97	56	57	2336	-2333	0	0
0.1502	795.81	2.409	-0.333	4956.3	500.00	1.44	4.44	45.44	1.03	0.97	56	57	2336	-2333	0	0
0.1503	796.31	2.410	-0.333	4956.3	500.00	1.44	4.44	45.44	1.03	1.07	56	57	2336	-2333	0	0
0.1504	795.80	2.411	-0.333	4956.2	500.00	1.44	4.44	45.44	1.03	1.12	55	57	2336	-2333	0	0
0.1505	797.30	2.412	-0.333	4956.2	500.00	1.44	4.44	45.44	1.03	1.16	55	57	2336	-2333	0	0
0.1506	797.79	2.413	-0.333	4956.2	500.00	1.44	4.44	45.44	1.03	1.21	55	57	2336	-2333	0	0
0.1507	798.29	2.414	-0.333	4956.2	500.00	1.44	4.44	45.44	1.03	1.24	55	57	2336	-2333	0	0
0.1508	798.79	2.415	-0.333	4956.2	500.00	1.44	4.44	45.44	1.03	1.29	55	57	2336	-2333	0	0
0.1509	799.29	2.416	-0.333	4956.2	500.00	1.44	4.44	45.44	1.03	1.31	55	57	2336	-2333	0	0
0.1510	799.78	2.416	-0.333	4956.2	500.00	1.44	4.44	45.44	1.03	1.34	55	57	2336	-2333	0	0
0.1511	800.27	2.417	-0.333	4956.2	500.00	1.44	4.44	45.44	1.03	1.36	55	57	2336	-2333	0	0
0.1512	800.77	2.418	-0.333	4956.2	500.00	1.44	4.44	45.44	1.03	1.34	55	57	2336	-2333	0	0
0.1513	801.25	2.418	-0.333	4956.1	500.00	1.44	4.44	45.44	1.03	1.40	55	57	2336	-2333	0	0
0.1514	801.76	2.419	-0.333	4956.1	500.00	1.44	4.44	45.44	1.03	1.41	55	57	2336	-2333	0	0
0.1515	802.25	2.420	-0.333	4956.1	500.00	1.44	4.44	45.44	1.03	1.42	55	57	2336	-2333	0	0
0.1516	802.75	2.421	-0.333	4956.1	500.00	1.44	4.44	45.44	1.03	1.43	55	57	2336	-2333	0	0
0.1517	803.25	2.422	-0.333	4956.1	500.00	1.44	4.44	45.44	1.03	1.43	55	57	2336	-2333	0	0
0.1518	803.74	2.422	-0.333	4956.1	500.00	1.44	4.44	45.44	1.03	1.43	55	57	2336	-2333	0	0
0.1519	804.24	2.423	-0.333	4956.1	500.00	1.44	4.44	45.44	1.03	1.43	55	57	2336	-2333	0	0
0.1520	804.73	2.424	-0.333	4956.1	500.00	1.44	4.44	45.44	1.03	1.42	55	57	2336	-2333	0	0
0.1521	805.23	2.425	-0.333	4956.1	500.00	1.44	4.44	45.44	1.03	1.41	55	57	2336	-2333	0	0
0.1522	805.72	2.425	-0.333	4956.1	500.00	1.44	4.44	45.44	1.03	1.41	55	57	2336	-2333	0	0
0.1523	806.22	2.426	-0.333	4956.1	500.00	1.44	4.44	45.44	1.03	1.41	55	57	2336	-2333	0	0
0.1524	806.72	2.427	-0.333	4956.1	500.00	1.44	4.44	45.44	1.03	1.41	55	57	2336	-2333	0	0
0.1525	807.21	2.428	-0.333	4956.1	500.00	1.44	4.44	45.44	1.03	1.41	55	57	2336	-2333	0	0
0.1526	807.71	2.429	-0.333	4956.1	500.00	1.44	4.44	45.44	1.03	1.41	55	57	2336	-2333	0	0
0.1527	808.20	2.429	-0.333	4956.1	500.00	1.44	4.44	45.44	1.03	1.41	55	57	2336	-2333	0	0
0.1528	808.70	2.430	-0.333	4956.1	500.00	1.44	4.44	45.44	1.03	1.41	55	57	2336	-2333	0	0
0.1529	809.19	2.431	-0.333	4956.1	500.00	1.44	4.44	45.44	1.03	1.41	55	57	2336	-2333	0	0
0.1530	809.69	2.432	-0.333	4956.1	500.00	1.44	4.44	45.44	1.03	1.41	55	57	2336	-2333	0	0
0.1531	810.18	2.433	-0.333	4956.1	500.00	1.44	4.44	45.44	1.03	1.41	55	57	2336	-2333	0	0
0.1532	810.68	2.434	-0.333	4956.1	500.00	1.44	4.44	45.44	1.03	1.41	55	57	2336	-2333	0	0
0.1533	811.18	2.435	-0.333	4956.1	500.00	1.44	4.44	45.44	1.03	1.41	55	57	2336	-2333	0	0
0.1534	811.67	2.436	-0.333	4956.1	500.00	1.44	4.44	45.44	1.03	1.41	55	57	2336	-2333	0	0
0.1535	812.17	2.437	-0.333	4956.1	500.00	1.44	4.44	45.44	1.03	1.41	55	57	2336	-2333	0	0
0.1536	812.66	2.438	-0.333	4956.1	500.00	1.44	4.44	45.44	1.03	1.41	55	57	2336	-2333	0	0
0.1537	813.15	2.439	-0.333	4956.1	500.00	1.44	4.44	45.44	1.03	1.41	55	57	2336	-2333	0	0
0.1538	813.65	2.440	-0.333	4956.1	500.00	1.44	4.44	45.44	1.03	1.41	55	57	2336	-2333	0	0
0.1539	814.15	2.441	-0.333	4956.1	500.00	1.44	4.44	45.44	1.03	1.41	55	57	2336	-2333	0	0
0.1540	814.64	2.442	-0.333	4956.1	500.00	1.44	4.44	45.44	1.03	1.41	55	57	2336	-2333	0	0
0.1541	815.14	2.443	-0.333	4956.1	500.00	1.44	4.44	45.44	1.03	1.41	55	57	2336	-2333	0	0
0.1542	815.63	2.444	-0.333	4956.1	500.00	1.44	4.44	45.44	1.03	1.41	55	57	2336	-2333	0	0
0.1543	816.13	2.445	-0.333	4956.1	500.00	1.44	4.44	45.44	1.03	1.41	55	57	2336	-2333	0	0
0.1544	816.63	2.446	-0.333	4956.1	500.00	1.44	4.44	45.44	1.03	1.41	55	57	2336	-2333	0	0
0.1545	817.12	2.447	-0.333	4956.1	500.00	1.44	4.44	45.44	1.03	1.41	55	57	2336	-2333	0	0
0.1546	817.62	2.448	-0.333	4956.1	500.00	1.44	4.44	45.44	1.03	1.41	55	57	2336	-2333	0	0
0.1547	818.11	2.449	-0.333	4956.1	500.00	1.44	4.44	45.44	1.03	1.41	55	57	2336	-2333	0	0
0.1548	818.61	2.450	-0.333	4956.1	500.00	1.44	4.44	45.44	1.03	1.41	55	57	2336	-2333	0	0
0.1549	819.11	2.451	-0.333	4956.1	500.00	1.44	4.44	45.44	1.03	1.41	55	57	2336	-2333	0	0
0.1550	819.61	2.452	-0.333	4956.1	500.00	1.44	4.44	45.44	1.03	1.41	55	57	2336	-2333	0	0

FLICHELLETTE GROUND POINT

PAGE 3-

T SEC	X FT	Y FT	Z FT	V FT/SEC	P P/SEC	ALPHA MACH	PHI DEG	ALPHA DEG	META DEG	L-A 1/SEC	L-P 1/SEC	4-3 1/SEC	M-P 1/SEC	5 IAU	K-T DEG
0.1650	818.60	2.455	-0.869	4957.7	500.00	1.44 4.44	45.51	1.43	-0.03	-55	-57	2337-2333	-0	0	1
0.1651	820.10	2.457	-0.870	4957.7	500.00	1.44 4.44	45.51	1.43	-0.15	-55	-57	2337-2333	-0	0	1
0.1652	820.55	2.459	-0.871	4957.7	500.00	1.44 4.44	45.51	1.43	-0.22	-55	-57	2337-2333	-0	0	1
0.1653	821.09	2.460	-0.873	4957.7	500.00	1.44 4.44	45.51	1.43	-0.23	-55	-57	2337-2333	-0	0	1
0.1654	821.59	2.462	-0.874	4957.7	500.00	1.44 4.44	45.51	1.43	-0.34	-55	-57	2337-2333	-0	0	1
0.1655	822.08	2.464	-0.875	4957.7	500.00	1.44 4.44	45.51	1.43	-0.43	-55	-57	2337-2333	-0	0	1
0.1656	822.57	2.466	-0.876	4957.7	500.00	1.44 4.44	45.50	1.43	-0.53	-55	-57	2337-2333	-0	0	1
0.1657	823.07	2.467	-0.877	4957.7	500.00	1.44 4.44	45.50	1.43	-0.63	-55	-57	2337-2333	-0	0	1
0.1658	823.57	2.469	-0.878	4957.7	500.00	1.44 4.44	45.49	1.43	-0.73	-55	-57	2337-2333	-0	0	1
0.1659	824.06	2.471	-0.880	4957.7	500.00	1.44 4.44	45.48	1.43	-0.83	-55	-57	2337-2333	-0	0	1
0.1660	824.55	2.473	-0.881	4957.7	500.00	1.44 4.44	45.47	1.43	-0.93	-55	-57	2337-2333	-0	0	1
0.1661	825.05	2.475	-0.882	4957.7	500.00	1.44 4.44	45.47	1.43	-1.03	-55	-57	2337-2333	-0	0	1
0.1662	825.55	2.477	-0.883	4957.7	500.00	1.44 4.44	45.46	1.43	-1.13	-55	-57	2337-2333	-0	0	1
0.1663	826.04	2.479	-0.884	4957.7	500.00	1.44 4.44	45.46	1.43	-1.23	-55	-57	2337-2333	-0	0	1
0.1664	826.54	2.480	-0.885	4957.7	500.00	1.44 4.44	45.45	1.43	-1.33	-55	-57	2337-2333	-0	0	1
0.1665	827.03	2.482	-0.886	4957.7	500.00	1.44 4.44	45.45	1.43	-1.43	-55	-57	2337-2333	-0	0	1
0.1666	827.53	2.484	-0.887	4957.7	500.00	1.44 4.44	45.45	1.43	-1.53	-55	-57	2337-2333	-0	0	1
0.1667	828.03	2.487	-0.888	4957.7	500.00	1.44 4.44	45.45	1.43	-1.63	-55	-57	2337-2333	-0	0	1
0.1668	828.52	2.489	-0.889	4957.7	500.00	1.44 4.44	45.45	1.43	-1.73	-55	-57	2337-2333	-0	0	1
0.1669	829.01	2.491	-0.890	4957.7	500.00	1.44 4.44	45.45	1.43	-1.83	-55	-57	2337-2333	-0	0	1
0.1670	829.51	2.493	-0.891	4957.7	500.00	1.44 4.44	45.45	1.43	-1.93	-55	-57	2337-2333	-0	0	1
0.1671	830.01	2.495	-0.892	4957.7	500.00	1.44 4.44	45.45	1.43	-2.03	-55	-57	2337-2333	-0	0	1
0.1672	830.50	2.497	-0.893	4957.7	500.00	1.44 4.44	45.45	1.43	-2.13	-55	-57	2337-2333	-0	0	1
0.1673	831.00	2.499	-0.894	4957.7	500.00	1.44 4.44	45.45	1.43	-2.23	-55	-57	2337-2333	-0	0	1
0.1674	831.50	2.501	-0.895	4957.7	500.00	1.44 4.44	45.45	1.43	-2.33	-55	-57	2337-2333	-0	0	1
0.1675	831.99	2.504	-0.896	4957.7	500.00	1.44 4.44	45.45	1.43	-2.43	-55	-57	2337-2333	-0	0	1
0.1676	832.48	2.506	-0.897	4957.7	500.00	1.44 4.44	45.45	1.43	-2.53	-55	-57	2337-2333	-0	0	1
0.1677	832.98	2.508	-0.898	4957.7	500.00	1.44 4.44	45.45	1.43	-2.63	-55	-57	2337-2333	-0	0	1
0.1678	833.47	2.510	-0.899	4957.7	500.00	1.44 4.44	45.45	1.43	-2.73	-55	-57	2337-2333	-0	0	1
0.1679	833.97	2.512	-0.900	4957.7	500.00	1.44 4.44	45.45	1.43	-2.83	-55	-57	2337-2333	-0	0	1
0.1680	834.47	2.515	-0.901	4957.7	500.00	1.44 4.44	45.45	1.43	-2.93	-55	-57	2337-2333	-0	0	1
0.1681	834.96	2.517	-0.902	4957.7	500.00	1.44 4.44	45.45	1.43	-3.03	-55	-57	2337-2333	-0	0	1
0.1682	835.46	2.519	-0.903	4957.7	500.00	1.44 4.44	45.45	1.43	-3.13	-55	-57	2337-2333	-0	0	1
0.1683	835.95	2.521	-0.904	4957.7	500.00	1.44 4.44	45.45	1.43	-3.23	-55	-57	2337-2333	-0	0	1
0.1684	836.45	2.523	-0.905	4957.7	500.00	1.44 4.44	45.45	1.43	-3.33	-55	-57	2337-2333	-0	0	1
0.1685	836.95	2.526	-0.906	4957.7	500.00	1.44 4.44	45.45	1.43	-3.43	-55	-57	2337-2333	-0	0	1
0.1686	837.44	2.528	-0.907	4957.7	500.00	1.44 4.44	45.45	1.43	-3.53	-55	-57	2337-2333	-0	0	1
0.1687	837.94	2.530	-0.908	4957.7	500.00	1.44 4.44	45.45	1.43	-3.63	-55	-57	2337-2333	-0	0	1
0.1688	838.43	2.532	-0.909	4957.7	500.00	1.44 4.44	45.45	1.43	-3.73	-55	-57	2337-2333	-0	0	1
0.1689	838.93	2.536	-0.910	4957.7	500.00	1.44 4.44	45.45	1.43	-3.83	-55	-57	2337-2333	-0	0	1
0.1690	839.43	2.538	-0.911	4957.7	500.00	1.44 4.44	45.45	1.43	-3.93	-55	-57	2337-2333	-0	0	1
0.1691	839.92	2.541	-0.912	4957.7	500.00	1.44 4.44	45.45	1.43	-4.03	-55	-57	2337-2333	-0	0	1
0.1692	840.42	2.543	-0.913	4957.7	500.00	1.44 4.44	45.45	1.43	-4.13	-55	-57	2337-2333	-0	0	1
0.1693	840.91	2.545	-0.914	4957.7	500.00	1.44 4.44	45.45	1.43	-4.23	-55	-57	2337-2333	-0	0	1
0.1694	841.41	2.547	-0.915	4957.7	500.00	1.44 4.44	45.45	1.43	-4.33	-55	-57	2337-2333	-0	0	1
0.1695	841.90	2.549	-0.916	4957.7	500.00	1.44 4.44	45.45	1.43	-4.43	-55	-57	2337-2333	-0	0	1
0.1696	842.40	2.551	-0.917	4957.7	500.00	1.44 4.44	45.45	1.43	-4.53	-55	-57	2337-2333	-0	0	1
0.1697	842.89	2.553	-0.918	4957.7	500.00	1.44 4.44	45.45	1.43	-4.63	-55	-57	2337-2333	-0	0	1
0.1698	843.39	2.555	-0.919	4957.7	500.00	1.44 4.44	45.45	1.43	-4.73	-55	-57	2337-2333	-0	0	1
0.1699	843.89	2.557	-0.920	4957.7	500.00	1.44 4.44	45.45	1.43	-4.83	-55	-57	2337-2333	-0	0	1



T SEC	X FT	Y FT	Z FT	V FT/SEC	P RAD/SEC	ALPHA DEC	PUL SEC	RST SEC	L-D 1/3 SEC	W-D 1/3 SEC	S 1/3 SEC	T-D 1/3 SEC	R-T SEC
0.1750	859.16	2.014	-0.973	4058.5	500.00	1.43	0.46	45.50	0.45	1.35	55	0	0
0.1751	869.64	2.015	-0.977	4954.5	500.00	1.43	0.46	45.50	0.45	1.32	55	0	0
0.1752	870.15	2.015	-0.978	4954.5	500.00	1.43	0.44	45.49	0.42	1.10	55	0	0
0.1753	870.65	2.017	-0.970	4955.5	500.00	1.43	0.44	45.49	0.43	1.25	55	0	0
0.1754	871.14	2.019	-0.970	4955.5	500.00	1.43	0.44	45.49	0.43	1.23	55	0	0
0.1755	871.66	2.019	-0.971	4955.5	500.00	1.43	0.44	45.49	0.43	1.19	55	0	0
0.1756	872.16	2.019	-0.972	4955.5	500.00	1.43	0.44	45.49	0.43	1.15	55	0	0
0.1757	872.63	2.020	-0.974	4955.5	500.00	1.43	0.44	45.49	0.42	1.15	55	0	0
0.1758	873.12	2.021	-0.974	4955.4	500.00	1.43	0.44	45.49	0.42	1.11	55	0	0
0.1759	873.62	2.022	-0.975	4955.4	500.00	1.43	0.44	45.49	0.42	1.11	55	0	0
0.1760	874.12	2.023	-0.976	4955.4	500.00	1.43	0.44	45.49	0.42	1.11	55	0	0
0.1761	874.61	2.024	-0.977	4955.4	500.00	1.43	0.44	45.49	0.42	1.11	55	0	0
0.1762	875.11	2.025	-0.978	4955.4	500.00	1.43	0.44	45.49	0.42	1.11	55	0	0
0.1763	875.60	2.026	-0.979	4955.4	500.00	1.43	0.44	45.49	0.42	1.11	55	0	0
0.1764	876.10	2.027	-0.980	4955.4	500.00	1.43	0.44	45.49	0.42	1.11	55	0	0
0.1765	876.60	2.028	-0.981	4955.4	500.00	1.43	0.44	45.49	0.42	1.11	55	0	0
0.1766	877.10	2.029	-0.982	4955.4	500.00	1.43	0.44	45.49	0.42	1.11	55	0	0
0.1767	877.59	2.031	-0.983	4955.4	500.00	1.43	0.44	45.49	0.42	1.11	55	0	0
0.1768	878.08	2.032	-0.984	4955.4	500.00	1.43	0.44	45.49	0.42	1.11	55	0	0
0.1769	878.57	2.033	-0.985	4955.4	500.00	1.43	0.44	45.49	0.42	1.11	55	0	0
0.1770	879.06	2.034	-0.986	4955.4	500.00	1.43	0.44	45.49	0.42	1.11	55	0	0
0.1771	880.56	2.037	-0.989	4955.4	500.00	1.43	0.44	45.49	0.42	1.11	55	0	0
0.1772	881.06	2.038	-0.991	4955.4	500.00	1.43	0.44	45.49	0.42	1.11	55	0	0
0.1773	881.56	2.040	-0.992	4955.4	500.00	1.43	0.44	45.49	0.42	1.11	55	0	0
0.1774	881.55	2.042	-0.993	4955.4	500.00	1.43	0.44	45.49	0.42	1.11	55	0	0
0.1775	882.05	2.043	-0.995	4955.4	500.00	1.43	0.44	45.49	0.42	1.11	55	0	0
0.1776	882.54	2.045	-1.000	4955.4	500.00	1.43	0.44	45.49	0.42	1.11	55	0	0
0.1777	883.04	2.046	-1.007	4955.4	500.00	1.43	0.44	45.49	0.42	1.11	55	0	0
0.1778	883.53	2.048	-0.994	4955.4	500.00	1.43	0.44	45.49	0.42	1.11	55	0	0
0.1779	884.03	2.051	-0.991	4955.4	500.00	1.43	0.44	45.49	0.42	1.11	55	0	0
0.1780	884.53	2.051	-0.992	4955.4	500.00	1.43	0.44	45.49	0.42	1.11	55	0	0
0.1781	885.02	2.053	-0.994	4955.4	500.00	1.43	0.44	45.49	0.42	1.11	55	0	0
0.1782	885.52	2.055	-0.994	4955.4	500.00	1.43	0.44	45.49	0.42	1.11	55	0	0
0.1783	886.01	2.057	-0.991	4955.4	500.00	1.43	0.44	45.49	0.42	1.11	55	0	0
0.1784	886.51	2.059	-0.995	4955.4	500.00	1.43	0.44	45.49	0.42	1.11	55	0	0
0.1785	887.00	2.060	-0.997	4955.4	500.00	1.43	0.44	45.49	0.42	1.11	55	0	0
0.1786	887.50	2.062	-0.994	4955.4	500.00	1.43	0.44	45.49	0.42	1.11	55	0	0
0.1787	887.99	2.064	-0.995	4955.4	500.00	1.43	0.44	45.49	0.42	1.11	55	0	0
0.1788	888.49	2.065	-0.993	4955.4	500.00	1.43	0.44	45.49	0.42	1.11	55	0	0
0.1789	889.99	2.070	-0.997	4955.4	500.00	1.43	0.44	45.49	0.42	1.11	55	0	0
0.1790	890.49	2.072	-0.993	4955.4	500.00	1.43	0.44	45.49	0.42	1.11	55	0	0
0.1791	890.97	2.074	-0.994	4955.4	500.00	1.43	0.44	45.49	0.42	1.11	55	0	0
0.1792	891.47	2.076	-0.995	4955.4	500.00	1.43	0.44	45.49	0.42	1.11	55	0	0
0.1793	891.96	2.078	-0.994	4955.4	500.00	1.43	0.44	45.49	0.42	1.11	55	0	0
0.1794	892.45	2.083	-0.993	4955.4	500.00	1.43	0.44	45.49	0.42	1.11	55	0	0
0.1795	892.95	2.085	-0.997	4955.4	500.00	1.43	0.44	45.49	0.42	1.11	55	0	0
0.1796	893.44	2.087	-0.995	4955.4	500.00	1.43	0.44	45.49	0.42	1.11	55	0	0
0.1797	893.94	2.087	-0.995	4955.4	500.00	1.43	0.44	45.49	0.42	1.11	55	0	0

COPY AVAILABLE TO LEO DOES NOT  
PERMIT FULLY LEGIBLE PRODUCTION

# FLECHETTE GROUND POINT

PAGE 37

SEC	T	X	Y	Z	V	P	ALPHA	WCH	PHI	ALPHA	BETA	L-D	L-P	M-N	N-O	S	T-U	W-V
SEC	FT	FT	FT	FT	FT/SEC	RAD/SEC	DEG	DEG	DEG	DEG	DEG	1/SEC	1/SEC	1/SEC	1/SEC	1/SEC	1/SEC	1/SEC
0.1700	893.96	2.689	-0.560	4955.9	500.00	1.43	4.44	43.57	3.42	-1.37	-55	-57	2337	-2337	-0	0	0	0
0.1700	894.43	2.551	-0.561	4955.6	500.00	1.43	4.44	43.57	3.35	-1.39	-55	-57	2337	-2337	-0	0	0	0
0.1700	894.90	2.413	-0.561	4955.6	500.00	1.43	4.44	43.57	3.28	-1.41	-55	-57	2337	-2337	-0	0	0	0
0.1700	895.37	2.275	-0.562	4955.6	500.00	1.43	4.44	43.57	3.21	-1.42	-55	-57	2337	-2337	-0	0	0	0
0.1700	895.84	2.137	-0.563	4955.6	500.00	1.43	4.44	43.57	3.14	-1.43	-55	-57	2337	-2337	-0	0	0	0
0.1700	896.31	2.000	-0.563	4955.6	500.00	1.43	4.44	43.57	3.07	-1.43	-55	-57	2337	-2337	-0	0	0	0
0.1700	896.78	1.862	-0.564	4955.6	500.00	1.43	4.44	43.57	3.00	-1.43	-55	-57	2337	-2337	-0	0	0	0
0.1700	897.25	1.725	-0.565	4955.6	500.00	1.43	4.44	43.57	2.93	-1.43	-55	-57	2337	-2337	-0	0	0	0
0.1700	897.72	1.587	-0.565	4955.6	500.00	1.43	4.44	43.57	2.86	-1.43	-55	-57	2337	-2337	-0	0	0	0
0.1700	898.19	1.450	-0.565	4955.6	500.00	1.43	4.44	43.57	2.79	-1.43	-55	-57	2337	-2337	-0	0	0	0
0.1700	898.66	1.312	-0.565	4955.6	500.00	1.43	4.44	43.57	2.72	-1.43	-55	-57	2337	-2337	-0	0	0	0
0.1700	899.13	1.175	-0.566	4955.6	500.00	1.43	4.44	43.57	2.65	-1.43	-55	-57	2337	-2337	-0	0	0	0
0.1700	899.60	1.037	-0.566	4955.6	500.00	1.43	4.44	43.57	2.58	-1.43	-55	-57	2337	-2337	-0	0	0	0
0.1700	900.07	0.900	-0.566	4955.6	500.00	1.43	4.44	43.57	2.51	-1.43	-55	-57	2337	-2337	-0	0	0	0
0.1700	900.54	0.762	-0.567	4955.6	500.00	1.43	4.44	43.57	2.44	-1.43	-55	-57	2337	-2337	-0	0	0	0
0.1700	901.01	0.625	-0.567	4955.6	500.00	1.43	4.44	43.57	2.37	-1.43	-55	-57	2337	-2337	-0	0	0	0
0.1700	901.48	0.487	-0.567	4955.6	500.00	1.43	4.44	43.57	2.30	-1.43	-55	-57	2337	-2337	-0	0	0	0
0.1700	901.95	0.350	-0.567	4955.6	500.00	1.43	4.44	43.57	2.23	-1.43	-55	-57	2337	-2337	-0	0	0	0
0.1700	902.42	0.212	-0.567	4955.6	500.00	1.43	4.44	43.57	2.16	-1.43	-55	-57	2337	-2337	-0	0	0	0
0.1700	902.89	0.075	-0.567	4955.6	500.00	1.43	4.44	43.57	2.09	-1.43	-55	-57	2337	-2337	-0	0	0	0
0.1700	903.36	0.000	-0.567	4955.6	500.00	1.43	4.44	43.57	2.02	-1.43	-55	-57	2337	-2337	-0	0	0	0
0.1700	903.83	0.000	-0.567	4955.6	500.00	1.43	4.44	43.57	1.95	-1.43	-55	-57	2337	-2337	-0	0	0	0
0.1700	904.30	0.000	-0.567	4955.6	500.00	1.43	4.44	43.57	1.88	-1.43	-55	-57	2337	-2337	-0	0	0	0
0.1700	904.77	0.000	-0.567	4955.6	500.00	1.43	4.44	43.57	1.81	-1.43	-55	-57	2337	-2337	-0	0	0	0
0.1700	905.24	0.000	-0.567	4955.6	500.00	1.43	4.44	43.57	1.74	-1.43	-55	-57	2337	-2337	-0	0	0	0
0.1700	905.71	0.000	-0.567	4955.6	500.00	1.43	4.44	43.57	1.67	-1.43	-55	-57	2337	-2337	-0	0	0	0
0.1700	906.18	0.000	-0.567	4955.6	500.00	1.43	4.44	43.57	1.60	-1.43	-55	-57	2337	-2337	-0	0	0	0
0.1700	906.65	0.000	-0.567	4955.6	500.00	1.43	4.44	43.57	1.53	-1.43	-55	-57	2337	-2337	-0	0	0	0
0.1700	907.12	0.000	-0.567	4955.6	500.00	1.43	4.44	43.57	1.46	-1.43	-55	-57	2337	-2337	-0	0	0	0
0.1700	907.59	0.000	-0.567	4955.6	500.00	1.43	4.44	43.57	1.39	-1.43	-55	-57	2337	-2337	-0	0	0	0
0.1700	908.06	0.000	-0.567	4955.6	500.00	1.43	4.44	43.57	1.32	-1.43	-55	-57	2337	-2337	-0	0	0	0
0.1700	908.53	0.000	-0.567	4955.6	500.00	1.43	4.44	43.57	1.25	-1.43	-55	-57	2337	-2337	-0	0	0	0
0.1700	909.00	0.000	-0.567	4955.6	500.00	1.43	4.44	43.57	1.18	-1.43	-55	-57	2337	-2337	-0	0	0	0
0.1700	909.47	0.000	-0.567	4955.6	500.00	1.43	4.44	43.57	1.11	-1.43	-55	-57	2337	-2337	-0	0	0	0
0.1700	910.00	0.000	-0.567	4955.6	500.00	1.43	4.44	43.57	1.04	-1.43	-55	-57	2337	-2337	-0	0	0	0
0.1700	910.53	0.000	-0.567	4955.6	500.00	1.43	4.44	43.57	0.97	-1.43	-55	-57	2337	-2337	-0	0	0	0
0.1700	911.06	0.000	-0.567	4955.6	500.00	1.43	4.44	43.57	0.90	-1.43	-55	-57	2337	-2337	-0	0	0	0
0.1700	911.59	0.000	-0.567	4955.6	500.00	1.43	4.44	43.57	0.83	-1.43	-55	-57	2337	-2337	-0	0	0	0
0.1700	912.12	0.000	-0.567	4955.6	500.00	1.43	4.44	43.57	0.76	-1.43	-55	-57	2337	-2337	-0	0	0	0
0.1700	912.65	0.000	-0.567	4955.6	500.00	1.43	4.44	43.57	0.69	-1.43	-55	-57	2337	-2337	-0	0	0	0
0.1700	913.18	0.000	-0.567	4955.6	500.00	1.43	4.44	43.57	0.62	-1.43	-55	-57	2337	-2337	-0	0	0	0
0.1700	913.71	0.000	-0.567	4955.6	500.00	1.43	4.44	43.57	0.55	-1.43	-55	-57	2337	-2337	-0	0	0	0
0.1700	914.24	0.000	-0.567	4955.6	500.00	1.43	4.44	43.57	0.48	-1.43	-55	-57	2337	-2337	-0	0	0	0
0.1700	914.77	0.000	-0.567	4955.6	500.00	1.43	4.44	43.57	0.41	-1.43	-55	-57	2337	-2337	-0	0	0	0
0.1700	915.30	0.000	-0.567	4955.6	500.00	1.43	4.44	43.57	0.34	-1.43	-55	-57	2337	-2337	-0	0	0	0
0.1700	915.83	0.000	-0.567	4955.6	500.00	1.43	4.44	43.57	0.27	-1.43	-55	-57	2337	-2337	-0	0	0	0
0.1700	916.36	0.000	-0.567	4955.6	500.00	1.43	4.44	43.57	0.20	-1.43	-55	-57	2337	-2337	-0	0	0	0
0.1700	916.89	0.000	-0.567	4955.6	500.00	1.43	4.44	43.57	0.13	-1.43	-55	-57	2337	-2337	-0	0	0	0
0.1700	917.42	0.000	-0.567	4955.6	500.00	1.43	4.44	43.57	0.06	-1.43	-55	-57	2337	-2337	-0	0	0	0
0.1700	917.95	0.000	-0.567	4955.6	500.00	1.43	4.44	43.57	0.00	-1.43	-55	-57	2337	-2337	-0	0	0	0
0.1700	918.48	0.000	-0.567	4955.6	500.00	1.43	4.44	43.57	0.00	-1.43	-55	-57	2337	-2337	-0	0	0	0

332

COPY AVAILABLE TO REG BATS NOT  
PERMIT FULLY LEGAL PRODUCTION



## FLECHETTE GROUND POINT

PAGE 39

T SEC	X FT	Y FT	Z FT	V FT/SEC	P RAG/SEC	ALPHA DEG	MACH	PMI DEG	ALPHA DEG	BETA DEG	L-N 1/500	L-N 1/500	M-N 1/500	4-P 1/500	S	TAU	M-T DEG
0.1899	943.47	2.628	-0.308	4554.8	500.00	1.43	4.44	45.49	1.43	0.01	-1.5	-57	2333-2335	-0	0	0	1
0.1900	943.07	2.629	-0.309	4554.8	500.00	1.43	4.44	45.48	1.43	0.01	-1.5	-57	2333-2335	-0	0	0	1
0.1901	942.67	2.631	-1.009	4554.7	500.00	1.43	4.44	45.48	1.43	0.01	-1.5	-57	2333-2335	-0	0	0	1
0.1902	942.27	2.632	-1.002	4554.7	500.00	1.43	4.44	45.48	1.43	0.01	-1.5	-57	2333-2335	-0	0	0	1
0.1903	941.87	2.634	-1.003	4554.7	500.00	1.43	4.44	45.48	1.43	0.01	-1.5	-57	2333-2335	-0	0	0	1
0.1904	941.47	2.635	-1.004	4554.7	500.00	1.43	4.44	45.48	1.43	0.01	-1.5	-57	2333-2335	-0	0	0	1
0.1905	941.07	2.637	-1.005	4554.7	500.00	1.43	4.44	45.48	1.43	0.01	-1.5	-57	2333-2335	-0	0	0	1
0.1906	940.67	2.638	-1.006	4554.7	500.00	1.43	4.44	45.48	1.43	0.01	-1.5	-57	2333-2335	-0	0	0	1
0.1907	940.27	2.640	-1.007	4554.7	500.00	1.43	4.44	45.48	1.43	0.01	-1.5	-57	2333-2335	-0	0	0	1
0.1908	939.87	2.641	-1.008	4554.7	500.00	1.43	4.44	45.48	1.43	0.01	-1.5	-57	2333-2335	-0	0	0	1
0.1909	939.47	2.642	-1.009	4554.7	500.00	1.43	4.44	45.48	1.43	0.01	-1.5	-57	2333-2335	-0	0	0	1
0.1910	939.07	2.643	-1.010	4554.7	500.00	1.43	4.44	45.48	1.43	0.01	-1.5	-57	2333-2335	-0	0	0	1
0.1911	938.67	2.644	-1.011	4554.7	500.00	1.43	4.44	45.48	1.43	0.01	-1.5	-57	2333-2335	-0	0	0	1
0.1912	938.27	2.645	-1.012	4554.7	500.00	1.43	4.44	45.48	1.43	0.01	-1.5	-57	2333-2335	-0	0	0	1
0.1913	937.87	2.646	-1.013	4554.7	500.00	1.43	4.44	45.48	1.43	0.01	-1.5	-57	2333-2335	-0	0	0	1
0.1914	937.47	2.647	-1.014	4554.7	500.00	1.43	4.44	45.48	1.43	0.01	-1.5	-57	2333-2335	-0	0	0	1
0.1915	937.07	2.648	-1.015	4554.7	500.00	1.43	4.44	45.48	1.43	0.01	-1.5	-57	2333-2335	-0	0	0	1
0.1916	936.67	2.649	-1.016	4554.7	500.00	1.43	4.44	45.48	1.43	0.01	-1.5	-57	2333-2335	-0	0	0	1
0.1917	936.27	2.650	-1.017	4554.7	500.00	1.43	4.44	45.48	1.43	0.01	-1.5	-57	2333-2335	-0	0	0	1
0.1918	935.87	2.651	-1.018	4554.7	500.00	1.43	4.44	45.48	1.43	0.01	-1.5	-57	2333-2335	-0	0	0	1
0.1919	935.47	2.652	-1.019	4554.7	500.00	1.43	4.44	45.48	1.43	0.01	-1.5	-57	2333-2335	-0	0	0	1
0.1920	935.07	2.653	-1.020	4554.7	500.00	1.43	4.44	45.48	1.43	0.01	-1.5	-57	2333-2335	-0	0	0	1
0.1921	934.67	2.654	-1.021	4554.7	500.00	1.43	4.44	45.48	1.43	0.01	-1.5	-57	2333-2335	-0	0	0	1
0.1922	934.27	2.655	-1.022	4554.7	500.00	1.43	4.44	45.48	1.43	0.01	-1.5	-57	2333-2335	-0	0	0	1
0.1923	933.87	2.656	-1.023	4554.7	500.00	1.43	4.44	45.48	1.43	0.01	-1.5	-57	2333-2335	-0	0	0	1
0.1924	933.47	2.657	-1.024	4554.7	500.00	1.43	4.44	45.48	1.43	0.01	-1.5	-57	2333-2335	-0	0	0	1
0.1925	933.07	2.658	-1.025	4554.7	500.00	1.43	4.44	45.48	1.43	0.01	-1.5	-57	2333-2335	-0	0	0	1
0.1926	932.67	2.659	-1.026	4554.7	500.00	1.43	4.44	45.48	1.43	0.01	-1.5	-57	2333-2335	-0	0	0	1
0.1927	932.27	2.660	-1.027	4554.7	500.00	1.43	4.44	45.48	1.43	0.01	-1.5	-57	2333-2335	-0	0	0	1
0.1928	931.87	2.661	-1.028	4554.7	500.00	1.43	4.44	45.48	1.43	0.01	-1.5	-57	2333-2335	-0	0	0	1
0.1929	931.47	2.662	-1.029	4554.7	500.00	1.43	4.44	45.48	1.43	0.01	-1.5	-57	2333-2335	-0	0	0	1
0.1930	931.07	2.663	-1.030	4554.7	500.00	1.43	4.44	45.48	1.43	0.01	-1.5	-57	2333-2335	-0	0	0	1
0.1931	930.67	2.664	-1.031	4554.7	500.00	1.43	4.44	45.48	1.43	0.01	-1.5	-57	2333-2335	-0	0	0	1
0.1932	930.27	2.665	-1.032	4554.7	500.00	1.43	4.44	45.48	1.43	0.01	-1.5	-57	2333-2335	-0	0	0	1
0.1933	929.87	2.666	-1.033	4554.7	500.00	1.43	4.44	45.48	1.43	0.01	-1.5	-57	2333-2335	-0	0	0	1
0.1934	929.47	2.667	-1.034	4554.7	500.00	1.43	4.44	45.48	1.43	0.01	-1.5	-57	2333-2335	-0	0	0	1
0.1935	929.07	2.668	-1.035	4554.7	500.00	1.43	4.44	45.48	1.43	0.01	-1.5	-57	2333-2335	-0	0	0	1
0.1936	928.67	2.669	-1.036	4554.7	500.00	1.43	4.44	45.48	1.43	0.01	-1.5	-57	2333-2335	-0	0	0	1
0.1937	928.27	2.670	-1.037	4554.7	500.00	1.43	4.44	45.48	1.43	0.01	-1.5	-57	2333-2335	-0	0	0	1
0.1938	927.87	2.671	-1.038	4554.7	500.00	1.43	4.44	45.48	1.43	0.01	-1.5	-57	2333-2335	-0	0	0	1
0.1939	927.47	2.672	-1.039	4554.7	500.00	1.43	4.44	45.48	1.43	0.01	-1.5	-57	2333-2335	-0	0	0	1
0.1940	927.07	2.673	-1.040	4554.7	500.00	1.43	4.44	45.48	1.43	0.01	-1.5	-57	2333-2335	-0	0	0	1
0.1941	926.67	2.674	-1.041	4554.7	500.00	1.43	4.44	45.48	1.43	0.01	-1.5	-57	2333-2335	-0	0	0	1
0.1942	926.27	2.675	-1.042	4554.7	500.00	1.43	4.44	45.48	1.43	0.01	-1.5	-57	2333-2335	-0	0	0	1
0.1943	925.87	2.676	-1.043	4554.7	500.00	1.43	4.44	45.48	1.43	0.01	-1.5	-57	2333-2335	-0	0	0	1
0.1944	925.47	2.677	-1.044	4554.7	500.00	1.43	4.44	45.48	1.43	0.01	-1.5	-57	2333-2335	-0	0	0	1
0.1945	925.07	2.678	-1.045	4554.7	500.00	1.43	4.44	45.48	1.43	0.01	-1.5	-57	2333-2335	-0	0	0	1
0.1946	924.67	2.679	-1.046	4554.7	500.00	1.43	4.44	45.48	1.43	0.01	-1.5	-57	2333-2335	-0	0	0	1
0.1947	924.27	2.680	-1.047	4554.7	500.00	1.43	4.44	45.48	1.43	0.01	-1.5	-57	2333-2335	-0	0	0	1
0.1948	923.87	2.681	-1.048	4554.7	500.00	1.43	4.44	45.48	1.43	0.01	-1.5	-57	2333-2335	-0	0	0	1

## FLECHETTE GROUND POINT

PAGE 10

T	X	Y	Z	V	P	ALPHA	PHI	ALPHA	ETA	L-N	L-P	M-N	L-M	S	T-M	F-T
SEC	FT	FT	FT	FT/SEC	FT/SEC	DIG	DIG	DIG	DIG	1/SEC	1/SEC	1/SEC	1/SEC	1/SEC	1/SEC	DIG
0.1959	988.24	2.628	-1.033	4053.2	500.00	1.43	4.74	45.49	-1.19	-0.47	-0.8	-57	233	-2335	-0	0
0.1950	988.74	2.630	-1.033	4053.2	500.00	1.43	4.74	45.49	-1.19	-0.47	-0.8	-57	233	-2335	-0	0
0.1951	989.23	2.632	-1.033	4053.2	500.00	1.43	4.74	45.49	-1.19	-0.47	-0.8	-57	233	-2335	-0	0
0.1952	989.73	2.634	-1.032	4053.2	500.00	1.43	4.74	45.49	-1.19	-0.47	-0.8	-57	233	-2335	-0	0
0.1953	990.22	2.635	-1.032	4053.1	500.00	1.43	4.74	45.49	-1.19	-0.47	-0.8	-57	233	-2335	-0	0
0.1954	990.72	2.637	-1.032	4053.1	500.00	1.43	4.74	45.49	-1.19	-0.47	-0.8	-57	233	-2335	-0	0
0.1955	991.21	2.639	-1.032	4053.1	500.00	1.43	4.74	45.49	-1.19	-0.47	-0.8	-57	233	-2335	-0	0
0.1956	991.71	2.641	-1.032	4053.1	500.00	1.43	4.74	45.49	-1.19	-0.47	-0.8	-57	233	-2335	-0	0
0.1957	992.21	2.642	-1.032	4053.1	500.00	1.43	4.74	45.49	-1.19	-0.47	-0.8	-57	233	-2335	-0	0
0.1958	992.70	2.644	-1.032	4053.1	500.00	1.43	4.74	45.49	-1.19	-0.47	-0.8	-57	233	-2335	-0	0
0.1959	993.20	2.646	-1.031	4053.1	500.00	1.43	4.74	45.49	-1.19	-0.47	-0.8	-57	233	-2335	-0	0
0.1960	993.69	2.647	-1.031	4053.1	500.00	1.43	4.74	45.49	-1.19	-0.47	-0.8	-57	233	-2335	-0	0
0.1961	994.19	2.648	-1.031	4053.0	500.00	1.43	4.74	45.49	-1.19	-0.47	-0.8	-57	233	-2335	-0	0
0.1962	994.68	2.649	-1.031	4053.0	500.00	1.43	4.74	45.49	-1.19	-0.47	-0.8	-57	233	-2335	-0	0
0.1963	995.18	2.652	-1.031	4053.0	500.00	1.43	4.74	45.49	-1.19	-0.47	-0.8	-57	233	-2335	-0	0
0.1964	995.67	2.653	-1.033	4053.0	500.00	1.43	4.74	45.49	-1.19	-0.47	-0.8	-57	233	-2335	-0	0
0.1965	996.17	2.655	-1.033	4053.0	500.00	1.43	4.74	45.49	-1.19	-0.47	-0.8	-57	233	-2335	-0	0
0.1966	996.66	2.657	-1.033	4053.0	500.00	1.43	4.74	45.49	-1.19	-0.47	-0.8	-57	233	-2335	-0	0
0.1967	997.16	2.657	-1.033	4053.0	500.00	1.43	4.74	45.49	-1.19	-0.47	-0.8	-57	233	-2335	-0	0
0.1968	997.65	2.659	-1.032	4053.0	500.00	1.43	4.74	45.49	-1.19	-0.47	-0.8	-57	233	-2335	-0	0
0.1969	998.15	2.660	-1.032	4053.0	500.00	1.43	4.74	45.49	-1.19	-0.47	-0.8	-57	233	-2335	-0	0
0.1970	998.65	2.661	-1.032	4053.0	500.00	1.43	4.74	45.49	-1.19	-0.47	-0.8	-57	233	-2335	-0	0
0.1971	999.14	2.662	-1.032	4053.0	500.00	1.43	4.74	45.49	-1.19	-0.47	-0.8	-57	233	-2335	-0	0
0.1972	999.64	2.663	-1.032	4053.0	500.00	1.43	4.74	45.49	-1.19	-0.47	-0.8	-57	233	-2335	-0	0
0.1973	1000.13	2.664	-1.032	4053.0	500.00	1.43	4.74	45.49	-1.19	-0.47	-0.8	-57	233	-2335	-0	0
0.1974	1000.63	2.665	-1.032	4053.0	500.00	1.43	4.74	45.49	-1.19	-0.47	-0.8	-57	233	-2335	-0	0
0.1975	1001.12	2.667	-1.032	4053.0	500.00	1.43	4.74	45.49	-1.19	-0.47	-0.8	-57	233	-2335	-0	0
0.1976	1001.62	2.668	-1.032	4053.0	500.00	1.43	4.74	45.49	-1.19	-0.47	-0.8	-57	233	-2335	-0	0
0.1977	1002.11	2.669	-1.032	4053.0	500.00	1.43	4.74	45.49	-1.19	-0.47	-0.8	-57	233	-2335	-0	0
0.1978	1002.61	2.670	-1.032	4053.0	500.00	1.43	4.74	45.49	-1.19	-0.47	-0.8	-57	233	-2335	-0	0
0.1979	1003.10	2.671	-1.032	4053.0	500.00	1.43	4.74	45.49	-1.19	-0.47	-0.8	-57	233	-2335	-0	0
0.1980	1003.60	2.672	-1.032	4053.0	500.00	1.43	4.74	45.49	-1.19	-0.47	-0.8	-57	233	-2335	-0	0
0.1981	1004.09	2.673	-1.032	4053.0	500.00	1.43	4.74	45.49	-1.19	-0.47	-0.8	-57	233	-2335	-0	0
0.1982	1004.59	2.674	-1.032	4053.0	500.00	1.43	4.74	45.49	-1.19	-0.47	-0.8	-57	233	-2335	-0	0
0.1983	1005.08	2.675	-1.032	4053.0	500.00	1.43	4.74	45.49	-1.19	-0.47	-0.8	-57	233	-2335	-0	0
0.1984	1005.58	2.676	-1.032	4053.0	500.00	1.43	4.74	45.49	-1.19	-0.47	-0.8	-57	233	-2335	-0	0
0.1985	1006.07	2.677	-1.032	4053.0	500.00	1.43	4.74	45.49	-1.19	-0.47	-0.8	-57	233	-2335	-0	0
0.1986	1006.57	2.678	-1.032	4053.0	500.00	1.43	4.74	45.49	-1.19	-0.47	-0.8	-57	233	-2335	-0	0
0.1987	1007.07	2.679	-1.032	4053.0	500.00	1.43	4.74	45.49	-1.19	-0.47	-0.8	-57	233	-2335	-0	0
0.1988	1007.56	2.680	-1.032	4053.0	500.00	1.43	4.74	45.49	-1.19	-0.47	-0.8	-57	233	-2335	-0	0
0.1989	1008.05	2.681	-1.031	4053.0	500.00	1.43	4.74	45.49	-1.19	-0.47	-0.8	-57	233	-2335	-0	0
0.1990	1008.55	2.682	-1.031	4053.0	500.00	1.43	4.74	45.49	-1.19	-0.47	-0.8	-57	233	-2335	-0	0
0.1991	1009.05	2.683	-1.031	4053.0	500.00	1.43	4.74	45.49	-1.19	-0.47	-0.8	-57	233	-2335	-0	0
0.1992	1009.54	2.684	-1.032	4053.0	500.00	1.43	4.74	45.49	-1.19	-0.47	-0.8	-57	233	-2335	-0	0
0.1993	1010.04	2.685	-1.032	4053.0	500.00	1.43	4.74	45.49	-1.19	-0.47	-0.8	-57	233	-2335	-0	0
0.1994	1010.53	2.686	-1.033	4053.0	500.00	1.43	4.74	45.49	-1.19	-0.47	-0.8	-57	233	-2335	-0	0
0.1995	1011.03	2.687	-1.033	4053.0	500.00	1.43	4.74	45.49	-1.19	-0.47	-0.8	-57	233	-2335	-0	0
0.1996	1011.52	2.688	-1.033	4053.0	500.00	1.43	4.74	45.49	-1.19	-0.47	-0.8	-57	233	-2335	-0	0
0.1997	1012.02	2.689	-1.035	4053.0	500.00	1.43	4.74	45.49	-1.19	-0.47	-0.8	-57	233	-2335	-0	0
0.1998	1012.51	2.690	-1.035	4053.0	500.00	1.43	4.74	45.49	-1.19	-0.47	-0.8	-57	233	-2335	-0	0



FLECHETTE GROUND POINT

PAGE 41

T SEC	X FT	Y FT	Z FT	V FT/SEC	P RAD/SEC	ALPHA DEG	MACH LEO	PHI DEG	ALPHA DEG	ETA DEG	L-N 1/SEC	L-P 1/SEC	4-V KNOTS	W-O KNOTS	3 TSU	K-T SEC
0.1999	993.01	2.987	-1.036	4953.6	500.00	1.43	4.44	45.48	0.49	1.33	-55	-57	233	233	0	1
0.2000	993.50	2.995	-1.037	4953.6	500.00	1.43	4.44	45.48	0.47	1.33	-55	-57	233	233	0	1
0.2001	994.00	2.998	-1.038	4953.4	500.00	1.43	4.44	45.48	0.33	1.33	-55	-57	233	233	0	1
0.2002	994.50	2.999	-1.038	4953.4	500.00	1.43	4.44	45.48	0.51	1.30	-55	-57	233	233	0	1
0.2003	995.00	2.999	-1.039	4953.4	500.00	1.43	4.44	45.48	0.56	1.27	-55	-57	233	233	0	1
0.2004	995.50	2.999	-1.040	4953.4	500.00	1.43	4.44	45.48	0.73	1.23	-55	-57	233	233	0	1
0.2005	996.00	2.999	-1.041	4953.4	500.00	1.43	4.44	45.48	0.79	1.20	-55	-57	233	233	0	1
0.2006	996.50	2.999	-1.042	4953.4	500.00	1.43	4.44	45.48	0.45	1.14	-55	-57	233	233	0	1
0.2007	997.00	2.999	-1.043	4953.4	500.00	1.43	4.44	45.48	0.30	1.11	-55	-57	233	233	0	1
0.2008	997.50	2.999	-1.044	4953.4	500.00	1.43	4.44	45.48	0.65	1.07	-55	-57	233	233	0	1
0.2009	998.00	2.999	-1.045	4953.4	500.00	1.43	4.44	45.48	1.11	1.02	-55	-57	233	233	0	1
0.2010	998.50	2.999	-1.046	4953.4	500.00	1.43	4.44	45.48	1.06	0.96	-55	-57	233	233	0	1
0.2011	999.00	2.999	-1.047	4953.4	500.00	1.43	4.44	45.48	1.11	0.91	-55	-57	233	233	0	1
0.2012	999.50	2.999	-1.048	4953.4	500.00	1.43	4.44	45.48	1.15	0.85	-55	-57	233	233	0	1
0.2013	1000.00	2.999	-1.049	4953.4	500.00	1.43	4.44	45.48	1.10	0.79	-55	-57	233	233	0	1
0.2014	1000.50	2.999	-1.050	4953.4	500.00	1.43	4.44	45.48	1.23	0.74	-55	-57	233	233	0	1
0.2015	1001.00	2.999	-1.051	4953.4	500.00	1.43	4.44	45.48	1.24	0.67	-55	-57	233	233	0	1
0.2016	1001.50	2.999	-1.052	4953.4	500.00	1.43	4.44	45.48	1.24	0.61	-55	-57	233	233	0	1
0.2017	1002.00	2.999	-1.053	4953.4	500.00	1.43	4.44	45.48	1.33	0.54	-55	-57	233	233	0	1
0.2018	1002.50	2.999	-1.054	4953.4	500.00	1.43	4.44	45.48	1.33	0.48	-55	-57	233	233	0	1
0.2019	1003.00	2.999	-1.055	4953.4	500.00	1.43	4.44	45.48	1.33	0.42	-55	-57	233	233	0	1
0.2020	1003.50	2.999	-1.056	4953.4	500.00	1.43	4.44	45.48	1.33	0.36	-55	-57	233	233	0	1
0.2021	1004.00	2.999	-1.057	4953.4	500.00	1.43	4.44	45.48	1.33	0.30	-55	-57	233	233	0	1
0.2022	1004.50	2.999	-1.058	4953.4	500.00	1.43	4.44	45.48	1.41	0.27	-55	-57	233	233	0	1
0.2023	1005.00	2.999	-1.059	4953.4	500.00	1.43	4.44	45.48	1.42	0.20	-55	-57	233	233	0	1
0.2024	1005.50	2.999	-1.060	4953.4	500.00	1.43	4.44	45.48	1.43	0.13	-55	-57	233	233	0	1
0.2025	1006.00	2.999	-1.061	4953.4	500.00	1.43	4.44	45.48	1.43	0.06	-55	-57	233	233	0	1
0.2026	1006.50	2.999	-1.062	4953.4	500.00	1.43	4.44	45.48	1.43	0.00	-55	-57	233	233	0	1
0.2027	1007.00	2.999	-1.063	4953.4	500.00	1.43	4.44	45.48	1.43	0.00	-55	-57	233	233	0	1
0.2028	1007.50	2.999	-1.064	4953.4	500.00	1.43	4.44	45.48	1.43	0.00	-55	-57	233	233	0	1
0.2029	1008.00	2.999	-1.065	4953.4	500.00	1.43	4.44	45.48	1.43	0.00	-55	-57	233	233	0	1
0.2030	1008.50	2.999	-1.066	4953.4	500.00	1.43	4.44	45.48	1.43	0.00	-55	-57	233	233	0	1
0.2031	1009.00	2.999	-1.067	4953.4	500.00	1.43	4.44	45.48	1.43	0.00	-55	-57	233	233	0	1
0.2032	1009.50	2.999	-1.068	4953.4	500.00	1.43	4.44	45.48	1.43	0.00	-55	-57	233	233	0	1
0.2033	1010.00	2.999	-1.069	4953.4	500.00	1.43	4.44	45.48	1.43	0.00	-55	-57	233	233	0	1
0.2034	1010.50	2.999	-1.070	4953.4	500.00	1.43	4.44	45.48	1.43	0.00	-55	-57	233	233	0	1
0.2035	1011.00	2.999	-1.071	4953.4	500.00	1.43	4.44	45.48	1.43	0.00	-55	-57	233	233	0	1
0.2036	1011.50	2.999	-1.072	4953.4	500.00	1.43	4.44	45.48	1.43	0.00	-55	-57	233	233	0	1
0.2037	1012.00	2.999	-1.073	4953.4	500.00	1.43	4.44	45.48	1.43	0.00	-55	-57	233	233	0	1
0.2038	1012.50	2.999	-1.074	4953.4	500.00	1.43	4.44	45.48	1.43	0.00	-55	-57	233	233	0	1
0.2039	1013.00	2.999	-1.075	4953.4	500.00	1.43	4.44	45.48	1.43	0.00	-55	-57	233	233	0	1
0.2040	1013.50	2.999	-1.076	4953.4	500.00	1.43	4.44	45.48	1.43	0.00	-55	-57	233	233	0	1
0.2041	1014.00	2.999	-1.077	4953.4	500.00	1.43	4.44	45.48	1.43	0.00	-55	-57	233	233	0	1
0.2042	1014.50	2.999	-1.078	4953.4	500.00	1.43	4.44	45.48	1.43	0.00	-55	-57	233	233	0	1
0.2043	1015.00	2.999	-1.079	4953.4	500.00	1.43	4.44	45.48	1.43	0.00	-55	-57	233	233	0	1
0.2044	1015.50	2.999	-1.080	4953.4	500.00	1.43	4.44	45.48	1.43	0.00	-55	-57	233	233	0	1
0.2045	1016.00	2.999	-1.081	4953.4	500.00	1.43	4.44	45.48	1.43	0.00	-55	-57	233	233	0	1
0.2046	1016.50	2.999	-1.082	4953.4	500.00	1.43	4.44	45.48	1.43	0.00	-55	-57	233	233	0	1
0.2047	1017.00	2.999	-1.083	4953.4	500.00	1.43	4.44	45.48	1.43	0.00	-55	-57	233	233	0	1
0.2048	1017.50	2.999	-1.084	4953.4	500.00	1.43	4.44	45.48	1.43	0.00	-55	-57	233	233	0	1

## REFERENCES

1. Fowler, R.M., Gallop, E.G., Lock, C.N.M., and Richmond, N.W., "Aerodynamic of a Spinning Shell" Phil. Trans. Royal Society, London, 1920.
2. Sterne, T.E., "On Jump Due to Bore Clearance," BRL Report No. 491, 28 Sept. 1944.
3. Murphy, C.H., "Comments on Projectile Jump," BRL Report No. 1071, April, 1957.
4. Kent, R.H., "First Memorandum Report on 3.3 inch Design Data Firings in Connection with O.B. Program 2627-3," BRL 14 May 1920.
5. Zaroodny, S.J., "On Jump Due to Muzzle Disturbances," BRL Report No. 703, June, 1949.
6. Murphy, C.H., Bradley, J.W., "Jump Due to Aerodynamic Asymmetry of a Missile with Varying Roll Rate," BRL Report No. 1077, May, 1959.
7. Nicolaidis, J.D., "On the Free Flight Motion of Missiles Having Slight Configurational Asymmetries," BRL Report No. 858, June, 1953.
8. Nicolaidis, J.D., McAllister, L.D., "A Note on the Contribution of Configurational Asymmetries to the Free Flight Motion of Missiles," Journal of the Aeronautical Sciences, Vol. 19, No. 12, Dec., 1952.
9. Nicolaidis, J.D., "Free Flight Dynamics," Text, Aerospace Engineering Department, University of Notre Dame, 1964.
10. Ingram, C.W., "A Computer Program for Integrating the Six-Degree-of-Freedom Equations of Motion of a Symmetrical Missile," Aerospace Engineering Dept., University of Notre Dame, 1970.
11. Ingram, C.W., Daniels, P., "A Spin Scale Theory for Rigid Body Integration Using the Frick Slip Frame," AIAA Journal, Vol. 5, No. 1, Jan. 1967.

REFERENCES (concluded)

12. Ingram, C.W., "Analytical Program for the Evaluation and Reduction of Dispersion and Jump of Fin Bodies," U.S. Army Frankford Arsenal Contract No. DAAA25-71-C0447, August, 1972.
13. Eikenberry, R.S., "Wobble, Analysis of Missile Dynamic Data," Prepared for Sandia Corp., Albuquerque, N.M., 1969.
14. Ingram, C.W., Nicolaides, J.D., Eikenberry, R.S., Lijewski, L.E., "A Computer Program to Fit the Initial Angular Data from Test Firing of Flechettes," Prepared for U.S. Army, Frankford Arsenal, Phila. Pa., 1973.
15. Piddington, M., "The Aerodynamic Characteristics of a Spin Projectile," BRL Memo Rpt. No. 1594, Ballistics Research Laboratory, Aberdeen Proving Ground, Md., Sept., 1964.
16. Garsik, M., "Dynamic Supersonic Wind Tunnel Testing," Masters Thesis, University of Notre Dame, Aerospace Dept., May, 1974.

## APPENDIX D

### FRANKFORD ARSENAL EXPERIMENTAL BALLISTICS FIRING PROGRAM OF FLECHETTES

During the spring and summer of 1974, eleven flechette firings were carried out in the Frankford Arsenal X-ray Ballistic Range. The data was measured from the x-ray plates by Frankford Arsenal personnel and is given in Figure D-1.

The flechette used in this test is very similar to the flechette used in lot 3 of the previous test data. It is assumed that the C.G. and the axial and transverse moments are the same. The C.G. is 0.94 inches from the nose; the axial moment is 0.0107 grain in<sup>2</sup> and the transverse moment is 1.78 grain in<sup>2</sup>. It is also assumed that the average spin rate is 2750 rev/sec.

The coordinate axis for the target data is defined as having plot (0,0) coincident with the aim point as established with a laser.

Times of flight were obtained between the first x-ray station and the sixth x-ray station. The baseline for determining the velocity was then a variable where the distance was measured between the flechette C.G. at the first station and at the sixth station.

The data used in the ND analysis is given in Figure D-2. The horizontal and vertical angles for Round 17 are plotted in D-3. In the case of Round 17 and Rounds 35, 23, 21 and 25 the motion was nearly 1d and therefore reductions and analysis could be carried out. The motions, however, on the

other rounds were highly 2 d and therefore computer fits were not possible. The results for Round 17 are presented herein in order to provide the reader with an example. Figure D-4 contains the original  $\alpha$ ,  $\beta$  data and the new data as determined by computer fit. The final  $\alpha$ ,  $\beta$  data is given in Figure D-5 which is used in the basic jump equation.

The trajectory data given in Figure D-1 is fitted on the computer with second degree, third degree and fourth degree polynomials as shown in Figure D-6. The third degree fit was used and a summary of the trajectory data is given in Figure D-7 which is also used in the basic jump equation.

Therefore, the  $\alpha$  and  $\beta$  data from Figure D-5 and the trajectory data from Figure D-7 is used with the basic jump equation to provide the results given in Figure D-8.

Figure D-8, therefore, is the final result of the firing program and the jump analysis which shows the agreement between the experimentally determined jump and the jump predicted from the translational ballistics motion parameters as determined in the Frankford Arsenal X-Ray Ballistics Range.

LOT YBR  
JUN 24 1976

Figure D-1

NOSE TO CG IS .940 INCHES

ROUND 17 TIME = 2031.4

FILM	X	Y	Z	ERR	VERT ANGLE	HOR ANGLE	ABS ANGLE	DIRECTION
1	-0.770	-1.1363	10.9339	.0366	-2.1564	1.0221	-2.3860	156.4353 .0001912
2	.0633	-1.137	33.6985	.0488	-5.2285	1.9080	-5.5622	161.8445 .0005742
3	.2172	-1.191	55.5981	-.0085	-5.3931	-.8609	-5.4606	172.9318 .0001727
4	.3963	-.2875	80.8581	-.0066	-1.8322	-.2348	-1.8472	-174.6961 .0014180
5	.5537	-.3637	103.8562	-.1123	2.6678	-.6549	2.5530	-15.6269 .0015160
6	.7172	-.4031	126.7605	-.2049	4.6416	-.4234	4.6607	-5.2615 .0022153

AVERAGE VELOCITY = 4752. FT/SEC

ROUND 35 TIME = 2029.5

FILM	X	Y	Z	ERR	VERT ANGLE	HOR ANGLE	ABS ANGLE	DIRECTION
1	-.1154	-1.1406	10.8052	.0301	-.9013	1.2915	-1.5747	126.3521 .0001970
2	-.0313	-1.1407	32.8870	.0282	-2.3030	.7494	-2.4216	163.8556 .0005750
3	-.1841	-1.1711	56.1766	-.0089	-.5331	.9839	-1.1190	119.8155 .0001830
4	.3364	-.2003	79.3832	-.0499	1.6433	.9455	1.8957	30.2541 .0012842
5	.4957	-.2078	103.6874	-.0435	2.6546	.0061	2.6546	.1327 .0014110
6	.6364	-.1778	126.4009	-.1251	2.2742	-.1278	2.2778	-3.2511 .0024180

AVERAGE VELOCITY = 4766. FT/SEC

ROUND 23 TIME = 2032.7

FILM	X	Y	Z	ERR	VERT ANGLE	HOR ANGLE	ABS ANGLE	DIRECTION
1	-.1640	-.1583	13.9515	-.0332	-.4711	-.0979	-.4812	-11.8711 .0002115
2	.0331	-.1488	33.6919	-.0046	-.0734	-.9900	-.9927	-95.3307 .0005740
3	.1912	-.1679	57.4623	-.0253	-1.4390	-.7920	-1.6336	-152.7508 .0010170
4	.3483	-.1776	80.3243	-.0158	-2.1346	-.0780	-2.1360	-179.9656 .0014574
5	.4870	-.1637	104.2197	-.1972	-1.1244	-.5813	-1.2685	154.1847 .0015146
6	.6360	-.1618	126.4914	-.1822	.2545	1.4928	1.5144	81.2546 .0022150

AVERAGE VELOCITY = 4694. FT/SEC

ROUND 2 TIME = 2033.8

FILM	X	Y	Z	ERR	VERT ANGLE	HOR ANGLE	ABS ANGLE	DIRECTION
1	-.0696	-.1638	10.8592	-.0108	-.0094	.3910	-.3911	92.4375 .0001873
2	-.0659	-.1694	33.3137	-.0769	-.1156	1.2257	-1.2311	96.4906 .0205765
3	-.2086	-.1793	55.7173	-.0155	-.1293	3.0829	-3.0856	93.4665 .0009812
4	-.3594	-.1917	80.0782	-.0415	-.1647	2.8075	2.8123	87.6873 .0013852
5	-.5340	-.1704	104.9778	-.0738	-.1934	1.6753	1.6884	84.3817 .0018161
6	-.7837	-.1529	128.0970	-.1210	-.2988	-.6213	-.6291	-81.8971 .0022160

AVERAGE VELOCITY = 4804. FT/SEC

ROUND 4 TIME = 2031.1

FILM	X	Y	Z	ERR	VERT ANGLE	HOR ANGLE	ABS ANGLE	DIRECTION
1	-.0877	-.1514	11.3160	-.0155	-.2499	.7507	-.7212	109.6656 .0001935
2	-.0866	-.1451	33.9186	-.0229	-.6793	.9779	-1.1900	126.1844 .0005800
3	-.2521	-.1558	56.6785	-.0133	-.8100	1.3149	-1.5480	123.3238 .0009490
4	-.4366	-.1599	82.7373	-.0041	-.8880	1.0144	-1.0511	105.9825 .0017147
5	-.6058	-.1533	106.0447	-.0408	-.4102	-.0312	-.4114	-4.3984 .0018123
6	-.7700	-.1336	129.6708	-.0841	-.5251	-.0261	-.5258	-2.8748 .0022159

AVERAGE VELOCITY = 4848. FT/SEC

ROUND 21 TIME = 1996.1

FILM	X	Y	Z	ERR	VERT ANGLE	HOR ANGLE	ABS ANGLE	DIRECTION
1	-.1109	-.1486	11.6143	-.0261	1.5107	.6916	1.6614	24.8773 .0001983
2	-.0324	-.1572	34.3057	-.0144	2.6938	1.9501	3.3240	36.3072 .0003666
3	-.1612	-.1628	57.3012	-.0249	3.3340	2.2342	3.9561	32.9843 .0009424
4	-.2396	-.1287	81.8297	-.0067	1.3399	1.3983	1.9363	46.7553 .0013492
5	-.4950	-.0898	105.2557	-.1631	-.2921	1.2987	-.4178	135.9067 .0017490
6	-.6488	-.0326	128.1421	-.1871	-.2826	-.7241	-.29205	-187.5308 .0021912

AVERAGE VELOCITY = 4865. FT/SEC

ROUND 5 TIME = 2031.8

FILM	X	Y	Z	ERR	VERT ANGLE	HOR ANGLE	ABS ANGLE	DIRECTION
1	-.0804	-.1666	11.1459	-.0056	2.1431	1.4189	2.5695	33.8883 .0001939
		-.1898	33.4874	-.0364	5.1425	2.1200	6.1186	20.4972 .0005625

Figure D-1 (continued)

2	.0500	-.1578	33.4674	.0364	5.7425	2.1260	6.1185	20.4472
3	.1923	-.1692	56.1273	.0102	6.8876	2.5060	7.3220	20.1627
4	.3561	-.1145	81.4707	.0145	4.2813	2.0130	4.7279	25.4419
5	.5199	-.0263	104.7454	-.0145	-.2779	-.3683	-.4614	128.5055
6	.6580	.0264	127.0880	-.0529	-.4.0700	-.8014	-.4.1477	-170.8303

AVERAGE VELOCITY = 4788. FT/SEC

ROUND 25 TIME = 2030.1

FILM	X	Y	Z	ERR	VERT ANGLE	HOR ANGLE	ABS ANGLE	DIRECTION
1	-.1253	-.1501	10.9129	.0343	.6746	1.5046	1.7401	67.5253
2	-.0110	-.1466	32.7991	.0480	1.5000	4.5882	4.9515	72.0126
3	.1336	-.1408	56.3469	.0405	1.9755	5.8165	6.1386	72.1167
4	.3120	-.1226	79.1842	-.0435	.9627	4.4618	4.5637	78.7452
5	.5126	-.0865	103.3855	-.1231	.2195	1.1622	1.1827	80.2229
6	.6852	-.0297	125.5950	-.2131	-.7632	-.2.0623	-.2.1987	-111.5758

AVERAGE VELOCITY = 4703. FT/SEC

ROUND 22 TIME = 1981.0

FILM	X	Y	Z	ERR	VERT ANGLE	HOR ANGLE	ABS ANGLE	DIRECTION
1	-.1164	-.1541	12.0050	.0208	-.5206	-.1123	-.5325	-169.7685
2	.0097	-.1676	33.7631	.0128	-.9490	-.9475	-1.3409	-136.6050
3	.1557	-.1883	57.4306	.0158	-.5403	-2.7707	-2.8227	-102.1945
4	.2767	-.2187	80.5107	-.0006	-.6122	-2.2402	-2.3826	-111.1919
5	.3712	-.2176	102.6521	-.2085	-.5678	-.1.9202	-1.0886	-113.0768
6	.4595	-.2498	123.7467	-.1795	.1003	1.3582	1.3519	86.7690

AVERAGE VELOCITY = 4701. FT/SEC

ROUND 20 TIME = 2031.9

FILM	X	Y	Z	ERR	VERT ANGLE	HOR ANGLE	ABS ANGLE	DIRECTION
1	-.0706	-.1522	10.9858	.0177	.4859	.3060	.5742	32.5670
2	.6937	-.1789	33.6055	.0075	.9567	-.4694	1.9746	-26.1987
3	.2396	-.2136	57.2682	-.0056	1.1981	-2.2065	-2.5103	-82.2175
4	.4180	-.2226	80.7352	-.0194	.4580	-1.9860	2.1554	-67.3041
5	.5145	-.1923	105.9170	-.0222	-.3738	-.3760	-.5302	-136.3904
6	.6327	-.1588	129.1871	-.0959	-.1.1776	1.8329	-2.1782	124.1322

AVERAGE VELOCITY = 4848. FT/SEC

Figure D-1 (continued)



Figure D-1 (continued)

ROUND 6 TIME = 2030.9

FILM	X	Y	Z	ERR	VERT ANGLE	HOR ANGLE	ABS ANGLE	DIRECTION
1	-0.0750	-0.1429	11.0242	-0.386	-1.3051	-0.5355	-1.4106	159.5169 .0001907
2	-0.0712	-0.1516	33.3521	-0.514	-2.2015	-0.5321	-2.2647	168.3413 .0006776
3	-0.2307	-0.1945	55.9890	-0.269	-0.507	-0.3150	-0.3191	-81.7950 .0000684
4	-0.4348	-0.2324	61.7539	-0.0202	-0.2448	-2.1247	3.0894	-43.9266 .0014152
5	-0.5390	-0.2384	104.8275	-0.0708	3.0944	-0.5440	3.1417	-30.8167 .0018152
6	-0.6706	-0.2111	127.9104	-0.0903	2.3496	-0.3856	2.3813	9.4220 .0022128

AVERAGE VELOCITY = 4736. FT/SEC

Figure D-2

R&D PARAMETERS

$$d = 0.00587 \text{ ft.}$$

$$m = 0.00004573 \text{ slugs}$$

$$I_x = 0.000 \ 000 \ 000 \ 330 \text{ slugs-ft}^2$$

$$I_y = 0.000 \ 000 \ 054 \ 883 \text{ slugs-ft}^2$$

$$p = 17279 \text{ rad/sec}$$

Round 17

Figure D-3

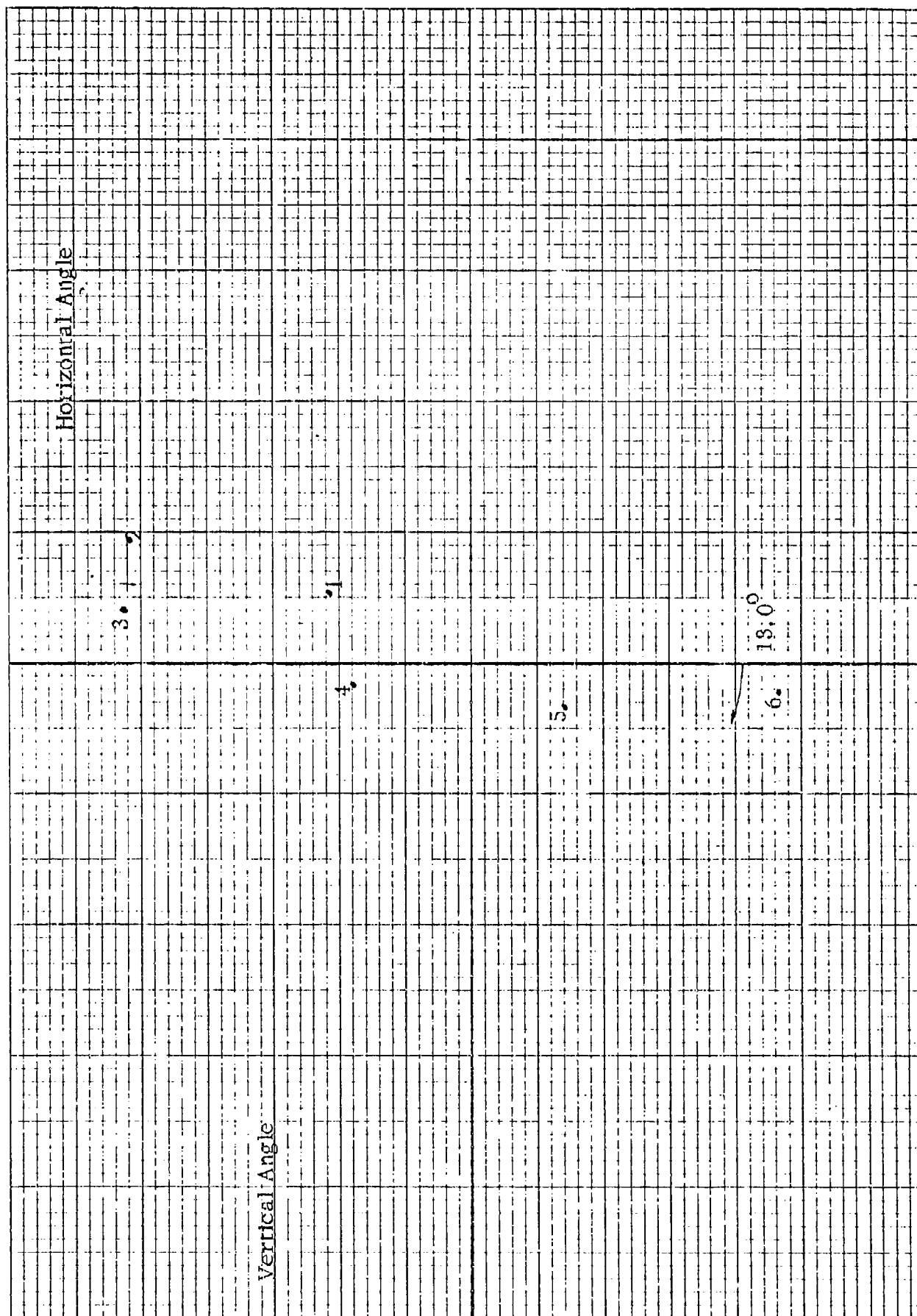


Figure D-4

5 AUG 12 1974

PAGE 2

ROUND 18

	ALPHA(DDU)	ANGLE(DDU)
1	-0.21500E 01	0.102210E 01
2	-0.22200E 01	0.100000E 01
3	-0.23000E 01	0.098000E 00
4	-0.23800E 01	0.096000E 00
5	-0.24600E 01	0.094000E 00
6	-0.25400E 01	0.092000E 00

ANGLE (RAD) ANGLE(DDU)

-0.20220E 01 -0.101710E 03

	PHI(DDU)	DELTA(DDU)
1	-0.250017E 01	-0.294090E 00
2	-0.250017E 01	-0.274090E 00
3	-0.250017E 01	-0.254090E 00
4	-0.250017E 01	-0.234090E 00
5	-0.250017E 01	-0.214090E 00
6	-0.250017E 01	-0.194090E 01

END PAGE 000 MI 1220  
 COMMENT JOB TIME 7.7 SEC  
 // FIN

TOTAL JOB TIME 11.3 SECS. 2 TOTAL PAGE(S)

PAGE 22 05/30/68 JOB 22 000 12, 1974

NUMBER 17

Figure 4 (continued)

T16L LPHN(NEW)

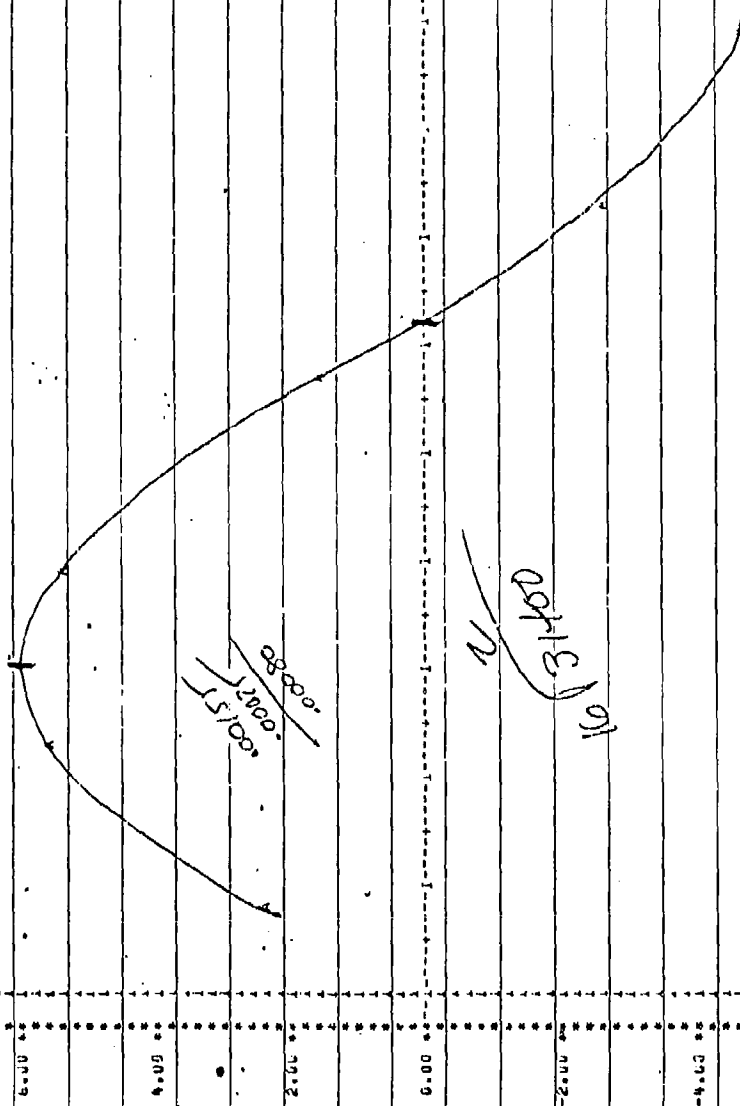
0.1913040000	0.250017	01
0.3752000000	0.350011	01
0.5727000000	0.350009	01
0.1413000000	0.250007	01
0.1110000000	0.250007	01
0.2210300000	0.350014	01

Figure D-4 (continued)

PAGE 23 0075XJUB JWB 22 AUG 121 1974

UALL 00 0.250-03 0.500-03 0.750-03 0.100-02 0.150-02 0.170-02 0.200-02 0.250-02

$k=6$   
 $W=2000$



UALL 00 0.250-03 0.500-03 0.750-03 0.100-02 0.150-02 0.170-02 0.200-02 0.250-02

DEKADON F. AT 1100  
 EAST PAUL JWS AT 1100

## Title

[illegible]

APPROXIMATIUS

KI	LI	a1	Li
U.S.BUSINESS U4	U.S.BUSINESS U6	U.S.BUSINESS U4	U.S.BUSINESS U4

REF	RI	LI	U1	SUS
B	0.653643E 01	-0.159249E 03	0.202000E 04	0.120470E 01

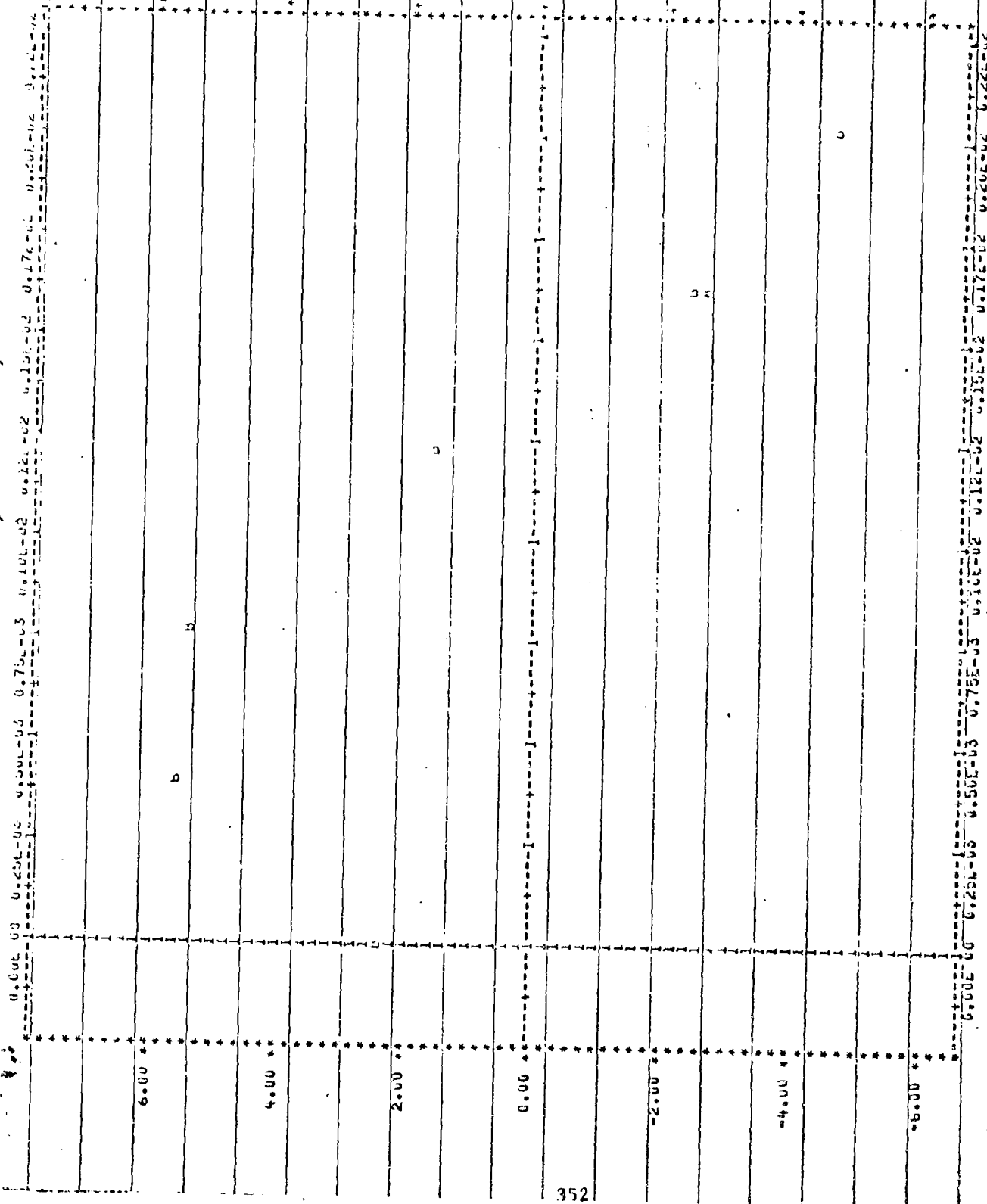
14-00000

[illegible]



Figure D-4 (continued)

PAGE 15 000000 000 52 AUG 12, 1974



ROUND 17

Figure D-5

Y	A	B	ALPHA	CA	DB	DALPHA
0.000191	-2.2214	0.7332	2.2399	-198.1504	65.5778	208.1700
0.000291	-3.2863	1.0876	3.4615	-172.3991	57.0554	181.5951
0.000391	-4.1853	1.3831	4.4086	-140.5085	46.5012	148.0033
0.000491	-4.8876	1.6175	5.1483	-103.9553	34.4039	109.5004
0.000591	-5.3778	1.7775	5.6573	-64.3590	21.2996	87.7920
0.000691	-5.6225	1.8678	5.9225	-23.4107	7.7478	24.6594
0.000791	-5.6398	1.8665	5.9406	17.1974	-5.6915	-18.1147
0.000891	-5.4292	1.7988	5.7188	55.8395	-18.4830	-58.8180
0.000991	-5.2665	1.6569	5.2735	91.0273	-30.1231	-95.8754
0.001091	-4.3953	1.4566	4.6297	121.4303	-40.1873	-127.9375
0.001191	-3.6261	1.2330	3.8195	145.9939	-48.3166	-153.7814
0.001291	-2.7349	0.9731	2.8908	163.9044	-54.2441	-172.6473
0.001391	-1.7614	0.5829	1.8554	174.6488	-51.7999	-183.9648
0.001491	-0.7475	0.2474	0.7874	178.0187	-58.9152	-187.5144
0.001591	0.2647	-0.0876	-0.2789	174.1094	-57.6214	-183.3966
0.001691	1.2346	-0.4036	-1.3004	163.3067	-54.0492	-172.0176
0.001791	2.1243	-0.7330	-2.2376	146.2620	-48.4053	-154.0638
0.001891	2.9035	-0.9539	-3.0552	123.8577	-40.9906	-130.4645
0.001991	3.5355	-1.1711	-3.7241	97.1649	-32.1567	-102.3478
0.002091	4.0081	-1.3265	-4.2219	67.3933	-22.3038	-70.9881
0.002191	4.3044	-1.4245	-4.5340	35.8394	-11.8610	-37.7511
0.002291	4.4187	-1.4621	-4.6536	3.8305	-1.2677	-4.0348
0.002391	4.3560	-1.4396	-4.5820	-27.3295	9.7447	28.7873
0.002491	4.1088	-1.3518	-4.3279	-56.4113	18.6693	59.4203
0.002591	3.7096	-1.2277	-3.9074	-82.3082	27.2399	86.6987
0.002691	3.1734	-1.0512	-3.3427	-104.0767	34.4441	109.6283
0.002791	2.5262	-0.8363	-2.6609	-120.9689	40.0346	127.4216
0.002891	1.7974	-0.5949	-1.8933	-132.4570	43.8366	139.5224
0.002991	1.0191	-0.3373	-1.0735	-138.2473	45.7329	145.6216
0.003091	0.2241	-0.0742	-0.2361	-139.2854	45.7655	145.6518
0.003191	-0.5350	0.1817	0.5846	-132.7499	43.9335	139.8309

Figure D-6

17X

THIRD DEGREE  
POLYNOMIAL COEFFICIENTS

$$C1 = -0.1258$$

$$C2 = 0.00175$$

$$C3 = 0.00000$$

THE PROBABLE ERROR OF FIT IS 0.024

THIRD DEGREE  
POLYNOMIAL COEFFICIENTS

$$C1 = -0.2441$$

$$C2 = 0.0014$$

$$C3 = 0.00000$$

$$C4 = -0.00000$$

$$\chi = -0.1441 + 0.3404t + 0.0398t^2 - 0.0083t^3$$

$$\dot{\chi} = 0.3404 + 0.0796t - 0.0249t^2$$

THE PROBABLE ERROR OF FIT IS 0.020

FOURTH DEGREE  
POLYNOMIAL COEFFICIENTS

$$C1 = -0.13452$$

$$C2 = 0.00175$$

$$C3 = 0.00000$$

$$C4 = -0.00000$$

$$C5 = 0.00000$$

Figure D-6 (continued)

17Y

COEFFICIENTS  
POLYNOMIAL FIT TO DATA

69

$$C1 = -0.07442$$

$$C2 = -0.00000$$

$$C3 = -0.00000$$

THE PROBABLE ERROR OF FIT IS 0.0136

THE COEFFICIENTS  
POLYNOMIAL FIT TO DATA

$$C1 = -0.00000$$

$$C2 = -0.00000$$

$$C3 = -0.00000$$

$$C4 = -0.00000$$

$$Y = -0.1551 + 0.1359t - 0.2526t^2 + 0.0628t^3$$

$$\dot{Y} = 0.1359 - 0.5024t + 0.1884t^2$$

THE PROBABLE ERROR OF FIT IS 0.0037

THE COEFFICIENTS  
POLYNOMIAL FIT TO DATA

$$C1 = -0.00000$$

$$C2 = -0.00000$$

$$C3 = -0.00000$$

$$C4 = -0.00000$$

$$C5 = -0.00000$$

Figure D-7

	X	Y	S	DX	DY	DS
0.000000	-0.012008	-0.012925	0.017642	0.028367	0.011325	0.030544
0.100000	-0.009139	-0.011997	0.015081	0.029059	0.007295	0.029912
0.200000	-0.006218	-0.011455	0.013059	0.029610	0.003580	0.029826
0.300000	-0.003219	-0.011270	0.011721	0.030170	0.000178	0.030170
0.400000	-0.000175	-0.011409	0.011411	0.030668	0.002910	0.030826
0.500000	0.002918	-0.011842	0.012196	0.031165	-0.005683	0.031679
0.600000	0.006056	-0.012536	0.013922	0.031600	-0.008143	0.032632
0.700000	0.009236	-0.013460	0.016324	0.031993	-0.010289	0.033607
0.800000	0.012454	-0.014583	0.019177	0.032345	-0.012120	0.034542
0.900000	0.015714	-0.015873	0.022329	0.032656	-0.013638	0.035389
1.000000	0.018983	-0.017300	0.025684	0.032925	-0.014842	0.036116
1.100000	0.022208	-0.018831	0.029178	0.033153	-0.015731	0.036696
1.200000	0.025612	-0.020436	0.032766	0.033339	-0.016307	0.037113
1.300000	0.028954	-0.022182	0.036414	0.033483	-0.016569	0.037358
1.400000	0.032308	-0.023739	0.040092	0.033586	-0.016516	0.037428
1.500000	0.035673	-0.025375	0.043775	0.033649	-0.016150	0.037323
1.600000	0.039036	-0.026959	0.047443	0.033668	-0.015470	0.037352
1.700000	0.042402	-0.028458	0.051067	0.033647	-0.014475	0.036628
1.800000	0.045764	-0.029843	0.054635	0.033584	-0.013167	0.036073
1.900000	0.049117	-0.031181	0.058125	0.033479	-0.011545	0.035414
2.000000	0.052458	-0.032142	0.061522	0.033333	-0.009608	0.034690
2.100000	0.055783	-0.032993	0.064899	0.033146	-0.007358	0.033953
2.200000	0.059086	-0.033603	0.067973	0.032917	-0.004794	0.033264
2.300000	0.062365	-0.033941	0.071002	0.032647	-0.001915	0.032703
2.400000	0.065614	-0.033975	0.073889	0.032335	0.001277	0.032350
2.500000	0.068833	-0.033675	0.076626	0.031981	0.004783	0.032337
2.600000	0.072009	-0.033108	0.079214	0.031586	0.008604	0.032737
2.700000	0.075146	-0.031944	0.081654	0.031150	0.012738	0.033654
2.800000	0.078237	-0.030450	0.083954	0.030672	0.017186	0.035159
2.900000	0.081279	-0.028496	0.086130	0.030153	0.021949	0.037295
3.000000	0.084267	-0.026150	0.088201	0.029592	0.027025	0.040075

CORE USAGE OBJECT CODE= 1720 BYTES, ARRAY AREA= 868 BYTES, TOTAL AREA AVAILABLE= 86112 BYTES

DIAGNOSTICS NUMBER OF ERRORS= 0, NUMBER OF WARNINGS= 0, NUMBER OF EXTENSIONS= 0

COMPILE TIME= 0.08 SEC, EXECUTION TIME= 0.15 SEC, WAITIV - VERSION 1 LEVEL 3 MARCH 1971 DATE= 74/225

Table D-8

DISPERSION ANALYSIS  
(127 ft. Target)

R O U N D	Position Downrange (ft)	Initial Conditions				Frankford Dispersion		6-D Dispersion	
		$u_o$ (ft./sec)	$P_o$ (rad/sec)	$\bar{S}_o$ (ft)	$\dot{S}_o$ (ft./sec)	$\bar{\alpha}_o$ (deg)	$\dot{\alpha}_o$ (rad/sec)	mils	mils
17	1			-0.006208	0.029610+	0.7352-	65.6-	-0.087	0.2657
	3			-0.011455i	0.003580i	2.2214i	198.2i	+0.251i	
	5	4752	17279	0.006056-	0.031600-	1.7775-	21.3-	-0.019	0.1472
	7			0.012536i	0.008143i	3.3708i	64.4i	+0.146-	
21	1			0.018983-	0.032925-	1.6569-	30.1	0.032-	0.0918
	3			0.017300i	0.014842i	5.0065i	+91.0i	0.086i	
	5	4865	17279	0.032308-	0.033586-	0.5829-	57.8	0.091-	0.2427
	7			0.023739i	0.016516i	1.7614i	+174.6i	0.225i	
23	1			-0.009130	0.029123-	1.1027+	73.6+	-0.098	0.1304
	3			-0.012263i	0.004831i	1.1028i	73.6i	-0.086i	
	5			0.002832-	0.030624-	2.3922+	34.5+	-0.035	0.0442
	7			0.013482i	0.001223i	2.3925i	34.5i	-0.027i	
25	1			0.015317-	0.031733-	2.5669+	19.7	0.0657+	0.0955
	3			0.013208i	0.002633i	2.5672i	19.7i	0.0683i	
	5	4696	17279	0.028167-	0.032451+	1.5643+	64.1	0.106+	0.1352
	7			0.011342i	0.006737i	1.5644i	64.1i	0.084i	
35	1			-0.009095	0.030700+	-0.0187	0.9-	-0.007	0.0099
	3			-0.012963i	0.00724i	+0.6239i	29.2i	+0.007i	
	5	4708	17279	0.003109-	0.030350-	0.0085-	1.4-	0.170+	0.1806
	7			0.013058i	0.001001i	0.2842i	47.1i	0.061i	
37	1			0.015208-	0.030175-	0.0403-	1.2-	0.005+	0.0344
	3			0.013608i	0.001558i	1.3458i	40.6i	0.034i	
	5			0.027273-	0.030176-	0.0574-	0.2	0.019+	0.0206
	7			0.014148i	0.000948i	1.9201i	5.1i	0.008i	
39	1			-0.010197	0.018419+	1.6128+	174.1+	-0.201	0.2163
	3			-0.012496i	0.000672i	0.5056i	54.6i	-0.080i	
	5	4708	17279	-0.000791	0.028081+	4.8205+	97.0+	-0.137	0.1379
	7			-0.012241i	0.000818i	1.5112i	30.4i	-0.016i	
41	1			0.011842-	0.034550+	5.8206+	11.1	-0.040	0.0408
	3			0.011667i	0.002275i	1.8247i	3.5i	-0.008i	
	5			0.026424-	0.037827+	4.4261+	104.6	0.154+	0.1594
	7			0.010247i	0.005044i	1.3875i	32.8i	0.041i	
43	1			-0.009245	0.031137+	0.2731-	10.1-	-0.027	0.0658
	3			-0.011629i	0.002960i	1.5468i	56.9i	+0.060i	
	5	4746	17279	0.003296-	0.031503-	0.3742-	1.9+	-0.007	0.0076
	7			0.011988i	0.004020i	2.1193i	10.6i	+0.003i	
45	1			0.015908-	0.031500-	0.1959-	12.7	0.043-	0.1089
	3			0.014258i	0.006690i	1.1094i	71.8i	0.100i	
	5			0.028446-	0.031129-	-0.1344	14.2	0.050-	0.1003
	7			0.016681i	0.004780i	+0.7614i	80.5i	0.087i	

DISTRIBUTION

Commander  
U.S. Army Armament Command  
Attn: AMCRD  
5001 Eisenhower Avenue  
Alexandria, VA 22333

Commander  
U.S. Army Armament Command  
Attn: AMSAR-RD  
Rock Island, IL 61202

Commander  
Ballistics Research Laboratories  
Attn: AMXRD-BEL  
Aberdeen Proving Ground, MD 21005

Defense Documentation Center (2)  
Attn: DDC-TCA  
Cameron Station  
Alexandria, VA 22314

Frankford Arsenal:

3 Attn: TSP-L/51-2  
(1 - Circulation copy  
1 - Reference copy  
1 - Record copy)

1 Attn: MDS-D/220-2  
Mr. Walter Schupp

Printing & Reproduction Division  
FRANKFORD ARSENAL  
Date Printed: 3 Sept. 1975

DEPARTMENT OF THE ARMY  
FRANKFORD ARSENAL  
PHILADELPHIA, PA. 19137

OFFICIAL BUSINESS  
PENALTY FOR PRIVATE USE \$300  
SARFA-TSP-T

POSTAGE AND FEES PAID  
DEPARTMENT OF THE ARMY  
E109-314

